AUGUST 1990
ENVIRONMENTAL SCIENCE & TECHNOLOGY

ES&T

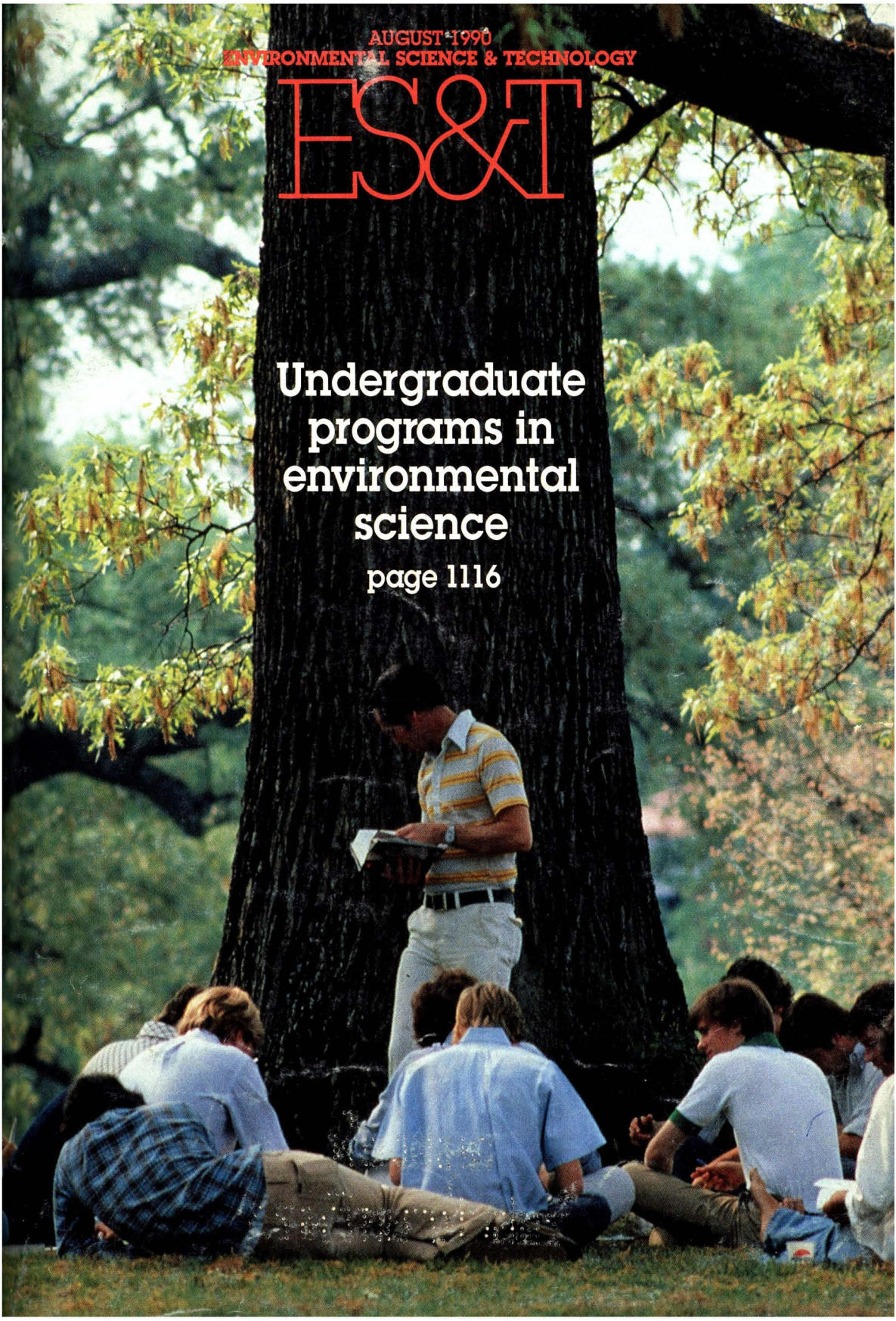

Undergraduate programs in environmental science

page 1116

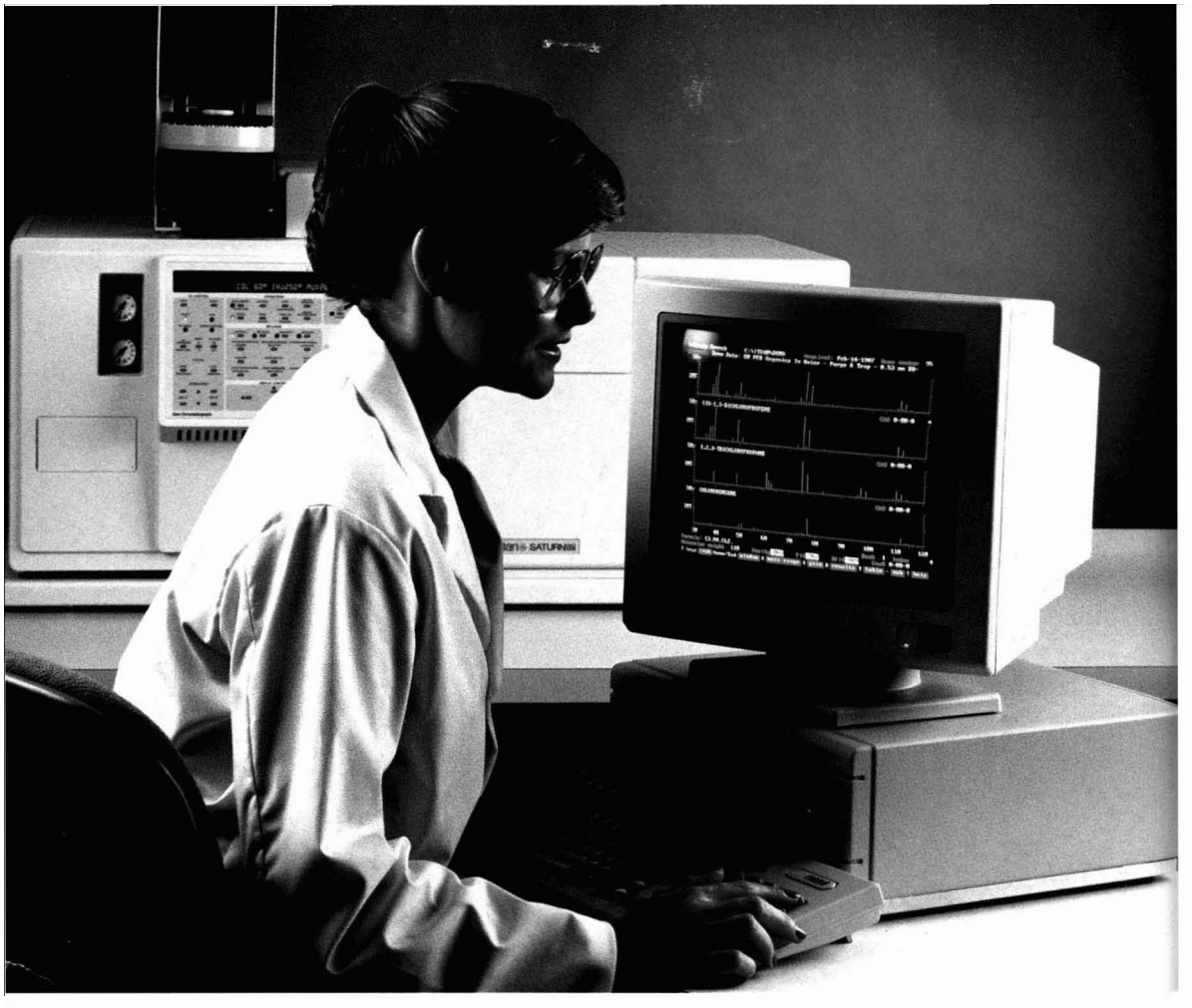

THE FUTURE OF GC/MS IS WITH VARIAN.

The best GC/MS, now and in the future, starts with chromatographic excellence. After all, if you don't start with expert chromatographic techniques, how can you trust the final results? Look to the company known for its expertise — from sample handling to the most sensitive detection — Varian.

The combination of our proven 3400 Gas Chromatograph with second generation ion trap technology brings the most sensitive and reliable benchtop GC/MS to the market.

The new Varian Saturn GC/MS System gives picture perfect spectra even at picogram levels, a significant advantage over conventional benchtop quadrupoles. It's important to know that you can count on the Saturn GC/MS to give you the whole picture when you're confirming compounds, because you're doing scientific analyses that affect our environment, our health, the products we use, and must meet regulatory protocols.

Chromatographic excellence and the most sensitive mass spec detector, coupled with Varian's renowned service and support throughout the world, make this the GC/MS with a future.

Let us show you why you should invest your GC/MS future with Varian. For more information, call **1-800-926-3000.**
In Canada, call **416-457-4130.**

CIRCLE 1 ON READER SERVICE CARD

GC WITH A FUTURE

varian

Environmental Science & Technology

Please send *research* manuscripts to Manuscript Reviewing, *feature* manuscripts to Managing Editor. For editorial policy, author's guide, and peer review policy, see the January 1990 issue, page 41, or write Yvonne D. Curry, Manuscript Reviewing Office, *ES&T.* A sample copyright transfer form, which may be copied, appears on the inside back cover of the January 1990 issue.

Environmental Science & Technology, ES&T (ISSN 0013-936X), is published monthly by the American Chemical Society at 1155 16th Street, N.W., Washington, D.C. 20036. Second-class postage paid at Washington, D.C., and at additional mailing offices. POSTMASTER: Send address changes to *Environmental Science & Technology,* Membership & Subscription Services, P.O. Box 3337, Columbus, Ohio 43210.

SUBSCRIPTION PRICES 1990: Members, $36 per year; nonmembers (for personal use), $67 per year; institutions, $276 per year. Foreign postage, $14 additional for Canada and Mexico, $29 additional for Europe including air service, and $36 additional for all other countries including air service. Single issues, $23 for current year; $24 for prior years. Back volumes, $282 each. For foreign rates add $3 for single issues and $14 for back volumes. Rates above do not apply to nonmember subscribers in Japan, who must enter subscription orders with Maruzen Company Ltd., 3-10 Nihon bashi 2 chome, Chuo-ku, Tokyo 103, Japan. Tel: (03) 272-7211.

SUBSCRIPTION SERVICE: Orders for new subscriptions, single issues, back volumes, and microform editions should be sent with payment to Office of the Treasurer, Financial Operations, ACS, 1155 16th St., N.W., Washington, D.C. 20036. Phone orders may be placed, using VISA, MasterCard, or American Express, by calling the ACS Sales Office at (614) 447-3776 or toll free (800) 333-9511 from anywhere in the continental U.S. (In the Washington, D.C., area call 872-4600.) Changes of address, subscription renewals, claims for missing issues, and inquiries concerning records and accounts should be directed to Manager, Membership and Subscription Services, ACS, P.O. Box 3337, Columbus, Ohio 43210. Changes of address should allow six weeks and be accompanied by old and new addresses and a recent mailing label. Claims for missing issues will not be allowed if loss was due to insufficient notice of change of address, if claim is dated more than 90 days after the issue date for North American subscribers or more than one year for foreign subscribers, or if the reason given is "missing from files."

ES&T CONTENTS

Volume 24, Number 8, August 1990

FEATURES

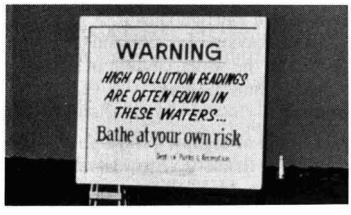

VIEWS

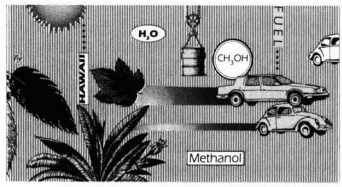

REGULATORY FOCUS

DEPARTMENTS

UPCOMING

RESEARCH

ESTHAG 24(8)1109–1270 (1990)
ISSN 0013 936X

Cover: SuperStock

Credits: p. 1122, International Joint Commission

1167
Effect of ten quaternary ammonium cations on tetrachloromethane sorption to clay from water. James A. Smith,* Peter R. Jaffé, and Cary T. Chiou

The molecular structure of quaternary ammonium cations substituted onto Wyoming bentonite affects both the magnitude and mechanism of tetrachloromethane sorption.

1173
Identification of solubility-controlling solid phases in a large fly ash field lysimeter. Jonathan S. Fruchter,* Dhanpat Rai, and John M. Zachara

Potential solubility controls for Al, Ba, Ca, Cr, Cu, Fe, S, Si, and Sr concentrations in leachates and pore waters from a large field fly ash lysimeter are identified by a geochemical model.

1179
Determination of polycyclic aromatic hydrocarbons in urban street dusts and their source materials by capillary gas chromatography. Hideshige Takada,* Tomoko Onda, and Norio Ogura

Detailed molecular distributions of PAHs suggest that PAHs in street dusts from heavily trafficked roads are derived mainly from traffic-related sources, probably automobile exhausts.

1186
Determination of optimal storage conditions for particle samples. George M. Sverdrup,* Bruce E. Buxton, Jane C. Chuang, and Gary S. Casuccio

Laboratory studies are conducted to show how to store particle samples to preserve them for chemical, physical, and biologic testing.

1196
An intercomparison of sampling techniques for nicotine in indoor environments. Fern M. Caka, Delbert J. Eatough,* Edwin A. Lewis, Hongmao Tang, S. Katherine Hammond, Brian P. Leaderer, Petros Koutrakis, John D. Spengler, Adam Fasano, Jack McCarthy, Michael W. Ogden, and Joellen Lewtas

The concentrations of nicotine in environmental tobacco smoke are determined and compared by using filter pack, annular denuder, sorbent bed, and passive sampling systems.

1203
Model of organic chemical uptake and clearance by fish from food and water. Kathryn E. Clark, Frank A. P. C. Gobas, and Donald Mackay*

A fugacity model is developed to describe uptake of organic chemicals by fish from water and food and loss to water and feces and by metabolism.

1214
Fluorescent polycyclic aromatic hydrocarbons as probes for studying the impact of colloids on pollutant transport in groundwater. Debera A. Backhus and Philip M. Gschwend*

A fluorescence quenching method, allowing examination of samples under in situ conditions, is tested using model organic colloids and then applied to groundwater samples.

1224
^{210}Po and ^{210}Pb remobilization from lake sediments in relation to iron and manganese cycling. Gaboury Benoit* and Harold F. Hemond

The behavior of ^{210}Po and ^{210}Pb is studied in the water column of an oligotrophic, dimictic lake.

1234
Adsorption of organic cations to natural materials. Bruce J. Brownawell, Hua Chen, John M. Collier, and John C. Westall*

The extent of adsorption of an amphiphilic organic cation on environmental sorbents depends strongly on concentrations of major cations and anions in solution, but pH has little effect.

1241
Structure–activity relationships for biodegradation of linear alkylbenzenesulfonates. Robert J. Larson

Results of studies to characterize the kinetics of biodegradation of a range of pure chain-length linear alkylbenzenesulfonate homologues in river water and river water/sediment systems are reported.

1246
Modeling the bioconcentration of organic chemicals in plants. Stefan Trapp,* Michael Matthies, Irene Scheunert, and Eva M. Topp

Uptake of several organic chemicals by growing barley is investigated in a closed laboratory model ecosystem.

1252
Reduction of phosphorus and chlorophyll *a* concentrations following $CaCO_3$ and $Ca(OH)_2$ additions to hypereutrophic Figure Eight Lake, Alberta. Ellie E. Prepas,* Tom P. Murphy, Jan M. Crosby, Dave T. Walty, Jit T. Lim, Jay Babin, and Patricia A. Chambers

Addition of lime to a hardwater hypereutrophic lake results in suppression of chlorophyll *a* and total phosphorus concentrations, and an enhancement of under-ice oxygen conditions.

1259
Inferred effects of lake acidification on *Daphnia galeata mendotae.* Wendel Keller,* Norman D. Yan, Keith E. Holtze, and J. Roger Pitblado

Lake acidification causes widespread effects on *Daphnia galeata mendotae* populations in Canada.

1261
Nonaqueous ion-exchange separation technique for use in bioassay-directed fractionation of complex mixtures: Application to wood smoke particle extracts. Douglas A. Bell,* Hani Karam, and Richard M. Kamens

The feasibility of an alternative method for separating acid/base/neutral fractions in pine wood smoke extract while achieving high mass and mutagenicity recovery required for bioassay-directed fractionation is explored.

1265
Selected organic pollutant emissions from unvented kerosene space heaters. Gregory W. Traynor,* Michael G. Apte, Harvey A. Sokol, Jane C. Chuang, W. Gene Tucker, and Judy L. Mumford

An exploratory study is performed to assess the semivolatile and nonvolatile organic pollutant emission rates from unvented kerosene space heaters.

* To whom correspondence should be addressed.

This issue contains no papers for which there is supplementary material in microform.

ES&T
EDITORIAL

Ecological research within EPA

There is increasing attention being given to the basic research program within EPA. It is generally conceded that EPA is primarily a regulatory agency, but many people feel that it must also be responsible for coordinating a high-quality research agenda for this country. This raises new questions about the ownership of environmental research within the federal government, the funding of basic research vis à vis research to support the regulatory agenda and, most recently, the relative priority to be given to research supporting human health versus ecological health.

Three public meetings were held recently in Chicago, Seattle, and Philadelphia to discuss ecological research at EPA, and at each meeting it became evident that the questions that needed to be resolved were much broader than the printed agenda. Each meeting included presentations by EPA officials representing the Office of Research and Development, invited speakers, and comments from the attending public. The purposes of the meetings were to respond to an EPA Science Advisory Board recommendation (*Future Risk: Research Strategies for the 1990s*) that EPA provide federal leadership in establishing an enlarged, better coordinated program of national ecological research, and to consider establishment of an "institute" to implement such an expanded program.

There is no doubt that more ecological research is needed, but the debate surrounding this issue raises many questions, including: How can the diverse ecological research programs within various federal agencies be accounted for and coordinated? Is EPA the appropriate agency in which to vest authority for an expanded ecological research agenda? Could EPA effectively articulate to budget planners and policy makers the need for an expanded, sustained ecological research program? Would such a program under EPA stewardship be tied too strongly to the EPA regulatory agenda?

Many people point out that EPA has not been a major sponsor of ecological research, either intra- or extramural, and in the agency there is not presently a tradition nor an infrastructure for such a program. It is perhaps significant that ecological research is not drawn out as a category in the EPA budget, though many program areas undoubtedly include some research in such a broad category. Nor do many people feel that EPA has the track record to suggest that it will foster the type of research, especially long-term research, that is needed in this and other areas.

For these reasons, some people are proposing a new super institute [Hubbell, Howe et al. in *National Institute for the Environment* (NIE)] that would be modeled on the NIH model. Such an institute would conduct intramural research through a staff of professional environmental scientists and would also sponsor extramural research through a peer review system such as that employed at NIH. Among the questions raised by this proposal are: What would be the relationship between the NIE and existing federal environmental programs, including EPA? Would the research agenda be influenced by the regulatory agenda and if so, by what mechanism? What would be the breadth and depth of the research program? Would the NIE take a very broad definition of "environmental" to include essentially all of the programs now covered by federal agencies? Or would its mission be more focused—and would the institute take a global view or one that was directed more towards the perceived needs of this country?

All of these issues and more will undoubtedly be debated within the next few months. It is reported that the National Academy of Sciences will empower a panel to discuss the NIE concept, but it is hoped that such a panel will take a much broader view. What is needed is for this country and (perhaps better) a consortium of developed countries to construct a mechanism for the support and sustenance of long- and short-term research and technology transfer in the areas of environmental sciences, engineering, and policy. Funding in all of these areas is woefully deficient, the personnel base is insufficient in quality and quantity, and the research agendas have been too tightly tied to the short-term regulatory agenda. Let us hope that the leadership in government, academia, and the private sector can combine to address this important problem for the benefit of future generations.

0013-936X/90/0924-1111$02.50/0

ES&T LETTERS

Protecting human health

Dear Sir: Jeffery Foran's summary of the procedures for deriving numeric criteria to protect human health from toxicants in surface water (*ES&T,* May 1990, p. 604) describes some of the variations in water pollution control that exist under the programs of the eight Great Lakes states. As he recognizes, the adoption by the states of unique state-specific procedures to develop human health criteria may result in different criteria for the same pollutant in the same lake. For example, Lake Superior is shared by Minnesota, Michigan, and Wisconsin (along with Ontario). Each state uses different assumptions in its procedures to develop water quality criteria. The three states have developed the following criteria for polychlorinated biphenyls (PCBs) in Lake Superior:

Michigan	.02 ng/L
Minnesota	.014 ng/L
Wisconsin	.15 ng/L

This problem of varying degrees of stringency in controlling pollution as a result of different numeric criteria can be compounded by the different assumptions the states make when they use their criteria to develop water quality-based effluent limits. For example, all Great Lakes states allow dilution when developing effluent limits, but in varying degrees. These differences can result in hundreds of times greater quantities of pollutants entering the lakes when comparing one state's dilution factors with another's.

Two initiatives are underway to address the continuing problem of toxic contamination in the Great Lakes and to bring about greater uniformity in water quality standards (WQS) and pollution control programs. In 1978, the United States and Canada signed the Great Lakes Water Quality Agreement, pledging to restore and maintain the Great Lakes basin ecosystem. The National Wildlife Federation's Great Lakes office is currently developing "Model" WQS for the Great Lakes, based on incorporating the goals of the agreement into domestic laws and regulations. Our research team is currently developing procedures and numeric criteria to protect sensitive wildlife species that have been adversely affected by toxic contamination in the Great Lakes food chain. We are also developing criteria to protect pregnant women, women of child-bearing age, and their offspring, taking into account recent evidence that babies born to mothers who consumed large quantities of Great Lakes fish were smaller and had impaired performance on short-term memory tests.

EPA has also recognized that current state and federal water quality criteria and pollution control programs are inadequate to achieve the goals of the Great Lakes Water Quality Agreement. In June of 1989, EPA and the Great Lakes states commenced the Great Lakes Water Quality Initiative. The objective of the initiative is to improve the United States' ability to implement the Agreement by developing water quality criteria and guidance on critical application issues like dilution for persistent, bioaccumulative toxic pollutants. The results of the initiative are to be published under Sections 303 and/or 304 of the Clean Water Act.

Despite past progress, particularly in the area of controlling conventional pollutants, levels of toxic contaminants in Great Lakes water and biota remain at unacceptably high levels. The International Joint Commission has repeatedly advised the United States and Canada that current approaches are inadequate and that a new, comprehensive focus on reducing total loads of toxic pollution from all sources toward the ultimate goal of virtual elimination of persistent toxic substances is necessary. The commission has recognized that the existing complex regulatory framework limits governments' ability to achieve the international agreement's goals. Efforts like NWF's Model standards and EPA's Initiative have the potential to reform the existing system toward that end.

Tim Eder
National Wildlife Federation
Great Lakes Natural Resource Center
Ann Arbor, MI 48104

0013-936X/90/0924-1112$02.50/0

ES&T CURRENTS

INTERNATIONAL

British Prime Minister Margaret Thatcher pledged that Britain would eliminate growth in carbon dioxide emissions over the next 15 years, if other industrialized countries would follow suit. This pledge represents a break with the Bush administration on the CO_2 issue. Thatcher made this pledge after the United Nations Intergovernmental Panel on Climate Change issued a report May 25 that forecasts global warming of 2 °F by 2025 and 6 °F by 2100. The U.N. report contrasts with the findings of a U.S. Agricultural Research Service (ARS) study that overall average temperatures in the United States actually have declined by about 0.3 °F since 1920. The findings are uneven, however; for instance, they indicate warming by 3.23 °F in Schenectady, NY, and cooling by as much as 3.40 °F in Oconee, SC. ARS physicist Sherwood Idso has characterized the ARS study as "inconclusive as to whether the climate is warming or cooling." In another development, the Bush administration announced June 15 that it was dropping its objections to the creation of a $100 million international fund to help developing nations end their use of chemicals suspected of harming the stratospheric ozone layer.

The European Commission (EC) proposes to control the evaporative emissions of gasoline from cars. The EC's main strategy is to require the installation of onboard enlarged carbon canisters "to control effectively refueling and evaporative losses in one step, including running losses. This strategy is more effective and energy-efficient than the alternative of restricting the composition of gasoline" (*Closing the Gasoline System; CONCAWE Report No. 3/90*). According to CONCAWE (Brussels), this approach also "is more effective. . . than restricting the quality and composition of gasoline" and limiting the benzene content of gasoline. The report says that enlarged carbon canisters can control evaporative emissions, including those of benzene, from parked cars by as much as 90% (also see *ES&T* feature, this issue, p. 1128).

FEDERAL

The Council on Environmental Quality's most recent report to Congress shows much success in environmental improvement, and stresses "the very long way" the nation has come, says CEQ chairman Michael Deland. He cites the enactment of 12 laws, more stringent enforcement, better data collection, improved international cooperation, and more enlightened response from American business leaders. Critics charge that the report fails to mention slower progress than expected under the Clean Air Act of 1970 and delays on the part of the United States in action on chlorofluorocarbons, which are suspected of depleting stratospheric ozone. A CEQ spokesperson says that the report does not try to cover up problems, but does take the position that much has been accomplished. Copies of the 494-page report are available for $17 from the Superintendent of Documents, U.S. Government Printing Office, Washington, DC 20402.

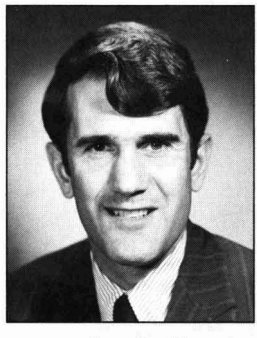

***Deland:** Pleased with progress*

EPA announced June 13 tighter regulations on emissions of volatile organic compounds (VOCs). VOCs are suspected of being precursors of tropospheric ozone and smog. Most affected are manufacturers of synthetic organic chemicals and managers of hazardous waste treatment, storage, and disposal facilities. Authorized under the Clean Air Act and the Resource Conservation and Recovery Act, the regulations aim at reducing VOC emissions by 30%. The capital costs of compliance for synthetic organic chemical makers are estimated at $35.8 million. EPA officials hope that these regulations will give chemical manufacturers incentive to recover and recycle more chemical ingredients, rather than vent them to the atmosphere. For more information on the new rules, contact the Emission Standards Division (MD-13), EPA, Research Triangle Park, NC 27711.

The public is not properly protected from neurotoxic substances, according to the congressional Office of Technology Assessment. In a report, *Neurotoxicity: Identifying and Controlling Poisons of the Nervous System*, OTA notes that most chemicals on the market have not been tested to determine whether they affect the nervous system adversely. Potentially neurotoxic chemicals include certain industrial chemicals, foods and food additives, pesticides, and heavy metals. Some occur naturally. The report says that there is evidence that some environmental agents may be responsible for increases in the number of cases of amyotrophic lateral sclerosis and Parkinson's disease. The report (stock no. 052-003-01184-1) is available for $15 from the Superintendent of Documents, U.S. Government Printing Office, Washington, DC 20402; (202) 783-3238.

The Federal Centers for Disease Control (CDC, Atlanta, GA) predict improved blood lead measurement will be needed. Private firms have a chance to make a cooperative research and development agreement (CRADA) with CDC to develop improved instrumentation. CDC's emphasis is on anodic stripping voltammetry, but other appropriate techniques also will be considered. The instruments are needed for the childhood lead poisoning screening programs. In addition to accuracy and precision, the goals are low detection limits, instrument ruggedness, and low cost. CDC's current recommended action level for blood lead in children is 25 μg/dL, but that level may be lowered after review by a panel of experts, to be completed this year. One cautionary note: CDC may not provide funds to non-CDC participants in a CRADA, but it may furnish staff, facilities, equipment, and

0013-936X/90/0924-0111302.50/0

supplies. For more information, contact Dayton Miller or Daniel Paschal, Centers for Disease Control, 1600 Clifton Road (F18), Atlanta, GA 30333; (404) 488-4026.

The National Institute of Standards and Technology and EPA have announced that sample preparation time can be cut by means of a heating device similar to a kitchen microwave oven. Normally, heating samples to test for environmentally hazardous trace elements requires hot plates and reflux systems. The process that uses these devices takes 8–24 h to complete. According to NIST and EPA spokespersons, the microwave system reduces sample preparation time to 10 min and saves costs commensurately.

STATES

The coast of Texas between Galveston and Corpus Christi was threatened by an oil spill that occurred after several explosions aboard the Norwegian supertanker *Mega Borg* in the Gulf of Mexico June 8. The U.S. Coast Guard estimated that 4.3 million gallons of Angolan light crude spilled. Coast Guard spokesmen added, however, that only about 14,000 gallons remained in the water; the rest burned or evaporated. Concentrated bacteria were spread in the Gulf to "eat" the oil, with the enthusiastic approval of Texas Land Commissioner Garry Mauro. He believes that if the bacteria work at sea as they did in the laboratory, "we are going to solve the problem of oil spills in the country." Many members of the environmental scientific community feel that the bacteria will not work fast enough to consume the oil in such a large spill. Others fear that the bacteria may break the crude down to toxic compounds such as naphthalenes and quinones.

Gasoline sold in New York State must have a Reid vapor pressure (RVP) not exceeding 9 lb/in.^{2}, under regulations announced May 31 by Environmental Conservation Commissioner Thomas Jorling. This rule will be in effect from May 1 to September 15 of every year. A lower RVP results in the release of less vapor from unburned gasoline (*ES&T*, this issue, p. 1128). The Department of Environmental Conservation (DEC) estimates that the new regulation will reduce hydrocarbon emissions in the state by about 45,000 tons, as compared with emissions in previous years. DEC officials expect that the lower RVP gasoline should not affect the performance of cars adversely.

California Air Resources Board (CARB) officials seem to be intrigued by a catalytic converter that reportedly reduces hydrocarbon (HC) emissions to 0.03 g/mi. Converters currently in use curtail HC emissions to 0.21 g/mi. The electrically heated converter is added to a car's catalytic converter system and is designed to clean pollutants out of the dirtiest exhaust, most of which is emitted during the first two to three miles of a car's journey. The new converter also reportedly reduces carbon monoxide emissions to 0.35 g/mi and benzene to 0.016 g/mi; for conventional converters, these figures are 2.83 g/mi and 0.076 g/mi, respectively. The electrical converter is made by Camet Co. (Hiram, OH). A spokesperson for General Motors said that the device would have to work for at least 50,000 mi before it would be acceptable to the automobile industry. Camet president Richard Cornelison expressed optimism that the converter could meet this goal.

Pennsylvania hosted a "first-ever" recycling market exchange in Harrisburg June 5. More than 300 buyers and sellers of recyclable materials met to exchange information and to learn about recycling markets in Pennsylvania. The meeting grew out of work by the Governor's Recycling Market Development Task Force that

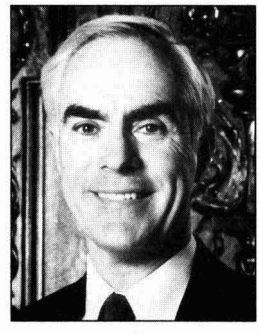

Casey: *Recycling good economics*

Gov. Robert Casey had established in April 1989. Casey and Lt. Gov. Mark Singel see recycling as "not just environmentally sound," but as offering the state "tremendous economic opportunities." The meeting and related efforts are authorized and mandated by Pennsylvania's recycling law, passed in July 1988. The law requires 407 communities to begin recycling by 1992. It also authorizes economic aids—such as an Environmental Technology Fund which had $755,000 in low-interest loan money available as of June 1—to fund recycling projects in the state.

Michigan has embarked on a project to use bacteria to clean up spilled oil in groundwater and soil. The emphasis is on developing improved techniques for removing compounds such as benzene, toluene, ethylbenzene, and xylene, that are commonly associated with petroleum leaks and spills. The 3-year, $1.5-million project involves the state Department of Natural Resources (DNR), the Michigan Universities Hazards Waste Management Consortium (MUC), and the Michigan Oil and Gas Association (MOGA). It is characterized as unique because of the close cooperation between public, private, and academic groups. MOGA is contributing $1 million, DNR is putting in $300,000, and MUC is adding $200,000. Field work will begin in 1991 at three Michigan locations provided by Shell Western.

SCIENCE

Why do trout from Lake Ontario continue to show levels of polychlorinated biphenyls that exceed the federal guideline of 2 ppb? After all, Lake Ontario water itself has lower concentrations of PCBs than do most public drinking-water supplies in the region, notes Rahul Ram, a Ph.D. candidate at Cornell University (*ICET News* 1990, *6*[1], 1, 2, 7). Moreover, several other species of fish do not seem to biomagnify PCBs. In this case, the PCBs seem to migrate from lake sediment to the bottom feeding crustacean, *Pontoporeia*, which serves as food for alewives. Salmonids, such as trout, feed on the alewives and thus obtain the PCBs. Rahul estimates that about 60% of PCB residues in salmonids originate in lake sediment. He has developed a mathematical formula that expresses the dynamics of a chemical in an individual organism and the rate at which the organism obtains the chemical.

Effects of ozone (O_3), SO_2, and the two gases in combination on six major crops were studied at Cornell University under contract with the Electric Power Research Institute (EPRI, Palo Alto, CA). The crops were alfalfa, corn, soybean, wheat, and a combination of timothy grass and clover. Outdoor fumigation exposure was carried out during three growing seasons—1983, 1984, and 1985. Seven levels of O_3 and four

levels of SO_2 were tried separately and in combination, as were varying time intervals of exposure. Ambient O_3 damaged all crops except alfalfa. Exposure to "realistic" doses of SO_2, however, appeared to reduce yield only for soybean. Normally interactive effects of O_3 and SO_2 appeared negligible. For soybean, however, the combination produced "less than additive effects," and for corn, interaction depended on the concentrations of the gases. O_3 often reduced rates of photosynthesis, and SO_2 sometimes affected conductance through leaf stomata.

The analysis of toxic substances, including dioxin congeners, becomes clearer with the aid of high-resolution and tandem mass spectrometers (HRMS and MS/MS). Joseph Pan of Southwest Research Institute (SwRI, San Antonio, TX) points out that HRMS can identify and differentiate between normally hard-to-isolate compounds—those nearly identical in molecular weight, for instance—that occur at concentrations far smaller than those normally detectable by conventional MS. HRMS also yields "excellent results" in determining the elemental composition of unknowns, says Pan. He adds that MS/MS then speeds up the analysis and takes out much of the chemical "noise" from background contaminants in a sample. Initial sample cleanup time therefore is reduced substantially, Pan says.

Who is using what kind of flue gas desulfurization (FGD) system and where? IEA Coal Research (London), an arm of the International Energy Agency, has published *FGD Installations on Coal-Fired Power Plants,* which reviews FGD type and use data, compiled from installations worldwide. The data are broken down according to process and sorbent, such as regenerable Wellman-Lord (sodium sulfite); lime, limestone, and dual-alkali; and lime and other spray dry technologies. For countries that are members of IEA Coal Research, the publication costs £60 (about $105); for nonmember countries, £180 (about $315). For more information, contact IEA Coal Research, Gemini House, 10-18 Putney Hill, London SW15 6AA, England, U.K.; Fax 081-780 1746.

Hydrocarbons in contaminated soil can be broken down in situ with bacteria, says Pete Mote, project manager for Harding Lawson Associates (HLA, Novato, CA). The technique uses nutrient- and oxygen-laden water to stimulate the growth of naturally occurring *Pseudomonas* species. Mote says that the gasoline "is converted into nonhazardous biomass, carbon dioxide, and water." Currently, HLA is using a system of 36 injection and extraction wells and 10 infiltration basins to clean up about 10,000 yd^3 of contaminated soil at a redevelopment site in Oakland, CA. Groundwater and soil are monitored regularly. An Oakland city official noted that bioremediation "averts the liability risk inherent in moving soil from a contaminated site," and Mote said that the process saved Oakland $2 million over conventional methods. HLA received the Grand Award from the American Consulting Engineers Council for the bacterial technique.

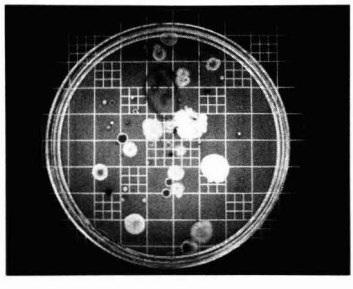

Hydrocarbon-eating microbes

Polyvinyl chloride (PVC) plastics for recycling can be separated from other plastics in municipal waste by means of a system developed at the Center for Plastics Recycling at Rutgers University (Piscataway, NJ). Recycled PVC has uses as drainage piping, garden hose, floor mats, and profile extrusions. The system also sorts out clear and green polyethylene terephthalate, and unpigmented and pigmented high-density polyethylene. A spokesperson for the Vinyl Institute (Wayne, NJ) sees widespread PVC recycling as "having come closer to practical reality. The markets for recycled vinyl already exist," he added.

Nonaqueous-phase liquid (NAPL) contaminants of aquifers can be flushed with carbon dioxide, alcohols, surfactants, or alkaline solutions, say G. R. Boyd and K. J. Farley of Clemson University (SC). At a meeting of the American Geophysical Union held in Baltimore May 29–June 1, the researchers said that flooding with alcohol—for example, 2-propanol—may be the better alternative because of alcohol's biodegradability. Experiments have shown that flushing with one pore volume of alcohol removed almost 100% of the residual NAPL. Subsequent flooding with water reduces alcohol concentrations to levels at which they can be biodegraded.

BUSINESS

Texaco spokespersons warn that alternative fuels required by the proposed Clean Air Act amendments "have never been made and we do not have any research data that demonstrates that such radical new fuel formulations of gasoline could be made. And even if they could be made, they could not become available to consumers in the time-frame mandated," according to a statement issued in response to clean air legislation passed by the U.S. House of Representatives. Amoco chairman Richard Morrow added his voice June 5 in opposition to "a mandated recipe for reformulated gasoline" and called for a flexible approach that would allow the industry to design fuels that would meet congressional goals without unnecessary costs. The House and Senate bills require oxygenated additives such as ethanol or methyl-*tert*-butyl ether (MTBE). Morrow says, "implementation of the relevant amendments would require more ethanol and MTBE than the entire production capacity of the United States."

The world total of nuclear power plants in commercial operation was 428 as of May 31, according to the U.S. Council for Energy Awareness (USCEA, Washington, DC). Moreover, 26 countries now produce electricity from nuclear energy; the latest to join this group was Mexico, when it completed tests at its Laguna Verde plant early this year. France, however, tops the list, with 74.6% of its electricity coming from 54 operating units. Belgium is the runner-up with 60.7%, and the Republic of Korea comes in third with 50.1%. The United States has 112 commercially licensed nuclear plants and got only 19.1% of its power from nuclear energy in 1989.

The U.S. bioremediation market could grow to more than $500 million by the year 2000, compared with $100 million in 1990, according to a forecast by Falmouth Associates (Falmouth, ME). The consulting firm says that treating waste by bioremediation costs $50–$80/ton. By contrast, incineration costs $250–$650/ton and landfill disposal costs $200 or more per ton.

The status of undergraduate programs in environmental science

Judith S. Weis
Rutgers University
Newark, NJ 07102

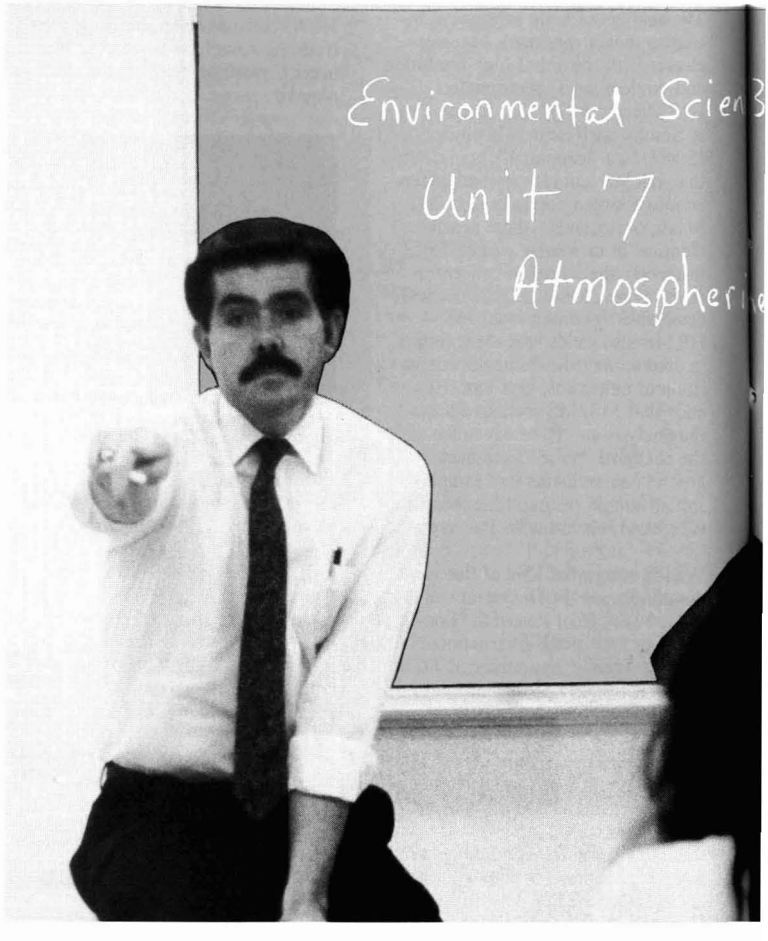

In the early 1970s, as a result of the increased public interest in the environment, many universities initiated courses dealing with the environment and some began to offer majors in the field. There are growing numbers of schools that now offer a major in the interdisciplinary area of environmental science. Given the magnitude and multiplicity of environmental problems, there is a need for broadly trained scientists. Narrowly trained specialists will be unable to come to grips with many of these problems, and there is a job market for environmental scientists at the bachelor's, master's, and Ph.D. degree levels.

In a recent editorial in this journal, W.H. Glaze said, "What is needed now is for universities and society as a whole to recognize that environmental science is one of the distinctive, essential features of the search for knowledge; that holistic, integrated approaches are necessary for research in this area to flourish; and that irregular, patchwork, cross-departmental programs are not enough. In short, environmental sciences must be 'canonized' into the structure of universities" *(1)*.

Environmental science is an important area in undergraduate education, but one in which curricular issues generally have not been examined. "Environmental education" efforts are focused on the curriculum for elementary and secondary schools. For example, the "Alliance for Environmental Education"—a broad coalition of diverse scientific, educational, industrial, and environmental groups—focuses on programs for schools and the general public and is developing networks for teacher training, dissemination of information, and outreach *(2)*. At the college level, faculty in the traditional disciplines of chemistry, physics, and so forth have professional societies which can provide mechanisms for discussion of curriculum issues, but there is no single professional society to which directors of environmental science programs are likely to belong. The National Association of Environmental Education and the National Association of Environmental Professionals are groups to which the majority of program directors do not belong.

A number of studies in the 1970s discussed the content and structure of environmental programs *(3–5)*. In recent years, the National Science Foundation has held undergraduate workshops to examine curriculum issues in the traditional disciplines *(6)*, but environmental science thus far has not been examined in NSF's undergraduate curriculum efforts.

0013-936X/90/0924-1116$02.50/0

I obtained a listing of the schools that offer a bachelor's degree in environmental science from the College Board's *Index of Majors (7)* and contacted coordinators of such programs in colleges and universities around the country. (Because the schools surveyed were only those listed in that publication as offering a bachelor's degree called "environmental science," many nondegree programs and programs in conservation, natural resources, forestry, fisheries, and wildlife are not included.) These schools were invited to provide information about the requirements of their program, its administrative status within the institution, placement of graduates upon completion of the bachelor's degree, and their views of the field and their program.

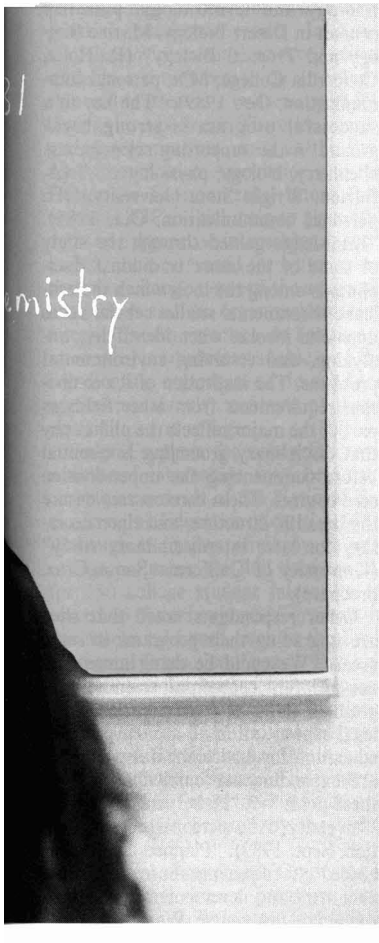

Of the 262 institutions listed as offering a bachelor's degree in environmental science, 76 supplied some information such as appropriate pages from the school catalog or a brochure. These institutions included major research universities, state colleges, and small private colleges. A number of program directors wrote letters expressing their views of the field and their particular program. I have summarized the information in Table 1.

Of the respondents, 40 were from "environmental science" programs, 28 were from "environmental studies" programs, 1 from an environmental conservation program, 6 from environmental health science programs, and 2 from environmental engineering programs. The environmental engineering programs were quite different from all the others and have not been included in the rest of the analysis. The other three types of programs were quite similar and are considered together.

Administrative arrangements

Half of the programs, 38, are interdepartmental; very few were in a department of environmental science. One was part of a college of environmental studies (Huxley College of Environmental Studies of Western Washington University). The others were housed within existing traditional departments: 13 in biology or life sciences, five in geology, two in geography, four in natural science, one in forestry, one in plant and soil science, and one in industrial studies. The administrative status of some programs could not be determined from the information supplied. Departmental status appears to give more resources and greater faculty commitment to the program and was considered preferable. "Over the years, we have found the 'department' approach to administration and management both effective and economical in terms of time and the use of resources" (W. Odum, University of Virginia, personal communication, Oct. 1989).

Curriculum requirements

Virtually all programs required courses in biology, chemistry, and earth science or physics. The majority of "environmental science," (23) as well as almost all the "environmental studies" programs also required courses in the social sciences or law. A total of 29 programs included a research component, and 35 indicated that internships were a part of their program. Environmental health programs were not especially different. "Curricula in environmental science, protection, and health are beginning to look similar as we realize that the problems of human health, protection of organisms and ecosystems, groundwater problems, and other areas are significantly related. We feel strongly that there is a need for workshops or conferences which will bring environmental science curricula in universities and colleges into integrated, multidisciplinary, problem-oriented programs" (G. Smith, Western Carolina University, personal communication, Oct. 1989).

As far as could be determined from the material supplied, laboratory courses were essential in the vast majority of the programs, whereas field work was required in only 32.

Enrollments

Some programs are shrinking, some are growing; many that were languishing are recently showing signs of revitalization. Some have not experienced a growth in the number of majors, but have seen a dramatic increase in the number of students taking their courses, probably caused by increased media coverage of environmental problems.

Of those who expressed views on the status of their program, 20 felt it was doing well, eight thought it was doing poorly, and six thought it was doing satisfactorily.

Directors' comments

Directors cited the following areas in which they were pleased with their programs.

Curriculum. Many directors of programs that had rigorous and demanding science courses felt that their curricula were "oriented toward solving environmental problems from a science perspective" and were "quite successful educating fairly broadly in the environmental area" (W. McFee, Purdue University, IN, personal communication, Oct. 1989). "Environmental studies" programs that included social, political, and economic areas stressed that those perspectives are very important. "I emphasize the word 'studies' in our title because we include social, political, and economic aspects of environmental management, perspectives that are crucial to effective problem-solving" (G. Godshalk, Alfred University, NY, personal communication, Oct. 1989).

"The aim of the Environmental Sciences group major is twofold: 1. an understanding of the physical environment, human impact on it, and the difficult choices that must be made at all levels of society as we move into an era of limits; and 2. developing tools with which to solve the critical environmental challenges facing the world" (University of California-Berkeley brochure). "Environmental problems are often multifaceted and contain biological, chemical, social, historical, psychological and economic elements which must be addressed" (University of Maine brochure).

"I think our program does a fairly good job helping students translate concern for the environment into recognition that few environmental problems

TABLE 1
Undergraduate environmental programs responding to survey

State	School	Name of program: Environmental	Department
Alabama	Livingston U.	science	Interdepartmental
Alabama	Troy State	science	Biology
Arizona	N. Arizona U.	science	Interdepartmental
Arkansas	U. Arkansas	health	Biology
California	U.C. Berkeley	science	Interdepartmental
California	U.C. Riverside	science	Soil & Env. Science
California	U.C. Santa Cruz	studies	Interdepartmental
California	CA State San Bernardino	studies	Geography
California	CA State Sacramento	studies	Interdepartmental
Connecticut	U. New Haven	science	Interdepartmental
Delaware	Wesley C.	science	Interdepartmental
Florida	FL Inst. Technology	science	Engineering
Florida	FL International U.	studies	Interdepartmental
Georgia	Savannah State	studies	Biology
Indiana	U. Evansville	studies	Interdepartmental
Indiana	Purdue U.	science	Interdepartmental
Iowa	Cornell C.	studies	Interdepartmental
Iowa	Simpson	studies	Biology/ES
Kentucky	U. Eastern KY	health	Health
Kentucky	Georgetown C.	science	Interdepartmental
Louisiana	McNeese State U.	science	Biology/ES
Maine	U. ME–Machias	studies	Interdepartmental
Maine	St. Joseph's C.	science	Earth/Natural Science
Maine	U. ME–Ft. Kent	studies	Interdepartmental
Maine	U. of New England	science	Life Science
Maryland	Hood College	studies	Interdepartmental
Massachusetts	U. Lowell	science	Earth Science
Massachusetts	Wellesley C.	science	Interdepartmental
Massachusetts	U. MA	science	Plant & Soil Science
Michigan	U. MI–Dearborn	science	Interdepartmental
Michigan	Lake Superior State C.	science	Interdepartmental
Michigan	MI Tech. U.	engineering	Engineering
Michigan	Northern MI U.	health	Interdepartmental
Michigan	Western MI	studies	Interdepartmental
Michigan	Aquinas C.	studies	Interdepartmental
Minnesota	U. MN–St. Paul	studies	College of Nat. Res.
Minnesota	Hamline U.	studies	Interdepartmental
Minnesota	Concordia C.	science	Interdepartmental
Minnesota	St. Cloud State U.	studies	Biology
Minnesota	Bemidji State U.	studies	Interdepartmental
Nebraska	Doane C.	studies	Interdepartmental
New Hampshire	U. NH	conservation	Interdepartmental
New Hampshire	Keene State C.	science	Interdepartmental
New Hampshire	Franklin Pierce C.	science	Interdepartmental
New Jersey	Rutgers State U.	science	Env. Science
New Jersey	Stockton State C.	studies	Geology/Env. Studies
New York	S.U.N.Y. Binghamton	studies	Geology & Env. Studies
New York	S.U.N.Y. Plattsburgh	science	Earth & Env. Science
New York	S.U.N.Y. Geneseo	studies	Interdepartmental
New York	Marist C.	science	Interdepartmental
New York	Alfred U.	studies	Interdepartmental
N. Carolina	U. NC–Asheville	studies	Interdepartmental
N. Carolina	W. Carolina U.	health	Health
Ohio	Wright State U.	health	Biology
Pennsylvania	Bucknell U.	science	Interdepartmental
Pennsylvania	Edinboro	studies	Geography
Pennsylvania	Marywood C.	science	Science
Pennsylvania	Drexel U.	science	Biology
Pennsylvania	E. Stroudsburg State	studies	Biology
Pennsylvania	Wilkes C.	science	Earth & Env. Science
Puerto Rico	Inter American U.	science	Biology
S. Carolina	Benedict C.	health	Physical Science
S. Dakota	S. Dakota State U.	science	Biology
Tennessee	Middle TN State U.	sci. & tech.	Industrial Studies
Texas	Sam Houston State U.	science	Interdepartmental
Texas	Concordia Lutheran C.	science	Interdepartmental
Texas	Stephen F. Austin State U.	science	School of Forestry
Vermont	St. Michael's C.	science	Interdepartmental
Vermont	Bennington C.	studies	Interdepartmental
Vermont	Middlebury C.	studies	Interdepartmental
Vermont	Johnson State C.	science	Env. & Health Science
Virginia	U. VA	science	Env. Science
Virginia	Clinch Valley C., U. VA	science	Natural Science
Wisconsin	St. Norbert C.	science	Biology
Wisconsin	U. WI–Green Bay	science	Natural & Appl. Science
Washington	Western WA U.	studies	College of Env. Studies

have easy solutions; most problems require thorough study by experts who can communicate effectively with people from other disciplines" (P. Thompson, Cornell College, IA, personal communication, Oct. 1989). "Economic activity within our biological ecosystems requires understanding of both subject areas, and development of policies and planning is essential to resolving environmental problems" (University of New Hampshire brochure).

Some programs were proud of their laboratory and field offerings. "Lab courses which have proven important in our major are Microbiology, Chemistry (2 or 3 years), and Geology. Important field courses include Field Biology, Ecology and Ornithology, plus trip courses in Desert Biology, Marine Biology and Tropical Biology" (R. Holtz, Concordia College, MN, personal communication, Oct. 1989). "The key to a successful program is strong background in the supporting sciences, e.g. chemistry, biology, physiology. . ." (A. Burton, Wright State University, OH, personal communication, Oct. 1989). "Knowledge gained through the study of some of the more traditional disciplines is among the tools which the critical environmental studies scholar relies upon and invokes when identifying, analyzing, and resolving environmental problems. The institution of lower-division requirements from other fields as part of the major reflects the philosophy that disciplinary grounding is essential before commencing the upper-division core courses. These core courses ensure the breadth, structure, and rigor necessary for later interdisciplinary study" (University of California–Santa Cruz, brochure).

Other respondents noted that they are upgrading their programs in some areas. "We could be doing more with our ES [environmental science] program in terms of field experience and legal aspects, all in all a more practical education for environmental work. We are expanding our curriculum toward these goals" (K. Haberyan, Troy State University, AL, personal communication, Sept. 1989). "Planned changes include. . . requiring more analytical chemistry and development of an environmental law course. We need to work in more computer experience and more remote sensing" (P. Shelton, Clinch Valley College of the University of Virginia, personal communication, Oct. 1989).

Internships. Program contacts expressed a high level of enthusiasm for internship programs. "Probably the most important part of our major is the required internship. Students find out what the work place is like and it adds

an important element to their resumes" (R. Holtz, Concordia College, MN, personal communication, Oct. 1989). Internships provide students with opportunities to grow personally and professionally and to become better qualified for placement in the job market. Their work can contribute to solving environmental problems.

Internships are available in government agencies, the nonprofit sector—consisting of regional, national, and international organizations—and in the private sector, including large and small corporations and environmental consulting firms. There are a number of foundations that provide financial support for environmental internships. Internships may or may not involve a stipend or academic credit. In some schools, environmental science/studies students are required to do an internship and to prepare a written report following the experience. There are coordinating organizations, such as the Student Conservation Association and the Center for Environmental Intern Programs (CEIP), which help to place students in appropriate internships. Nevertheless, there is a need for better information exchange between the academic institutions and the organizations using interns. Faculty members do not always know of opportunities available, and the coordinating organizations do not have appropriate faculty contacts at many universities and colleges.

Federal support for enhancing environmental internships may be forthcoming as a result of the National Environmental Education Act (S. 1076). Although it focuses primarily on precollege programs, this bill does provide for 150 college student interns to be placed in federal agencies involved in environmental issues, such as the Environmental Protection Agency, Fish and Wildlife Service, National Oceanic and Atmospheric Administration, National Park Service, U.S. Forest Service, Council on Environmental Quality, and Soil Conservation Service. These internships would be for up to six months, and students would be paid by the hiring agency.

Placement of graduates. Graduates of environmental science programs have been obtaining jobs in state and federal regulatory agencies, planning departments, environmental health departments, parks, as well as consulting firms, testing laboratories, and industry. Some pursue further academic study in law, environmental planning, and the sciences. A number of respondents noted that employers have been pleased with their graduates. McCormick and Barrett in 1979 *(5)* and Disinger and Schoenfeld in 1987 *(8)* felt that career opportunities in the environmental field would be better for graduates of such interdisciplinary programs than for those with a disciplinary major who had taken some environmental courses. A recent study of the status of environmental programs indicated that student and employer interest in interdisciplinary studies is still strong *(8)*.

Perceived problems

Despite the positive feelings expressed about the programs by many directors, there are a number of perceived problems.

Identity. Respondents commented on the generally low level of understanding by students and faculty of the nature of environmental sciences. "Some degree of standardization of curricula, or even standardization of curricular nomenclature, might help in raising the level of understanding of the environmental sciences" (R. Parnell, Northern Arizona University, personal communication, Sept. 1989). Respondents noted that high school teachers are aware of biology and chemistry as fields of science but most are not aware of environmental science, and thus direct students into the traditional fields. Because of the diversity within this interdisciplinary field, there is no central leadership in matters of education.

"I obtained a listing of the schools that offer a bachelor's degree in environmental science . . . and contacted coordinators of such programs . . . around the country."

Even within the environmental science community there is disagreement over whether public health or ecological issues are the most important. "A major problem in any environmental curriculum is the term itself. It is used in fields as diverse as psychology, interior design, ecology, engineering, and physics. We consider forestry as the original environmental science. The same can be said for ecology" (K. Watterston, Stephen F. Austin State University, TX, personal communication, Oct. 1989). There also exists in the general public some confusion with "environmental activism," which is a political position; the general public often has a very unclear view of what an environmental scientist is. "We all have been misguided and confused by nearly 20 years of ill defined 'environmental' activities" (F. O. Blackwell, Eastern Kentucky University, personal communication, Sept. 1989).

Job market. Though not addressed by respondents, graduates of environmental science/studies programs may not be as competitive in the job market as traditional majors. A possible explanation for any problems in employment experienced by environmental science graduates was suggested by Rajagopal *(9)*. He felt that environmental science graduates do not fare as well in the job market as traditional majors [contrary to the views of McCormick and Barrett *(5)* and Disinger and Schoenfeld *(8)*], because most entry-level positions in government and industry require a certain disciplinary background. He felt that specialized programs such as environmental health or environmental engineering, which have roots in existing occupational categories, are more likely to lead to employment. Rajagopal analyzed job descriptions from EPA and internships with various organizations and concluded that broadly trained environmental science students would be at a disadvantage. He recommended vigorous efforts by faculty and administrators to encourage employers to fully tap the potential of these students.

NSF data *(10)* show that in 1986 the unemployment rate of environmental scientists was 4.4%, the highest of any of the sciences, while the overall unemployment rate for scientists and engineers was 1.5%. This study also examined the underemployment rate, defined as those who are qualified to work in science or engineering but are not, or who want to work full time but are working part-time. By combining unemployment and underemployment data, the "underutilization rate" was calculated. The overall underutilization rate for scientists and engineers was 4.1%, while that for environmental scientists was the highest, almost 10%—slightly higher than that of social scientists.

The report itself is unclear as to exactly who are included in the category of "environmental scientists." However, those who put together the report defined environmental scientists as geologists, atmospheric scientists, and oceanographers—a very different group than I am considering in this paper. This mismatch emphasizes again the problems of identity described above, of exactly who are considered "environmental scientists." The NSF definition can be detrimental to the reputation and

health of the field because the high unemployment rate attributed to it could discourage students from pursuing study in this area.

It is likely that the recent upsurge of interest in the environment and the realization that environmental problems are pervasive and not easily solved will improve the employment situation for environmental scientists.

Students. Students who express an interest in the field may not have a strong science background and may be unprepared for rigorous courses. "During the early years of the program (1970–1980) our majors numbered over 100 but the attrition rate was high and only about 50% completed the rigorous program. Today our rate of graduation is much higher because our students are less influenced by what I call the 'Earth Day syndrome,' but are more realistic about their plans for a career in science. I expect to see a rise in enrollment over the next few years, principally due to increased media coverage of environmental problems. . ." (S. Spigarelli, Bemidji State University, MN, personal communication, Sept. 1989). Minority students are greatly underrepresented in the field.

Breadth versus depth. Traditional science departments may view environmental science programs as somewhat "soft." The necessity for breadth of training may lead to perceptions of (or in some cases real problems of) inadequate depth and rigor. "Programs must involve a continuous compromise in the tension between the interdisciplinary breadth and the depth of disciplinary knowledge demanded for understanding and solution of environmental problems. Such tensions may always be part of any interdisciplinary program" (J. Lemons, University of New England, ME, personal communication, Nov. 1989). "Equally dangerous is to let the synthetic nature of such programs, the necessity of breadth, lead to a loss of expectation for advanced focus work; such programs have led to the perception of environmental studies programs as 'soft'" (K. Woods, Bennington College, VT, personal communication, Oct. 1989).

"[Environmental science] is hampered because of the tremendous diversity within the field. However, that could also be a strength. Environmental Science encompasses aspects of engineering as well as biological, agricultural, and natural resources sciences on campus. Therefore the division into one departmental function is difficult and has been a roadblock thus far" (G. Arnold, South Dakota State University, personal communication, Sept. 1989). Some programs have developed "tracks" within the interdisciplinary framework of the major so that students may concentrate in certain aspects of environmental science. Although providing for greater depth, such curricula tend to have very extensive requirements, thus reducing the number of electives available to the students. Some environmental scientists (though none of the respondents) feel that the field is more appropriate at the graduate level and that undergraduates should get in-depth preparation in a standard major such as biology, geology, or chemistry, rather than a major in environmental science.

Lack of sufficient laboratory and field training. "I think our greatest liability is the lack of sufficient laboratory training for our undergraduates" (R. Maples, McNeese State University, LA, personal communication, Sept. 1989). Experience with instrumentation is hindered by lack of resources. In some schools, undergraduate research experiences are very limited. However, it is possible that these problems were campus-wide rather than program-specific.

"[Environmental science] is hampered because of the tremendous diversity within the field. However, that could also be a strength."

Staffing and resource problems. Although interdisciplinary programs prepare students to confront problems in the "real world" that are not separable into disciplines, they run against the grain of university structure. Difficulties arise in philosophy, faculty, students, curriculum, research, funding, and evaluation *(4)*. These problems are particularly acute in programs that are competing with "home" departments of the faculty members.

"Good and effective faculty for Environmental Studies are also good researchers. They are needed by their 'home' departments and not willingly released to participate in the Environmental Studies program" (R. Lougeay, S.U.N.Y. Geneseo, personal communication, Sept. 1989). "We do have conflicts with our home departments, teaching and advising overloads, and feelings of divided loyalty" (S. Trombulak, Middlebury College, VT, personal communication, Oct. 1989).

"I am well aware of the turf battles which develop between more traditional disciplines over such programs, and the commonly held view that any interdisciplinary program cannot possibly be rigorous or valuable. Without a strong support structure, interdisciplinary majors soon lose out" (P. Kotila, Franklin Pierce College, NH, personal communication, Oct. 1989). It is interesting to note that similar problems were noted in the earlier study by Aldrich and Kormondy *(3)*, who mentioned that personnel decisions were generally made by the "home department, a euphemism which indicates where the bread is really buttered."

Additional problems arise when the college's administration does not recognize the importance of the program. "Despite the growing interest in environmental studies, the university administration does not seem to recognize the importance of our program. We are limping along financially, while more traditional departments with fewer students are receiving greater support" (R. Sherman-Huntoon, Western Michigan University, personal communication, Oct. 1989).

Conclusions

Over the past 20 years, many universities and colleges have developed programs in environmental science that attempt to give students an interdisciplinary approach, one that many agree is necessary to deal successfully with our diverse local, regional, and global environmental problems. However, these programs generally lack departmental status and are at a disadvantage compared to the traditional university departments. There is inadequate understanding of the field on the part of other faculty members and students.

A persistent curricular issue is how to achieve the proper breadth of education in this interdisciplinary field and at the same time provide students with adequate depth of understanding in certain areas. Some programs suffer from inadequate resources for laboratory and field work, and are dependent on, and often competing with, traditional departments for staffing their courses. As Francis *(11)* said, "Academic institutions, already caught up in a growing debate about their proper role in a changing world, can either demonstrate their potential or reveal their impotence. The challenge of working toward environmentally sustainable development is one they must meet. It will require balancing the best from the traditional disciplines and professions with a variety of new integrative endeavors."

There has not been enough communication and discussion among directors of such programs in the past. As one respondent said, "I know of no journal or coherent literature to help us navigate through this politically, administratively, and pedagogically complex matter" (B. Marsh, Bucknell University, PA, personal communication, Oct. 1989). As we enter the "environmental decade" of the 1990s and the third decade of existence of environmental science programs, there is a need for workshops and conferences in which directors of these programs can share ideas and strategies with one another. Such a workshop is being planned in conjunction with the American Institute of Biological Sciences meeting in August 1991.

Acknowledgments

I am grateful to the directors of the environmental science/studies programs at the various institutions of higher education who took the time to give their thoughts about the status of their programs.

References

(1) Glaze, W. H. *Environ. Sci. Technol.* **1989,** *23,* 1173.
(2) Paulk, J. *Environ. Sci. Technol.* **1988,** *22,* 25–27.
(3) Aldrich, J. L.; Kormondy, E. J. *J. Environ. Educ.* **1973,** *3,* 1–4.
(4) Wolman, M. G. *Science* **1977,** *198,* 800–04.
(5) McCormick, F. J.; Barrett, G. W. *BioScience* **1979,** *29,* 419–24.
(6) "Report on the National Science Foundation Disciplinary Workshops on Undergraduate Education"; National Science Foundation: Washington, DC, 1989.
(7) *Index of Majors, 1987–88*; 10th ed.; College Board: New York, pp. 266–67.
(8) Disinger, J.; Schoenfeld C., Eds. *The Environmental Professional* **1987,** *9,* 185–274.
(9) Rajagopal, R. *Environ. Conserv.* **1983,** *10,* 225–30.
(10) *Science and Engineering Indicators—1987*; No. 87-1; National Science Board: Washington, DC, 1987.
(11) Francis, G. R. *The Environmental Professional* **1987,** *9,* 211–14.

Judith S. Weis *is a professor in the Department of Biological Sciences at Rutgers University, Newark, NJ. She was on leave (1988–90) to the National Science Foundation in Washington, DC, working in the Division of Undergraduate Science, Engineering, and Math Education.*

Regional water quality

Evaluation of data for assessing conditions and trends

Janet Hren
Carolyn J. Oblinger Childress
J. Michael Norris
Thomas H. Chaney
Donna N. Myers
U.S. Geological Survey

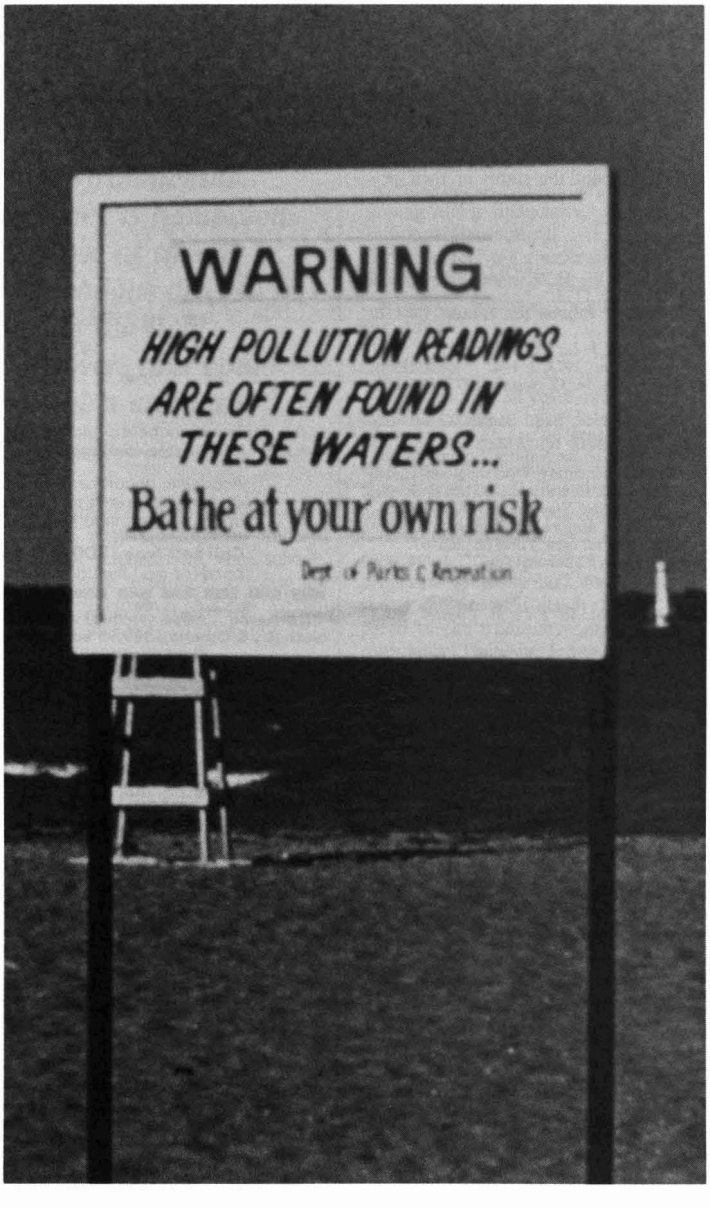

Although large amounts of water quality data have been collected, the problems of aggregating them into one data base for broad water quality assessments are unknown. The U.S. Geological Survey in 1984 undertook a study in Colorado and Ohio to determine how well these data could be used to address such questions as, What are existing water quality conditions? How have they changed? and How do these conditions and changes relate to natural and human-induced activities?

The major finding of this study was that few areas in either state had adequate numbers of samples or sampling sites for the constituents evaluated. This was because the benefits of aggregating data collected by various agencies were limited due to either the nature (e.g., effluent samples) or quality of the data with respect to regional assessments. Furthermore, more data were collected for gross indicators of water quality (e.g., dissolved solids) than for constituents specifically related to toxic contamination (e.g., organic compounds).

Have U.S. rivers benefited from the expenditure of $40 billion since the passage of the Clean Water Act in 1972? With the reauthorization of the Act in 1987, it is estimated that an additional $60 to $70 billion will be required to meet its goals. Recent drought has caused shortages in some areas of the country, and contamination of supplies has increased the need to better determine the quantity and quality of the nation's water resources. Despite this need, only a small part of existing data can be used to assess the status, trends, and causes of water quality conditions on regional and national scales.

Blodgett *(1)* described monitoring programs as "fragmented, duplicative and wasteful, and in many cases. . . devoid of scientific validity and leadership." Other studies have criticized programs as inadequate for effective management *(2, 3, 4)*. The need for a national water quality monitoring and assessment program has been expressed by a number of federal, state, local, and private agencies *(5)*. This need has been recognized by recent plans of the Department of Interior for full-scale implementation of the National Water Quality Assessment Program (NAWQA) by the U. S. Geological Survey *(6)*.

In 1986, a pilot NAWQA program was begun to develop, test, and refine methods useful for a full-scale national water quality assessment program. In late 1989 the Bush administration determined that the U.S. Geological Survey (USGS) should proceed with implementation of the NAWQA program in FY 1991 and requested that Congress appropriate $18 million to begin the full program, which is planned to increase in four years to about $60 million annually. The goals of the NAWQA program are, first, to describe the status and trends in the water quality of the nation's streams and aquifers and second, to provide an understanding of the natural and human causes of the observed conditions and trends. Study unit investigations will be conducted in 60 areas throughout the nation to provide a framework for national and regional water quality assessments. The study unit areas are stream aquifer systems thousands to tens of thousands of square miles in extent. The study unit investigations will consist of intensive assessment activity for 4–5 years followed by 5 years of less intensive activity. Twenty study units will be in an intensive data collection and analysis phase during each fiscal year, and the first cycle of intensive investigations covering the 60 study units will be completed in FY 2002.

Prior to the initiation of the NAWQA program, the USGS undertook a comprehensive examination of programs in Colorado and Ohio to determine the characteristics of data collection activities of federal, state, and local agencies and universities and to determine the adequacy of resulting data. The goals were to improve the ability of USGS to define current water quality conditions, determine water quality changes, and establish cause and effect relationships between current conditions and anthropogenic activities.

The programs were studied in three phases; objectives of the phases are shown in the box.

Phase I—Identify existing programs

USGS compiled an inventory of 1984 data collection activities for all public agencies and academic institutions in Colorado and Ohio. Forty-eight organizations in Colorado with 115 programs were identified, and in Ohio 42 organizations with 88 programs.

Each program was screened using the following criteria: (1) Were data collected from natural sources (e.g., streams, wells, lakes, etc.) as opposed to "in-line" sources (e.g., treated drinking water, sewage effluent)? Only natural sources were used in this USGS study. (2) Were data available for public use? (3) Were sampling sites readily located? (4) Was quality assurance documentation available? (5) Were data in accessible computer files?

"Have U.S. rivers benefited from the expenditure of $40 billion since the passage of the Clean Water Act in 1972?"

Sources of samples. Most samples were from surface water sources. Groundwater represented only 9% of the samples reported from Colorado and 4% of those from Ohio. The dominance of surface water samples reflected its greater public use in both states (e.g., drinking water). The predominance of surface water sampling may also reflect the opinion that because groundwater moves more slowly than surface water its quality should change more slowly (assuming no introduction of contaminants). Therefore, less frequent sampling would be needed to detect changes in groundwater quality. In addition, much of the sampling effort in both states was for mandated purposes, such as meeting permit requirements for monitoring drinking water or wastewater effluent. Most of these permits involve surface waters and require repetitive sampling.

Data collection purposes. Water quality data collected by identified organizations were classified by purpose: to meet permit requirements, to fulfill compliance and enforcement needs, or to characterize ambient water quality conditions. The data collection purposes largely dictated the location and frequency of sample collection, methods used, and the constituents analyzed. These data attributes, in turn, affect the availability and applicability of the data for broad-scale studies. As indicated in Figure 1, 46% of the Colorado samples and 84% of the Ohio samples were collected to meet permit requirements.

None of the samples from programs required for permits passed the initial screening test primarily because they did not represent ambient water conditions. We recognized that when used with predictive techniques and in-stream data, these analyses are useful for conducting certain water quality evaluations. For example, effluent analyses are useful for modeling certain constituents (e.g., dissolved oxygen) in specific waste load allocation studies and for evaluating alternative wastewater treatment technologies.

However, for many other constituents (e.g., heavy metals and pesticides), knowledge of in-stream reactions and processes was inadequate for sound modeling-based assessments. Therefore, samples required for permits were considered inappropriate for constructing a data base to define ambient conditions and to address fundamental water quality issues.

Property and constituent groups. Usefulness of the existing data for addressing critical water quality issues depends largely on the specific constituents that

Objectives of the USGS water quality assessment program

Phase I—Identify, inventory, and estimate costs of the 1984 water quality data collection programs in Colorado and Ohio and identify specific programs producing data that satisfy requirements for broad-scale water quality assessment.

Phase II—Evaluate the quality assurance of programs that meet the broad criteria of Phase I; only data meeting the Phase I criteria were evaluated in Phase II

Phase III—Compile the data resulting from Phase II and evaluate the extent to which it can be used to address selected water quality issues for the two states.

We have reported in detail elsewhere on results of Phase I *(7)*, Phase II *(8)*, and Phase III *(9)*. Major findings of all three phases are summarized in this article.

have been measured. For this study, 11 major groups were evaluated (Figure 2). Of the total number of samples passing the screening criteria, relatively few were directed at concerns about toxic pollution. For example, priority pollutants, pesticides, and radiochemicals amounted to only 0.5% of the Colorado samples and 5% of the Ohio samples.

Screening results. Of about 308,000 samples reported for Colorado and about 1 million samples reported for Ohio, only a fraction met all the screening criteria. Thirty-four percent of the samples reported for Colorado and 5% of the Ohio samples met all five of the Phase I screening criteria. Most of the data failed the screening step because of the ambient conditions criterion; that is, they did not represent generally prevailing water quality conditions.

Laboratory costs. An estimated $13.5 million was spent during 1984 in Colorado and $49.6 million in Ohio for the laboratory analyses. Of this amount, about $6.1 million for Colorado and $35.7 million for Ohio were spent specifically to meet permit requirements. These samples accounted for 45% of the total estimated laboratory costs for Colorado and 72% of the total for Ohio. For Colorado, 17% of the total estimated laboratory costs was for samples for compliance and enforcement activities, and the remaining 38% for samples to characterize ambient conditions. For Ohio, 2% of the estimated laboratory costs was for compliance and enforcement activities and the remaining 26% for characterization of ambient conditions.

FIGURE 1
Regional water quality samples reported in 1984, by collection purpose

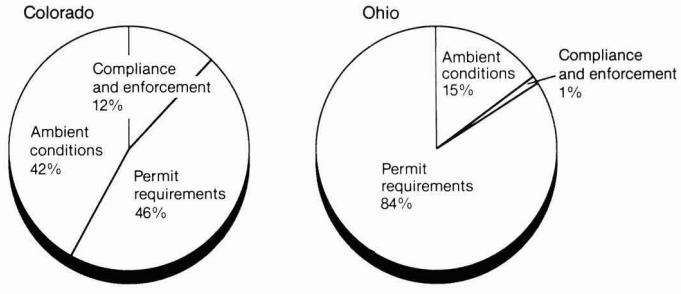

Source: U.S. Geological Survey.

Of an estimated $21.3 million spent on analyses of samples collected to characterize ambient conditions or for compliance and enforcement activities in the two states, about $7.1 million represents data from samples that met all Phase I screening criteria. Thus, only about 11% of the total estimated laboratory costs (of $63.1 million) produced data that are readily available and are considered to be potentially applicable to fundamental, broad water quality issues. These laboratory costs, of course, represent only a part of the total expenditures of data collection programs.

Phase II—Quality assurance

Water quality data are collected by many organizations for diverse purposes that range from meeting statutory requirements to basic research. Combining these individual data bases is an appealing and potentially cost-effective way to develop a data base adequate for regional or national assessments. However, to combine data from diverse sources, field and laboratory procedures used to produce the data need to be equivalent and need to meet specific quality assurance standards. A total of 44 programs in Colorado and 29 programs in Ohio passed the Phase I screen and were examined in Phase II. These programs accounted for an estimated 165,000 analyses in Colorado and 76,300 analyses in Ohio for 20 constituents selected for Phase II.

Each of the eight criteria that comprise the Phase II screen fall into one of two major categories: field practices or laboratory practices. Field practices included the use of documented sample collection techniques, collection of samples representative of stream or aquifer

FIGURE 2
Number of surface and groundwater samples reported in 1984 before and after Phase 1 screening, by property and constituent group

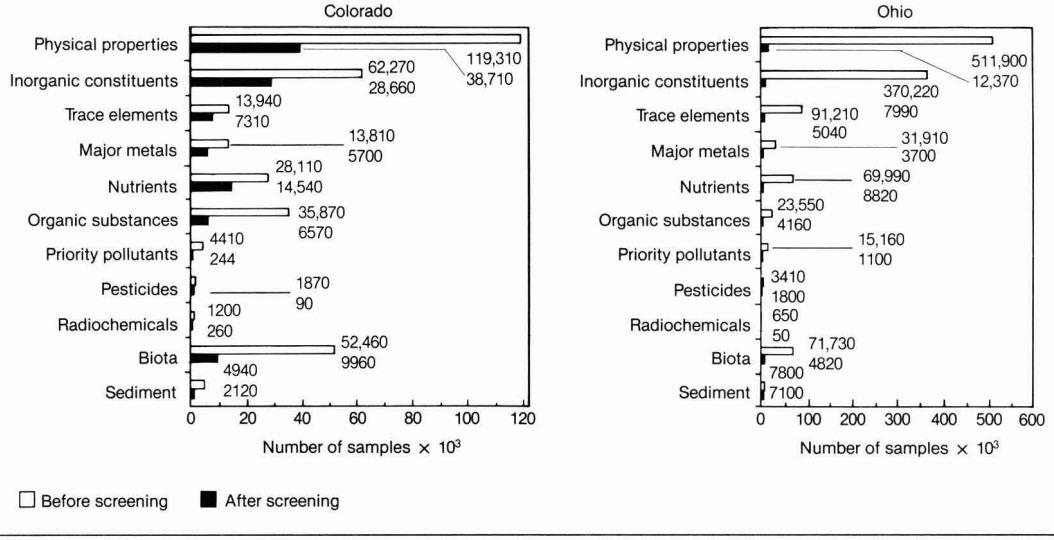

Emerging Developments in Environmental Science

ES&T

ENVIRONMENTAL SCIENCE & TECHNOLOGY

Enter your own monthly subscription to ES&T and be among the first to get the most authoritative technical and scientific information on environmental issues.

☐ **YES! I want my own one-year subscription to ENVIRONMENTAL SCIENCE & TECHNOLOGY at the rate checked below:**

1990 Published Monthly	U.S.	Canada & Mexico	Europe	All Other Countries
ACS members:	☐ $ 36	☐ $ 50	☐ $ 65	☐ $ 72
Nonmembers Personal	☐ $ 67	☐ $ 81	☐ $ 96	☐ $103
Nonmembers-Institutional	☐ $276	☐ $290	☐ $305	☐ $312

☐ Payment Enclosed (Payable to American Chemical Society)
☐ Bill Me ☐ Bill Company
Charge my ☐ ViSA/MasterCard
☐ Diners Club/Carte Blanche

Card No. _____

Expires _____ Signature _____

Name _____

Title _____ Employer _____

Address ☐ Home
☐ Business _____

City, State, Zip _____

Employer's Business: ☐ Manufacturing ☐ Academic ☐ Government
☐ Other _____

Member rates are for personal use only.
Subscriptions outside the U.S., Canada, and Mexico are delivered via air service.
Foreign payment must be made in U.S. currency by international money order, UNESCO coupons, or U.S. bank draft. Orders accepted through your subscription agency. For nonmember rates in Japan, contact Maruzen Co., Ltd. Please allow 45 days for your first copy to be mailed.

Redeem until December 31, 1990.

680 **MAIL THIS POSTAGE-PAID CARD TODAY!** 5454J

(800) 227-5558 (U.S. only)

NO POSTAGE
NECESSARY
IF MAILED
IN THE
UNITED STATES

BUSINESS REPLY MAIL

FIRST CLASS PERMIT NO. 10094 WASHINGTON, D.C.

POSTAGE WILL BE PAID BY ADDRESSEE

American Chemical Society
Marketing Communications Department
1155 Sixteenth Street, N.W.
Washington, D.C. 20077-5768

(800) 227-5558 (U.S. only)

NO POSTAGE
NECESSARY
IF MAILED
IN THE
UNITED STATES

BUSINESS REPLY MAIL

FIRST CLASS PERMIT NO. 10094 WASHINGTON, D.C.

POSTAGE WILL BE PAID BY ADDRESSEE

American Chemical Society
Marketing Communications Department
1155 Sixteenth Street, N.W.
Washington, D.C. 20077-5768

conditions, use of other established field practices, use of established sample handling and sample preservation procedures, and use and maintenance of analytical instruments in the field in accordance with established procedures.

Laboratory practices included maintenance of a quality assurance program, maintenance of laboratory quality control procedures, and use of appropriate analytical methods. About 11% of analyses reported for Colorado and 14% of analyses reported for Ohio passed both Phase I and Phase II screening steps.

Effect of screening criteria. The smallest percentage of analyses met the representative-sampling criterion. Analyses that failed this criterion were from stream samples that could not be verified as being representative. Generally, these were point (or "grab") samples; that is, samples collected from a single point near the water surface without any knowledge of mixing conditions. Point samples may be collected for several reasons, but savings of time and cost probably are dominant factors.

A representative stream sample is best obtained by combining depth integrated samples collected at several locations in the stream cross section. For Colorado, about 115,000 surface water analyses met all of the field and laboratory practices criteria except the representative-sample criterion. For Ohio, about 118,000 analyses met all the criteria except the representative-sample criterion. The sample handling and sample preservation criterion was met by the second smallest percentage of analyses for both states.

In contrast to the field practices criteria, most analyses in both states met each of the laboratory practices criteria. This was because of more detailed description and widespread publication of guidelines for laboratory practices compared with guidelines for field collection practices. Few of these field guidelines emphasize the need for, or methods of, collecting representative samples. Furthermore, little has been published about the sources and magnitude of errors associated with collection of water samples for chemical analysis.

Most of the data passing both the Phase I and Phase II screening were pH, alkalinity, specific conductance, and dissolved oxygen—factors that broadly characterize water quality. Therefore, the Colorado and Ohio data bases contain a relatively large amount of data needed to address issues of long-standing concern (e.g., sanitary quality and salinity). The fewest acceptable analyses were for trace constituents (atrazine, polychlorinated biphenyl, and lead). As a result, these data bases contain relatively few analyses that are needed to address current issues of contamination by potentially toxic substances.

The Phase II screening had little effect on the few groundwater analyses identified in Phase I. Sixty-nine percent of the groundwater analyses for Colorado and 100% of those for Ohio passed the Phase II screen.

Phase III—Utility of data

Phase III evaluated the extent to which ambient water quality data that met the Phase I and Phase II criteria can be used to answer major regional and national questions such as: What are existing water quality conditions? Has water quality changed? and How do the existing water quality conditions and trends relate to natural versus anthropogenic factors? This evaluation focused on the first two questions by examining the number of measurements of different constituents at sampling sites and site areal distributions.

In Phase III, 12 of the 20 constituents evaluated in Phase II were selected for further study. To define existing conditions, both surface water and groundwater data collected during 1980–84 were used. For defining changes or trends, the period 1977–84 was used for surface water and 1972–84 was used for groundwater.

Number of measurements at each data collection site. The number of measurements made at each of the data collection sites has a large effect on meeting the goals of ambient water quality assessments. Single or a few measurements at sites may be adequate for describing current groundwater quality conditions and are useful for reconnaissance level assessments of streams. However, because of the inherent variability of streams, measurements with concurrent streamflow data are needed to develop models of seasonal variation and long-term trends at a site.

Most (75% or more) data from surface water sites in both Colorado and Ohio also had concurrent streamflow measurements. Although no single frequency of sampling or number of measurements is ideal for all conditions, 10 analyses were considered the minimum number needed to define existing conditions. Because groundwater quality changes more slowly than surface water quality, only one observation for the period 1980–84 was considered necessary to define existing groundwater conditions.

For the different constituents evaluated in Phase III, an average of 123 (26%) of the surface water sites in Colorado and 36 (12%) of the sites in Ohio yielded 10 or more analyses and concurrent streamflow data for the period 1980-84. All groundwater sites that met the Phase II criteria in Colorado and Ohio yielded at least one analysis and were suitable for defining existing conditions.

Estimates of constituent load (mass per unit time) also are used to compare contributions of various constituents from different streams and to estimate rates of erosion, deposition, and reservoir sedimentation. Accurate calculation of loads requires daily streamflow data and frequent water quality measurements. For this study, a minimum of 10 water quality measurements and daily streamflow data were required for estimating loads. In Colorado, 105 sites (22%) and in Ohio only 30 sites (10%) met this requirement.

Computation of changes or trends in conditions generally requires uniform data collection over a long period of time *(10, 11, 12)*. For this study, at least quarterly surface water quality measurements and concurrent streamflow data collected over 5 years were used. Fewer than 10% of the sites in both states met this requirement. For groundwater, only 1%, or 10 sites, in Colorado and 13%, or 23 sites, in Ohio had at least one sample per year over at least 5 years.

Areal distribution of data collection sites. Data collection sites with an adequate number of measurements were mostly in relatively small areas with known or suspected water quality problems and/or high water use. For example, in Colorado, most sites with streamflow data and 10 or more dissolved-solids and suspended-sediment measurements were clustered in the northwestern part of the state, in response to concerns about salinity and mining effluent effects on the Colorado River (Figure 3). In Ohio, sites with streamflow data and 10 or more total phosphorus measurements were more concentrated in the Lake Erie basin, a heavily populated, high-water-use area (Figure 4).

Although important to specific water resource management objectives, the focus on known or suspected water quality problem areas and high-water-use areas results in a biased assessment of conditions and trends. For an unbiased assessment, additional data collection sites are needed so that the full range of hydrologic and land use conditions in the states are represented.

Implications of study results

This study was undertaken in part because of concerns and criticism raised that existing monitoring programs were "fragmented, duplicative, and wasteful" and inadequate for effective management of water resources. Accordingly, the U.S. Geological Survey examined water quality programs in Colorado and

Ohio to determine whether existing data can be aggregated into a consistent and technically sound data base that is appropriate for assessments on the regional or national scale. Although the study results were specific to Colorado and Ohio, many of the conclusions have implications for a national assessment.

Expenditures for data collection activities in the nation were large and difficult to estimate. In Colorado and Ohio during 1984, an estimated $63 million was spent for laboratory analyses of water samples. Laboratory costs represent generally less than 50% of the total costs of data collection programs. Assuming that these costs are representative, an estimated $2.5–3.0 billion was spent annually on water quality data collection activities in the United States.

The magnitude of funding for these activities fails to reliably indicate the quantity or usefulness of data for assessing regional and national conditions and trends. There are several major reasons for this conclusion. First, most of the funding is for programs that have limited potential for producing the kinds of data needed for regional ambient assessment. Environmental laws and sampling programs initiated in the 1970s focused on pollution discharges rather than on the receiving waters. The result has been large expenditures for end-of-pipe effluent sampling.

For example, in 1984, 45% of the estimated laboratory costs in Colorado and 72% of the costs in Ohio were for samples that represented effluent or treated water conditions rather than ambient stream or groundwater conditions. These programs have not provided the kind of information necessary to answer the types of regional and national questions facing the nation. More emphasis on in-stream sampling both upstream and downstream of discharge points, combined with effluent sampling, would increase our ability to determine improvements in water quality resulting from expenditures on treatment facilities.

Second, several key aspects of these programs seemed to be out of balance. One aspect of this imbalance was that more than 90% of the samples inventoried for this study were from surface water sources. Increased effort needs to be focused on groundwater to address growing concerns about groundwater contamination.

Another area of imbalance was the limited effort directed toward the determination of potentially toxic constituents. Of the samples meeting Phase I screening criteria, samples for the determination of priority pollutants, pesticides, and radiochemicals amounted to 0.5% of the samples in Colorado and 5% of those samples in Ohio. In contrast, most of the samples were analyzed for traditional constituents and properties associated with acidification, sanitary quality, salinity, and eutrophication.

There was also an apparent imbalance in the areal and temporal scales of the assessments. Most of the programs in Colorado and Ohio were directed to-

FIGURE 3
Location of Colorado sites with 10 or more suspended sediment samples and streamflow data, 1980–84

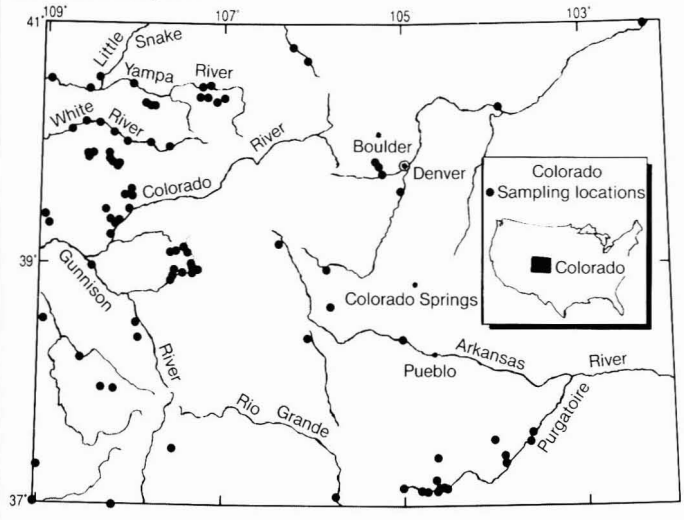

FIGURE 4
Location of Ohio sites with 10 or more total phosphorus samples and streamflow data, 1980–84

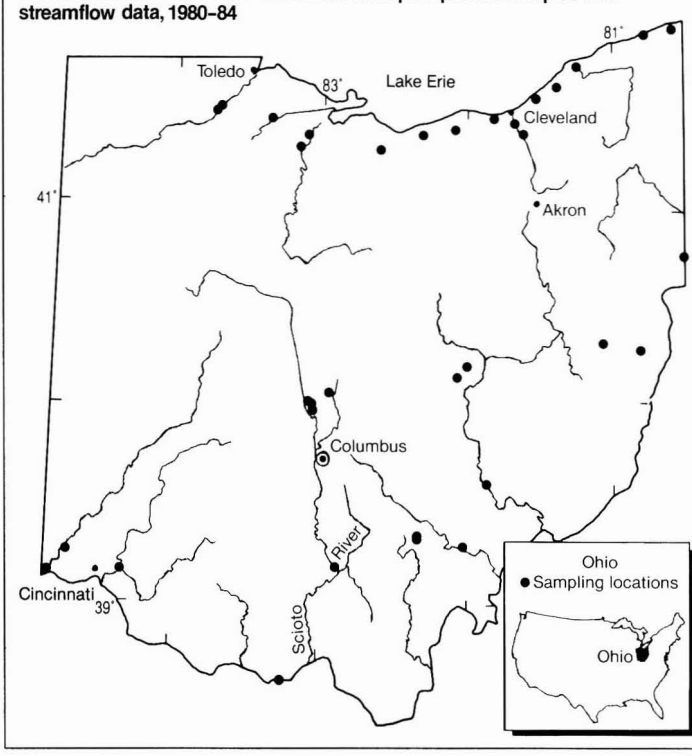

ward small-scale, transient assessments that characterized individual problem areas associated with known or suspected point and nonpoint sources of contaminants. For large areas information was inadequate to perform an unbiased assessment of regional surface water and groundwater quality conditions.

Similarly, there were relatively few sites in either state where samples were collected over a long enough period to define trends in water quality. A critical factor in understanding water quality is the ability to make comparisons among different locations and over time.

The third finding of this study was the increased need to define field procedures, especially the collection of representative water samples. Improvements to field procedures would result in more reliable data suitable for water quality assessments. Maintaining high quality assurance standards in the laboratory is equally important, but precise laboratory analysis is of little benefit if the samples are unrepresentative.

In spite of the criticisms of long-term networks *(4)*, these networks provide adequate data for regional-scale assessments of conditions and changes. At many of the sites in these networks, samples were collected only once each month, but the record of surface water flow was long enough that the range of flows generally was well represented. The data were adequate to define not only the water quality at a site but also, in conjunction with synoptically collected data around a river basin, were adequate for describing general water quality conditions and changes for a number of constituents in a basin.

References

(1) Blodgett, J. E. Summary of hearings on "National Environmental Monitoring"; Congressional Research Service: Washington, DC, 1983.

(2) *Environmental Monitoring, Volume 4, Analytical Studies for the U.S. Environmental Protection Agency*; National Academy of Sciences: Washington, DC, 1977.

(3) Council on Environmental Quality. "Final report of the interagency task force on environmental data and monitoring"; National Technical Information Service, U.S. Department of Commerce: Springfield, VA, 1980.

(4) "Better Monitoring Techniques Are Needed to Assess the Quality of Rivers and Streams"; Report CED-81-30; General Accounting Office: Washington, DC, 1981.

(5) National Research Council. "National Water Quality Monitoring and Assessment—Report on a Colloquium Sponsored by the Water Science and Technology Board 1986"; National Academy Press: Washington, DC, 1987.

(6) Leahy, P. P.; Rosenshein, J. S.; Knopman, D. S. "Implementation Plan for the National Water-Quality Assessment Program"; U.S. Geological Survey Open-File Report 90-174; USGS: Washington, DC, 1990.

(7) Hren, J. et al. "Water-Quality Data-Collection Activities in Colorado and Ohio: Phase I—Inventory and Evaluation of 1984 Programs and Costs"; U.S. Geological Survey Water-Supply Paper 2295-A; USGS: Washington, DC, 1987.

(8) Childress, C.J.O. et al. "Water-Quality Data-Collection Activities in Colorado and Ohio: Phase II—Evaluation of 1984 Field and Laboratory Quality-Assurance Practices"; U.S. Geological Survey Water-Supply Paper 2295-B; USGS: Washington, DC, 1989.

(9) Norris, J. M. et al. "Water-Quality Data Collection Activities in Colorado and Ohio: Phase III—Evaluation of Existing Data for Use in Assessing Regional Water-Quality Conditions and Trends"; U.S. Geological Survey Water-Supply Paper 2295-C; USGS: Washington, DC, in press.

(10) Hirsch, R. M.; Slack, J. R.; Smith, R. A. *Water Resour. Res.* **1982,** *18,* 107-21.

(11) Hirsch, R. M., *Water Resour. Bull.* **1988,** *24,* 493-503.

(12) Lettenmaier, D. P. *Water Resour. Bull.* **1978,** *14,* 884-902.

Janet Hren *is a hydrologist with the U.S. Geological Survey, Water Resources Division, Western Region Office in Menlo Park, CA. She has a B.S. degree in biology from Kent State University and an M.S. degree in biology from the University of Akron, OH.*

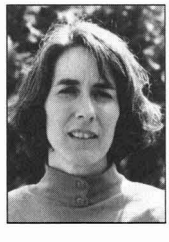

Carolyn J. Oblinger Childress *is a hydrologist with the U.S. Geological Survey, Water Resources Division district office in Columbus, OH. She received an M.S. degree in environmental health from the University of Michigan and a B.S. degree in zoology from the University of Massachusetts in Amherst.*

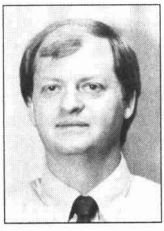

J. Michael Norris *is a hydrologist for the U.S. Geological Survey in Lakewood, CO. He has an M.S. degree in hydrology and water resources from Colorado State University. For the past 10 years his work has focused on various aspects of water quality, hydrologic modeling, and hazardous waste contamination in both surface water and groundwater.*

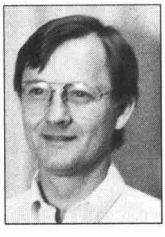

Thomas H. Chaney *is a hydrologist with the Water Resources Division of the U.S. Geological Survey in Denver, CO. He has B.S. degrees in zoology from Ohio State University, Columbus, OH, and in invertebrate zoology from Wright State University, Dayton, OH. His current interests include application of quality assurance protocols to scientific investigations.*

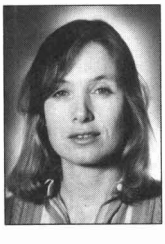

Donna N. Myers *is a hydrologist and project manager with the U.S. Geological Survey-Water Resouces Division in Columbus, OH. She received an M.S. degree in biological sciences from Kent State University, OH, and a B.S. degree in zoology from Ohio State University, Athens, OH. During the last 10 years she has worked in quality assurance and quality control in the field of water resources.*

Controlling emissions from motor vehicles

A benefit–cost analysis of vehicle emission control alternatives

Lester B. Lave
Carnegie Mellon University
Pittsburgh, PA 15213

William E. Wecker
Winthrop S. Reis
Duncan A. Ross
William E. Wecker Associates
Novato, CA 94945

U.S. ozone levels exceed the National Ambient Air Quality Standard (NAAQS) of 0.12 ppm in virtually every major urban area and in many nonurban areas in the East *(1)*. Hydrocarbon emissions are a primary contributor to the photochemical reactions that produce ozone *(2)*. These emissions from cars and light duty trucks (LDTs) account for approximately 35% of total man-made hydrocarbon emissions *(1)*.

This article reports the results of a benefit–cost analysis of alternative strategies for controlling emissions from hydrocarbon refueling and evaporative emissions from cars and LDTs. Our analysis accounts for interactions among the different control methods that influence both the costs and benefits of the available strategies. It also examines the role played by variations in temperature conditions and pollution levels across regions and seasons in estimating the costs and benefits. (A detailed report of the analysis is available from the authors.)

We have found that the most economically efficient control of refueling and evaporative hydrocarbon emissions from cars and LDTs would result from a mixed strategy that includes fuel volatility controls and controls on service station pumps. The most cost-effective control strategy involves fuel volatility and gasoline pump controls, which can be tailored to each region; the former can be changed with each season. Such flexible controls can be targeted to the specific regions and season where they will do the most good, while avoiding the wasteful cost of controls when and where ozone is not a problem. Vehicle-based controls do not have these advantages.

Sources of emissions

In a vehicle's fuel system, gasoline may be heated and vaporized by diurnal ambient temperature deviations (excursions) as well as by the engine and exhaust system after the engine is turned off ("hot soak") or when it is operated under extreme conditions ("running loss") *(3)*. Evaporative emissions occur when the amount of gasoline vapors exceeds the capacity of the vehicle's emission control system.

Refueling emissions occur primarily when liquid fuel from the gas pump displaces the vapor in the fuel tank. These vapors escape through the vehicle fuel tank fillpipe. A secondary source of refueling emissions is the escape of vapor from the service station's underground fuel tank. When liquid fuel is pumped from the underground tank, it is replaced by outside air. The increased concentration of air reduces the partial pressure of the gasoline vapor in the tank. More gasoline evaporates to return the liquid–vapor system in the underground tank to equilibrium. The

0013-936X/90/0924-1128$02.50/0

Types of evaporative emissions

Diurnal emissions may occur while a vehicle is parked and its fuel tank is heated by an increase in ambient temperature. Ambient temperature varies greatly by region and by season; therefore, diurnal emissions vary greatly by region and season.

"Hot soak" emissions may occur following engine shutdown; they are caused by heat transferred from the engine and exhaust system to the fuel.

"Running loss" emissions may occur while the engine is running under extreme conditions, such as operating at low speeds using high-volatility fuel on a very hot day. Under these conditions, the rate of vapor generation from the fuel tank can exceed the rate at which the engine can consume the vapors.

evaporation increases the pressure in the underground tank, pushing some of the vapor–air mixture out a vent to the atmosphere. Gasoline spills also contribute to refueling emissions.

Controlling emissions

The four main approaches to controlling evaporative and refueling emissions are "enhanced" versions of current canister controls on vehicles; "onboard" refueling emission controls on vehicles; "Stage II" refueling emission controls on service station pumps; and control of gasoline volatility. (Stage I controls route the displaced air from the underground storage tank to the delivery truck when the underground tank is being filled.)

Enhanced vehicle controls. The evaporative emission control system of vehicles includes a canister to contain the vapors generated by diurnal heating of the fuel. If the vehicle remains parked for several days, the capacity of the 1-L canister can be exceeded. EPA has investigated whether to increase the size of the canister to 5 L. Enhanced vehicle controls are not designed to control refueling vapors; that requires additional plumbing and valves (onboard vehicle controls).

Onboard vehicle controls. EPA has investigated controlling refueling emissions using a system on board the vehicle. Like the enhanced system, the onboard system would require a 5-L canister. In addition, the onboard system has plumbing and valves to route refueling vapors to the canister when the vehicle is being refueled. As occurs now, the canister would be purged when the engine is running, providing fuel for the vehicle.

Stage II controls. The Stage II control system uses specially designed gasoline-dispensing nozzles to collect vapor displaced during refueling and route it to the gasoline stations' underground fuel storage tanks. The Stage II controls considered in our analysis are part of a program similar to that used in California that includes rigorous emission-control system inspection and maintenance. Currently, Stage II refueling controls are in use in most of California, in St. Louis, and in Washington, DC, and are mandated in portions of New York and New Jersey.

Early Stage II control systems used a dual hose system and gasket that were criticized as clumsy and difficult to use. Successive generations of fuel-dispensing hoses and nozzles have performed better and have been easier to use. The current technology includes a hose nozzle that is virtually indistinguishable from a conventional (non-Stage II) nozzle.

Fuel volatility controls. Evaporative and refueling emissions can be reduced by changing the composition of gasoline. Its evaporation rate depends on the proportions of the components of the gasoline. Fuel volatility is often referred to as "RVP" because Reid vapor pressure is a commonly used index of the evaporation rate of gasoline *(4)*. RVP reductions are most often achieved by reducing the amount of butane, a volatile hydrocarbon, in the gasoline.

Implementation rates. Fuel volatility controls could be implemented within one year. Stage II controls could be fully implemented within five years *(5)*. Vehicle controls would take much longer to implement because all existing cars and LDTs would have to be retired before the full effects of vehicle controls are realized. Ten years after onboard controls were installed on all new vehicles, only 65% of cars and light trucks on the road would be equipped. It would take 15 years for 90% of the vehicle fleet to be so equipped *(6)*.

Regional and seasonal flexibility. The control alternatives described above vary in degree of regional and seasonal flexibility. Because ozone levels vary greatly by region and by season, there is an advantage to using flexible controls such as RVP that can be targeted to the regions and seasons in which the problem is the greatest. Stage II controls can be installed only in regions in which ozone levels are severe enough to warrant their year-round presence. Because enhanced or onboard vehicle controls lack regional and seasonal flexibility, they would be installed on vehicles operating in regions and seasons with good air quality. Vehicles with different control system designs could, in principle, be produced for use in different regions of the country, but the estimated extra cost of designing, certifying, and licensing multiple systems apparently has persuaded EPA, Congress, and automobile manufacturers not to propose multiple control system designs *(7)*.

Benefit–cost analysis

Identifying an efficient national control strategy requires four basic steps: defining the relevant control regions; defining the control strategy choices for each of those regions; calculating the nationwide benefits and costs of the many combinations of regional control strategies; and selecting the national control strategy that has the greatest overall (nationwide) benefit.

To define our control strategy, we have partitioned the nation into eight regions and three seasons, as shown in Tables 1 and 2. Except for the Los Angeles region, our "regions" are not contiguous areas of the United States. Rather, they represent areas with simi-

TABLE 1
Characteristics of U.S. vehicle control strategy regions

Region	Number of vehicles	Ambient temperature, °F (Peak ozone concentration, ppm) Summer	Shoulder season[a]	Winter
Los Angeles	9,067,000	72–96 (0.35)	72–96 (0.24)	60–84 (0.14)
Class 1	3,415,000	84–108 (0.23)	72–96 (0.18)	60–84 (0.14)
Class 2	26,164,000	72–96 (0.21)	72–96 (0.13)	60–84 (0.06)
Class 3	9,149,000	84–108 (0.16)	72–96 (0.13)	60–84 (0.06)
Class 4	17,063,000	72–96 (0.16)	60–84 (0.09)	48–72 (0.04)
Class 5	8,231,000	84–108 (0.13)	60–84 (0.09)	48–72 (0.04)
Class 6	14,950,000	72–96 (0.13)	60–84 (0.09)	48–72 (0.04)
Attainment[b]	79,154,000	60–84 (0.06)	48–72 (0.04)	48–72 (0.04)

[a]March, April, September, and October.
[b]Attainment areas are those not included in the Los Angeles region or in regions in Classes 1–6 (see Table 2).

lar temperatures and ozone concentrations. We define summer as May through August; the "shoulder" season as March, April, September, and October; and winter as November through February.

Each regional control strategy is composed of a choice of RVP controls (9.0, 10.5, or 11.5 psi); a choice of whether to have Stage II (service station pump) controls; and a choice of current, enhanced (with 5-L canister), or onboard (with 5-L canister plus plumbing) vehicle controls. A different regional control strategy is allowed for each of the three seasons in a region. For example, "9.0 RVP, no Stage II, and onboard refueling vehicle controls" would be one possible regional control strategy.

A national control strategy is composed of a regional control strategy for each of the three seasons and for each region in the nation. For example, just one of many possible control strategies would require 9 RVP in all regions and all seasons, Stage II in all regions, plus onboard refueling controls nationwide (the "abatement by all possible means" strategy).

Our current model with eight regions, each with three seasons, thus contains approximately 10^{30} distinct national control strategies, less the following "unallowed" strategies (constraints): Stage II controls are not allowed to change with the season, and vehicle controls must be the same for all new vehicles in all regions and all seasons. These two constraints reduce the number of distinct national control strategies to approximately 10^{14}.

The cost of a regional control strategy depends on the choices of emission control. Because estimates of the costs of onboard and enhanced controls are controversial, we use three different base cases, each with different control cost assumptions. We calculate the incremental cost of each regional control strategy beyond a reference case of 11.5 RVP with no Stage II controls and current vehicle controls. Note that our reference case of 11.5 RVP with no Stage II controls and current vehicle controls bears no relationship to, and should not be confused with, the controls actually in place in a region.

Four basic steps are needed for our calculation of control strategy benefits: predicting the level of hydrocarbon abatements obtained by a given control strategy; estimating the fuel cost savings of that strategy; calculating the ozone concentration reductions based on the hydrocarbon abatement; and assigning a monetary value to that reduction.

First, we calculate the hydrocarbon emissions per vehicle for each of the 18 possible regional control strategies at each of the ambient temperature levels shown in Table 1. Next, we calculate the reduction of ozone concentration that results from the reduction of hydrocarbon emissions for each regional control strategy. We assume that a reduction in volatile organic compound (VOC) emissions will result in an approximately proportional reduction in VOC concentration.

In addition, we assume that a reduction in VOC concentration will result in an approximately proportional reduction in ozone concentration. EPA's Empirical Kinetic Modeling Approach model of ozone formation shows the validity of this assumption for a wide range of NO_x concentrations and VOC:

TABLE 2
Populations and seasonal peak ozone concentrations in nonattainment MSAs[a,b]

MSA	Population[c] (1000s)	Peak ozone concentrations, ppm[d] Summer	Shoulder[e]	Winter[f]
	Los Angeles region			
Los Angeles, CA	13,075	0.36	0.24	0.14
	Class 1 region			
Houston, TX	3,634	0.25	0.19	0.17
Sacramento, CA	1,291	0.18	0.17	0.07
Total	**4,925**			
Population-weighted average		**0.23**	**0.18**	**0.14**
	Class 2 region			
Atlantic City, NJ	297	0.19	N/A	N/A
Chicago, IL	8,116	0.20	0.09	0.04
Greater Conn, CT	2,206	0.23	N/A	N/A
New York, NY	17,968	0.22	0.15	0.06
Philadelphia, PA	5,833	0.18	0.12	0.04
Providence, RI	1,108	0.18	0.10	0.04
San Diego, CA	2,201	0.21	0.20	0.09
Total	**37,729**			
Population-weighted average		**0.21**	**0.13**	**0.05**
	Class 3 region			
Bakersfield, CA	494	0.16	0.11	0.07
Baton Rouge, LA	546	0.16	0.12	0.10
Beaumont, TX	376	0.16	0.12	0.08
Dallas, TX	3,655	0.16	0.11	0.06
El Paso, TX	562	0.16	0.13	0.11
Fresno, CA	588	0.17	0.13	0.08
Longview, TX	200	0.15	N/A	N/A
Memphis, TN	960	0.15	0.10	0.05
Phoenix, AZ	1,900	0.16	0.13	0.09
Salt Lake City, UT	1,041	0.15	0.09	0.04
St. Louis, MO	2,438	0.16	0.10	0.04
Stockton, CA	433	0.15	0.11	0.06
Total	**13,193**			
Population-weighted average		**0.16**	**0.11**	**0.06**
	Class 4 region			
Atlanta, GA	2,561	0.16	N/A	N/A
Baltimore, MD	2,280	0.17	0.10	0.04
Boston, MA	4,056	0.16	0.08	0.04
Cincinnati, OH	1,690	0.17	0.09	0.05
Louisville, KY	963	0.15	0.10	0.06
Milwaukee, WI	1,552	0.17	0.10	0.04
Modesto, CA	317	0.15	0.10	0.05
New Bedford, MA	200	0.16	N/A	N/A
Portland, ME	200	0.16	N/A	N/A
San Francisco, CA	5,878	0.17	0.08	0.03
Santa Barbara, CA	339	0.16	0.14	0.09
Seaford, DE	200	0.15	0.09	N/A
Washington, DC	3,563	0.16	N/A	N/A
Worcester, MA	408	0.15	0.10	N/A
York Co., ME	398	0.15	N/A	N/A
Total	**24,605**			
Population-weighted average		**0.16**	**0.09**	**0.04**

Calculating the number of vehicle emission control strategies

The formulae for calculating the number of strategies are as follows.

Without accounting for "unallowed strategies":

(3 RVP control options × 2 Stage II control options × 3 vehicle control options)$^{(8\ \text{regions} \times 3\ \text{seasons})} = 18^{24} = 1.34 \times 10^{30}$.

When accounting for "unallowed strategies":

(3 vehicle control options) × [(2 Stage II control options) × (3 RVP control options)$^{(3\ \text{seasons}]^{8\ \text{regions}})} = 3 \times [2 \times 3^3]^8 = 3 \times 54^8 = 2.17 \times 10^{14}$.

MSA	Populations[c] (1000s)	Peak ozone concentrations, ppm[d] Summer	Shoulder[e]	Winter[f]
	Class 5 region			
Birmingham, AL	911	0.13	N/A	N/A
Iberville Parish, LA	200	0.13	0.09	0.06
Jacksonville, FL	853	0.14	N/A	N/A
Kansas City, MO	1,518	0.14	N/A	N/A
Lake Charles, LA	200	0.14	N/A	N/A
Miami, FL	2,912	0.13	N/A	N/A
Nashville, TN	931	0.14	0.08	0.05
Pointe Coupee, LA	200	0.13	N/A	N/A
Richmond, VA	810	0.13	N/A	N/A
St. James Parish, LA	200	0.13	N/A	N/A
Tampa, FL	1,914	0.13	N/A	N/A
Tulsa, OK	734	0.13	N/A	N/A
Visalia, CA	287	0.13	N/A	N/A
Yuba City, CA	200	0.13	N/A	N/A
Total	**11,870**			
Population-weighted average		**0.13**	**0.08**	**0.05**
	Class 6 region			
Acadia Natl Park, ME	200	0.13	N/A	N/A
Allentown, PA	657	0.14	0.09	0.05
Beloit, WI	200	0.13	0.09	N/A
Charleston, WV	266	0.14	0.09	0.06
Charlotte, NC	1,065	0.13	0.10	0.06
Cleveland, OH	2,766	0.14	0.09	0.03
Dayton, OH	934	0.13	0.09	0.05
Denver, CO	1,847	0.13	0.09	0.07
Detroit, MI	4,601	0.13	0.09	0.05
Dover, DE	200	0.14	0.09	0.04
Erie, PA	279	0.13	0.10	0.05
Gardiner, ME	200	0.14	N/A	N/A
Grand Rapids, MI	649	0.13	0.09	0.04
Hancock Co., ME	200	0.13	N/A	N/A
Harrisburg, PA	577	0.13	0.10	0.05
Huntington, WV	328	0.14	N/A	N/A
Indianapolis, IN	1,213	0.13	N/A	N/A
Lancaster, PA	377	0.13	0.10	0.06
Muskegon, MI	200	0.14	N/A	N/A
Northampton Co., VA	200	0.14	0.09	0.02
Pittsburgh, PA	2,316	0.13	N/A	N/A
Portland, OR	1,364	0.13	N/A	N/A
Portsmouth, NH	200	0.13	N/A	N/A
Reading, PA	321	N/A	N/A	N/A
York, PA	398	0.13	N/A	N/A
Total	**21,558**			
Population-weighted average		**0.13**	**0.09**	**0.05**

[a]Metropolitan statistical areas.
[b]MSAs whose populations were not listed in the *Statistical Abstract* were assumed to have a population of 200,000.
[c]Source: Reference 8.
[d]Source: Reference 9.
[e]March, April, September, and October; data source: Reference 10.
[f]November, December, January, and February; data source: Reference 10.

NO_x ratios *(11)*, especially where the NO_x concentration is less than 0.28 ppm and the VOC:NO_x ratio is less than 10:1, as it is in most of the nation. Where the VOC:NO_x ratio is greater than 10:1, hydrocarbon abatement will cause smaller reductions in ozone concentration and therefore will have less benefit.

Thus a 20% reduction in total hydrocarbon emissions in a region is assumed to lead to a 20% reduction in ozone concentration for that region. Because hydrocarbon emissions from motor vehicles make up approximately 35% of total man-made hydrocarbon emissions, a 20% reduction of hydrocarbon emissions from motor vehicles would lead to approximately a 7% decrease in ozone, if hydrocarbon emissions from other sources remain constant (20% × 35% = 7%).

We assume that every abatement of hydrocarbon emissions from motor vehicles—and therefore every reduction in ozone concentration—has value. The value is greatest in regions with high ozone concentrations. Our assumptions about the marginal benefit of ozone concentration reductions are shown in Figure 1.

The decreasing marginal benefit curve (Figure 1) conforms to intuition and current experience. Los Angeles has instituted the most stringent and expensive program for abating hydrocarbon emissions. The expense and inconvenience of some control measures imply that a high value is placed on achieving small reductions in hydrocarbon emissions. Residents in other parts of the country with much lower peak ozone levels display a willingness to pay to reduce hydrocarbon emissions by a small amount that is related, roughly, to the ozone concentration.

Hydrocarbons not emitted remain in the vehicle or underground tank as fuel. We value this increased fuel availability at $0.32/kg, the pre-tax price for gasoline.

Emission controls may have benefits other than ozone reduction and increased fuel availability. EPA's Office of Air and Radiation (OAR) assumes that the abatement of refueling emissions has the additional benefit of causing fewer cancers because it reduces exposure to toxic substances during the refueling process *(7)*. This assumption is controversial *(12, 13)*. In our OAR case, we calculate this source of benefits assuming that the number of cancers, and thus the dollar benefit of abatement, is proportional to hydrocarbons abated.

EPA and independent analyses have suggested that lowering in-use fuel volatility may reduce the levels of exhaust hydrocarbon and exhaust carbon monoxide emissions significantly under some driving conditions. By not including the benefits of reduced levels of exhaust emissions, we may have underestimated the number of areas that should have fuel volatility controls. Similarly, the model presented here does not take account of potential changes in accident risks associated with Stage II and onboard refueling emissions controls.

The accident-risk issues surrounding OAR's 1987 proposals are potentially important, but also are the source of considerable controversy. Proponents of in-use fuel volatility controls argue, for example, that historical data show reduced incidence of vehicle fires when lower volatility fuels are available—a claim that is disputed by representatives of the gasoline-marketing industry. Likewise, opponents of onboard refueling emissions controls argue that these controls increase the risk of vehicle fires and other accidents in crash and noncrash settings. In contrast, proponents sometimes claim that some onboard control systems may reduce the incidence of injury due to fuel siphoning. The onboard accident risk issue has been examined by consultants retained by the National Highway Traffic Safety Administration. When they are clarified, these accident-risk issues could be encompassed in our benefit-cost model.

Selecting the optimal strategy

The benefits of reducing ozone are more valuable the sooner they are

achieved. We account for this time value of benefits by using a discount rate for future benefits and costs to value them in current dollars. The optimal national control strategy is the one with the greatest present value of net benefits.

Evaluating the control alternatives requires an estimate of the hydrocarbon emissions in each of the regional control strategies for each of the temperature levels. Our model for estimating emissions is based on a modified form of EPA's PT (powertrain) Evaporative Emissions model. It is designed to account for driving patterns, vapor generation, and carbon canister characteristics. In May 1989 EPA published engineering data and analysis indicating that the canister and purge modules of the published PT model are not verifiable. We replaced the PT model's purge schedule and canister model with a purge schedule and canister model based on laboratory measurements. We believe that these modifications to the PT model help clear up recognized deficiencies in the original model. The PT model also does not provide a method of predicting the rate or quantity of tank vapor generation; we are able to do that, however, with a model based on a study by Reddy *(14)*.

In its 1987 proposals, OAR claimed that the size of canister currently in use is inadequate for handling evaporative emissions but that a larger canister would be adequate *(7)*. However, OAR based this claim on their PT model, which has proven to be inaccurate. Our modified version of the PT model shows that a larger canister would do little to control evaporative emissions from a vehicle fueled with 11.5 RVP fuel, contrary to OAR's claim. In addition, the modified PT model shows that the current size of canister can handle virtually all evaporative emissions from a broad range of vehicle driving patterns when the vehicle uses 9 RVP fuel.

Three "base cases"

The Motor Vehicle Manufacturers Association (MVMA), the Congressional Office of Technology Assessment (OTA), and OAR disagree on the costs of enhanced and onboard vehicle controls, in part due to different assumptions and methods. MVMA estimates that onboard controls will cost $1 billion in capital and $35 per vehicle and that enhanced controls will cost $250 million in capital and $16.50 per vehicle. OTA estimates the capital costs will be negligible for both onboard and enhanced controls and the costs per vehicle will be $25 and $10, respectively. OAR also assumes the capital costs will be negligible and puts the costs of onboard at $19 per vehicle. EPA's rule making does not discuss costs of enhanced controls, so we use the same costs of $10 per vehicle for enhanced controls in the OAR case as in the OTA case. We examine the implications of each cost estimate below.

FIGURE 1
Marginal benefit of ozone concentration reduction.

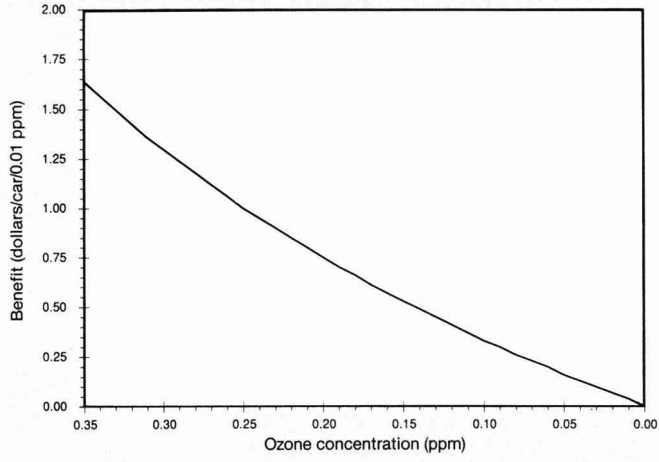

Refueling emissions expose people to low levels of benzene, a chemical known to cause leukemia. OAR assumes that 67 cancers per year result, at a social cost of $7.5 million per cancer. Because the dose–response relationship is assumed to be a fixed proportion, an 80% reduction in the 280 million kg of refueling emissions is assumed to result in an 80% reduction in the 67 associated cancers.

We use the same (EPA-estimated) Stage II costs for all three cases: $5,700–$23,200 capital cost per service station plus $1,300–$3,100 per year maintenance cost (depending on the size of the station). We use the same (EPA-estimated) cost in all three cases for RVP reductions: $0.006 per gallon for reducing RVP from 11.5 to 10.5, and $0.025 per gallon for reducing RVP from 11.5 to 9.0.

Efficient control strategies

The national control strategy (choice of RVP, Stage II, and vehicle controls for each region in each season) with the largest net benefit is shown in Table 3 for each of the three assumptions about control costs. (Net social benefit of controlling evaporative and refueling emissions subtracts the costs from estimated benefits.) Using MVMA's assumptions, the volatility of fuel is controlled below 11.5 RVP in all nonattainment regions in summer; in the Los Angeles, Class 1, and Class 2 regions during the shoulder seasons; and in none of the regions in winter. The strategy calls for Stage II controls in the Los Angeles, Class 1, and Class 2 regions. Neither onboard nor enhanced vehicle controls are part of MVMA's optimal strategy.

Despite the different assumptions about onboard and enhanced control costs, the OTA case calls for the same strategy as the MVMA case does. The OAR case, with its still lower vehicle control costs and assumed benefits from cancer reduction, calls for a similar strategy. The only difference is that Stage II controls are required in the OAR case for all regions, instead of just the Los Angeles, Class 1, and Class 2 regions. The need for additional Stage II controls results from the large cancer reduction benefits assumed in the OAR case. Like the MVMA cost estimates, the OTA and OAR estimates do not indicate that onboard or enhanced controls would be part of the best control strategy.

Lost net benefits

Although onboard controls are not part of the best control strategy, Congress appears headed toward requiring them. Theoretically, requiring onboard controls could involve a minuscule social loss compared with the best strategy. To investigate this possibility, we assumed that onboard controls were required and then calculated the best control strategy for the remaining choices.

Under the MVMA cost assumptions, the best unconstrained strategy produces net social benefits worth $5.45 billion, which indicates that society has been too slow in controlling refueling losses. But requiring onboard controls rather than the best control strategy lowers the value of this net benefit by $3.48 billion, a 64% loss. If enhanced rather than onboard controls are required, the lost net benefit is $1.42 bil-

TABLE 3

Optimal national vehicle emission control strategies for three cost scenarios[a]

Region	Stage II controls	Reid vapor pressure: Summer	Reid vapor pressure: Shoulder season[b]	Reid vapor pressure: Winter
Motor Vehicle Manufacturers Association case				
Los Angeles	Yes	9.0	10.5	11.5
Class 1	Yes	10.5	10.5	11.5
Class 2	Yes	10.5	10.5	11.5
Class 3	No	10.5	10.5	11.5
Class 4	No	10.5	11.5	11.5
Class 5	No	10.5	11.5	11.5
Class 6	No	10.5	11.5	11.5
Attainment[c]	No	11.5	11.5	11.5
Office of Technology Assessment case				
Los Angeles	Yes	9.0	10.5	11.5
Class 1	Yes	10.5	10.5	11.5
Class 2	Yes	10.5	10.5	11.5
Class 3	No	10.5	10.5	11.5
Class 4	No	10.5	11.5	11.5
Class 5	No	10.5	11.5	11.5
Class 6	No	10.5	11.5	11.5
Attainment[c]	No	11.5	11.5	11.5
Office of Air and Radiation case				
Los Angeles	Yes	9.0	10.5	11.5
Class 1	Yes	10.5	10.5	11.5
Class 2	Yes	10.5	10.5	11.5
Class 3	Yes	10.5	10.5	11.5
Class 4	Yes	10.5	11.5	11.5
Class 5	Yes	10.5	11.5	11.5
Class 6	Yes	10.5	11.5	11.5
Attainment[c]	Yes	11.5	11.5	11.5

[a]All cost scenarios assume current vehicle controls.
[b]March, April, September, and October.
[c]The remainder of the continental United States.

lion, a 26% loss. Under the OTA cost assumptions, the unconstrained net social benefit of $5.45 billion would be reduced by $1.60 billion (29%) and $0.55 billion (10%), respectively, by requiring onboard or enhanced controls. For the OAR assumptions, the unconstrained net social benefit of $10.32 billion is reduced by $1.89 billion (18%) and $0.90 billion (9%) for onboard and enhanced controls, respectively. As this article goes to press, Congress is debating whether to require both onboard and Stage II controls. To assess the efficiency of this proposal we have analyzed two specific control strategies.

Stage II required in all nonattainment areas. In the first strategy we require Stage II in nonattainment areas but not in attainment areas. We do not require the controls for retail service stations that pump less than 25,000 gallons of gasoline per month or nonretail service stations that pump less than 10,000 gallons of gasoline per month. We choose RVP by season and by region and nationwide vehicle controls to maximize present-value net benefit, subject to the constraints described above. Onboard vehicle controls are not part of the optimal solution under this set of constraints.

Stage II required in all nonattainment areas plus onboard controls required nationwide. This strategy has the constraints described in the previous case plus the requirement that onboard controls be installed in cars and LDTs nationwide. Also in this case, we assume that Stage II maintenance costs are zero and that Stage II in-use efficiency will not be lowered by the absence of maintenance.

One congressional proposal in the Clean Air reauthorization bill would phase out Stage II after onboard controls are in widespread use. Our conservative assumption of zero maintenance cost is intended to reflect the reduced maintenance costs that would be brought about by a phaseout of Stage II.

The choices of RVP by season and by region are made to maximize present-value net benefit, subject to the constraints previously described. The optimal solution under this set of constraints calls for the same levels of RVP control as in the previous case.

For the MVMA cost assumptions, the cost to the nation of imposing the requirements of the first strategy would be $0.40 billion. The cost to the nation of requiring onboard controls as well (the second strategy) is $3.34 billion. The difference, $2.94 billion, is the cost to the nation of requiring onboard in addition to requiring Stage II controls in nonattainment areas. For the OTA and OAR cases, the cost of requiring onboard in addition to Stage II controls is $1.35 billion and $1.03 billion, respectively.

Sensitivity analyses

Our sensitivity analyses for the three base cases considered changes in capital and unit costs of onboard vehicle controls; capital and unit costs of enhanced vehicle controls; installation and maintenance cost of Stage II controls; the benefits of ozone abatement; the first year of vehicle control implementation; and the discount rate.

Estimates of the costs of onboard controls are controversial; therefore, we calculated what capital cost or what cost per vehicle would justify the choice of onboard controls. If all other model parameters are held constant for the MVMA case, the cost per vehicle could not be greater than $4.87 if onboard controls are to be worth introducing. In other words, the per-vehicle cost would have to be four times lower than the costs estimated by MVMA, OTA, or OAR. At a cost of $35 per vehicle, the capital cost would have to be a negative $3.73 billion for onboard controls to be attractive. For the OTA case, these figures are $10.98 per vehicle and negative $2.20 billion, respectively. For the OAR case, the costs would have to be $2.49 per vehicle and negative $2.59 billion. Thus, for all three cases, the costs of onboard controls would have to be far lower than those estimated by MVMA, OTA, or OAR for this control strategy to be attractive.

We then examined the sensitivity of our analysis to changes in the costs of Stage II controls for the three base cases. The installation and maintenance costs of Stage II controls would have to be increased by more than 350% before Stage II would cease to be a part of the optimal national strategy in the MVMA and OTA cases. In the OAR case, the installation and maintenance costs of Stage II controls would have to be increased by more than 510% before Stage II would cease to be a part of the optimal national strategy. The OAR case has a higher break-even cost for Stage II than do the MVMA and OTA cases because the cancer-avoidance benefits in the OAR case increase the benefits of Stage II controls.

Next we checked how sensitive our calculation was to alternative assumptions about the marginal benefit of ozone reduction. We continued to assume that the social benefit of abating the last tiny amount of ozone is zero, but assumed that the social benefit of abating ozone at 0.35 ppm would be much larger. We investigated marginal values of abatement more than six times greater than the vertical intercept shown in Figure 1, implying values of abating hydrocarbons of up to $20,000 per ton. For none of these values are onboard controls part of the best solution.

If society gained nothing from ozone

abatement, requiring onboard controls would lead to a net benefit loss (loss of value of the benefit) of $4.25 billion (essentially the cost of the controls). As the value of abatement increases (see Figure 2), the social net benefit loss from requiring onboard controls diminishes a bit but is never less than $3.40 billion for the MVMA assumptions (or less than $1.50 billion for the OTA assumptions or $1.30 billion for the OAR assumptions). Stage II and RVP controls can be implemented more quickly than onboard controls. Once Stage II and fuel RVP reductions are in place, there is no additional benefit from adding onboard controls. The results are detailed in Figure 2 in terms of the social losses from requiring onboard controls.

Figure 3 shows the effect of varying the discount rate when other factors are held constant. For real discount rates in the range of 5–15% percent, there is no change in the optimal strategy under any of the three cases. The lost net benefit of requiring onboard controls increases as the real discount rate is decreased because a lower discount rate increases the net benefits of both the optimal strategy and the best strategy that requires onboard controls. The difference in present-value net benefits between these two strategies also is increased.

FIGURE 2
Lost net benefit of requiring onboard vehicle emission controls[a]

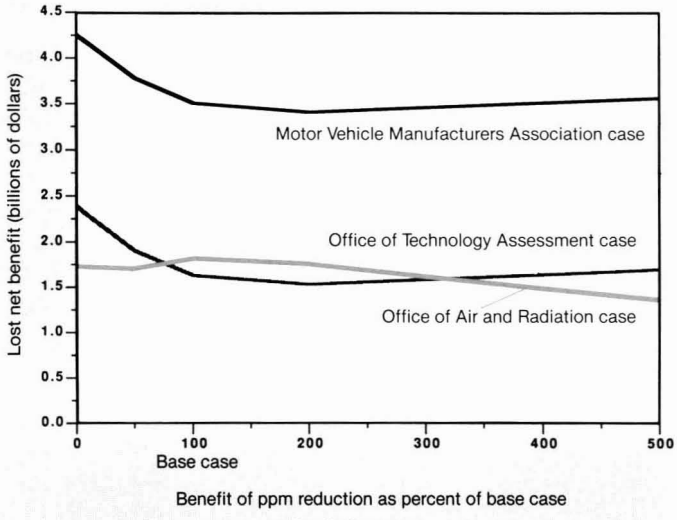

[a](Net benefit of optimal national strategy) – (net benefit of best strategy requiring onboard controls). Each case uses different values of the benefit of ozone abatement.

FIGURE 3
Lost net benefit of requiring onboard vehicle emission controls[a] using different discount rates

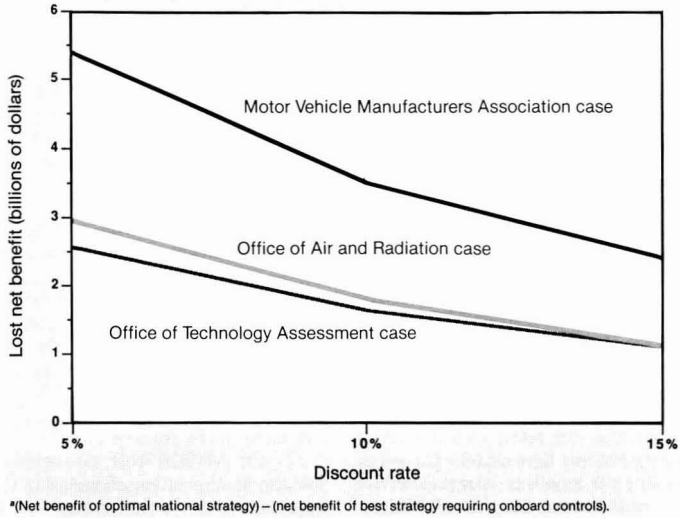

[a](Net benefit of optimal national strategy) – (net benefit of best strategy requiring onboard controls).

The most efficient approach

Hydrocarbon emissions from motor vehicles can be abated most efficiently by adopting a mixed strategy of RVP controls and Stage II controls. Additional vehicle-based controls would impose large costs on society without commensurate increases in benefits. Vehicle-based controls are not only more expensive per gram of hydrocarbon emissions abated than a combination of RVP and Stage II controls, but they take longer to implement, thereby causing persons who live in urban areas to breathe more polluted air for almost a decade longer than they would if strategies of combined RVP and Stage II controls were implemented.

Acknowledgments

This research was supported by the Motor Vehicle Manufacturers Association. The opinions are those of the authors. We thank the referees for their helpful comments.

This article was reviewed for suitability as an *ES&T* feature by Richard Morgenstern, EPA, Washington, DC 20460; Robert W. Hahn, American Enterprise Institute, Washington, DC 20036; and Joseph Norbeck, Ford Motor Company, Dearborn, MI 48121.

References

(1) Friedman, R.M., et al. "Urban Ozone and the Clean Air Act: Problems and Proposals for Change"; U.S. Office of Technology Assessment: Washington, DC, April, 1988.

(2) Abelson, P. H. *Science* **1988,** *241*(4873), 1569.

(3) Patterson, D.; Henein, N. *Emissions from Combustion Engines and their Control;* Ann Arbor Science: Ann Arbor, MI, 1972.

(4) *Fed. Regist.* **1989,** *54,* 11867-928.

(5) "Comments on the Environmental Protection Agency's Proposed Rules Limiting the Volatility of Gasoline and Refueling Emissions"; U.S. Office of Management and Budget: Washington, DC, 1987.

(6) *MVMA Facts and Figures '88;* Motor Vehicle Manufacturers Association of the United States, Inc.: Detroit, MI, 1988.

(7) *Fed. Regist.* **1987,** *52,* 31161-271.

(8) *1988 Statistical Abstract of the United States*; Bureau of the Census, U.S. Department of Commerce: Suitland, MD, 1989; pp. 28–30.

(9) "Urban Ozone and the Clean Air Act: Problems and Proposals for Change"; Congress of the United States, Office of Technology Assessment: Washington, DC, 1988; pp. 24–25.

(10) Baugues, K. *A Review of Non-Methane Organic Compound, NO_x, and NMOC/NO_x Ratios Measured in 1984 and 1986*; U.S. Environmental Protection Agency: Washington, DC, 1986.

(11) Seinfeld, J. H. *Science* **1989**, *243*, 745-52.
(12) *Fed. Regist.* **1987**, *52*, 31161, 31273.
(13) *Fed. Regist.* **1987**, *52*, 31162, 31274.
(14) Reddy, S. R. Paper 861556; In SAE Transactions 1986, Vol. 95, Sec. 6, pp. 760–78; Society of Automotive Engineers: Warrendale, PA, 1986.

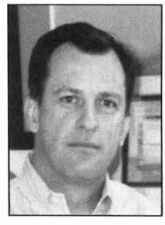

Lester B. Lave *(l) is the James Higgins Professor of Economics at Carnegie Mellon University (Pittsburgh, PA). He has a Ph.D. in economics from Harvard University and has done research on regulation and risk analysis for more than a decade. Lave is a past president of the Society for Risk Analysis.*

William E. Wecker *(r) is president of the consulting firm of William E. Wecker Associates, Inc. (Novato, CA). He received his Ph.D. in statistics and management science from the University of Michigan in 1972 and has served on the faculties of the University of Chicago and of the University of California–Davis from 1972 to 1989.*

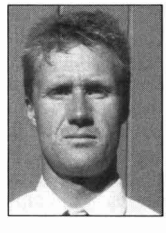

Winthrop S. Reis *(l) is a consultant with William E. Wecker Associates, Inc. He received his B.S. degree in mathematical and computational sciences, with honors in statistics, from Stanford University in 1988.*

Duncan A. Ross *(r) is a consultant with William E. Wecker Associates, Inc. He received his B.S. degree in mathematical and computational engineering and his A.B. degree in psychology from Stanford University in 1988.*

ES&T VIEWS

Methanol from biomass

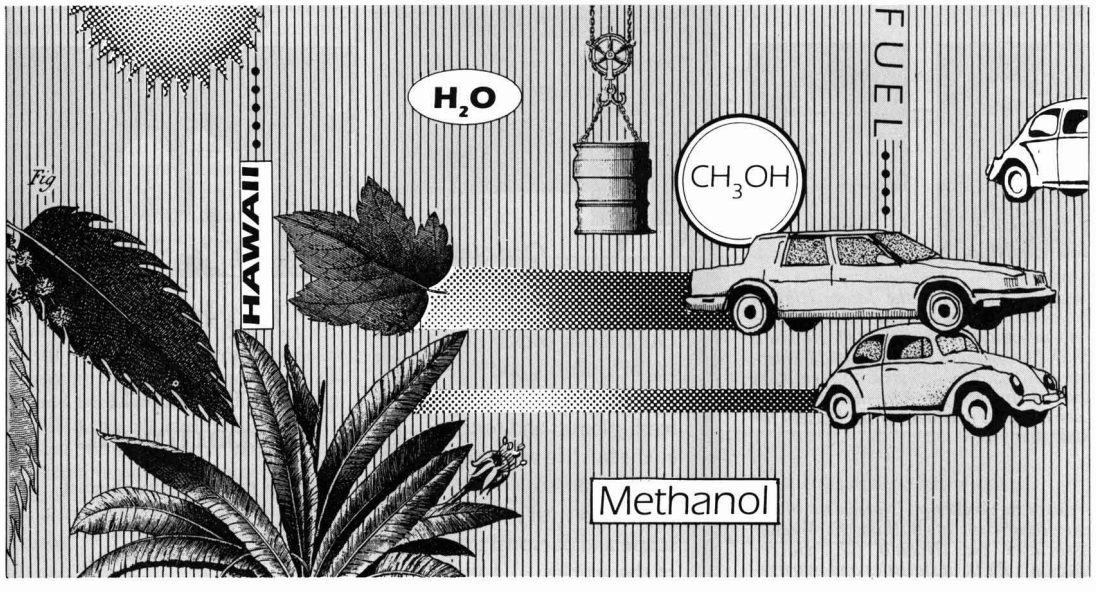

By Victor D. Phillips and Patrick K. Takahashi

Methanol has been identified by most experts as the fuel of choice to replace gasoline and diesel fuel because it costs less than other alternative fuels (when it is produced from natural gas); it is an oxygenated fuel, which burns cleaner; it has a higher octane rating, which enhances engine performance; and it is safer (methanol fires are extinguishable with water) *(1, 2)*.

Methanol is currently manufactured worldwide by the conversion of synthesis gas ("syngas") derived from natural gas, refinery off-gas, petroleum, or coal. However, research scientists at the Hawaii Natural Energy Institute (HNEI) have identified methanol from biomass as the most cost-effective, near-term, indigenous, and renewable liquid fuel alternative to replace gasoline and diesel fuel for ground transportation. It is manufactured by partial oxidation of biomass feedstocks into syngas, followed by catalytic conversion into methanol.

Views are insightful commentaries on timely environmental topics, represent an author's opinion, and do not necessarily represent a position of the society or editors. Contrasting views are invited.

Hawaii is uniquely suited to be an international showcase for the development, production, and utilization of methanol from biomass for several reasons. Hawaii has no indigenous fossil fuels, and thus needs an alternative fuel. The environmental conditions for high yields of biomass feedstocks are ideal. A wealth of experience and expertise exists in the Hawaiian agricultural industry and university community to develop the required technology. Gaseous and liquid fuels such as methane, methanol, and ethanol manufactured locally from biomass feedstocks are the most viable alternatives to gasoline and diesel fuels for transportation in Hawaii. Short driving distances on the islands allow for convenient refueling at nearby methanol fueling stations *(3)*.

The Hawaii Integrated Biofuels Research Program is an integrated research and development effort which combines biomass production research to evaluate the potential of several biomass resources, including woody crops such as eucalyptus and leucaena and herbaceous crops like sugarcane and napiergrass; analyses of feedstock handling and processing; and thermochemical conversion to a biofuel product, methanol from biomass *(4)*.

The goal of this program is to provide a technological and economic data base for use by private industry to manufacture liquid fuels commercially from Hawaiian-grown biomass feedstocks for transportation. The results are directly applicable in the American territories throughout the Pacific Basin and Caribbean and in many parts of the United States and the world.

The tasks of the program are organized into two research components: biomass production and feedstock preparation, and biomass conversion. The first component focuses on identifying the tree and grass species that grow fastest and yield the highest biomass energy. These crops are matched with suitable and available sites. This research will improve biomass yields through plant breeding techniques and will develop cost-efficient biomass plantation management strategies and least-cost feedstock harvesting, processing, and transport systems. The information from this research will be integrated in yield and economic models for manufacturing methanol.

The second research component in biomass conversion emphasizes the analysis and testing of several thermochemical processes, such as pyrolysis, oxygen and steam gasification, and solvolysis, used in the conversion of biomass feed-

0013-936X/90/0924-1136$02.50/0

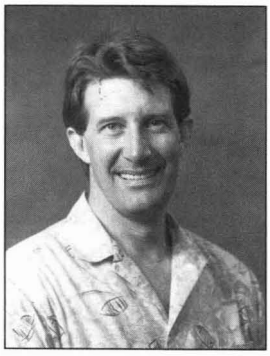

Victor Phillips

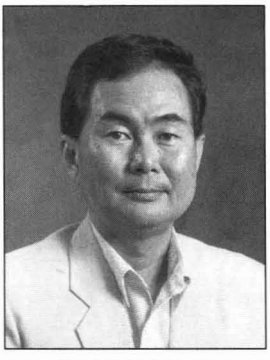

Patrick Takahashi

stocks to gaseous and liquid fuels, especially methanol.

During more than a decade of biofuels research conducted at HNEI, an emerging attribute of biomass energy is its ability to increase economic and environmental security both locally—by eliminating the export of over $1 billion annually from Hawaii's economy for imported oil for transportation fuels—and globally by replacing gasoline and diesel fuel with biofuels (especially methanol from biomass). The use of biomass energy can reduce atmospheric carbon dioxide from the transportation sector, help reverse the greenhouse effect, and avoid oil spills.

The overall energy in CO_2 equivalents for the biomass conversion process is not yet available. A total fuel cycle auditing of the energy in versus energy out (and subsequent conversion to CO_2 units) for methanol from biomass has not been made. We are in the process of developing methodologies for incorporating externalities into the real or "green" economic costs for energy products and services.

During testimony presented before a congressional hearing in June 1988 on the role of renewable energy technologies in helping remediate the greenhouse effect, Phillips said, "I spell relief from global greenhouse warming R-E-L-E-A-F" *(5)*. In the fall of 1988 the American Forestry Association adopted as the motto for its tree-planting promotion "Global ReLeaf."

Not only do biofuels help reverse the greenhouse effect, they can be produced in virtually every state and nation and are the only renewable energy resource readily available in convenient liquid form. For example, by taking advantage of its ideal conditions for plant growth, Hawaii can harvest sufficient fast-growing trees and grasses on less than 5% of its land area to provide all of the state's liquid fuel as methanol from biomass for ground transportation *(6)*.

Renewable energy technologies offer flexible, affordable, locally available, and sustainable alternatives to fossil and nuclear fuels and ultimately enhance our democratic values and individual freedom *(7)*. The human race is at a crossroads, but the direction to take is clear.

Continued use of fossil and nuclear fuels may lead us to an irreparable economic and environmental breakdown. Biofuels will enable us to drive more responsibly on the highway of life toward a bright future.

References

(1) Phillips, V. D. et al. *Appl. Energy* **1990,** *35,* 167–75.
(2) Browne, S. H. et al. *Solar Today* **1989,** July/August, 18–19, 26.
(3) Phillips, V. D. In *Proceedings of the Third Pacific Basin Biofuels Workshop;* Hawaii Natural Energy Institute: Waianae, Oahu, HI, March, 1989, pp. 32–42.
(4) Hawaii Natural Energy Institute. "Hawaii Integrated Biofuels Research Program-Phase 1 Final Report;" U.S. Department of Energy/Solar Energy Research Institute Subcontract No. XK-8-18000-1; 1989.
(5) Phillips, V. D.; Mackenzie, F. T.; Takahashi, P. K. Testimony before U. S. House of Representatives Subcommittees on Natural Resources, Agricultural Research, and Environment, and Science, Space, and Technology; Joint Hearing on Technologies for Remediating Global Warming; June 29, 1988, Washington, DC.
(6) Phillips, V. D.; Neill, D. R.; Takahashi, P. K. Presented at VIII International Symposium on Alcohol Fuels; Tokyo, Japan, November, 1988.
(7) Phillips, V. D.; Takahashi, P. K. *Environ. Sci. Technol.* **1989,** *23,* 10–13.

Victor D. Phillips is the manager of bioresources and environmental research at HNEI of the University of Hawaii at Manoa (Honolulu). He has a Ph.D. in ecology from the University of Colorado.

Patrick K. Takahashi is director of HNEI and vice president for development of the Pacific International Center for High Technology Research. He has a Ph.D. in chemical engineering from Stanford University.

What to do about greenhouse warming

By S. Fred Singer

Earth Day celebrations and a White House Environment Conference held in April 1990 focused attention on the possibility of greenhouse warming (GHW) being the issue of the 1990s. The easing of international tension with the Soviet Union could make GHW one of the most important foreign policy issues.

The wide acceptance of the Montreal Protocol—which limits and rolls back the manufacture of chlorofluorocarbons (CFCs), considered a threat to the stratospheric ozone layer—has encouraged environmental activists at conferences in Toronto (1988) and The Hague (1989) to call for similar controls on carbon dioxide. They have expressed disappointment with the White House for not supporting immediate action on CO_2, which is produced by the burning of oil, gas, and coal and is presumed to be the major greenhouse gas. But should the United States assume "leadership" in this campaign, or would it be wiser to first ensure through scientific research that the problem is both real and urgent?

The scientific base for GHW includes some facts, lots of uncertainty, and just plain ignorance; it needs more observations, better theories, and more extensive calculations. Specifically, there is consensus about an increase in so-called greenhouse gases (CO_2, CFCs, methane, nitrous oxide, ozone) in the Earth's atmosphere as a result of human activities. There is some uncertainty about the strength of sources and sinks for these gases and their rates of generation and removal.

There is major uncertainty and disagreement about whether this increase has caused a change in the climate during the past 100 years; observations simply don't fit the theory. There is also major disagreement in the scientific community about predicted changes from further increases in greenhouse gases; the models used to calculate future climate are not yet refined enough to simulate nature. As a consequence, we cannot be sure whether the next century will bring a warming that is negligible or a warming that is significant.

Finally, even if there is a warming and associated climate changes, it is debatable whether the consequences will be good or bad; likely we will get some of each. (The good consequences of GHW would be more rapid plant growth, longer growing seasons, and improved global food production.)

0013-936X/90/0924-1138$02.50/0

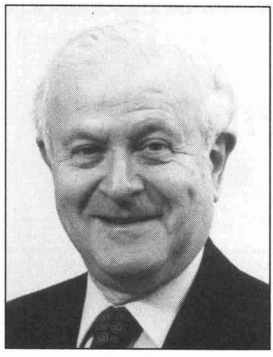

S. Fred Singer

The climate record

Has there been a climate effect caused by the observed increase of greenhouse gases in the last decades—about 50%, when expressed in CO_2-equivalent terms? The data are ambiguous to say the least. Advocates of immediate action profess to see a global warming of about 0.5 °C since 1880 and point to record temperatures experienced in the 1980s. Others, especially scientists, tend to be more cautious. They call attention to the fact that there has been no increasing-temperature trend during the 1980s (as recently confirmed by satellite observations); the strongest increase occurred before 1940, before the major rise in greenhouse gas concentration, and it was followed by a quarter-century decrease, between 1940 and 1965, when concern arose about an approaching ice age.

It is therefore fair to say that we haven't seen the expected greenhouse warming in the temperature record. But why not? Suggested solutions to this scientific puzzle include the following.

- The GHW has been "soaked up" by the ocean and will appear after a delay of some decades. Plausible, but there is no evidence to support this theory.
- The GHW exists as predicted, but has been hidden by offsetting climate changes caused by volcanoes, solar variations, or other causes as yet unspecified—such as the cooling from an approaching ice age. Some scientists consider the warming observed before 1940 to be a recovery from the "Little Ice Age" that prevailed from 1600 to about 1850. Each of these causes has vocal proponents and opponents in the scientific community, but the jury is out until better data become available.
- The GHW has been overestimated by the existing models. Meteorologists Hugh Ellsaesser and Richard Lindzen demonstrate that the models cannot properly account for tropical convection and thereby overestimate the amplifying effects of water vapor—the most important greenhouse gas. Other atmospheric scientists suggest that the extent of cloudiness may increase as ocean temperatures try to rise and as evaporation increases. Clouds reflect incoming solar radiation; the resultant cooling could off-set much of the greenhouse warming.

My conclusion can be summed up in a simple message: *The scientific base for a greenhouse warming is too uncertain to justify drastic action at this time.* There is little risk in delaying policy responses to this century-old problem because there is every expectation that scientific understanding will be substantially improved within a few years. Instead of taking premature actions that are likely to be ineffective, we may prefer to use the same resources—a few trillion dollars by some estimates—to increase our economic resilience so that we can then apply specific remedies if and as necessary. That is not to say that some steps cannot be taken now; indeed, many kinds of energy conservation and efficiency increases make economic sense even without the threat of greenhouse warming.

Drastic, precipitous, and especially, unilateral steps to delay the putative greenhouse impacts can cost jobs and prosperity without being effective. Yale economist William Nordhaus, one of the few who has been trying to deal quantitatively with the economics of the greenhouse effect, has pointed out that ". . .those who argue for strong measures to slow greenhouse warming have reached their conclusion without any discernible analysis of the costs and benefits. . . ." (His paper was presented at an AAAS symposium in New Orleans, February 1990.)

It would be prudent to complete the ongoing and recently expanded research so that we will know what we are doing before we act. "Look before you leap" may still be good advice.

S. Fred Singer, professor of environmental sciences at the University of Virginia, has served as chief scientist of the Department of Transportation, as deputy assistant administrator of the Environmental Protection Agency, and as the first director of the U.S. weather satellite program in the Department of Commerce. An atmospheric and space physicist, he developed satellites and instruments and predicted the increase of atmospheric methane due to human activities. His most recent book is Global Climate Change, *published by Paragon House, New York, NY, 1989.*

The "mixed waste" dilemma

By Marion Elliott Deerhake

Definition of mixed waste

"An issue of immediate concern in managing low-level radioactive waste (LLW) is the regulation of 'mixed' LLW—waste that is both radioactive, as defined in the Low-Level Radioactive Waste Policy Amendments Act, and hazardous, as defined by the Resource Conservation and Recovery Act (RCRA). This waste is regulated by both the Nuclear Regulatory Commission (NRC) and the Environmental Protection Agency (EPA). . . . No disposal facility for mixed LLW has been available since 1985."

U.S. Office of Technology Assessment *(1)*

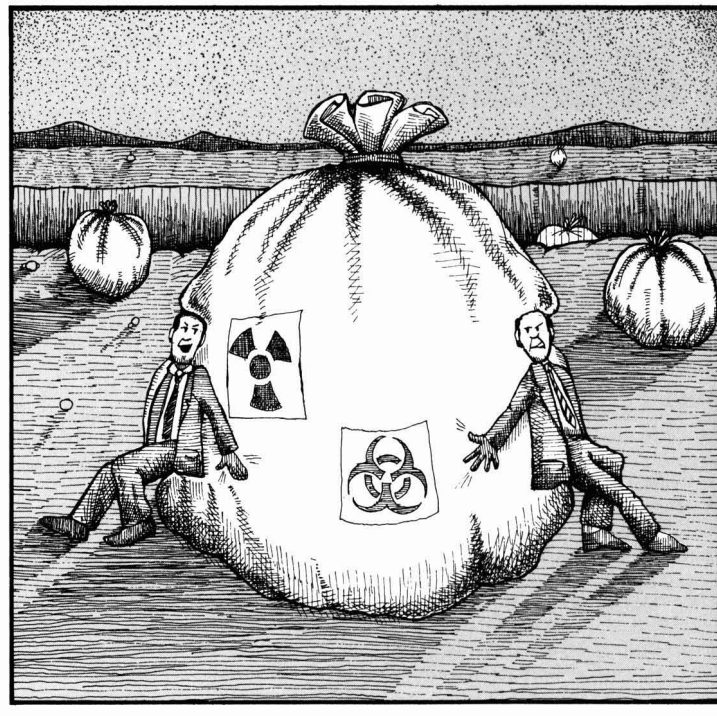

There is an immediate need for finding both technically and economically feasible solutions to the mixed waste management issue. The absence of commercial waste management capacity will force some generators of such waste to enter into expensive and time-consuming permitting procedures for this single stream of waste, which makes up only a small fraction of the hazardous wastes generated in the United States.

Regulatory background

On July 3, 1986, EPA published its interpretation of state authorization to regulate the hazardous components of radioactive mixed wastes under RCRA *(2)*. EPA published a clarification of interim status qualification requirements for mixed waste on September 23, 1988 *(3)*. In that announcement, EPA stated that facilities managing mixed wastes in states with basic RCRA authorization would not be subject to RCRA regulations until the state program is authorized to issue RCRA permits for mixed waste. The effective date of a state's RCRA authorization would serve as the date its facilities become subject to permitting requirements for mixed wastes. Currently 14 states are fully authorized for RCRA mixed waste programs. The effective date for states not previously authorized under RCRA to issue permits (i.e., their programs were overseen by EPA) was July 3, 1986.

Mixed waste generators who cannot find off-site management and are forced to store the waste on site must submit a RCRA Part A permit application to the state no later than six months after the state receives RCRA mixed waste authorization *(4)*. Mixed waste generators currently operating under RCRA interim status for other hazardous wastes must submit a revised Part A application by this date. Some generators are being forced to submit Part A applications because they have one waste stream—mixed waste—for which off-site management cannot be found. These generators are otherwise exempt from permitting because they ship other hazardous wastes off site in less than 90 days. Both parties are potentially subject to the RCRA section 3004(j) storage prohibition for wastes regulated under the Land Disposal Restrictions.

As of April 1990, no commercial waste management capacity was available for mixed waste. In fact, mixed waste has been banned from off-site commercial waste management facilities in certain regional LLW compact states and regional hazardous waste agreement states. [A compact is formed when a group of states agree to share their waste management capacity with each other. For example, South Carolina now accepts LLW waste from several southeastern U.S. states. When it reaches capacity, North Carolina will begin accepting the region's LLW for management.] The bans have been imposed by the compacts, by state legislation, and/or by facility owners. Such bans conflict with Congress's mandate under Section 104(c)(9) of the Comprehensive Emergency Response Compensation and Liability Act (CERCLA) that requires all states to provide management capacity no later than October 17, 1989, for hazardous wastes generated in their boundaries.

Estimated number of generators

Little data are available on mixed waste generation. Preliminary results of EPA's 1989 "National Survey of Hazardous Waste Generators" indicate approximately 200 mixed waste generators. Included in this group are teaching hospitals and research and development laboratories that conduct toxicology re-

0013-936X/90/0924-1140$02.50/0

Marion Deerhake

search. Other mixed waste generators include federal facilities (e.g., the Department of Energy) and power companies.

Even fewer data are available on the quantity of mixed waste generated annually. The OTA report quoted above states that less than 10% of the LLW generated is mixed waste. The fraction of RCRA-regulated hazardous waste that is mixed waste has not been documented.

Obtaining a RCRA permit

The three steps required to receive a simple container storage permit for hazardous waste are typically submittal of a Part A permit application (1–6 months); drafting the more extensive Part B permit application (4–6 months); and agency review and decision on the Part B application (1.5–2 years). In total, a mixed waste generator would require 1.9–3 years to receive a RCRA storage permit at an expense ranging from $25,000 to $50,000. Estimates are based on 40 CFR Part 270 and discussions with industry and consulting representatives familiar with the RCRA permitting process. In addition, the applicant must make funds available for facility closure and liability insurance coverage of up to $6 million annually.

The permit applicant's potential liabilities also increase greatly because of the large increase in the number of regulations with which the generator/applicant must comply.

Closure during interim status

Assuming off-site capacity becomes available in the next 2–3 years, the generator may close the facility and not seek a final RCRA permit. Generators who choose to close as RCRA interim status facilities are subject to closure regulations under 40 CFR 265 and potentially subject to the Corrective Action Orders of Section 3008(h) of RCRA. EPA's final Land Disposal Restrictions (55 FR 22520) grant a two-year variance for radioactive wastes that are mixed with first-third, second-third, and third-third wastes, assuming that adequate treatment capacity will become available after this time. Radioactive wastes that are mixed with spent solvents, dioxins, or California-listed wastes are subject to Land Disposal Restrictions; however, commercial treatment capacity is also currently inadequate. Facilities and ventures are already under development—for example, two facilities in Tennessee.

The five activities that could occur if an interim status facility closed before receiving its final RCRA permit include notifying authorities of closure and submittal of a closure plan (1–2 months); receiving the agency's decision on closure plan adequacy (3 months); performing a RCRA Facility Assessment for site contamination (too variable to estimate time); implementing and completing closure (6 months); and last, certifying closure (2 months). Estimates for a simple container storage facility are based on 40 CFR Part 264 and review of closure plans.

In total, closure of a simple container storage facility with no corrective action measures may take up to 10 months from initial notification to approved certification of closure. The cost of this closure scenario may range from $2000 to $5000 depending on the volume of waste stored and rates charged by commercial waste facilities. The cost estimate reflects only the cost of waste removal to off-site management and decontamination of a container storage facility. It does not reflect the cost of administrative responsibilities required to receive certification of closure. However, if contamination were discovered on the generator's site, the cost of closure and time consumed would be unpredictable because the extent of corrective action could vary widely.

Recommendations

Two approaches are suggested to relieve both the regulatory and economic burden on the small number of mixed waste generators who require storage permits only for that waste.

- Approach 1—Designate interim off-site storage facilities. Until commercial mixed waste treatment capacity becomes available (within two years), an existing commercial radioactive or hazardous waste storage facility could be designated to store this relatively small volume of waste temporarily for a region or state. This approach is consistent with the intent of Section 104(c) of CERCLA.
- Approach 2—Grant an extension in the Part A permit application deadline to applicants for mixed waste management permits only. First, extend the deadline for Part A application submittal to a reasonable date that allows generators to find off-site waste management capacity, or second, grant a deadline variance to the small number of generators who must request a RCRA permit for only the mixed waste.

These actions could be implemented using one of two regulatory vehicles:

- 40 CFR 262.34—This regulation grants extensions to the 90-day accumulation period if "hazardous wastes must remain on-site for longer than 90 days due to unforeseen, temporary, and uncontrollable circumstances."
- 40 CFR Part 268—This regulation grants two-year variances when treatment capacity is unavailable.

If these recommendations are not followed, an authorized state must go through the time-consuming and expensive processing of permit applications and, most likely, interim status closure procedures for these few facilities generating small amounts of mixed waste. Because 1992 permitting deadlines exist for other categories of hazardous waste management facilities [Hazardous and Solid Waste Amendments Section 3005(c)*(2)*], the mixed waste permit applications will be, chronologically, on the lower end of the list for permit review anyway. Therefore, by the time a final decision is made on mixed waste permit applications (e.g., 1992 at earliest), off-site treatment capacity is likely to be available, and storage permits would be unnecessary in many cases.

References

(1) "Partnerships Under Pressure: Managing Commercial Low-Level Radioactive Waste (Summary)"; Office of Technology Assessment: Washington, DC, November 1989; p. 3.
(2) *Fed. Regist.* **1986,** *51,* 24505.
(3) *Fed. Regist.* **1988,** *53,* 37045.
(4) *Code of Federal Regulations,* **1989,** *40,* 270.10(e).

Marion Elliott Deerhake is a senior environmental scientist at Research Triangle Institute in Research Triangle Park, NC. She received her B.S. degree in chemistry from Salem College and her M.S.P.H. degree in environmental chemistry from the University of North Carolina at Chapel Hill. She is currently a member of the North Carolina Governor's Waste Management Board's Technical Committee on Hazardous Waste.

POLYMERS & PLASTICS

New books from the American Chemical Society

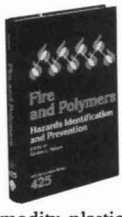

Fire and Polymers: Hazards Identification and Prevention

Gordon L. Nelson, Editor

This new volume provides an examination of the ongoing research in fire and-polymers. Thirty-four chapters are divided into five sections covering: fire toxicity; fire retardants and fire retardant commodity plastics; fire retardancy in engineering plastics; fire and cellulosics; fire performance, test, and risk.

ACS Symposium Series No. 425
640 pages (1990) Cloth.
ISBN 0-8412-1779-3
$99.95

Barrier Polymers and Structures

William J. Koros, Editor

Provides solid coverage on this rapidly changing field. Offers discussions on structure–property relationships of Saran materials and nylons, approaches to engineering around the sensitivity of barrier polymers to humidity, characterization of sorption kinetics in several glassy polymers for a broad spectrum of penetrants, complex barrier structures, and flavor scalping.

ACS Symposium Series No. 423
416 pages (1990) Cloth.
ISBN 0-8412-1762-9
$89.95

Sound and Vibration Damping with Polymers

Robert D. Corsaro and L.H. Sperling, Editors

This state-of-the-art volume examines blends and interpenetrating networks for their ability to damp over broad temperature and frequency ranges. Background material is presented as well as information on fillers, plasticizers, additives, new instrumentation, and theory.

ACS Symposium Series No. 424
480 pages (1990) Cloth.
ISBN 0-8412-1778-5
$99.95

Handbook of Plastics Testing Technology

Vishnu Shah

Offers up-to-date methods and guidelines for testing plastics. Provides step-by-step methods for accurately testing the five basic properties of plastics: mechanical, thermal, electrical, weathering, and optical. Covers tests for tensile strength, elevated temperature performance, electrical resistance, dielectric strength, photoelasticity, flammability, and water absorption.

Published by Wiley-Interscience
493 pages (1984) Cloth.
ISBN 0-471-07871-9
$89.95

Bonding Energetics in Organometallic Compounds

Tobin J. Marks, Editor

A broad, up-to-date, and in-depth overview of the current state of knowledge in this field is the focus of this new volume. It brings together carefully reviewed contributions from leading experimental researchers studying organometallic bonding energetics in the gas phase, in solution, and on well-characterized surfaces. The latest theoretical developments are also presented.

ACS Symposium Series No. 428
292 pages (1990) Cloth.
ISBN 0-8412-1719-2
$64.95

Rubber-Toughened Plastics

C. Keith Riew, Editor

Examines the development of theoretical and practical approaches of toughness and improvements for both thermosets and thermoplastics. Three major themes focus on fracture mechanics and failure mechanisms vs. toughness; morphology and mechanical properties vs. toughness; and chemistry and physics of toughening vs. toughness.

Advances in Chemistry Series No. 222
468 pages (1989) Cloth.
ISBN 0-8412-1475-1
$89.95

Agricultural and Synthetic Polymers: Biodegradability and Utilization

J. Edward Glass and Graham Swift, Editors

Offers an unbiased review of biodegradable synthetic polymers and polymers from renewable resources. Examines the state-of-the-art in commodity plastics degradation and disposal, and the greater utilization of agricultural polymers in industrial applications. Biodegradation, photodegradation, and chemical degradation are addressed and various uses for agricultural polymers are explored.

ACS Symposium Series No. 433
328 pages (1990) Cloth.
0-8412-1816-1
$69.95

To order CALL TOLL FREE 1-800-227-5558
In Washington D.C. area call 872-4363 or mail payment to: American Chemical Society, Distribution Office, Dept. 75, 1155 Sixteenth Street, NW, Washington, DC 20036

Elevating EPA to cabinet rank

Jay D. Hair

There is no better way to mark our entry into the decade of the environment than to bring a Department of the Environment into the president's cabinet this year.

For the past four years the National Wildlife Federation has urged that EPA be given cabinet rank. Two years ago bipartisan legislation was introduced in the Senate to accomplish this end. When President George Bush embraced the idea, success seemed assured.

But as these lines are written the EPA–Cabinet bill has yet to be acted upon. Partisan differences, jurisdictional rivalries, and concern over who will get the credit if the act passes have combined to slow the process down. Before we lose the bill, let's keep our eye on the ball: the environment needs an advocate in the counsels of the cabinet.

With the end of the Cold War, our national security is increasingly defined in environmental terms. The environmental decisions we make and the leadership the United States provides in this next decade will decide whether the course of the 21st century is one of environmental renaissance or unprecedented deterioration.

If there are still skeptics, let them consider:

- We will bequeath a potentially disastrous global warming to future generations if we do not curb the production of gases that trap the sun's heat in an atmospheric thermal blanket. Carbon dioxide, produced from burning fossil fuels, is the largest contributor to global warming gases, and the United States leads the world in CO_2 emissions.
- The planet's paper-thin stratospheric ozone shield is being ripped open by man-made chlorofluorocarbons. Intact, this shield filters out ultraviolet rays that can cause cancer in humans and mutations at the anchor leg of the food chain.
- The cost estimates for coping with our solid, toxic, and hazardous waste sites begin at $20 billion and soar to more than $100 billion.
- In 1987 alone, 500 U.S. manufacturers released 7.5 billion pounds of toxic pollutants, including 39 known or probable carcinogens, into our environment.

No other area of our national life requires rising to greater challenges. To meet them, a Department of the Environment should join the voices of the State, Defense, and Treasury departments in directly advising the president.

The United States alone among the industrialized nations has a representative of less than cabinet rank address environmental concerns. Creation of a Department of the Environment will send a clear message at home and abroad of our resolve to confront our environmental agenda.

President Bush has placed a respected environmentalist, William K. Reilly, at the helm of EPA, who stands ready to steer the agency confidently into its new responsibilities.

The right idea, the leadership, and wide public support have all converged at the same time to take this necessary step forward. Why then the delay?

Some observers say the Democrats don't want to give the president an easy environmental victory. Others claim the White House isn't pushing the legislation hard enough. Then there are turf disputes between the Senate committees handling the bill. And finally, some fear that so many "bells and whistles" are being tacked on that the whole thing may fall of its own weight.

The victory we are all seeking is for the American people. The environment is not a partisan possession. There will be credit enough to go around once the environmental agenda is placed squarely on the cabinet table.

Certainly in an ideal world a new Department of the Environment might encompass many new ideas. A bureau of environmental statistics is a sound suggestion. So too is the call to place all federal facilities under national environmental regulations. The entire point of the exercise, however, is to get a majority of votes to create the Department of the Environment. If necessary, other battles can be fought at other times. There is one primary idea here and it must not be jeopardized in disagreements over secondary matters.

The irony is that the people, the president, and the Congress all agree on the main objective. That being the case, let's stick to it.

This is the year to create the Department of the Environment!

Guest Regulatory Focus columnist Jay D. Hair has been president and chief executive officer of the National Wildlife Federation in Washington, DC, since May 1981. NWF is the largest U.S. conservation and education organization with 5.8 million members and supporters nationwide. Hair received B.S. and M.S. degrees from Clemson University and a Ph.D. in zoology from the University of Alberta, Canada.

0013-936X/90/0924-1143$02.50/0

ES&T BOOKS

The Greenhouse Trap: What We're Doing to the Atmosphere and How We Can Slow Global Warming. Francesca Lyman et al. Beacon Press, 25 Beacon St., Boston, MA 02108-2800. 1990. 190 pages. $21.95, cloth; $9.95, paper.

The Greenhouse Trap was written to explain "in plain English" what the greenhouse effect is and what causes it. The book forecasts how much the Earth's temperature will rise even if preventive measures are taken now and why the increase is more devastating than it appears. *The Greenhouse Trap* also examines the relationship between the greenhouse effect and the Antarctic ozone hole, and explains how energy conservation could help mitigate the greenhouse effect and what actions individuals can take.

Worker Protection During Hazardous Waste Remediation. Lori P. Andrews, Ed. Van Nostrand Reinhold, 7625 Empire Dr., Florence, KY 41042. 1990. xxi + 391 pages. $44.95, cloth.

This guide explains how workers should recognize hazards, handle wastes, prevent accidents, and treat exposure victims. The hazard recognition section deals with subjects such as noise, oxygen deficiency, chemical dangers, radiation, risk assessment, and control. Other topics in *Worker Protection* include medical surveillance, toxicology, safe sampling techniques, and protective equipment. The book was written by the Center for Labor Education and Research.

The Complete Book of Home Environmental Hazards. Roberta Altman. Facts On File, Inc., 460 Park Ave. S., New York, NY 10016. 1990. 304 pages. $24.95.

This book explains how to purify drinking water, test for radon, and remove asbestos. It also tells how to detect health hazards when one is considering buying or renting a house or apartment. Other topics include the control of insects without dangerous pesticides, lead in the plumbing and paint of old houses (especially those built before 1950), and potential asbestos problems from old insulation. The author currently is with the Cancer Information Service of Sloan-Kettering Hospital (New York).

Detection of Subsurface Hazardous Waste Containers by Nondestructive Techniques. Arthur E. Lord, Jr., and Robert M. Koerner. Noyes Data Corporation, Mill Rd. at Grand Ave., Park Ridge, NJ 07656. 1990. 83 pages. $39, cloth.

Nondestructive testing (NDT) involves remote sensing. This book discusses the latest NDT methods such as eddy currents, microwaves, electrical resistivity, sonar, infrared radiometry, induced polarization, and optical techniques. It deals with experimental evaluation of NDT techniques at various field sites and presents conclusions and recommendations. The authors are with Drexel University.

PAH-XI: Polynuclear Aromatic Hydrocarbons: Measurements, Means, and Metabolism. Marcus Cooke, Kurt Loening, and Joy Merritt, Eds. Battelle Press, 505 King Ave., Columbus, OH 43201-2693. 1990. 1220 pages. $82.50.

One in a series of books of proceedings of international PAH symposia, *PAH-XI* features advanced DNA adduct research, air pollution studies (including indoor air pollution), synthesis of new molecules, nitrated mutagens, and source characterization. It includes a special nomenclature guide on enzyme terminology. *PAH-XI* contains papers from a symposium on polynuclear aromatic hydrocarbons.

Continuous Emission Monitoring: Present and Future Applications. Air & Waste Management Association, P.O. Box 2861, Pittsburgh, PA 15230. 1990. 412 pages. $60 ($40 for association members), paper.

Continuous Emission Monitoring reviews current knowledge and describes new technology for future systems. Its 33 papers deal with topics such as federal and state enforcement and quality assurance policies. They also discuss applications of technologies at electric utilities and incineration facilities and review successes and limitations. The application of electrooptical techniques and of new instrumentation also is presented.

Heavy Metals in Soils. Brian J. Alloway, Ed. Wiley, Dept. 1-9501, P.O. Box 6792, Somerset, NJ 08875-9976. 1990. 339 pages. $95, cloth.

Heavy Metals in Soils reviews 18 metals in soils and their impact on the environment. The book also presents methods of analysis. Topics include soil processes; the behavior of metals in soils; and the analysis of individual metals such as arsenic, chromium, mercury, lead, and other metals and metalloids.

Nutrient Cycling in Terrestrial Ecosystems. A. F. Harrison, P. Ineson, and O. W. Heal, Eds. Elsevier Science Publishing Co., P.O. Box 882, Madison Square Station, New York, NY 10159. 1990. 462 pages. $81, cloth.

Nutrient Cycling deals mainly with inputs, turnover, losses, and plant uptake. It covers inputs of nutrients to, and losses of nutrients from, ecosystems; turnover of nutrients in ecosystems; and uptake of nutrients from soils.

RnR_x: Radon Remedies, Vol. 1. Radon Remedies, Inc., P.O. Box 44234, Columbus, OH 43204. 1989. Videotape. $49.95 + $3 shipping.

Radon Remedies consists of computer animations with narration that are designed to explain how radon gets into a building, how its health effects increase with increasing concentration, and what can be done to abate indoor radon.

Waste Reduction Advisory System, Version 2.3. Hazardous Waste Research & Information Center, One East Hazelwood Dr., Champaign, IL 61820. 1990. IBM-compatible software, available in 5 1/4-in. or 3 1/2-in. format. $95. Updates, less than $30.

This software provides individualized waste reduction assistance via a series of questions in an audit checklist. The system also includes an information bibliography with literature abstracts and case studies on current technologies, some of which are not available elsewhere, according to the publisher.

0013-936X/90/0924-1145$02.50/0

ES&T PRODUCTS

AIR POLLUTION

Non-CFC solvent. Terpene-based solvents are being developed as substitutes for chlorofluorocarbon (CFC) solvents for cleaning processes in the electronics and precision metals industries. Bush Boake Allen **110**

Weather station. Microelectronic weather station is designed to measure wind velocity, temperature, precipitation, and other meteorological factors unattended. System is IBM PC-compatible. Climatronics **111**

Smoke elimination. POLYTUBE electrostatic precipitation system is designed to control condensable organic, highly corrosive, saturated, and gaseous emissions. Precipitation can be wet or dry. Beltran **112**

CFC loss reduction. ZER-O-COIL is a low-temperature system designed to condense fumes and vapors and to reduce CFC-113 losses by up to 40%. Principle is a cold-air blanket. Ultronix **113**

HAZARDOUS MATERIALS

Plastics recycling. Facility is designed to use Belgian technology to make SYNTAL "lumber" from used plastic. Initially, it will accept wastes from New York City and Long Island, NY. National Waste Technologies **114**

Solvent recovery. Vacuum Assist System is designed to recover solvents and remove contaminants by means of vacuum distillation. Often these solvents cannot be safely recovered by conventional means. Solvent Kleene **115**

INSTRUMENTATION

Chromatography aids. Many columns, accessories, and standards for gas and liquid chromatography and solid phase extraction are available, including special columns for dioxin analysis. J & W Scientific **116**

Conductivity controllers. A complete line of conductivity controllers is available for water analysis applications. They range from 0.055 μs to 99.9 ms. Omega Engineering **117**

Indoor contaminant warning. 4-WARN warns of the presence of indoor contaminants in air and drinking water. It also warns of the presence of radon and of high noise levels. Envir Alert **118**

Groundwater sampling. Groundwater sampling is eased with the Well Wizard 1500 Power Pump, which allows purging and sampling with the same pump. QED **119**

High-resolution MS. Company announces "the world's first" high-resolution inductively coupled plasma (ICP) mass spectrometer; it can be used in major, minor, trace, and ultratrace analysis. VG Instruments **120**

Gas-hazard detector. TRIPLE 84TR Multifunction gas-hazard detector warns of life-threatening situations caused by poisonous or explosive gases or by high or low levels of oxygen. Crowcon Instruments **121**

Wastewater samplers. The 3700 Series automatic wastewater samplers include refrigerated samplers and samplers that can hold several sampling programs in the instrument's internal memory. ISCO Environmental Division **122**

Soil gas sampling pump. Model 150 Syringe Pump is designed to obtain uncontaminated soil gas samples and to store them in 1-L to 10-L Tedlar bags for future analysis. A battery-powered kit allows up to 8 h of sampling. KVA Analytical Systems **123**

Organic vapor analyzers. CENTURY OVA portable organic vapor analyzers are designed for heavy field use. Applications include groundwater monitoring, leak detection from tanks, and fugitive emissions in industrial plants. Foxboro **124**

Clarity monitors. Explosion-proof clarity monitor detects conditions of fluids, even in hazardous environments, and warns of out-of-limit readings. McNab **125**

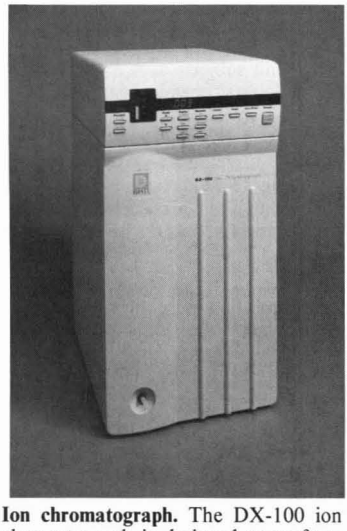

Ion chromatograph. The DX-100 ion chromatograph is designed to perform all types of isocratic IC separation using conductivity detection. Applications include many types of anion and cation analysis. Dionex **128**

Need more information about any items? If so, just circle the appropriate numbers on one of the reader service cards bound into this issue and mail in the card. No stamp is necessary.

Companies interested in a listing in this department should send their release directly to Environmental Science and Technology, *Attn: Products, 1155 16th St., N.W., Washington, DC 20036.*

0013-936X/90/0924-1146$02.50/0

Thermal hazard screening. RADEX-Solo is designed to warn of the occurrence of a dangerous decomposition reaction. It works from ambient temperatures to 400 °C with PC-AT control and data analysis. Astra Scientific International **126**

Flame/furnace AA spectrometer. Smith-Hieftje 8000 atomic absorption spectrometer is compatible with flame and furnace atomization and may be used for elemental analysis of water, oil, metal, and other materials. Thermo Jarrell Ash **127**

Supercritical fluid extraction. Company says that supercritical fluid extraction offers far greater speed for environmental sampling with diminished costs. Scott Specialty Gases **129**

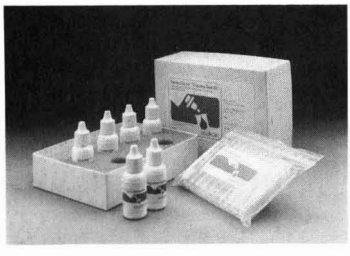

Pesticide detection. EnviroGard Test Kit is designed to detect residues of pesticides such as Aldicarb, 2,4-D, Carbofuran, cyclodienes, and Triazine. Results are available in 7–120 min, depending on the pesticide(s). Millipore **130**

High-purity gas generators. Gas generators are designed to convert "house" air into dry, high-purity gases. One generator supplies clean nitrogen; another furnishes hydrocarbon-free air. Balston **131**

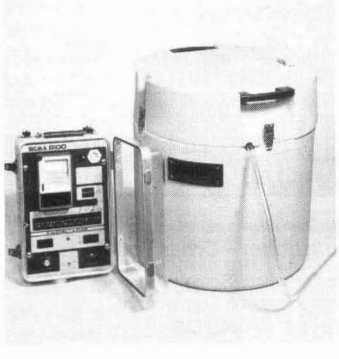

Wastewater sampling. STREAMLINE 700/702 portable wastewater sampler adjusts its intake rate to flow rate. With a flow computer, it can do flow proportional sampling. American Sigma **132**

Organic carbon analyzer. DC-190 total organic carbon (TOC) analyzer measures TOC in wastewater and saltwater samples. Range is 0.2–50,000 mg/L; particles up to 0.5 mm in diameter are handled. Rosemount Analytical **133**

Acid precipitation sampler. Model APS is designed to sample total precipitation episodes and total dry particulates for later laboratory analysis. Andersen Instruments **134**

Supercritical fluid extraction. Model SFE-50 is designed to combine the speed and cost advantages of supercritical fluid extraction with the ability to be coupled directly to a gas chromatograph. Applications include sampling organic contaminants. Suprex **135**

PUBLICATIONS

Acid precipitation. *Acid Precipitation Digest* presents a summary of current news, research, and events. Annual subscription (12 issues) is $235. Elsevier Science Publishers **136**

Risk assessment critique. *Toxicological Risk Assessment Distortions* by Jay H. Lehr, points up misconceptions Americans have about the quality of their water supplies. The American Ground Water Trust **137**

Design for recycling. *Annual Report for 1989* discusses design and goals for recycling, especially in Europe. BIR **138**

SERVICES

Environmental news tracking. Environmental NewsNow offers round-the-clock news on regulation, compliance, project finance, liability, citizens' initiatives, and other matters. UPI **139**

Contamination surveys. Company offers services in surveying for contamination over broad areas, reckoned in square miles, using detection methods that work "where conventional monitoring techniques have failed." Tracer Research **140**

Form R preparation. Company offers assistance in preparing Form R under SARA, Title III, Section 313, for reporting listed chemical releases. Geraghty & Miller **141**

SOFTWARE

Organic analysis. Enviroforms/Organic CLP is designed to generate deliverable data packages according to EPA's Contract Laboratory Program (CLP) protocol. Telecation Associates **142**

Hazardous material reporting. Software programs support hazardous material reporting and management and earthquake emergency response. Gaia Systems **143**

Hazard identification. HAZOPtimizer program is designed to facilitate hazard identification and risk analysis studies. Package includes hazard, failure, and "what-if" analyses. Arthur D. Little **144**

Hazardous waste sites. CERCLIS is a hazardous waste site data base compiled by EPA, which contains data on more than 30,000 U.S. sites that have been proposed or approved for cleanup under Superfund. CIS **145**

Geological modeling. LYNX 3D Geotechnical System software models the geological environment in three dimensions. Applications include mining, reclamation, and remediation. Lynx Geosystems **146**

WATER TREATMENT

Inoculant. MUNOX bacterial inoculant is designed to enhance wastewater treatment. Microlife Technics **147**

Filter aids. Celite marine diatomite is a filter aid that company says offers greater filtration efficiency and porosity than freshwater diatomite and perlite. Manville **148**

Sludge dewatering. DREWFLOC 2400 series emulsion flocculants consist of cationic polymers designed to dewater industrial sludge and clarify industrial wastewater. It also is designed to work at lower dosages than conventional emulsion flocculants. Drew **149**

Sludge flocculation controller. Sludge conditioning controller (SCC) is designed to measure the exact polymer dosage needed to produce optimum sludge flocculation. Company says that using SCC can lead to savings of up to 40% of polymer costs. Zenon Water Systems **150**

CIRCLE
NUMBERS
FOR FREE
INQUIRY
SERVICE

ES&T

Reader Service Reply Card

It's computer processed for fast response to your inquiries AND, IT'S FREE

JOURNAL OF CHEMICAL AND ENGINEERING DATA

Get A World Of Precise, Accurate Data In This International, Quarterly Journal

Multidisciplinary in nature and international in scope, the *Journal of Chemical and Engineering Data* (*JCED*) features contributions by distinguished physicists, chemists, chemical engineers, mechanical engineers, biological scientists, and applied mathematicians from the world over. Their expert reports represent numerical data bases for private technical information systems, particularly in industry, that will broaden your scientific horizons and improve the quality of your work.

This unique journal offers you precise, accurate data on physical, thermodynamic and transport properties of well-defined materials. It also keeps you informed about the latest international standards on symbols, terminology and units of measurement for reporting data properly.

You'll find numerical property data measurements on:

- pure substances of defined purity
- well-defined gaseous, liquid and solid mixtures
- semi-empirical and theoretical correlations useful in interpolating, extrapolating and predicting properties of scientific and technological importance
- new substances — the physical and spectral properties of inorganic, organic, and biochemical substances and other complex substances prepared by established synthetic procedures that may have major scientific and technological applications

1990 SUBSCRIPTION INFORMATION

Volume 35
4 Issues Per Year

		U.S.	Canada and Mexico	Europe (Air Service Included)	All Other Countries (Air Service Included)
ACS Members	1 year	$ 30	$ 35	$ 37	$ 40
	2 years	$ 54	$ 64	$ 68	$ 74
Nonmembers	1 year	$207	$212	$214	$217
Supplementary Material on Microfiche		$ 12	$ 16	$ 16	$ 16

Member subscription rates are for personal use only.
For nonmember rates in Japan, contact Maruzen Co., Ltd.

Journal subscriptions start January 1990 and are based on a calendar year.

Address your orders or inquiries to:
American Chemical Society
Sales and Distribution Department
1155 Sixteenth Street, N.W.
Washington, DC 20036

Toll free (800) 227-5558
Outside U.S. (202) 872-4363
Telex: 440159 ACSPUI or
892582 ACSPUBS
Fax: (202) 872-4615

This publication is available on microfilm, microfiche, and electronically through Chemical Journals Online on STN International.

Our people make the world a better place to live.

We all share this planet, so a clean environment is as important to us as business people as it is to the community at large.

At Hart Crowser, we provide innovative and creative solutions to environmental problems. Our continued growth is creating excellent opportunities for caring and dedicated professionals in the following areas:

- Hydrogeology
- Chemistry
- Chemical Engineering
- Environmental Engineering
- Geotechnical Engineering
- Environmental Science
- Mechanical Engineering
- Environmental Regulatory Analysis

We offer challenging opportunities, a stimulating and supportive work environment, and a comprehensive salary and benefits package.

For consideration, please forward your resume to us at

HARTCROWSER

Hart Crowser, Inc.
1910 Fairview Avenue East
Seattle, WA 98102

SEATTLE, WA • PORTLAND, OR • SAN FRANCISCO, CA • ANCHORAGE, AK • RICHLAND, WA

AFFIRMATIVE ACTION EMPLOYER, M/F/V/H

CLASSIFIED SECTION

Research Scientist

Battelle, Pacific Northwest Laboratories, is the preeminent multiprogram national laboratory for rapid advancement of science and development of technology. This laboratory is located in southeastern Washington, which boasts a favorable climate and is completely devoid of traffic congestion and smog. Battelle's 1000+ research projects per year are handled by over 3300 staff members.

PNL presently has an opportunity for a Research Scientist to support the Contaminant Transport Geochemistry Group's activities; conduct research in estimation of chemical properties of environmentally important compounds; and interface with contaminant transport model development and application studies.

The successful candidate will also research the transport of organic contaminants, involving the development and application of data estimation techniques and computer models. Acitivities will include computer programming, database development, and model application.

The position requires a PhD in Geochemistry, Environmental Chemistry, Civil Engineering, Chemical Engineering, or other related field. Two to three years postdoctoral experience in transport of organic contaminants is preferred. Experience in the application of computer modeling techniques to waste disposal problems and knowledge of FORTRAN and its application on IBM Personal Computers is required.

Send resume to: **Battelle, Pacific Northwest Laboratories, Dept. RZ6, P.O. Box 1406, Richland, WA 99352.** U.S. Citizenship required. Equal Opportunity Employer.

Battelle
Pacific Northwest Laboratories

ENVIRONMENTAL ENGINEERS

Our Career Opportunities will bring you to Idaho ....Our Quality of Life will keep you here.

Westinghouse Idaho Nuclear Company, Inc.

We offer outstanding opportunities for Environmental Engineers. You'll find great professional opportunities and a superb all-around lifestyle at Westinghouse Idaho Nuclear Company in Idaho Falls, Idaho.

WINCO operates the Idaho Chemical Processing Plant at the Idaho National Engineering Laboratory. Located in Southeastern Idaho, the INEL employs about 10,000 people. The area provides a broad range of recreational and cultural activities, and we are in close proximity to Yellowstone, the Tetons, Sun Valley and other outstanding features.

For immediate consideration, send a resume with a copy of this advertisement to: **Ace Ballard, Ref ES, Westinghouse Idaho Nuclear Company, Inc., P. O. Box 4000, Idaho Falls, ID 83403. U.S. Citizenship Required. Candiates who hold or qualify for a DOE 'L' Clearance are preferred. An Equal Opportunity Employer.**

Westinghouse

Wanted Chemical Laboratory Technician to analyze foods, water and soils for hazardous chemicals like PCB's, pesticides, petroleum hydrocarbons and priority pollutant metals using Gas Chromatograms. Infrared Spectrophotometers and Atomic Absorption Spectrophotometers. Require BS degree in Chemistry, Bio Chemistry, or Food Science, plus 6 months experience or 6 months related experience in Laboratory Instrumentation. Salary $23,000 per year, 40 hour week. Qualified applicants contact in person or by resume **Georgia Department of Labor, 1275 Clarendon Avenue, Avondale Estates, Georgia 30002,** or to the nearest Georgia Job Service Center. Control #GA 5435267.

Environmental Engineer/Specialist

Cement Company (ten plants) based in Allentown, Pa., seeks an individual to report to Unit Head, assist in compliance, field visits, agency contact. B.S.-scientific background preferred, 3–5 yrs. experience. Some travel, competitive benefit package.

Salary: Up to mid $40's. Send resume to: Elizabeth Mikols, Lehigh Portland Cement Company, P.O. Box 1882, Allentown, PA 18105-1882.

CLASSIFIED ADVERTISING RATES

Rate based on number of insertions used within 12 months from date of first insertion and not on the number of inches used. Space in classified advertising cannot be combined for frequency with ROP advertising. Classified advertising accepted in inch multiples only.

Unit	1-T	3-T	6-T	12-T	24-T
1 Inch	$105	$100	$95	$90	$85

(Check Classified Advertising Department for rates if advertisement is larger than 10″.)
SHIPPING INSTRUCTIONS: Send all material to

Environmental Science & Technology
Classified Advertising Department
500 Post Road East
P.O. Box 231
Westport, CT 06881
(203) 226-7131, FAX: (203) 454-9939

The University of Queensland

Equal Opportunity in Employment is University Policy

Lecturer/Senior Lecturer (Tenurable)

Environmental Engineering/ Waste Management

Chemical Engineering Department

A candidate with a higher degree and a commitment to teaching and research. Relevant industrial experience is viewed favourably. The Department would be particularly interested in an applicant with experience, expertise and an interest in research related broadly to environmental issues and or waste management.

Duties: The successful applicant will be expected to participate in teaching and co-ordinating two new degree programs — an undergraduate environmental engineering degree and a masters level environmental management program.

Salary: Lecturer $33,163 – $43,096 and Senior Lecturer $43,984 – $51,015 per annum.

Closing Date: 31 August 1990. **Ref. No:** 33390.

Please forward an original plus seven copies of application and resume to the Director, Personnel Services, The University of Queensland, Q. 4072.

Geochemistry Section Manager

Battelle, Pacific Northwest Laboratories, invites applications for Manager of the Geochemistry Section in the Geosciences Department. Qualifications include a Ph.D. in Geochemistry, Soil Chemistry, Hydrogeology, or related field with a minimum of 8 years experience. We are seeking an established Researcher with demonstrated ability to develop and direct basic and applied research programs. Applicants should have line management experience with excellent communication/interpersonal skills. This position is responsible for the technical direction and administrative oversight for approximately 45 researchers.

Battelle is enjoying a significant increase in opportunities for conducting applied and basic research related to subsurface chemical and hydrologic processes and their control on contaminant form, mobility, and environmental fate. The new research programs are focused on testing and validating new scientific concepts, new computer models, advanced measurement and sampling technologies, and innovative in situ remediation techniques. The successful applicant will have the opportunity to pursue independent research in these areas.

For consideration, submit resume and three references to: **Battelle, Pacific Northwest Laboratories, Dept. RZ8, P.O. Box 1406, Richland, WA 99352.** Equal Opportunity Employer. U.S. citizenship required.

Battelle
Pacific Northwest Laboratories

Hydrology Section Manager

Battelle, Pacific Northwest Laboratories, the preeminent multiprogram national laboratory for environmental technology development, currently has an opening for Manager of the Hydrolcgy Section in the Geosciences Department.

We are seeking an established Researcher with a demonstrated ability to develop and direct basic and applied research programs. The position is responsible for the technical and administrative management of approximately 35 researchers.

The qualified individual will have a Ph.D. in Hydrology, Hydrogeology, Civil Engineering, or a related field with a minimum of 8 years experience. Line management experience and excellent communication/interpersonal skills essential.

Battelle is currently enjoying a significant increase in opportunities for conducting applied and basic reasearch related to subsurface hydrologic and chemical processes and their control on contaminant type, mobility, and environmental consequences. The new research programs are focused on testing and validating new scientific concepts, new computer models, advanced measurement and sampling technologies, and innovative *in situ* remediation techniques. The successful applicant will have the opportunity to pursue independent research in these areas.

For consideration, submit resume and three references to: **Battelle, Pacific Northwest Laboratories, Dept. RZ9, P.O. Box 1406, Richland, WA 99352. FAX (509) 376-9099.** U.S. Citizenship is required. Battelle is an equal opportunity employer, M/F.

Battelle
Pacific Northwest Laboratories

POSITIONS AVAILABLE
ENVIRONMENTAL ORGANIC CHEMISTS
U.S. Geological Survey
Water Resources Division

The U.S. Geological Survey, Water Resources Division, is seeking candidates for research positions investigating the fate and transport of organic contaminants in the environment. Candidates' research interests should focus on the biological and chemical processes that control the distribution and transformation of organic contaminants in hydrological environments. The research should combine field and laboratory investigations in collaboration with other scientists. The Division seeks to strengthen its capability in this field to support its programs in Toxic Substances Hydrology and National Water Quality Assessment.

At least one position will be available in the National Research Program in Menlo Park, CA, Denver, CO, or Reston, VA. Requirements are U.S. citizenship, Ph.D. degree or equivalent research experience, and proven ability or demonstrated potential for independent research in analytical organic geochemistry, and knowledge of hydrologic environments.

The starting position will be at GS-12 to GS-14 level ($35,825–$65,444), depending on the candidate's qualifications. Applicants should submit resume, bibliography, brief description of research interests, and Standard Form 171 (Application for Federal Employment—available from the address below or any Federal Personnel Office) to U.S. Geological Survey, 215 National Center, Reston, VA 22092. Direct inquiries to John B. Weeks, Chairman, Search Committee, U.S. Geological Survey, Mail Stop 418, Box 25046, Federal Center, Lakewood, CO 80225-0046, phone (303) 236-5021. Applications will be accepted until August 31, 1990. The USGS is an equal opportunity employer.

professional consulting services directory

INDEX TO THE ADVERTISERS IN THIS ISSUE

Advertising Management for the American Chemical Society Publications

CENTCOM, LTD.

President
James A. Byrne

Executive Vice President
Benjamin W. Jones

Clay S. Holden, *Vice President*
Robert L. Voepel, *Vice President*
Joseph P. Stenza, *Production Director*

500 Post Road East
P.O. Box 231
Westport, Connecticut 06880
(Area Code 203) 226-7131
Telex No. 643310
Fax No. (203) 454-9939

ADVERTISING SALES MANAGER
Bruce E. Poorman

ADVERTISING PRODUCTION MANAGER
Jane F. Gatenby

SALES REPRESENTATIVES

Philadelphia, Pa. . . . CENTCOM, LTD., GSB Building, Suite 405, 1 Belmont Ave., Bala Cynwyd, Pa. 19004 (Area Code 215) 667-9666, FAX: (215) 667-9353

New York, N.Y. . . . John F. Raftery, CENTCOM, LTD., 60 E. 42nd Street, New York 10165 (Area Code 212) 972-9660

Westport, Ct. . . . Edward M. Black, CENTCOM, LTD., 500 Post Road East, P.O. Box 231, Westport, Ct 06880 (Area Code 203) 226-7131, FAX: (203) 454-9939.

Cleveland, OH. . . . Bruce E. Poorman, John C. Guyot, CENTCOM, LTD., 325 Front St., Berea, OH 44017 (Area Code 216) 234-1333, FAX: (216) 234-3425

Chicago, Ill. . . . Michael J. Pak, CENTCOM, LTD., 540 Frontage Rd., Northfield, Ill 60093 (Area Code 708) 441-6383, FAX: (708) 441-6382

Houston, Tx. . . . Michael J. Pak, CENTCOM, LTD., (Area Code 708) 441-6383

San Francisco, Ca. . . . Paul M. Butts, CENTCOM, LTD., Suite 1070, 2672 Bayshore Frontage Road, Mountainview, CA 94043 (Area Code 415) 969-4604

Los Angeles, Ca. . . . Clay S. Holden, CENTCOM, LTD., 3142 Pacific Coast Highway, Suite 200, Torrance, CA 90505 (Area Code 213) 325-1903

Boston, Ma. . . . Edward M. Black, CENTCOM, LTD., (Area Code 203) 226-7131

Atlanta, GA. . . . John C. Guyot, CENTCOM, LTD., (area Code 216) 234-1333

Denver, Co. . . . Paul M. Butts, CENTCOM, LTD., (Area Code 415) 969-4604

Environ. Sci. Technol. 1990, 24, 1157–1164

ES&T RESEARCH

Measurement of in Situ Rates of Selenate Removal by Dissimilatory Bacterial Reduction in Sediments

Ronald S. Oremland,*,† Nisan A. Steinberg,† Ann S. Maest,† Laurence G. Miller,† and James T. Hollibaugh‡

U.S. Geological Survey, 345 Middlefield Road, Menlo Park, California 94025, and Tiburon Center, San Francisco State University, Tiburon, California 94920

■ A radioisotope method for measurement of bacterial respiratory reduction of selenate to elemental selenium in aquatic sediments was devised. Sediments were labeled with [^{75}Se]selenate, incubated, and washed, and $^{75}Se^0$(s) was determined as counts remaining in the sediment. Core profiles of selenate reduction, sulfate reduction, and denitrification were made simultaneously in the sediments of an agricultural wastewater evaporation pond. Most of the in situ selenate reduction (85%) and all the denitrification activities were confined to the upper 4–8 cm of the profile, whereas sulfate reduction was greatest below 8 cm (89% of total). The integrated areal rate of selenate reduction was 301 μmol m^{-2} day^{-1}, which results in a turnover of water column selenate in 82.4 days.

Introduction

Oxyanions of selenium have been identified as toxic constituents in drainage waters from irrigated, seleniferous agricultural soils (*1*). This environmental problem is apparently quite common in many regions of the western United States (*2*). Therefore, methods that address the question of removal of selenium oxyanions from soils and/or drainage waters by various means have received considerable attention because they offer the prospect of restoring water or soil quality while allowing for the continuation of irrigated farming. With regard to possible microbiological methods, volatilization of selenium by formation of alkylated gases (e.g., dimethyl selenide) has been suggested for treatment of soils (*3*) or impacted marsh waters, such as those of the Kesterson Wildlife Refuge (*4*, *5*).

Recently, we reported on a novel process by which anaerobic bacteria respire selenate, which in turn biochemically reduces this oxyanion to selenite and ultimately to elemental selenium (*6*). This dissimilatory reduction was demonstrated to occur in sediments, was independent of sulfate, and was inhibited by nitrate and chromate. Bacterial cultures capable of selenate respiratory growth have been isolated (*6*, *7*). Although we were able to show that this process holds the potential to rapidly remove and sequester considerable quantities (millimolar) of added selenate from sediment slurries, the questions remained as to how rapidly it proceeds in nature, and what was its vertical distribution in sediments relative to other forms of anaerobic bacterial respiration. An understanding of how the process of dissimilatory selenate reduction operates in these respects should ultimately aid the design of treatment schemes and the rehabilitation of selenium-contaminated regions. In order to answer these questions and to achieve these long-term goals, it was first necessary to devise a method for measuring in situ selenate reduction.

In situ measures of bacterial activities have been a focus of microbial ecology for the past 25 years. A variety of techniques employing radioisotopes, gas chromatography, and/or enzyme inhibitors or analogues have been exploited to assess environmental rates of methanogenesis (*8*), denitrification (*9*, *10*), nitrogen fixation (*11*), and sulfate reduction (*12*). This latter process is analogous to the methods we report herein to measure selenate reduction. However, in the case of selenate reduction, our task was simplified because ^{75}Se is a γ-emitting radioisotope ($t_{1/2}$ = 120 days), which circumvents the quenching/efficiency problem associated with liquid scintillation counting of weak β-emitters like ^{35}S. Thus, there was no need to volatilize and trap the product $^{75}Se^0$(s) as there is for [^{35}S]sulfide, but merely to wash away the added [^{75}Se]-selenate. Our results with core profiles from a selenium-rich agricultural wastewater evaporation pond represent "quasi" in situ assays because they were incubated in the laboratory under conditions approximating the field. However, our results indicate that selenate reduction occurs in the surficial layers of these sediments, in proximity to the region of active denitrification, yet spatially separated from sulfate reduction occurring deeper in the core. Areal rates of selenate removal obtained from this core indicate its rapid removal by reduction to Se^0(s), and a quick turnover of water column selenate. When combined with previous observations with regard to inhibitors and stimulators of selenium reduction, the conceptual design of an efficient anaerobic selenate "digestor" can be discerned.

Experimental Section

Sites and Sampling. Surficial (upper ~20 cm) sediments were collected from Hunter Drain, an agricultural drain located in Stillwater, NV, where selenium contamination is documented (*2*), as well as from the littoral zone of Big Soda Lake, an alkaline/saline environment (*13*) having a diversity of microbial activities (*14*, *15*). Grabs of anoxic sediments were placed in Mason jars (completely

† U.S. Geological Survey.
‡ San Francisco State University.

filled) and were used in the preliminary experiments to determine the practicality of the method. They were stored at 6 °C for up to 8 weeks prior to use. Subsequently, intact cores for determination of in situ activities were taken from a selenium-impacted agricultural waste evaporation pond in the San Joaquin Valley (*6*). Cores (1 m × 8.25 cm) were collected by hand, stored at 6 °C, and processed within 24 h of collection. These sediments were generally characterized by having a brown surface layer (<10-cm depth), which made a transition to a black, reduced layer at depths below 10 cm. However, in some cores, alternating sequences brown, grey, and black occurred with no predictable pattern. The evaporation pond was sampled during late September and again in early November 1988, when midday water temperature was 25 and 19 °C, respectively. The salinities of the evaporation pond, Hunter Drain sites, and Big Soda Lake were respectively 64, 60, and 27‰. The pH values for these environments were respectively 9.5, 7.6, and 9.7.

Experimental Protocol. Hunter Drain and Big Soda Lake sediments were allowed to reach room temperature (~3 h), after which a jar was opened and the porous sediments were hand stirred (to achieve consistency) with a spatula. The sediment was then drawn into 5-mL Plastipak syringes (hub end removed; volume of sediment, 3 mL) and capped with a rubber serum cap. Killed controls consisted of twice-autoclaved sediments (121 °C and 250 kPa for 30 min, followed 14 h later by a 20-min treatment just prior to the start of the experiment), which were cooled and syringe-filled as described above. Samples were injected with 2.0 μCi/100 μL [^{75}Se]selenate ($H_2{}^{75}SeO_4$, specific activity = 8033 mCi/mmol; New England Nuclear, Boston, MA) or 0.08 μCi/100 μL [^{75}Se]selenite (8365 mCi/mmol) in isotonic solutions of NaCl under N_2 adjusted to the ambient pH. An additional experimental treatment consisted of injecting unlabeled selenate with the radioisotope to yield a final sediment selenate concentration of 17 nmol/mL of sediment. During the incubation, triplicate sets of samples were extruded into disposable centrifuge tubes (15 mL) containing 7 mL of the isotonic NaCl solution (pH = 7.5 for Hunter drain and 9.2 for Big Soda Lake) plus an unlabeled chase of 10 mM Na_2SeO_4 or Na_2SeO_3 ("stop" solutions) for the respective ^{75}Se injections. The tubes were capped and vortexed (to disperse the sediment), and 1 mL of the slurry was withdrawn to determine the total counts added. The remaining slurry was centrifuged (4000*g* for 5 min), the supernatant discarded, and the pellet rinsed twice with small volumes of the stop solution before being resuspended in 3 mL of the wash solution and centrifuged again. After the second centrifugation, the bottom section of the tube containing the pellet was placed in a scintillation vial, severed, and counted.

The ability of nitrate or chromate ions to inhibit selenate reduction was examined in another experiment. Duplicate syringes filled with Hunter Drain sediments (see above) were injected with a final concentration of 25 μM selenate plus 0.03 μCi of [^{75}Se]selenate, and in addition, other samples received 20 mM (final) levels of either $NaNO_3$ or $NaCrO_4$, both of which inhibit selenate reduction in slurries (*6*). The samples were processed at zero time and after a 3-h incubation.

Formation of $^{75}Se^0$(s) in samples incubated with [^{75}Se]selenate was followed by using sediments from Hunter Drain and Big Soda Lake. Triplicate sets of sediments were prepared as indicated above (25 μM final selenate concentration) and extracted for red, amorphous elemental selenium by procedures used previously in experiments with estuarine sediments (*6*). Briefly, after 0 and 96 h of incubation, sediment samples were extruded into isotonic stop solutions (see above), vortexed, and centrifuged. The stop solution was discarded. Next the pellet was washed and counts were extracted (vortexing/centrifugation/decanting) with a series of solvents of decreasing polarity (water, ethanol, ethyl acetate, carbon disulfide). The supernatant from each extraction was counted, as was the total activity of the initial slurry and that in the resulting final pellet of sediment.

To determine if any sediment-related quenching occurred in the samples, duplicate unlabeled sediment pellets (Hunter Drain) were injected with 0.03 μCi/100 μL $^{75}SeO_4{}^{2-}$. Counts in the samples were compared with equivalent amounts of isotope in duplicate vials containing the following: (1) resuspended sediments, (2) without sediment but with 5 mL of stop solution, or (3) with only the 100 μL of isotope. In another experiment with Hunter Drain sediments, the distribution of label in duplicate samples at the beginning and after a 16.5-h incubation was followed. In addition to the pellet and the 1-mL slurry subsample, counts remaining on the syringes, stoppers, and rinse solutions were determined. In addition, a 5-mL sample of the headspace volumes over the initial sediment slurries was injected into a serum-capped scintillation vial to determine if volatile products were present.

Cores from the San Joaquin Valley site were vertically extruded in 2- or 4-cm sections, from which samples were taken for chemical analysis of porewaters and porosity (*6*). Subcores were also taken for measurement of sulfate reduction, denitrification, and selenate reduction. For denitrification and sulfate reduction, 10-mL Plastipak syringes (hub ends removed) were employed to subsample 3 (2-cm sections) or 7 mL (4-cm sections) vertically extruded from the core. These subcores were plugged with recessed no. 1 butyl rubber stoppers. Selenate reduction samples were collected in either 1 (2-cm sections) or 2 mL (4-cm sections) as outlined above.

Sulfate reduction subcores were injected with either 3 or 6 μCi (2- or 4-cm sections, respectively) of carrier-free sodium [^{35}S]sulfate (ICN Radiochemicals, Irvine, CA) in 100- or 200-μL volumes (depending on core section size) of an anaerobic stock solution. Three samples from each depth were incubated at 20 °C for 42 h, after which time activity was stopped by freezing the samples. Subsequent acid-volatilization/flushing-train trapping and liquid scintillation counting of [^{35}S]sulfide was performed within 72 h by methods described elsewhere (*16*, *17*). Denitrification (endogenous and potential) was assayed by the acetylene block technique (*9*, *10*). Subcores were extruded into wide-mouth test tubes (total volume, 50 mL) with an equal volume of either tap water or surface water supplemented with 0.5 mM $NaNO_3$. Tubes were sealed with serum stoppers, flushed for 5 min with N_2, and then injected with 15% headspace volume of C_2H_2 (5–7 mL). Tubes were incubated at 20 °C with constant reciprocal shaking (~150 rpm). Nitrous oxide in the headspace was determined by electron-capture gas chromatography (*18*). Subcores for selenate reduction assays were injected with 0.04 μCi/100 μL sodium [^{75}Se]selenate solution and incubated at 22 °C. Four or five subcores (from the same core used for the denitrification/sulfate reduction assays) were taken at each depth horizon and incubated in a progressive time course. Activity was stopped by freezing at −20 °C or by immediate processing. Processing consisted of extruding subcores into a 50-mL serum bottle, which initially contained 20 mL of filtered (1.2 μm) pond surface water plus 1 mM Na_2SeO_4. The volume was brought to 25 mL

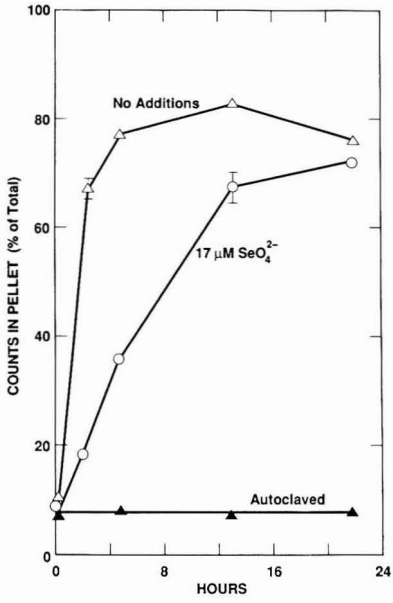

Figure 1. Selenate reduction time course experiment with live, autoclaved, and selenate-amended live Hunter Drain sediments. Points represent the mean of three samples and bars indicate ±1 SE. Absence of bars indicates error was smaller than the symbol.

with additional pond water and then the bottles were crimp-sealed and vigorously shaken. A 2-mL subsample of the slurry was then counted to determine total counts, after which it was centrifuged, decanted, and rinsed once (see above) prior to determining counts incorporated into the sediments.

Analysis. Porewaters were analyzed for the anions Cl^- and SO_4^{2-} by ion chromatography (*6*), NO_3^- and NO_2^- by autoanalyzer (*19*), and SeO_4^{2-} and SeO_3^{2-} by boiling acid reduction and hydride generation atomic absorption spectroscopy (*20*, *21*). Detection limits were 30 nM for [SeO_4^{2-} + SeO_3^{2-}] and 2.5 nM for SeO_3^{2-}. No precautions were taken against interference of selenite analyses by dissolved organic carbon (*22*) or nitrite (*23*), and therefore, our reported values for both selenium oxyanions may be underestimates. Samples containing ^{75}Se were counted in a Beckman Model 8000 γ-counter. Ammonium and free sulfide were determined by the methods of Solorazano (*24*) and Cline (*25*), respectively. Methane was determined on 2-mL subcore samples by their extrusion into 37-mL serum bottles containing 16 mL of NaCl-saturated water, followed by shaking (0.5 h) and analysis by flame-ionization gas chromatography (*26*).

Results

Hunter Drain Sediments. Time course experiments demonstrated incorporation of ^{75}Se into "live" sediments and that this activity was blocked by autoclaving (Figure 1). Live samples removed ~80% of the added counts within the first 5 h of incubation, after which no further significant uptake occurred. By contrast, no activity was observed in the killed controls over the course of the experiment. Amendment of samples with 17 μM selenate slowed the rate of isotope incorporation by ~6-fold (due to isotope dilution), and uptake persisted over a longer duration than in the unamended samples. The uptake rate for the selenate-amended samples over the first 13.2 h of incubation was 0.74 nmol mL^{-1} h^{-1}, calculated by a first-order linear regression (r = 0.995). In the inhibitor experiment, the rate of selenate reduction in uninhibited samples was 0.46 (SE = 0.003) nmol mL^{-1} h^{-1}, while it was 0.15 (SE = 0.03) and 0.20 (SE = 0.011) nmol mL^{-1} h^{-1} in the chromate (67% inhibition) and nitrate (56% inhibition) controls. In the extraction experiment, recovery in the polar solvents and in the final sediment pellet greatly increased after the 96-h incubation for both the Hunter Drain and Big Soda Lake sediments (Table I). Percent recoveries of the injected label after 96 h in the CS_2 and pellet fractions were 55.5% for Hunter Drain and 94% for Big Soda Lake.

Table I. Recovery of ^{75}Se in Extracted Fractions of Hunter Drain and Big Soda Lake Sediments Incubated with [^{75}Se]Selenate

fraction	DPM[a] 0 h	DPM[a] 96 h
Hunter Drain Sediments[b]		
water	1197 (21)	386 (2)
ethanol	866 (37)	9604 (714)
ethyl acetate	504 (26)	5505 (345)
carbon disulfide	916 (40)	12310 (377)
pellet	1391 (150)	6976 (436)
Big Soda Lake Sediment[b]		
water	1135 (83)	
ethanol	429 (16)	992 (75)[c]
ethyl acetate	303 (23)	1099 (83)
carbon disulfide	558 (59)	5817 (42)
pellet	719 (51)	26863 (342)

[a] Values represent the mean of three samples and parentheses indicated 1 SE. [b] Total [^{75}Se]selenate injected was 48350 (Hunter Drain) and 37937 dpm (Big Soda Lake). [c] Value for combined water and ethanol extractions.

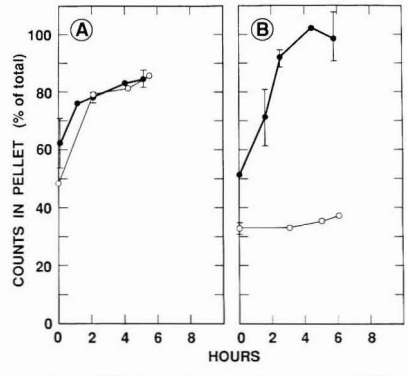

Figure 2. Uptake of [^{75}Se]selenite by sediments from (A) Hunter Drain and (B) Big Soda Lake. Live samples (●), autoclaved controls (○); results represent the mean of three samples and bars indicate ±1 SE. Absence of bars indicates error was smaller than the symbol.

Uptake of [^{75}Se]selenite by autoclaved and live Hunter Drain sediments (pH = 7.6) was similar, with increased counts occurring with time (Figure 2A). However, sediments from Big Soda Lake (pH 9.7) demonstrated an obvious biological effect. Live samples incorporated all of the injected [^{75}Se]selenite by 5 h, whereas autoclaved controls did not increase significantly above ~30–35% for the duration of the incubation (Figure 2B).

No observable quenching occurred when $^{75}SeO_4^{2-}$ was injected into pellets or suspended sediments. Average counts of duplicates were as follows (dpm): isotope only, 48876; isotope plus chase solution, 46038; isotope plus suspended sediments, 45494; and isotope injected into pellets, 47704. Student's t test indicated there was no

Table II. Sediment Characteristics and Porewater Chemical Profiles of a Core Collected from the San Joaquin Valley Evaporation Pond on September 28, 1988

depth, cm	color[a]	P,[b] g/mL	concn,[c,d] μmol/L of porewater					
			CH_4	NH_4^+	NO_3^-	NO_2^-	SeO_4^{2-}	SeO_3^{2-}
water			ND	ND	2500	131	7.28	1.930
0–4	LBr	0.63	6	1156	78	3.4	0.03	0.013
4–8	Blk		26	1841	6	0.6	BDL	0.012
8–12	Blk	0.50	50	1792	7	0.7	BDL	0.007
12–16	LBr		11	1142	4	0.5	BDL	0.012
16–20	MBlk	0.51	16	641	5	1.0	BDL	0.012
20–24	Grey		20	466	6	0.8	BDL	0.005
24–28	LBr	0.36	16	332	7	0.7	BDL	0.007

[a] LBr, light brown; Blk, black; MBlk, black mottled with brown. [b] P, porosity. [c] ND, not determined. [d] BDL, below detection limit (0.03 μM).

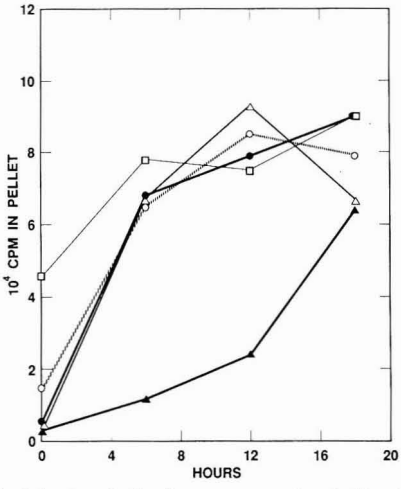

Figure 3. Selenate reduction time course experiment with sediments from various depths in a San Joaquin Valley evaporation pond core collected 9/28/88. Symbols: 0–4 cm (O), 4–8 cm (□), 8–12 cm (●), 16–20 cm (△), 24–28 cm (▲). Amount isotope injected, 0.05 μCi. Similar uptake was also observed at 12–16 and 16–20 cm (not shown). Note that vertical axis is given as total counts rather than as a percent of added counts.

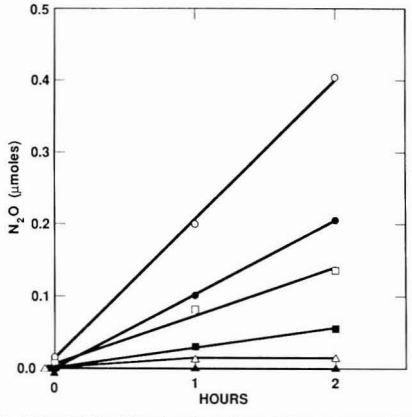

Figure 4. Potential denitrification in sediments from evaporation pond core collected on 9/28/88. Assay tubes contained a total of 21 μmol (3 mM) of nitrate. Symbols: 0–4 cm (O), 4–8 cm (□), 8–12 cm (●), 16–20 cm (△), 20–24 cm (■), 24–28 cm (▲); not shown is the 12–16-cm sample, but its time course was nearly identical with the 20–24-cm sample.

significant difference at the 95% confidence level between any of these conditions. In the experiment with distribution of label, at the start and after 16.5 h of incubation, respectively, counts were located as follows (percent of total): initial wash, 67.2 and 1.7; other washes and rinses, 15.5 and 1.2; 1-mL subsample of initial suspension, 10.2 and 9.8; pellet 6.5 and 84.4; syringes and stopper, 0.4 and 2.1; upper portion of centrifuge tube 0.2 and 0.8; gas phase, 0 and 0.

San Joaquin Valley Cores. The characteristics and porewater chemistry of a core taken from the evaporation pond in September 1988 are given in Table II. The water column had abundant nitrate (2.5 mM) and high levels of selenate (7.28 μM) and selenite (1.93 μM). These oxyanions were rapidly depleted down the length of the core. In contrast, reduced substances (methane and ammonium) were prevalent in the core and were most abundant in the visually highly reduced black layers between 4- and 12-cm depth. Free sulfide was not detected at any depth in the core (detection limit, 0.1 mM).

In an initial experiment, incorporation of ^{75}Se into sediments proceeded rapidly in all the samples (Figure 3). Although the percent incorporated for each individual sample was not measured in this experiment, calculated uptake by the first sampling (6 h) indicated that 54–92% of the added [^{75}Se]selenate was recovered in the pellets. Rates of isotope incorporation into the pellets decreased or leveled off after 6 h. The only exception was the 24–28-cm samples in which only ~15% of the added label was recovered in the pellet at that time. Potential denitrification rates were linear for the 2-h assay, activity was present at all depths except for the 24–28-cm interval, and minimal activity was observed at the 16–20-cm interval (Figure 4). Highest activity was observed in the surficial layer. In contrast, endogenous activity (no added nitrate) was only observed in the surface layer, at a rate comparable (~75%) with the nitrate-supplemented 0–4-cm interval (data not shown).

A second core was retrieved from this site on November 9, 1988. Because of the rapid uptake of [^{75}Se]selenate by the sediments in the September core, sampling intervals with much shorter incubation periods were conducted for the selenate respiration experiments. In general, uptake of label was rapid, with >50% of the added [^{75}Se]selenate incorporated into the sediments after less than 1 h of incubation (Figure 5). The only exception was in the surface layer (0–2 cm) where turnover was 8.9%/h. As in the previous experiment, uptake rates leveled off or ceased after the initial samplings. In a few cases, however, the results were somewhat erratic, with some of the later samplings having less incorporation than the initial or previous points. The most erratic uptake observed was for the 2–4-cm layer (Figure 5). This was probably caused by the inhomogenous nature of the sample (e.g., some

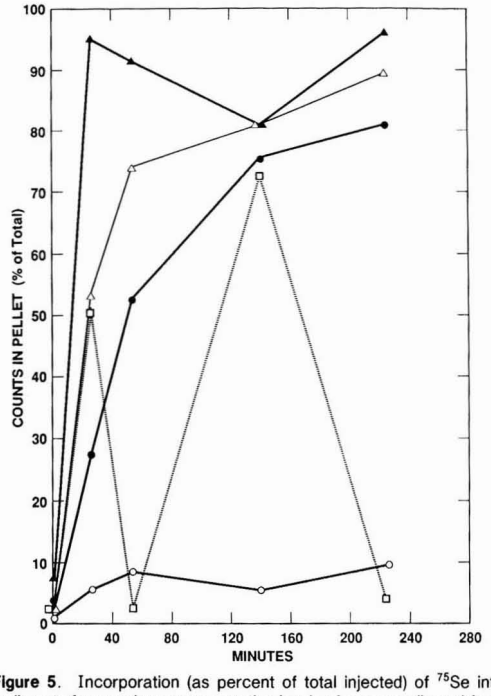

Figure 5. Incorporation (as percent of total injected) of ^{75}Se into sediments from various representative levels of a core collected from the evaporation pond on 11/8/88. Symbols: 0–2 cm (O), 2–4 cm (□), 8–12 cm (▲), 12–16 cm (△), 24–28 cm (●); not shown are the 4–8-, 16–20-, and 20–24-cm samples.

fibrous plant debris was evident in this layer). To a much lesser extent, some erratic kinetics (decreased total uptake) were noted after the 25-min sampling for the 8–12-cm samples (Figure 5) as well as for the 4–8-cm samples (not shown); however, these are explained by variability associated with maximum uptake (Figure 1). Therefore, in order to calculate the percent turnover per hour (turnover rate constant) of the added [^{75}Se]selenate in erratic cases, the incorporation by the first incubation sampling (25 min) was used. In all other cases, the turnover rate constant was calculated from the initial linear portion (0–51 min) of the uptake curves.

Table III. Selenate Pool Turnover and Selenate Reduction Rates with Depth in a Core Taken from the San Joaquin Valley Pond on November 9, 1988

depth, cm	k,[a] h^{-1}	P,[b] g/mL	Se concn,[c] μM	rate, nmol/(mL·h)
0–2	0.089	0.63	6.510	0.365
2–4	1.190[d]	0.53	0.056	0.035
4–8	1.860[d]	0.62	0.061	0.070
8–12	2.200[d]	0.59	0.012	0.015
12–16	0.842	0.56	0.017	0.008
16–20	1.040	0.61	0.014	0.009
20–24	0.963	0.51	0.024	0.012
24–28	0.573	ND[e]	ND[e]	ND[e]

[a] k, turnover rate constant. [b] P, porosity. [c] Selenate plus selenite; depths below 4 cm as only selenite due to the dilution factor required for converting selenate to selenite. [d] Determined from first incubation sampling interval (25 min). [e] ND, not determined.

Selenate turnover constants and reduction rates for the various depths are given in Table III. Turnover below the surface layer was very rapid, the highest being 2.2 h^{-1} at 8–12-cm depth. In contrast, the total selenium oxyanion pool decreased rapidly with depth to values approaching the detection limit for selenite. The changes in selenium oxyanions contributed to the observed decrease in selenate reduction with depth. The vertical profiles of selenate reduction, endogenous denitrification (without added nitrate), and sulfate reduction are shown in Figure 6. Most of the sulfate reduction (89.4%) occurred at depths below 8 cm (Figure 6A), whereas all the denitrification occurred above 4 cm (Figure 6B), and 86% of the selenate reduction took place in the 0–8-cm interval (Figure 6C). Maximal rates of sulfate reduction were ~10-fold greater than those for denitrification and selenate reduction.

Discussion

Some incorporation of ^{75}Se into sediments from Hunter Drain occurred in all samples at the initial time point (Figure 1). This uptake was presumably due to a combination of some adsorption onto the sediments (*27*) plus any interstitial volume of [^{75}Se]selenate not removed by the rinsing procedure. These factors accounted for less than 10% of the total amount of isotope added. After an incubation interval, considerably more uptake was evident in the live samples but not in autoclaved controls, thereby underscoring the biological nature of the process. Final

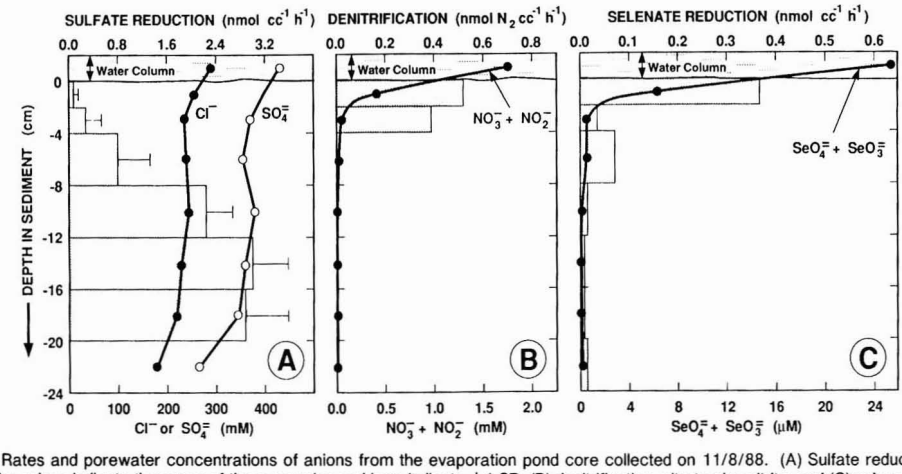

Figure 6. Rates and porewater concentrations of anions from the evaporation pond core collected on 11/8/88. (A) Sulfate reduction, sulfate and chloride; values indicate the mean of three samples and bars indicate +1 SD; (B) denitrification, nitrate plus nitrite; and (C) selenate reduction, selenate plus selenite.

counts incorporated into the pellet were generally 80–90% of the total added, with the remaining minor quantities present in the washes and residual on the syringes, discarded centrifuge tubes, and stoppers. Thus, because no significant quantities were detected in the gas phase or in the washes, sediment incorporation was total, and volatiles (e.g., dimethyl selenide) or soluble organoselenium compounds were not produced.

Bacterial reduction of selenate results in the appearance of a selenite intermediate (*6*, *7*). Thus, incorporation of counts could be explained by the strong adsorptive properties (*27*, *28*) of this first bacterial reduction product binding to sediment surfaces rather than by further reduction to the insoluble, elemental state. In contrast to the results with [^{75}Se]selenate, different patterns were observed with [^{75}Se]selenite (Figure 2). Biological activity was indistinguishable from adsorption in the circumneutral pH Hunter Drain sediments (Figure 2A); however, there was a very obvious biological effect with the higher pH Big Soda Lake sediments (Figure 2B). Because selenite adsorption onto mineral surfaces greatly decreases above pH 9 (*28*), these results suggest that the observed increased counts in the live samples were due to formation of a more reduced, insoluble product rather than adsorptive effects of selenite. This was confirmed in the extraction and inhibition experiments (see below).

In the extraction experiments, counts greatly increased in the nonpolar fraction and in the extracted pellet after 96-h of incubation (Table I). These results are consistent with the formation of elemental selenium as the major end product of selenate reduction and are similar to results observed with estuarine sediments (*6*). Because both red, amorphous Se^0(s) (soluble in CS_2) and crystalline, hexagonal Se^0(s) (insoluble in CS_2) are produced by bacterial selenate reduction (*6*), the high counts observed in the residual pellet fraction can be explained by the formation of the crystalline form. Formation of significant quantities of insoluble selenides are unlikely because of inhibition of this reaction by the very high levels of sulfate (*29*) present in these sediments (58 mM Big Soda Lake; 90–100 mM Hunter Drain). In addition, the inhibition of [^{75}Se]selenate reduction by nitrate and chromate (see Results), both of which inhibited bacterial dissimilatory selenate reduction (*6*), further indicates that similar bacterial processes were operative in this current study. The above results demonstrate that bacterial dissimilatory selenate reduction to Se^0(s) was responsible for the incorporation of ^{75}Se into the sediment fraction during the incubations. Because of the chemical similarities of Big Soda Lake and the San Joaquin Valley evaporation pond, these conclusions could be extended to the experiments conducted in the latter environment.

All the depths assayed for selenate reduction in the pond sediments demonstrated activity, with the least occurring in the 24–28-cm section (Figure 3). Likewise, all the depths assayed for "potential" denitrification showed activity, with the exception of the 24–28-cm interval (Figure 4). Actual "endogenous" denitrification was confined to the surface section (0–4 cm) where nitrate was still present (Table II), as was obtained in studies with San Francisco Bay sediments (*18*). Because the bacteria that respire selenate are denitrifiers (*6*), there should be a correlation between the presence of potential denitrification and selenate reduction, and we observed this phenomenon in the pond sediments (Figures 3 and 4). The absence of significant quantities of nitrate from other than the very surface layer of the sediment (Table II) restricts the actual extent of in situ denitrification. Likewise, the absence of significant quantities of selenium oxyanions below the surface layers of the cores restricts the extent of selenate reduction.

Selenate reduction in the pond sediments proceeded quite rapidly, although there was some erratic activity in a few (primarily the 2–4-cm horizon) of the samples (Figure 5). Such erratic behavior can be explained by inhomogeneity of the cores (e.g., Table II), even within the same depth horizon where a "mottling" of colors (light brown interspersed with black) was sometimes observed. By contrast, hand-blended sediments displayed very low sample-to-sample variability (Figures 1 and 2), which underscores this explanation. The turnover rate constants calculated from these data indicated that the selenium oxyanion pool was cycled rapidly within these sediments (Table III). The lowest value for turnover (0.089 h^{-1}) was measured in the very surface layer where selenium oxyanion concentrations were >100-fold higher than in the rest of the core. However, because of the high levels of selenium oxyanions therein, the rate of selenate reduction was highest in the 0–2-cm layer. This situation is analogous to the selenate-amended Hunter Drain samples (Figure 1).

Calculation of selenate reduction rates at the lower depths of the core was complicated by the detection limits imposed for analysis of [SeO_4^{2-} + SeO_3^{2-}]. Because this step consists of a chemical reduction of selenate to selenite and requires a dilution of the sample, it is quite possible that the pools of selenium oxyanions below 8 cm were as much as twice that reported, which would have doubled some of the selenate reduction rates. However, in comparison with the rates observed at the surface, selenate reduction below 8 cm would still account for <30% of the total activity of the sediment column. Thus, because of an analytical limitation, this radioisotopic procedure for measuring selenate reduction tends to slightly underestimate the in situ transformation rates. Furthermore, because we took no precautions against analytical interferences by nitrite or organic carbon (*22*, *23*), we may have underestimated the selenate/selenite pool sizes. Higher pools would increase the rates, which further emphasizes the conservative nature of our estimates.

The zone of active selenate reduction coincided with that of denitrification and the presence of appreciable (0.4 mM at 0–2 cm) nitrate (Figure 6). This finding appears to contradict the observation that nitrate is an inhibitor of selenate reduction in sediment slurries and cultures (*6*). However, the levels of nitrate employed in those experiments were very high (10 mM) and it is possible that a lower "threshold" value exists whereby the two processes can occur simultaneously. Alternatively, there can also be nitrate-free microzones occurring in the surficial sediments that allow for selenate reduction to proceed, or there are species of selenate-reducing bacteria that do not reduce nitrate. We observed only a partial (56%) inhibition of selenate reduction by nitrate in our experiments with Hunter Drain sediments (see Results), which can be explained by any of the above reasons. The rate of denitrification in the 0–2-cm horizon (~0.5 nmol of N_2 mL^{-1} h^{-1} or ~1.0 nmol of NO_3^- consumed mL^{-1} h^{-1}) was somewhat higher than the rate of selenate reduction (~0.37 nmol mL^{-1} h^{-1}). This is a bit perplexing because the nitrate concentration in the 0–2-cm horizon was ~70-fold greater than that of the selenate. However, nitrate is also an electron sink for dissimilatory reduction to ammonium, which competes with denitrification and limits its extent (*18*, *30–32*). Highest rates of sulfate reduction were ~ 10-fold greater than those observed for denitrification or selenate reduction and were spatially separated from these

Table IV. Turnover of Sulfate, Nitrate, and Selenate in the Water Column of the Evaporation Pond

process	rate, mol/(m^2·day)	concn,[a] mmol/m^2	turnover time, days
sulfate reduction	8.72	429000	49197
denitrification	0.876[b]	1760	2009
selenate reduction	0.301	25	82

[a] Amount of oxyanion in 1 m^3 of water; water depth, ~1 m. [b] As millimoles of nitrate consumed.

processes (Figure 6). This observation reinforces previous results, which concluded that despite the chemical similarity of selenium and sulfur, the process of selenate reduction to elemental selenium is independent of sulfate and unrelated to sulfate reduction (*6*).

Integrated areal estimates for the magnitude of the sediment as a sink for sulfate, nitrate, and selenate are given in Table IV. Although sulfate reduction rates were 10-fold greater than either denitrification or selenate reduction and hence were more significant in terms of carbon mineralization, the pool size of sulfate was so large that a turnover time of over 49 000 days was calculated. This does not factor in any sulfate reduction occurring below 20-cm depth (Figure 6) or any ^{35}S incorporated into the pyrite fraction, which would tend to decrease the sulfate turnover time. In contrast, the turnover for nitrate was 2009 days. However, because of the competitive action of dissimilatory nitrate reduction, denitrification can account for removal of only a few percent of the available nitrate (*18*), thereby making its turnover from denitrification comparable to that for selenate reduction. The turnover of selenate, however, is clearly quite rapid and holds the capacity to remove all the selenium oxyanions from the surface water in a matter of months. This turnover estimate ignores potential recycling reactions, such as microbial oxidation (*33*) or further reduction by thiols (*34*).

It is relevant to compare the magnitude of our selenate dissimilatory reduction estimate with volatilization sinks (*3*, *5*). Cooke and Bruland (*4*) estimated an average loss of ~6.6 μmol m^{-2} day^{-1} (highest value, ~66 μmol m^{-2} day^{-1}) from the flooded Kesterson Wildlife Refuge, an environment similar to our evaporation pond site. Thus, our sediment sink of 301 μmol m^{-2} day^{-1} is 5–50-fold higher than that for dimethyl selenide. In addition, the potential for rapid bacterial demethylation of dimethyl selenide in these shallow Kesterson surficial sediments, resulting in production of methane, carbon dioxide, and hydrogen selenide (*35*) has been generally overlooked in studies suggesting selenium biomethylation as a mechanism for loss or restoration of impacted soils or waters (*4–6*). Demethylation is significant not only because it would lower outward flux of dimethyl selenide, but also because it converts this gas into the much more toxic and reactive hydrogen selenide. Hydrogen selenide not escaping to the atmosphere would be either oxidized back to selenium oxyanions in the water column or complexed with Fe^{2+} and precipitated into the sediments, thereby contributing to retention of selenium by a salt marsh.

Presumably, the rate of selenate reduction by natural sediments can be enhanced. This was achieved in laboratory experiments (*6*) by provision of the proper electron donors (e.g., acetate, lactate, hydrogen, etc.). When this is done in conjunction with removal of competitive electron acceptors like fertilizer-derived nitrate (*6*), a treatment scheme can be envisioned. Such a treatment process should also prevent the reoxidation or subsequent chemical/biological reduction of the elemental selenium. An enclosed, flow-through anaerobic digestor preceded by an algal treatment step (to remove nitrate and provide the ultimate source of electron donor) could represent a conceptual design for a practical waste treatment process to remove selenium oxyanions from impacted agricultural drainage waters.

Acknowledgments

We are grateful to S. Luoma, D. Lovley, and M. Sylvester for helpful comments and critical reviews of the manuscript, and to S. Hager for technical assistance.

Registry No. Methane, 74-82-8; ammonium, 14798-03-9.

Literature Cited

(1) Presser, T. P.; Barnes, I. U.S. Geological Survey Water Resources Investigations Report 85-4220, 1984.
(2) Sylvester, M. A.; Deason, J. P.; Feltz, H. R.; Engberg, R. A. *Proceedings on Planning Now for Irrigation Drainage Studies*; Americal Society of Civil Engineers: New York, 1988; pp 665–667.
(3) Karlson, U.; Frankenberger, W. T., Jr. *Sci. Total Environ.*, in press.
(4) Cooke, T. D.; Bruland, K. W. *Environ. Sci. Technol.* **1987**, *21*, 1219–1224.
(5) Thompson-Eagle, E. T.; Frankenberger, W. T., Jr.; Karlson, U. *Appl. Environ. Microbiol.* **1989**, *55*, 1406–1413.
(6) Oremland, R. S.; Hollibaugh, J. T.; Maest, A. S.; Presser, T. S.; Miller, L. G.; Culbertson, C. W. *Appl. Environ. Microbiol.* **1989**, *55*, 2333–2343.
(7) Macy, J. M.; Michel, T. A.; Kirsch, D. G. *FEMS Microbiol. Lett.* **1989**, *61*, 195–198.
(8) Conrad, R.; Schultz, H. In *Methods in Aquatic Bacteriology*; Austin, B. Ed.; John Wiley & *Sons*: New York, 1988; pp 301–343.
(9) Balderston, W. L.; Sherr, B.; Payne, W. J. *Appl. Environ. Microbiol.* **1976**, *31*, 504–508.
(10) Chain, Y.-K.; Knowles, R. *Appl. Environ. Microbiol.* **1979**, *37*, 1067–1072.
(11) Stewart, W. D. P.; Fitzgerald, N. G. P.; Burris, R. H. *Proc. Natl. Acad. Sci. U.S.A.* **1967**, *58*, 2071–2078.
(12) Jørgensen, B. B. *Geomicrobiol. J.* **1978**, *1*, 11–27.
(13) Kharaka, Y. K.; Robinson, S. W.; Law, L. M.; Carothers, W. W. *Geochim. Cosmochim. Acta* **1984**, *48*, 823–835.
(14) Oremland, R. S.; Cloern, J. E.; Sofer, Z.; Smith, R. L.; Culbertson, C. W.; Miller, L.; Cole, B.; Harvey, R.; Iversen, N.; Klug, M.; Des Marais, D. J.; Rau, G. In *Lacustrine Petroleum Source Rocks*; Fleet, A. J.; Kelts, K.; Talbot, M. R. Eds.; 1988, *Geol. Soc. Spec. Publ. (London)* **1988**, *40*, 59–76.
(15) Zehr, J. P.; Harvey, R. W.; Oremland, R. S.; Cloern, J. E.; George, L. H.; Lane, J. L. *Limnol. Oceanogr.* **1987**, *32*, 781–793.
(16) Smith, R. L.; Klug, M. J. *Appl. Environ. Microbiol.* **1981**, *41*, 1230–1237.
(17) Smith, R. L.; Oremland, R. S. *Limnol. Oceanogr.* **1987**, *32*, 794–803.
(18) Oremland, R. S.; Umberger, C.; Culbertson, C. W.; Smith, R. L. *Appl. Environ. Microbiol.* **1984**, *47*, 1106–1112.
(19) Peterson, D. H. In *The Urbanized Estuary*; Conomos, T. J., Ed.; Pacific AAAS: San Francisco, CA, 1979; pp 175–194.
(20) Vijan, P. N.; Leung, D. *Anal. Chim. Acta* **1980**, *120*, 141–146.
(21) Brimmer, S. P.; Fawcett, W. R.; Kulhavy, K. A. *Anal. Chem.* **1987**, *59*, 1470–1471.
(22) Roden, D. R.; Tallman, D. E. *Anal. Chem.* **1982**, *54*, 307–309.
(23) Cutter, G. A. *Anal. Chim. Acta* **1983**, *149*, 391–394.
(24) Soloranzano, L. *Limnol. Oceanogr.* **1969**, *14*, 799–801.
(25) Cline, J. D. *Limnol. Oceanogr.* **1969**, *14*, 454–459.
(26) Oremland, R. S. *Appl. Environ. Microbiol.* **1981**, *42*, 122–129.
(27) Bar-Yosef, B.; Meek, D. *Soil Sci.* **1987**, *144*, 11–19.
(28) Hayes, K. F.; Papelis, C.; Leicke, J. O. *J. Colloid Interface Sci.* **1988**, *125*, 717–726.
(29) Zehr, J. P.; Oremland, R. S. *Appl. Environ. Microbiol.* **1987**, *53*, 1365–1369.

(30) Sørensen, J. *Appl. Environ. Microbiol.* **1978**, *35*, 301–305.
(31) Koike, I.; Hattori, A. *Appl. Environ. Microbiol.* **1978**, *35*, 278–282.
(32) Rehr, B.; Klemme, J.-H. *FEMS Microbiol. Ecol.* **1989**, *62*, 51–58.
(33) Doran, J. W. *Adv. Microbiol. Ecol.* **1982**, *6*, 17–32.
(34) Weres, O.; Jaouni, A. R.; Tsao, L. *Appl. Geochem.* **1990**, *4*, 543–563.
(35) Oremland, R. S.; Zehr, J. P. *Appl. Environ. Microbiol.* **1986**, *52*, 1031–1036.

Received for review September 18, 1989. Accepted January 30, 1990. This work was funded by and conducted at the USGS. J.T.H. was supported by an interagency personnel agreement with the USGS. Mention of brand-name products does not constitute and endorsement by the USGS.

The Surface Area of Soil Organic Matter

Cary T. Chiou*

U.S. Geological Survey, Box 25046, MS 408, Denver Federal Center, Denver, Colorado 80225

Jiunn-Fwu Lee† and Stephen A. Boyd

Department of Crop and Soil Sciences, Michigan State University, East Lansing, Michigan 48824

■ The previously reported surface area for soil organic matter (SOM) of 560–800 m^2/g as determined by the ethylene glycol (EG) retention method was reexamined by the standard BET method based on nitrogen adsorption at liquid nitrogen temperature. Test samples consisted of two high organic content soils, a freeze-dried soil humic acid, and an oven-dried soil humic acid. The measured BET areas for these samples were less than 1 m^2/g, except for the freeze-dried humic acid. The results suggest that surface adsorption of nonionic organic compounds by SOM is practically insignificant in comparison to uptake by partition. The discrepancy between the surface areas of SOM obtained by BET and EG methods was explained in terms of the "free surface area" and the "apparent surface area" associated with these measurements.

Introduction

In spite of the general acceptance that sorption of organic pollutants and pesticides from water by soils (or sediments) is controlled primarily by the organic matter content of the soil (*1–7*), the mechanistic function of the soil organic matter (SOM) in uptake of the organic compound has been a subject of active discussion (*3–15*). Before 1979, most studies regarded the SOM as a high-surface-area adsorbent in analogy with other traditional solid adsorbents (*1*, *16–18*). This assumption appeared to result partially from the suggested apparent surface area for the SOM (of the order of 560–800 m^2/g), as first reported by Bower and Gschwend (*19*) and propagated subsequently by others (*16–20*). The reported surface area of SOM was derived from the retention of ethylene glycol (EG) by this material at room temperature, the assumption of monolayer surface adsorption, and the area–mass conversion factor obtained from the EG uptake by reference clay minerals of known BET (Brunauer–Emmett–Teller) surface areas. In more recent studies, however, Chiou and co-workers (*3*, *6–10*) took close account of the aqueous-sorption and vapor-sorption behavior of soils and soil humic acids and suggested that SOM functioned primarily as a partition medium rather than as an adsorbent in the uptake of (nonionic) organic compounds. Evidence supporting the partition model consists of linear sorption isotherms of organic solutes (or organic vapors) to high relative concentrations, low heats of sorption, no competitive effects in uptake of binary solutes, and the general compliance of the sorption data with the Flory–Huggins theory (*21*, *22*) for solute solubility behavior in (amorphous) polymers and macromolecular substances.

Although the partition model has successfully explained a wide variety of observations (*3*, *6–10*, *13*, *15*, *23*), the surface adsorption concept is still being advocated by some researchers as the mechanistic basis for organic compound uptake by SOM (*11*, *12*, *14*, *20*, *24*, *25*). Since the magnitude of the SOM surface area would serve as a primary indicator of the adsorption power of SOM, reexamination of the previously reported surface area for SOM by a generally accepted method is necessary, because the basic assumptions for the surface-area determination of SOM by EG retention have not been rigorously confirmed, despite the conventional use of EG retention in characterizing clay minerals. In other words, if the observed EG retention by SOM were due primarily to monolayer adsorption rather than other contributions, one would expect similar monolayer adsorption of nitrogen at liquid nitrogen temperature. In this study, we used the standard BET method (*26*) to measure the surface areas of high organic content soils and extracted soil humic acids and discussed the mechanistic uptake of organic compounds by SOM in terms of the surface areas as determined by the BET and EG methods.

Experimental Section

The BET surface areas were determined by nitrogen adsorption at liquid nitrogen temperature for the following organic soils and purified soil humic acids: a Florida peat soil from Everglades, FL, which contains 86.4% organic matter (OM) on a dry weight basis; a Houghton muck soil from the Michigan State University Muck Research Farm, Laingsburg, MI (91.9% OM content); a purified soil humic acid in freeze-dried form (98.8% OM) isolated from Sanhedron soil in the Mattole River Valley of northern California (*9*); and the oven-dried soil humic acid obtained from the alkaline solution of the above freeze-dried humic acid, followed by dialysis of the sample to bring the pH to 6.5, and then drying at 65–70 °C. A Quantasorb Jr. surface area analyzer (Quanta Chrome Corp.) was used to measure the monolayer capacity of nitrogen gas at liquid ntirogen temperature. All samples were outgassed under vacuum at 105 °C for 6 h before N_2 adsorption. Helium was used as the carrier and dilution gas to fix the relative pressure of N_2 in the range of 0.05–0.25, the region where the data conformed to a linear BET plot (*8*). The molecular surface area of 16.2×10^{-20} m^2 for nitrogen was used

†Present address: Department of Environmental Engineering and Water Resources, Tamkang University, Taipei, Taiwan 10620, Republic of China.

 0013-936X/90/0924-1164$02.50/0

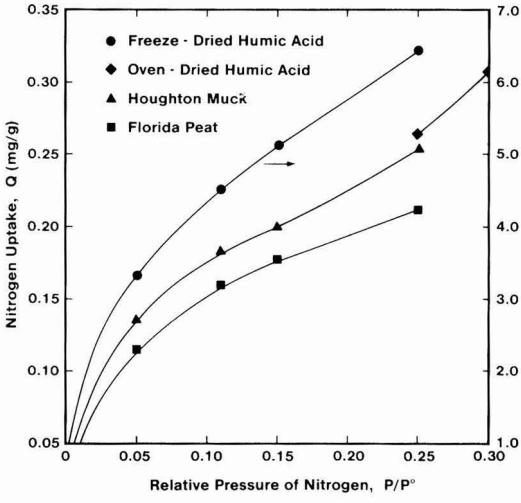

Figure 1. Adsorption isotherms of nitrogen vapor at liquid nitrogen temperature on selected organic soils and soil humic acids.

in the surface area determination of the test samples.

Results and Discussion

The adsorption data of nitrogen on four test samples at liquid nitrogen temperature are given in Figure 1. To obtain the surface area, the data in Figure 1 were expressed in a linear BET form as

$$\frac{1}{Q(P^\circ/P - 1)} = \frac{C - 1}{CQ_m}\frac{P}{P^\circ} + \frac{1}{CQ_m} \qquad (1)$$

in which P/P° is the relative pressure of nitrogen, Q is the amount of nitrogen adsorbed at given P/P°, Q_m is the monolayer adsorption capacity, and C is a constant related to the net heat of monolayer adsorption. The Q_m value for each sample was determined from the slope, $(C - 1)/CQ_m$, and the intercept, $1/CQ_m$, of the plot of $1/Q(P^\circ/P - 1)$ against P/P°; the BET surface area was then calculated from the Q_m value and the molecular surface area of nitrogen. Plots of $1/Q(P^\circ/P - 1)$ vs P/P° for the freeze-dried humic acid, Houghton muck, and Florida peat are shown in Figure 2, in which the data exhibit a good fit to the BET equation. Because of the very small sample size of the oven-dried humic acid used in this study (~0.05 g), the adsorption data with this sample at low P/P° could not be accurately measured. The surface area of this sample was estimated from the data points at $P/P^\circ = 0.25$ and 0.30 by the one-point approximation method (*27*):

$$Q_m = Q(1 - P/P^\circ) \qquad (2)$$

which generally gives a good estimate of Q_m for systems with $C > 10$ and $P/P^\circ = 0.05 - 0.3$; the present data for the other three samples ($C > 20$) fit eq 2 reasonably well over the stated P/P° range.

The determined BET surface areas for the above samples were as follows: 0.61 m^2/g for the Florida peat, 0.73 m^2/g for the Houghton muck, 18 m^2/g for the freeze-dried soil humic acid, and ~0.70 m^2/g for the oven-dried soil humic acid. These values are extremely small in comparison with the surface area previously reported for SOM. In this study, the much larger area for the freeze-dried humic acid sample relative to the oven-dried sample may be attributed to the freeze-drying process, which frequently increases surface areas of low-surface substances. That the surface areas for the two organic-rich soils are comparable to that of the oven-dried soil humic acid suggests

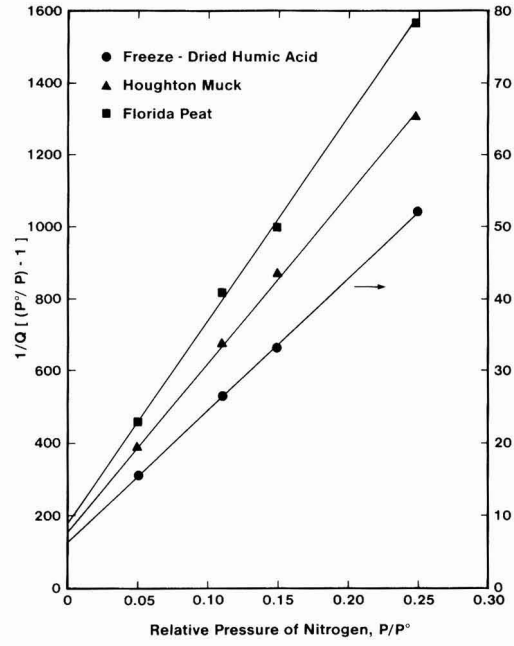

Figure 2. Plots of nitrogen adsorption data in a linear BET equation.

that the minor mineral fractions in these soils are not readily accessible to vapor adsorption, presumably because they are deeply enclosed by the organic matter. In light of the notably low surface areas for these samples, surface adsorption of nonionic organic compounds by SOM should be extremely small.

The discrepancy of the determined surface areas for the SOM by the BET and EG methods may be put into perspective in terms of the "free surface area" and "apparent surface area" associated with these measurements. The free surface area corresponds to the solid–vacuum interfacial area of a solid, which exists before adsorption and is unequivocally measured by an adsorbate that does not change the structure of the solid. Determination of free surface areas by the BET method is based on the assumptions that (i) only physical adsorption is involved, (ii) surface area is not changed by the adsorption process, and (iii) no solution is formed by the adsorbate in the solid. The apparent surface area of a solid is the one measured by the uptake of an "adsorbate" that either changes the structure of the solid, dissolves in it, or both. For example, the very large so-called "total surface area" of a smectite determined by the uptake of polar liquids (such as water and EG) (*28*) results from creation of interlamellar surfaces by lattice swelling; it does not exist before the liquid uptake. Similarly, amorphous organic polymers or macromolecular substances also give rise to large apparent surface areas when they are calculated from the uptake of solvents of similar polarities that form solutions in the solid amorphous material. Solutions of the vapors of benzene in natural rubber (*29–32*) and poly(isobutylene) (*33*), cyclohexane in poly(isobutylene) (*34*), and *n*-pentane in poly(isobutylene) (*35*) are just a few well-known systems in which the polymers have negligible BET surface areas (except those polymers specially made to produce porosity) but take up large amounts of solvents by partition (solubility). In general, the apparent surface area is not well-defined and can be ambiguous, because it does not refer to the surface area of the solid before the measurement

is taken; in many cases, it is difficult to make a distinction between true surface adsorption and such phenomena as expansion of the solid lattice by the adsorbate, accessibility of the adsorbate to a presumed "internal surface", and solubility of the "adsorbate" in the solid. In a rigorous manner, one should limit the concept of "surface area" to those cases in which the surface area of the solid remains invariant to the adsorption measurement.

The enormously large surface area reported by Bower and Gschwend (*19*) for SOM is presumably an artifact of their calculation method, which assumed only surface adsorption of EG on SOM and the absence of significant bulk solubility of the compound. In the study of Bower and Gschwend (*19*), the assumed monolayer capacity of EG on SOM (corresponding to 17–25% by weight) was empirically obtained from a single retention data point rather than determined from isotherms; these data give no evidence for exclusive monolayer adsorption of EG by SOM. There are good reasons to believe that the relatively high EG retention by SOM at room temperature is due essentially to partition, when one considers the polar nature of both EG and amorphous SOM. For example, ethanol, a polar liquid similar in composition to EG, has been shown to partition effectively in soil humic acid and to give rise to a practically linear isotherm, with the limiting partition capacity approaching 35% by weight (*9*) (also note that there is no theoretical basis for deriving a surface area from a practically linear isotherm). Water uptake by soil humic acid exhibits similar results (*9*). The difference in magnitude between surface adsorption and solubility is further illustrated for a nonpolar solid sorbent–vapor system by the uptake of benzene vapor on a specially made poly(styrene-*co*-divinylbenzene), as Chromosorb 101 from Supelco, Inc., with 30–35 m^2/g BET surface area (technical data from Manville Corp., Lompoc, CA). Here one finds a relatively linear isotherm with a limiting capacity of ~30% by weight (*9*), while the monolayer surface adsorption of benzene would correspond to less than 1.5% by weight. Thus, the benzene uptake in this case is still predominantly by bulk solubility in the polymer.

In conclusion, our findings on SOM are consistent with the well-known behavior of polymers and are best accounted for by solution of organic vapors or solvents in (solid) amorphous, macromolecular substances (*21*, *22*, *29–35*). To insist on the primacy of surface adsorption of EG on SOM, one would be forced to postulate some sort of poorly defined "inner surface" with SOM that is accessible to EG and ethanol but that somehow excludes smaller molecules like N_2; this hypothesis would however seem rather excessive, especially when one is faced with linear isotherms and other noted effects that are characteristic of solubility. The partition model reconciles the large uptake of polar liquids (such as ethanol and EG) by SOM with the relatively low BET surface area for the SOM. The low BET areas for the samples tested in this study and the various other sorption characteristics of organic compounds on SOM (*3*, *4*, *6–10*, *13*, *15*, *23*) suggest that it is no longer tenable to ascribe the sorption of organic pollutants and pesticides by soil organic matter to a high-surface area that it in fact does not possess.

Acknowledgments

We thank Ronald L. Malcolm, U.S. Geological Survey, Denver, CO, for the soil humic acid used in this study. The use of trade and product names in this article is for identification purposes only and does not constitute endorsement by the U.S. Geological Survey.

Literature Cited

(1) Hamaker, J. W.; Thompson, J. M. In *Organic Chemicals in the Soil Environment*; Goring, C. A. I., Hamaker, J. W., Eds.; Dekker: New York, 1972; pp 49–143.
(2) Lambert, S. M. *J. Agric. Food Chem.* **1968**, *16*, 340.
(3) Chiou, C. T.; Peters, L. J.; Freed, V. H. *Science (Washington, D.C.)* **1979**, *206*, 831.
(4) Karickhoff, S. M.; Brown, D. S.; Scott, T. A. *Water Res.* **1979**, *13*, 241.
(5) Kenaga, E. E.; Goring, C. A. I. In *Aquatic Toxicology*; Eaton, J. C., Parrish, P. R., Hendricks, A. C., Eds.; American Society for Testing and Materials: Philadelphia, 1980; pp 78–115.
(6) Chiou, C. T.; Porter, P. E.; Schmedding, D. W. Environ. *Sci. Technol.* **1983**, *17*, 227.
(7) Chiou, C. T.; Shoup, T. D.; Porter, P. E. *Org. Geochem.* **1985**, *8*, 9.
(8) Chiou, C. T.; Shoup, T. D. *Environ. Sci. Technol.* **1985**, *19*, 1196.
(9) Chiou, C. T.; Kile, D. E.; Malcolm, R. L. *Environ. Sci. Technol.* **1988**, *22*, 298.
(10) Chiou, C. T. In *Reactions and Movement of Organic Chemicals in Soils*; Sawhney, B. L., Brown, K., Eds.; Special Publication No. 22; Soil Science Society of America: Madison, WI, 1989; pp 1–29.
(11) Mingelgrin, U.; Gerstl, Z. *J. Environ. Qual.* **1983**, *12*, 1.
(12) MacIntyre, W. G.; Smith, G. L. *Environ. Sci. Technol.* **1984**, *18*, 295.
(13) Gschwend, P. M.; Wu, S.-C. *Environ. Sci. Technol.* **1985**, *19*, 90.
(14) Hassett, J. J.; Banwart, W. L. In *Reactions and Movement of Organic Chemicals in Soils*; Sawhney, B. L., Brown, K., Eds.; Special Publication No. 22; Soil Science Society of America: Madison, WI, 1989; pp 31–44.
(15) Boyd, S. A.; Mikesell, M. D.; Lee, J.-F. in *Reactions and Movement of Organic Chemicals in Soils*; Sawhney, B. L., Brown, K., Eds.; Special Publication No. 22; Soil Science Society of America: Madison, WI, 1989; pp 209–228.
(16) Bailey, G. W.; White, L. L. *J. Agric. Food Chem.* **1964**, *12*, 324.
(17) Haque, R. In *Environmental Dynamics of Pesticides*; Haque, R., Freed, V. H., Eds.; Plenum: New York, 1975; pp 97–114.
(18) Browman, M. G.; Chesters, G. In *Fate of Pollutants in the Air and Water Environments*; Suffet, I. H., Ed.; Wiley: New York, 1977; Part I, pp 49–105.
(19) Bower, C. A.; Gschwend, F. B. *Soil Sci. Proc.* **1952**, *16*, 342.
(20) Valsaraj, K. T.; Thibodeaux, L. J. *J. Hazard. Mater.* **1988**, *19*, 79.
(21) Flory, P. J. *J. Chem. Phys.* **1942**, *10*, 51.
(22) Huggins, M. L. *Ann. N.Y. Acad. Sci.* **1942**, *43*, 1.
(23) Chin, Y.-P.; Weber, W. J., Jr. *Environ. Sci. Technol.* **1989**, *23*, 978.
(24) Sabljic, A. *J. Agric. Food Chem.* **1984**, *32*, 243.
(25) Sabljic, A. *Environ. Sci. Technol.* **1987**, *21*, 358.
(26) Brunauer, S.; Emmett, P. H.; Teller, E. *J. Am. Chem. Soc.* **1938**, 60, 309.
(27) Adamson, A. W. *Physical Chemistry of Surfaces*, 2nd ed.; Interscience Publishers: New York, 1967; pp 584–588.
(28) Bower, C. A.; Goertzen, J. O. *Soil Sci.* **1959**, *87*, 289.
(29) Gee, G.; Treloar, L. R. G. *Trans. Faraday Soc.* **1942**, *38*, 147.
(30) Gee, G.; Orr, J. C. R. *Trans. Faraday Soc.* **1946**, *42*, 507.
(31) Gee, G.; Herbert, J. M. B.; Roberts, R. C. *Polymer* **1965**, *6*, 541.
(32) Eichinger, B. E.; Flory, P. J. *Trans. Faraday Soc.* **1968**, *64*, 2035.
(33) Eichinger, B. E.; Flory, P. J. *Trans. Faraday Soc.* **1968**, *64*, 2053.
(34) Eichinger, B. E.; Flory, P. J. *Trans. Faraday Soc.* **1968**, *64*, 2061.
(35) Eichinger, B. E.; Flory, P. J. *Trans. Faraday Soc.* **1968**, *64*, 2066.

Received for review August 10, 1989. Accepted January 24, 1990.

Environ. Sci. Technol. **1990**, *24*, 1167–1172

Effect of Ten Quaternary Ammonium Cations on Tetrachloromethane Sorption to Clay from Water

James A. Smith*

U.S. Geological Survey, 810 Bear Tavern Road, Suite 206, West Trenton, New Jersey 08628

Peter R. Jaffé

Department of Civil Engineering and Operations Research, Princeton University, Princeton, New Jersey 08544

Cary T. Chiou

U.S. Geological Survey, MS 408, Denver Federal Center, Denver, Colorado 80225

■ The mineral surface of Wyoming bentonite (clay) was modified by replacing inorganic ions by each of 10 quaternary ammonium compounds, and tetrachloromethane sorption to the modified sorbents from water was studied. Tetrachloromethane sorption from solution to clay modified with tetramethyl-, tetraethyl-, benzyltrimethyl-, or benzyltriethylammonium cations generally is characterized by relatively high solute uptake, isotherm nonlinearity, and competitive sorption (with trichloroethene as the competing sorbate). For these sorbents, the ethyl functional groups yield reduced sorptive capacity relative to methyl groups, whereas the benzyl group appears to have a similar effect on sorbent capacity as the methyl group. Sorption of tetrachloromethane to clay modified with dodecyldimethyl(2-phenoxyethyl)-, dodecyltrimethyl-, tetradecyltrimethyl-, hexadecyltrimethyl-, or benzyldimethylhexadecylammonium bromide is characterized by relatively low solute uptake, isotherm linearity, and noncompetitive sorption. For these sorbents, an increase in the size of the nonpolar functional group(s) causes an increase in the organic carbon normalized sorption coefficient (K_{oc}). No measurable uptake of tetrachloromethane sorption by the unmodified clay or clay modified by ammonium bromide was observed.

Introduction

Wyoming bentonite, which is predominantly a montmorillonitic clay, is commonly used as a liner for waste-disposal ponds and as a principal component of slurry walls. Montmorillonite is characterized by alternating layers of tetrahedral silica and octahedral aluminum coordinated with oxygen atoms. The isomorphous substitution of Al^{3+} for Si^{4+} in the tetrahedral layer and Mg^{2+} or Zn^{2+} for Al^{3+} in the octahedral layer results in a net negative surface charge on the clay (*1*). This charge imbalance is offset by exchangeable cations (typically Na^+ or Ca^{2+}) at the clay surface. The layered structure of the clay allows expansion (swelling) after wetting, which in turn exposes additional mineral surface capable of cation adsorption. These factors, in combination with its small particle size, cause montmorillonite to exhibit a high cation-exchange capacity relative to other natural soils. However, the mineral surfaces of montmorillonite and most other natural soils are relatively ineffective sorbents for nonionic organic compounds in aqueous systems, primarily because of the strong dipole interaction of water with the negatively charged mineral surface (*2–9*).

In aqueous systems, quaternary ammonium cations can be retained by both the outer and interlayer surfaces of an expandable clay particle by an ion-exchange process and are not easily displaced by smaller cations such as H^+, Na^+, or Ca^{2+}. The sorptive properties of the modified clay surface may be significantly altered by this substitution reaction. For example, Smith and Bayer (*10*) described semiquantitatively the effect of five quaternary ammonium cations on the sorption of diuron to natural soil from water. They showed that the presence of these cations in the soil–water mixture increased the percent removal of diuron from the aqueous phase relative to soil–water mixtures with no quaternary ammonium cations present. More recently, Boyd et al. (*11*) suggested that the substitution of Na^+ and Ca^{2+} ions by quaternary ammonium ions with large alkyl groups in expandable clays creates an organic medium at the mineral surface through a conglomeration of alkyl chains. This medium may be capable of sorbing nonionic organic contaminants from water by a partition process. These investigators (*11*) found a linear uptake of benzene and trichloroethene from water by bentonite saturated with hexadecyltrimethylammonium cations (HTMA). The resulting sorption coefficients normalized to the organic content of the HTMA-modified clay are of comparable magnitude to the heptane–water partition coefficients of the respective solutes. On the other hand, clays substituted with small tetramethylammonium (TMA) cations show a strong, nonlinear uptake of benzene and small aromatic molecules from water, which is attributed to adsorption onto the TMA-treated surface (*12*, *13*). Adsorption of these solutes by TMA–clay from water also exhibits a size- and shape-selective effect, disfavoring sorption of large solute molecules. These results may have great practical utility, as the use of clay treated with quaternary ammonium ions as a liner for waste-disposal facilities and as a component of slurry walls at groundwater-contamination sites is likely to increase the attenuation of dissolved nonionic organic contaminants.

The present study further analyzes the effect of the molecular structure of quaternary ammonium cations associated with a montmorillonitic clay on the sorption of a nonionic organic contaminant, tetrachloromethane. Ten quaternary ammonium cations composed of various alkyl and aromatic groups were selected for study to provide a wide range of molecular sizes and configurations. In addition to the practical value of optimizing the effect of these cations on the uptake of contaminants by clay, the purpose of this research is to provide a better understanding of the mechanistic interaction of nonionic organic compounds and organic matter at the mineral–water interface.

Experimental Section

The sorbent used in this study, Wyoming bentonite, was obtained from the American Colloid Co. It contains 3.6% sand, 7.3% silt, and 89.1% clay. The organic carbon content is 0.1%, and the cation-exchange capacity is 78.5 mequiv/100 g. This sorbent will be referred to as "clay" throughout this paper. A total of 250 μCi of [^{14}C]tetra-

0013-936X/90/0924-1167$02.50/0

Table I. Organic Carbon Contents, Langmuir-Type Isotherm Parameters, and Regression Correlation Coefficients for Tetrachloromethane Sorption to Four Organoclay Sorbents

	sorbent			
	TMA–clay	TEA–clay	BTMA–clay	BTEA–clay
organic C content, %	1.80	3.49	4.21	5.75
a, mmol/g	0.14	0.08	0.15	0.11
b, L/mmol	1.46	2.11	2.23	3.69
corr coeff	0.992	0.997	0.996	0.998

chloromethane (specific activity equal to 4.3 mCi/mmol) and 50 μCi of [^{14}C]tetraethylammonium (TEA) bromide (specific activity equal to 3.0 mCi/mmol) was obtained from Du Pont NEN. A total of 100 μCi of [^{14}C]trichloroethene (specific activity equal to 4.1 mCi/mmol) was obtained from Sigma Chemical Co. [^{14}C]tetrachloromethane and [^{14}C]trichloroethene were mixed with nonradioactive tetrachloromethane and trichloroethene, respectively, to yield net volumes of 4.0 mL of each pure liquid. Similarly, [^{14}C]tetraethylammonium bromide was mixed with nonradioactive tetraethylammonium bromide to yield a net mass of 5.0 g. The resultant chemical and radiochemical purity of each radioisotope was greater than 99%. All quaternary ammonium compounds were obtained from Aldrich Chemical Co. and were used as received. Their chemical purities, molecular structures, and abbreviations are given in Figure 1.

The addition of a quaternary ammonium cation to an aqueous clay suspension resulted in strong uptake of the cation by the clay. The resultant cation–clay complexes were considered to be unique sorbents and are specified by the cation abbrevation in Table I followed by "–clay." For example, combining dodecyltrimethylammonium bromide (DTMA) with clay and water produced a modified clay identifiable as DTMA–clay. With the exception of ammonium–clay, these sorbents will be generally referred to as "organoclay complexes" or simply "organoclays."

The sorption of tetrachloromethane, trichloroethene, and TEA to unsubstituted clay, ammonium–clay, and organoclay complexes from water was quantified by using a conventional batch equilibration method. For tetrachloromethane sorption to DTMA–, TTMA–, HTMA–, DDPA–, and BDHA–clay, 6.0 g of clay, 55 mL of deionized water, the appropriate organic cation, and tetrachloromethane were combined in 50-mL (nominal volume) disposable glass centrifuge tubes with Teflon-lined septum caps. For TEA sorption to clay, 2 g of clay, 55 mL of deionized water, and TEA were combined in the 50-mL glass centrifuge tubes described above. For tetrachloromethane and trichloroethene sorption to ammonium–, TMA–, TEA–, BTMA–, and BTEA–clay complexes, 0.5 g of clay, 15 mL of deionized water, the appropriate cation, and tetrachloromethane were combined in 15-mL (nominal volume) disposal glass centrifuge tubes. The amount of quaternary ammonium cation added was based on the desired organic carbon content or percentage of cation-exchange capacity of the resultant ammonium– or organoclay complex.

The effect of a competing solute, trichloroethene, on the sorption of tetrachloromethane to each of the organoclay complexes also was studied. For these cases, equal volumes of trichloroethene and [^{14}C]tetrachloromethane were added to each centrifuge tube.

The centrifuge tubes were equilibrated in the dark at 20 °C. During equilibration, the tubes were rotated continuously to facilitate mixing. Kinetic experiments conducted over a 30-day period indicated that solute equilibrium between the aqueous and solid phases was reached after approximately 12 h of incubation. Nevertheless, in all experiments a 48-h incubation time was used to ensure equilibrium. After incubation, the tubes were centrifuged for 60 min at 2000*g* (g = 9.81 m/s^2). A 1.0-mL aliquot of the supernatant was removed from each centrifuge tube and combined with 10 mL of scintillation cocktail in a 20-mL glass scintillation vial. The radioactivity in the sample was quantified subsequently by use of a Packard Tri-Carb 1900CA liquid scintillation analyzer. All radioactivity measurements were corrected for quench by using an external standard. The equilibrium solute concentration (C_e) in the supernatant from the centrifuge tube was then determined from a standard curve relating disintegrations per minute to aqueous concentration. The equilibrium concentration of the solute on the clay or organoclay complex (C_s) was determined by difference.

To ensure the quality of the data, one "background" and two "blank" samples were prepared and handled in parallel with the previously described centrifuge tubes for each isotherm. A background sample consisted of clay, water, and quaternary ammonium cation combined in a centrifuge tube without a radioisotope. These samples were used to quantify the ambient, or background, radiation, and to ensure that the glassware, clay, water, and cation were not contaminated with radioactivity. A blank sample consisted of water, quaternary ammonium cation, and radioisotope combined in a centrifuge tube without the clay. These samples were used to determine losses of the solute caused by sorption to glassware, biodegradation, volatilization, etc. In general, solute recovery was from 95 to 105%. If solute recovery was less than 90%, the accompanying experimental isotherm was repeated. Because solute recovery generally was high, the isotherm data were not adjusted

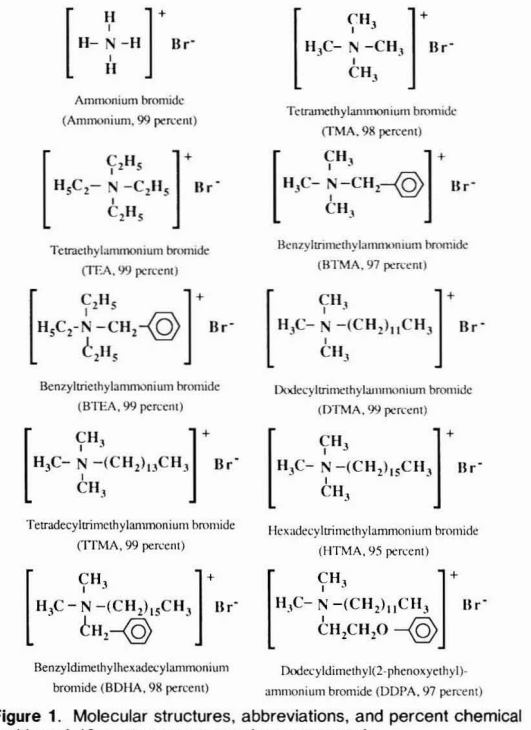

Figure 1. Molecular structures, abbreviations, and percent chemical purities of 10 quaternary ammonium compounds.

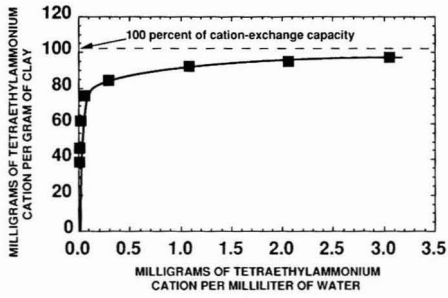

Figure 2. Tetraethylammonium (TEA) uptake by clay from water.

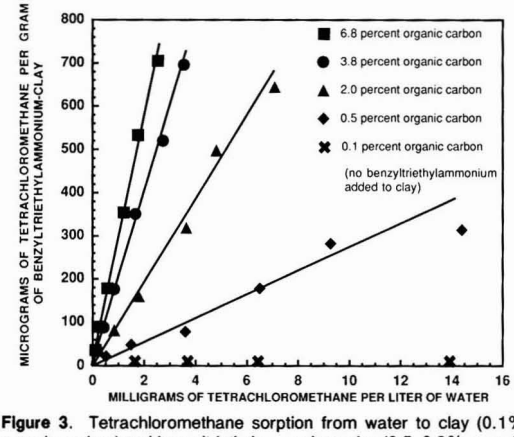

Figure 3. Tetrachloromethane sorption from water to clay (0.1% organic carbon) and benzyltriethylammonium–clay (0.5–6.8% organic carbon).

to account for the percent recovery.

The organic carbon content of the clay and organoclay complexes and the cation-exchange capacity of the clay were quantified by Huffman Laboratories, Golden, CO.

Results

Figure 2 shows the strong retention of the TEA cation by the clay. The independent variable in the graph is the equilibrium aqueous TEA concentration, C_e, and the dependent variable is the equilibrium sorbed TEA concentration, C_s.

The isotherms in Figure 3 shows the effect of one of the organic cations, benzyltriethylammonium bromide (BTEA), on the sorption of tetrachloromethane to clay from water at relatively low aqueous solute concentrations. The lower isotherm in Figure 3 (0.1% organic carbon) quantifies the sorption of tetrachloromethane to clay in the absence of BTEA. The remaining isotherms (0.5–6.8% organic carbon) quantify tetrachloromethane sorption to clays exchanged with increasing amounts of BTEA.

The graphs shown in Figure 4 quantify tetrachloromethane sorption to BTMA–clay (graph A) and HTMA–clay (graph B) in both the presence and absence of a binary solute (trichloroethene). The organic carbon contents of the BTMA–clay and the HTMA–clay are 3.8 and 6.2%, respectively. In contrast to Figure 3, the isotherm data extend to C_e values greater than 50% of the aqueous solubility of tetrachloromethane. Tetrachloromethane sorption from water to BTMA–clay (graph A) is characterized by isotherm nonlinearity, competitive sorption, and relatively strong solute uptake. Tetrachloromethane sorption from water to HTMA–clay (graph B) is characterized by isotherm linearity, noncompetitive sorption, and relatively weak solute uptake.

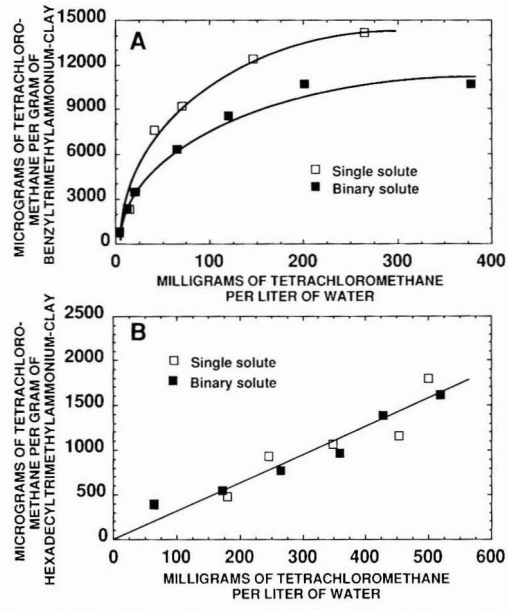

Figure 4. Tetrachloromethane sorption to benzyltrimethylammonium–clay with 3.8% organic carbon (A) and hexadecyltrimethylammonium–clay with 6.16% organic carbon (B). The binary solute is trichloroethene.

With the exception of ammonium–clay, the characteristics of tetrachloromethane sorption to different organoclay complexes are similar to the characteristics of the isotherms of either graph A or graph B in Figure 4. Tetrachloromethane sorption to TMA–, TEA–, BTMA–, and BTEA–clay generally was characterized by isotherm nonlinearity, competitive sorption, and relatively high solute uptake. Tetrachloromethane sorption to DTMA–, TTMA–, HTMA–, BDHA–, and DDPA–clay was characterized by isotherm linearity, noncompetitive sorption, and relatively low solute uptake. Therefore, these two groups of sorption data were separated for analysis. No measurable uptake of tetrachloromethane by ammonium–clay was observed.

The data for all nonlinear single- and binary-solute isotherms have been fit to the linear, Langmuir-type equation given by

$$\frac{C_e}{C_s} = \frac{1}{ba} + \frac{C_e}{a} \tag{1}$$

where C_e and C_s are in millimoles per liter and millimoles per gram, respectively. The values of the parameters a and b are determined by a linear regression of C_e versus C_e/C_s. The slope and intercept of the plot are $1/a$ and $1/ba$, respectively. The parameters a and b for the single-solute isotherms are given in Table I, along with the organic carbon contents of the sorbents and the regression correlation coefficients. The single- and binary-solute isotherm data were compared statistically by use of a multiple-regresion analysis with a dummy variable (*14*). Results of this analysis indicate that the presence of the binary solute reduces tetrachloromethane sorption to TEA–, BTMA–, and BTEA–clay relative to the single-solute case at a p value of 0.05. No competitive effect was observed for tetrachloromethane sorption to TMA–clay in the presence of trichloroethene.

Table II. Linear Isotherm Parameters, Organic Carbon Contents, and Regression Correlation Coefficients for Tetrachloromethane Sorption to Five Organoclay Sorbents

	sorbent				
	DTMA–clay	TTMA–clay	HTMA–clay	BDHA–clay	DDPA–clay
sorption coeff, K_d, kg/L	1.36	1.51	3.12	6.56	7.64
organic C content, %	7.56	6.97	6.16	7.13	6.57
log K_{oc}	1.26	1.34	1.70	1.96	2.07
corr coeff	0.94	0.81	0.95	0.94	0.94

For the remaining linear isotherms, a regression model that presupposes a zero contaminant concentration on the clay in response to a zero aqueous contaminant concentration was used and is given by

$$C_s = K_d C_e \tag{2}$$

where K_d is the sorption (distribution) coefficient. For a set of n data points of the form (C_e^i, C_s^i), $i = 1, n$, differentiation of the sum of the squares of the residuals (SSR) with respect to K_d is given by

$$\frac{\partial(\mathrm{SSR})}{\partial K_d} = -2\sum_{i=1}^{n} C_e^i (C_s^i - K_d C_e^i) \tag{3}$$

The SSR is minimized by setting eq 3 equal to zero. The value of K_d can then be calculated as follows:

$$K_d = \sum_{i=1}^{n} C_e^i C_s^i / \sum_{i=1}^{n} (C_e^i)^2 \tag{4}$$

The sorption coefficient can be normalized by the organic carbon content of the sorbent with

$$K_{oc} = K_d / f_{oc} \tag{5}$$

where K_{oc} is the organic carbon normalized sorption coefficient and f_{oc} is the organic carbon fraction of the sorbent, which is equal to the percent organic carbon divided by 100. The values of K_d, percent organic carbon, log K_{oc}, and the sample correlation coefficient for the linear tetrachloromethane sorption isotherms are presented in Table II. Analysis of single- and binary-solute isotherm data shows that the isotherm pairs are coincident for each sorbate–sorbent system in Table II at a p value of 0.05.

For the sorbents given in Table I, the mass of added organic cation equals 41% of cation-exchange capacity. For the sorbents in Table II, the mass of added organic cation was chosen to give an organic carbon content of about 7%, which corresponds to cation-exchange capacities of about 30 (DDPA) to 50% (DTMA).

Discussion

The cationic quaternary ammonium compounds shown in Figure 1 are solids at room temperature. With the exception of ammonium bromide, they are classified as surface-active agents (surfactants) because each molecule has a nonpolar hydrocarbon group and an ionic, polar component. The molecular structures of the selected compounds are diverse, with alkyl-chain lengths ranging from 0 to 16 carbon atoms. Four of the selected quaternary ammonium compounds have an aromatic functional group.

Unlike nonionic organic compounds, large organic cations can effectively displace inorganic ions such as Ca^{2+} and Na^+ from the negatively charged mineral surfaces of clay and natural soil by ion exchange (*7*, *15–22*). As a result, organic cations are strongly retained by the clay surface until the concentration of the cation on the clay approaches the cation-exchange capacity. This observation is supported by the isotherm data for TEA in Figure 2. The data in Figure 2 indicate that essentially 100% of the TEA is retained by the clay when the number of moles of added TEA is less than 90% of the cation-exchange capacity.

Similarly, the organic carbon content data in Tables I and II and Figure 3 agree well with the clay organic carbon content predicted by assuming that 100% of the added quaternary ammonium cation is retained by the clay. The predicted organic carbon contents for TMA–, TEA–, BTMA–, and BTEA–clay (Table I) are 1.6, 3.1, 3.9, and 5.1%, respectively. The predicted organic carbon contents for DTMA–, TTMA–, HTMA–, BDHA–, and DDPA–clay (Table II) are all 7%. Similarly, the predicted organic carbon contents for the BTEA–clay isotherms in Figure 3 are 0.5, 1.8, 3.4, and 6.8%. The agreement between predicted and measured organic carbon contents is indicative of the strong uptake of the quaternary ammonium cations by the clay from water.

The isotherms in Figure 3 were generated at equilibrium aqueous tetrachloromethane concentrations less than 2% of its solubility [800 mg/L at 25 °C (*23*)]. These trace concentrations are representative of concentrations typically observed in the field. As such, these isotherms illustrate several important characteristics. First, the lowest isotherm (0.1% organic carbon) describes the sorption of tetrachloromethane to clay that has not been amended with quaternary ammonium cations. As evidenced by the data, sorption to the clay is negligible. The hydrated mineral surface of the clay prevents tetrachloromethane adsorption and the low organic carbon content of the clay (0.1%) results in negligible solute uptake by partition. By contrast, the addition of a relatively small amount of BTEA (0.5–6.8% organic carbon) causes a dramatic increase in the uptake of tetrachloromethane relative to the untreated clay. These results encourage continued investigation into the feasibility of the treatment of clay with quaternary ammonium cations for use in slurry walls and as liners at waste disposal sites.

Second, consider the magnitude of uptake and linearity of the isotherms in Figure 3. If tetrachloromethane uptake by BTEA–clay was the result of a partition interaction between water and an organophilic medium created by the organic cation at the clay surface, the resulting organic carbon normalized partition coefficient (K_{oc}) for each isotherm in Figure 3 would be expected to be of a magnitude comparable to the octanol–water partition coefficient (K_{ow}) of tetrachloromethane. However, the values of K_{oc} for the isotherms of Figure 3 range from 5000 to 6000, whereas the K_{ow} for tetrachloromethane is 440 (*23*). This discrepancy suggests that tetrachloromethane sorption to the BTEA–clay is caused primarily by adsorption rather than by partition alone. For partition equilibria, the isotherm should be linear over a wide range of C_e values relative to the aqueous solubility of the solute. Although the isotherms in Figure 3 are highly linear, the C_e values are less than 2% of the aqueous solubility of tetrachloromethane. This linearity may be attributed to a Henry's law type effect at dilute concentration. Therefore, experimental extension of the isotherm for BTEA–clay to C_e values greater than 50% of the aqueous solubility of

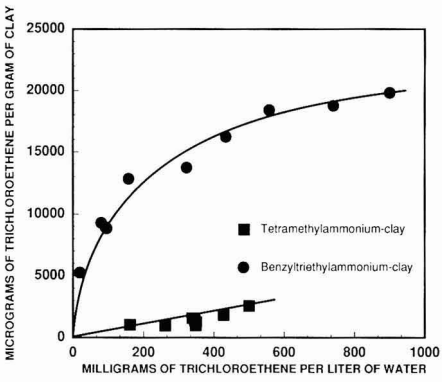

Figure 5. Trichloroethene sorption to benzyltriethylammonium–clay and tetramethylammonium–clay.

tetrachloromethane was conducted, and a distinctly nonlinear isotherm was observed (data not shown).

Considering the data in Figure 4 and Tables I and II, it is apparent that the molecular structure of the quaternary ammonium cation affects both the magnitude and the mechanism of tetrachloromethane sorption to the organoclay complex. Tetrachloromethane sorption to TEA–, BTMA–, and BTEA–clay (Table I) is characterized by distinctly nonlinear isotherms, relatively strong solute uptake, and a competitive effect. This behavior is typical of an adsorption process wherein the nonionic solute is attracted by London (van der Waals) forces to an organic surface formed by the quaternary ammonium cations. The cations are retained on the mineral surface by electrostatic forces.

Sorption of tetrachloromethane to TMA–clay also was characterized by isotherm nonlinearity and relatively strong solute uptake. No competitive sorption effect was observed, however. In an attempt to explain this result, sorption of the competitive solute, trichloroethene, to TMA–, TEA–, BTMA–, and BTEA–clay was quantified. Some of these data are shown in Figure 5, which compares the sorption of trichloroethene to TMA– and BTEA–clay. For both cases, the mass of retained organic cation is 41% of cation-exchange capacity. These results indicate that trichloroethene uptake by TMA–clay is very weak relative to uptake by BTEA–clay. Trichloroethene uptake by TEA– and BTMA–clay is similar to the uptake by BTEA–clay. Therefore, tetrachloromethane sorption to TMA–clay does not exhibit a strong competitive effect. The reason for the weak uptake of trichloroethene by TMA–clay is not exactly known. As the uptake of aromatic organic solutes by TMA–clay has been shown to be size and shape selective (*12*), it is possible that the larger molecular dimension of trichloroethene relative to tetrachloromethane reduces solute association with the small methyl groups in the $N(CH_3)_4^+$ tetrahedron.

In contrast to the data discussed above, tetrachloromethane sorption to DTMA–, TTMA–, HTMA–, BDHA–, and DDPA–clay (Table II) is characterized by linear isotherms, relatively weak solute uptake, and noncompetitive sorption. In addition, it has been shown previously that the sorption of seven nonionic solutes to natural soil treated with HTMA cations decreases with increasing solute solubility (*24*). This behavior is typical of a partition process, wherein the nonionic solute distributes itself between an aqueous and organic phase in proportion to its solubility in the two phases. In addition, the log K_{oc} values given in Table II (1.26–2.07) are less than the log K_{ow} value of 2.64 for tetrachloromethane.

The difference in sorption mechanism between the two groups of organoclay complexes appears to be related to the alkyl-chain length rather than to the presence of an aryl functional group. All the organic cations that led to contaminant adsorption effects (Table I) have short alkyl functional groups (two carbon atoms or less), whereas the organic cations that caused a partition-like contaminant uptake (Table II) have at least one large alkyl functional group (12 carbon atoms or more). Therefore, the presence of one or more large alkyl groups appears to prevent the organic cations from forming a modified clay surface capable of strong adsorption. Presumably, such large chains cannot be effectively "anchored" to the clay surface (*13*) because their lack of polarity and charge prevents a strong interaction with the polar, interlamellar mineral surface. Conglomeration of these long and flexible alkyl chains produces an organic medium for solute partition (*11*). This explanation is supported by the data of Table II, which show that as the length of the cations' hydrocarbon chain increases from 12 to 16 carbon atoms (DTMA to HTMA), the sorption coefficient increases from 1.36 to 3.12 kg/L. Smaller and more rigid functional groups (e.g., methyl, ethyl, benzyl) may be expected to be tightly anchored to the clay surface. The size and rigidity of these groups prevent them from forming an effective partition medium. The modified clay surface reduces the hydrophilicity of the mineral and thereby allows the nonionic solute to compete effectively with water for adsorption.

TMA– and BTMA–clay have distinctly higher capacities for tetrachloromethane than TEA– and BTEA–clay, indicating that, in the absence of a large alkyl group, the substitution of ethyl for methyl functional groups reduces the effectiveness of the organic cation to act as an adsorbent surface at the clay–water interface. The benzyl group appears to have a similar effect as the methyl group in this regard, as evidenced by the similar sorptive capacities of the TMA–clay and BTMA–clay. The result suggests that an increase in chain length reduces the rigidity of the organic surface and consequently weakens adsorption of tetrachloromethane. While the partition effect should increase with alkyl-chain length, the ethyl group appears to be too small to form an effective partition medium.

It is also important to note the difference in the sorption of tetrachloromethane to ammonium–clay versus TMA–clay. No measurable uptake of tetrachloromethane by the ammonium–clay was observed, but tetrachloromethane was strongly adsorbed by the TMA–clay. Much like Ca^{2+} or Na^+ ions, a dipole is induced in the ammonium ion from the electric field created by the negative charge at the clay surface. As a result, the ammonium ion is strongly hydrated and significant sorption of the nonionic solute is prohibited because of the hydration effect and the absence of an organic moiety in the cation.

The data in Table II also indicate that substitution of an aromatic functional group (BDHA) or an ethylene oxide aromatic functional group (DDPA) for a methyl group in organoclays containing a large alkyl group results in a further increase in the sorption coefficient to values of 6.56 and 7.64 (log K_{oc} equal to 1.96 and 2.07), respectively, indicating that these functional groups also increase the solvency of the organic medium for tetrachloromethane. The log K_{oc} value for the sorption of tetrachloromethane to soil organic matter is estimated to be 1.9 (*2*), indicating that DTMA, TTMA, and HTMA are slightly less effective sorbent media than soil organic matter when applied to the clay in an amount equal to 7% organic carbon. However, application of BDHA and DDPA to the clay (also at 7% organic carbon) produced sorbents with an organic

phase that shows a similar partition effect as natural soil organic matter with regard to the sorption of tetrachloromethane.

The log K_{oc} value for the sorption of tetrachloromethane to the HTMA–clay used in this study compares well with the value of 1.7 for the sorption of trichloroethene to HTMA–clay (about 7% organic carbon) reported by Boyd et al. (*11*). This is not suprising given the similar water solubilities of these two solutes. The work of Boyd et al. (*11*) also indicates that the K_{oc} values of benzene and trichloroethene are a function of the amount of HTMA on the clay. At organic carbon contents greater than 13%, the K_{oc} values are comparable to heptane–water partition coefficients, which are 5–10 times greater than the K_{oc} values for soil organic matter. These differences may be attributed to the density of alkyl chains in the organic medium formed by the different amounts of HTMA incorporated into the interlamellar spaces of the clay. Thus, the closer correspondence of the K_{oc} values from Table II with K_{oc} data for natural soil organic matter can be better explained by the size and alkyl-chain density of the organic medium formed in organoclays rather than by the composition and polarity of the organic medium in comparison with soil organic matter.

Finally, these results can be related to natural soil–water systems. The organic matter fraction of natural soil has been correlated repeatedly to the sorption of nonionic organic contaminants from water (*25–30*), and the sorption process has been attributed to solute partition between water and the soil organic matter (*2–9, 31*). The data for many organoclay systems comply with these observations. Natural soil organic matter is known to be a complex mixture of macromolecular organic substances of different sizes that generally are classified as humic and fulvic acids and humin (*32*). The relatively diverse macromolecules present in natural organic matter lead to the formation of a highly amorphous organic substance, which acts as a partition medium for the sorption of nonionic organic solutes.

Acknowledgments

We thank Robert Mueller and Wesley Go for technical assistance.

Registry No. Tetrachloromethane, 56-23-5; trichloroethane, 79-01-6.

Literature Cited

(1) Stumm, W.; Morgan, J. J. *Aquatic Chemistry. An Introduction Emphasizing Chemical Equilibria in Natural Waters*; John Wiley and Sons: New York, 1981.
(2) Chiou, C. T.; Porter, P. E.; Schmedding, D. W. *Environ. Sci. Technol.* **1983**, *17*, 227.
(3) Chiou, C. T.; Shoup, T. D. *Environ. Sci. Technol.* **1985**, *19*, 1196.
(4) Chiou, C. T.; Shoup, T. D.; Porter, P. E. *Org. Geochem.* **1985**, *8*, 9.
(5) Witkowski, P. J.; Smith, J. A.; Fusillo, T. V.; Chiou, C. T. *Geol. Surv. Circ. (U.S.)* **1987**, *No. 993*.
(6) Witkowski, P. J.; Jaffé, P. R.; Ferrara, R. A. *J. Contam. Hydrol.* **1988**, *2*, 249.
(7) Smith, J. A.; Witkowski, P. J.; Chiou, C. T. *Rev. Environ. Contam. Toxicol.* **1988**, *103*, 127.
(8) Smith, J. A.; Witkowski, P. J.; Fusillo, T. V. *Geol. Surv. Circ. (U.S.)* **1988**, *No. 1007*.
(9) Smith, J. A.; Chiou, C. T.; Kammer, J. A.; Kile, D. E. *Environ. Sci. Technol.* **1990**, *24*, 676.
(10) Smith, L. W.; Bayer, D. E. *Soil Sci.* **1967**, *103*, 328.
(11) Boyd, S. A.; Mortland, M. M.; Chiou, C. T. *Soil Sci. Soc. Am. J.* **1988**, *52*, 652.
(12) Lee, J.-F.; Mortland, M. M.; Boyd, S. A.; Chiou, C. T. *J. Chem. Soc., Faraday Trans. 1* **1989**, *85*, 2953.
(13) Lee, J.-F.; Mortland, M. M.; Chiou, C. T.; Kile, D. E.; Boyd, S. A. *Clays Clay Miner.* **1990**, *38*, 113.
(14) Kleinbaum, D. G.; Kupper, L. L. *Applied Regression Analysis and Other Multivariable Methods*; Duxbury Press: North Scituate, MA, 1978.
(15) Khan, S. U. *Environ. Lett.* **1972**, *3*, 1.
(16) Hayes, M. H. B.; Pick, M. E.; Toms, B. A. *Res. Rev.* **1975**, *57*, 1.
(17) El-Dib, M. A.; Aly, O. A. *Water Res.* **1976**, *10*, 1051.
(18) Karickhoff, S. W.; Brown, D. S. *J. Environ. Qual.* **1978**, *7*, 246.
(19) Juo, A. S. R.; Oginni, O. O. *J. Environ. Qual.* **1978**, *7*, 9.
(20) Zierath, D. L.; Hassett, J. J.; Banwart, W. L.; Wood, S. G.; Means, J. C. *Soil Sci.* **1980**, *129*, 277.
(21) Senesi, N.; Testini, C. *Soil Sci.* **1980**, *130*, 314.
(22) Narine, D. R.; Guy, R. D. *Soil Sci.* **1982**, *133*, 356.
(23) Verschueren, K. *Handbook of Environmental Data on Organic Chemicals*; Van Nostrand Reinhold: New York, 1983.
(24) Lee, J.-F.; Crum, J. R.; Boyd, S. A. *Environ. Sci. Technol.* **1989**, *23*, 1365.
(25) Spencer, W. F.; Cliath, M. M.; Farmer, W. J.; Sheperd, R. A. *J. Environ. Qual.* **1974**, *3*, 126.
(26) Herbes, S. E. *Water Res.* **1977**, *11*, 493.
(27) Rao, P. S. C.; Davidson, J. M. *Water Res.* **1979**, *13*, 375.
(28) Hassett, J. J.; Means, J. C.; Banwart, W. L.; Wood, S. G.; Ali, S.; Khan, A. *J. Environ. Qual.* **1980**, *9*, 184.
(29) Hassett, J. J.; Anderson, M. A. *Environ. Sci. Technol.* **1982**, *16*, 681.
(30) Nkedi-Kizza, P.; Rao, P. S. C.; Johnson, J. W. *J. Environ. Qual.* **1983**, *12*, 195.
(31) Chiou, C. T.; Peters L. J.; Freed, V. H. *Science* **1979**, *206*, 831.
(32) Stevenson, F. J. *Humus Chemistry*; Wiley: New York, 1982.

Received for review December 1, 1989. Revised manuscript received March 13, 1990. Accepted March 22, 1990. This research was performed by the U.S. Geological Survey in cooperation with the Division of Science and Research of the New Jersey Department of Environmental Protection. The use of trade or firm names in this report is for identification purposes only and does not constitute endorsement by the U.S. Geological Survey.

Environ. Sci. Technol. 1990, 24, 1173–1179

Identification of Solubility-Controlling Solid Phases in a Large Fly Ash Field Lysimeter

Jonathan S. Fruchter,* Dhanpat Rai, and John M. Zachara

Battelle, Pacific Northwest Laboratories, Battelle Boulevard, Richland, Washington 99352

■ Samples of pore fluids and leachates were obtained from a large fly ash field lysimeter in central Pennsylvania. The fly ash in the lysimeter was usually only partially saturated, and only 0.3 pore volumes of water leached through the lysimeter during the 3-year study period. The samples were analyzed for major and trace inorganic anions and cations. The resulting analyses were modeled by using an equilibrium speciation/solubility code to test the hypothesis that the solubilities of at least some species in the fly ash leachate were controlled by solid phases. Potential solubility-controlling solids were identified for Al, Ba, Ca, Cr, Cu, Fe, S, Si, and Sr in the pore waters and leachates. Solid solutions appear to play an important role in controlling the concentrations of Ba, Sr, and Cr. The activity relationships were independent of location within the lysimeter and time of sampling. A laboratory experiment showed that equilibration times between these nine elements and their solubility-controlling solids were on the order of days or less. Geochemical reactions controlling the concentrations of As, B, Cd, Mo, and Se were not identified.

Introduction

The electric utility industry produces approximately 75 million tons of solid waste annually (*1*). This amount may double by the turn of the century. The vast majority of this waste consists of fly ash and bottom ash produced during the combustion of coal. In the United States, about 80% of these wastes are disposed of on land, either in landfills or ponds. Both the fly ash and the bottom ash are enriched in certain major and trace elements that have the potential to alter nearby groundwater and surface-water quality if released in sufficient concentrations. These elements include arsenic, boron, cadmium, chromium, copper, molybdenum, selenium, sulfur, and zinc. It is, therefore, important to understand those chemical processes in the ash/water system that control the concentrations of these elements in the resulting leachate.

A number of recent studies have concentrated on various aspects of fly ash characterization in the laboratory. These have included leaching studies (*2–5*) and mineralogical and chemical analyses (*6–9*). Much of this past work has been summarized in a recent review (*10*). Several of the leaching studies have documented solubility and adsorption phenomena that control leachate composition and have shown that different mineralogical transformations occur with time and environmental exposure.

Published accounts of fly ash leaching under field conditions are limited. In one such study of a midwestern bituminous fly ash pond, six metals (Cd, Cr, Cu, Ni, Pb, and Zn) were investigated (*11*). Possible solubility controls were identified for Cr, Cu, and Pb, including $Cr(OH)_3$, malachite [$Cu_2(OH)_2CO_3$], and $Pb(OH)_2$. Another study documented the migration of As, Cr, Mo, Pb, and Se from a lignite fly ash landfill in North Dakota (*12*). This study found elevated concentrations of all of these elements in groundwaters below the landfill.

This paper reports on the characteristics of pore waters and leachates from a large field lysimeter at the Montour Power Station, Pennsylvania, under natural rainfall conditions. The lysimeter was well instrumented and equipped with several sampling devices. Aqueous samples were obtained from different depths in the field lysimeter over a 3-year period starting in 1985, with the objectives of (1) identifying geochemical reactions controlling pore-water concentration over the study period, (2) determining whether laboratory-derived data were applicable to a field situation, and (3) identifying inadequacies in current understanding of the leaching process and in current descriptive thermodynamic constants for the solubility reactions that were postulated to occur.

A previous study (*13*) has described leachate concentrations and trends from this lysimeter.

Site Description

The Montour field lysimeter, located in central Pennsylvania, was designed to model a dry coal fly ash disposal facility (*14*). It was constructed aboveground in the shape of a truncated pyramid, with a 30.5 m × 30.5 m base and an 18.3 m × 18.3 m top. The 3.05-m-high lysimeter was constructed of 10 0.305-m layers of compacted fly ash. The fly ash was produced by the combustion of bituminous coal mined in western Pennsylvania. The side slopes were 2:1 horizontal to vertical and vegetated. The top was left bare but covered with a 10-cm layer of bottom ash to prevent wind erosion of the fly ash. A 50-cm layer of bottom ash was also placed at the bottom to facilitate drainage. The lysimeter was equipped with a leachate collection system and a pore-water sampling system, described below.

Because the lysimeter was constructed aboveground and is not irrigated, conditions are only partially saturated except after major precipitation events. Leachate is produced during only part of each year, generally from October to May. The cumulative volume of leachate that exited the base of the lysimeter over the 3-year study period amounted to only 0.3 pore volumes. Thus it seems likely that the ash is still largely unweathered, indicating that the data from the lysimeter should be suitable for comparison with data from laboratory studies performed on freshly collected ash.

Water-Sampling Procedures

Pore-water samples were obtained with ceramic porous cups installed in multiple-instrument installations or nests. In these installations, ceramic porous cups were set into slurried ash to ensure good hydraulic connection between the porous cups and the fly ash at the borehole wall. Samples were taken by first drawing water into the ceramic cups under vacuum and then pressurizing the ceramic cups from the lysimeter surface to force the water out into 1-L polyethylene bottles.

Leachate samples represented lysimeter drainage and were collected directly from a leachate drain located in the southwest corner of the lysimeter. Aliquots of both leachate and pore waters were subsequently sealed in polyethylene vials after appropriate preservation procedures and transferred to the laboratory for analysis. The sam-

0013-936X/90/0924-1173$02.50/0

pling procedures are described in greater detail elsewhere (*14*).

Solid-Sampling Procedures

Two sets of solid samples were collected. One set consisted of 10 samples from each of the individual lysimeter construction layers that were set aside in 1984 when the test cell was being constructed. These samples were stored in a field-moist condition until they were analyzed.

The second set consisted of samples from three continuous cores collected from the lysimeter in late 1987 after 3 years of exposure. The cores were collected by using a hollow-stem auger with a lined 1.5-m core barrel. Two cores collected fly ash only. The third core collected 3.05 m of fly ash and 0.45 m of the bottom ash drainage blanket at the base of the test cell. All of the core segments contained significant moisture but none were saturated. Visual inspection of these cores did not reveal any horizontal stratification of the ash. The 0.76-m core segments were capped immediately after collection, taped, and coated with paraffin wax to prevent gas or moisture exchange during shipping. The cores were shipped by overnight express in core boxes specially constructed to minimize disturbance. The cores were refrigerated in storage.

Laboratory Procedures

Extraction of Construction-Layer Samples. The 10 construction-layer samples were equilibrated in deionized/distilled water, and the solutions were analyzed for comparison with the compositions of the pore waters. Replicate 100-g samples of each construction-layer composite were placed in 250-mL plastic centrifuge tubes; 100 g of water was then added. The 1:1 mixtures were rotated on a shaker for 4 h at 25 °C, after which pH was measured on the settled suspension over a 15-min time span. The mixtures were returned to the shaker for 1 week at 25 °C and then were centrifuged at 4812*g* for 30 min. After centrifugation, the pH, Eh and conductivity of the supernatant were measured under air. The supernatant was then filtered through a prewashed 0.1-μm filter.

Core Subsampling, and Extraction and Analysis of Pore Waters. The three cores were subsampled in a glovebox under N_2 gas within 60 h of collection. Selected subsamples were taken in each core at depths of 2.5–20, 60–90, 135–165, 210–240, and 277.5–297.5 cm. Additional subsamples were taken in the deeper core at 302.5–312.5 and 312.5–327.5 cm. First, small cores of known volume were removed for determination of bulk density and moisture content. Then the rest of the subsample was homogenized, and two 200-g samples were put in individual 250-mL plastic centrifuge tubes. One of these 200-g samples was then freeze-dried, and the other was used in extracting pore water, as described below. The remaining core material was archived.

Freon 113 (200 g) was added to the samples, which were centrifuged for 4 h at 4812*g* under N_2 atmosphere to displace pore water (*15*). The displaced water was recovered from the surface of the Freon and its mass recorded.

Analysis of Water Samples. The various types of water samples obtained by the methods described above are summarized in Table I. The samples were analyzed for 23 elements and species by a combination of atomic absorption spectroscopy (AAS), inductively coupled plasma-atomic emission spectroscopy (ICP-AES), ion chromatography (IC), and specific ion electrodes (SIE). Ranges of data for each analyte are shown in Table II. The samples represent various types of samples from various locations within the lysimeter taken over a 3-year period. Most of the analytes range over at least 2 orders of magnitude in aqueous concentrations.

Table I. Summary of Aqueous Samples Used in This Study

sample name	sample type	location
AB	pore water	sampler nest AB
CD	pore water	sampler nest CD
composite	pore water	composite of sampler nests AB and CD
leachate	leachate	leachate collection cistern
construction layers	1:1 fly ash/water extract	samples of fly ash layers used in lysimeter construction
extracted pore fluid	pore water extracted by immiscible displacement	fly ash cores taken from the lysimeter 3 years after construction

Table II. Ranges of Concentrations for Montour Lysimeter Aqueous Samples (in mg/L Except pH)[a]

analyte	range	analyte	range
Al	0.40–9.8	K	1.4–740
As	0.007–0.78	Mg	0.3–42
B	0.27–31	Mn	0.006–27
Ba	<0.007–0.27	Mo	0.15–48
CO_3^{2-}	25–210	Na	0.56–210
Ca	72–800	Se	<0.004–0.79
Cl	1.5–99	Si	0.70–18
Cr	0.041–3.2	SO_4^{2-}	140–9600
Cd	<0.004–0.14	Sr	0.55–11
Cu	<0.008–0.50	Zn	<0.002–24
F	0.08–11	pH	6.14–10.2
Fe	<0.01–0.56		

[a] For 92 samples.

Geochemical Calculations

Our first strategy for interpreting the concentration data for the aqueous samples from the lysimeter was to look for evidence of elements whose concentrations appeared to be controlled by solubility reactions. Elements that could not be interpreted in this simple fashion would then be interpreted in terms of adsorption or kinetic controls. To this end, the analytical data defining the chemical composition (pH, major and minor cations and anions) of each individual sample were input to the geochemical code MINTEQ (*16*) for the purpose of calculating ionic strength, ion speciation, single ion activity coefficients, single ion activities for aqueous solute species, and ion activity products and saturation indexes for mineral solids. The use of MINTEQ for these purposes as well as other applications is described in two user's manuals (*17*, *18*).

Results

The discussion that follows emphasizes the elements Al, Ba, Ca, Cr, Cu, Fe, S, Si, and Sr, for which the aqueous concentrations can be interpreted or related to specific solubility reactions. Those elements (As, B, Cd, Mo, and Se) for which controlling solubility reactions were not identified are also briefly discussed.

Major Ash Constituents. Aluminum. Measured Al concentrations varied by more than 2 orders of magnitude in the various samples from the large field lysimeter site. Previous laboratory studies (*5*) implied that in many fly ashes Al is controlled by the solubility of $Al(OH)SO_4$ when pH values are less than ~6.0, by amorphous $Al(OH)_3$ when pH is between ~6.0 and 9.0, and by crystalline $Al(OH)_3$ (gibbsite) when pH is greater than 9.0. Since the pH of all samples from the field lysimeter was above 6.0, it was expected that amorphous $Al(OH)_3$ and gibbsite would

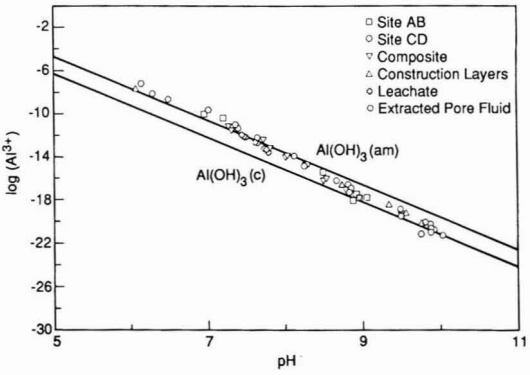

Figure 1. Plot of calculated Al^{3+} activity vs pH for various fly ash lysimeter samples, compared to activities predicted (solid lines) from control by crystalline $Al(OH)_3$ (gibbsite) and amorphous $Al(OH)_3$.

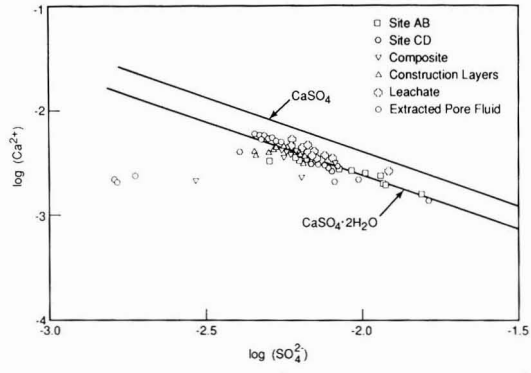

Figure 2. Plot of calculated log Ca^{2+} activity vs calculated log SO_4^{2-} activity for various fly ash lysimeter samples, compared to activities predicted (solid line) from control by $CaSO_4$ (anhydrite) and $CaSO_4 \cdot 2H_2O$ (gypsum).

control the solubility of Al. The computed Al^{3+} activities (Figure 1) varied as a smooth function of pH, regardless of the origin of samples. Comparison of the observed Al^{3+} activities with those predicted to be in equilibrium with the $Al(OH)_3$(am) and $Al(OH)_3$(c) (Figure 1) indicated that the activities observed at pH values of less than ~8.5 and greater than 9 were similar to those in equilibrium with $Al(OH)_3$(am) and $Al(OH)_3$(c), respectively. These results were consistent with the experimental data for fly ashes reported by several authors (*5*, *19*, *20*).

Calcium and Sulfur. Ca and S were the major soluble elements in the pore waters and leachates. Analytical measurements showed that reduced S species (SO_3^{2-}, $S_2O_3^{2-}$) were present in negligible quantities and that SO_4^{2-} was the dominant species. The presence of SO_4^{2-} as the dominant species was consistent with the oxidizing redox potentials and the presence of other highly oxidized aqueous species, such as CrO_4^{2-}. Concentrations of SO_4^{2-} were high, with an average concentration of ~0.02 M, commensurate with the high S concentrations typically present in bituminous coals and their ashes. Calcium concentrations in fly ashes may be controlled by $CaSO_4/CaSO_4 \cdot 2H_2O$, $CaCO_3$, or $Ca(OH)_2$ (*10*). Among these compounds, $Ca(OH)_2$ is expected only at very high pH values (greater than ~12). Calcium activities were essentially independent of pH in the measured pH range (6–10), suggesting that $CaCO_3$ and $Ca(OH)_2$ are not the solubility-controlling solids. The plot of Ca^{2+} activity as a function of SO_4^{2-} activity (Figure 2) shows that Ca^{2+} activity decreased as sulfate activity increased, as would be expected if Ca concentrations were controlled by calcium sulfate. Both $CaSO_4$ and $CaSO_4 \cdot 2H_2O$ have been identified in fly ashes by many researchers (*6*, *10*, *21*, *22*). The Ca^{2+} activities observed were similar to those predicted from $CaSO_4 \cdot 2H_2O$ (Figure 2). Because $CaSO_4 \cdot 2H_2O$ (gypsum) rather than $CaSO_4$ (anhydrite) usually precipitates below 42 °C from aqueous solutions of an ionic strength less than that of seawater (*23*), this result was expected.

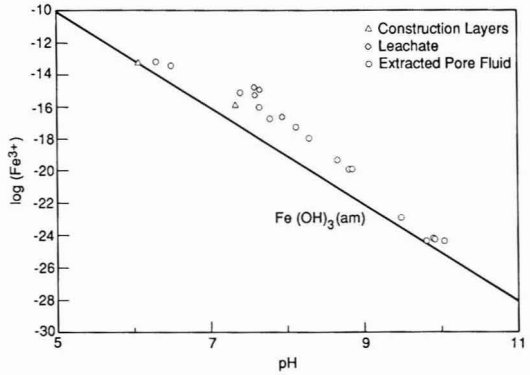

Figure 3. Plot of calculated log Fe^{3+} activity vs pH for various fly ash lysimeter samples, compared to activities predicted (solid line) from control by amorphous $Fe(OH)_3$.

Iron. Aqueous Fe was present in measurable quantities only in the leachate, construction layers, and extracted pore water; it was below detection limits in all other samples. Speciation measurements made by ion chromatography indicated that all of the detectable Fe in these samples was in the Fe(III) state. The similarity of the measured Fe^{3+} activities to those calculated in equilibrium with $Fe(OH)_3$(am) (Figure 3) in some of the samples and the reported presence of amorphous $Fe(OH)_3$(am) in other fly ashes (*6*) together suggest that Fe concentrations may be controlled by $Fe(OH)_3$(am). However, between pH 7 and 9, the calculated iron activities are almost 2 orders of magnitude higher than those expected from reported values for $Fe(OH)_3$(am). Possible explanations for this discrepancy are (1) that despite the fact that 0.0030-μm filters were used on the construction layer and extracted fluid samples (0.1 μm was used on the leachate sample), some colloidal iron still remained in the filtrates, and (2) that the published thermochemical data for amorphous iron hydroxides are not accurate.

Silicon. Si was one of the major matrix elements of the fly ash. Aqueous Si concentrations were measured in selected samples only (composite pore-water samples, extracted pore water, leachate, and construction-layer samples). The computed aqueous activities of H_4SiO_4 (Figure 4) indicated that SiO_2 (amorphous or quartz) was not controlling the Si concentrations in the test-cell pore waters. The similarity of the measured activities to those predicted in equilibrium with wairakite (Figure 5) suggested that wairakite might be the solubility-controlling aluminosilicate. Wairakite ($CaAl_2Si_4O_{12} \cdot 2H_2O$) is the Ca analogue of the more common sodium zeolite, analcite. It has been reported in altered/weathered volcanic tuff. Whether this solid can or will form in utility fly ash is not known at present. Other studies have suggested other aluminosilicates, such as proto-imogolite (*6*), laumontite (*10*), or mullite (*11*).

Minor Ash Constituents. Barium and Strontium. Ba and Sr form sparingly soluble compounds with carbo-

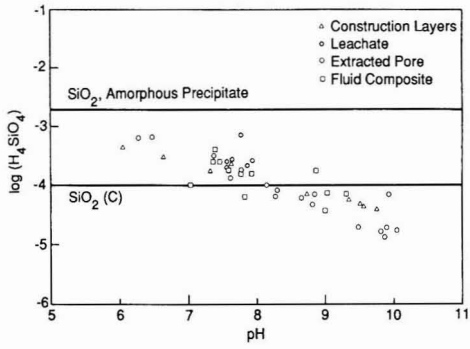

Figure 4. Plot of calculated log H_4SiO_4 activity for various fly ash lysimeter samples, compared to activities predicted (solid line) from control by SiO_2(c) (quartz) and amorphous SiO_2.

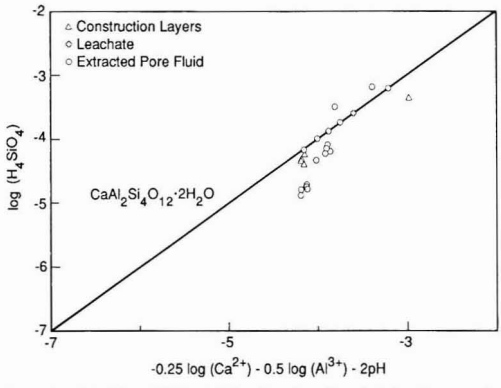

Figure 5. Plot of log H_4SiO_4 activity of various fly ash lysimeter samples vs the logarithm of the equilibrium expression for the formation of $CaAl_2Si_4O_{12}{\cdot}2H_2O$ (wairakite). Only those samples from Figure 4 that had measured Al^{3+} concentrations above the detection limit are included in this figure.

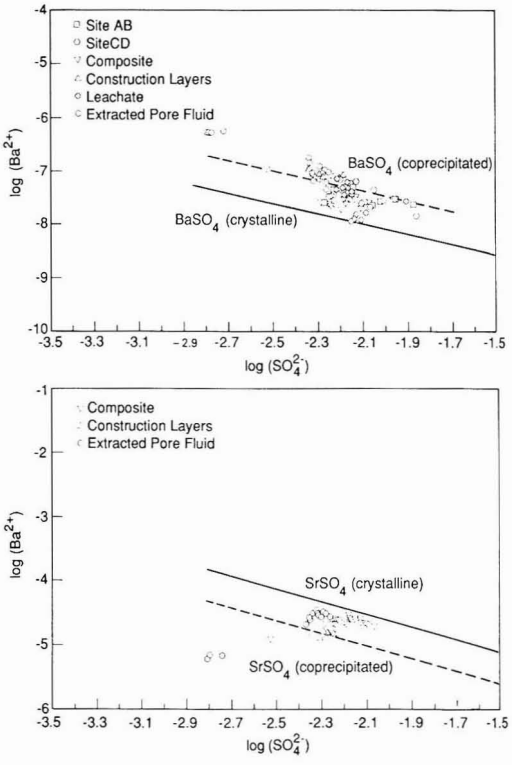

Figure 6. Plots of calculated log Ba^{2+} activity and calculated log Sr^{2+} activity vs calculated log SO_4^{2-} activity for various fly ash lysimeter samples, compared to activities predicted (solid lines) from control by $BaSO_4$(c) (barite) and $SrSO_4$(c) (celestite).

nates and sulfates. The total concentrations of Ba varied by about an order of magnitude, while those of Sr were nearly constant in the pore waters and leachates. The concentrations of Ba and Sr were essentially independent of pH throughout the measured pH range, suggesting that $BaCO_3$ and $SrCO_3$ were not the solubility-controlling solids. Because the dominant pore-water anion was SO_4^{2-}, the activities of Ba^{2+} and Sr^{2+} were plotted as a function of the activity of SO_4^{2-} (Figure 6) to determine if celestite ($SrSO_4$) and barite ($BaSO_4$) control pore-water concentrations. The results for Ba showed that Ba^{2+} activities were up to an order of magnitude higher than those in equilibrium with $BaSO_4$(c). In addition, the results for Sr^{2+} in Figure 6 showed that Sr^{2+} was slightly undersaturated with respect to celestite ($SrSO_4$). These results for Ba and Sr are similar to those reported for a large number of unweathered fly ashes (*5*).

Recent experiments in our laboratory with the freshly coprecipitated (Ba,Sr)SO_4 also showed a similar behavior. This laboratory-observed behavior was found to be not the result of thermodynamic equilibrium with a (Ba,Sr)SO_4 solid solution, but instead a result of perhaps a stronger interaction between Ba and SO_4 than between Sr and SO_4. In the Ba-substituted $SrSO_4$, this stronger interaction would reduce the solubility of $SrSO_4$, and in Sr-substituted $BaSO_4$, it would increase the solubility of $BaSO_4$. With aging of the coprecipitates, however, the Ba and Sr activities were seen to approach that of the pure end members. Total Ba and Sr were present in equimolar ratios in the ash. The fact that the observed Ba and Sr behavior in lysimeter samples was similar to the 14-day equilibrated–coprecipitated $(Ba_{0.5}Sr_{0.5})SO_4$ (Figure 6) indicates that the lysimeter fly ash was relatively unweathered. The results collectively show that Ba and Sr concentrations are controlled by their sulfate solids, currently more likely by coprecipitated (Ba,Sr)SO_4 than by $BaSO_4$ or $SrSO_4$.

Chromium. Oxidation-state analyses of the samples showed that the soluble Cr was present as Cr(VI). Because of the very high sulfate concentrations and near-neutral to alkaline pH values, adsorption was not expected to control Cr concentrations. Studies have shown that CrO_4^{2-} adsorption is significantly depressed in the presence of SO_4 (*24*). It has also been shown that $BaCrO_4$ and Ba(S,Cr)O_4 have relatively low solubilities and rapid precipitation/dissolution kinetics, and that they could form and control Cr(VI) concentrations in geologic environments (*25*). These solids may be important in the large field lysimeter, where there are significant total concentrations of Ba and SO_4^{2-}. A comparison of measured CrO_4^{2-} activity with that in equilibrium with $BaCrO_4$ (Figure 7) showed that $BaCrO_4$ was not the solubility-controlling solid. The reported results (*25*) demonstrated that Ba(S,Cr)O_4 was more stable than $BaCrO_4$. Additionally, this solid solution was found to control Cr(VI) levels in an oxidizing SO_4^{2-}-containing soil. To evaluate whether Ba(S,Cr)O_4 is the solubility-controlling solid, the specific composition of the Ba(S,Cr)O_4 in the ash must be known. At present, techniques are not available to characterize the small quantities of Ba(S,Cr)O_4 in the fly ash.

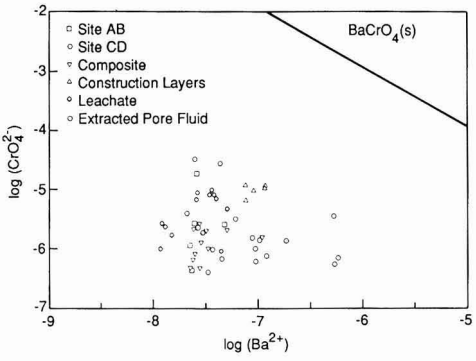

Figure 7. Plot of calculated log CrO_4^{2-} activity vs calculated log Ba^{2+} activity for various fly ash lysimeter samples, compared to activities predicted (solid line) from control by $BaCrO_4$(s).

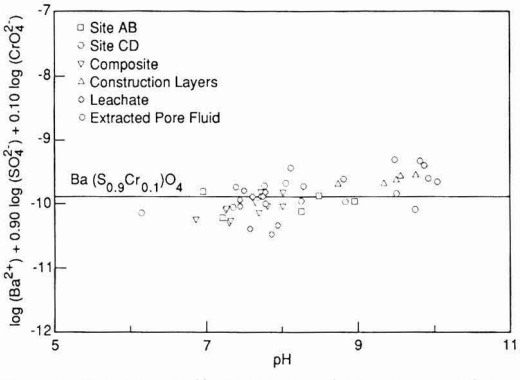

Figure 8. Plot of [log (Ba^{2+}) + 0.9 log (SO_4^{2-}) + 0.1 log (CrO_4^{2-})] vs pH observed in different solutions. The solid line is based on activities in equilibrium with $Ba(S_{0.9}Cr_{0.1})O_4$ reported by Rai et al. (*25*).

Figure 8 shows a $Ba(S,Cr)O_4$ solid solution that, if present, could be controlling the chromate concentrations. The various aqueous analyses could be fit by solid-solution composition of $Ba(S_{0.9}Cr_{0.1})O_4$. Whether this solid solution in fact controlled the aqueous Cr(VI) concentrations in Montour samples could not be definitely assessed with this set of data. The $Ba(S_{0.9}Cr_{0.1})O_4$ solid solution is a plausible solubility control because the large variability in Cr(VI) concentrations as a function of depth, time, and pH is well explained by this single hypothesized solid phase (Figure 8). There was also enough Ba, Cr, and SO_4^{2-} present in the ash that $Ba(S_{0.9}Cr_{0.1})O_4$ could form.

One study of fly ash disposal in a marine environment showed the Cr to be present in that system largely as Cr(III) (*26*). Studies have shown (*25*) that Cr(III) in fly ash systems generally forms solid solutions with iron hydroxides [$(Fe,Cr)(OH_3)$]. These solid solutions show very low solubilities ($<10^{-7}$ M) at the pH levels of the samples used in this study. Therefore, very low leachate Cr concentrations can be expected in those fly ash systems where Cr(III) is the major redox species.

Copper. Detectable aqueous Cu concentrations were observed in the pore-water sampler nest composite samples, the construction-layer samples, and pore waters from the ash cores. Tenorite (CuO) and malachite [$Cu_2(OH)_2CO_3$] have been predicted to be present in fly ash samples (*20*, *27*). It has been reported (*10*) that under oxidizing conditions, like those present in the field lysimeter, and in the pH range measured at the test cell, CuO is the most likely solubility-controlling phase among the

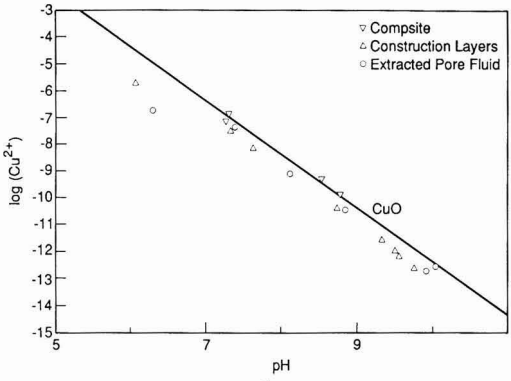

Figure 9. Plot of calculated log Cu^{2+} activity vs pH for various fly ash lysimeter samples, compared to activities predicted (solid line) from control by CuO (tenorite).

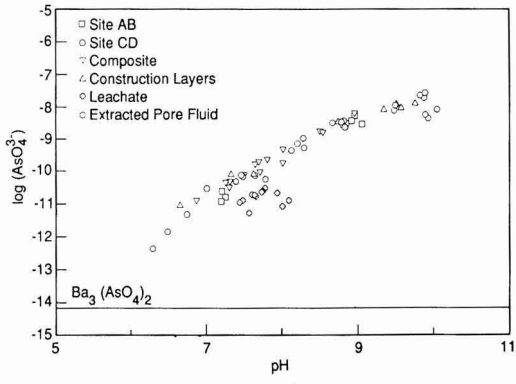

Figure 10. Plot of calculated log AsO_4^{3-} activity vs pH for various fly ash lysimeter samples, compared to activities predicted (solid line) from control by $Ba_3(AsO_4)_2$ when Ba^{2+} is fixed at $10^{-7.5}$ M.

solids that may be present in near-surface geologic environments [the others are $Cu_4SO_4(OH)_6$, $Cu_2(OH)_2CO_3$, and $Cu(OH)_2$]. CuO has also been reported as a common ore mineral in oxidized systems (*23*). These findings, along with the fact that measured Cu^{2+} activities are similar to those predicted from CuO (Figure 9), indicate that the aqueous Cu concentrations in the field lysimeter samples were controlled by CuO (tenorite). Our extensive laboratory studies (unpublished results) with four different fly ashes that were equilibrated at different pH values with and without the addition of CuO and Cu^{2+} also indicate that CuO is the solubility-controlling solid.

Other Trace Elements. In addition to the elements discussed above, aqueous concentrations of several other trace elements (As, B, Cd, Mo, and Se) were also measured. Using the existing thermochemical data, attempts were made to determine whether their concentrations could be related to precipitation/dissolution reactions. These attempts were unsuccessful. Therefore, it was not clear whether the aqueous concentrations of these elements were controlled by precipitation/dissolution, adsorption/desorption, or rates of dissolution of fly ash matrix.

Calculations using the standard redox potentials for As(III) and As(V) suggested that As should be in the As(V) state at the Eh levels found in the test cell solutions. Speciation measurements have not been performed to test this hypothesis. Barium arsenate $[Ba_3(AsO_4)_2]$ has been proposed as a solubility-controlling phase for As(V) (*28*). However, the plots of AsO_4^{3-} activity against pH in Figure

Table III. Summary of Inferred Solubility-Controlling Solids

element	solubility-controlling solid: formula	solubility-controlling solid: name
Al	$Al(OH)_3$(am) (pH 6–9)	amorphous aluminum hydroxide
	$Al(OH)_3$(c) (pH >9)	gibbsite
Fe	$Fe(OH)_3$(am)	amorphous ferric hydroxide
Ca,S	$CaSO_4 \cdot 2H_2O$	gypsum
Ba,Sr	$(Ba,Sr)SO_4$	barium and strontium coprecipitates
Cu	CuO(c)	tenorite
Cr	$Ba(S,Cr)O_4$	barium sulfate/barium chromate solid solution

10 do not appear to support that hypothesis for these samples. Similar results were reported by another study (*29*).

No conclusive statements regarding the mechanisms that control Cd behavior can be made. The observed aqueous concentrations of Cd were near their detection limits and were similar to those reported in a previous study of a large number of fly ashes (*5*).

Measured B, Mo, and Se concentrations were well above detection limits, varied widely, and were essentially independent of pH. The estimated thermochemical data for several borate minerals (pinnoite, inderite, inyoite, colemanite, inderborite, hungchaoite, borax, sborgite, McAllisterite, kaliborite, and nobleite) has shown that these B minerals are very soluble and could not control B concentrations in the field lysimeter (*30*). The observed B concentrations fell within the range of values for B reported for a large number of fly ash extracts (*5*). In the case of Mo, powellite ($CaMoO_4$) appears to control Mo concentrations in hot-water extracts of many fly ashes (*5*). However, the observed activities of MoO_4^{2-} in the large field lysimeter samples were about an order of magnitude higher than the activities in equilibrium with $CaMoO_4$, suggesting that $CaMoO_4$ was not the solubility-controlling solid. The mechanisms that may control B, Mo, and Se concentrations are not understood.

Summary of Results. Collectively, these results indicate that the observed aqueous concentrations of Al, Ba, Ca, Cr, Cu, Fe, S, Si, and Sr were controlled by solubility phenomena. Regardless of the origin of the aqueous samples (i.e., their location, depth, and when they were taken at the large field lysimeter site), the aqueous concentrations of these elements in all of these samples were explained by specific solubility reactions. The solubility-controlling solids for different elements are listed in Table III. To draw definite conclusions regarding these inferred solid phases, further experiments must demonstrate their existence. Plausible geochemical reactions that could control the aqueous concentrations of As, B, Cd, Mo, and Se were not identified.

Discussion

The solubility controls identified in this paper for various elements were based on matching calculated single ion activities for elements with activities expected in equilibrium with different solid phases. Such evidence is by its nature circumstantial. Therefore, this type of analysis should be considered as a guide to further experimentation to confirm the presence of these solid phases, rather than as a definitive proof. This confirmation can be done by either direct or indirect methods. Direct methods include X-ray diffraction and various electron spectroscopies. Indirect methods include observing the pH behavior of the element over a wider pH range or approaching equilibrium for the proposed solid in the sample from both oversaturation and undersaturation. In most cases, indirect methods will be most applicable because trace-element solids are present in low concentrations.

Hypothesized reactions pertaining to the solubility-controlling solids have been discussed in the previous section. In inferring that the concentrations of several elements (e.g., Al, Ba, Ca, Cu, Fe, S, Sr) are controlled by solubility limits, it was assumed that the observed elemental concentrations were governed by equilibrium reactions and that the solubility-controlling solids were present in the ash. Before the conclusions can be relied upon, the validity of these assumptions must be ascertained.

Most of the solubility-controlling solids expected to be present in the Montour ash are sulfate and hydroxide compounds (Table III), which are known to have rapid precipitation/dissolution kinetics. Most environmentally important aqueous complexation reactions that would affect the final concentrations in equilibrium with solubility-controlling solids are also rapid. Therefore, it is reasonable to hypothesize that equilibrium reactions control the aqueous concentrations of elements contained in sulfate and hydroxide compounds. The validity of this equilibrium assumption was tested through laboratory batch equilibration experiments of the construction-layer samples. As can be seen by examination of Figures 1–10, solubility reactions that controlled aqueous concentrations in the lysimeter pore waters developed in the laboratory in 7 days or less.

Conclusions

A variety of solid and aqueous samples from a large field lysimeter site were analyzed, and the resulting data were modeled by using an equilibrium geochemical code (MINTEQ). Despite the caveats discussed in the preceding section, several conclusions are supported by the results of these studies.

The concentrations of Al, Fe, Cu, S, Ba, Sr, Cu, and Cr appear to be determined by solubility-controlling solids. Solid solutions appear to play an important role in controlling the concentrations of Ba, Cr, and Sr. Geochemical reactions controlling the aqueous concentrations of As, B, Cd, Mo, and Se were not identified. For elements for which a solubility control is hypothesized, the different types of aqueous samples all show similar activity relationships, regardless of location, depth, time of sampling, or equilibration time.

Registry No. Al, 7429-90-5; As, 7440-38-2; B, 7440-42-8; Ba, 7440-39-3; Zn, 7440-66-6; Ca, 7440-70-2; Cl, 7782-50-5; Cr, 7440-47-3; Cd, 7440-43-9; Cu, 7440-50-8; F, 7782-41-4; Fe, 7439-89-6; K, 7440-09-7; Mg, 7439-95-4; Mn, 7439-96-5; Mo, 7439-98-7; Na, 7440-23-5; Se, 7782-49-2; Si, 7440-21-3; Sr, 7440-24-6.

Literature Cited

(1) Murarka, I. P.; McIntosh, D. A. *Solid Waste Environmental Studies (SWES): Description, Status, and Available Results*; EPRI EA-5322-SR; Electric Power Research Institute: Palo Alto, CA, 1987.

(2) Warren, C. J.; Dudas, M. J. *J. Environ. Qual.* **1984**, *13*, 530–538.

(3) Theis, T. L.; Wirth, J. L. *Environ. Sci. Technol.* **1977**, *11*, 1096–1100.

(4) Roy, W. R.; Griffin, R. A.; Dickerson, D. R.; Schuller, R. M. *Environ. Sci. Technol.* **1984**, *18*, 734–739.

(5) Ainsworth, C. C.; Rai, D. *Chemical Characterization of Fossil Fuel Wastes*; EPRI EA-5321; Electric Power Re-

search Institute: Palo Alto, CA, 1987.
(6) Warren, C. J.; Dudas, M. J. *J. Environ. Qual.* **1985**, *14*, 405-410.
(7) Bauer, C. F.; Natusch, D. F. S. *Environ. Sci. Technol.* **1981**, *15*, 783-788.
(8) Hansen, L. D.; Silberman, D.; Fisher, G. L. *Environ. Sci. Technol.* **1981**, *15*, 1057-1062.
(9) Mattigod, S. V.; Ervin, J. O. *Fuel* **1983**, *62*, 927-931.
(10) Rai, Dhanpat; Ainsworth, C. C.; Eary, L. E.; Mattigod, S. V.; Jackson, D. R. *Inorganic and Organic Constituents in Fossil Fuel Combustion Residues. A Critical Review*; EPRI EA-5176; Electric Power Research Institute: Palo Alto, CA, 1987; Vol. 1.
(11) Theis, T. L.; Richter, R. O. *Environ. Sci. Technol.* **1979**, *13*, 219-224.
(12) Groenewald, G. H.; Hassett, D. J.; Koob, R. D.; Manz, O. E. In *Fly Ash and Coal Conversion By-Products: Characterization, Utilization and Disposal I*; McCarthy, G. J., Lauf, R. J., Eds.; Materials Research Society: Pittsburgh, PA, 1985; Vol. 43, pp 213-226.
(13) Villaume, J. F.; Bell, J. W.; LaBuz, L. L. In *Fly Ash and Coal Conversion By-Products: Characterization, Utilization and Disposal IV*; McCarthy, G. J., Glasser, F. P., Roy, D. M., Hemmings, R. T., Eds.; Materials Research Society: Pittsburgh, PA, 1988; Vol. 133, pp 325-332.
(14) Rehm, B. W.; Christel, B. J.; Stolzenburg, T. R.; Nichols, D. G. *Field Evaluation of Instruments for the Measurement of Unsaturated Hydraulic Properties of Fly Ash*; EPRI EA-5011; Electric Power Research Institute: Palo Alto, CA, 1987.
(15) Kinniburgh, D. G.; Miles, D. L. *Environ. Sci. Technol.* **1983**, *17*, 362-368.
(16) Felmy, A. R.; Girvin, D. C.; Jenne, E. A. *MINTEQ—A Computer Program for Calculating Aqueous Geochemical Equilibria*; EPA 600/3/84/032; U.S. Environmental Protection Agency, Office of Research and Development: Athens, GA, 1984.
(17) Brown, D. S.; Allison, J. D. *MINTEQ A1, An Equilibrium Metal Speciation Model: User's Manual*; EPA 600/3-87/012; U.S. Environmental Protection Agency, Athens Environmental Research Laboratory: Athens, GA, 1987.
(18) Peterson, S. R.; Hostetler, C. J.; Deutsch, W. J.; Cowan, C. E. *MINTEQ User's Manual*; NUREG/CR-4808 (PNL-6101); U.S. Nuclear Regulatory Commission: Washington, DC, 1987.
(19) Roy, W. R.; Griffin, R. A. *Environ. Sci. Technol.* **1984**, *18*, 739-742.
(20) Talbot, R. W.; Anderson, M. A.; Andren, A. W. *Environ. Sci. Technol.* **1978**, *12*, 1056-1062.
(21) Simons, H. S.; Jeffery, J. W. *J. Appl. Chem.* **1960**, *10*, 328-336.
(22) Scheetz, B. E.; White, W. B. In *Fly Ash and Coal Conversion By-Products: Characterization, Utilization, and Disposal I*; McCarthy, G. J., Lauf, R. J., Eds.; Materials Research Society: Pittsburgh, PA, 1985; Vol. 43, pp 53-60.
(23) Mason, B.; Berry, L. G. *Elements of Mineralogy*; W. H. Freeman & Co.: New York, 1968.
(24) Zachara, J. M.; Girvin, D. C.; Schmidt, R. L.; Resch, C. T. *Environ. Sci. Technol.* **1987**, *21*, 589-594.
(25) Rai, D.; Zachara, J. M.; Eary, L. E.; Ainsworth, C. C.; Amonette, J. E.; Cowan, C. E.; Szelmeczka, R. W.; Resch, C. T.; Schmidt, R. L.; Girvin, D. C.; Smith, S. C. *Chromium Reactions in Geologic Materials*; EPRI EA-5741; Electric Power Research Institute: Palo Alto, CA, 1988.
(26) Hjelmar, O. In *Proceedings of the International Conference on Coal Fired Power Plants and the Aquatic Environment Copenhagen, Denmark*; International Association of Water Pollution Research: London, 1982.
(27) Theis, T. L.; Halvorsen, M.; Levein, A.; Stankunas, A.; Unites, D. Fly Ash Leachate Attenuation Mechanisms. Draft report; TRC Environmental Consultants, Inc: East Hartford, CN, 1982.
(28) Wageman, R. *Water Res.* **1978**, *12*, 139-145.
(29) Turner, R. R. *Environ. Sci. Technol.* **1981**, *15*, 1062-1066.
(30) Mattigod, S. V. *Soil Sci. Soc. Am. J.* **1983**, *47*, 654-655.

Received for review October 31, 1989. Accepted March 19, 1990. We gratefully acknowledge the Pennsylvania Power and Light Co. for their cooperation and assistance throughout this project. The research was funded by the Electric Power Research Institute, Inc. (EPRI) under Contract RP2485-08, "Leaching Chemistry".

Determination of Polycyclic Aromatic Hydrocarbons in Urban Street Dusts and Their Source Materials by Capillary Gas Chromatography

Hideshige Takada,* Tomoko Onda, and Norio Ogura

Department of Environmental Science and Conservation, Faculty of Agriculture, Tokyo University of Agriculture and Technology, Fuchu, Tokyo 183, Japan

■ Molecular distributions of polycyclic aromatic hydrocarbons (PAHs) in street dust samples collected from the Tokyo metropolitan area were determined by capillary gas chromatography following HPLC fractionation. Sixty-four compounds including three- to six-ring PAHs and sulfur heterocyclics were identified by capillary GC/MS. Total PAH concentrations were in the range of a few micrograms per gram of dust. The source materials (automobile exhaust, asphalt, fuel-oil combustion products) were also analyzed. The PAH profile, especially relative abundance of alkyl-PAHs and sulfur-containing heterocyclics, indicated that PAHs in the street dusts on the heavily trafficked streets are strongly affected by automobile exhausts and those in the residential area have a somewhat more significant contribution from combustion products in stationary sources. With both types of dusts, asphalt is thought to contribute only a minor part of their PAHs.

Introduction

Polycyclic aromatic hydrocarbons (PAHs) have long been recognized as hazardous environmental chemicals. Some PAHs are known to be carcinogenic to man (*1*). PAHs are mainly formed during the combustion of coal and petroleum (*2*) and are widely distributed in soils and sediments throughout the world (*3-9*). Their sources and transport mechanisms have been the subject of a number of recent investigations (*10-19*). On urban street surfaces, PAHs of various origins (e.g., weathered materials of street surfaces, automobile exhaust, lubricating oils, gasoline, diesel fuel, tire particles, and atmospherically deposited materials) are present as street dust. The street dust material is washed from roads during heavy rain storms and transported to rivers, wastewater treatment plants, and estuaries (*17*, *18*). Therefore, street dust is considered to be one of the important sources of PAHs in the aquatic environment, but the data available on PAHs in street dusts are limited (*14*, *20*, *21*). In particular, their detailed molecular compositions were rarely given (*14*, *20*), although PAH profiles are useful to estimate their sources and fates. For example, Wakeham et al. (*14*) extensively characterized PAH profiles for lacstrine sediments, street dust, and plausible source materials (asphalt, automobile exhaust,

0013-936X/90/0924-1179$02.50/0

tire-wear particles) in Switzerland. On the basis of a comparison of their PAH profiles, they suggested that asphalt particles in street dust may be an extremely important contributor to the PAH content of lake sediments. There are not, however, any other available data on the detailed molecular compositions of PAHs in street dusts. This can probably be ascribed to analytical difficulties.

The detailed molecular compositions of PAHs in environmental samples are generally determined by high-resolution gas chromatography, whose utility for estimating the sources and fates of PAHs has been demonstrated through many studies (*3*, *11–15*). The capillary gas chromatographic determination, however, requires prior thorough purification of an aromatic fraction. Normal-phase open-column liquid chromatography (LC) on silica gel is conventionally used to isolate the aromatic fraction from sediment extracts (e.g., refs 20 and 22). But this technique is time consuming and inadequate to purify the aromatic fraction of street dusts, in which PAHs are present at trace levels in the highly complex mixture of polar and apolar materials derived from automobile exhaust, asphalt, lubricating oils, gasoline, diesel fuel, tire particles, and atmospheric fallout (*23*). Recently, normal-phase HPLC using a cyano/amino bonded silica stationary phase, which has a larger capacity than a conventional silica gel open column, has been developed (*24*, *25*) and used to isolate PAH fractions from sediment extracts (*26*, *27*) and aerosols in a roadway tunnel (*28*). In the present study, the HPLC method was applied to the purification of PAHs in extracts from street dust samples.

Polycyclic aromatic hydrocarbons in street dust samples from the Tokyo metropolitan area as well as the source materials (automobile exhaust, asphalt, fuel-oil combustion products) were determined by capillary gas chromatography following fractionation by normal-phase HPLC on cyano/amino bonded silica stationary phase. The sources of PAHs in dusts are discussed on the basis of their PAH profile, especially relative abundances of alkyl-PAHs and sulfur-containing heterocyclics.

Experimental Section

Sample Collection. Street dusts were taken from a heavily trafficked street (Setagaya Avenue; 36 000 vehicles/day) and a residential street (Seijo-gakuen cho; ca. 10 vehicles/day) in Tokyo, Japan. Both sampling sites are paved by asphalt. To examine the contribution of asphalt to PAHs in street dusts, street dust samples were also taken from both an asphalt-paved part and a concrete-paved part of a heavily trafficked street (National Road Route 20; 64 000 vehicles/day) in Tokyo. Street dust samples were collected on prebaked glass-fiber filters (TOYO Roshi GB100R; nominal pore size 0.6 μm) by vacuuming the road surface (160 cm^2) with a constant flow rate of 15 L/min. The street dusts were collected at 1-month intervals from January to September 1988. Automobile exhaust samples were taken from six types of automobiles of Japanese make. Automobiles A–E were equipped with diesel engines having piston displacements of 2300, 1500, 3300, 6400, and 14 000 cc, respectively. Automobile F was equipped with a spark-ignition engine (1600 cc). On the sample collection, the engines were rotated at ca. 3000 rpm with no load. The exhaust from each automobile was introduced into a 300-L chamber and the automobile exhaust particles were collected on the prebaked glass-fiber filter by 30 min of vacuuming (15 L/min) with the same vacuum cleaner as used for sampling of the street dust. A combustion product of fuel oil was taken from a steam generator. Soot from the steam generator was collected on the glass-fiber filter by similarly vacuuming the smoke near the top of a 20-m chimney. Three asphalt samples were taken by breaking pieces from the surfaces of the asphalt-paved streets. The back sides of the broken asphalt were ground with a stainless steel file, with care taken to avoid contamination of street dust from the surfaces of the piece.

Extraction and Isolation Procedures. The street dust (ca. 2 g) together with the glass-fiber filter was Soxhlet extracted in a prebaked glass-fiber thimble with 500 mL of benzene for 18 h. The source materials were similarly Soxhlet extracted. The cycling rate for the extraction was 30 min/cycle. The extracts were concentrated to 5 mL in a rotary evaporator at 30 °C and then applied to a Florisil column (60–100 mesh; Wako Fine Chemicals; 1.0 cm i.d. × 8 cm). Prior to use, Florisil had been baked at 450 °C, activated at 155–160 °C for 5 h, and stored in benzene. PAHs were eluted from the column with 30 mL of benzene.

The benzene eluate from the Florisil column was evaporated just to dryness under reduced pressure below 30 °C, and then the residue was dissolved in 250 μL of *n*-hexane/dichloromethane (7:3). Sample aliquots of 50–240 μL were then injected into the HPLC. HPLC conditions as reported by Killops and Readman (*26*) were modified and used in this study. HPLC fractionation was performed on a 25 cm × 6 mm i.d. Partisil 5-μm PAC column (Whatman; 1:2 cyano/amino bonded-phase column) connected in series with two identical precolumns (1 cm × 4.6 mm i.d.; packed with Partisil 5-μm PAC), using a Shimadzu LC 5A liquid chromatograph with Rheodyne 7125 valve injector (1000-μL loop) and Shimadzu SPD-2AM UV detector (monitoring 254-nm adsorption). A binary solvent (*n*-hexane and dichloromethane) was employed in the Shimadzu SGR-1A stepwise solvent delivery system. The proportion of *n*-hexane was programmed as follows: 3 min at 100%, 3 min at 96%, 2 min at 88%, 2 min at 82%, 2 min at 76%, 3 min at 70%, and then a reversed gradient over a 15-min period with *n*-hexane, at a flow rate of 3 mL/min. PAHs (three-ring to seven-ring) were shown to elute between 6 and 13 min by using a PAH standard mixture containing phenanthrene, anthracene, 1-methylphenanthrene, fluoranthene, pyrene, benzo[*a*]fluorene, chrysene, benzo[*a*]pyrene, benzo[*e*]pyrene, perylene, benzo[*ghi*]perylene, and coronene. Then the eluent between 6 and 13 min was collected as the PAH fraction. To ensure PAH detection, the eluent of each sample was monitored with the UV detector (254 nm). To keep column activity, the precolumns were repacked every 10–15 runs. At the same time, the resolution column was washed for 30 min with dichloromethane and for 30 min with methanol at a rate of 3 mL/min. It was then flushed for 30 min with dichloromethane and for a final 30 min with *n*-hexane at the same flow rate. The resolution was checked by injecting the PAH standard mixture after each cleaning of the resolution column. The fluctuations of the retention time of the PAH standards on the liquid chromatograph were within 1 min throughout ca. 150 isolations. The repacking of the precolumns and extensive cleaning restored the column to its original activity throughout our work (ca. 150 isolations).

The PAH fraction isolated by HPLC was evaporated to dryness, taken up in 0.5 mL of benzene/methanol (6:4), and subjected to column chromatography on Sephadex LH-20 (Pharmacia Fine Chemicals; 5 g; 1.0 cm i.d. × 23 cm) using benzene/methanol (6:4). Sephadex LH-20 had been previously conditioned in benzene/methanol (6:4) and washed with the same solvent after wet packing into the column. The first 10 mL of the eluent was discarded and

then a 10–20-mL fraction was collected as the PAH fraction.

Gas Chromatography and GC/MS. The PAH fraction was evaporated just to dryness under reduced pressure at 30 °C and taken up in an appropriate volume (30–200 μL) of isooctane solution containing 1-chlorotetradecane (40 mg/L) and dotriacontane (45 mg/L) as internal injection standards. Sample aliquots of 1 μL were then injected into a Shimadzu 9A gas chromatograph equipped with a flame ionization detector (FID) and a 30 m × 0.25 mm i.d. DB-5 fused-silica column in the splitless mode at 70 °C. The column was maintained at 70 °C for 2 min, followed by heating to 150 °C at 30 °C/min, then temperature programmed from 150 to 200 °C at 5 °C/min and 200 to 310 °C at 4 °C/min, and maintained 5 min with He as carrier gas (flow rate 3mL/min). The FID and injection port were maintained at 310 °C. PAHs were identified by GC/MS. The mass spectra were recorded with a HP 5990A + 5970B GC/MS system. GC column, column and injection temperature, and carrier gas were same as those used in the gas chromatography. The other operating conditions were as follows: MS in the electron impact (EI) mode at 70 eV with scanning from 50 to 350 amu; temperature of ionization chamber, 310 °C.

All quantitative data were obtained by GC peak height with an Hitachi D-2500 integrator. 1-Chlorotetradecane was used as an internal injection standard for the quantification of PAHs ranging from dibenzothiophene (peak 1; cf Figure 1 and Table I) to methylpyrene (peak 46), and dotriacontane for PAHs from benzo[*b*]naphtho[2,1-*d*]-thiophene (peak 47) to benzo[*ghi*]perylene (peak 64). Individual PAHs were quantified by using the response factor of corresponding standards relative to each internal injection standard. The response factors were determined from a gas chromatographic run of the standards on the same day.

Procedure Blank and Reproducibility. An empty thimble was extracted in the Soxhlet apparatus with 500 mL of benzene for 18 h. The extract was then carried through the entire procedure as described above. The resultant gas chromatogram did not display any peaks interfering with the compounds of interest.

The reproducibility was determined by triplicate analyses of the benzene extracts from 2 g of a street dust sample from Setagaya Avenue containing 1–300 ng of individual PAH per gram of dry material. In order to test PAH recovery, 1 μg each of the PAH standards was added to the benzene extracts and analyzed at the same time as the nonspiked extracts. The relative standard deviation each PAH concentration by triplicate analyses ranged from 8.3% for benzo[*ghi*]perylene to 19.4% for phenanthrene. Recovery ranged from 73.2% for benzo[*ghi*]perylene to 97.6% for fluoranthene, by triplicate analyses. The precision of the method is most acceptable considering that the concentration levels are in the tenth of a microgram per gram range in a complex sample matrix requiring sophisticated separation techniques. The precision attained is certainly adequate for applications in environmental investigation. Anthracene was, however, excluded from the quantification, because the reproducibility (relative standard deviation: 43%, $n = 3$) and recovery (58%) was lower than others.

Results and Discussion

Identification of PAHs in Street Dusts. Street dust is a mixture of automobile exhaust, asphalt, lubricating oils, gasoline, diesel fuel, tire particles, atmospheric fallout, and soils. Organic extracts of street dusts, therefore, contain a large amount of polar and nonpolar materials

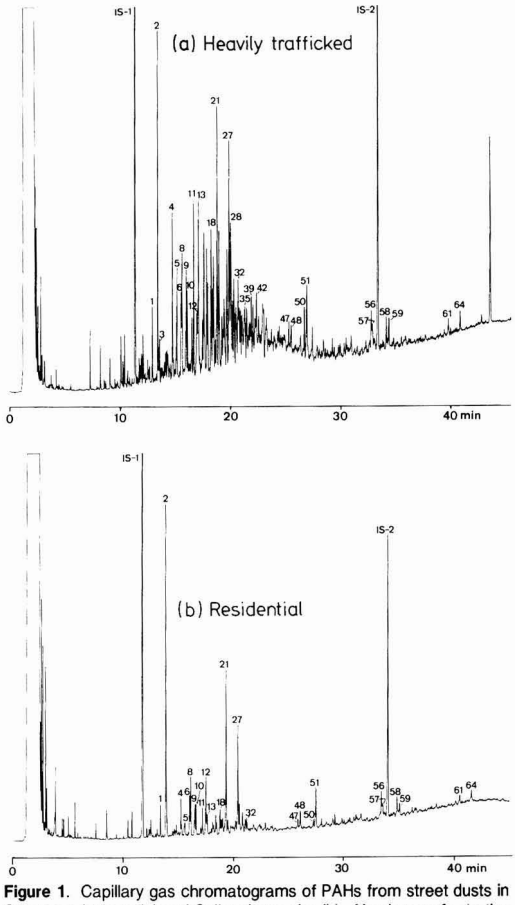

Figure 1. Capillary gas chromatograms of PAHs from street dusts in Setagaya Avenue (a) and Seijogakuen-cho (b). Numbers refer to the compounds listed in Table I. IS-1: internal injection standard-1, 1-chlorotetradecane. IS-2: internal injection standard-2, dotriacontane. GC conditions: 25 m × 0.3 mm i.d. DB-5 fused-silica column; column was maintained at 70 °C for 2 min, followed by heating to 150 °C at 30 °C/min, and then temperature programmed from 150 to 200 °C at 5 °C/min and 200 to 310 °C at 4 °C/min and maintained 5 min with He as carrier gas (flow rate 3 mL/min) (see text for the other conditions).

together with PAHs. Conventional open-column chromatography is not adequate to isolate PAHs from this complex mixture, since its capacity is small and its activity is lowered by the polar materials. The impurities in the PAH fraction obtained by conventional open-column chromatography interfere in the quantification of PAHs by gas chromatography. Thus, in the present study, normal-phase HPLC using cyano/amino bonded silica stationary phase was applied to the fractionation. Normal-phase HPLC have been found to be useful for the separation of PAHs (*24, 25*). In particular, cyano/amino bonded silica stationary phase has a strongly basic surface, which makes it possible to separate PAHs from the polar compounds, and selectivity for a number of the fused aromatic rings. As a consequence, normal-phase HPLC succeeded in isolating a sufficiently purified PAH fraction from organic extracts of street dusts, as shown in Figure 1.

Table I lists the PAHs identified in the street dust samples. GC retention data with the reference standards and literature data (*29–32*) were also used for the identification as well as GC/MS. Three-ring PAHs (phenan-

Table I. Polycyclic Aromatic Hydrocarbons Identified in Street Dusts

peak no.	retention index[a]	MW[b]	identification
1	294.90 ± 0.20	184	dibenzothiophene
2	300.00	178	phenanthrene
3	301.17 ± 0.07	178	anthracene
4	309.83 ± 0.11	198	methyldibenzothiophene
5	312.68 ± 0.10	198	methyldibenzothiophene
6	315.61 ± 0.10	192	3-methylphenanthrene
7	316.04 ± 0.11	198	methyldibenzothiophene
8	316.40 ± 0.09	192	2-methylphenanthrene
9	319.17 ± 0.08	192	9-methylphenanthrene
10	319.96 ± 0.07	192	1-methylphenanthrene
11	324.20 ± 0.10	212	C_2-dibenzothiophene
12	326.51 ± 0.10	204	2-phenylnaphthalene
13	327.46 ± 0.12	212	C_2-dibenzothiophene
14	330.13 ± 0.11	212	C_2-dibenzothiophene
15	331.68 ± 0.09	206	C_2-phenanthrene[c]
16	333.13 ± 0.11	206/212	C_2-phenanthrene[c]/C_2-dibenzothiophene
17	333.73 ± 0.12	206/212	C_2-phenanthrene[c]/C_2-dibenzothiophene
18	335.95 ± 0.11	206	C_2-phenanthrene[c]
19	336.90 ± 0.08	206	C_2-phenanthrene[c]
20	337.67 ± 0.07	206	C_2-phenanthrene[c]
21	340.11 ± 0.06	202	fluoranthene
22	341.27 ± 0.11	226	C_3-dibenzothiophene
23	343.23 ± 0.11	202	benz[*e*]acenaphthylene
24	343.96 ± 0.12	226	C_3-dibenzothiophene[d]
25	344.59 ± 0.09	226	C_3-dibenzothiophene[d]
26	346.65 ± 0.05	226	C_3-dibenzothiophene[d]
27	348.09 ± 0.05	202	pyrene
28	349.03 ± 0.10	218/226	methylphenylnaphthalene/C_3-dibenzothiophene[d]
29	350.40 ± 0.09	240	C_4-dibenzothiophene[d]
30	351.40 ± 0.13	218/226	methylphenylnaphthalene/C_3-dibenzothiophene[d]
31	352.87 ± 0.19	220	C_3-phenanthrene[c,d]
32	354.01 ± 0.13	218/220	methylphenylnaphthalene[d]/C_3-phenanthrene[c]
33	355.71 ± 0.06	220/240	C_3-phenanthrene[c]/C_4-dibenzothiophene[d]
34	356.67 ± 0.07	220/240	C_3-phenanthrene[c]/C_4-dibenzothiophene[d]
35	358.56 ± 0.10	216/240	methylfluoranthene/C_4-dibenzothiophene[d]
36	359.84 ± 0.09	220/240	C_3-phenanthrene[c,d]/C_4-dibenzothiophene[d]
37	361.59 ± 0.12	216/240	methylpyrene[d,e]/C_4-dibenzothiophene[d]
38	362.11 ± 0.06	216/240	methylpyrene[d,e]/C_4-dibenzothiophene[d]
39	362.79 ± 0.14	216/240	methylpyrene[d,e]/C_4-dibenzothiophene[d]
40	364.08 ± 0.14	240	C_4-dibenzothiophene[d]
41	365.38 ± 0.09	216/240	methylpyrene[d,e]/C_4-dibenzothiophene[d]
42	366.33 ± 0.08	216/234/254	methylpyrene[e]/C_4-phenanthrene[c,d]/C_5-dibenzothiophene[d]
43	367.87 ± 0.10	232	C_2-phenylnaphthalene[d]
44	369.96 ± 0.09	216	methylpyrene[d,e]
45	370.47 ± 0.17	234/254	C_4-phenanthrene[c,d]/C_5-dibenzothiophene[d]
46	371.18 ± 0.12	216/234/254	methylpyrene[e]/C_4-phenanthrene[c,d]/C_5-dibenzothiophene[d]
47	388.05 ± 0.07	234	benzo[*b*]naphtho[2,1-*d*]thiophene
48	389.64 ± 0.09	226	benzo[*ghi*]fluoranthene
49	397.36 ± 0.20	226	cyclopenta[*cd*]pyrene
50	398.41 ± 0.08	228	benz[*a*]anthracene
51	400.00	228	chrysene/triphenylene
52	407.69 ± 0.20	242	methylchrysene[f]
53	411.05 ± 0.09	242	methylchrysene[f]
54	416.92 ± 0.06	242	methylchrysene[f]
55	418.24 ± 0.08	242	methylchrysene[f]
56	442.69 ± 0.09	252	benzofluoranthene
57	443.55 ± 0.15	252	benzofluoranthene
58	452.65 ± 0.12	252	benzo[*e*]pyrene
59	454.33 ± 0.13	252	benzo[*a*]pyrene
60	457.45 ± 0.08	252	perylene
61	493.59 ± 0.03	276	indeno[1,2,3-*cd*]pyrene
62	495.05 ± 0.12	278	dibenz[*a,c*]anthracene
63	499.02 ± 0.20	278	dibenz[*a,h*]anthracene
64	501.32	276	benzo[*ghi*]perylene

[a] Retention index: $I = [RT(\text{substance}) - RT(\text{std } z)]/[RT(\text{std } z+1) - RT(\text{std } z)] \times 100 + 100 \times z$, where RT(substance) is the retention time of the substance for which the retention index is to be determined, RT(std z) and RT(std $z+1$) are the retention times for the PAH standards that bracket the substance of interest, and z is the number of aromatic fused rings in the PAH standard that elute just prior to the substance of interest. As the PAH standards, naphthalene, phenanthrene, chrysene, and picene were used, whose retention indexes are defined as 200.00, 300.00, 400.00, 500.00, respectively. [b] Molecular weight assignment based on highest mass ion of significant relative abundance observed in electron impact mass spectrum. [c] Or -anthracene. [d] Tentatively identified. [e] Or methylfluoranthene. [f] Or methylbenz[*a*]anthracene.

threne) to six-ring PAHs (benzo[*ghi*]perylene) and their alkyl-substituted homologues were identified. Dibenzothiophene and methyl- and dimethyl-/ethyl- (C_2-) dibenzothiophenes were also confirmed in the samples. In addition, compounds with m/z 226, 240, and 254 of molecular ion were found by GC/MS analysis. These com-

Table II. PAHs in Street Dusts in Tokyo

	no. of samples	PAH concn				
		$\sum 63$,[c] μg/g	$\sum 63$,[c] μg/m²	$\sum$COMB,[d] μg/g	MP/P[a]	MDBTP/MP[b]
Setagaya Avenue (heavily trafficked)	12	5.35 ± 2.65	2323 ± 1859	1.62 ± 0.93	1.24 ± 0.20	0.52 ± 0.16
Seijyogakuen-cho (residential)	7	3.20 ± 1.57	25 ± 13	1.44 ± 0.71	0.65 ± 0.27	0.26 ± 0.10
National Road Route 20						
concrete-paved part	7	7.27 ± 7.01	890 ± 766	2.25 ± 1.55	1.14 ± 0.16	0.37 ± 0.08
asphalt-paved part	6	8.16 ± 2.77	651 ± 250	3.02 ± 0.83	0.93 ± 0.06	0.39 ± 0.04

[a] Ratio of the sum of the concentrations of 3-methylphenanthrene (peak 6), 2-methylphenanthrene (peak 8), 9-methylphenanthrene (peak 9), and 1-methylphenanthrene (peak 10) relative to the concentration of phenanthrene. [b] Ratio of the sum of the concentrations of methyldibenzothiophenes (peak 4 + peak 5) relative to the sum of the concentrations of methylphenenthrenes. [c] Sum of the concentrations of 63 PAHs identified (Table I), excluding anthracene. [d] Sum of the concentrations of pyrene, fluoranthene, benz[*a*]anthracene, chrysene, benzofluoranthenes, benzo[*a*]pyrene, benzo[*e*]pyrene, indeno[*cd*]pyrene, and benzo[*ghi*]perylene.

pounds were tentatively assigned as C_3-, C_4-, and C_5-dibenzothiophene, respectively.

Characteristics of PAHs in the Urban Street Dusts. Table II indicates the concentrations of PAHs in the street dust samples. Total PAH contents (i.e., the sum of 63 PAHs identified in this study, excluding anthracene; $\sum 63$) in the street dusts are in the range of a microgram per gram for both heavily trafficked and residential roads. The sum of concentrations of nine major nonalkylated compounds (fluoranthene, pyrene, benz[*a*]anthracene, chrysene, benzofluoranthenes, benzo[*a*]pyrene, benzo[*e*]pyrene, indeno[*cd*]pyrene, and benzo[*ghi*]perylene), which is expressed as $\sum$COMB, has often been used as an indicator of PAHs from combustion (*5*, *16*). $\sum$COMB in the street dusts is a few micrograms per gram. Herrmann (*21*) reported that the street dusts in West Germany contain 1.0 ± 1.6 μg/g fluoranthene and 0.53 ± 0.77 μg/g benzo[*a*]pyrene. PAH contents in the street dusts in Tokyo are comparable to these values. That is, the fluoranthene and benzo[*a*]pyrene contents for Tokyo are 0.33 ± 0.20 and 0.10 ± 0.06 μg/g (Setagaya Avenue; n = 12), respectively. However, these values for Tokyo are lower by 1 order of magnitude than those for Switzerland (fluoranthene, 10 μg/g; benzo[*a*]pyrene, 2.7 μg/g; ref 20).

PAH contents in the street dusts in Tokyo are comparable to those for Tokyo Bay sediments. Yun et al. (*6*) reported that PAH contents (sum of phenanthrene, fluoranthene, pyrene, chrysene, benzofluoranthenes, and benzopyrenes) for Tokyo Bay sediments range from 0.2 to 1.3 μg/g of dry sediment with an average of 0.8 ± 0.3 μg/g (n = 19). The values for the street dusts are 1.7 ± 1.0 μg/g (Setagaya Avenue; n = 12). Thus, the PAH contents in the street dusts suggest that they are a potential major contributor to the PAHs of the bay sediments. However, dilution of street dusts and the aquatic sediments by soils and sands, which contain less PAHs, makes it difficult to simply compare PAH contents in both types of samples. The comparison of their PAH profiles may be an alternative tool to evaluate the contribution of street dusts to PAHs in the aquatic sediments.

Figure 1 shows gas chromatograms of the PAH fraction isolated from street dusts collected from the heavily trafficked street and the residential road. For PAHs in both dust samples, unsubstituted ring systems (i.e., parent PAH) ranging from phenanthrene (three aromatic rings) to benzo[*ghi*]perylene (six aromatic rings) were the primary components. In particular, three- and four-ring PAHs (i.e., phenanthrene, fluoranthene, and pyrene) were predominant. These PAH profiles are similar to those observed in sediments from Tokyo Bay (*7*) and throughout the world (*3*), in that unsubstituted PAHs are predominant components. This agreement indicates the possibility that the street dusts significantly contribute to PAHs in Tokyo Bay sediments. Molecular distributions of PAHs in the street dust, however, shift to low molecular weights compared with those in the aquatic sediments, in which four- and five-ring PAHs predominate. The proportion of pyrene + fluoranthene to $\sum$COMB was reported to be 20% for Tokyo Bay sediment (*7*), whereas that for the dust samples was 40 ± 4%. Lower molecular weight PAHs having higher hydrophilicity may selectively dissolve in water on the way to the sediments.

Sources of PAHs in Street Dusts. On the heavily trafficked road, much larger amounts of PAHs (on an unit area basis) were present than on the residential one, whereas no significant differences were noted in weight-based PAH contents of street dusts between both types of roads (Table II). This fact indicates that vast amounts of particles containing PAHs are discharged by traffic. Also, clear compositional differences were noted between PAHs in the both types of street dusts, as is obvious from Figure 1, parts a and b. The samples collected from the heavily trafficked road are more abundant in alkyl-substituted PAHs (e.g., peaks 6, 8–10, and 18) than those from the residential area. The compositional difference is expressed as the relative abundance of total methylphenanthrenes to phenanthrene (MP/P), which has been used for source identification of PAHs (*5*, *10*, *11*). Table II indicates that MP/P for the sample from the heavily trafficked street is 1.24 ± 0.20 (average of 12 samples), while that from the residential street is 0.65 ± 0.27 (average of 7 samples). In addition, the dusts from the heavily trafficked road contain more alkyldibenzothiophenes. To express the relative abundance of alkyl-substituted benzothiophenes, for convenience, a ratio of concentration of methyldibenzothiophenes (peaks 4 + 5) relative to that of methylphenanthrenes (peaks 6 + 7 + 9 + 10) is defined as MDBTP/MP, since these peaks are clearly resolved on gas chromatograms. MDBTP/MP is 0.52 ± 0.16 for street dusts from the heavily trafficked street and 0.26 ± 0.10 for that from the residential street. These features in the PAH profiles indicate that the PAH assemblage abundant in alkyl-PAHs and alkyldibenzothiophenes is derived from mobile sources.

Automobile exhaust is proposed as one of the traffic-related sources of PAHs. As shown in Figure 2a, the gas chromatogram of PAHs in automobile exhaust is similar to that in heavily trafficked street dust, particularly in the abundance in alkyl-substituted PAHs and sulfur heterocyclics. This suggests that automobile exhausts are one major source of PAHs in the street dust from the highly trafficked road. As indicated in Table III, MP/P ratios for the automobile exhausts range from 0.7 to 8.2. The range of MP/P for the exhausts overlapped with those for the street dust samples (0.7–1.2). Also, their MDBTP/MP ratios range from 0.2 to 0.6, agreeing with those for the dust samples (0.3–0.5). Some of the exhaust samples, however, have higher MP/P ratios than those for the dust samples.

Table III. PAHs in the Plausible Sources of Street Dust[a]

	PAH concn, μg/g			MDBTP/
	Σ63	ΣCOMB	MP/P	MP
automobile exhaust				
A (diesel, 2300 cc)	415	62	1.73	0.55
B (diesel, 1500 cc)	1072	129	5.00	0.50
C (diesel, 3300 cc)	6639	332	8.17	0.46
D (diesel, 6400 cc)	2558	102	7.60	0.47
E (diesel, 14000 cc)	8868	177	3.46	0.21
F (spark ignition, 1600 cc)	240	100	0.69	0.26
asphalt				
1	4.32	0.39	2.29	0.67
2	8.82	1.06	3.76	0.71
3	7.08	0.71	2.52	0.97
combustion products from steam generator	413	200	0.95	0.05

[a] MP/P, MDBTP/MP, Σ63, and ΣCOMB are defined in Table II.

These higher MP/P ratios might be attributed to a sampling artifact, for the following reason. Various conditions (e.g., fuel composition, fuel to air ratio, engine combustion temperature, and fuel injection timing) affect the PAH composition in the exhaust. Especially, combustion temperature largely affects the relative abundance of alkyl-substituted PAHs (*10*). It was reported that the content of alkyl-substituted PAHs in automobile exhaust decreases as engine load increases and cylinder exhaust temperature increases (*33*). In the present study, the automobile exhaust samples were collected under no engine load. Thus, the relative abundance of alkyl-PAHs (e.g., MP/P) discharged from the automobiles actually running on streets, whose engines are loaded, is probably lower than those in the exhausts collected in the present study (no load). Further extensive collection of automobile exhausts should be conducted.

Asphalt particles have been proposed as a primary contributor of PAHs in street dusts in Switzerland (*14*). For the case of Tokyo area, however, PAH contents in the asphalt samples are lower than those in the street dusts. ΣCOMB in the asphalt particles range from 0.4 to 1.1 μg/g (Table III), compared to from 1.4 to 3.0 μg/g for the street dusts (Table II). Therefore, if asphalt contributed to a major portion of the PAHs in the street dusts, the street dust would have to consist mostly of asphalt particles. But microscopic observation showed that asphalt particles are minor components in the street dusts, suggesting that asphalt is not primary source of street dust PAHs.

Furthermore, the PAH profiles give clear evidence for the above statements. Alkyl-substituted PAHs and benzothiophenes are much more abundant in asphalt than in street dust, as is obvious from Figure 2b. MP/P for the asphalt samples range from 2.3 to 3.8 (Table III). These values reasonably fall within the reported range of MP/P (2–8) for unburned fossil organic material, such as petroleum, oil shales, and their refined products (*10*). These MP/P ratios for the asphalt samples have no overlap with the range for the dust samples. Also, MDBTP/MP ratios of 0.67–0.97 for asphalt (Table III) are higher than the value for the street dusts (0.52 ± 0.16). These much higher MP/P and MDBTP/MP ratios compared with those in the street dusts exclude asphalt from being the primary contributor of PAHs to the street dusts in the Tokyo area. This conclusion was further supported by the similarity of PAH profiles of street dusts between the asphalt-paved part and the concrete-paved part of National Road Route 20, as shown in Figure 3. The MP/P ratio and the

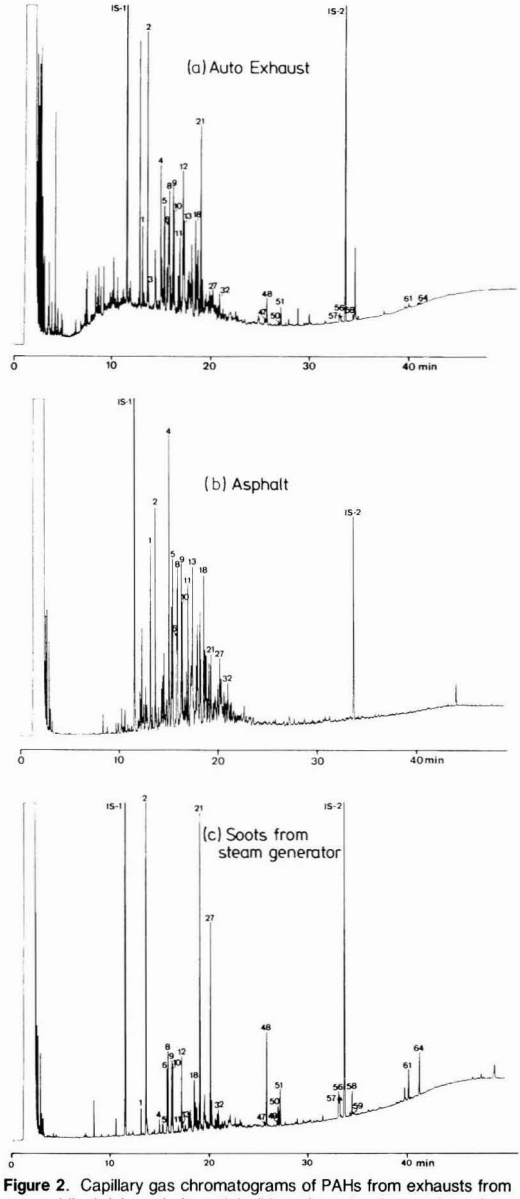

Figure 2. Capillary gas chromatograms of PAHs from exhausts from automobile A (a), asphalt particle (b), and combustion products from a steam generator (c). Numbers refer to identified compounds listed in Table I. IS-1: internal injection standard-1, 1-chlorotetradecane. IS-2: internal injection standard-2, dotriacontane. GC conditions as for Figure 1.

MDBTP/MP ratio in the samples from the concrete-paved material were 1.14 ± 0.16 and 0.37 ± 0.08, respectively. If asphalt particles contributed a major portion of the PAHs in the street dusts, they should have higher MP/P and MDBTP/MP ratios. But MP/P and MDBTP/MP ratios for the asphalt-paved part were similar to those for the concrete-paved part (Table II). Consequently, it is concluded that asphalt is a minor contributor to PAHs in the street dusts in the Tokyo area. The lower contribution of asphalt particles to the street dusts in Tokyo might be attributable to the fact that road surfaces are less abraded by spiked tires due to the infrequent showfall in this area.

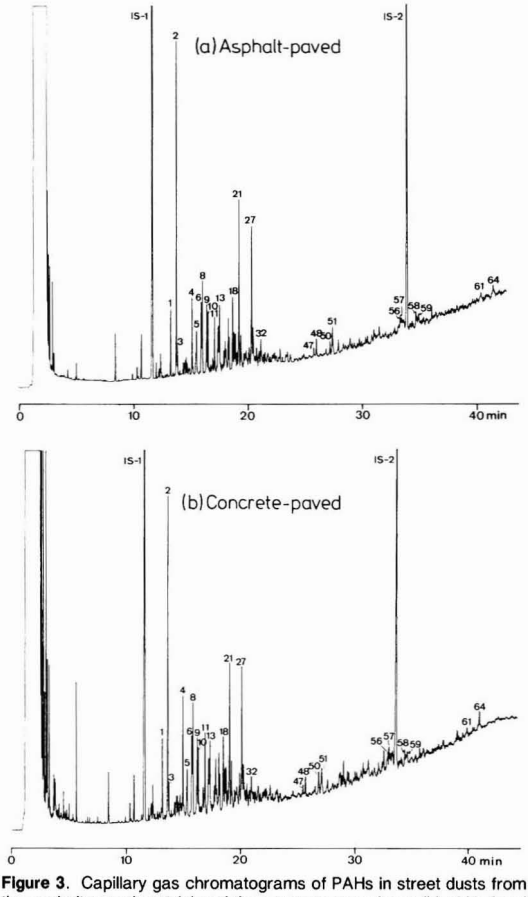

Figure 3. Capillary gas chromatograms of PAHs in street dusts from the asphalt-paved part (a) and the concrete-paved part (b) of National Road Route 20. Numbers refer to identified compounds listed in Table I. IS-1: internal injection standard-1, 1-chlorotetradecane. IS-2: internal injection standard-2, dotriacontane. GC conditions as for Figure 1.

On the other hand, for the street dusts from the residential area, PAHs were depleted in alkyl-substituted homologues and sulfur heterocyclics, as shown in Figure 1b. MP/P for the sample from the residential street is 0.65 ± 0.27. This indicates that residential areas have a more significant contribution from PAH assemblies depleted in alkyl-PAHs and sulfur heterocyclics. The abundance of alkyl-PAHs relative to parent PAHs in combustion products is known to decrease with increasing combustion temperature, and values of MP/P in PAHs generated at high-temperature combustion of fossil fuel are generally <1 (*10*). Thus, PAHs in residential streets may be chiefly derived from stationary combustion sources, where fuel is burning at higher temperatures, than from mobile sources. As an example of combustion PAHs from stationary sources, the gas chromatogram of PAHs in soots from a steam generator burning fuel oil is illustrated in Figure 2c. Its PAH profile resembles that of street dust from the residential street, in the depletion in alkyl-substituted PAHs and benzothiophenes. The MDBTP/MP ratio for the soots is, however, much lower than those for the street dusts in the residential area. Their lower sulfur heterocyclic contents might be due to the lower sulfur content in the fuel (0.06%). Extensive samples of combustion products from various stationary sources should be analyzed to quantitatively evaluate their contribution to PAHs on street surfaces.

Conclusion

The present study demonstrated the detailed molecular composition of PAHs in street dust samples collected from the Tokyo metropolitan area. Unsubstituted ring systems (i.e., parent PAH) ranging from phenanthrene (three aromatic rings) to benzo[*ghi*]perylene (six aromatic rings) were the primary components. In particular, three- and four-ring PAHs (i.e., phenanthrene, fluoranthene, and pyrene) are predominant. Total PAH concentrations were in the range of a few micrograms per gram of dust. On the basis of the PAH profile, it is estimated that PAHs in the street dusts on the heavily trafficked streets arise mainly from automobile exhausts. On the other hand, residential areas appear to have a somewhat more significant contribution from stationary sources. In both types of dusts, asphalt was thought to contribute only a minor part of their PAHs. Higher PAH contents in the street dusts and their PAH profiles suggested that street dusts may be one of major contributors to the PAHs in Tokyo Bay sediments. The impacts of PAHs in street dusts to aquatic environments should be quantitatively evaluated by determining the PAH contents and profiles in runoff samples from the street surfaces.

Acknowledgments

We are most grateful to Dr. S. Sakata, Geological Survey of Japan, for recording the GC/MS.

Registry No. Dibenzothiophene, 132-65-0; phenanthrene, 85-01-8; anthracene, 120-12-7; methyldibenzothiophene, 30995-64-3; 3-methylphenanthrene, 832-71-3; 2-methylphenanthrene, 2531-84-2; 9-methylphenanthrene, 883-20-5; 1-methylphenanthrene, 832-69-9; C_2-dibenzothiophene, 132-65-0; 2-phenylnaphthalene, 612-94-2; C_2-phenanthrene, 85-01-8; fluoranthene, 206-44-0; benz[*e*]acenaphthylene, 201-06-9; pyrene, 129-00-0; methylphenylnaphthalene, 97232-29-6; methylfluoranthene, 30997-39-8; methylpyrene, 27577-90-8; C_2-phenylnaphthalene, 35465-71-5; benzo[*b*]naphtho[2,1-*d*]thiophene, 239-35-0; benzo[*ghi*]fluoranthene, 203-12-3; cyclopenta[*cd*]pyrene, 27208-37-3; chrysene, 218-01-9; triphenylene, 217-59-4; methylchrysene, 41637-90-5; benzofluoranthene, 56832-73-6; benzo[*e*]pyrene, 192-97-2; benzo[*a*]pyrene, 50-32-8; perylene, 198-55-0; indeno[1,2,3-*cd*]pyrene, 193-39-5; dibenz[*a,c*]anthracene, 215-58-7; dibenz[*a,h*]anthracene, 53-70-3; benzo[*ghi*]perylene, 191-24-2; benz[*a*]anthracene, 56-55-3.

Literature Cited

(1) *Particulate Polycyclic Organic Matter*; National Academy of Sciences: Washington, DC, 1972.
(2) Neff, J. M. *Polycyclic Aromatic Hydrocarbons in the Aquatic Environment. Sources, Fates and Biological Effects*; Applied Science Publishers Ltd.: London, 1979.
(3) Laflamme, R. E.; Hites, R. A. *Geochim. Cosmochim. Acta* **1978**, *42*, 289–303.
(4) Platt, H. M.; Mackie, P. R. *Nature* **1979**, *280*, 576–578.
(5) Barrick, R. C.; Prahl, F. G. *Estuarine, Coastal, Shelf Sci.* **1987**, *25*, 175–191.
(6) Yun, S.-J.; Ishiwatari, R.; Shioya, M.; Matsumoto, E. *Chikyu Kagaku (Geochemistry)* **1983**, *17*, 53–59.
(7) Takada, H.; Ishiwatari, R.; Yun, S.-J. *Jpn. J. Water Pollut. Res.* **1984**, *7*, 172–181.
(8) Handa, N.; Ohta, K. *Chikyu Kagaku (Geochemistry)* **1983**, *17*, 60–67.
(9) Ohta, K.; Handa, N. Matsumoto, E. *Geochim. Cosmochim. Acta* **1983**, *47*, 1651–1654.
(10) Youngblood, W. W.; Blumer, M. *Geochim. Cosmochim. Acta* **1975**, *39*, 1303–1314.
(11) Prahl, F. G.; Crecelius, E.; Carpenter, R. *Environ. Sci. Technol.* **1984**, *18*, 687–693.

(12) Broman, D.; Colmsjo, A.; Ganning, B.; Naf, C.; Zebuhr, Y. *Environ. Sci. Technol.* **1988**, *22*, 1219–1228.
(13) Lee, M. L.; Prado, G. P.; Howard, J. B.; Hites, R. A. *Biomed. Mass Spectrom.* **1977**, *4*, 182–186.
(14) Wakeham, S. G.; Schaffner, C.; Giger, W. *Geochim. Cosmochim. Acta* **1980**, *44*, 403–413.
(15) Gschwend, P. M.; Hites, R. A. *Geochim. Cosmochim. Acta* **1981**, *45*, 2359–2367.
(16) Prahl, F. G.; Carpenter, R. *Geochim. Cosmochim. Acta* **1983**, *47*, 1013–1023.
(17) Hoffman, E. J.; Mills, G. L.; Latimer, J. S.; Quinn, J. G. *Environ. Sci. Technol.* **1984**, *18*, 580–587.
(18) Hoffman, E. J.; Latimer, J. S.; Hunt, C. D.; Mills, G. L.; Quinn, J. G. *Water, Air, Soil Pollut.* **1985**, *25*, 349–364.
(19) Bates, T. S.; Murphy, P. P.; Curl, H. C.; Feely, R. A. *Environ. Sci. Technol.* **1987**, *21*, 193–198.
(20) Giger, W.; Schaffner, C. *Anal. Chem.* **1978**, *50*, 243–249.
(21) Herrmann, R. *Water, Air, Soil Pollut.* **1981**, *16*, 445–467.
(22) Takada, H.; Ishiwatari, R. *J. Chromatogr.* **1985**, *346*, 281–290.
(23) Novotny, V.; Sung, H. M.; Bannerman, R.; Baum, K. *J. Water Pollut. Control Fed.* **1985**, *57*, 339–348.
(24) Wise, S. A.; Chesler, S. N.; Hertz, H. S.; Hilpert, L. R.; May, W. E. *Anal. Chem.* **1977**, *49*, 2306–2310.
(25) Miller, R. *Anal. Chem.* **1982**, *54*, 1742–1746.
(26) Killops, S. D.; Readman, J. W. *Org. Geochem.* **1985**, *8*, 247–257.
(27) Readman, J. W.; Mantoura, R. F. C.; Rhead, M. M. *Sci. Total Environ.* **1987**, *66*, 73–94.
(28) Benner, B. A., Jr.; Gordon, G. E.; Wise, S. A. *Environ. Sci. Technol.* **1989**, *23*, 1269–1278.
(29) Lee, M. L.; Vassilaros, D. L.; White, C. M.; Novotny, M. *Anal. Chem.* **1979**, *51*, 768–773.
(30) Wise, S. A.; Benner, B. A.; Byrd, G. D.; Chesler, S. N.; Rebbert, R. E.; Schantz, M. M. *Anal. Chem.* **1988**, *60*, 887–894.
(31) Lee, M. L.; Novotny, M.; Bartle, K. D. *Anal. Chem.* **1976**, *48*, 1566–1572.
(32) Radke, M.; Willsch, H.; Leythaeuser, D.; Teichmuller, M. *Geochim. Cosmochim. Acta* **1982**, *46*, 1831–1848.
(33) Jensen, T. E.; Hites, R. A. *Anal. Chem.* **1983**, *55*, 594–599.

Received for review November 8, 1989. Accepted March 27, 1990.

Determination of Optimal Storage Conditions for Particle Samples

George M. Sverdrup,* Bruce E. Buxton, and Jane C. Chuang

Battelle Memorial Institute, 505 King Avenue, Columbus, Ohio 43201-2693

Gary S. Casuccio

R. J. Lee Group, 350 Hochberg Road, Monroeville, Pennsylvania 15146

■ Results are presented from laboratory studies on how to store particle samples to preserve them for chemical, physical, and biologic testing. Surrogate samples for power plant plume fly ash were created by using electrostatic precipitator (ESP) hopper ash. Particles of diameters less than 10 μm were suspended and mixed with three polycyclic aromatic hydrocarbons (PAH), one nitro-PAH, salt, and sulfuric acid. The particle mixture was then collected on filters to create surrogate samples. Samples were stored for periods of 30 and 120 days at either 20 or −79 ± 1 °C as well as under a set of variable conditions of temperature, light, and humidity. Gas chromatography/mass spectrometry and scanning electron microscopy with energy dispersive analysis were used to characterize changes in organic and elemental composition, particle size distribution, and particle morphology. Preservation of organic compounds in the samples was best achieved when the samples were packaged in Teflon-wrapped glass dishes. Both storage temperature and duration of storage can influence sample stability. In many cases storage at −79 °C provided statistically significant enhancement of organic compound stability after 120 days compared to storage at 20 °C. Particle agglomeration in some samples was suggested by microscopy results. Sulfuric acid had a deleterious effect on two of the spiked PAH. Considering all factors, the most favorable storage conditions were −79 °C in the dark. Under these conditions, loss of the lightest PAH (fluorene) was minimized; the heaviest PAH (chrysene) was stable for at least 120 days.

To assess the biologic effects of plume fly ash, samples of particulate matter need to be collected from plumes and later tested in the laboratory. Realistic biologic assessment requires that the test results on collected samples are equivalent to the biologic effects of particles in the atmosphere. This, in turn, requires equivalency between the properties of both collected and airborne particles that give rise to biologic effects. Clearly, one of the tasks in biologic assessment is, after collection, to store samples in such a manner as to minimize changes in their properties between the times of collection and analysis.

Both chemical and physical changes in samples can influence their biologic activity. Possible chemical changes include (a) thermal reactions involving the storage container, atmosphere, other sample constituents, and the collection medium; (b) photochemical reactions; (c) state of hydration; and (d) contamination from the atmosphere, container, and collection medium. Possible physical changes include (a) vaporization and (b) morphological change resulting from fracturing and agglomeration.

To provide protocols and equipment to store environmental samples for biologic testing (*1*) we investigated several different sample packaging techniques and the subsequent stability of surrogate samples under different storage conditions. The storage conditions can be classified according to three experimental factors: storage temperature, storage time, and the presence or absence of sulfuric acid in the samples. In the investigation of storage temperature, the primary storage condition was defined to be −79 °C in the dark. Two additional conditions considered were storage at 20 °C in the dark and "worst case" conditions of variable temperature, humidity, and light. We assumed that changes would occur in the samples stored under worst case conditions, and we used these samples to assess our ability to detect changes. In the investigation of storage time, samples were stored for either 30 or 120 days. Together these various storage conditions represent the range of conditions at which researchers have stored samples (*2–14*).

The storage stability experiments were designed to address five groups of questions. The first three groups, listed below, pertain to organic material on fly ash. In particular we investigated the stability of polycyclic aro-

 0013-936X/90/0924-1186$02.50/0

matic hydrocarbons (PAH). The last two questions pertain to elemental composition, morphology, and particle size distribution as determined by computer-controlled scanning electron microscopy (CCSEM).

1. Is storage at −79 °C better than storage at 20 °C? That is, do the concentrations of the PAH decrease with time, and if so, do they decrease more quickly for samples stored at 20 °C than for samples stored at −79 °C?

2. Does sulfuric acid affect either the starting concentrations of the PAH in samples or the rate of decrease of those concentrations during storage?

3. How does PAH stability under the −79 °C, 20 °C, and worst case storage conditions compare? Can we detect changes in PAH concentrations if they occur? Do the concentrations of the PAH decrease more quickly for samples stored in any of these three conditions?

4. Does storage at −79 °C or under worst case conditions influence the elemental composition and morphology of samples as determined by CCSEM?

5. Does the presence of sulfuric acid influence the elemental composition and morphology of samples stored at −79 °C, as determined by CCSEM?

The sample packaging, surrogate samples, experimental design, apparatus, procedures, and results from our experiments are provided in the following sections.

Sample Packaging Techniques

As an initial step in our study, we developed procedures for handling and packaging samples that preserve their integrity. A series of experiments was conducted by spiking the following six PAH onto clean quartz filters: naphthalene, fluorene, phenanthrene, pyrene, chrysene, and benzo[*a*]pyrene. The filters were cleaned by heating them in a muffle furnace for 16 h at 400 °C. The PAH-laden filters were handled, packaged, and stored in various ways for periods up to 1 month. The PAH content of filters was then compared to their content prior to packaging and storing. Results of the investigations are summarized below.

In one group of tests we evaluated cotton and vinyl gloves. Following a series of handling procedures with forceps, the quartz filters that were exposed to vinyl gloves were found to contain ethyl hexyl phthalate (a plasticizer). The filters that were handled with cotton gloves and forceps showed no significant signs of chemical contamination. Therefore, all subsequent work with filters was conducted with cotton gloves.

A series of tests was conducted to develop a satisfactory packaging scheme for individual samples. Variations of the following techniques and materials were examined: polyethylene bags, aluminum foil, glass Petri dishes, glass plates, crimping aluminum foil, wrapping containers with Teflon tape, and marking containers with various ink pens and labels. The optimal method of packaging consists of enclosing a folded quartz filter in a clean glass Petri dish, wrapping the exterior joint between the dishes with three turns of Teflon tape, and enclosing the assembly in aluminum foil. For storage in the dark at −79 °C, the aluminum foil served as an added, though unnecessary, barrier. Permanent pens and standard sticky labels did not contaminate the samples.

These results are consistent with work by others (*2–4*). Our results indicated that the polyethylene bags were both a source of contamination and a sink for PAH. Kalkwarf found that polyethylene envelopes were a perfect sink for PAH that had been adsorbed onto electrostatic precipitator (ESP) hopper ash (*2*). In accord with the practice of others (*3*, *4*), our investigations demonstrated that aluminum foil provided a practical outer barrier for sample packaging. Our experience with sample handling and packaging leads us to recommend the following packaging technique: samples stored in Teflon-wrapped, glass Petri dishes, with or without (if the samples are stored in the dark) an outer covering of aluminum foil.

Table I. Model Compounds and Classes of Change They Represent for the Storage Stability Study

compound	class of change
2-nitrofluorene	biologic activity resulting from chemical change
fluorene	organic chemical change by decomposition and volatilization
chrysene	volatilization (comparatively less than fluorene)
cyclopenta[*cd*]pyrene	oxidation
sulfuric acid	inorganic chemical changes in oxidation state of sulfur by reaction with ammonia
epsom salt	chemical changes in hydration during storage
	physical changes such as fracturing during freezing and agglomeration

Surrogate Samples

The samples that we used for this study were designed with two primary considerations. First, our surrogate samples were to possess the physical characteristics of field samples. This was accomplished by using filter samples prepared in the laboratory. Second, the surrogate samples were to possess properties that could represent various classes of change during the storage of field samples. For this purpose model compounds were applied to size-fractionated (particle diameter less than 10 μm) ESP hopper ash, which was then collected on filters.

The model compounds and the classes of change that they represent are listed in Table I. Three PAH and one nitro-PAH were used to model the behavior of organic components. Epsom salt was added to evaluate the influence of freezing and thawing on particles (analysis by polarized light microscopy). This analysis is not reported in this paper. Sulfuric acid was used to model the influence of sulfuric acid in stack and plume samples.

Our use of surrogate samples follows the practice of other researchers (*4–22*). We expanded the range of model compounds beyond the PAH and nitro-PAH used in the studies cited above in an effort to represent the field samples. A model system such as ours does, of course, have limitations in its portrayal of reality. For example, this system does not account for aging and reaction of plume particles with coemitted gases; nor are possible interactive effects between constituents in field samples accounted for if these constituents are absent in the model system. Finally, adsorption of organic compounds on fly ash particles is strongly dependent upon the composition of the adsorbate material. This dependence is expected to influence the stability of stored samples (*5*). Consequently, the ESP hopper ash that was used for this study approximates the adsorptive properties of field samples to an unknown degree.

We do expect that our model system provides a qualitative surrogate for field samples for three reasons (*1*). First, the filters are identical with those commonly used for field collections. Second, the ESP hopper ash consists of particles with the size range of importance to inhalation (less than 10 μm) and with about the same loadings as we collected in plumes. Third, the concentrations of model organic compounds and sulfuric acid are representative of environmental samples.

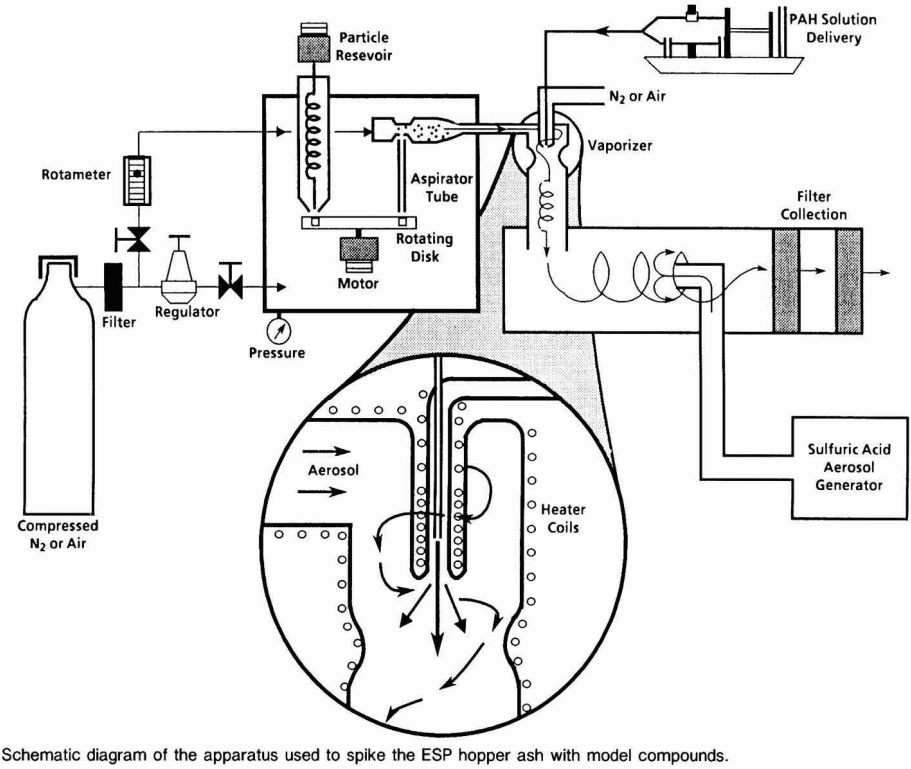

Figure 1. Schematic diagram of the apparatus used to spike the ESP hopper ash with model compounds.

Experimental Design

Each set of filters that was prepared for the storage stability study consisted of a quartz filter for study of PAH and nitro-PAH degradation and a polycarbonate filter for study of elemental composition and morphology by CCSEM.

The experiments proceeded in three steps. First, various combinations of fly ash compounds were collected on several different filters to create three levels of spiking. *Unspiked filters* have ESP hopper ash only; *partially spiked filters* have ESP hopper ash, epsom salt, and model PAH; and *fully spiked filters* have ESP hopper ash, epsom salt, model PAH, and sulfuric acid.

Second, after the compounds were deposited, each filter was quartered into individual samples that were then stored under different conditions before chemical analysis. There were *three storage conditions* under which individual samples were stored: −79 ± 1 °C in the dark, 20 ± 1 °C in the dark, or worst case conditions (changing temperatures from −79 to 60 °C, changing humidity, and changing light). There were also *three time periods* for which individual samples were stored at 20 and −79 °C, 0 (the sample was analyzed soon after filter preparation), 30, or 120 days.

Last, after storage the quartz filter samples were extracted and the extracts were chemically analyzed for fluorene, cyclopenta[*cd*]pyrene, chrysene, and 2-nitrofluorene. The response variables of interest are the concentrations of these compounds on each sample filter.

A total of 33 quartz samples was included in the storage stability experiment. Those samples can be classified according to three experimental factors: the type of spiking (none, partial, full), the storage time (0, 30, 120 days), and the storage conditions (−79 °C, 20 °C, worst case). For each unique combination of these three factors, three replicate filters were stored and analyzed. The classification of the individual samples by the experimental factors is shown in Table II. A single quartz filter can be identified by four characters of the sample ID, for example, 95-Q1. The fifth character of the sample ID is either A, B, C, or D and denotes a specific one-quarter piece of an individual filter. Although each of the first three study questions can be addressed with the data, no question can be addressed across all experimental factors: Question 1 can be addressed by examining all full spike data except for those samples stored under worst case conditions; question 2 can be addressed by examining the data for samples stored at −79 °C and then comparing the data for samples that were fully spiked with the data for samples that were partially spiked; and question 3 can be addressed by examining all full spike data for samples stored no more than 30 days.

The experimental design employed here balances the ability to examine several study questions with practical limits on the number of chemical analyses that could be performed.

Thirty-three polycarbonate filters were prepared alongside the quartz filters. Seven of these filters were analyzed by CCSEM. The quartz filters that correspond to the seven polycarbonate filters analyzed by CCSEM are denoted with asterisks in Table II.

Apparatus

The apparatus that we used to generate the surrogate samples is shown schematically in Figure 1. Four parts make up the apparatus: aerosol dust generator, PAH/nitro-PAH generator and vapor–particle aging chamber, sulfuric acid aerosol generator, and filter unit.

The aerosol dust generator is a mechanical generator. Particles are delivered by gravity feed to a circular me-

Table II. Experimental Design for the Quartz Filter Samples

storage time, days	type of spiking[a,b]			
	no spike	partial spike	full spike	
0	98-Q.A[c]*	95-Q1A*	92-Q1A*	92-Q4A
		95-Q2A	92-Q2A	92-Q5A
		95-Q3A	92-Q3A	92-Q6A
		−79 °C	−79 °C	20 °C
30	98-Q.B*	95-Q1B*	92-Q1C*	92-Q4B
		95-Q2B	92-Q2C	92-Q5B
		95-Q3B	92-Q3C	92-Q6B
			worst case	
			92-Q1B*	
			92-Q2B	
			92-Q3B	
		−79 °C	−79 °C	20 °C
120	98-Q.C	95-Q1C	92-Q1D	92-Q4C
		95-Q2C	92-Q2D	92-Q5C
		95-Q3C	92-Q3D	92-Q6C

[a] Sample ID is listed by the following type of spiking (no spike, partial spike, full spike), storage time (0, 30, 120 days), storage condition (−79 °C, 20 °C, worst case). [b] * Denotes that CCSEM analysis was conducted on a polycarbonate filter sample that corresponds to the highlighted quartz filter sample. [c] The three "no spike" filters were combined for analysis.

tering groove in a rotating plastic (Lexan) disk. The particles in the groove are carried beneath an aspiration tube, where they are sucked up and dispersed into a stream of nitrogen. The aerosol particle concentration in the nitrogen stream is controlled by the rotational speed of the disk and the size of the metering groove. The dust generator is enclosed in a plastic compartment to exclude ambient air from the generator.

The PAH vapor generator consists of a microsyringe pump and heating zone. A single solution of 2-nitrofluorene, fluorene, chrysene, and cyclopenta[*cd*]pyrene in an aliphatic solvent was fed from the syringe pump reservoir through a 0.25 mm internal diameter fused-silica (deactivated with Carbowax 20M) capillary tube to the vaporization zone. The aerosol stream was preheated to ~75 °C before it entered the vaporization zone. The vaporization zone was heated to produce a thermal gradient of 150 °C at the upstream end to 275 °C at the vapor exit.

The vapor–particle aging chamber is made of Pyrex glass. It is silylated by gas-phase treatment with hexamethyldisilazane at 200 °C for several hours in a vacuum oven before use.

A sulfuric acid aerosol was generated by atomization and then mixed with the PAH-spiked aerosol. This mixed aerosol was collected on filters.

Sample Preparation

The following five procedures were used to prepare and store the samples.

1. About 8 L of ESP hopper ash was collected from TVA's Cumberland Fossil Plant. A Donaldson classifier was used to classify the raw (as collected) ESP hopper ash into two size fractions: less than and greater than roughly 10 μm particle aerodynamic diameter.

2. We prepared three types of samples for the storage study: unspiked, partially spiked, and fully spiked ESP hopper ash on filters. (1) About 20 g of epsom salt that had been ground and sieved to generate a sample of crystals with diameters less than 50 μm was mixed with ~200 g of ESP hopper ash. The mixture of particles was suspended in the nitrogen stream. (2) The model PAH were vapor deposited onto the surface of the suspended mixture of salt and ESP hopper ash at a concentration of ~2 μg of each PAH/g of ESP hopper ash. (3) Sulfuric acid aerosol was mixed with the parially spiked aerosol (2% spike) and collected on filters to generate the fully spiked samples. Filter loadings of 700–800 mg/quartz filter were achieved.

3. We weighed each quartz filter and then cut each filter (quartz, Nuclepore, Millipore) into quarters. The quarter sections were each enclosed in a clean glass Petri dish that was wrapped three times around with Teflon tape and then encased in aluminum foil.

4. Samples were transported to the analytical laboratories by courier for a time zero analysis.

5. The remaining sections were stored according to the specified protocol for 30 and 120 days.

At time zero, 30, and 120 days filters were analyzed by GC/MS for the organic model compounds. To prepare the samples for analysis, they were extracted with 5% methanol/95% benzene (v/v) for 16 h. Each extract was concentrated to ~500 μL by rotoevaporation and nitrogen evaporation. A 50-μL aliquot of each extract was removed to determine residue weights. Half of each extract was used for chemical analysis, and the other half was used for bioassay analysis. The portion used for bioassay analysis was evaporated to dryness under a gentle nitrogen stream, and the sample vial was purged with nitrogen and then sealed with Teflon tape. These residue samples were packed in dry ice and sent to SRI for bioassay testing (bioassay results are not reported here). The internal standard 9-phenylanthracene was added to each sample portion for chemical analysis at a constant concentration level of 1 ng/μL. These extracts were analyzed by gas chromatography/electron impact ionization mass spectrometry. The average response factors for the target compounds in standard solutions were used to quantify the four compounds in the extracts.

Gravimetric analysis of the quartz filters yielded an average particulate mass loading of 745 mg/filter with a relative standard deviation of 17%. Total extractable material with the benzene/methanol solvent averaged 97 μg/quarter filter with a relative standard deviation of 30%. These results were achieved after a development effort that consisted of repeated trials and analysis to improve uniformity of sample loading.

Ion chromatography analyses were made on five samples to determine their sulfate content. Analyses were made of the organic solvent extracts as well as the sample remaining on the filter after organic extraction.

The unspiked samples contained ~3% sulfate by mass. The epsom salt did not contribute significantly to the sulfate content of the samples. The maximum concentration of sulfate that could be expected from the epsom salt component is ~4% (because sulfate is 39% of the mass of epsom salt and the salt was blended into the ESP hopper ash at a 1:10 ratio). Operators of the generation apparatus noted significant amounts of dust on the walls of the apparatus. It is likely that a substantial fraction of the large salt particles was not captured by the filter. This statement is supported by the CCSEM analyses, which showed negligible particle mass comprising particles with diameters greater than 10 μm and also negligible concentrations of magnesium. These findings are acceptable in terms of the experimental design because epsom salt was added solely for the analysis of changes in hydration of the samples.

Table III. Concentration of Spiked PAH and Nitro-PAH during the Storage Stability Study

sample ID	spike type	storage cond, °C	storage time, days	ng of PAH/mg of particles			
				fluorene	2-nitrofluorene	cyclo[a]	chrysene
98Q.A	none			0.31	<0.01	<0.01	0.08
98Q.B	none	−79	30	0.34	<0.01	<0.01	0.12
98Q.C	none	−79	120	0.19	<0.01	<0.01	0.31
95Q1A	part		0	10	59	2.1	26
95Q2A	part		0	14	91	2.1	34
95Q3A	part		0	18	41	1.5	22
95Q1B	part	−79	30	5.5	34	0.096	19
95Q2B	part	−79	30	7.9	39	2.8	26
95Q3B	part	−79	30	11	27	1.6	17
95Q1C	part	−79	120	10	17	1.1	21
95Q2C	part	−79	120	12	14	0.31	29
95Q3C	part	−79	120	15	8.1	<0.01	15
92Q4A	full		0	0.55	53	0.019	21
92Q5A	full		0	14	27	0.011	11
92Q6A	full		0	12	40	0.014	8.8
92Q4B	full	20	30	0.43	43	<0.01	18
92Q5B	full	20	30	6.9	9.8	<0.01	7.2
92Q6B	full	20	30	3.5	17	<0.01	5.9
92Q4C	full	20	120	0.43	24	<0.01	21
92Q5C	full	20	120	1.1	2.3	<0.01	6.4
92Q6C	full	20	120	2.1	8.1	<0.01	4.4
92Q1A	full		0	0.49	90	0.075	28
92Q2A	full		0	0.49	110	0.009	40
92Q3A	full		0	0.60	52	0.069	17
92Q1C	full	−79	30	0.52	52	<0.01	26
92Q2C	full	−79	30	0.61	73	<0.01	33
92Q3C	full	−79	30	0.52	35	<0.01	16
92Q1D	full	−79	120	0.33	30	<0.01	30
92Q2D	full	−79	120	0.61	52	0.80	46
92Q3D	full	−79	120	0.47	15	0.19	16
92Q1B	full	WC	30	0.36	43	<0.01	22
92Q2B	full	WC	30	0.10	54	<0.01	30
92Q3B	full	WC	30	0.084	27	<0.01	13

[a] Cyclo, cyclopenta[*cd*]pyrene.

Stability of Organic Components

Analysis of the organic storage stability data was made to estimate the effects of the three experimental factors (type of spiking, storage time, and storage condition) on the stability of the organic compounds. The process of loading the filters with ESP hopper ash, epsom salt, PAH, and sulfuric acid, does not place the same amount of these compounds onto each filter (see Table III). Therefore, there is variation in the concentrations of the PAH on the samples due to initial loading, as well as to the effects of the three experimental factors. The statistical analysis is focused on the effects of storage condition and storage time by first controlling the effect of the initial loading (filter effect). For all data analyses, the initial loading effect is controlled by explicitly including in the statistical model terms that quantify the variability in PAH concentrations from filter to filter.

Study Question 1. The first question asks whether or not the concentrations of the PAH decrease with time, and if so, whether they decrease more quickly for samples stored at 20 °C than for samples stored at −79 °C. The corresponding concentration data for each PAH were modeled with the analysis of variance model shown in eq 1, where Y_{ijkm} is the concentration for the mth sample from

$$Y_{ijkm} = \mu + \alpha_i + \beta_j + (\alpha\beta)_{ij} + \gamma_{k(i)} + (\beta\gamma)_{jk(i)} + \epsilon_{ijkm} \quad (1)$$

the kth filter stored in the ith storage condition for the jth storage time; μ is the overall average concentration for all samples; α_i is the main effect for storage condition i, i = 1 is storage at −79 °C, i = 2 is storage at 20 °C; β_j is the main effect for storage time j, j = 1 is storage for 0 days, j = 2 is storage for 30 days, j = 3 is storage for 120 days; $(\alpha\beta)_{ij}$ is the interaction effect for storage condition i and storage time j; $\gamma_{k(i)}$ is the main effect for filter k, nested within storage condition i; $(\beta\gamma)_{jk(i)}$ is the interaction effect for storage time j and filter k; and ϵ_{ijkm} is the independent error term.

An examination of question 1 was made by estimating the effect of storage condition (storage at −79 or 20 °C) and storage time (30 or 120 days) on PAH concentration. The storage condition effect is estimated for a given PAH by comparing the average concentration for all samples stored at −79 °C to the average concentration for all samples stored at 20 °C. Similarly, the storage time effect is estimated by comparing the average concentration for all samples stored for 0, 30, or 120 days. If the storage time effect depends on the storage condition (or vice versa), then the two experimental factors are said to interact. In the presence of an interaction, the effect of one experimental factor can only be estimated after conditioning on the level of the other factor. For example, if a significant interaction effect is identified, then the effect of storage condition is estimated separately for samples stored 0, 30, and 120 days.

For question 1, the statistical analysis proceeds in two steps.

1. The presence or absence of a significant interaction effect (e.g., between storage condition and storage time) is judged with an analysis of variance F test. If an interaction effect exists, then the main effects can be analyzed with multiple pairwise comparisons between the average concentrations for all combinations of the experimental factors.

2. If no interaction effect is found, then the presence of main effects is estimated with another analysis of variance F test. If a significant main effect is found (e.g., due to storage condition), then the effect is quantified by

Table IV. Analysis of Variance Comparison of Means for Study Question 1[a]

analyte	storage condn, °C	storage time, days 0	30	120	av
fluorene	−79	0.53	0.55	0.47	0.52
	20	**8.85**	**3.61**	**1.21**	4.56
	av	4.69	2.08	0.84	
2-nitrofluorene	−79	**84.0**	**53.3**	**32.3**	56.5
	20	**40.0**	**23.3**	**11.5**	24.9
	av	62.0	38.3	21.9	
cyclopenta[*cd*]pyrene	−79	0.05	0.01	0.33	0.13
	20	0.01	0.01	0.01	0.01
	av	0.03	0.01	0.17	
chrysene	−79	28.3	25.0	30.7	28.0
	20	13.6	10.4	10.6	11.5
	av	21.0	17.7	20.6	

[a] Bold-face type denotes effects judged to be either significant or marginally significant.

comparing the average concentrations for each level of the experimental factor (e.g., the average concentration for storage at −79 °C versus the average concentration for storage at 20 °C).

We have chosen to group the results of the statistical analysis in three categories of observed significance level (p): significant ($p \leq 0.05$), marginally significant ($0.05 < p \leq 0.10$), and not significant ($p > 0.10$). This approach is used because with only three replicate samples for each data point, we need to be cautious in arbitrarily setting a cutoff (such as $p < 0.05$) for stated statistical significance.

The significance level can be interpreted for a given effect as the probability of observing simply by chance a greater difference in the averages of the data calculated for each level of that effect. The highlights of the analysis results are the following (see Table IV):

1. For fluorene there was a marginally significant interaction effect between storage condition and storage time (i.e., observed significance level p of 0.074). That is, the loss of fluorene over time was different for samples stored at −79 and 20 °C. With a marginally significant interaction effect, the main effect of storage time must be judged separately for samples stored at −79 °C and samples stored at 20 °C. As shown by the bold-faced data for fluorene in Table IV, fluorene concentrations in samples stored at −79 °C did not appear to change over time, while the fluorene concentrations in samples stored at 20 °C steadily decreased from an average of 8.85 ng/mg before storage to an average of 1.21 ng/mg after storage for 120 days. However, it should also be noted that, as indicated by the samples that were stored for 0 days, the samples stored at −79 °C had low initial loadings and therefore had much less PAH to lose during storage. Therefore, it is possible that the statistically significant differences found in the data are attributable to storage temperature or to the initial loadings. Visual comparison of the stability of fluorene at −79 and 20 °C can be made by referring to Figure 2. A plot of the average ratio of concentrations at 30 and 120 days compared to the initial value is shown.

2. For 2-nitrofluorene there was a significant interaction effect between storage condition and storage time (i.e., $p = 0.024$). Samples stored at both −79 and 20 °C lost 2-nitrofluorene during storage. However, as in the case of fluorene, the initial loadings for samples stored at −79 °C are quite different from those stored at 20 °C, and therefore the same precaution applies in attributing the differences seen in the data to storage conditions or to the initial loadings.

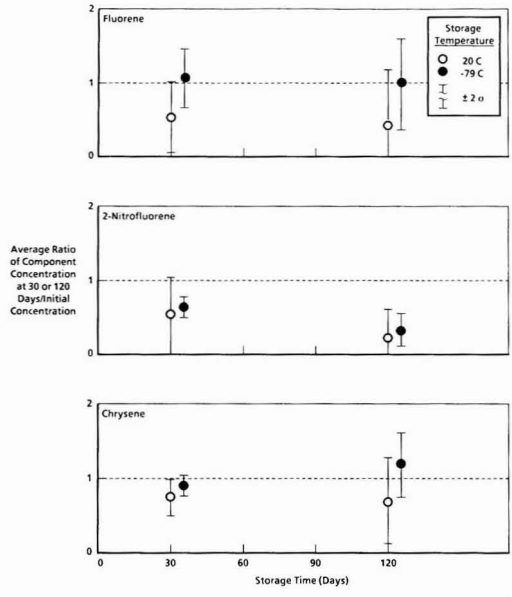

Figure 2. Stability of selected organic compounds in spiked ESP hopper ash samples during storage.

3. For both cyclopenta[*cd*]pyrene and chrysene, no significant interaction or main effects were observed. For cyclopenta[*cd*]pyrene, many measured concentrations were close to the method detection limit, making it difficult to discern any significant effects in the data.

Study Question 2. The second question asks whether or not adding sulfuric acid to the filters affects either the starting concentrations of the PAH or the rate of decrease of those concentrations during storage. This question can be addressed by comparing the data for fully spiked samples stored at −79 °C with those for partially spiked samples stored at −79 °C. The concentration data for each PAH were modeled with an analysis of variance model shown in eq 2, where Y_{ijkm} is the concentration for the mth

$$Y_{ijkm} = \mu + \alpha_i + \beta_j + (\alpha\beta)_{ij} + \gamma_{k(i)} + (\beta\gamma)_{jk(i)} + \epsilon_{ijkm} \quad (2)$$

sample from the kth filter receiving the ith type of spiking and stored for the jth storage time; μ is the overall average concentration for all samples; α_i is the main effect for type of spiking i, $i = 1$ is full spiking (with sulfuric acid), $i = 2$ is partial spiking (without sulfuric acid); β_j is the main effect for storage time j, $j = 1$ is storage for 0 days, $j = 2$ is storage for 30 days, $j = 3$ is storage for 120 days; $(\alpha\beta)_{ij}$ is the interaction effect for type of spiking i and storage time j; $\gamma_{k(i)}$ is the main effect for filter k, nested within type of spiking i; $(\beta\gamma)_{jk(i)}$ is the interaction effect for storage time j and filter k; and ϵ_{ijkm} is the independent error term.

The analysis of variance was conducted in the same two steps as for question 1. Highlights of the analysis results are the following (see Table V):

1. For fluorene there was a significant interaction effect ($p = 0.0001$) between type of spiking and storage time. That is, the average fluorene concentration in fully spiked samples was significantly lower than that in partially spiked samples; however, the difference depended on the storage time of the samples. The data for samples stored 0 days indicate that fully spiked samples (i.e., with sulfuric acid) lose their fluorene either before initial loading or immediately after loading. The data for samples stored

Table V. Analysis of Variance Comparison of Means for Study Question 2[a]

analyte	type spiking	storage time, days 0	30	120	av
fluorene	full	**0.53**	**0.55**	**0.47**	0.52
	part	**14.0**	**8.1**	**12.3**	11.5
	av	7.3	4.3	6.4	
2-nitrofluorene	full	84.0	53.3	32.3	56.5
	part	63.7	33.3	13.0	36.7
	av	**73.8**	**43.3**	**22.7**	
cyclopenta[*cd*]pyrene	full	0.05	0.01	0.33	**0.13**
	part	1.90	1.50	0.47	**1.29**
	av	0.98	0.75	0.40	
chrysene	full	28.3	25.0	30.7	28.0
	part	**27.3**	**20.7**	**21.7**	23.2
	av	27.8	22.8	26.2	

[a] Bold-face type denotes effects judged to be either significant or marginally significant.

0 days from filters 92Q4, 92Q5, and 92Q6 were not included in this analysis of variance; however, they suggest that the difference might be attributed to initial loading.

2. For 2-nitrofluorene the interaction effect was not significant. Therefore, the main effects were evaluated in the second analysis step. We found a significant effect due to storage time ($p = 0.0001$), but not due to type of spiking ($p = 0.24$). That is, the average concentration of 2-nitrofluorene in fully spiked samples was not significantly different from that for partially spiked samples. Both fully spiked and partially spiked samples lost ~40% of their 2-nitrofluorene after storage for 30 days and ~70% of their 2-nitrofluorene after storage for 120 days.

3. For cyclopenta[*cd*]pyrene there was a significant main effect due to type of spiking ($p = 0.008$), but not due to storage time ($p = 0.40$). The average concentration of cyclopenta[*cd*]pyrene in fully spiked samples (i.e., 0.13 ng/mg) was an order of magnitude below that for partially spiked samples (i.e., 1.29 ng/mg). However, the concentration of cyclopenta[*cd*]pyrene did not decrease significantly during storage.

4. For chrysene there was a marginally significant interaction effect between type of spiking and storage time ($p = 0.071$). The initial concentrations of chrysene were approximately the same for fully spiked and partially spiked samples. During storage the fully spiked samples did not appear to lose chrysene; however, the partially spiked samples did lose ~20% of their chrysene after storage for 30 or 120 days.

Study Question 3. The third study question asks whether or not the concentrations of the PAH decrease after storage for 30 days, and if so, do they decrease more for samples stored at −79 °C, 20 °C, or worst case conditions. This question can be addressed by examining all full spike data for samples stored no more than 30 days. Because for question 3 there were only three filters stored under worst case conditions, the statistical analysis proceeds in two different steps.

1. To compare storage under worst case conditions with storage at −79 °C, a paired t test is performed on the data for the three fully spiked filters stored 30 days under each of these conditions. The paired test can be used because both sets of samples were quartered from the 92Q1, 92Q2, and 92Q3 filters (see Table II).

2. To compare storage under worst case conditions with storage at 20 °C, the analysis is performed in the same two steps described above for study questions 1 and 2.

Table VI. Comparison of Means for Study Question 3[a]

Storage at Worst Case versus −79 °C Condition

analyte	worst case	−79 °C
fluorene	**0.18**	**0.55**
2-nitrofluorene	**41.3**	**53.3**
cyclopenta[*cd*]pyrene	0.01	0.01
chrysene	**21.7**	**25.0**

Storage at Worst Case versus 20 °C Condition

analyte	storage condn	storage time, days 0	30	av
fluorene	WC	0.53	0.18	0.35
	20 °C	8.85	3.61	6.23
	av	**4.69**	**1.90**	
2-nitrofluorene	WC	**84.0**	**41.3**	62.7
	20 °C	**40.0**	**23.3**	31.6
	av	62.0	32.3	
cyclopenta[*cd*]pyrene	WC	0.05	0.01	0.03
	20 °C	0.01	0.01	0.01
	av	**0.03**	**0.01**	
chrysene	WC	28.3	21.7	25.0
	20 °C	13.6	10.4	12.0
	av	**21.0**	**16.0**	

[a] Bold-face type denotes effects judged to be either significant or marginally significant.

For the comparison of storage at −79 °C and worst case conditions, directly comparable data were available from filters 92Q1, 92Q2, and 92Q3. Quarters labeled "B" from those filters were stored at worst case conditions, and quarters labeled "C" were stored at −79 °C. The corresponding concentration data for each PAH were modeled with the following one-way analysis of variance model, which is equivalent to a paired t-test model:

$$Y_{ik} = \mu + \alpha_i + \epsilon_{ik} \quad (3)$$

where Y_{ik} is the concentration after storage for 30 days for the kth sample stored in the ith storage condition; μ is the overall average concentration for all samples; α_i is the main effect for storage condition i, $i = 1$ is storage at −79 °C, $i = 2$ is storage at worst case conditions; and ϵ_{ik} is the independent error term.

For the comparison of storage at 20 °C and worst case conditions, an analysis of variance model similar to eq 1 was employed:

$$Y_{ijkm} = \mu + \alpha_i + \beta_j + (\alpha\beta)_{ij} + \gamma_{k(i)} + (\beta\gamma)_{jk(i)} + \epsilon_{ijkm} \quad (4)$$

where α_i is the main effect for storage condition i, $i = 1$ is storage at 20 °C, $i = 2$ is storage at worst case conditions; β_j is the main effect for storage time j, $j = 1$ is storage for 0 days, $j = 2$ is storage for 30 days; and the other six terms are as defined for eq 1.

Highlights of the analysis results are the following (see Table VI):

1. In the comparison of storage at −79 °C and worst case conditions, marginally significant storage condition effects were found for fluorene ($p = 0.074$) and 2-nitrofluorene ($p = 0.076$), and a significant effect was found for chrysene ($p = 0.010$). For all three of these compounds, the average concentration in samples stored at −79 °C was greater than the average concentration in samples stored under worst case conditions. No statistical analysis could be performed

Table VII. Elemental Composition of Fully Spiked ESP Hopper Ash Samples Before and After 30 Days of Storage at Worst Case Conditions and −79 °C

	percent of X-ray counts[a]		
element	time zero 090-N1-A	worst case 090-N1-B	−79 °C 090-N1-C
C	0.1	0.0	0.8
O	15.6	9.5	16.2
Na	0.0	0.1	0.0
Mg	0.0	0.0	0.1
Al	20.5	22.2	21.0
Si	41.8	45.7	44.5
P	0.3	0.3	0.0
S	6.9	3.5	4.4
Cl	0.0	0.0	0.1
K	2.4	3.3	2.2
Ca	4.8	3.8	4.0
Ti	0.5	0.8	0.4
V	0.1	0.1	0.0
Fe	6.9	8.4	6.3

[a] Less than 0.1% of total counts for Cr, Mn, Ni, Cu, Zn, As, Se, Br, Cd, Sb, Ba, Pb, and Sc.

for cyclopenta[*cd*]pyrene because this compound was undetected in all six samples considered.

2. In the comparison of storage at 20 °C and worst case conditions, the only evidence of a storage condition effect was found in a marginally significant interaction effect for 2-nitrofluorene ($p = 0.060$). However, the data in Table VI indicate that the average concentration of 2-nitrofluorene is actually higher in samples stored under worst case conditions than in those stored at 20 °C. The data for samples stored 0 days indicate that this apparent storage condition effect may actually be caused by unequal initial loadings.

3. Also regarding the comparison of storage at 20 °C and worst case conditions, evidence of at least marginally significant storage time effects was found for all four PAH compounds. For 2-nitrofluorene this effect was found in an interaction effect with storage condition. Significance levels for fluorene, cyclopenta[*cd*]pyrene, and chrysene were 0.098, 0.098, and 0.005, respectively. For all four compounds the average concentration in samples stored for 30 days at both 20 °C and worst case conditions was reduced from the average concentration measured before storage.

Elemental Composition and Morphology

To address questions 4 and 5, we evaluated samples after their preparation (time zero) and then after 30 days of storage. CCSEM was not used after 120 days of storage because the high stability of the samples during the first 30 days of storage combined with the analytical expense made the benefit/cost ratio for the 120-day information too low for us to undertake the additional analysis.

Question 4 can be addressed by examining all full spike data and then comparing the changes after 30 days storage in samples stored at −79 °C versus the changes in samples stored under worst case conditions, and question 5 can be addressed by examining the data for samples stored at −79 °C and then comparing the data for samples that were fully spiked with the data for samples that were partially spiked.

Study Question 4. The fourth question turns attention from the stability of organic constituents in stored samples to elemental and morphological constituents. Data on the fully spiked samples in Table VII suggest a possible change in sulfur content. First note that significant differences (qualitative evaluation) appear to exist between samples for the elements O and S. Because each sample has a relative elemental distribution listed, any change in one element will influence the entire distribution. This may be the cause for slight variations in the Al and Si data. The oxygen data are equivalent for time zero and storage at −79 °C, but the relative oxygen counts are substantially less for the sample stored under worst case conditions.

The sulfur data indicate a possible decrease in sulfur content for the stored samples. This may be attributable to loss of spiked epsom salt and sulfuric acid. Note that the relative sulfur content for the 30-day spiked samples stored at −79 °C and under worst case conditions approaches the unchanging unspiked levels.

Table VIII. Morphological Classification of Particles in Fully Spiked ESP Hopper Ash Samples Before and After 30 Days of Storage at Worst Case Conditions and −79 °C

	weight distribution, %		
		30 days of storage	
morphological class	time zero 090-N1-A	worst case 090-N1-B	−79 °C 090-N1-C
round	18	15	5.9
round agglomerated	47	35	71
fused	30	40	19
acicular	0	0	0
crystalline	0	0	0
ambiguous	5.3	4.8	3.5
ambiguous agglomerated	0	4.5	0

Table IX. Summary of Calculated Physical Mass Distribution Results (Weight Percent)

BEPFA sample	spiking level	storage	particle diameter range, μm 0.1–1.0	1.0–2.5	2.5–5.0	5–10
096-N2-A	none	none	1.0	22	47	30
096-N1-B	none	−79 °C	1.0	23	45	31
090-N1-A	full	none	0.9	19	50	30
090-N1-B	full	20 °C	0.5	21	54	25
090-N1-C	full	−79 °C	0.9	13	34	53
093-N1-A	part	none	2.9	23	51	23
093-N1-B	part	−79 °C	2.9	23	49	27

Morphological characteristics of the samples were studied by classifying particles into the seven categories that are given in Table VIII (*1*). This information is coupled with calculated mass size distributions for samples in Table IX. The fraction of particles that are classified as round agglomerated compared to round is significantly higher for the 30-day, −79 °C sample than for the time zero sample. Also, from Table IX the calculated mass fraction in the particle diameter range 5–10 μm increases at the expense of the 1.0–2.5 and 2.5–5 μm size ranges for the full spike, −79 °C sample compared to the full spike, time zero sample. No other significant differences in the size distributions presented in Table IX are evident. The results in these two tables indicate the possibility of growth (i.e., agglomeration) in particles that were stored at −79 °C.

Study Question 5. The fifth question asks whether or not the sulfuric acid spiked onto the samples influenced either the elemental composition or size distribution of samples stored 30 days at −79 °C. Comparison of results shown in Table VII (fully spiked samples) and Table X (partially spiked samples, i.e., without sulfuric acid) is needed to address the question of elemental composition. Results in Table IX can be used to compare size distributions.

The elemental data indicate that, with the possible exception of sulfur, no significant changes in elemental composition occurred in the partially spiked sample. Addition of sulfuric acid did not influence the stability of the relative composition of major elements.

Table X. Elemental Composition of Partially Spiked ESP Hopper Ash Samples Before and After 30 Days of Storage at −79 °C

element	percent of X-ray counts[a] time zero 093-N1-A	30 days 093-N1-B	element	percent of X-ray counts[a] time zero 093-N1-A	30 days 093-N1-B
C	0.6	2.2	K	2.0	2.0
O	16.1	17.5	Ca	6.2	5.9
Mg	0.1	0.0	Ti	0.5	0.6
Al	19.4	19.5	Cr	0.5	0.1
Si	40.2	42.0	Fe	7.3	6.5
P	0.0	0.4	Ni	0.1	0.0
S	6.8	3.2	Cu	0.1	0.0

[a] Less than 0.1% of total counts for Na, Cl, V, Mn, Zn, As, Se, Br, Cd, Sb, Ba, Pb, and Sc.

Note from Table X that the S decreased from 6.8 to 3.2% of total X-ray counts. This decrease cannot be attributed to sulfuric acid because the partially spiked sample did not have it added. The decrease may reflect changes in the epsom salt that was spiked onto the ESP hopper ash. Presumably, this would also be the explanation for the sulfur decrease in the fully spiked sample (Table VII).

The size distribution of the partially spiked samples given in Table IX indicates no significant change during storage for 30 days at −79 °C. Comparison with the size distribution data for the fully spiked samples suggests that spiking sulfuric acid may have influenced the size distribution during storage for 30 days at −79 °C. The duplicate and triplicate samples were not analyzed to confirm or reject this tentative finding.

Discussion

Summarizing the results from the analyses of the first three study questions, four conclusions can be made about the addition of sulfuric acid to the spiking mixture for the samples with PAH and about the storage of samples with PAH at different storage conditions.

1. **For fluorene**, storage at −79 °C did not appear to affect the samples, but storage at 20 °C or under worst case conditions did. Storage at 20 °C resulted in a loss of 86% of the starting concentration after 120 days. Furthermore, addition of sulfuric acid to the samples appears to have resulted in a significant loss of fluorene. However, as discussed earlier, both of these conclusions may be attributable to unequal initial loadings on the samples, rather than to storage conditions or the presence of sulfuric acid in the spiking mixture.

2. **For 2-nitrofluorene**, storage at −79 and 20 °C resulted in a loss of approximately 62 and 71% of the starting concentration after 120 days. However, as with fluorene, this conclusion may be attributable to unequal loadings rather than to storage condition. In addition, the adding of sulfuric acid to the samples resulted in no loss of 2-nitrofluorene.

3. **For cyclopenta[*cd*]pyrene**, the measured concentrations were almost always close to the method detection limit. However, it appears that there was a substantial loss of cyclopenta[*cd*]pyrene when sulfuric acid was added to the samples, or when the samples were stored, under worst case conditions.

4. **For chrysene**, storage at −79 °C did not affect fully spiked samples. However, partially spiked samples stored at −79 °C and fully spiked samples stored at either 20 °C or worst case conditions do appear to have lost chrysene during storage.

Results of this sample stability storage test for the PAH and nitro-PAH compounds indicate that both storage temperature and duration of storage can be important factors that influence sample stability. These results are in qualitative agreement with earlier investigations of changes in biologic activity (*11*, *12*) and physicochemical properties (*24*, *25*) of environmental samples.

Our results indicate that a very cold storage temperature is preferable to 20 °C storage. This is consistent with the findings of ref 24 for coal samples wherein experiments at 4, 20, and −150 °C were carried out over 18 months. Temperature was found to be the most important variable (storage atmospheres of air, nitrogen, and argon were also used) affecting changes in the coal sample composition and properties. The −150 °C temperature was the optimal storage temperature of the three temperatures that were used.

Our optimal temperature storage condition is the same as used by the contemporary "Integrated Air Cancer Project", which used storage of filter samples at −80 °C for 2, 4 and 8 months. Storage under this temperature condition produced no changes in extractable mass or mutagenic activity (*27*).

Our results are also consistent with studies on the stability of S(IV) species in particulate matter that had been collected on quartz fiber filters and stored in sealed Petri dishes. Richter (*25*) found that some or all of the S(IV) species were lost from the samples during storage at 5 °C over a period of 4–6 months. However, when stored at −80 °C for up to 8 weeks, the concentrations of both inorganic and organic S(IV) were essentially unchanged.

Results from this study also indicate that various PAH differ in their storage stability. Not an unexpected conclusion, it is in accord with the work of Korfmacher et al. (*5*), who found that out of 14 model PAH they studied, 6 decomposed in the dark during storage over 2000 h. Fluorene decomposed during storage; it partially disappeared during the current study also. The stability results for fluorene and chrysene at 20 and −79 °C are consistent with propensity for volatilization of PAH by virtue of their relative vapor pressures (*28*).

Chuang et al. (*10*) studied the stability of field samples on quartz filters stored for 0, 10, 20, and 30 days at room temperature in the dark. The samples were collected by filtration over 24-h periods in homes. They found that cyclopenta[*cd*]pyrene was the most labile PAH of the 12 they analyzed. It decomposed over 30 days to 51% of its initial value. The current study found that this compound was unstable during preparation of samples for storage. Chuang et al. found the other 11 PAH to be stable as judged by plots of the data. The current data indicate that of the three PAH and one nitro-PAH investigated, only chrysene was stable for 120 days and then only when stored at −79 °C.

In conclusion, the results of this study indicate that particle samples should be stored at a temperature well below 0 °C to minimize changes in their chemical and physical properties. Samples can be packaged in Teflon-wrapped, glass dishes, with an inorganic covering (e.g., clean aluminum foil) over the dishes to shield the samples from light. Of the various storage conditions that we evaluated in this study, we found that storage at −79 °C in the dark is the optimal storage condition to preserve samples for at least a few months.

Registry No. C, 7440-44-0; O, 7782-44-7; Na, 7440-23-5; Mg, 7439-95-4; Al, 7429-90-5; Si, 7440-21-3; P, 7723-14-0; S, 7704-34-9; Cl, 7782-50-5; K, 7440-09-7; Ca, 7440-70-2; Ti, 7440-32-6; V, 7440-62-2; Fe, 7439-89-6; Cr, 7440-47-3; Ni, 7440-02-0; Cu, 7440-50-8; 2-nitrofluorene, 607-57-8; fluorene, 86-73-7; chrysene,

218-01-9; cyclopenta[*cd*]pyrene, 27208-37-3; sulfuric acid, 7664-93-9; epsom salts, 7487-88-9; polyethylene, 9002-88-4; Teflon, 9002-84-0.

Literature Cited

(1) Biologic Effects of Plume Fly Ash: Preliminary Studies—Collection, Storage, Chemistry, and Physics. Battelle report to the Electric Power Research Institute under RP2482-5, 1990.

(2) Kalkwarf, D. R.; Garcia, S. R. Pollutant Transformations in the Atmosphere. In *Pacific Northwest Laboratory Annual Report for 1979 to the DOE Assistant Secretary for Environment. Part 3—Atmospheric Sciences*; Pacific Northwest Laboratory Report No. PNL-3300 PT3; February 1980; pp 22–25.

(3) Pitts, J. N., Jr.; Winer, A. M. Particulate and Gas Phase Mutagens in Ambient and Simulated Atmospheres. University of California at Riverside Final Report to California Air Resources Board, Contact No. A3-049-32, December 1984.

(4) Pitts, J. N., Jr.; Paur, H. R.; Zielinska, B.; Arey, J.; Winer, A. M.; Ramdahl, T.; Mejia, V. *Chemosphere* **1986**, *15*, 675–685.

(5) Korfmacher, W. A.; Natusch, D. F. S.; Taylor, D. R.; Mamantov, G.; Wehry, E. L. *Science* **1980**, *207*, 763–765.

(6) Kalkwarf, D. R.; Garcia, S. R. Pollutant Transformation in the Atmosphere. In *Pacific Northwest Laboratory Annual Report for 1978 to the DOE Assistant Secretary for Environment. Part 4—Physical Sciences*; Pacific Northwest Laboratory Report No. PNL-2850 PT4; 1979; pp 1.3–1.5.

(7) Butler, J. P.; Kneip, T. J.; Daisey, J. M. *Atmos. Environ.* **1987**, *21*, 883–892.

(8) Masclet, P.; Bresson, M. A.; Mouvier, G. *Fuel* **1987**, *66*, 556–562.

(9) De Raat, W. K.; Kooijman, S. A. L. M.; Gielen, J. W. J. *Sci. Total Environ.* **1987**, *66*, 95–114.

(10) Chuang, J. C.; Hannan, S. W.; Wilson, N. K. *Environ. Sci. Technol.* **1987**, *21*, 798–804.

(11) Huisingh, J.; et al. Application of Bioassay to the Characterization of Diesel Particle Emissions. In *Application of Short-Term Bioassays in the Fractionation and Analysis of Complex Environmental Mixtures*; Waters, M. D., Nesnow, S., Huisingh, J. L., Sandhu, S. S., Claxton, L., Eds.; Plenum Publishing Corp.: New York, 1979; pp 381–418.

(12) Mizusaki, S.; Takashima, T.; Tomaru, K. *Mutat. Res.* **1977**, *48*, 29–36.

(13) Davis, P. B. Ames Test Mutagenicity of Fly Ash Samples from the "Gelderland" Power Plant of the PEGM in Nijmegen. TNO Report No. TNO-HMT-R--83/159A; June 1985.

(14) Yokley, R. A.; Garrison, A. A.; Wehry, E. L.; Mamantov, G. *Environ. Sci. Technol.* **1986**, *20*, 86–90.

(15) *Conversion of Adsorbed Benzo(a)pyrene (^{14}C) and Benz(a)anthracene (^{14}C) on Fly Ash in the Presence of Light and Air Pollution Components*; Toegepast-Natuarwetenschappelijk Onderzoek: s'Gravenhage, The Netherlands, TNO-HMT-R--85-268; October 1985.

(16) Kalkwarf, D. R. Transformation of Energy—Related Pollutants. In *Pacific Northwest Laboratory Annual Report for 1981 to the DOE Office of Energy Research. Part 3—Atmospheric Sciences*. Pacific Northwest Laboratory Report No. PNL-4100 PT3; February 1982; pp 15–17.

(17) Korfmacher, W. A.; Mamantov, G.; Wehry, E. L.; Natusch, D. F. S.; Mauney, T. *Environ. Sci. Technol.* **1981**, *15*, 1370–1375.

(18) Soltys, P. A.; Mauney, T.; Natusch, D. F. S.; Schure, M. R. *Environ. Sci. Technol.* **1986**, *20*, 175–180.

(19) Miguel, A. H.; Korfmacher, W. A.; Wehry, E. L.; Mamantov, G.; Natusch, D. F. S. *Environ. Sci. Technol.* **1986**, *13*, 1229–1232.

(20) Mumford, J. L.; Tejada, S. B.; Jackson, M.; Lewtas, J. *Environ. Res.* **1986**, *40*, 427–436.

(21) Pitts, J. N., Jr.; Winer, A. M.; Atkinson, R.; Arey, J.; Biermann, H. W.; Harger, W. P.; Zielinska, B. Photochemical and Thermal Reactions of Combustion-Related Particulate Matter: A Combined Chemical and Microbiological Approach. Final Report to U.S. Department of Energy, Contract No. DE-AM03-76F0034; DOE/EV/10048--T1; University of California, Riverside, 1986.

(22) Griest, W. H.; Tomkins, B. A. *Environ. Sci. Technol.* **1986**, *20*, 291–295.

(23) Sousa, J. A.; Houck, J. E.; Cooper, J. A.; Daisey, J. M. *JAPCA*, **1987**, *37*, 1439–1444.

(24) *Development of Techniques for Obtaining and Storing Premium Coal Samples*; GRI-85/0008; Gas Research Institute: Chicago, IL, June 1985.

(25) Richter, B. E. S(IV) and Alkylating Agents in Airborne Particulate Matter. Ph.D. Dissertation, Department of Chemistry, Brigham Young University, 1981.

(26) Lewis, C. W.; Baumgardner, R. E.; Stevens, R. K.; Claxton, L. D.; Lewtas, J. *Environ. Sci. Technol.* **1988**, *22*, 968–971.

(27) Integrated Air Cancer Project—Status Report. U.S. Environmental Protection Agency, Research Triangle Park, February 1989.

(28) Coutant, R. W.; Brown, L.; Chuang, J. C.; Riggin, R. M.; Lewis, R. G. *Atmos. Environ.* **1988**, *22*, 403–409.

Received for review May 31, 1989. Revised manuscript received March 9, 1990. Accepted March 22, 1990. This work was conducted for the Electric Power Research Institute (EPRI) under RP2482-5. Dr. Blakeman S. Smith was the EPRI project manager. Dr. James O. Jackson provided valuable recommendations for the design of the storage studies and their reporting.

Environ. Sci. Technol. **1990**, *24*, 1196–1203

An Intercomparison of Sampling Techniques for Nicotine in Indoor Environments

Fern M. Caka, Delbert J. Eatough,* Edwin A. Lewis, and Hongmao Tang

Chemistry Department, Brigham Young University, Provo, Utah 84602

S. Katherine Hammond

Department of Family and Community Medicine, University of Massachusetts Medical School, Worcester, Massachusetts 01655

Brian P. Leaderer

John B. Pierce Foundation and Yale University School of Medicine, New Haven, Connecticut 06519

Petros Koutrakis, John D. Spengler, Adam Fasano, and Jack McCarthy

School of Public Health, Harvard University, Boston, Massachusetts 02115

Michael W. Ogden

R. J. Reynolds Tobacco Company, Winston-Salem, North Carolina 27102

Joellen Lewtas

U.S. Environmental Protection Agency, Research Triangle Park, North Carolina 27711

■ A study using several types of sampling systems was conducted in the chamber facility at the Pierce Laboratory to compare the determination of nicotine in environmental tobacco smoke generated by volunteer smokers. The sampling systems used included filter packs, annular denuders, sorbent beds, and passive samplers. Total nicotine determined by the various sampling systems was generally in good agreement. Agreement among samplers was also generally good for gas-phase nicotine. The most notable exception was the determination of nicotine with a stainless steel passive sampler where the results were low due to adsorption of nicotine by the sampler. Agreement, but with poor precision, was seen for the determination of particulate-phase nicotine with a Tenax microtube sorbent sampling system and two different annular denuder systems. However, loss of particulate nicotine to the gas phase occurred during sampling with the filter pack system, and determination of particulate-phase nicotine by these systems was in error. Because greater than 95% of the nicotine was in the gas phase, this loss of particulate nicotine did not significantly affect the determination of gas-phase nicotine with a filter pack sampling system.

Introduction

There is an increased emphasis on the accurate determination of exposure to environmental tobacco smoke (ETS) due to the prevalence of ETS in indoor environments and due to the suspected adverse health effects associated with ETS exposure for the nonsmoker (*1*, *2*). In the past, nicotine has been extensively used as a marker and tracer to assess ETS exposure.

The determination of nicotine in indoor environments with ETS present has been reported in studies that either measure the airborne concentration of nicotine (*3–13*) or monitor nicotine and cotinine in the urine of exposed populations (*14–20*). The results of a workshop to compare the techniques available for the determination of nicotine and cotinine in body fluids have been reported (*21*). However, no intercomparison studies on the determination of airborne nicotine have been reported.

In the indoor environment, nicotine is primarily found in the gas phase (*3*, *22–25*). It is now clear that early data based on collection of nicotine on a filter significantly underestimated the concentration of nicotine present in the environments studied. Several recent studies have attempted to monitor only gas-phase nicotine or to use a sampling procedure that collects both gas- and particulate-phase nicotine. It is possible that the different methods of sampling may result in substantial differences in the concentration of nicotine reported in indoor environments. The sampling method itself could, for example, influence the apparent gas-phase–particulate-phase distribution for nicotine. Hence, a need exists to directly compare the sampling and analysis methods used to determine nicotine in indoor environments.

In the past, the major sampling techniques that have been used for the determination of nicotine in ETS have been the following:

1. Filter pack sampling systems where particles are removed on a filter, and gas-phase nicotine collected on acid-saturated filters (*6*, *8–10*, *24*).
2. Passive samplers for the specific collection of gas-phase nicotine after diffusion to the sampling surface (*7*, *26*, *27*, *34*).
3. Diffusion denuder sampling systems where gas-phase nicotine is first collected on an acidic surface by diffusion denuding followed by collection of particulate-phase nicotine by a filter pack designed to collect particles and any nicotine lost from particles during sampling (*3*, *22–24*, *28*).
4. Sorbent bed sampling systems that collect gas-phase nicotine (*4*, *11*, *12*, *23*, *29*).

An intercomparison study of nicotine determination was conducted to evaluate the precision and equivalency of examples of each of the sampling techniques presently being used. Results from the study for the determination of airborne gaseous and particulate-phase nicotine are given here.

Experimental Section

Four laboratories participated in the study using the sampling techniques and analysis procedures described below.

Sampling Procedures. Brigham Young University. The group from BYU used four sampling techniques:

1. The annular diffusion denuder (BYU AD) has been described (*26*). This sampling system determines gas- and particulate-phase nicotine by collection of gas-phase nic-

 0013-936X/90/0924-1196$02.50/0

otine in an acid-coated annular diffusion denuder, followed by collection of particulate nicotine. The inlet to the sampler is a Teflon cyclone with a cut of 2.5 μm to remove coarse particles. The inlet is followed by two annular denuder sections (*30*) to collect gaseous nicotine. The surfaces of the denuders are prepared by coating with an aqueous 5% (w/w) benzenesulfonic acid (BSA) solution. The collection efficiency for gas-phase nicotine is determined by comparing the amount collected on the two denuder sections. Two BSA-coated glass fiber filters follow the denuder sections. The filters collect particulate nicotine and any gas-phase nicotine that evolves from the collected particles plus gas-phase nicotine not collected by the denuder. Thus, the results obtained with the annular denuder give gas-phase, particulate-phase, and total nicotine concentrations. Flow through the system was controlled at 20 standard L/min (sLpm; at 25 °C and 1 atm) by Tylan mass flow controllers.

2. The filter pack (BYU FP) sampling system consists of a 47-mm Teflon filter followed by two BSA-coated glass fiber filters. Particulate nicotine is collected on the Teflon filter, and the BSA-coated filters collect gas-phase nicotine as well as any nicotine lost from particles collected on the first filter. Data generated from the filter pack include particulate-phase (assumed to be the nicotine collected on the Teflon filter), gas-phase, and total nicotine. Flow through the sampler for the study was controlled at 5 sLpm by a Tylan mass flow controller.

3. The passive sampling device (BYU PAS) collected gas-phase nicotine on a BSA-coated glass fiber filter. The design of the passive sampler used was originally described by Lewis et al. (*31*) and is marketed by Scientific Instrumentation Specialists (Moscow, ID). A description of the sampler and its flow calibration has been published (*26*). The effective collection rate for the sampler is 50 mL/min.

4. The Tenax semi-real-time sampler (BYU TEN) has been described by Tang et al. (*32*). It consists of two glass microtubes in sequence. For the intercomparison study, the first tube contained 3 mg of silanized glass wool to collect particulate nicotine. The second tube contained a 20-mg bed of Tenax sorbent, 35/60 mesh, to collect gas-phase nicotine. Up to 24 sets of tubes can be put into the multiport sampling box. The sampling time for each port can be varied from 1 to 60 min. During the intercomparison study, data were obtained by sampling over 10- or 20-min intervals. Flow rate through the system was controlled at 0.10 sLpm by a Tylan mass flow controller.

The Tylan mass flow controllers were calibrated for the intercomparison study by use of dry gas meters, mass flowmeters, and bubble flowmeters.

Harvard University. The group from Harvard used two sampling systems:

1. The miniannular denuder (HAR AD) is a personal annular denuder including a Teflon-coated glass impactor, which serves as a size-selective inlet, and a Teflon filter pack to collect particulate nicotine (*33*). The Harvard denuder system contains a single diffusion annular denuder section coated with an aqueous 4% (w/w) citric acid (CA) solution. Data previously reported (*33*) indicate that the expected efficiency of the denuder section for nicotine collection is 98.6%. The filter pack following the denuder section contains a 37-mm Teflon filter followed by a CA-coated glass fiber filter. Flow rate through the system was controlled by a modified Kurz Model 250 mass flow controller at 2 L/min.

2. The Millipore cassette (HAR FP) consists of a Teflon filter followed by a CA-coated glass fiber filter. Particulate-phase nicotine is collected on the Teflon filter; gas-phase nicotine and any nicotine lost from the particles are collected on the acid-coated filter. Flow through the system was controlled by a modified Kurz Model 250 mass flow controller at 2 L/min. Flow was calibrated for the denuder and cassette sampling systems by using rotameters.

R. J. Reynolds. The group from Reynolds used two sampling systems:

1. The normally used configuration for the XAD-IV sampler (REY XAD) has been described (*12*, *29*). It consists of a 7 cm × 0.6 cm glass tube containing two sections of 20/40 mesh XAD-IV sorbent (80 mg primary, 40 mg backup) separated by a glass wool spacer (no. 226-30-11-04, SKC Inc., Eighty Four, PA). Flow through the sorbent bed is controlled at 1 L/min by an SKC (Model 224-PCXR7) personal sampling pump. The data from the two XAD-IV sorbent sections allow determination of the efficiency of the XAD sorbent bed for the collection of gas-phase nicotine.

The Reynolds sampling procedure normally entails connecting the outlet end of the XAD-IV sorbent tube directly to the sampling pump with rubber tubing. To provide a check on the amount of nicotine passing the two sorbent beds, in the experiments reported here, the XAD-IV sorbent tubes were followed by a 25-mm BSA-coated glass fiber filter prepared and subsequently analyzed by BYU. A threaded Delrin filter holder was connected in-line between the tube and the pump. The filter holder used a rubber O-ring to seal the BSA-coated 25-mm glass filter in place. The XAD-IV sorbent tube was connected directly to the inlet of the filter holder with a $^1/_4$-in. Swagelok–$^1/_8$-in. NPT Teflon union using a $^1/_4$-in. Teflon 2-piece ferrule. Since the ferrule is slightly larger than the outside diameter of the sorbent tube, leaks will occur at this junction if the Swagelok nut is not tightened with a wrench. Also, leaks will occur within the Delrin filter holder if the two halves are either under- or overtightened or if the O-ring is placed on the downstream side of the filter. With the exception of experiment 1, samples for this intercomparison study were not collected by RJR scientists. Flow calibration of the sampling pumps for this system was done with a rotameter.

2. The passive sampling device (REY PAS) consists of a stainless steel diffusion sampler (*34*) available from Scientific Instrumentation Specialists containing a 600-mg bed of XAD-IV sorbent. The sampling rate used for nicotine in this device was 62.5 mL/min.

University of Massachusetts Medical School/Yale University. The group from the University of Massachusetts and Yale University used two sampling systems:

1. The active sampler (UM/Y FP) has been described (*6*, *8*). A polystyrene air sampling cassette (Millipore) contains a 37-mm Teflon coated glass fiber filter (Pallflex) followed by a Teflon-coated glass fiber filter coated with an aqueous 4% (w/w) $NaHSO_4$ solution. Particulate-phase nicotine is collected on the first filter and gaseous nicotine is collected on the acid-coated filter. Flow through the systems was controlled by Gilian personal sampling pumps at 3 L/min. Flow rate for the UM/Y samplers was calibrated by using rotameters.

2. The passive sampling device (UM/Y PAS) and its flow calibration (24 mL/min) have been described (*7*, *27*). The collection surface is a $NaHSO_4$-coated, Teflon-coated glass fiber filter held in a modified 37-mm-diameter polystyrene air sampling cassette (Millipore) protected with a PTFE filter (S&S) used as a windscreen.

Sampling. Six experiments were conducted during the week of December 14–18, 1987, in the chamber facility

Table I. Experimental Conditions in Each of the Six Experiments.

expt	expected total nicotine concn, nmol/m³	expected total nicotine concn, μg/m³	sampling time, h	av RSP,[a] μg/m³
1	800	125	6	930
2	200	30	3	196
3	200	30	2	184
4	200	30	6	190
5	800	125	3	930
6	800	125	1	990

[a] RSP, respirable suspended particles.

described by Leaderer (*35*, *36*) and Hammond (*6*). Environmental tobacco smoke was generated in the chamber by four smokers at a rate of one cigarette smoked every 10 min. The commercial cigarette used has an FTC tar rating of 17 mg and a nicotine rating of 1 mg. Steady state was achieved by controlling the air circulation and ventilation rates (*36*). In order to simulate typical indoor environments, nicotine concentrations were varied in the experiments by changing the fraction of air exchanged. The sampling time at two different nicotine concentrations was varied in the six experiments conducted. Details of the experiments are given in Table I with the location of the various samplers relative to the smokers shown in Figure 1. The lower expected concentration of nicotine used in this study (200 nmol/m³ or 30 μg/m³) represents the higher concentrations found in indoor environments where smoking is present, including homes (*3*, *18*), work environments (*5*, *6*, *37*), and restaurants (*4*, *7*). The higher concentration of nicotine used (800 nmol/m³ or 125 μg/m³) has been reported in indoor environments (*3*, *9*) but in practice is seldom seen (*38*). The amount of nicotine collected in the high- and low-concentration experiments was altered by varying the sampling time. Sampling was started 1 h after the start of smoking to allow time to establish steady state in the chamber.

During the experiments each sampler was run in triplicate with the exception of BYU TEN. Only one Tenax sampler was used in all the experiments, with a sample being obtained every 10 or 20 min. Appropriate blank samples were obtained by each participant during the experiments. The results reported by each investigator have been corrected by using the data from these blank samples.

Analyses. Analyses were done on the samples in the four organizations' respective laboratories. A summary of analytical techniques is given below.

Brigham Young University. BYU analyzed all collected samples by gas chromatography. Nicotine collected on the BSA-coated annular denuder surface was removed by extraction of the annular surfaces with 5 mL of water. Filters from all BYU samplers were extracted with 5 mL of water for 30 min in an ultrasonic bath. The resulting solutions were made basic with 0.25 M NaOH. A 2-mL sample of the basic solution was extracted with 4 mL of dichloromethane. Recovery of nicotine in the dichloromethane extraction is 80 ± 4% (*39*). Results obtained in the GC analysis (FID detector) of the dichloromethane solutions were corrected for this extraction efficiency. The technique for analyzing the Tenax samples (GC-NPD detector) has been described by Tang et al. (*32*). The nicotine collected on Tenax or on the silanized glass wool was thermally desorbed and collected on a capillary column submerged in liquid nitrogen. Upon completion of desorption, the cold trap was removed and the column was ramped through a temperature program. The nicotine

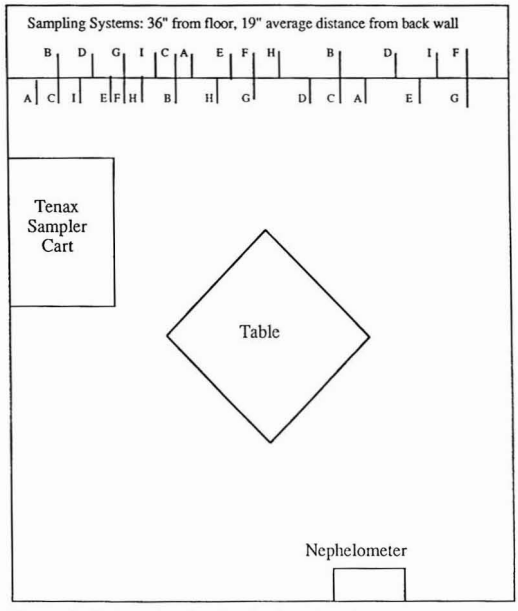

Figure 1. Schematic showing the location of the table where the smokers were located and the location of the various sampling systems in the chamber Key: A, BYU AD; B, BYU FP; C, BYU PAS; D, HAR AD; E, HAR FP; F, REY PAS; G, REY XAD; H, UM/Y FP; I, UM/Y PAS.

concentrations were corrected for the experimentally determined 88 ± 3% collection efficiency of the Tenax trap (*40*).

Harvard University. Collected nicotine was recovered from the denuder surfaces by an aqueous extraction technique. The inlet, impaction plate, and filter pack were removed and one end of the denuder was capped. By use of a micropipet, 500 μL of ethanol was added dropwise to the denuder to wet the inside surfaces. After the denuder surface had been coated with ethanol, 1 mL of extraction solvent was added. The solvent was prepared by dissolving 0.17 g of $NaHSO_4$ in 100 mL of water. The other end was then capped and the denuder was rotated, coating all internal surfaces. The extract was then transferred to a 5-mL Wheaton vial. A second and third extraction were then made following the same procedure and the extracts were combined; however, the ethanol was added only prior to the first extraction. The Teflon and citric acid coated filters were extracted by the same procedure. The denuder or filter extracts were transferred to a 50-mL Erlenmeyer flask. Ten milliliters of 10 M NaOH was then added. The solution was mixed for 5 min with a magnetic stirrer and Teflon-coated stirring bar. Ammoniated heptane (5 mL) was then added and the mixture stirred for an additional 10 min. The ammoniated heptane was prepared by bubbling anhydrous NH_3 through reagent/GC grade heptane for 2–3 min. The flask was removed from the mixer and the organic and aqueous layers were allowed to separate. An aliquot of the organic layer was decanted into a Wheaton vial. The extract was then analyzed for nicotine content by using gas chromatography with an NPD detector. The nicotine extracts were stored at 5 °C. If the extracts were stored more than 24 h, the ammoniation process was repeated. Recovery of nicotine in the analytical procedure was 100% for the denuder and 95% for the filter.

R. J. Reynolds. RJR determined nicotine by using capillary column gas chromatography as described by

Ogden (*29*, *41*). Nicotine was extracted from the XAD-IV with ethyl acetate modified to contain 0.01% (v/v) triethylamine. Nicotine recovery by this procedure is 100.1 ± 2.2% (*41*). The resulting extract solutions were analyzed directly by GC using nitrogen-selective detection with quinoline as an internal standard. Primary and backup sections of the XAD-IV sorbent were analyzed separately to enable assessment of any breakthrough.

Although ETS contains trace amounts of quinoline (~ 1% of the nicotine concentration), the use of quinoline as an internal standard in this method is appropriate in most circumstances. In field-sampling situations, the volume of air sampled in conjunction with typical nicotine concentrations results in 0.1–2.0 μg of nicotine collected on the XAD-IV resin (*29*). For samples in this range, the mass of quinoline also collected on the resin is below the limit of detection and poses no interference with the 5 μg of quinoline added as internal standard. However, in these experiments, the nicotine mass collected on XAD-IV ranged as high as 40 μg, thus imposing a low bias as great as 8% (0.4 μg of ETS quinoline collected; 5 μg of quinoline added). The results presented in Table II have been corrected for any bias attributable to quinoline. If this method is used routinely for large quantities of collected nicotine (>10 μg), the standard method should be modified. Recommended modifications are either an increased amount of quinoline or use of *N*-ethylnornicotine as internal standard (*41*).

University of Massachusetts Medical School/Yale University. The $NaHSO_4$-treated filters from both the UM/Y FP and UM/Y PAS samplers were placed in centrifuge tubes containing 2 mL of water and 60 μL of ethanol and mixed for 1 min. A 2-mL aliquot of 10 M sodium hydroxide was added and the resultant solution mixed for 1 min. Nicotine was concentrated into 500 μL of ammoniated heptane by liquid/liquid extraction. Nicotine recovery by this method was 95 ± 5% (*6*). An aliquot of the heptane solution was injected into a Hewlett-Packard 5890 gas chromatograph with nitrogen-selective detection for quantification of nicotine. Details of the analytical procedure have been published (*6*).

Spiked Samples. To compare analytical techniques for the various laboratories involved, spiked $NaHSO_4$-coated filters were prepared with a known amount of nicotine. Each group was given a set of coded spiked filters. The Reynolds laboratory did not analyze the spiked filters because the acid-coated filters were not compatible with their analytical scheme. The filters, provided by the U.S. Environmental Protection Agency, National Environmental Research Center, Research Triangle Park, NC, were prepared by addition of 100 μL of a standard 1 mg/mL or 20 μg/mL nicotine solution in ammoniated heptane to a Teflon-coated glass fiber filter. The filter had been coated with $NaHSO_4$ following the procedure outlined by Hammond et al. (*6*). Samples were prepared containing 2.0 and 100 μg of nicotine to provide each laboratory with three filters at each concentration. A set of three blank filters was also given each laboratory. In addition, as part of their standard protocol, spiked filters were prepared daily by this same procedure by the University of Massachusetts for independent analysis by that group.

Results

Results from the intercomparison study are given in Table II and are shown as bar graphs in Figures 2–4. The bar graphs give the average and standard deviation of an observation for the replicate samples for each sampling system except for the BYU TEN sampler. For this sampler, the average concentration of nicotine over the time period corresponding to operation of the other samplers was calculated from the sequential time data points. An estimated uncertainty was assigned to this average based on previously reported results (*32*, *40*). Results from analysis of the spiked samples are given in Table III.

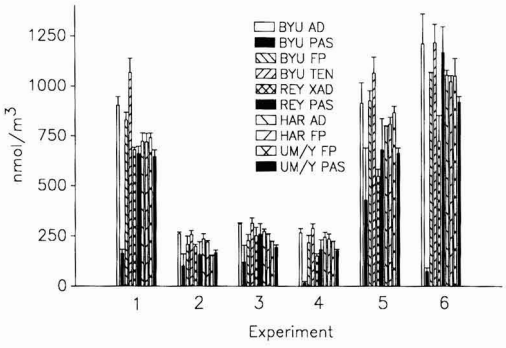

Figure 2. Gas-phase nicotine concentrations obtained with the various samplers.

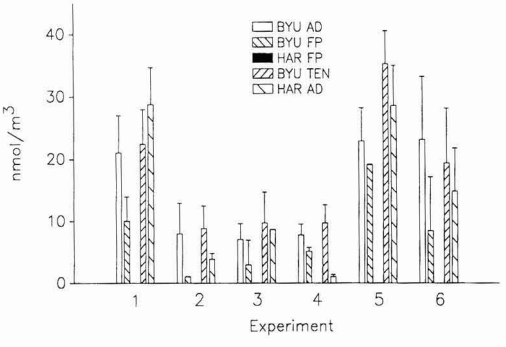

Figure 3. Particulate-phase nicotine concentrations obtained with the various samplers.

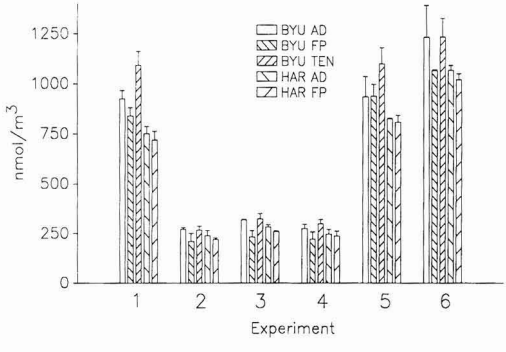

Figure 4. Total nicotine concentrations obtained with the various samplers.

Discussion

Collection Efficiencies of the Sampling Systems. The collection efficiency of the samplers was evaluated for three of the systems by determining the amount of nicotine present in two sequential, identical collection units. These included the XAD-IV sorbent bed in the REY XAD sampler, the BSA-coated denuder sections in the BYU AD sampler, and the two BSA-coated filters in the BYU AD sampler. If X_1 and X_2 are the amounts of nicotine found

Table II. Results of the Intercomparison Study for the Determination of Nicotine in Environmental Tobacco Smoke. Uncertainties Are Reported as the Standard Deviation of an Observation for Three Replicates[a]

expt	phase	BYU AD	BYU FP	BYU TEN	BYU PAS	HAR AD	HAR FP	REY PAS	REY XAD[b]	UM/Y FP	UM/Y PAS	"best"[c,d]
1	gas	903 ± 43	829 ± 39	1069 ± 70	164 ± 20	722 ± 42	719 ± 44	660 ± 37	680 ± 12	741 ± 23	645 ± 33	716 ± 26 (116)
	particle	21.0 ± 6.0	10.0 ± 3.9	22.4 ± 5.6		28.8 ± 5.9	0.1					24.1 ± 4.1 (3.9)
	total	924 ± 42	839 ± 42	1091 ± 70		751 ± 36	719 ± 44					865 ± 150 (140)
2	gas	262 ± 9	209 ± 41	258 ± 20	101 ± 61	235 ± 27	221 ± 7	157 ± 65	199 ± 10	152 ± 4	166 ± 14	219 ± 38 (36)
	particle	7.9 ± 5.0	1.0 ± 0.1	8.8 ± 3.7		3.9 ± 0.9	0.1					6.9 ± 2.6 (1.1)
	total	270 ± 9	210 ± 41	267 ± 20		239 ± 27	221 ± 7					241 ± 27 (39)
3	gas	310 ± 5	229 ± 30	315 ± 25	121 ± 83	274 ± 12	260 ± 3	260 ± 52	252 ± 43	223 ± 4	195 ± 12	266 ± 36 (43)
	particle	7.0 ± 2.6	2.9 ± 4.0	9.7 ± 5.0		8.6 ± 0.0	0.1					8.5 ± 1.3 (1.4)
	total	317 ± 6	232 ± 32	325 ± 26		282 ± 12	260 ± 3					283 ± 39 (46)
4	gas	267 ± 22	218 ± 38	290 ± 22	18 ± 8	246 ± 25	237 ± 25	171 ± 49	152 ± 11	223 ± 4	178 ± 7	247 ± 27 (40)
	particle	7.7 ± 1.8	5.1 ± 0.6	9.7 ± 2.9		1.0 ± 0.4	0.1					8.7 ± 1.4 (1.4)
	total	275 ± 21	222 ± 36	300 ± 22		247 ± 25	237 ± 25					256 ± 31 (42)
5	gas	914 ± 103	927 ± 50	1066 ± 80	430 ± 259	798 ± 3	809 ± 35	679 ± 157	549 ± 34	866 ± 32	663 ± 29	897 ± 98 (145)
	particle	22.9 ± 5.3	19.1 ± 0.1	35.3 ± 5.3		28.6 ± 6.5	0.1					28.9 ± 6.2 (4.7)
	total	937 ± 101	940 ± 59	1101 ± 80		826 ± 5	809 ± 35					923 ± 117 (150)
6	gas	1212 ± 148	1068 ± 3	1217 ± 92	74 ± 19	1055 ± 25	1023 ± 30	1167 ± 130	724 ± 129	1050 ± 87	918 ± 29	1104 ± 87 (179)
	particle	23.1 ± 10.2	8.4 ± 8.7	19.3 ± 8.8		14.8 ± 6.9	0.1					19.1 ± 4.2 (3.1)
	total	1235 ± 157	1069 ± 5	1236 ± 92		1070 ± 24	1023 ± 30					1127 ± 101 (183)

[a] Results are in nmol/m^3. [b] Includes nicotine collected by both the XAD sorbent bed and BSA-saturated filter; see text. [c] See text for details on how the "best" average concentration was obtained. Note that total nicotine is based only on the results obtained with the sampling systems that determined both gas- and particulate-phase nicotine. [d] The values in parentheses are in μg/m^3.

Table III. Results of Spike Sample Analysis

EPA-Prepared Samples[a]

	nicotine, μg		
	BYU	Harvard	UMMC
high	108	108	156
	103	103	127
	99.3	92.2	122
low	2.16	1.35	1.64
	1.59	1.59	1.46
	1.37	1.20	0.77
blank	0.11	<0.02	0.02
	0.00	<0.02	0.02
	0.00	<0.02	0.01

UMMC-Prepared Samples

taken, μg of nicotine	no. of filters	rec, %
0.1	5	95 ± 4
1.0	29	95 ± 4
10	10	96 ± 6
50	2	93 ± 1
200	6	95 ± 2

[a] Expected results: high, 100 μg; low, 2.0 μg; blank, zero.

in the first and second sections, respectively, then the efficiency of collection of nicotine by any collection unit is

$$E = (X_1 - X_2)/X_1 \quad (1)$$

and the total amount entering the first unit is

$$T = X_1/E = X_1^2/(X_1 - X_2) \quad (2)$$

By use of eq 1, the amount of nicotine collected by the primary section of the XAD-IV sorbent bed in the REY XAD sampler was calculated to be 99.1 ± 0.2% of the total collectable by XAD-IV. The two sequential XAD-IV sections are predicted to have captured 100.0% of the nicotine. However, nicotine was found on the acid-saturated filter after the XAD sorbent at concentrations much higher (8–15% of the total nicotine) than could be attributed to particulate-phase nicotine based on the particulate-phase nicotine results with either of the denuder samplers (0.4–4% of total nicotine) (Table II). These results suggest that there was a leak between the second XAD-IV section and the filter, which was added for this study but which is not normally used for field sampling (*12*). The gas-phase data in Table II have been corrected for this apparent leak by combining the XAD and BSA-saturated filter results to give a corrected gas-phase concentration.

The collection efficiency of the BYU AD annular denuder sections for nicotine is calculated from eq 1 to be 93 ± 3% for each of the two sections. The concentration of gas-phase nicotine was calculated from eq 2 for each data set. The collection efficiency of the BSA-saturated filters in the BYU AD sampler is calculated from eq 1 to be 96 ± 4%. The concentration of particulate-phase nicotine was calculated from eq 2 by using the data for the two BSA-saturated filters and correcting for calculated denuder breakthrough of gas-phase nicotine. The breakthrough was calculated as the total gas-phase nicotine (calculated from eq 2) minus the experimental amount collected on the two denuder sections.

The calculated collection efficiency of the HAR AD sampling system for gas-phase nicotine is 98.6% (*33*). This value was used to correct the data for denuder break-

through, giving the results in Table II.

Statistical Comparisons of the Results Obtained by the Sampling Systems. The results obtained with the various sampling techniques were compared by both Bonferoni and Scheffe pairwise tests at a 95% confidence level for each experiment. One-way analysis of variance was also performed for each experiment for gas-phase, particulate-phase, and total nicotine. The results from these statistical tests are that the concentrations of gas-phase and total nicotine were in agreement for all samplers with the exception of all BYU PAS samples (gas phase only); the BYU AD, BYU TEN, and BYU FP (gas phase only) samples from experiment 1; the UM/Y PAS (gas phase only) samples from experiments 4 and 5; the REY PAS (gas phase only) sample from experiment 4; and REY XAD samples for the last three experiments (gas phase only). The data from the REY PAS and UM/Y PAS were generally the lowest concentrations measured, but the results of the statistical tests indicated that the concentrations were not statistically different from those obtained with the active samplers except as noted. The average value of all data obtained with the active sampling systems, omitting the statistical outliers, was assumed to give the "best" concentration for gas-phase nicotine and total nicotine for each experiment. These "best" concentrations are given in Table II.

The results of the statistical analyses showed that the HAR FP particulate nicotine results were not in agreement with the other data. Rank ordering showed a consistent trend for the BYU FP results for particulate nicotine to be lower than the corresponding denuder or Tenax sampling system concentrations. However, the difference was not statistically significant because of the large variance in the data. All other results were in agreement except for the HAR AD result for experiment 4.

Collection of particulate-phase nicotine can be complicated in two ways: (1) by loss of nicotine from particles during sampling in a filter pack system resulting in erroneously low concentrations, or (2) by incomplete collection of nicotine by a denuder or sorbent sampler resulting in artifically high concentrations. Tang et al. (*32*, *40*) showed that loss of particulate-phase nicotine from the silanized glass wool in the BYU TEN sampler was only a problem for collection times longer than 20 min. Therefore, agreement among the BYU AD, BYU TEN, and HAR AD sampling systems is expected. For particulate nicotine, the average of BYU AD, BYU TEN, and HAR AD (except for experiment 4) was used as the reference "best" value. The collection of particulate nicotine by the coated filters of the denuder systems should be quantitative, while analysis of particles collected by the filter pack samplers could underestimate particulate-phase nicotine due to stripping of nicotine from particles during sampling.

Linear Regression Analyses of the Results. Linear regression analyses were done to compare the results for gas-phase, particulate-phase, and total nicotine obtained with each of the sampling systems to the average "best" concentrations outlined above. The results of these analyses are given in Table IV. For all samplers, the uncertainty in the linear regression intercept includes (or nearly includes) zero for all comparisons, indicating no significant constant bias exists in any of the data sets. The magnitude and uncertainty of the slope is a measure of how well each measurement by any given sampling system agreed with the calculated average.

BYU TEN results for gas-phase nicotine were high by 16% (Table IV). Location of the sampler and errors in the calibration used in the analysis could be two factors

Table IV. Results of Linear Regression Analysis of the Average Concentration (See Text) As Compared to the Results Obtained with Each Sampler

sampler	nicotine species	slope	intercept, nmol/m^3	R^2
BYU AD	total	1.06 ± 0.03	9 ± 30	1.00
	gas	1.07 ± 0.08	28 ± 67	0.98
	particle	0.81 ± 0.16	2.0 ± 3.3	0.87
BYU FP	total	1.06 ± 0.03	−39 ± 29	1.00
	gas	1.04 ± 0.07	−19 ± 63	0.98
	particle	0.65 ± 0.12	−2.7 ± 2.5	0.88
BYU PAS	gas	0.17 ± 0.17	56 ± 146	0.19
BYU TEN	total	1.16 ± 0.07	5 ± 58	0.99
	gas	1.17 ± 0.14	33 ± 116	0.95
	particle	1.08 ± 0.14	0.2 ± 2.9	0.94
HAR AD	total	0.90 ± 0.04	17 ± 31	0.99
	gas	0.91 ± 0.04	31 ± 33	0.99
	particle	1.24 ± 0.20	−5.5 ± 4.1	0.91
HAR FP	total	0.87 ± 0.03	8 ± 27	1.00
	gas	0.91 ± 0.03	22 ± 28	0.99
	particle	0.0		
REY PAS	gas	1.01 ± 0.12	−62 ± 104	0.94
REY XAD	gas[a]	0.96 ± 0.01	8 ± 6	1.00
	gas[b]	0.65 ± 0.05	−15 ± 29	1.00
UM/Y FP	gas	1.01 ± 0.04	−40 ± 36	0.99
UM/Y PAS	gas	0.84 ± 0.06	−20 ± 48	0.98

[a] First three experiments. [b] Last three experiments.

contributing to the high results. The Tenax sampler was located against a side wall in the chamber (Figure 1). It was also closer to the table where the smokers were seated than the other samplers. Location analyses of all the samplers showed random distribution of the variation among replicate sampling techniques, with the exception of the first and last experiments (higher concentrations), where there was a suggestion that concentrations were ~10% higher than normal at the wall closest to the location of the Tenax sampler. If the trend observed in these experiments indicates a concentration gradient in the region of the Tenax sampler, then part of the high results may thus be accounted for.

Concentrations of gas-phase nicotine determined with the BYU PAS sampler were clearly low. Subsequent experiments have shown that the low results are due to adsorption of nicotine by the passive filter holder itself. The passive stainless steel sampling device effectively scrubbed out a portion of the gas-phase nicotine before it reached the filter inside. This same problem was not seen for the REY PAS sampler, which was also constructed of stainless steel by the same manufacturer, but which had a passivation surface treatment applied by the manufacturer.

Concentrations of gas-phase nicotine determined with the REY XAD sampler agreed with the average for the first three experiments but were low by 35% for the last three experiments (Table IV). Results obtained in previous intercomparison studies show the REY XAD sampler as typically used (without a backup filter) agreed well with those obtained with the annular denuder sampler system (*23*) and with a thermal desorption based Tenax trapping system (*42*). As mentioned previously, the REY XAD data have been corrected for an apparent leak between the XAD tube and the filter pack holder by summing the total collected by the two parts of the system.

The BYU FP and HAR FP filter packs gave concentrations of particulate-phase nicotine that averaged 47 ± 19% and <1%, respectively, the particulate-phase nicotine concentrations determined with the annular denuder and Tenax sampling system (Table IV). This suggests that particulate-phase nicotine is lost from the particles to the gas phase as air is drawn through the filter. This artifact

nicotine would then be collected by the acid-coated filter following the particle Teflon filter. The artifact will have negligible effect on the filter pack data for gas-phase nicotine because >95% of the nicotine was in the gas phase in the environmental tobacco smoke sampled (Table III).

Spiked Sample Results. The results obtained for the spiked samples prepared by EPA (Table III), agreed with the expected values with the exception of the results from the University of Massachusetts/Yale. The results from UM/Y averaged 32% higher in the 100-μg nicotine spikes than was expected. However, for the experimental results, UM/Y samplers compared well with the other samplers and were in agreement with the UMMC-prepared spikes (95 ± 5% recovery) prepared at low amounts of nicotine (Table III).

The results from the EPA high-concentration spiked samples for the other two laboratories agreed with the expected concentrations with an average variance in the data of 5%. For all laboratories, the results obtained for the low-concentration spiked samples gave results that were generally low by from 15 to 35% of the expected value. The variance in these data ranged from 12 to 29% for the three laboratories. This is higher than the variance of 11 ± 8% for collection of 2 μg of nicotine by the passive samplers. In addition, as discussed above, the concentrations obtained with the REY and UM/Y passive samplers are comparable to those obtained with the active samplers and do not show a low bias. This suggests that the low results obtained for the low-concentration spikes prepared by EPA may reflect variability in the preparation of spikes with small amounts of nicotine. A possible source of error might be the loss of some nicotine during the application and drying of the standard nicotine solution. No analytical work was done by EPA to verify the constancy of spikes prepared in their laboratory.

Summary

The intercomparison study compared several types of sampling systems being used for the determination of nicotine in ETS. Total nicotine determined with the various sampling systems was generally in good agreement. Because >95% of the nicotine is present in the gas phase, agreement among samplers was also seen for this species. The most notable exception was the determination of nicotine with a stainless steel passive sampler where the results were low due to adsorption of nicotine by the sampler. Surface passivation of the sampler helps minimize this problem. Good agreement was seen for the determination of gas-phase and particulate-phase nicotine by using two different annular denuder systems, and also a semi-real-time Tenax sampling system. The precision of the particulate nicotine data was poor because only 2–3% of the total nicotine was present as particulate-phase nicotine. However, the study also indicates that loss of particulate-phase nicotine to the gas phase occurs in a filter pack sampling system, and that determination of particulate-phase nicotine by these systems can be expected to be in error due to loss of nicotine from particles during sampling. This volatilization of particulate-phase nicotine did not significantly affect determined gas-phase nicotine concentrations for the environment sampled in this study. The low concentrations of particulate-phase nicotine resulted in total and gas–phase nicotine generally not being significantly different (Table II) where both were determined.

Acknowledgments

Appreciation is expressed to R. Williams, EHRT, for assistance in preparing spiked filters.

Registry No. BSA, 98-11-3; XAD-4, 37380-42-0; $NaHSO_4$, 7681-38-1; Tenax, 24938-68-9; Teflon, 9002-84-0; citric acid, 77-92-9; nicotine, 54-11-5.

Literature Cited

(1) The health consequences of involuntary smoking. A report of the Surgeon General, U.S. Dept. of Health and Human Services, 1986.
(2) *Environmental tobacco smoke. Measuring exposure and assessing health effects*; National Research Council, National Academy Press: Washington DC, 1986.
(3) Eatough, D. J.; Benner, C. L.; Tang, H.; Landon, V.; Richards, G.; Caka, F. M.; Crawford, J.; Lewis, E. A.; Hansen, L. D.; Eatough, N. L. The chemical composition of environmental tobacco smoke III. Identification of conservative tracers of environmental tobacco smoke. *Environ. Int.* **1989**, *15*, 19–25.
(4) Eudy, L.; Heavner, D.; Stancill, M.; Simmons, J. S.; McConnell, B. *Indoor Air '87. Proceedings of the Fourth International Conference on Indoor Air Quality and Climate*; Seifert, B., Esdorn, H., Fischer, M., Ruden, H., Wegner, J., Eds.; Berlin (West), 17–21 August 1987; Institute for Water, Soil and Air Hygiene, 1987; Vol. 2, pp 126–130.
(5) Hammond, S. K.; Smith, T. J.; Woskie, S. R.; Leaderer, B. P.; Bettinger, N. *Am. Ind. Hyg. Assoc. J.* **1988**, *49*, 516–522.
(6) Hammond, S. K.; Leaderer, B. P.; Roche, A. C.; Schenker, M. *Atmos. Environ.* **1987**, *21*, 457–462.
(7) Hammond, S. K.; Coghlin, J. *Indoor Air '87. Proceedings of the Fourth International Conference on Indoor Air Quality and Climate*; Seifert, B., Esdorn, H., Fischer, M., Ruden, H., Wegner, J., Eds., Berlin (West), 17–21 August 1987; Institute for Water, Soil and Air Hygiene, 1987; Vol. 2, pp 131–136.
(8) Hammond, S. K.; Leaderer, B. P.; Roche, A. C.; Schenker, M. *Proceedings, 1985 EPA/APCA Symposium on Measurement of Toxic Air Pollutants*; Air Pollution Control Association, 1985; pp 16–24.
(9) Löfroth, G.; Burton, R. M.; Forehand, L.; Hammond, S. K.; Sella, R. L.; Zweidinger, R. B.; Lewtas, J. *Environ. Sci. Technol.* **1989**, *23*, 610–614.
(10) McCarthy, J.; Spengler, J.; Chang, B.-H.; Coultas, D.; Samet, J. *Indoor Air '87. Proceedings of the Fourth International Conference on Indoor Air Quality and Climate*; Seifert, B., Esdorn, H., Fischer, M., Ruden, H., Wegner, J., Eds.; Berlin (West), 17–21 August 1987; Institute for Water, Soil and Air Hygiene, 1987; Vol. 2, pp 142–146.
(11) Muramatsu, M.; Umemura, S.; Okada, T.; Tomita, H. *Environ. Res.* **1984**, *35*, 218–227.
(12) Oldaker, G. B., III; Conrad, F. W., Jr. *Environ. Sci. Technol.* **1987**, *21*, 994–999.
(13) Sterling, T. D.; Collett, C. W.; Sterling, E. M. *J. Occup. Med.* **1987**, *29*, 57–62.
(14) Curvall, M.; Kazemi-Vala, E.; Enzell, C. R.; Olander, L.; Johansson, J. *Indoor Air '87. Proceedings of the Fourth International Conference on Indoor Air Quality and Climate*; Seifert, B., Esdorn, H., Fischer, M., Ruden, H., Wegner, J., Eds.; Berlin (West), 17–21 August 1987; Institute for Water, Soil and Air Hygiene, 1987; Vol. 2, pp 57–60.
(15) Feyerabend, C.; Higgenbottam, T.; Russell, M. A. H. *Br. Med. J.* **1982**, *284*, 1002–1004.
(16) Foliart, D.; Benowitz, N. L.; Becker, C. E. *N. Engl. J. Med.* **1983**, *308*, 1105.
(17) Greenberg, R. A.; Haley, N. J.; Etzel, R. A.; Loda, F. A. *N. Engl. J. Med.* **1984**, *310*, 1075–1078.
(18) Henderson, F. W.; Morris, R.; Reid, H. F.; Hu, P. C.; Mumford, J. L.; Forehand, L.; Burton, R.; Lewtas, J.; Hammond, S. K.; Haley, N. J. *Indoor Air '87. Proceedings of the Fourth International Conference on Indoor Air Quality and Climate*; Seifert, B., Esdorn, H., Fischer, M., Ruden, H., Wegner, J., Eds.; Berlin (West), 17–21 August 1987; Institute for Water, Soil and Air Hygiene, 1987; Vol. 2, pp 18–21.
(19) Matsukura, S.; Taminato, T.; Kitano, N.; Seino, Y.; Hamada, H.; Uchihashi, M.; Nakajima, H.; Hirata, Y. *N. Engl.*

J. Med. **1984**, *311*, 828–832.
(20) Yanagisawa, Y.; Matsuki, H.; Spengler, J. D. *Indoor Air '87. Proceedings of the Fourth International Conference on Indoor Air Quality and Climate*; Seifert, B., Esdorn, H., Fischer, M., Ruden, H., Wegner, J., Eds.; Berlin (West), 17–21 August 1987; Institute for Water, Soil and Air Hygiene, 1987; Vol. 2, pp 115–118.
(21) Watts, R. R.; Langone, J. J.; Knight, G. J.; Lewtas, J. *Env. Health Perspect.*, in press.
(22) Eatough, D. J.; Hansen, L. D.; Lewis, E. A. *Proceedings, APCA Specialty Conference on Indoor Air Quality*; September 27–29, 1988; Niagara Falls, NY, 1988; pp 183–200.
(23) Eatough, D. J.; Woolley, K.; Tang, H.; Lewis, E. A.; Hansen, L. D.; Eatough, N. L.; Ogden, M. W. *Proceedings, EPA/APCA Symposium on Measurement of Toxic and Related Air Pollutants*; 1988; pp 739–749.
(24) Eatough, D. J.; Benner, C. L.; Mooney, R. L.; Bartholomew, D.; Steiner, D. S.; Hansen, L. D.; Lamb, J. D.; Lewis, E. A. *Proceedings, 79th Annual Meeting of the Air Pollution Control Association*; 22–27 June 1986, Minneapolis, MN, 1986; Paper 86-68.5.
(25) Eudy, L. W.; Thome, F. A.; Heavner, D. L.; Green, C. R.; Ingebrethsen, B. J. *Proceedings, 79th Annual Meeting of the Air Pollution Control Association*; 22–27 June 1986; Minneapolis, MN, 1986; Paper 86-38.7.
(26) Eatough, D. J.; Benner, C. L.; Bayona, J. M.; Caka, F. M.; Tang, H.; Lewis, L.; Lamb, J. D.; Lee, M. L.; Lewis, E. A.; Hansen, L. D. *Proceedings, EPA/APCA Symposium on Measurement of Toxic and Related Air Pollutants*; Air Pollution Control Association, 1987; pp 132–139.
(27) Hammond, S. K.; Leaderer, B. P. *Environ. Sci. Technol.* **1987**, *21*, 494–497.
(28) Thome, F. A.; Heavner, D. L.; Ingebrethsen, B. J.; Eudy, L. W.; Green, C. R. *Proceedings, 79th Annual Meeting of the Air Pollution Control Association*; 23–27 June 1986; Minneapolis, MN, 1986; Paper 86-37.6.
(29) Ogden, M. W. *J. Assoc. Off. Anal. Chem.* **1989**, *72*, 1002–1006.
(30) Possanzini, M.; Febo, A.; Liberti, A. *Atmos. Environ.* **1983**, *17*, 2605–2610.
(31) Lewis, R. G.; Mulik, J. D.; Coutant, R. W.; Wooten, G. W.; McMillan, C. R. *Anal. Chem.* **1985**, *57*, 214–219.
(32) Tang, H.; Richards, G.; Gunther, K.; Crawford, J.; Lee, M. L.; Lewis, E. A.; Eatough, D. J. *HRC & CC, J. High Resolut. Chromatogr. Chromatogr. Commun.* **1988**, *11*, 775–782.
(33) Koutrakis, P.; Fasano, A. M.; Slater, J. L.; Spengler, J. D.; McCarthy, J. F.; Leaderer, B. P. *Atmos. Environ.* **1989**, *23*, 2767–2773.
(34) Ogden, M. W.; Nystrom, C. W.; Oldaker, G. B., III; Conrad, F. W., Jr. *Proceedings, EPA/AWMA Symposium on Measurement of Toxic and Related Air Pollutants*; Air and Waste Management Association: Raleigh, NC, 1989; pp 552–558.
(35) Leaderer, B. P. *Science* **1982**, *218*, 1113–1115.
(36) Leaderer, B. P.; Cain, W. S.; Isseroff, R.; Bergulund, L. G. *Atmos. Environ.* **1984**, *18*, 99–106.
(37) Vaughn, W. M., Hammond, S. K. *Proceedings, 82nd Annual Meeting of the Air and Waste Management Association*; 25–30 June 1989, Anaheim, CA, 1989; Paper 89-159.6.
(38) Kirk, P. W. W.; Hunter, M.; Baek, S. O.; Lester, J. N.; Perry, R. *Indoor and Ambient Air Quality*; Perry, R., Kirk, P. W. W., Eds.; Selper Ltd.: London, 1988, pp 99–112.
(39) Eatough, D. J.; Benner, C. L.; Bayona, J. M.; Caka, F. M.; Richards, G.; Lamb, J. D.; Lewis, E. A; Hansen, L. D. *Environ. Sci. Technol.* **1989**, *23*, 688–699.
(40) Tang, H.; Benner, C. L.; Richards, G.; Lee, M. L.; Lewis, E. A.; Hansen, L. D.; Eatough, D. J. *Int. J. Environ. Anal. Chem.* **1988**, *33*, 197–208.
(41) Ogden, M. W.; Eudy, L. W.; Heavner, D. L.; Conrad, F. W., Jr.; Green, C. R. *Analyst* **1989**, *114*, 1005–1008.
(42) Jenkins, R. A.; Thompson, C. V.; Higgins, C. E. *Indoor and Ambient Air Quality*; Perry, R., Kirk, P. W. W., Eds.; Selper Ltd.: London, 1988; pp 557–566.

Received for review June 28, 1989. Accepted March 12, 1990.

Model of Organic Chemical Uptake and Clearance by Fish from Food and Water

Kathryn E. Clark, Frank A. P. C. Gobas, and Donald Mackay*

Department of Chemical Engineering and Applied Chemistry, University of Toronto, Toronto, Ontario, M5S 1A4 Canada

■ A comprehensive model is presented that describes the bioaccumulation of organic chemicals by fish from food and water, using size- and species-dependent parameters describing transport and transformation "resistances" and parameters for metabolic conversion and bioavailability. Uptake of a nonmetabolizing chemical from water tends to result in the chemical adopting a fugacity in the fish approaching that in the water, as expressed by a bioconcentration factor. Uptake from food may result in a fish fugacity that is higher than the food or water fugacity, corresponding to biomagnification. This is postulated to be due to food digestion causing a fugacity increase in the gastrointestinal tract. This biomagnification phenomenon is most significant for very hydrophobic, slowly clearing, nonmetabolizing chemicals. The model also describes food chain biomagnification, the dependence of fish concentration on rates of metabolism and growth, and the effect of reduced bioavailability.

Introduction

One of the most important environmental transport and partitioning processes is bioaccumulation. This process may result in concentrations of toxic chemicals in fish that are large multiples of those of the water in which the fish dwell. The phenomenon of bioconcentration is generally considered to be an equilibrium partitioning or "thermodynamic" process in which the fish/water concentration ratio is a reflection of the different affinities of the chemical for water and for the lipids of the fish and is usually well correlated with the chemical's octanol–water partition coefficient K_{OW} (*1–5*). The fish and water thus approach a state in which the chemical's fugacities or chemical potentials in fish and water are equal. This phenomenon is readily investigated in the laboratory in uptake–depuration experiments. When loss of correlation occurs, it may be due to the slow kinetics of uptake, fish growth, reduced bioavailability of the chemical due to sorption in the water, unusual resistances to transfer, or metabolism of the chemical (*5–13*).

In real situations the fish receives chemical both from water by gill transfer and from food by ingestion. The latter process may lead to biomagnification, or a fish/water concentration ratio that exceeds the bioconcentration ratio. Connolly and Pedersen (*14*) and Oliver and Niimi (*15*)

0013-936X/90/0924-1203$02.50/0

demonstrated the existence of a biomagnification phenomenon by comparing concentrations and fugacities of fish of various trophic levels with those of the water. Apparently the fish achieves a fugacity that may be a multiple (e.g., 3) of the food or water fugacity as a result of food uptake. If the food and water are at similar fugacities, the fish must thus be in a state in which the chemical is being taken up against a fugacity gradient, i.e., transport is from low to high fugacity. In principle there must be simultaneous loss by depuration, but the rate is presumably too slow to allow equilibrium to be reestablished.

Successful "kinetic" models have been developed to describe entire food chains (*16–19*) in which the concentration achieved in the fish is a balance between input and output rates expressed in terms of rate constants. In such models it is not necessary to consider the thermodynamic issue. Notable is the recent model by Thomann (*19*), which involved analysis of a large data base and elucidates the dependence of food chain biomagnification on K_{OW}.

In this paper we review and suggest mechanisms for these processes and assemble a comprehensive model describing uptake of chemical from water and food and losses to water and feces and by metabolism. The model brings together several existing models that have been individually validated for components of the overall process. The model is presented as a hypothesis in the hope that it may be tested and improved as a result of future experimental studies. The approach is to develop the model in fugacity format, suggest equations containing chemical-specific and fish-specific parameters that may be used to correlate or predict process rates, and test the model with available data. Many of these equations have been suggested in previous studies (*7*, *8*, *20*). It is shown that the "kinetic" and "thermodynamic" models of bioaccumulation, which are occasionally viewed as being inconsistent or competitive, are in reality merely different methods of expressing the same phenomena. Finally, the model is used to explore how differences in chemical properties affect the relative importance of food and water as sources of chemical, and how metabolism and bioavailability influence bioaccumulation.

Model Development in Fugacity Format

Figure 1A shows the fish uptake and loss processes in fugacity terms, in which each process is expressed as a product of a fugacity (f, in Pa) and a rate parameter or D value with units of (mol/Pa·h), thus Df has units of mol/h. Equilibrium is characterized by Z values (mol/m^3·Pa) that relate concentration C (mol/m^3) to fugacity (f) by equating C to Zf. Z values are estimated for the phases of water, lipid, octanol, and whole fish (denoted with subscripts W, L, O, and F, respectively). A dimensionless partition coefficient is merely the ratio of Z values. The calculation of Z and D values has been described in detail elsewhere (*21*), but briefly, three types of D values can apply.

For reactions (such as metabolism) D is the product $V_F Z k$, where k is the reaction rate constant, V_F is fish volume, and Z is for the fish. For bulk flow of chemical D is GZ, where G is the phase flow rate (m^3/h), and Z is for the flowing fluid. This is applied to water flow into and out of the gills, ingestion and egestion. Diffusive processes, for example transfer across membranes, can be expressed as $D(f_1 - f_2)$ where $(f_1 - f_2)$ is the fugacity difference or driving force. The D value can be viewed as a product KAZ where K is a mass-transfer coefficient (m/h), A is area (m^2), and Z is that of the chemical in the medium in which diffusion is occurring. K may be further viewed as a diffusivity divided by a diffusion path length. The

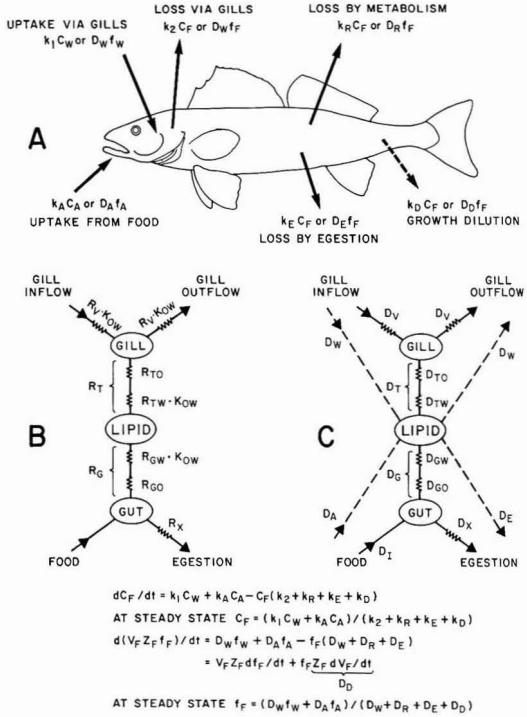

$$dC_F/dt = k_1 C_W + k_A C_A - C_F(k_2 + k_R + k_E + k_D)$$

$$\text{AT STEADY STATE } C_F = (k_1 C_W + k_A C_A)/(k_2 + k_R + k_E + k_D)$$

$$d(V_F Z_F f_F)/dt = D_W f_W + D_A f_A - f_F(D_W + D_R + D_E) = V_F Z_F df_F/dt + f_F Z_F dV_F/dt$$

$$\text{AT STEADY STATE } f_F = (D_W f_W + D_A f_A)/(D_W + D_R + D_E + D_D)$$

Figure 1. Schematic diagram of chemical transport in a fish (A), with flows expressed in resistance terms (B) and fugacity terms (C).

diffusion may be in a fluid boundary layer or in a stationary membrane.

As shown in Figure 1A, the rates of chemical transfer (in mol/h) may be expressed either in the form of products of rate constants and concentrations or as fugacities and D values. The corresponding differential equations are also given in Figure 1. Included is a term for growth dilution describing the change in concentration attributable to fish growth. The rates are defined as applying to transport into the fish body, i.e., through the epithelium, thus chemical that is in the gill cavity or the gastrointestinal (GI) tract is not included in the fish concentration, C_F. The terms k_1 or D_W, thus include an efficiency of uptake from the gill, and k_A or D_A a similar gut absorption efficiency. The differential equation can be integrated and various boundary conditions applied to give equations expressing C_F as a function of time, which can be fitted to experimental data. At constant exposure conditions dC_F/dt eventually becomes zero, steady state is reached, and C_F can be expressed as shown. The ratio C_F/C_W, the bioaccumulation factor K_B, then becomes dependent on k_A and k_E or D_A and D_E and, if metabolism occurs, on k_R or D_R. Steady state is thus not necessarily a true equilibrium (equifugacity) condition. When these terms are significant, it is expected that purely thermodynamically based correlations between K_B and K_{OW} will break down.

Inherent in this model is the use of the concept of resistance to transfer. These resistances add when they are in series. As has been discussed by Flynn and Yalkowsky (*22*) and Mackay and Hughes (*7*), when resistances in two different phases (e.g., organic and water) are in series, it is necessary to include the phase partition coefficient, usually the octanol–water partition coefficient. Large resistances tend to occur in phases (usually water) in which concentrations are low. Diffusive flux is proportional to

concentration, thus low concentrations constrain fluxes and result in high resistances. Since a D value is a conductivity, its reciprocal, $1/D$, is the resistance.

Equilibrium. At thermodynamic equilibrium K_B or C_F/C_W becomes Z_F/Z_W. If L_F is the lipid or octanol-equivalent volume fraction of the fish, Z_F is $L_F Z_O$, where Z_O is the fugacity capacity of octanol and Z_O/Z_W is K_{OW}; thus K_B is $L_F K_{OW}$. As discussed by Mackay (*5*), L_F is typically approximately 0.05.

Gill Transfer. The upper part of Figure 1C shows a model of gill-transfer processes, which is essentially that of Gobas and Mackay (*8*). It is assumed that the gill acts as a continuous-stirred tank reactor or well-mixed compartment into and out of which water flows, with chemical (and oxygen) being transferred to the fish by diffusion. The fish, enclosed within epithelial tissue, is treated as being at pseudo-steady-state composition and fugacity f_F. D_T contains terms for blood flow resistance and blood-to-lipid transfer as well as gill membrane resistances. The ventilation flow rate G_V (m^3/h) can be used to estimate D_V as $G_V Z_W$. A steady-state mass balance over the gill cavity gives

$$D_V f_W = D_V f_V + D_T(f_V - f_F) \quad (1)$$

thus

$$f_V = (D_V f_W + D_T f_F)/(D_V + D_T) \quad (2)$$

where f_V is the fugacity of the chemical in the water in the gill.

The gill uptake efficiency, E_T, is then given by the ratio of uptake to input:

$$E_T = D_T(f_V - f_F)/D_V f_W = D_T(f_W - f_F)/[(D_V + D_T)f_W] \quad (3)$$

This implies that gill uptake efficiency depends on the state of the fish, having a maximum value E_{TM} of $D_T/(D_V + D_T)$ when the fish is uncontaminated; falling to zero when the fish is in equilibrium with the water and $(f_W - f_F)$ is zero. Measurement of E_T is a convenient method of estimating D_T, because D_V can be measured (with difficulty) from the water flow rate past the gills. For example, a 50% efficiency implies that D_V and D_T are equal.

Following Gobas and Mackay (*8*) and Mackay and Hughes (*7*), it is suggested that D_T is a conductivity or reciprocal resistance made up of resistances in series, which are either "organic" (characterized by octanol) or water phase in nature, thus

$$1/D_T = 1/D_{TO} + 1/D_{TW} \quad (4)$$

Further, D_{TO} and D_{TW}, the organic and water D values, can be expressed as GZ products where G is a fictitious flow rate of organic matter or water, i.e.

$$D_{TO} = G_{TO} Z_O \quad (5)$$

and

$$D_{TW} = G_{TW} Z_W \quad (6)$$

These G values were designated Q_O and Q_W by Gobas and Mackay (*8*).

The relationship between the overall parameter, D_W, and D_T and D_V can now be established by equating the net uptake rates through the gill membrane, using eq 2 as

$$D_W(f_W - f_F) = D_T(f_V - f_F) = D_T D_V(f_W - f_F)/(D_V + D_T) = E_T D_V f_W \quad (7)$$

It follows that

$$D_W = D_T D_V/(D_V + D_T) \quad (8)$$

or

$$1/D_W = 1/D_V + 1/D_T = 1/D_V + 1/D_{TW} + 1/D_{TO} = 1/(G_V Z_W) + 1/(G_{TW} Z_W) + 1/G_{TO} Z_O = (1/G_V + 1/G_{TW})/Z_W + 1/G_{TO} Z_O \quad (9)$$

The overall resistance $(1/D_W)$ is thus the sum of three resistances in series, two of which contain Z_W and the third Z_O.

It is noteworthy, as discussed by Gobas and Mackay (*8*), that when K_{OW} or Z_O/Z_W is relatively small, e.g., 10^2, the term $1/D_{TO}$ dominates and transfer is lipid phase controlled. When K_{OW} is larger, e.g., 10^6, the term $1/D_{TO}$ is negligible and transfer is controlled by water-phase flow and diffusion. The reason for this is the constraint introduced by the low concentration in the water phase relative to that in the organic phase.

Gastrointestinal Tract. A similar approach is taken for the GI tract as shown in the lower part of Figure 1C, but in this case it is not feasible to assign the same D value to food ingestion and egestion because digestion causes the food to lose mass and change composition. We follow Gobas et al. (*20*) and Amidon et al. (*23*) by suggesting that absorption be described by assuming that the gut is a well-mixed reactor. A steady-state mass balance gives

$$D_I f_A = D_X f_G + D_G(f_G - f_F) \quad (10)$$

and

$$f_G = (D_I f_A + D_G f_F)/(D_G + D_X) \quad (11)$$

where f_G is the fugacity of the chemical in the gut contents, D_I is the food intake D value, D_X is the egestion value, and D_G expresses resistances to transfer through the gut wall and blood to the lipid tissues, which are the ultimate destination of the chemical. D_I is not equivalent to D_A, nor is D_X equivalent to D_E, because the mass balance is now over the gut contents, not the fish.

The food uptake efficiency is given by the ratio of uptake to input:

$$E_A = D_G(f_G - f_F)/D_I f_A = D_G(f_A - D_X f_F/D_I)/[(D_G + D_X)f_A] \quad (12)$$

Again it follows that E_A depends on the condition of the fish. When the fish is uncontaminated and f_F is zero, the uptake efficiency is a maximum E_{AM} of $D_G/(D_G + D_X)$. As with gill absorption, E_A may be used to estimate D_G if the feeding rate is known. Note that if D_I and D_X were equal, the algebraic form would be identical with that for the gills, the common D value in that case being D_V. In practice it is suspected that D_X is considerably smaller than D_I due to food absorption and especially to fat hydrolysis and absorption.

Following Gobas et al. (*20*), it is suggested that D_G may be treated similarly to D_T, as being comprised of organic and water resistances, i.e.

$$1/D_G = 1/D_{GO} + 1/D_{GW} = 1/G_{GO} Z_O + 1/G_{GW} Z_W \quad (13)$$

The relationship between D_A and D_E, and D_I, D_X, and D_G can now be established by equating the net food uptake rate as

$$D_A f_A - D_E f_F = D_G(f_G - f_F) = [D_G D_I/(D_G + D_X)]f_A - [D_X D_G/(D_G + D_X)]f_F \quad (14)$$

thus

$$D_A = D_G D_I/(D_G + D_X) = E_{AM} D_I \quad (15)$$

$$D_E = D_G D_X/(D_G + D_X) = E_{AM} D_X \quad (16)$$

or

$$1/D_E = 1/D_G + 1/D_X = 1/D_{GO} + 1/D_{GW} + 1/D_X \quad (17)$$

If it is assumed that egestion of chemical is in association with an organic medium which can be expressed in terms of an equivalent octanol flow G_{XO}, then D_X is $G_{XO}Z_O$ and $1/D_E$ can be expressed in water and organic terms as

$$1/D_E = (1/G_{GO} + 1/G_{XO})/Z_O + 1/G_{GW}Z_W \quad (18)$$

The initial or maximum food uptake efficiency is given by

$$E_{AM} = D_G/(D_G + D_X) = (1/D_X)/(1/D_G + 1/D_X) \quad (19)$$

These $1/D$ terms reflect the resistance to egestion $1/D_X$, and gut absorption resistance $1/D_G$. Absorption is thus viewed as a competitive process between absorption and egestion with absorption efficiency being high when $1/D_X$ is large compared to $1/D_G$. Substances of very large K_{OW}, e.g., exceeding 10^7, may be absorbed inefficiently as discussed by Gobas et al. (*20*).

A steady state may be reached at which there is no net gut transfer because f_G equals f_F. Thus, from eq 10, $D_I f_A$ equals $D_X f_G$ and $D_X f_F$, and the ratio of fish to food fugacity becomes D_I/D_X, which we call the "digestion coefficient" and designate as Q. Combining eq 15 and 16

$$D_A/D_E = D_I/D_X = Q = f_F/f_A \text{ (at steady state)} \quad (20)$$

The digestion coefficient, Q, represents the maximum biomagnification factor, or ratio of fish to food fugacity, and has an expected magnitude of 3–10 as discussed by Connolly and Pedersen (*14*).

Metabolism. The D value for metabolism, D_R, can be expressed as $V_F Z_F k_R$.

Overall Mass Balance. The gill, gut, and metabolism D values may be combined to give the overall equation given in Figure 1. If growth is included, it may be treated as a pseudo-D value (D_D), as shown. Clearly, it is possible for the fish fugacity to achieve values ranging up to Q times the food fugacity depending on the relative magnitudes of the D values.

Equivalence of Fugacity and Rate Constant Models

Examination of the fugacity and rate constant equations shows that they are algebraically equivalent as follows:

$$k_1 = D_W/V_F Z_W = k_2 L_F K_{OW} \quad (21)$$

$$k_2 = D_W/V_F Z_F \quad (22)$$

$$k_R = D_R/V_F Z_F \quad (23)$$

$$k_D = D_D/V_F Z_F = (dV_F/dt)/V_F \quad (24)$$

$$k_A = D_A/V_F Z_A = G_I E_A/V_F \quad (25)$$

$$k_E = D_E/V_F Z_F \quad (26)$$

where G_I is the feeding rate and Z_A is the fugacity capacity of the food.

Resistance Parameters

If a set of D values or rate constants is available, the steady- and unsteady-state concentrations in the fish can be determined for various exposure regimes. There is an incentive to devise correlations, and thus a predictive ability, by expressing D values and rate constants in terms of parameters that are separately specific to the fish and to the chemical. This is conveniently done by using resistances, denoted R, which have units of time (h). They can be viewed as the time required to achieve a certain degree of chemical transfer. Thus, a long time implies a high resistance and slow transfer. A schematic diagram of a fish in terms of resistances is shown in Figure 1B. The resistances are related to D values and rate constants as follows.

gill water flow resistance:

$$R_V = V_L/G_V = V_L Z_W/D_V \quad (27)$$

gill membrane water resistance:

$$R_{TW} = V_L/G_{TW} = V_L Z_W/D_{TW} \quad (28)$$

gill membrane organic resistance:

$$R_{TO} = V_L/G_{TO} = V_L Z_O/D_{TO} \quad (29)$$

gut membrane water resistance:

$$R_{GW} = V_L/G_{GW} = V_L Z_W/D_{GW} \quad (30)$$

gut membrane organic resistance:

$$R_{GO} = V_L/G_{GO} = V_L Z_O/D_{GO} \quad (31)$$

egestion resistance:

$$R_X = V_L/G_{XO} = V_L Z_O/D_X \quad (32)$$

The water and organic flow rates G_{TW}, G_{TO}, G_{GW}, G_{GO}, and G_{XO} are fictitious and represent the product of an area and a mass-transfer coefficient. Substituting these expressions into the rate constant equations (eq 21–26) gives

$$1/k_2 = (R_V + R_{TW})K_{OW} + R_{TO} \quad (33)$$

$$1/k_E = R_X + R_{GO} + R_{GW}K_{OW} = R_X + R_G \quad (34)$$

$$E_{TM} = R_V K_{OW}/[(R_V + R_{TW})K_{OW} + R_{TO}] \text{ (maximum value)} \quad (35)$$

$$E_{AM} = R_X/(R_X + R_{GO} + R_{GW}K_{OW}) = R_X/(R_X + R_G) = 1/(1 + R_G/R_X) \text{ (maximum)} \quad (36)$$

or

$$1/E_{AM} = 1 + R_{GO}/R_X + (R_{GW}/R_X)K_{OW}$$

These reciprocal rate constants are thus the sum of resistances in series and the efficiencies are ratios of resistances. The six resistances are specific to the fish, but are believed to vary systematically with fish size and apply to all chemicals that transfer by passive diffusion. The chemical specificity is contained entirely in K_{OW}, at least to a first approximation, and in k_R if metabolism occurs. The parameters required for the model are summarized in Table I.

An analogous resistance term, R_I, could be defined for food uptake as V_L/G_{IO} where G_{IO} is the octanol-equivalent inflow of food such that D_I is $G_{IO}Z_O$. It then follows that Q, which is the ratio D_I/D_X and D_A/D_E, is also R_X/R_I and G_{IO}/G_{XO}, i.e., it is the ratio of the egestion resistance to the feeding resistance. A high value of Q implies that the fish experiences difficulty in egesting the chemical, thus having a tendency to retain and biomagnify it.

Bioavailability in the Water Column

McCarthy and Jimenez (*24*) and Landrum et al. (*25*) have convincingly demonstrated that the presence of sorbing material such as humic acids in the water column reduces bioavailability and hence uptake of chemicals by aquatic organisms. The effect is particularly important for substances of high K_{OW}. To quantify this we assume that the chemical is partly in sorbed state in the water with a dimensionless partition coefficient K_{PW}, and the con-

Table I. Model Parameters

	Fundamental Parameters
K_{OW}	octanol–water partition coefficient (chemical specific)
L_F	fish lipid or octanol-equivalent volume fraction
L_A	food lipid or octanol-equivalent volume fraction
R_V	gill ventilation flow rate resistance (h)
R_{TW}	gill membrane water-phase resistance (h)
R_{TO}	gill membrane organic-phase resistance (h)
k_R	metabolism rate constant (h^{-1})
G_I/V_F	feeding rate (m^3 food/h)/(m^3 fish volume) or (h^{-1})
R_{GW}	gut absorption water resistance (h)
R_{GO}	gut absorption organic resistance (h)
Q	digestion coefficient (ratio of ingestion to egestion D values)
k_D	growth dilution rate constant (h^{-1})
	Secondary or Derived Parameters
K_B	equilibrium bioconcentration factor
E_{TM}	gill uptake efficiency (eq 35)
E_{AM}	food uptake efficiency (eq 36)
R_T	gill membrane total resistance
R_G	gut membrane total resistance
R_X	egestion resistance (eq 32)
k_1	gill uptake rate constant (eq 21)
k_2	gill depuration rate constant (eq 22)
k_A	food uptake rate constant (eq 25)
k_E	excretion rate constant (eq 26)

centration of sorbent is a volume fraction X (typically 10^{-5}). A mass balance gives

$$C_W = C_T/(1 + K_{PW}X) \quad (37)$$

where C_T and C_W are, respectively, the total and dissolved concentrations. Conventionally X is expressed in units of kg/L and K_{PW} in units of L/kg. K_{PW} is usually related to organic carbon content and K_{OW}.

DiToro (*26*) suggested that the organic carbon be treated as equivalent to octanol, i.e., K_{PW} is yK_{OW} where y is the organic carbon content (g/g) of the suspended matter. There is some controversy about the dependence of K_{PW} on sorbent concentrations (*27*, *28*), but there is no doubt that the presence of appreciable quantities of sorbent reduces bioavailability, i.e., C_W is less than C_T, or equivalently, the fugacity of the chemical in the water is reduced.

This issue is peripheral to the central task of describing the kinetics of chemicals in fish, but it can become an important determinant of bioaccumulation. We suggest the simple expedient of employing an "octanol-equivalent" sorbent concentration Y (volume fraction) in the water such that the sorptive capacity $K_{PW}X$ is equal to $K_{OW}Y$. Following DiToro, Y is then approximately the concentration (kg/L) of suspended organic carbon in the water. We thus sidestep the issue of determining K_{PW}, or relating X to Y, but we quantify the effect by introducing Y, a typical range of environmental values being 10^{-6}–10^{-5} kg/L. The water fugacity is thus controlled by the dissolved concentration, C_W. We assume that only the dissolved chemical is available for transfer through the gill surface, the sorbed chemical passing through the gill cavity unchanged.

Fish Size Dependence

It is suggested that the resistances are dependent on fish size. As discussed by Gobas and Mackay (*8*), it appears that diffusion, volumetric ventilation, and circulation rates increase as fish size increases but at a rate less than proportional to volume. Since the resistances can be regarded as ratios of fish volume to a flow rate, resistance is expected to increase with fish volume. It is thus postulated that the terms R_V, R_{TW}, R_{TO}, R_{GO}, and R_{GW} increase in proportion to fish volume raised to a low power, n, possibly in the range 0.2–0.4. The feeding rate (G_I/V_F) may also fall with increasing fish volume (V_F). For each resistance, an appropriate correlation is

$$R_i = A_i V_i^n \quad (38)$$

where A_i is a constant.

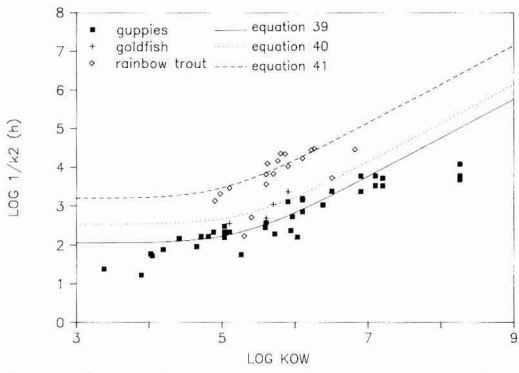

Figure 2. Plot of the log of the inverse elimination rate constant ($1/k_2$) as a function of log K_{OW}, for guppies, goldfish, and rainbow trout. The lines refer to eqs 39–41 in the text.

Fitting Parameters

The following procedure may be used to fit the model to experimental data.

From fish uptake-clearance experiments k_1, k_2, and K_B can be estimated by conventional procedures. If data are available for a series of chemicals, with a range of K_{OW}, the parameters R_{TO} and ($R_V + R_{TW}$) can be determined as the intercept and slope, respectively, of a plot of $1/k_2$ (the inverse elimination rate constant) versus K_{OW} (eq 33). Care must be taken in this regression to assign correct weights to the data points, because $1/k_2$ may vary by many orders of magnitude. We prefer to fit initially by inspection, i.e., "by eye", but a nonlinear regression technique may be used. If gill uptake efficiency data into clean fish are available, R_V and R_{TW} may be estimated by using eq 35, otherwise subsequent calculations can be performed using the sum of these terms.

Food uptake efficiency data into clean fish, for chemicals with a range of K_{OW}, may be used to estimate the ratios R_{GO}/R_X and R_{GW}/R_X (eq 36). Estimating the absolute values of R_{GO}, R_{GW}, and R_X requires a determination of Q. There are two options. If the flows and properties of the food and the feces are known, Q may be estimated as the ratio of octanol-equivalent flows G_{IO}/G_{XO}, but this may not be possible because of the complex nature of these phases. Gobas et al. (*20*) measured the fecal rate to be 37% of the volumetric food consumption rate for guppies fed Tetramin at 2% of fish volume per day. Thus, if the sorptive characteristics of food and feces are similar, a Q of approximately 3 is expected. The second method uses eq 20 and is to measure the fish and food fugacities after prolonged exposure to a conservative chemical, as was essentially done by Connolly and Pedersen (*14*). This yields a value of 3–10. For the purposes of this study we select a value of 3, recognizing that it may be in error.

The metabolic transformation rate is best estimated by comparison of bioconcentration data for the metabolizing chemical with that of a chemical of similar K_{OW}, which is known to be conservative.

Table II presents experimentally measured inverse elimination rate constants ($1/k_2$) and food absorption efficiencies (E_A) for guppies, goldfish, and rainbow trout, for

Table II. Experimentally Measured Inverse Elimination Rate Constants ($1/k_2$) and Food Absorption Efficiencies for Guppies, Goldfish, and Rainbow Trout[a]

chemical	log K_{OW}	$1/k_2$, day	E_A	chemical	log K_{OW}	$1/k_2$, day	E_A
				Guppies			
1,4-dibromobenzene	3.89 (*31*)	0.708 (*29*)		2,2′,3,3′,4,4′,5,5′-octachlorobiphenyl	7.1 (*32*)	250 (*12*)	
1,3,5-tribromobenzene	5.26 (*31*)	2.40 (*29*)		decachlorobiphenyl	8.26 (*32*)	500 (*12*)	
4,4′-dibromobiphenyl	5.72 (*31*)	8.13 (*29*)		2-monochloronaphthalene	4.19 (*9*)	3.24 (*9*)	
2,4,6-tribromobiphenyl	6.03 (*31*)	6.76 (*29*)		1,4-dichloronaphthalene	4.88 (*9*)	9.12 (*9*)	
2,2′,5,5′-tetrachlorobiphenyl	6.1 (*32*)	61.7 (*29*)		1,8-dichloronaphthalene	4.41 (*9*)	6.31 (*9*)	
2,2′,5,5′-tetrabromobiphenyl	6.5 (*31*)	102 (*29*)		2,3-dichloronaphthalene	4.71 (*9*)	7.08 (*9*)	
2,2′,4,4′,6,6′-hexabromobiphenyl	7.2 (*31*)	141 (*29*)		2,7-dichloronaphthalene	4.81 (*9*)	7.08 (*9*)	
				1,3,7-trichloronaphthalene	5.59 (*9*)	12.0 (*9*)	
2,4,5-trichlorobiphenyl	5.6 (*32*)	15.8 (*29*)		1,2,3,4-tetrachloronaphthalene	5.94 (*9*)	10.0 (*9*)	
decachlorobiphenyl	8.26 (*32*)	200 (*29*)		1,3,5,7-tetrachloronaphthalene	6.38 (*9*)	45.7 (*9*)	
mirex	6.9 (*33*)	219 (*29*)		1,3,5,8-tetrachloronaphthalene	5.96 (*9*)	22.4 (*9*)	
pentachlorobenzene	5.03 (*34*)	6.61 (*12*)		pentachlorobenzene	5.03 (*34*)	12.9 (*9*)	
2,5-dichlorobiphenyl	5.1 (*32*)	9.12 (*12*)		2,3′,4′,5-tetrachlorobiphenyl	5.9 (*32*)	55.0 (*9*)	
2,2′,5,5′-tetrachlorobiphenyl	6.1 (*32*)	66.1 (*12*)	0.51 (*12*)	1,4-dichlorobenzene	3.38 (*34*)	1.00 (*35*)	
2,2′,4,4′,5,5′-hexachlorobiphenyl	6.9 (*32*)	251 (*12*)	0.51 (*12*)	1,2,3-trichlorobenzene	4.04 (*34*)	2.24 (*35*)	
				1,3,5-trichlorobenzene	4.02 (*34*)	2.51 (*35*)	
2,2′,3,3′,4,4′,5,5′-octachlorobiphenyl	7.1 (*32*)	141 (*12*)	0.31 (*12*)	1,2,3,5-tetrachlorobenzene	4.65 (*34*)	3.89 (*35*)	
				pentachlorobenzene	5.03 (*34*)	9.12 (*35*)	
decachlorobiphenyl	8.26 (*32*)	251 (*12*)	0.19 (*12*)				
2,2′,5,5′-tetrachlorobiphenyl	6.1 (*32*)	30.3 (*12*)					
2,2′,4,4′,5,5′-hexachlorobiphenyl	6.9 (*32*)	100 (*12*)					
				Goldfish			
2,5-dichlorobiphenyl	5.1 (*32*)	15.2 (*11*)	0.56 (*11*)	2,2′,5,5′-tetrachlorobiphenyl	6.1 (*32*)	66.7 (*11*)	0.53 (*11*)
2,2′,5-trichlorobiphenyl	5.6 (*32*)	20.8 (*11*)	0.49 (*11*)	2,3′,4′,5-tetrachlorobiphenyl	5.9 (*32*)	99.9 (*11*)	0.48 (*11*)
2,4′,5-trichlorobiphenyl	5.7 (*32*)	47.6 (*11*)	0.6 (*11*)				
				Rainbow Trout			
3,3′-dichlorobiphenyl	5.3 (*32*)	7.22 (*36*)	0.62 (*36*)	2,4,6,2′,5′-pentachlorobiphenyl	6.22 (*37*)	1184 (*36*)	0.75 (*36*)
3,5-dichlorobiphenyl	5.4 (*32*)	21.7 (*36*)	0.80 (*36*)	2,3,4,2′,5′-pentachlorobiphenyl	6.5 (*32*)	224 (*36*)	0.75 (*36*)
2,2′-dichlorobiphenyl	4.9 (*32*)	57.7 (*36*)	0.79 (*36*)	2,4,6,3′,4′-pentachlorobiphenyl	6.58 (*37*)	>1443 (*36*)	0.80 (*36*)
2,3-dichlorobiphenyl	4.97 (*37*)	88.0 (*36*)	0.77 (*36*)	2,4,6,2′,6′-pentachlorobiphenyl	5.81 (*37*)	>1443 (*36*)	0.73 (*36*)
2,5-dichlorobiphenyl	5.1 (*32*)	123 (*36*)	0.73 (*36*)	2,3,4,5,6-pentachlorobiphenyl	6.3 (*32*)	>1443 (*36*)	0.85 (*36*)
2,5,2′-trichlorobiphenyl	5.6 (*32*)	274 (*36*)	0.77 (*36*)	2,4,5,2′,5′-pentachlorobiphenyl	6.4 (*32*)	>1443 (*36*)	0.78 (*36*)
2,5,4′-trichlorobiphenyl	5.7 (*32*)	283 (*36*)	0.78 (*36*)	2,3,4,5,2′,5′-hexachlorobiphenyl	6.82 (*37*)	1227 (*36*)	0.84 (*36*)
3,4,3′,4′-tetrachlorobiphenyl	6.1 (*32*)	63.5 (*36*)	0.68 (*36*)	2,3,4,6,2′,4′-hexachlorobiphenyl	6.67 (*37*)	>1443 (*36*)	0.77 (*36*)
2,3,2′,3′-tetrachlorobiphenyl	5.6 (*32*)	154 (*36*)	0.73 (*36*)	2,3,4,2′,3′,4′-hexachlorobiphenyl	6.74 (*37*)	>1443 (*36*)	0.78 (*36*)
2,3,4,5-tetrachlorobiphenyl	5.9 (*32*)	450 (*36*)	0.78 (*36*)	2,4,6,2′,4′,6′-hexachlorobiphenyl	7.0 (*32*)	>1443 (*36*)	0.64 (*36*)
2,5,2′,6′-tetrachlorobiphenyl	5.62 (*37*)	527 (*36*)	0.75 (*36*)	2,4,5,2′,4′,5′-hexachlorobiphenyl	6.9 (*32*)	>1443 (*36*)	0.75 (*36*)
2,3,2′,4′-tetrachlorobiphenyl	5.76 (*37*)	620 (*36*)	0.66 (*36*)	2,3,4,5,3′,4′-hexachlorobiphenyl	7.18 (*37*)	>1443 (*36*)	0.76 (*36*)
2,5,2′,5′-tetrachlorobiphenyl	6.1 (*32*)	722 (*36*)	0.74 (*36*)	2,3,4,5,2′,3′,4′,5′-octachlorobiphenyl	7.1 (*32*)	>1443 (*36*)	0.78 (*36*)
2,3,5,6-tetrachlorobiphenyl	5.86 (*37*)	938 (*36*)	0.77 (*36*)	2,3,4,5,6,2′,3′,4′,5′-nonachlorobiphenyl	7.2 (*32*)	>1443 (*36*)	0.80 (*36*)
2,4,3′,4′-tetrachlorobiphenyl	5.8 (*32*)	967 (*36*)	0.83 (*36*)				
2,5,3′,5′-tetrachlorobiphenyl	6.26 (*37*)	1285 (*36*)	0.76 (*36*)	decachlorobiphenyl	8.26 (*32*)	>1443 (*36*)	0.63 (*36*)

[a] References shown in parentheses.

chemicals of log K_{OW} 3.4–8.3. Figure 2 is a plot of the logarithm of the inverse elimination rate constants as a function of log K_{OW} for each organism. Regression to estimate k_2 is best done for chemicals of relatively low log K_{OW} (i.e., <6.5), since as Gobas et al. (*29*) have shown, fecal elimination (k_E) may exceed k_2 for very hydrophobic chemicals. The lines on Figure 2 represent the results of the following linear regressions (95% confidence intervals in parentheses).

guppies:

$$1/k_2 = 5.80\ (\pm 1.03) \times 10^{-4} K_{OW} + 115\ (\pm 310)\ \text{h} \quad (39)$$

goldfish:

$$1/k_2 = 1.39\ (\pm 0.77) \times 10^{-3} K_{OW} + 343\ (\pm 668)\ \text{h} \quad (40)$$

rainbow trout:

$$1/k_2 = 1.42\ (\pm 0.33) \times 10^{-2} K_{OW} + 1585\ (\pm 7012)\ \text{h} \quad (41)$$

Figure 3 presents a plot of the inverse of the experimental food absorption efficiencies as a function of log K_{OW} for the data set in Table II. The lines in the figure represent the following linear regressions (95% confidence intervals in parentheses).

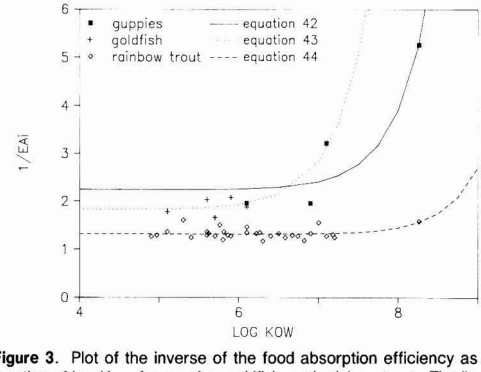

Figure 3. Plot of the inverse of the food absorption efficiency as a function of log K_{OW}, for guppies, goldfish, and rainbow trout. The lines refer to eqs 42–44 in the text.

guppies:

$$1/E_A = 1.67\ (\pm 0.43) \times 10^{-8} K_{OW} + 2.25\ (\pm 0.66) \quad (42)$$

goldfish:

$$1/E_A = 1.02\ (\pm 2.25) \times 10^{-7} K_{OW} + 1.83\ (\pm 0.19) \quad (43)$$

rainbow trout:

$$1/E_A = 1.39\ (\pm 0.57) \times 10^{-9} K_{OW} + 1.32\ (\pm 0.10) \quad (44)$$

These correlations are regarded as only tentative in view of the paucity of data, especially for high-K_{OW} chemicals. The term containing K_{OW} only becomes significant when log K_{OW} exceeds 6.5. The other term almost certainly has a value in the range 1.3–2.5, corresponding to absorption efficiencies ranging from 40 to 77%.

The resistances calculated for guppies, goldfish, and rainbow trout in eq 39–44 are summarized in Table III. The values of R_X were calculated by assuming that the digestion coefficient Q was 3 for each organism.

Resistances may then be related by fish size with eq 38. Figure 4 shows a plot of log resistance as a function of log fish volume. A linear regression for each resistance (95% confidence interval in parentheses) yielded (for R in h, V in m^3)

aqueous gill resistance

$$\log R_W = \log (R_V + R_{TW}) = 0.36\ (\pm 0.05) \log V - 0.81\ (\pm 0.15) \quad (45)$$

or

$$R_W = 0.15 V^{0.36}$$

organic gill resistance

$$\log R_{TO} = 0.29\ (\pm 0.003) \log V + 4.1\ (\pm 0.01) \quad (46)$$

or

$$R_{TO} = 1.26 \times 10^4 V^{0.29}$$

The slopes in Figure 4, and equivalently the power on V, must be regarded as of questionable accuracy or even significance. The values should be regarded as only illustrative, but they are consistent with the analysis by Gobas and Mackay (*8*), who suggested that the gill resistances are related to the organism volume raised to a power between 0.2 and 0.4.

The regressed slopes of the R_{GO} and R_{GW} points are 0.12 and −0.04, respectively, which are believed to differ insignificantly from zero. Thus, in the absence of more data, the simplest expedient is to assume that R_{GO} and R_{GW} are independent of organism size, R_{GO} has a value of 2000 h, and R_{GW} is 3×10^{-5} h.

Additional data are needed to test the assumption for the digestion coefficient, Q. It is emphasized that our present aim is not to fit the model rigorously to all available data, or even to test it thoroughly. Our primary objective is to obtain reasonable parameter values and then to examine and disscuss the model's ability to reproduce observed phenomena.

Discussion

We now discuss several features of the model and its ability to reproduce observed bioaccumulation phenomena.

Limitations. The model treats neutral organic chemicals and is not suitable for substances such as chlorinated phenols that ionize or display unusual phase-partitioning behavior. It is likely that the resistances are dependent to some extent on the diffusivity of the chemical in water and organic media. This dependence is not included but could be, given sufficient data. Processes of renal, biliary, or reproductive loss or dermal exchange are not included.

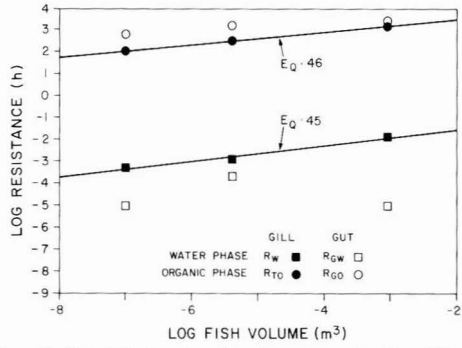

Figure 4. Plot of the log of each resistance as a function of the log of the organism volume, showing eqs 45 and 46. The symbols refer to the following: R_{GO}, organic gut resistance; R_{TO}, organic gill resistance; R_{GW}, aqueous gut resistance; R_W, aqueous gill resistance.

The equations reflect a situation of regular food intake and may be invalid if food consumption is highly intermittent.

The following discussion treats the "steady-state" condition. No true steady state can be achieved if growth occurs, but a "pseudo steady state" can be postulated by setting the differential equation to zero as shown in Figure 1. A problem then arises because the resistance parameters are size dependent and the condition of a growing fish depends not only on the current resistances but also on the (lower) resistances that occurred when the fish was smaller. This is not regarded as a serious limitation, except when the fish is growing rapidly. Accurate simulation is then best done by solving the differential equation numerically.

Simple Bioconcentration. After prolonged exposure, the fish concentration settles at a value

$$C_F = (k_1 C_W + k_A C_A)/(k_2 + k_R + k_E + k_D) \quad (47)$$

and equivalently, the fugacity at

$$f_F = (D_W f_W + D_A f_A)/(D_W + D_R + D_E + D_D) = (D_W f_W + E_{AM} D_I f_A)/(D_W + D_R + E_{AM} D_I/Q + D_D)$$

If water is the only source of chemical (C_A and f_A are zero), the chemical is not metabolically transformed, and there is no growth, then

$$C_F/C_W = k_1/(k_2 + k_E) \quad (48)$$

or

$$f_F/f_W = D_W/(D_W + D_E)$$

This suggests that C_F/C_W should approach a limit that is smaller than $L_F K_{OW}$ by an amount controlled by the relative magnitude of k_E and k_2 or D_E and D_W. The success of K_B–K_{OW} correlations suggests that in many cases k_E is small compared to k_2, or D_E is small compared to D_W, i.e., the resistance to exchange through the gills is small compared to that by excretion.

Biomagnification. Recently, Connolly and Pedersen (*14*) and Oliver and Niimi (*15*) suggested that C_F/C_W values in lakes may exceed $L_F K_{OW}$, or equivalently, that fish fugacities exceed that of water, the increase being largest at high trophic levels, and for high-K_{OW} chemicals. The model accounts for this effect, which can be attributed to the term $k_A C_A$. Ignoring growth dilution and metabolism the steady-state BCF will be

$$C_F/C_W = [k_1 + k_A(C_A/C_W)]/(k_2 + k_E) \quad (49)$$

This ratio can exceed k_1/k_2, especially if C_A/C_W becomes large. The amount of excess depends on how k_A, k_2, and

Table III. Resistances (h) and Volumes (cm^3) for Three Fish Species

organism	V_F	L_F	L_A	G_I[a]	$R_V + R_{TW}$	R_{TO}	R_{GW}	R_X	R_{GO}	Q
guppies	0.10	0.02	0.10	2.4	0.00058	115	1.0×10^{-5}	600	750	3
goldfish	4.0	0.029	0.10	1	0.0014	343	2.1×10^{-4}	2088	1733	3
rainbow trout	900	0.097	1	0.1	0.0142	1586	1.0×10^{-5}	7200	2326	3

[a] In % V_F/day.

k_E decrease relative to each other as K_{OW} increases. Rearranging the fugacity differential equation and ignoring metabolism and growth gives

$$f_F/f_W = [D_W + D_A(f_A/f_W)]/(D_W + D_E) \quad (50)$$

Now if the food fugacity is equal to the water fugacity, as is likely for small food organisms, then

$$f_F/f_W = (D_W + D_A)/(D_W + D_E) \quad (51)$$

Clearly, if D_A exceeds D_E, a f_F/f_W ratio greater than unity is expected. Further, when a steady state is reached then $(f_G - f_F)$ in eq 14 will become zero and

$$D_A f_A = D_E f_F \quad (52)$$

and

$$f_F/f_A = D_A/D_E = Q$$

Now, it is likely that D_E is considerably smaller than D_A because the volume of food egested is less than that ingested, and the lipid content is also reduced. If, for example, D_E was 20% of D_A, f_F would approach a value Q of 5 times f_A. Q is thus also the maximum fugacity ratio for the system of food and fish. This high fugacity will drive chemical across the gut wall and induce a high fish fugacity and thus biomagnification. We suggest that biomagnification may be caused by the increase in chemical fugacity in the gut, caused by food digestion. This effect is present, but is not observed, at low K_{OW} because of rapid gill exchange. Only when the gill resistance becomes large, and transfer is slow, is biomagnification apparent. It may be possible to define Q values and hence characterize biomagnification for each fish–food combination.

Detailed Kinetics. We now examine the detailed chemical flows using a hypothetical example of a fish with properties listed in Table IV, exposed to a slowly metabolizing chemical (half-life of 3 years) of log K_{OW} 6, as illustrated in Figure 5. The total inflow of chemical in the gill water is 2.10 nmol/h, of which 1.05 is in dissolved form (available for transfer) and 1.05 is in sorbed form (i.e., equipartitioning). The water fugacity is 0.250 mPa and the total water concentration is 0.001 g/m^3. At steady state (infinite time) the fish concentration and fugacity reach 0.199 mol/m^3 (39.7 g/m^3) and 0.397 mPa, respectively. The fish/water concentration ratio is then 39 700. Since the fish achieves a higher fugacity than the water there is a tendency for the fish to lose chemical by diffusion through the gills. The gill water settles at an intermediate fugacity of 0.312 mPa, resulting in diffusion across the membrane (in units of nmol/h) of 0.442 in, 0.703 out, and 0.261 net diffusion from fish to gill water.

Similarly in the GI tract, when the fugacity of the food is equal to the fugacity of the water, the food input is 1.04 nmol/h. Digestive processes cause the fugacity of the chemical in the gut to increase, by a factor of 2, to 0.525 mPa, a value sufficient to achieve rates of transport to the fish and feces that equal the input rate. These transfer rates (in nmol/h) are 0.729 to the feces, 0.666 from the GI tract to the fish, and 0.353 from the fish to the GI tract, resulting in a net absorption of 0.313 nmol/h.

Table IV. Properties of Hypothetical Fish used in Figure 5

fish properties: $V_F = 10\ cm^3 = 1 \times 10^{-5}\ m^3$
$L_F = 0.05$
$L_A = 0.05$
$R_V + R_{TW} = 2.38 \times 10^{-3}$ h, assume that R_V and R_{TW} are equal (i.e., 1.19×10^{-3} h each)
$R_{TO} = 447$ h
$R_{GW} = 3.0 \times 10^{-5}$ h
$R_{GO} = 2000$ h
$Q = 3$
$G_I/V_F = 2\%$/day
$T_R = 3$ years
$k_D = 0\ h^{-1}$
molecular weight of chemical = 200
$H = 100\ Pa \cdot m^3/mol$
[water] = 1 mg/m^3
[sorbent] = 1 ppm

Metabolism results in a loss of 0.052 nmol/h, finalizing the mass balance.

The overall picture is thus of a fish having net input of chemical only from food and output through the gills and feces, and by metabolism. There is "negative" gill uptake.

The situation when the fish has an initial zero chemical concentration is quite different. The inflows of chemical are the same as above, but there is absorption from the gills of 0.442 nmol/h and absorption through the gut of 0.666 nmol/h. The uptake routes and efficiencies thus change with the changing contamination status of the fish. Initially uptake is through the gills; then this reverses as the fish becomes contaminated. There is thus an inherent difficulty in using data from laboratory experiments involving exposure of "clean" fish to assess the toxicokinetics of "field" fish, which are in a near-steady-state contamination condition.

The bioconcentration literature frequently questions and discusses the relative roles of water and food as sources of exposure of chemical to the fish. This analysis suggests that the roles change with level of contamination. It is important to define "exposure" because there is always exposure through the gills, but that exposure may not lead to uptake. It is also necessary to define "the fish", i.e., whether or not the gill cavity and GI tract are included in the fish. Different definitions lead to quite different answers; thus the question must be posed carefully.

The contributions of food and water can be explored by running the model with uptake from food and water, food only, and water only. Because the equations are linear, the concentrations and fluxes obtained from combined exposure equal the sum of the individual contributions, i.e., "linear additivity" applies as has been discussed by Stiver and Mackay (*38*). In this case the steady-state fish concentrations and fugacities are

	concn, g/m^3	fugacity, mPa
food exposure only	23.9	0.239
water exposure only	15.8	0.158
food and water exposure	39.7	0.397

Since the water fugacity is 0.250 mPa, it is clear that exposure to water results in the fish fugacity approaching

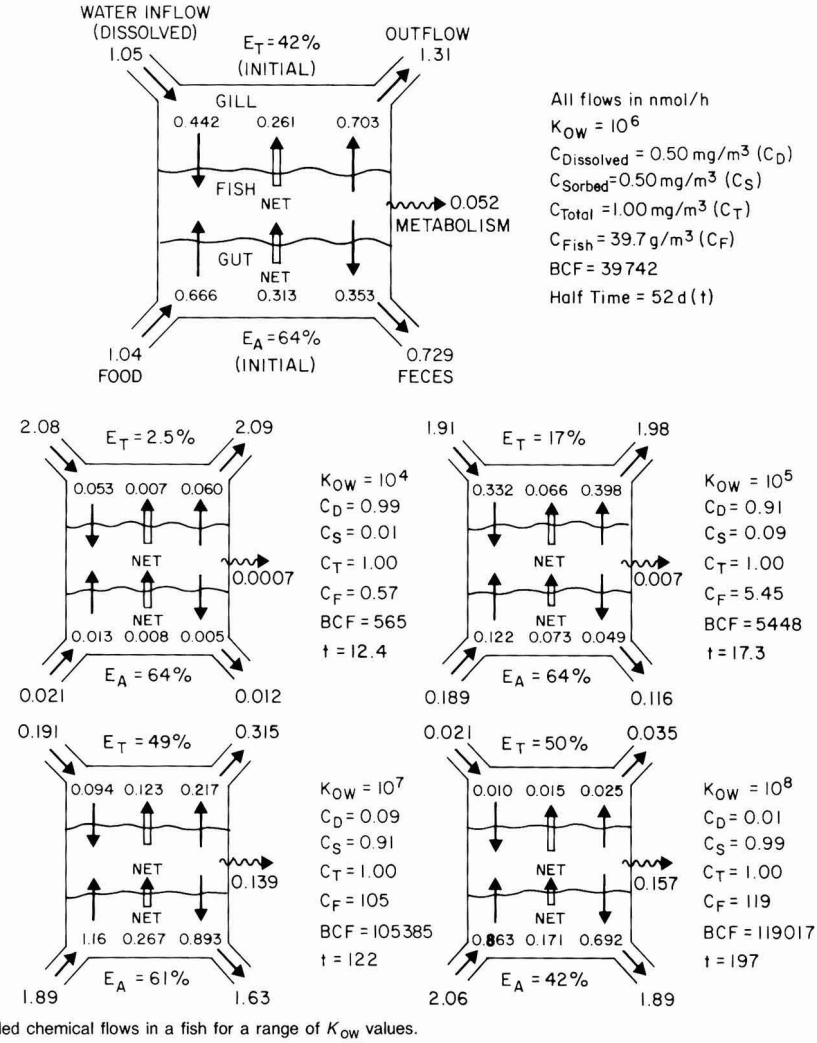

Figure 5. Detailed chemical flows in a fish for a range of K_{OW} values.

the water fugacity, but it is prevented from reaching the water fugacity as a result of loss by egestion. Food ingestion causes the fugacity to increase and exceed that of the water.

The overall half-time to achieve steady state is 52 days. This figure is controlled by the overall rate constant for loss of 5.58×10^{-4} h^{-1}, which comprises 3.54×10^{-4} loss from gills, 1.78×10^{-4} loss by egestion, and 0.26×10^{-4} loss by metabolism. Gill exchange and egestion thus control the uptake and clearance times.

Effect of Hydrophobicity. We now explore the effects of changing the chemical's K_{OW} on the contaminant dynamics in the fish. This is shown as a series of mass balances in Figure 5. The total water concentration is constant at 0.001 g/m³, but the extent of sorption increases with increasing K_{OW}, as shown in the figure. Thus, the bioavailable fraction of the chemical is reduced, although the total gill water inflows are constant. The fugacity of the chemical in the food is equal to the fugacity in the water in all cases and, thus, as K_{OW} increases the concentration in the food increases, but not in proportion to K_{OW} because of the bioavailability or sorption effect. Therefore, although the quantity of food ingested is constant, the intake of chemical from the food increases only slightly with increasing K_{OW}. Indeed, the principal effect of reduced bioavailability is to control food concentration and hence intake rather than control gill exchange.

When K_{OW} is low (10^4–10^5), virtually all the chemical is in dissolved form in the water; at log K_{OW} of 6, half is sorbed and half is dissolved; and at log K_{OW} 8, nearly all the chemical is in sorbed form. This difference in bioavailable fraction is reflected in the flow of bioavailable chemical in the gill water. At a log K_{OW} of 4, the flow of bioavailable chemical in and out of the gills is 2.08 and 2.09 nmol/h, respectively. These flows decline to 0.021 and 0.035 nmol/h for a chemical of log K_{OW} of 8, although the total water concentration remains constant at 1.00 mg/m³, as does the total chemical flow.

The ratio of the fish to water concentration increases from 565 at a log K_{OW} of 4 to 105 385 at a log K_{OW} of 7 and remains approximately constant (119 017 at a log K_{OW} of 8). The declining bioavailable fraction of the chemical is the principal reason for the loss of the linear relationship between bioconcentration factor and K_{OW}. Reduction in gut uptake efficiency also plays a role. In all steady-state cases the flow of chemical out of the gills exceeds the flow in, so that the net movement of chemical is from the gills to the water. The ratio of the fugacity of the fish to that

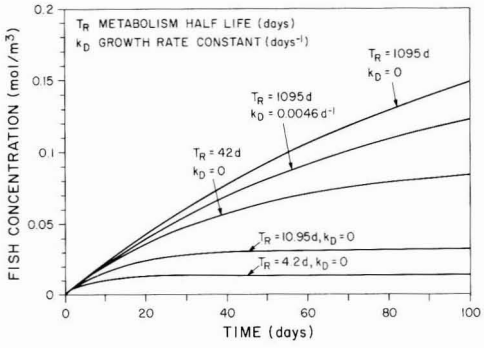

Figure 6. Effect of metabolism on fish concentration, T_R being the chemical half-life (days) and of growth rate, expressed as a growth rate constant (day^{-1}), (k_D = 0.0046 day^{-1} representing a doubling of volume in 150 days).

of the water increases from nearly unity (1.14 at a log K_{OW} of 4) to 2.40 at a K_{OW} of 8.

The fugacity of the food was set equal to that of the water. As K_{OW} increases the concentration of the chemical in the food increases, so that the flow of chemical from food to the GI tract increases from 0.021 nmol/h at a log K_{OW} of 4 to 2.06 nmol/h at a log K_{OW} of 8. This 100-fold increase is the net result of an increase in food–water partitioning, and a decrease in chemical bioavailability. The net flow of chemical from the GI tract increases from 0.008 nmol/h at log K_{OW} of 4 to 0.267 nmol/h at a log K_{OW} of 7. At a higher K_{OW} (10^8), uptake of chemical from the GI tract to the fish declines to 0.171 nmol/h due to increased gut membrane resistance. This increased resistance is also reflected in the initial uptake efficiencies for the gut, which are steady at ~64% for log K_{OW} up to 7 and then decline to 42% at log K_{OW} of 8.

The overall half-time to steady state, representing the time delay in uptake of chemical, increases with K_{OW} from 12.4 days at a log K_{OW} of 4, to 197 days at a log K_{OW} of 8. The metabolism half-time for the hypothetical chemicals is constant at 1095 days (3 years). As the half-time to steady state increases and approaches the metabolism half-time, metabolism becomes an increasingly important route of chemical elimination. At a log K_{OW} of 4, only 0.0007 nmol/h of chemical is metabolized, while at a log K_{OW} of 8, 0.157 nmol/h is metabolized. Thus, at very high K_{OW}'s more chemical is removed by metabolism than through the gills.

Effect of Metabolic Half-Time. Figure 6 illustrates the effect of altering the metabolism half-time on the fish concentration. The hypothetical chemical has a log K_{OW} of 6. The fish properties are listed in Table IV. The upper line in Figure 6 represents a near-conservative chemical with a metabolic half-time of 1095 days (3 years), which is essentially an infinite half-time. The overall half-time for chemical uptake in the fish is much smaller (52 days), and metabolism is thus not an important route of chemical elimination. When the metabolic half-time is decreased to 42 days, the fish concentration at steady state is reduced. Also, less time is required to reach steady state. When the rate of metabolism is rapid (half-time of 4.2 days), the fish concentration and the time required to reach steady state are greatly reduced.

Effect of Growth Dilution. In the other examples, the fish is assumed to have a constant volume. If a growth dilution term is included corresponding to a doubling in volume in 150 days, i.e., a rate constant k_D of 0.0046 day^{-1}, the effect is as shown in Figure 6. The concentrations (or fugacities) are lower in the growing fish. Growth dilution plays a role similar to metabolism and is most important for high K_{OW} chemicals, which exchange slowly with water.

Table V. Application of the Model to a Hypothetical Food Chain[a]

large fish	V_F = 10000 cm^3	f_4 = 13.8 × 10^{-4} Pa
↑		
medium fish	V_F = 100 cm^3	f_3 = 5.93 × 10^{-4} Pa
↑		
small fish	V_F = 1 cm^3	f_2 = 3.30 × 10^{-4} Pa
↑		
plankton		$f_1 = f_W$
↑		
water		f_W = 2.50 × 10^{-4} Pa

[a] Resistances for fish were calculated by using eqs 45 and 46. Feeding rate for fish is 5% of V_F per day and Q = 3. Lipid contents for all levels, 5%. Each level is food for the one above, with f_1 set equal to f_W.

Food Chain Biomagnification. Connolly and Pedersen (*14*) observed that the chemical fugacity in fish, in the field, was higher than the fugacity in the water in which the fish lived. The fugacity also increased with each level of the food chain. To test if the model reflects these observations, a trophic level simulation may be set up as shown in Table V by running the model sequentially using fish from one level as food for the next, and a chemical of log K_{OW} of 6. The first-level food (plankton) is assumed to be in equilibrium with the water (fugacity 2.50 × 10^{-4} Pa). A small fish (1 cm^3) consumes the plankton at a rate of 5% of the fish's volume per day and reaches a steady-state fugacity of 3.30 × 10^{-4} Pa. A medium fish (100 cm^3) then consumes the small fish, also at a rate of 5% of fish volume per day. The medium fish has a fugacity of 5.93 × 10^{-4} Pa at steady state. The largest fish (10 000 cm^3) consumes the medium fish at a rate of 5% per day and reaches a fugacity of 13.8 × 10^{-4} Pa. It is therefore apparent that the model accounts for the observation, described by Connolly and Pedersen (*14*), that fugacity increases with trophic level. At each stage of the food chain the fish fugacity becomes an increasing multiple of the water fugacity. As has been discussed by Clark et al. (*30*), a further increase in fugacity occurs for fish-eating birds, which achieve a fugacity considerably higher than the fish they consume.

Conclusions

A comprehensive model has been developed describing the processes of exchange of organic chemicals between water, food, and fish. The model can be used in the form of rate constants that are dependent on resistances. These resistances have been shown to have physiological significance using a fugacity model and expressions for size dependence have been suggested. The model has been shown to give a satisfactory description of the phenomena of bioconcentration, biomagnification, metabolism, bioavailability, and food chain magnification for a range of chemical hydrophobicities. It demonstrates that the detailed flows of contaminant to and from the fish, through the gills and gut, vary considerably in relative magnitude and direction as the fish becomes contaminated. It is hoped that the model will be tested and, if necessary, modified by fitting to new experimental data.

Registry No. 1,3,5-Tribromobenzene, 626-39-1; 4,4′-dibromodiphenyl, 92-86-4; 2,4,6-tribromobiphenyl, 59080-33-0; 2,2′,5,5′-tetrachlorobiphenyl, 35693-99-3; 2,2′,5,5′-tetrabromobiphenyl, 59080-37-4; 2,2′,4,4′,6,6′-hexabromobiphenyl, 59261-08-4; 2,4,5-trichlorobiphenyl, 15862-07-4; decachlorobiphenyl, 2051-24-3; mirex, 2385-85-5; 2,5-dichlorobiphenyl, 34883-39-1;

2,2′,4,4′,5,5′-hexachlorobiphenyl, 35065-27-1; 2,2′,3,3′,4,4′,5,5′-octachlorobiphenyl, 35694-08-7; 1,4-dichloronaphthalene, 1825-31-6; 1,8-dichloronaphthalene, 2050-74-0; 2,3-dichloronaphthalene, 2050-75-1; 2,7-dichloronaphthalene, 2198-77-8; 1,3,7-trichloronaphthalene, 55720-37-1; 1,2,3,4-tetrachloronaphthalene, 20020-02-4; 1,3,5,7-tetrachloronaphthalene, 53555-64-9; 1,3,5,8-tetrachloronaphthalene, 31604-28-1; pentachlorobenzene, 608-93-5; 2,3′,4′,5-tetrachlorobiphenyl, 32598-11-1; 1,2,3-trichlorobenzene, 87-61-6; 1,3,5-trichlorobenzene, 108-70-3; 1,2,3,5-tetrachlorobenzene, 634-90-2; 2,2′,5-trichlorobiphenyl, 37680-65-2; 2,4′,5-trichlorobiphenyl, 16606-02-3; 3,3′-dichlorobiphenyl, 2050-67-1; 3,5-dichlorobiphenyl, 34883-41-5; 2,2′-dichlorobiphenyl, 13029-08-8; 2,3-dichlorobiphenyl, 16605-91-7; 3,4,3′,4′-tetrachlorobiphenyl, 32598-13-3; 2,3,2′,3′-tetrachlorobiphenyl, 38444-93-8; 2,3,4,5-tetrachlorobiphenyl, 33284-53-6; 2,5,2′,6′-tetrachlorobiphenyl, 41464-41-9; 2,3,2′,4′-tetrachlorobiphenyl, 36559-22-5; 2,3,5,6-tetrachlorobiphenyl, 33284-54-7; 2,4,3′,4′-tetrachlorobiphenyl, 32598-10-0; 2,5,3′,5′-tetrachlorobiphenyl, 41464-42-0; 2,4,6,2′,5′-pentachlorobiphenyl, 60145-21-3; 2,3,4,2′,5′-pentachlorobiphenyl, 38380-02-8; 2,4,6,3′,4′-pentachlorobiphenyl, 56558-17-9; 2,4,6,2′,6′-pentachlorobiphenyl, 56558-16-8; 2,3,4,5,6-pentachlorobiphenyl, 18259-05-7; 2,4,5,2′,5′-pentachlorobiphenyl, 37680-73-2; 2,3,4,5,2′,5′-hexachlorobiphenyl, 52712-04-6; 2,3,4,6,2′,4′-hexachlorobiphenyl, 56030-56-9; 2,3,4,2′,3′,4′-hexachlorobiphenyl, 38380-07-3; 2,4,6,2′,4′,6′-hexachlorobiphenyl, 33979-03-2; 2,3,4,5,3′,4′-hexachlorobiphenyl, 38380-08-4; 2,3,4,5,6,2′,3′,4′,5′-nonachlorobiphenyl, 40186-72-9; water, 7732-18-5.

Literature Cited

(1) Tulp, M.; Hutzinger, O. *Chemosphere* **1978**, *10*, 849.
(2) Neely, W. B. *Environ. Sci. Technol.* **1979**, *13*, 1506.
(3) Veith, G. D.; DeFoe, D. L.; Bergstedt, B. V. *J. Fish. Res. Board Can.* **1979**, *36*, 1040.
(4) Spacie, A.; Hamelink, J. L. *Environ. Toxicol. Chem.* **1982**, *1*, 309.
(5) Mackay, D. *Environ. Sci. Technol.* **1982**, *16*, 274.
(6) Gobas, F. A. P. C.; Shiu, W. Y.; Mackay, D. Factors Determining Partitioning of Hydrophobic Organic Chemicals in Aquatic Organisms. In *QSAR in Environmental Toxicology*; II, Kaiser, K. L. E., Ed.; D. Reidel: Dordrecht, The Netherlands, 1987; Vol. II, p 107.
(7) Mackay, D.; Hughes, A. I. *Environ. Sci. Technol.* **1984**, *18*, 439.
(8) Gobas, F. A. P. C.; Mackay, D. *Environ. Toxicol. Chem.* **1987**, *6*, 495.
(9) Opperhuizen, A.; van den Velde, E. W.; Gobas, F. A. P. C.; Liem, D. A. K.; van der Steen, J. M. D.; Hutzinger, O. *Chemosphere* **1985**, *14*, 1871.
(10) Hawker, D. W.; Connell, D. W. *Chemosphere* **1985**, *14*, 1205.
(11) Bruggeman, W. A.; Matron, L. B. J.; Kooiman, D.; Hutzinger, O. *Chemosphere* **1981**, *10*, 811.
(12) Bruggeman, W. A.; Opperhuizen, A.; Wijbenga, A.; Hutzinger, O. *Toxicol. Environ. Chem.* **1984**, *7*, 173.
(13) Barber, M. C.; Suarez, L. A.; Lassiter, R. R. *Environ. Toxicol. Chem.* **1988**, *7*, 545.
(14) Connolly, J. P.; Pedersen, C. J. *Environ. Sci. Technol.* **1988**, *22*, 99.
(15) Oliver, B.; Nimi, A. *Environ. Sci. Technol.* **1988**, *22*, 388.
(16) Thomann, R. V. *Can. J. Fish. Aquat. Sci.* **1981**, *38*, 280.
(17) Thomann, R. V.; Connolly, J. P. *Environ. Sci. Technol.* **1984**, *18*, 65.
(18) Connolly, J. P.; Tonelli, R. *Estuarine, Coastal Shelf Sci.* **1985**, *20*, 349.
(19) Thomann, R. V. *Environ. Sci. Technol.* **1989**, *23*, 699.
(20) Gobas, F. A. P. C.; Muir, D. C. G.; Mackay, D. *Chemosphere* **1988**, *17*, 943.
(21) Mackay, D.; Paterson, S. *Environ. Sci. Technol.* **1982**, *16*, 654A.
(22) Flynn, G. L.; Yalkowsky, S. H. *J. Pharm. Sci.* **1972**, *61*, 838.
(23) Amidon, G. L.; Kou, J.; Elliot, R. L.; Lightfoot, E. N. *J. Pharm. Sci.* **1980**, *12*, 1369.
(24) McCarthy, J. F.; Jimenez, B. D. *Environ. Toxicol. Chem.* **1985**, *4*, 511.
(25) Landrum, P. F.; Reinhold, M. D.; Nihart, S. R.; Eadie, B. J. *Environ. Toxicol. Chem.* **1985**, *4*, 459.
(26) DiToro, D. M. *Chemosphere* **1985**, *14*, 1503.
(27) O'Connor, D. J.; Connolly, J. P. *Water Res.* **1980**, *14*, 1517.
(28) Mackay, D.; Powers, B. *Chemosphere* **1987**, *16*, 745.
(29) Gobas, F. A. P. C.; Clark, K. E.; Shiu, W. Y.; Mackay, D. *Environ. Toxicol. Chem.* **1989**, *8*, 231.
(30) Clark, T.; Clark, K.; Paterson, S.; Mackay, D.; Norstrom, R. *Environ. Sci. Technol.* **1988**, *22*, 120.
(31) Gobas, F. A. P. C.; Lahitette, J. M.; Garofalo, G.; Mackay, D. *J. Pharm. Sci.* **1988**, *77*, 265.
(32) Shiu, W. Y.; Mackay, D. *J. Phys. Chem. Ref. Data* **1986**, *15*, 911.
(33) Suntio, L. R.; Shiu, W. Y.; Mackay, D.; Seiber, J. N.; Glotfelty, D. *Rev. Environ. Contam. Toxicol.* **1988**, *103*, 1.
(34) Miller, M. M.; Wasik, S. P.; Huang, G. L.; Shiu, W. Y.; Mackay, D. *Environ. Sci. Technol.* **1985**, *19*, 522.
(35) Konemann, H.; van Leeuwen, K. *Chemosphere* **1980**, *9*, 3.
(36) Niimi, A. J.; Oliver, B. G. *Can. J. Fish. Aquat. Sci.* **1983**, *40*, 1388.
(37) Hawker, D. W.; Connell, D. W. *Environ. Sci. Technol.* **1988**, *22*, 382.
(38) Stiver, W.; Mackay, D. *Chemosphere* **1989**, *19*, 1187.

Received for review November 21, 1988. Revised manuscript received November 13, 1989. Accepted April 20, 1990. This work was supported by the Wildlife Toxicology Fund of Environment Canada and the World Wildlife Fund and the Natural Sciences and Engineering Research Council.

Environ. Sci. Technol. **1990**, *24*, 1214–1223

Fluorescent Polycyclic Aromatic Hydrocarbons as Probes for Studying the Impact of Colloids on Pollutant Transport in Groundwater

Debera A. Backhus and Philip M. Gschwend*

R. M. Parsons Laboratory for Water Resources and Hydrodynamics, Department of Civil Engineering, Massachusetts Institute of Technology, Cambridge, Massachusetts 02139

■ A fluorescence-quenching method was developed to assess the hydrophobic organic pollutant binding potential of organic colloids (OC) in unaltered natural waters. This method allows (1) direct assessment of the importance of OC-enhanced pollutant transport for environmental samples under in situ water chemistry conditions, without requiring the isolation of OC or separation of equilibrated phases; (2) testing of chemicals that suffer substantial wall losses from aqueous solutions; and (3) examination of unstable water samples such as anoxic samples. Our experiments show that some OC (Aldrich humic acids) fully quench OC-associated perylene fluorescence, but others (bovine serum albumin) do not. This implies that fluorescence-quenching results collected for a single [OC] or over a limited [OC] range provide only a lower limit estimate of the potential for OC association. Tests with groundwater, recharged with secondarily treated sewage and containing OC at ~1 mg of C/L, showed temporal variation in the ability of OC present to quench or bind perylene.

Introduction

Organic colloids or inorganic colloids with organic coatings (both referred to herein as OC) may enhance the transport of hydrophobic organic pollutants in groundwater (*1–4*). For such facilitated transport to be significant, not only must OC be present and mobile in the subsurface, but they must also be sufficiently capable of sorbing hydrophobic organic contaminants to augment the mobile load. Literature evidence suggests OC exist in uncontaminated groundwaters at approximately ppm levels (*5–8*) and in contaminated groundwaters at levels up to hundreds of ppm (*9, 10*). Some examples suggest that at least a portion of this OC may be mobile in groundwater. Reinhard (*9*) reported milligram per liter quantities of OC (MW 500–10 000) in groundwater, necessarily derived from a wastewater reclamation facility 140 m upgradient, as these macromolecules were chlorinated. Robertson et al. (*10*) detected up to 780 mg/L tannin and lignin in groundwater 900 m downgradient of a waste pulp liquor disposal pit, apparently traveling at the same rate as conservative constituents in the contaminant plume.

This paper focuses on the issue of sorption of hydrophobic organic pollutants to OC. For the purposes of this study, OC are operationally defined as organic matter that will not pass through a 500 molecular weight cutoff (MWCO) ultrafiltration membrane. Such matter may include humic and fulvic acids, other macromolecules such as proteins or carbohydrates, microorganisms, or organic coatings on inorganic colloids. The first objective of this study was to develop a nonintrusive method that could be used to determine the extent of sorptive interactions between hydrophobic organic compounds and unaltered groundwater OC. After testing with model OC, the technique was applied to groundwater samples. These were obtained from a site contaminated by the recharge of secondarily treated sewage and known to contain suspended colloids (*2*). The results allow assessment of the potential impact of colloid-facilitated transport at this site.

Fluorescence Quenching in Whole Water Samples. The key to using fluorescence to determine OC–water partitioning behavior, and directly assessing the importance of OC association in natural waters, is the observation that the fluorescence of a polycyclic aromatic hydrocarbon (PAH) is quenched on association with OC (*11–14*). This allows a distinction between dissolved PAH and OC-sorbed PAH without having to separate equilibrated phases. However, to date fluorescence-quenching studies have been performed after the OC were removed from the soil or natural water of interest. Isolation and concentration steps could change the character of these colloidal sorbents or may collect only a fraction of the OC sorbents present. Further, since pH, ionic strength, or specific cations may affect the magnitude of the observed K_{oc} (*14–17*), if the isolated OC are not rediluted with ultrafiltrate with in situ pH and ion conditions, the relevant K_{oc} value may be incorrectly estimated. To avoid such difficulties, we use a relatively simple adaptation of the fluorescence-quenching method to provide direct assessment of OC-enhanced transport for a given pollutant using whole groundwater samples under in situ conditions.

As derived by Gauthier et al. (*12*), the ratio of PAH probe fluorescence in the absence of OC quencher, F_0, (e.g., ultrafiltered groundwater) to that observed in the presence of OC, F, (e.g., untreated groundwater sample) can be used to determine the K_{oc} of the PAH probe:

$$\frac{F_0}{F} = \frac{[PAH_T]}{[PAH_d]} = (1 + K_{oc}[OC]) \qquad (1)$$

where $[PAH_T]$ is the total PAH mass per unit volume of sample, $[PAH_d]$ is the dissolved PAH concentration of the sample, and K_{oc} is the OC–groundwater partition coefficient for the PAH probe. Gauthier et al. (*12*) measured the fluorescence ratio as a function of [OC] to determined K_{oc} as the resulting slope. K_{oc} can be determined from a single fluorescence ratio if the [OC] of the sample is known (eq 1). The fluorescence ratio provides a direct assessment of OC-enhanced "solubility" even in the absence of [OC] estimates, as the ratio represents the total (OC-associated plus dissolved) mobile load relative to the truly dissolved load. For a given groundwater sample, the OC concentration cannot be adjusted without altering the sample by concentration or dilution. Therefore, to observe a decrease in fluorescence, the PAH probe used must be carefully chosen. If an estimate of the sample's [OC] is available, the proper PAH can be chosen on the basis of the compound's hydrophobicity. For example, to observe a $[PAH_T]/[PAH_d]$ ratio of at least 2.0, the PAH probe must have a $K_{oc} \geq [OC]^{-1}$. If the [OC] is unknown, a suite of PAH probes with a range of tendencies to sorb can be used to maximize the chance of observing quenching between the extremes of fully and insignificantly quenched. If there is no observable difference in PAH fluorescence between the ultrafiltered and unaltered samples ($F_0/F = 1$), significant association with OC is probably not occurring for the probe compound of interest (with the caveat concerning quenching efficiency discussed below); and by implication there would be no association of OC with other

 0013-936X/90/0924-1214$02.50/0

nonpolar pollutants of similar hydrophobicity. Hence the observed fluorescence ratio is a direct indication of the potential importance of colloid-enhanced transport for both the PAH probe under investigation and pollutants of similar hydrophobicity.

Considerations in Applying Fluorescence Quenching to Unaltered Samples. Use of this method with unaltered samples complicates the analysis and requires that a few concerns be addressed to obtain valid data. These concerns include (1) the possibility that other types of quenchers exist in the natural sample, (2) the need to account for sorption of the PAH probes to experimental vessels in a rigorous way for samples containing low levels of OC requiring the use of very hydrophobic probes and (3) the possibility that the quenching efficiency of OC for PAH probes may not be 100% for all types of OC capable of binding PAH in natural samples. Provided that only OC are removed by the ultrafilter, other quenchers such as oxygen, aromatic amines, metals, or heavy atoms like I^- will be accounted for by using the sample ultrafiltrate to obtain F_0. The other two concerns are discussed below.

(A) PAH Probe Partitioning to Glass Vessels. Preliminary experiments indicated that for very hydrophobic probes, such as perylene, substantial wall losses occurred. Gauthier et al. (*12*) dealt with the possibility of PAH sorption to cuvette walls by preequilibrating cuvettes with aqueous PAH probe solutions. This approach assumes that PAH sorbed to the cuvette wall does not desorb as the dissolved PAH concentration in the cuvette decreases on PAH/OC association. We do not believe this is a good assumption. Sorption to experimental vessel walls can be handled in a more rigorous way by either equilibrium or kinetic methods. Both approaches rely on the assumption that the PAH probe itself, rather than OC-associated probe, is partitioning to the vessel surface.

In the equilibrium approach, the mass balance equation is modified to allow for PAH partitioning to the vessel walls as well as to OC. Defining the equilibrium partition coefficient for the vessel wall as follows

$$K_w = \frac{[\text{PAH–wall}]}{[\text{PAH}_d](\text{SA}/V)}\ (\text{mL/cm}^2) \tag{2}$$

where [PAH–wall] is the mass of PAH associated with the wall per unit volume of sample, and SA/V is the surface area to volume ratio of the vessel estimated from its geometry, the mass balance equation can be simplified and rearranged to

$$\frac{[\text{PAH}_T]}{[\text{PAH}_d]} = 1 + K_{oc}[\text{OC}] + K_w(\text{SA/V}) \tag{3}$$

K_w can be obtained from a series of fluorescence measurements on wall-equilibrated aliquots of the sample following sequential exposure of the sample to new surfaces. If probe molecules are significantly lost to the vessel walls, the inverse of measured fluorescence, yielding measures of $1/[\text{PAH}_d]$, vs cumulative SA/V should decrease linearly with slope $K_w/[\text{PAH}_T]$ and intercept $(1 + K_{oc}[\text{OC}])/[\text{PAH}_T]$. Note that $[\text{PAH}_T]$ cannot be measured directly when wall loss is substantial, but this quantity can be estimated by extrapolation of data from the ultrafiltered sample to $\text{SA}/V = 0$. If both the ultrafiltered and unaltered samples are spiked with the same quantity of PAH, then this estimate of $[\text{PAH}_T]$ is valid for the OC-containing vessel as well. Substituting this value of $[\text{PAH}_T]$ into the expressions for the slope and the intercept of the unaltered sample yields values for K_w and $(1 + K_{oc}[\text{OC}])$.

An alternative approach is to use observations of the kinetics of wall loss. This approach requires the additional assumption that the kinetics of PAH partitioning to OC is fast relative to the kinetics of PAH adsorption to the vessel wall. Assume that the sorption process can be represented as

$$\text{PAH}_d \underset{k_{-w}}{\overset{k_w}{\rightleftharpoons}} \text{PAH–wall} \tag{4}$$

where k_w and k_{-w} are first-order forward and backward rate constants for wall adsorption. Fluorescence as a function of time is described by

$$F = \frac{k_{-w}F_0'}{k_w + k_{-w}} + \frac{k_wF_0'}{k_w + k_{-w}}e^{-(k_w + k_{-w})t} \tag{5}$$

where $F_0' = [\text{PAH}_T] - [\text{PAH–OC}]$ at time zero (*18*). A nonlinear least-squares curve-fitting program can be used to determine k_w, k_{-w}, and F_0' from fluorescence measurements obtained as a function of time. The ratio of fluorescence values extrapolated to $t = 0$ for the ultrafiltered sample relative to that for the unaltered sample allows calculation of the quantity $K_{oc}[\text{OC}]$. K_w can be estimated from the ratio of rate constants and vessel SA/V.

(B) Efficiency of Static Quenching by OC. The analysis thus far has also relied on the assumption that only the $[\text{PAH}_d]$ species is quantified by measured fluorescence. This assumption is valid if static quenching of PAH fluorescence by OC results in complete quenching of PAH fluorescence. If this is not the case, the formulation must incorporate the possibility that the OC-associated PAH contributes to the observed fluorescence. Ignoring wall losses for the purposes of this derivation and assuming only one type of OC exists in the sample

$$F = F_0[(\text{fraction dissolved}) + (\text{fraction sorbed})\phi] \tag{6}$$

where ϕ is the fluorescence quantum yield of OC-bound PAH. In this case, the fluorescence ratio reflects

$$\frac{F}{F_0} = \frac{1 + \phi K_{oc}[\text{OC}]}{1 + K_{oc}[\text{OC}]} \tag{7}$$

For groundwaters with a given quantity of OC of unknown composition, ϕ cannot be determined directly. If, however, the groundwater OC are concentrated, ϕ and K_{oc} can be determined by observing fluorescence as a function of [OC]. Unfortunately, it is uncertain how the concentration procedure might affect the sorbent properties of the OC or how estimation of the K_{oc} under other than in situ conditions may affect the magnitude of the product, $K_{oc}[\text{OC}]$. We have examined this issue indirectly by using model OC (Aldrich humic acids and bovine serum albumin, BSA), as discussed later.

Methods

Apparatus. Fluorescence measurements were obtained on a Perkin-Elmer LS-5 spectrofluorometer with slit widths set at 3 nm (ex)/10 nm (em). Fluorescence data were collected at the following wavelength pairs (nm) (ex/em): 434/466, 250/350, 340/460, 492/519, and 605/600. These wavelengths monitor perylene, phenanthrene, OC, rhodamine 110, and light scattering, respectively. The wavelength pairs were chosen to maximize each fluorophore signal and minimize background interference.

Absorbance measurements were obtained on a Beckman DU-7 spectrophotometer. Data were collected at the following wavelengths (nm): 519, 492, 466, 460, 434, 350, 340, and 250 to allow for inner-filter-effect correction of fluorescence data.

Materials. (A) Test Solutions. Concentrated stock solutions of PAH were made up in methanol. Experimental solutions for fluorescence studies were spiked with 10–25 μL of the stock PAH solution per 20–50 mL of test

Table I. Groundwater Chemistry

sample	pH	E_h, mV	O_2, ppm	conductivity, μS	[TOC], mg of C/L	[OC],[a] mg of C/L	laser light scattering, counts/s
well F242-77							
Oct 87	5.2	+120	5.0	84	0.8	0.1	120
Apr 88	4.7	+130	5.1	77	1.1	0.2	34
well F350-77							
Oct 87	5.5	+65	0.7	330	2.5	1.4	240
July 88	5.6	+70	1.7	210	2.6	1.3	140
well F343-57							
Apr 88	6.4	−70	0.7	450	2.9	1.1	380
July 88	6.3	−80	1.0	300	3.3	1.5	590

[a] Established as the decrease in TOC after ultrafiltration.

solution. The resulting spiked test solutions contained combinations of the following: 0.3–1 μg/L perylene (Aldrich, 99%, Gold Label), 26–65 μg/L phenanthrene (Eastman), 10–26 μg/L rhodamine 110 (Kodak, Lasergrade), and 200–500 mg/L methanol (EM Science, Omnisolve glass distilled). We do not believe such low levels of methanol (5×10^{-3} volume fraction) will affect PAH aqueous activities (*19–21*) enough to cause observable effects on PAH sorption by OC. Note the resulting perylene concentration of some test solutions exceeded the reported solubility of 0.4 μg/L (*22*). Substantial losses to glass walls were expected, so some samples were overspiked to maximize the fluorescent signal remaining after equilibration. For most experiments, perylene, phenanthrene, and rhodamine 110 were spiked concurrently. The fluorescence spectra of these probes do not overlap substantially. Partition coefficients observed for perylene to OC were indistinguishable in the presence and absence of the other two probes. Some test solutions received only methanol. These solutions allowed for background subtraction of fluorescence due to sample components. Rhodamine 110 was included in test solutions to normalize probe responses to account for slight differences in spike level. Rhodamine 110 has a strong fluorescence signal at wavelengths that do not interfere with the PAH used in this study and is soluble enough that sorption to glass walls and OC was not expected.

(B) Samples. Initial equilibrium-approach experiments were carried out using distilled water and 5 mg/L Aldrich humic acid solutions (Techgrade, Aldrich, Milwaukee, WI) at pH 4.5 Aldrich humic acids were used as received. Subsequent kinetic experiments were carried out with Norganic water (Millipore Corp., Bedford, MA) at pH 7, and 1.3 mg/L Aldrich humic acid solutions at pH 7. For these experiments Aldrich humic acid was cleaned prior to use by repeated dissolution in base, precipitation in acid, centrifugation, redissolution, and filtration through a 100-nm Nuclepore filter. For experiments involving BSA, distilled water dilutions of a 1 g/L bovine serum albumin stock were used.

Groundwater samples used in experiments were collected from three U.S. Geological Survey monitoring wells located near Otis Air Base, Cape Cod, MA. At this site, recharge of secondarily treated sewage to a sand and gravel aquifer for more than 50 years (*23*) has created an extensive plume of "dissolved" organic carbon (DOC, Figure 1), a portion of which is expected to be OC (Table I). Well F242-77 is outside the plume, and so relatively low levels of DOC and OC would be expected. Well F343-57 is near the contamination source, where higher levels of OC were anticipated. Well F350-77 is in the middle of a detergent plume. Half of the total DOC at the latter well consists of detergents (*24*); we expected a portion of the remainder

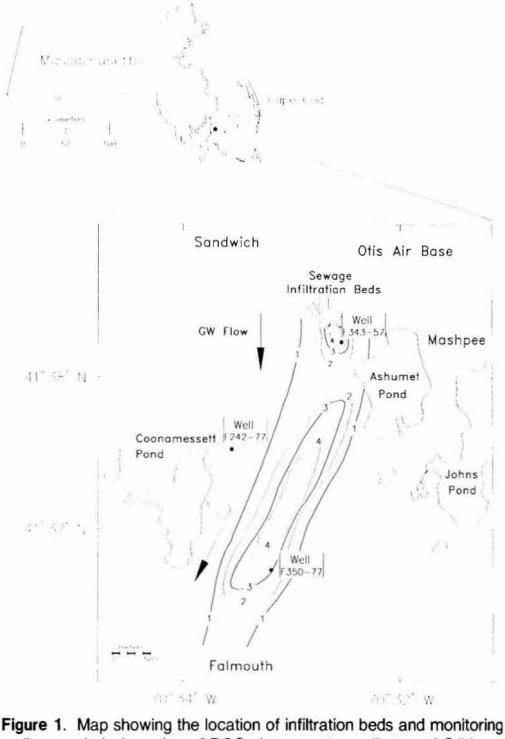

Figure 1. Map showing the location of infiltration beds and monitoring wells sampled. Location of DOC plume contours (in mg of C/L) are from Thurman et al. (*24*). Arrows indicate the general direction of groundwater flow.

to consist of OC. Groundwater samples were obtained from the three wells with a submersible gear-driven pump (Fultz Pump Inc., Lewistown, PA) at very low flow rates (100 mL/min) to minimize shearing of aquifer material. Samples were pumped to the surface through polypropylene tubing and collected in glass Luerlok syringes or in argon-filled biological oxygen demand (BOD) bottles in argon-filled zipper-lock bags. Samples were stored in the dark at slightly below groundwater temperature. Subsequent sample transfers were made in a glovebox in which commercial grade argon (<2 ppm O_2) was used to maintain an inert atmosphere. The pH, E_h, conductivity, dissolved oxygen (DO), and laser light scattering intensity (N4 submicron particle analyzer, Coulter Electronics, Hialeah, FL) of the samples were measured while sampling in the field, on subsampling in the laboratory, and after fluorescence-quenching studies were conducted to determine whether groundwater samples maintained their in

situ conditions through storage and experimentation. These parameters are reported for each well in Table I. For a given sample, these parameters were found to remain constant throughout storage and experimentation.

(C) Glassware. Fluorescence-quenching experiments were carried out in 100-mL round-bottom flasks with ground-glass stoppers or 50-mL glass Luerlok syringes. Reverse-phase separation equilibrations were carried out in 20-mL glass syringes. Quartz cuvettes (1 cm × 1 cm × 4 cm) were used for both fluorescence and absorbance measurements. Flasks and cuvettes were cleaned for use by soaking in concentrated chromic/sulfuric acid followed by rinsing with distilled water. Glass syringes were cleaned by soaking in persulfate solution (5 g/L potassium persulfate and 0.5% phosphoric acid in distilled water) at 90–100 °C for at least 1 h. This was followed by rinsing and soaking in distilled water.

(D) Ultrafiltration. Groundwater samples were ultrafiltered by using an Amicon ultrafiltration cell with a 76-mm 500 MWCO YCO5 ultrafiltration membrane. Ultrafilters were prepared for use by soaking overnight in Norganic water, rinsing with 100 mL of Norganic water, and then rinsing with 50 mL of the sample. A new filter was used for samples from each well. Roughly 350 kPa argon back-pressure forced the sample through the membrane.

(E) Organic Carbon Analysis. OC levels were established as the difference in total organic carbon (TOC) measured in the unaltered groundwater and the organic carbon measured in the ultrafiltered groundwater. Samples were acidified with phosphoric acid and purged of inorganic carbon by a nitrogen stream. Aliquots (50–200 μL) of purged samples were injected directly into the high-temperature combustion chambers of an Ionics total carbon analyzer (Watertown, MA). This instrument utilizes a platinum catalyst to facilitate organic matter oxidation at 900 °C and an infrared detector to measure CO_2 produced. Dilutions of a 1000 mg of C/L potassium biphthalate (Mallinckrodt, reagent grade) solution prepared with Norganic water were used to obtain a calibration curve.

Typical Procedure. (A) Kinetic Approach. A 50-mL glass syringe containing either a humic acid solution, ultrafiltered humic acid solution, Norganic water, whole groundwater, or ultrafiltered groundwater and a small Teflon stir bar was spiked with 10 μL of a methanol solution containing perylene, phenanthrene, and rhodamine 110 or 10 μL of methanol. Immediately after spiking, the syringe was placed on a stir plate. Syringes were covered with foil during experiments to minimize photodegradation of PAH, and samples were spiked with sodium azide to minimize biodegradation. The sample was allowed to mix 3 min; then aliquots were withdrawn sequentially in time for fluorescence and absorbance measurements. At each time point, 5 mL of sample was expelled from the syringe for rinsing and filling the cuvette. Four integrated fluorescence readings were immediately recorded for each of the wavelength pairs listed. Readings were recorded first for the least soluble PAH to minimize the effect of losses to the cuvette walls. After all the fluorescence measurements were obtained, the cuvette was transferred to the spectrophotometer for absorbance measurements. Absorbance measurements were used to calculate inner-filter-effect correction factors for fluorescence measurements (*12*). This correction was largest for fluorescence wavelengths used to monitor phenanthrene, but never exceeded 1.4. Corrected fluorescence measurements were normalized by rhodamine 110 fluorescence measurements for a given data set to account for slight variation in spiking volume. These data, along with the difference in measured organic carbon concentration in the whole and ultrafiltered samples, allow determination of K_{oc} values.

(B) Equilibrium Approach. Samples were transferred from BOD bottles to 100-mL flasks and spiked under an argon atmosphere in a glovebox. These flasks were then incubated in the dark at 22 °C for 3 days. Preliminary experiments indicated that PAH sorptive equilibrium between flask walls and sample was reached in less than 3 days (*18*). Following this equilibration period, an aliquot of the sample was removed from the flask in the glovebox. A portion of this subsample was used to rinse the pipet and cuvette, and then the remainder was transferred to the cuvette for measurement of fluorescence and absorbance. The remainder of the sample in the 100-mL flask was transferred to a clean flask. The sample was then allowed to reequilibrate with this fresh glass surface for 3 days. This sequence was repeated at least four times to obtain fluorescence observations as function of cumulative SA/V.

(C) Reverse-Phase Separation. For comparative purposes partition coefficients were determined by the method of Landrum et al. (*25*). The basis for the method is that dissolved PAH are retained by a C_{18} cartridge while OC (humic materials in particular) and associated PAH pass through the cartridge. Glass syringes (20 or 50 mL) were filled with Aldrich humic acid or BSA solutions, distilled water, or groundwater samples. Syringes were spiked with 10–25 μL of the PAH spiking solutions or methanol (for determination of background fluorescence) and 10 μL of saturated sodium azide solution. Syringes containing distilled water were used to ensure PAH were retained by the cartridge in the absence of OC. Samples in syringes were equilibrated with PAH spikes in the dark with a stir bar on a stir plate for several hours or without a stir bar for at least 18 h. An 8-mL aliquot was then taken to obtain a measure of total PAH (dissolved + OC-associated). The sample was then passed through the C_{18} cartridge at a flow rate of 12 mL/min (Maxi Clean cartridge, Alltech Associates, cleaned with 10 mL of methanol and at least 30 mL of distilled water before use) and an 8-mL aliquot of the effluent was taken to determine OC-associated PAH content. These aliquots were extracted with 4 mL of hexane (EM Science, Omnisolve, glass distilled) and analyzed by fluorometry. The dissolved PAH content was determined by difference. The K_{oc} (mL/g of C) was calculated as $[PAH\text{–}OC]/[PAH_d][OC]$.

Results and Discussion

Method Verification Using Model OC. Aldrich humic acids and bovine serum albumin were used as model OC to test the fluorescence-quenching method, verifying assumptions inherent in the derivation, as well as to allow comparison of partitioning data obtained by fluorescence quenching with results obtained by more traditional methods.

(A) Perylene/Aldrich Humic Acids: Equilibrium Approach. According to eq 3, the reciprocal of observed perylene fluorescence obtained via the equilibrium approach should vary directly with the vessel SA/V ratio. This is observed for perylene fluorescence in the presence of 1.4 mg of C/L Aldrich humic acids as well as for distilled water samples (Figure 2a). The fluorescence measurements obtained in the presence of Aldrich humic acids lie on a distinctly different line than those obtained for the distilled water sample, indicating fluorescence quenching is occurring due to association of perylene with the humic acids. The average K_w obtained from the slopes of the

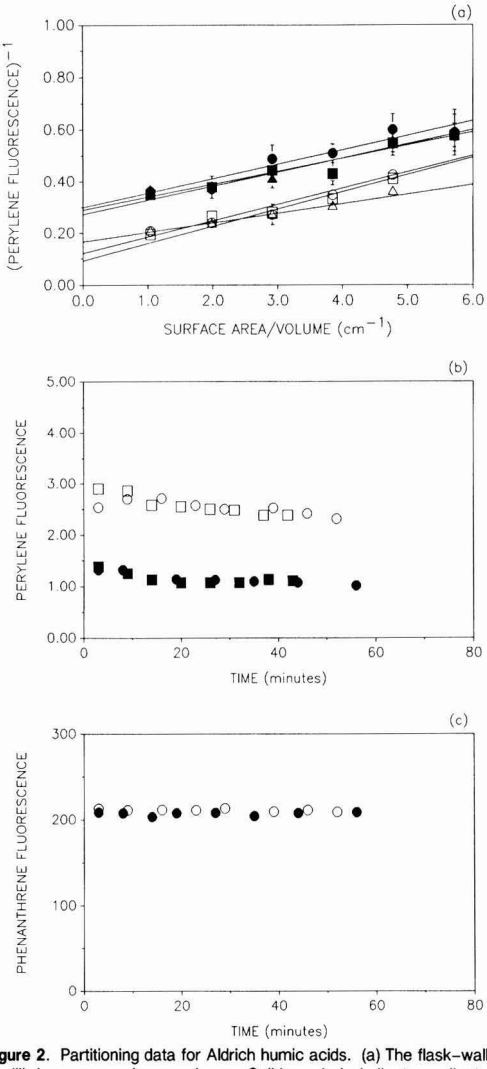

Figure 2. Partitioning data for Aldrich humic acids. (a) The flask–wall equilibrium approach: perylene. Solid symbols indicate replicate Aldrich humic acid solutions, 1.4 mg of C/L; open symbols indicate replicate distilled water samples. (b) The kinetic approach: perylene. Solid symbols indicate 0.47 mg of C/L clean Aldrich humic acid solutions: (■) spiked with perylene/phenanthrene/rhodamine, (●) spiked with perylene only. (○) Norganic water spiked with perylene, (□) ultrafiltered humic acid solution spiked with perylene/phenanthrene/rhodamine. (c) The kinetic approach: phenanthrene. (●) 0.47 mg of C/L clean and filtered humic acids, (○) ultrafiltered humic acid solution.

replicate Aldrich humic acid samples (K_w = 0.36 mL/cm^2) is virtually identical with that obtained for the replicate distilled water samples (K_w = 0.39 mL/cm^2). This supports the assumption that the PAH probe is partitioning directly to the glass surface. The Aldrich humic acid OC show no tendency to associate with the glass surface. Further substantiation of this assumption is provided by Backhus (*18*).

(B) Perylene/Aldrich Humic Acids: Kinetic Approach. When the kinetic approach is used, perylene fluorescence measurements for both the OC–void and humic acid samples show an exponential decrease in time, asymptotically approaching the solution–glass surface equilibrium value (Figure 2b). The fluorescence measurements obtained for the OC–void and humic acid samples lie on distinct curves, indicating quenching occurs in the presence of OC. The similarity of the average K_w values for replicates calculated from the ratio of the rate constants obtained from the curve-fitting program for the distilled water samples (K_w = 0.35 mL/cm^2) and humic acid samples (K_w = 0.33 mL/cm^2) supports both the assumptions that OC is not partitioning to the glass surface and that PAH–OC partitioning is fast relative to PAH–wall partitioning. Further evidence substantiating these assumptions is provided by Backhus (*18*).

(C) Phenanthrene/Aldrich Humic Acids. Current concepts of hydrophobic organic compound partitioning to OC lead to the prediction that partitioning behavior is proportional to the hydrophobicity of the organic compound, for example, as reflected by K_{ow}. To test this assumption, phenanthrene was included as a second probe in some samples. At low OC levels (0.47 mg of C/L) the phenanthrene fluorescence measured for the Aldrich humic acid samples is virtually identical with that measured for the OC–void samples (Figure 2c), indicating that phenanthrene, unlike the more hydrophobic perylene, shows little if any association to OC. This result could be predicted from the expected ratio of dissolved to total phenanthrene of 0.996 calculated from the K_{oc} of 8.3 × 10^3 mL/g of C (*25*). Not only does phenanthrene show less tendency to associate with OC, but the fluorescence readings in Figure 2c show no significant decrease with time, suggesting no interactions with glass surfaces. This allows the use of phenanthrene to further verify our assumptions regarding the absence of dynamic quenching and losses due to volatilization or biodegradation.

(D) Fluorescence-Quenching Efficiency. One final assumption inherent in the derivation of both the equilibrium and kinetic approaches is that the probe fluorescence is totally quenched on association with OC, i.e., $\phi \cong 0$. This assumption was examined by measuring probe fluorescence at various model OC concentrations. The data were analyzed according to eq 7 after accounting for wall losses. The curve should asymptotically approach ϕ as [OC] $\Rightarrow \infty$. The K_{oc} estimate from these data can be deduced from the curve as the inverse of the [OC] where $F/F_0 = (1 + \phi)/2$. Results for perylene with clean and filtered Aldrich humic acids and with BSA are shown in Figure 3a and b. For the Aldrich humic acids, the curve asymptotically approaches a ϕ value of –0.033, which is not significantly different from zero; the fit K_{oc} is 2.4 × 10^6. This K_{oc} is similar to the K_{oc} value obtained by the kinetic approach for clean unfiltered Aldrich humic acids at a single [OC] (Table II). For BSA, however, the curve asymptotically approaches a ϕ value of 0.58, which is significantly different from zero, and K_{oc} is found to be 3.4 × 10^5. This nonzero value of ϕ may reflect the diminished overlap of BSA's allowed electronic transitions (e.g., as exhibited by its shorter wavelength absorption spectrum as compared to Aldrich humic acids, Figure 4) with perylene's fluorescent emission energies. Determining a K_{oc} value for perylene partitioning to BSA by use of the equilibrium or kinetic approach and a single concentration of [BSA] would give too small a result if the nonzero value of ϕ were not taken into account. Similarly, since ϕ may not be zero for all types of OC found in groundwaters, K_{oc}[OC] estimates obtained by observing diminished probe fluorescence due to quenching by groundwater OC yield only a lower limit on probe–OC association. If concentration and dilution steps do not affect the OC sorbent properties, groundwater OC could be diluted or concen-

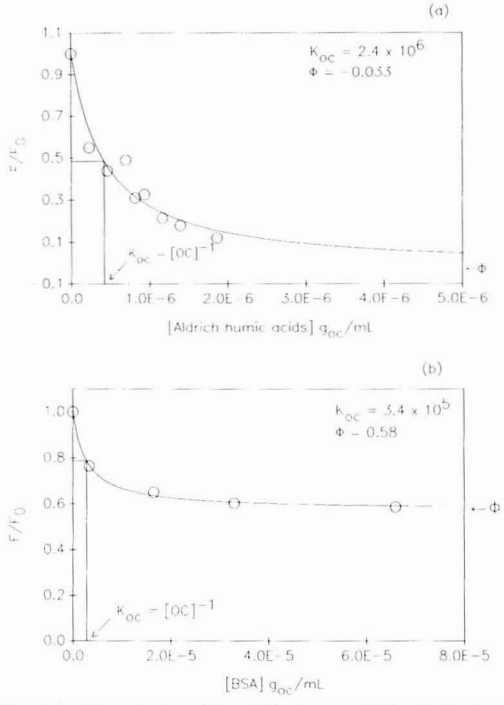

Figure 3. Determination of ϕ and K_{oc} for model OC. (a) Clean and filtered Aldrich humic acids, (b) BSA; each data point obtained by back-extrapolation to SA = 0 using kinetic approach.

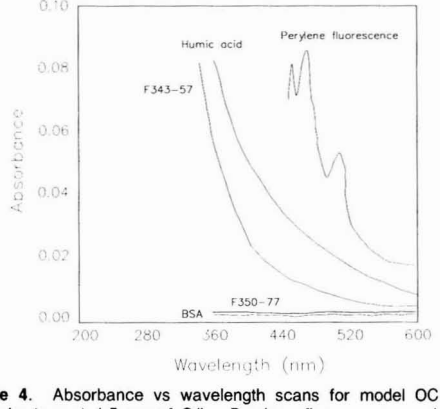

Figure 4. Absorbance vs wavelength scans for model OC and groundwaters at 1.5 mg of C/L. Perylene fluorescence emission wavelength scan excitation λ = 434.

trated to a wide range of [OC] levels to allow direct assessment of ϕ and K_{oc}. The results of Gauthier et al. (*13*) suggest that ϕ values of zero are found for a wide variety of humic and fulvic materials. Caution must be exercised in interpretation of the linearity of Stern–Volmer plots as an indication that $\phi = 0$, as deviations from linearity may not be apparent over limited OC ranges.

Static quenching in general can occur if there is significant overlap of the quencher absorbance spectrum and the fluorescent probe emission spectrum (*26*). Perhaps there is a correlation between degree of overlap and ϕ. There was a greater degree of overlap for perylene fluorescence energies with the absorption spectra of Aldrich humic acids than with BSA (Figure 4). Further work with a greater variety of OC and probes is required to substantiate such a correlation.

Table II. K_{oc}'s[a] (± rel. std. error) Found Using Model OC in This Work and Reported Previously

sorbent concn and technique	sorbate: phenanthrene	sorbate: perylene	sorbate: benzo[a]pyrene
Aldrich humic acid as received			
1.4 mg of C/L by equilibrium approach		8.8×10^5 (±55%)	
Aldrich humic acid after cleanup			
0.47 mg of C/L by kinetic approach	$<6 \times 10^4$ [b]	1.7×10^6 (±8.2%)	
0–1.9 mg of C/L by kinetic approach		2.4×10^6 (±32%)	
1.15 mg of C/L by reverse-phase approach		8×10^5 (±4.3%)	
11.5 mg of C/L by reverse-phase approach	9.8×10^3 (±1.4%)		
1–16 mg of C/L by reverse-phase approach (*25*)	8.3×10^3		8.9×10^5
0.7–40 mg of C/L by dialysis approach (*11*)			1.6×10^6
bovine serum albumin			
0–66 mg of C/L by kinetic approach		3.4×10^5 (±11%)	
2.8 mg of C/L by reverse-phase approach		1.4×10^4 (±50%)	
K_{ow} (*27*)	3.7×10^4	3.2×10^6	9.6×10^5

[a] Numbers in parentheses, ± relative standard error. [b] Indicates no quenching observed, and calculated upper limit K_{oc} value based on the [OC] present and the precision of the fluorescence measurements (generally <3% for phenanthrene estimates and perylene reverse-phase estimates) or the standard deviation of the back-extrapolated fluorescence estimates for perylene (generally <6%).

(E) Summary of K_{oc} Results and Comparisons with Other Investigators. After accounting for wall effects and determining that $\phi = 0$ for Aldrich humic acids, K_{oc} values can be calculated from the data presented in Figure 2. These K_{oc} estimates for perylene and upper estimates for phenanthrene (calculated from our fluorescence detection precision and observed [OC] since no quenching was observed) are reported in Table II. The standard deviations reported are based on variability of replicates. Both the kinetic and equilibrium approaches provide reproducible K_{oc} estimates (Table II and Figure 2a and b). Concurrent spiking of perylene, phenanthrene, and rhodamine did not affect the estimated perylene–OC partitioning constants (Figure 2b). Since fluorescence measurements for perylene in ultrafiltered humic acid solutions are the same as those obtained in Norganic water, either insignificant quantities of quenchers other than OC are present in the OC-containing samples or ultrafiltration removes only OC from the Aldrich humic acid solutions. We believe the difference in K_{oc} found for cleaned versus used-as-received Aldrich humic acids is due to real differences in the mixture of OC in these solutions, as indicated by the shift in maximum emission wavelength (Figure 5). Further discussion of the differences in humic acid solutions is provided by Backhus (*18*).

A comparison of these K_{oc} values obtained by fluorescence quenching with K_{oc} obtained by other techniques provides further verification of our method. K_{oc} values for perylene and phenanthrene with Aldrich humic acids were measured by a reverse-phase separation technique (Table II). The K_{oc} value for perylene with clean Aldrich humic acids measured by the reverse-phase technique is only $^1/_2$ to $^1/_3$ that obtained by the fluorescence-quenching method. Invalid assumptions in the fluorescence-quenching method should lead to underestimation rather than overestimation of the K_{oc} value; problems involved in the separation of equilibrated phases using reverse-phase cartridges may

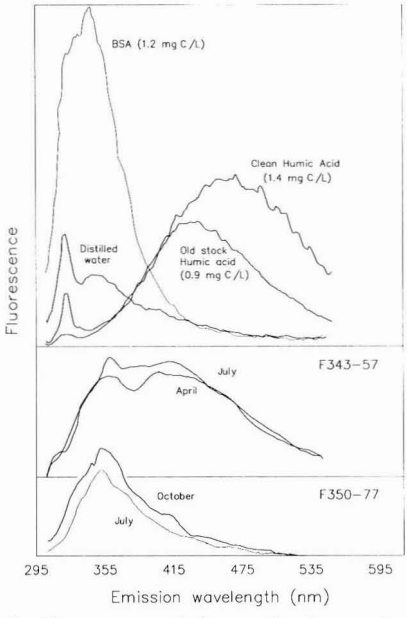

Figure 5. Fluorescence emission wavelength scans (excitation wavelength λ = 290) for model OC and groundwater OC. Note groundwater scans represent the difference between the whole and ultrafiltered scans.

account for the observed discrepancy in K_{oc} values. Though no data exist in the literature regarding perylene partitioning to Aldrich humic acids, comparison of our results with those obtained by others for benzo[*a*]pyrene (B[*a*]P), a five-ring PAH of similar hydrophobicity (but markedly greater carcinogenicity), is instructive. The K_{oc} values obtained for perylene by the fluorescence-quenching method are in the same range as those obtained by others for B[*a*]P (Table II). The K_{oc} values obtained by the reverse-phase method for phenanthrene are consistent with the upper limit K_{oc} estimated by considering the precision of the fluorescence-quenching method and match the K_{oc} value obtained by Landrum et al. (*25*) using a reverse-phase method. Thus, the fluorescence-quenching method appears consistent with other approaches.

Fluorescence Quenching To Quantify the Impact of OC in Groundwater. The fluorescence-quenching method was applied to several groundwater samples to investigate the potential importance of OC-sorbed species in such waters. Three wells were tested on two separate occasions. The groundwater properties vary substantially between these wells (Table I); most notably, wells F343-57 and F350-77 contain water with ~10 times more OC than the background well F242-77. The TOC does not vary so strongly. The groundwater nearest the infiltration beds had the highest pH, the lowest E_h, and the highest conductivity. Oxygen was present at or below detection limits in groundwater from both wells in the contamination plume, and laser light scattering intensity was greatest near the sewage beds. This level of light scattering, a few times above our background, suggests less than 1 mg/L inorganic colloids, possibly organic coated, was present (based on a polystyrene bead standard). Previous samples recovered from this particular site contained much greater inorganic colloid concentrations (*2*). Both wells F343-57 and F350-77 showed significant temporal changes in conductivity, further indicating the variable nature of the groundwater plume.

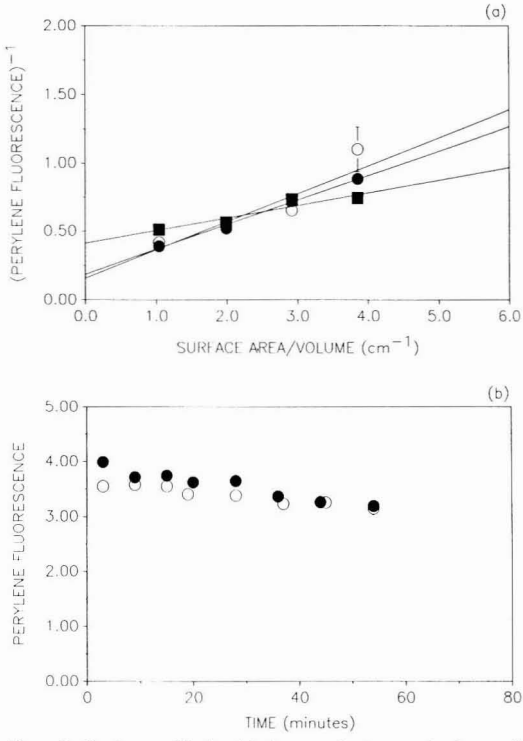

Figure 6. Perylene partitioning data for groundwater samples from well F242-77. Solid symbols indicate whole groundwater samples; open symbols indicate ultrafiltered groundwater samples. (a) Equilibrium approach: samples collected in October 1987. (b) Kinetic approach: samples collected in April 1988.

Maintenance of in situ conditions, especially anoxia, was especially challenging for samples from the groundwater contamination plume. Introduction of even slight amounts of oxygen into these samples quickly led to precipitation of iron oxides. By filling 50-mL glass syringes in the field, and using the kinetic approach for determining partitioning, we were able to observe fluorescence quenching while avoiding such water chemistry changes. With the most sensitive samples from well F343-57, the transfer steps involved in the equilibrium approach resulted in precipitation of ferric oxides. Hence, for well F343-57 only data obtained with the kinetic approach are reported here.

Fluorescence-quenching results for perylene, added to the whole and ultrafiltered groundwater from these three wells, are shown in Figures 6–8. We note that perylene fluorescence in the ultrafiltered water (containing between 0.7 and 1.8 mg of C/L residual DOC) never differed from that observed in Norganic water, indicating that this ultrafilterable organic matter did not participate in binding. Thus, calculations using TOC values to deduce K_{oc} will underestimate the true result. Using the measured OC concentration and assuming $\phi = 0$, K_{oc} values for these samples can be calculated. No evidence for any association of either perylene or phenanthrene with OC was ever observed for samples obtained from the background well F242-77, either via fluorescence quenching (Figure 6) or via reverse-phase separation (Table III). Similarly, no association of the more water soluble probe, phenanthrene, was observed for any sample obtained from well F343-57 or F350-77 regardless of the method used to quantify partitioning (Table III). The results for the more hydrophobic probe, perylene, for the wells within the contam-

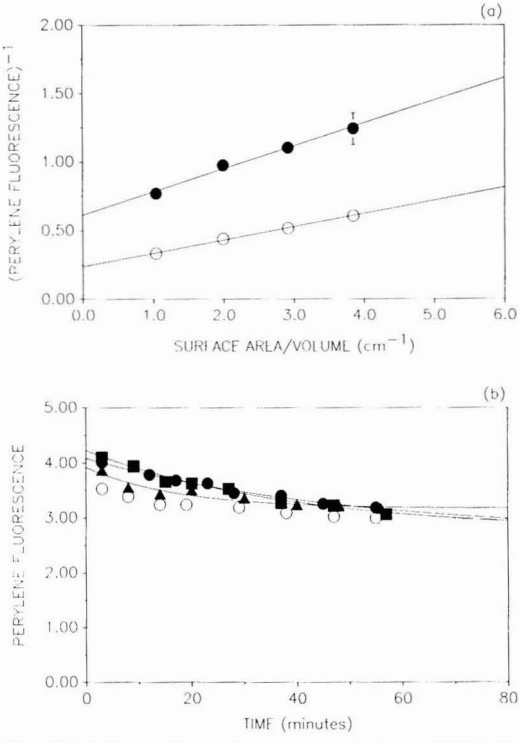

Figure 7. Perylene partitioning data for groundwater from well F350-77. Solid symbols indicate whole groundwater samples; open symbols indicate ultrafiltered groundwater samples. (a) Equilibrium approach: sample collected in October 1987. (b) Kinetic approach: sample collected in July 1988.

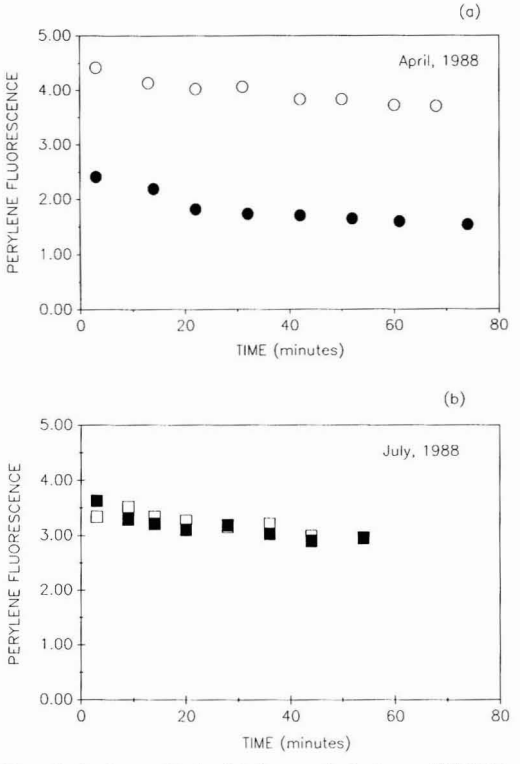

Figure 8. Perylene partitioning data for groundwater from well F343-57: kinetic approach. Solid symbols indicate whole groundwater samples; open symbols indicate ultrafiltered groundwater samples. (a) Sample collected in April 1988; (b) sample collected in July 1988.

Table III. PAH Partitioning Behavior to Groundwater OC[a]

sample and method	[OC], mg of C/L	K_{oc}, mL/g of C perylene	K_{oc}, mL/g of C phenanthrene
F343-57, Apr 88			
kinetic	1.1	$6.7 \times 10^5 \pm 3.6 \times 10^5$	$<1.8 \times 10^{5*}$
reverse-phase	1.1	$2.6 \times 10^5 \pm 2 \times 10^4$	$<2 \times 10^{3*}$
F343-57, July 88			
kinetic	1.5	$<4.1 \times 10^{4*}$	$<6.5 \times 10^{4*}$
reverse-phase	1.5	$<1.7 \times 10^{4*}$	$<1.2 \times 10^{4*}$
F350-77, Oct 87			
equilibrium	1.4	1.1×10^6	
F350-77, July 88			
kinetic	1.3	$<4 \times 10^{4*}$	$<4 \times 10^{4*}$
reverse-phase	1.3	$<1.6 \times 10^{4*}$	$<7 \times 10^{3*}$
F242-77, Oct 87			
equilibrium	0.1	$<5.5 \times 10^{6*}$	
F242-77, Apr 88			
kinetic	0.2	$<3 \times 10^{5*}$	$<8.4 \times 10^{4*}$
reverse-phase	0.2	$<1.4 \times 10^{5*}$	$<8.1 \times 10^{4*}$

[a] Asterisk indicates no quenching observed, and calculated upper limit K_{oc} value based on the [OC] present and the precision of the fluorescence measurements (generally <3% for phenanthrene estimates and perylene reverse-phase estimates) or the standard deviation of the back-extrapolated fluorescence estimates for perylene (generally ≤6%).

inant plume demonstrate temporal variability. Fluorescence measurements for the October 1987 samples from well F350-77 exhibited perylene quenching by OC (Figure 7a). The April 1988 samples from well F343-57 also demonstrated perylene association with OC both via fluorescence quenching (Figure 8a) and via reverse-phase methods (Table III); the two K_{oc} estimates agree reasonably well. In contrast, perylene showed no tendency to associate with OC in the July 1988 samples obtained from either of these wells, when measured by fluorescence quenching (Figures 7b and 8b) or by reverse-phase methods (Table III).

The magnitudes of the computed K_{oc} values for most cases seem reasonable. The lack of association of phenanthrene or perylene with OC in samples from the background well could have been predicted given the low OC concentrations. Calculations suggest only 5–9% of the perylene and less than 0.2% of the phenanthrene would be associated with OC in these samples (assuming K_{oc} values of 5×10^5 and 8×10^3, respectively). Similarly, phenanthrene is insufficiently hydrophobic to be significantly bound even at the higher OC concentrations found in wells F343-57 and F350-77 (less than 1% association predicted).

For the first set of samples collected from wells F343-57 (April 1988) and F350-77 (October 1987), the perylene K_{oc} estimates agree with values that might have been predicted. Both proteins and humic materials can be important components of secondary sewage effluent (*28*, *29*), leading us to expect K_{oc} values somewhere between those measured for the two model OC; the measured groundwater K_{oc} values are comparable to those measured for BSA and about half that measured for the clean Aldrich humic acids. If, however, the ϕ values for the groundwater OC were greater than zero, the true K_{oc} values would be greater than those reported in Table III. Using the K_{ow} value for perylene as an upper estimate of the true K_{oc} for OC in these groundwaters indicates that the $\phi = 0$ assumption leads to at most a factor of 3–5 underestimation of the true K_{oc} value.

It is difficult to interpret the temporal variability in the K_{oc} values measured for samples from wells F343-57 and F350-77. Conceivably, the OC in the July 1988 samples differed in composition and ϕ values from that previously collected from these wells; for example, they could have been rich in hydrophilic polysaccharides or consisted of quite small macromolecules. Other workers have previously shown how differences in the character of OC, for example C/O ratios or aliphatic/aromatic proportions can significantly affect K_{oc} (*13*, *30*, *31*). We briefly examined this possibility by comparing the fluorescence emission spectra of the July samples with the earlier samples (Figure 5). Both the fluorescent intensities and the overall spectral response did not appear significantly different for the samples collected at any one well, tending to counter the hypothesis that the OC was compositionally different. Another possibility is that the groundwater composition was varying so as to effect differential OC–perylene interactions. For both July 1988 samples, the electrical conductivity was lower than previously seen. Although this decrease in salt content would increase the solubility of perylene in the water, the Setchenow relationship (e.g., refs 32 and 33) suggests this effect would be quite small. Using a value of the Setchenow constant, K_s, similar to that reported for other PAH (0.4 M^{-1}) and converting conductivity measures to ionic strengths (10^{-2} M) by using Langmuir's equation (*34*), we find

$$\frac{\text{solubility}_{\text{saltwater 2}}}{\text{solubility}_{\text{saltwater 1}}} = 10^{-(K_s)(\Delta[\text{salt}])} = 10^{-0.004} \cong 0.99 \quad (8)$$

The corresponding change in perylene's aqueous activity coefficient due to these changing concentrations is insufficient to explain the observed lack of OC association. The observed differences in conductivities or specific ion concentrations (*14*) could also signal a shift in the macromolecular configuration of the OC. Increasing ionic strength has been shown to cause organic polyelectrolytes like humic acids and proteins to take on a more globular configuration (*35*). Chiou et al. (*30*) demonstrated that organic macromolecules occurring in a stretched-out configuration (e.g., polyacrylic acid) do not act as sorbents for hydrophobic chemicals. Conceivably, the OC present in the July 1988 groundwaters, although present at roughly the same concentrations and composed of similar structural elements as in the early samples, were simply "denatured" and unable to bind perylene. Further work is necessary to substantiate this hypothesis or other explanations.

Implication to Subsurface Transport. The quenching results for groundwater obtained within the plume at Otis Air Base suggest that sufficient OC is, at least sometimes, present to augment the mobile load of very hydrophobic chemicals. Assuming that OC moves at the groundwater seepage velocity, and that immobile organic matter has a K_{oc} value similar to mobile OC, an adjusted retardation coefficient can be calculated for such OC-interactive species:

$$\text{retardation factor} = 1 + \frac{\text{fraction immobilized in soil}}{\text{fraction dissolved} + \text{fraction OC-bound}}$$

$$= 1 + \frac{\rho_b f_{oc} K_{oc}}{n + n[\text{OC}]K_{oc}} \quad (9)$$

where ρ_b is the soil bulk density, f_{oc} is the organic carbon content of the soil, and n is the soil porosity. Obviously, for cases where the product $[\text{OC}]K_{oc}$ is small compared to 1, that is, when the mobile OC concentration is low or pollutants of concern exhibit low K_{oc} values, the retardation expression simplifies to that derived for the two-phase transport case (e.g., ref 36).

The significance of OC association to transport of compounds like perylene in the sewage plume at Otis Air Base can be illustrated as follows. Barber et al. (*37*) found for these aquifer solids, $n \simeq 0.3$, $\rho_b = 1.8$ g/cm^3, and $f_{oc} \cong 5\%$ fines at 0.1% organic content = 5×10^{-5}. For perylene with $K_{oc} \cong 7 \times 10^5$ and groundwater [OC] $\sim$ 1 mg C/L, we find

$$\text{retardation factor} = 1 + \frac{63}{0.3 + 0.2} \cong 130 \quad (10)$$

In other words, the presence of OC in the flowing groundwater approximately doubles the mobile load (halves the retardation factor calculated in the absence of OC) of a contaminant with hydrophobicity similar to perylene. The presence of OC could be even more important than the retardation coefficient predicts if size exclusion effects allow colloids to travel faster than the seepage velocity (*38*).

Conclusion

The fluorescence-quenching method described in this paper provides an alternative method for determination of partition coefficients between OC and fluorescent sorbates in environmental samples, allowing direct assessment of the possibility of OC-enhanced pollutant transport. The advantages of this method are that it requires no separation of equilibrated phases, and partition coefficients can be determined under in situ conditions. The method allows determination of partition coefficients for all OC that quench the fluorescence of PAH probes on association. Partition coefficients and the possibility of enhanced transport for nonfluorescent pollutants can be determined by inference. The main limitation of this method is the assumption that probe fluorescence is completely quenched on association with OC ($\phi = 0$). Bounds can be placed on the true K_{oc} value by using the probe K_{ow}, as an upper limit, and the K_{oc} calculated by assuming $\phi = 0$, as the lower bound. Determination of the actual groundwater $[\text{OC}]K_{oc}$ requires further sample manipulation by dilution or OC concentration to determine ϕ. The limitation of this method imposed by this assumption (factor of 3–5 underestimation of K_{oc}) must be weighed against the possible errors in other methods due to OC concentration and separation schemes that may change the nature of the OC or collect only a fraction of the OC present. The fluorescence-quenching method described is useful for screening/determining the K_{ow} range of contaminants for which OC in the sample will significantly increase the mobile load. The method was used successfully on samples from an aquifer contaminated by recharge of secondarily treated sewage. The data indicate the presence of OC in this case will approximately double the mobile load of hydrophobic pollutants such as perylene or B[*a*]P, but will have little effect on the mobility of less hydrophobic pollutants. The temporal variability observed in PAH–OC association in these groundwaters indicates that, unlike organic contaminant partitioning to soil organic matter, partition coefficients for OC may not be a simple function of OC organic carbon content. Understanding this variability will be necessary to estimate accurately the transport of OC-associated hydrophobic organic pollutants through the subsurface. Additionally, groundwater samples from this site indicate that OC may represent a significant fraction of the TOC in environmental samples (e.g., 40–60% for groundwater within the plume) or a minor fraction (e.g., 10–20% at well F242-77). This indicates that use of TOC in calculation of K_{oc} values will underestimate

the true K_{oc}, as ultrafilterable DOC (for the samples in this study) does not quench PAH fluorescence and therefore does not appear to bind.

Acknowledgments

We gratefully acknowledge the generous assistance of the following: Lynn Roberts, Francois Morel, Karen Hronek, Thomas Carlin, John MacFarlane, and Joe Ryan for their invaluable assistance in manuscript preparation and groundwater sampling. We also gratefully acknowledge the field site support provided by the U.S. Geological Survey Toxic Waste Groundwater Contamination Research Program.

Registry No. C, 7440-44-0; perylene, 198-55-0; phenanthrene, 85-01-8; benzo[*a*]pyrene, 50-32-8.

Literature Cited

(1) McDowell-Boyer, L. M.; Hunt, J. R.; Sitar, N. *Water Resour. Res.* **1986**, *22*, 1901.
(2) Gschwend, P. M.; Reynolds, M. D. *J. Contam. Hydrol.* **1987**, *1*, 309.
(3) Enfield, C. G.; Bengtsson, G. *Groundwater* **1988**, *26*, 64.
(4) McCarthy, J. F.; Zachara, J. M. *Environ. Sci. Technol.* **1989**, *23*, 496.
(5) Leenheer, J. A.; Malcolm, R. L.; McKinley, P. W.; Eccles, L. A. *J. Res. U.S. Geol. Surv.* **1974**, *2*, 361.
(6) West, C. C. Ph.D. Dissertation, Rice University, 1984.
(7) Thurman, E. M. *Organic Geochemistry of Natural Waters*; Kluwer: Hingham, MA, 1985.
(8) Ryan, J. N.; Gschwend, P. M. *Water Resour. Res.* **1990**, *26*, 307.
(9) Reinhard, M. *Environ. Sci. Technol.* **1984**, *18*, 410.
(10) Robertson, W. D.; Barker, J. F.; Lebeau, Y.; Marcoux, S. *Groundwater* **1984**, *22*, 192.
(11) McCarthy, J. F.; Jimenez, B. D. *Environ. Sci. Technol.* **1985**, *19*, 1072.
(12) Gauthier, T. D.; Shane, E. C.; Guerin, W. F.; Seitz, W. R.; Grant, C. L. *Environ. Sci. Technol.* **1986**, *20*, 1162.
(13) Gauthier, T. S.; Seitz, W. R.; Grant, C. L. *Environ. Sci. Technol.* **1987**, *21*, 243.
(14) Traina, S. J.; Spontak, D. A.; Logan, T. J. *J. Environ. Qual.* **1989**, *18*, 221.
(15) Boehm, P. D.; Quinn, J. G. *Geochim. Cosmochim. Acta* **1973**, *37*, 2459.
(16) Carter, C. W.; Suffett, I. H. *Environ. Sci. Technol.* **1982**, *16*, 735.
(17) Means, J. C.; Wijayaratne, R. *Science* **1982**, *215*, 968.
(18) Backhus, D. A. Ph.D. Dissertation, Massachusetts Institute of Technology, 1990.
(19) Yalkowsky, S. H.; Valvani, S. C.; Amidon, G. L. *J. Pharm. Sci.* **1976**, *65*, 1488.
(20) Munz, C.; Roberts, P. V. *Environ. Sci. Technol.* **1986**, *20*, 830.
(21) Morris, K. R.; Abramowitz, R.; Pinal, R.; Davis, P.; Yalkowsky, S. H. *Chemosphere* **1988**, *17*, 285.
(22) Mackay, D.; Shiu, W. Y. *J. Chem. Eng. Data* **1977**, *22*, 399.
(23) LeBlanc, D. R. Sewage plume in a sand and gravel aquifer, Cape Cod, Massachusetts. *U.S. Geol. Surv. Water-Supply Pap.* **1984**, *No. 2218*.
(24) Thurman, E. M.; Barber, L. B.; LeBlanc, D. R. *J. Contam. Hydrol.* **1986**, *1*, 143.
(25) Landrum, P. F.; Nihart, S. R.; Eadie, B. J.; Gardner, W. S. *Environ. Sci. Technol.* **1984**, *18*, 187.
(26) Schulman, S. G. *Fluorescence and Phosphorescence Spectroscopy: Physiochemical Principles and Practice*; Pergamon Press: New York, 1977.
(27) Miller, M. M.; Wasik, S. L.; Huang, G.-L.; Shiu, W.-Y.; Mackay, D. *Environ. Sci. Technol.* **1985**, *19*, 522.
(28) Rebhun, M.; Manka, J. *Environ. Sci. Technol.* **1971**, *5*, 606.
(29) Manka, J.; Rebhun, M.; Mandelbaum, A.; Bortinger, A. *Environ. Sci. Technol.* **1974**, *8*, 1017.
(30) Chiou, C. T.; Malcolm, R. L.; Brinton, T. I.; Kile, D. E. *Environ. Sci. Technol.* **1986**, *20*, 502.
(31) Garbarini, D. R.; Lion, L. W. *Environ. Sci. Technol.* **1986**, *20*, 1263.
(32) May, W. E.; In *Petroleum in the Marine Environment*; Petrakis, L., Weiss, F. T., Eds.; Advances in Chemistry Series 185; American Chemical Society: Washington, DC, 1980; Chapter 7.
(33) Whitehouse, B. *Mar. Chem.* **1984**, *14*, 319.
(34) Langmuir, D. Geochemistry of iron in a coastal-plain groundwater of the Camden, New Jersey area. *U.S. Geol. Surv. Prof. Pap.* **1969**, *No. 650-C*, C224.
(35) Ghosh, K.; Schnitzer, M. *Soil. Sci.* **1980**, *129*, 226.
(36) Freeze, R. A.; Cherry, J. A. *Groundwater*; Prentice-Hall Inc.: Englewood Cliffs, NJ, 1979; p 404.
(37) Barber, L. B.; Thurman, E. M.; Shroeder, M. P.; LeBlanc, D. R. *Environ. Sci. Technol.* **1988**, *22*, 205.
(38) Harvey, R. W.; George, L.; Smith, R. L.; LeBlanc, D. R. *Environ. Sci. Technol.* **1989**, *23*, 51.

Received for review September 26, 1989. Revised manuscript received March 21, 1990. Accepted April 23, 1990. This work was initiated with support from the U.S. Air Force and the U.S. Environmental Protection Agency under Contract No. CR812466-01-0 and completed under the continuing sponsorship of the Office of Health and Environmental Research, Ecological Research Division, U.S. Department of Energy under Contract No. DE-FG02-86ER60413. Although the research described in this paper has been funded in part by the U.S. Environmental Protection Agency, it has not been subjected to the Agency's required peer and policy review. Therefore, it does not necessarily reflect the views of the Agency and no official endorsement should be inferred.

Environ. Sci. Technol. 1990, 24, 1224–1234

^{210}Po and ^{210}Pb Remobilization from Lake Sediments in Relation to Iron and Manganese Cycling

Gaboury Benoit* and Harold F. Hemond

Department of Civil Engineering, Massachusetts Institute of Technology, Cambridge, Massachusetts 02139

■ The behavior of ^{210}Po and ^{210}Pb was studied in the water column of an oligotrophic, dimictic lake. Direct uptake of the radionuclides by sediments was negligible compared to removal on particles, and ^{210}Pb scavenging was 4 times that of ^{210}Po. Both nuclides were found to be significantly remobilized from sediments into the stratified, anoxic water column. Releases seem to be linked to the cycling of the transition metals, iron and possibly manganese. The distribution of both iron and ^{210}Pb in stratified, anoxic waters can be modeled as constant release and rapid horizontal mixing/dilution; vertical turbulent transport had a negligible effect on element distributions. Upon contact with oxygen, iron rapidly reprecipitates, forming a particulate maximum and rescavenging ^{210}Pb. Unlike ^{210}Pb, much ^{210}Po is released from sediments before overlying water becomes completely anoxic, leading to unsupported ^{210}Po. ^{210}Po cycling in the stratified water column is more complex than that of ^{210}Pb, and additional removal mechanism(s) may be active, including perhaps oxidation of soluble Po(II) to insoluble Po(IV).

Introduction

^{210}Po and ^{210}Pb are the final two long-lived daughters in the ^{238}U decay series. Since the source function of these two radionuclides is often known or easily measurable, they can serve as useful tracers of metal cycling in aquatic systems. Being radioactive ($t_{1/2}$ 138 days and 22 years), they can be used to determine removal rates as well as pathways. In a closed system at secular equilibrium, ^{210}Po is present at the same activity as ^{210}Pb. Differences from secular equilibrium, either positive or negative, reveal information about the behavior of the two radionuclides.

^{210}Pb has found special utility as a geochronometer of recent sedimentation. ^{210}Pb dating schemes all depend on the assumption that the radionuclide is immobile in sediments, and the many successes of ^{210}Pb dating are implicit evidence that this assumption is usually justified. Still, explicit tests of immobility are lacking.

We report here on a detailed study of the cycling of ^{210}Pb and ^{210}Po in the water column of a typical temperate lake. The purpose of this paper is twofold. First, we report the finding that ^{210}Pb is remobilized from sediments to the water column in significant amounts under reducing conditions. Release of lead from sediments raises the possibility of ^{210}Pb redistribution in sediments, and possible problems with ^{210}Pb dating in some lakes. Released lead also is more bioavailable and can be toxic to aquatic organisms.

Second, and just as importantly, we present biogeochemical data that helps to explain the radionuclides' behavior in terms of inputs and outputs, scavenging in the water column, redox conditions, transport processes, and the cycles of more abundant chemical components: transition metals, alkalinity, and sulfide. As such, this is one of few examples of a comprehensive study of trace-element behavior in lakes. The data help to elucidate trace-metal cycling in general. In this paper we focus on water column processes. Sedimentary data, and a discussion of the possible effect of ^{210}Pb remobilization on geochronology, will be published elsewhere (*1*).

Study Site and Methods

The study site is described in detail elsewhere (*2*) and is shown in Figure 1. The lake has an area of 60 ha, a maximum depth of 13 m, and a mean depth of 6 m. Bickford Reservoir has been the subject of detailed mass balance studies of major ion chemistry (*3*, *4*) and ^{210}Pb/^{210}Po (*2*).

Except as noted below, methods of sample collection, preparation, and analysis have been described previously (*2*). Water column samples were collected at approximately 20-day intervals from June through October 1985, though more frequent sampling was carried out whenever radionuclide levels changed rapidly, either as the result of anoxia or fast erosion of the metalimnion. Samples were collected from all levels in the water column, but the sampling interval spacing was longest in the mixed part of the water column, and shortest (≤10 cm) near the oxic–anoxic interface. Many of the samples were anoxic or suboxic, and special care was taken to filter these samples during collection, before exposure to the atmosphere.

Suspended particulate matter (SPM) was determined in duplicate, gravimetrically, by measuring material collected on preweighed 47 mm diameter 0.45-μm Millipore Durapore filters mounted in an in-line holder during collection. Throughout this paper the term "dissolved" refers to material that passes a 0.45-μm filter, including both colloids and material that is in true solution. Similarly, "particulate" means any material that is trapped on a 0.45-μm filter.

Settling particulate matter was collected in an all-plastic sediment trap. The inside of the trap was painted with antifouling paint to inhibit the growth of biota. The top of the trap was filled with 10-cm lengths of plastic drinking straws held under their own elastic forces in a space-filling honeycomb pattern, giving the sediment trap an effective aspect ratio greater than the recommended 5:1 (*5*). The lower end of the funnel was glued into a hole cut in the cap of a 100-mL Nalgene wide-mouth jar, which was harvested by scuba divers.

^{210}Po (and indirectly, ^{210}Pb) were measured by α spectrometry of silver planchets (*6*). The 1 standard deviation statistical counting error was always less than 10% for ^{210}Po, and less than 12% for ^{210}Pb. Duplicate samples had identical activities within the limits of the statistical error.

Sulfide was measured in the field by the methylene blue colorimetric method. Fe, Mn, and stable lead were measured by graphite furnace atomic absorption spectrophotometry. Alkalinity was determined by acidimetric titrimetry monitored on a pH meter to an end point characterized by a maximum in d(pH)/d(acid).

Results

Temperature and Dissolved Oxygen. The lake had stratified before the start of the study period in June 1985 (Figure 2) and remained stratified until fall overturn on about the 1st of November. During this period, the

* Present address: Dept. of Marine Sciences, Texas A&M University, 5007 Ave. U., Galveston, TX 77551.

 0013-936X/90/0924-1224$02.50/0

Table I. ^{210}Pb in the Water Column[a,b]

depth, m		June 14	July 4	July 24	Aug 14	Sept 4	Sept 11	Sept 19	Sept 26	Oct 9	Oct 12	Oct 19	Oct 24
1	diss	3.1	6.3	2.8	1.5			4.1[c]		6.1[d]			5.9[e]
	part	8.1	12.2	6.2	9.2			7.1[c]		8.2[e]			8.6[e]
11	diss			6.9[f]		5.6	7.8	5.7	14.2	10.3		14.2	
	part			12.5[f]		20.0	17.0	12.2	13.3	10.0		6.9	
12	diss	8.2	11.7	10.7	3.6	13.4	25.8	32.8	30.7	54.4	70.4	67.0[g]	5.9[h]
	part	8.1	11.8	20.1	22.7	20.7	20.6	30.2	33.0	30.4	35.2	53.1[g]	9.7[h]

[a] Units: dpm/100 kg. [b] Data from intermediate depths not listed. [c] 3 m. [d] 4 m. [e] 2 m. [f] 10 m. [g] 12.3 m. [h] 12.2 m.

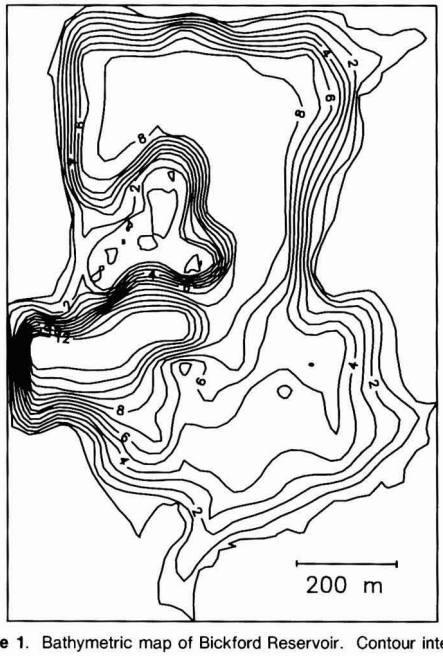

Figure 1. Bathymetric map of Bickford Reservoir. Contour interval is 1 m.

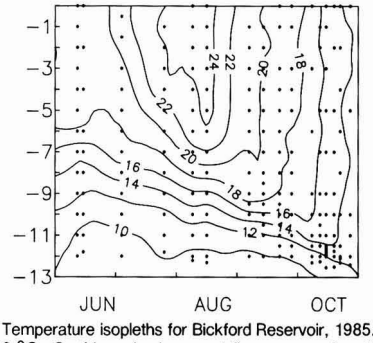

Figure 2. Temperature isopleths for Bickford Reservoir, 1985. Contour interval is 2 °C. On this and subsequent figures, sampling depths and dates are marked by dots.

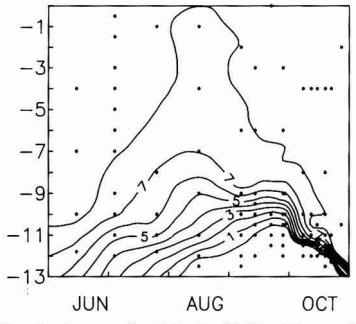

Figure 3. Dissolved oxygen isopleths for Bickford Reservoir. Contour interval is 1 mg of O_2/L.

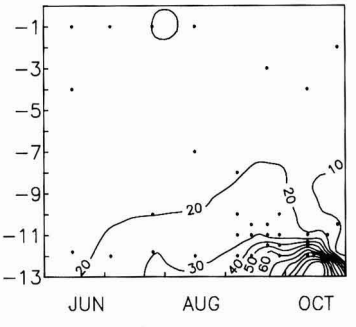

Figure 4. Isopleths of total ^{210}Pb. Contour interval is 10 dpm/100 kg.

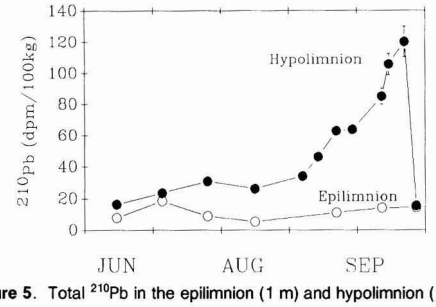

Figure 5. Total ^{210}Pb in the epilimnion (1 m) and hypolimnion (12 m).

thermocline deepened from 6 m to ~12 m. Anoxia started near the bottom in mid-August and continued until fall overturn, reaching progressively higher levels in the water column until attenuated by erosion of the metalimnion (Figure 3). Full anoxia was attained in 5 of the 6 years (1981–1986) that we have collected data at Bickford. In the other year (1983), oxygen decreased but never dropped below 1 mg/L, even at the sediment–water interface (2).

^{210}Pb. Dissolved and particulate ^{210}Pb data are summarized in Table I and total ^{210}Pb in Figure 4. In the upper water column, ^{210}Pb was low and relatively constant, with a little less than half passing a 0.45-μm filter. The samples above 10 m had an average ^{210}Pb concentration of 12.9 ± 3.1 dpm/100 kg; 32 ± 9% of that total was dissolved. This finding is in agreement with an earlier, year-long study at the same site (2).

The difference between total ^{210}Pb levels in surface and bottom waters is striking (Figure 5). In the epilimnion, ^{210}Pb remained nearly constant, while in the hypolimnion, it increased steadily and reached levels an order of magnitude higher than base-line values before fall overturn

Table II. ^{210}Po in the Water Column[a,b]

depth, m		June	July		Aug	Sept				Oct			
		14	4	24	14	4	11	19	26	9	12	19	24
1	diss	4.2	2.6	1.2	2.3			4.1[c]		5.4[d]			6.1[e]
	part	5.3	4.2	3.7	2.5			3.6[c]		4.1[d]			4.2[e]
11	diss			6.3[f]		14.9	15.5	20.6	26.9	6.5		4.4	
	part			8.6[f]		29.0	19.9	17.3	21.1	4.3		4.7	
12	diss	5.4	9.9	10.9	21.8	38.5	30.3	17.4	29.5	32.6	30.9	34.4[g]	4.3[h]
	part	6.6	6.6	20.6	29.7	52.9	70.6	83.8	77.0	57.1	61.2	64.6[g]	5.5[h]

[a] Units: dpm/100 kg. [b] Data from intermediate depths not listed. [c] 3 m. [d] 4 m. [e] 2 m. [f] 10 m. [g] 12.3 m. [h] 12.2 m.

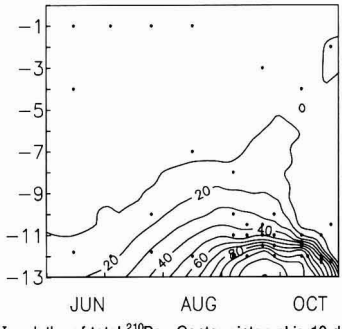

Figure 6. Isopleths of total ^{210}Po. Contour interval is 10 dpm/100 kg.

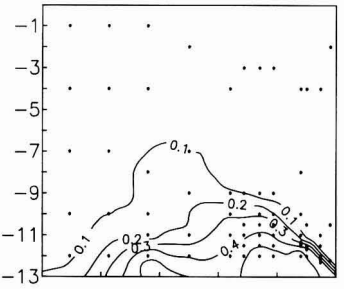

Figure 7. Total manganese isopleths. The contour interval is 0.1 mg of Mn/L. Manganese showed little tendency to reprecipitate in the water column, and $[Mn]_{dissolved}/[Mn]_{total}$ = 94.6%, averaged for all samples.

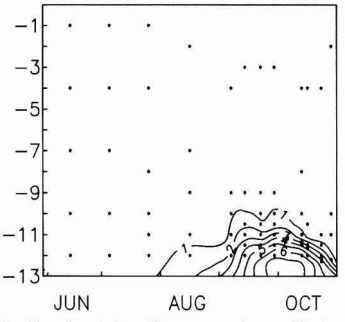

Figure 8. Total iron isopleths. The contour interval is 1 mg of Fe/L.

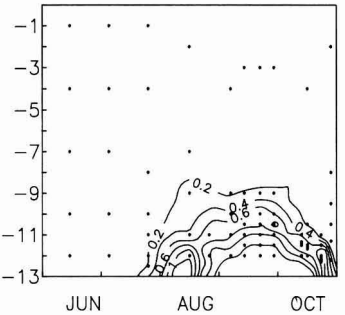

Figure 9. Isopleths of iron retained by 0.45-μm filters (particulate iron). The contour interval is 0.2 mg of Fe/L. Note that a maximum occurs at a distance from the sediment–water interface and at the same depth as the oxycline.

halted the rise. A single sample with elevated ^{210}Pb and ^{210}Po was reported in Bickford for October 1982, but no anomalous levels were recorded in 1983, a year when bottom water did not become oxygen depleted (*2*). The cooccurrence of high ^{210}Pb and anoxia, and the absence of elevated levels in 1983, support the interpretation that ^{210}Pb is released from sediments under the influence of reducing conditions. To our knowledge, these data are the first reported measurements of ^{210}Pb in anoxic freshwaters and show that substantial remobilization is possible under such conditions.

^{210}Po. For the most part, ^{210}Po followed the same pattern as ^{210}Pb, with low values in the epilimnion and levels increasing in the hypolimnion with time (Table II and Figure 6). In the epilimnion, ^{210}Po was slightly lower than ^{210}Pb (8.0 ± 2.2 dpm/100 kg), and it had a somewhat lesser tendency to be associated with particles (dissolved fraction 47 ± 10%) than did ^{210}Pb.

In the epilimnion, total ^{210}Po was never in excess of its progenitor, ^{210}Pb, but in bottom waters, ^{210}Po exceeded ^{210}Pb by as much as a factor of 3.8 from mid-August through early September. The magnitude of this excess is proof that the high water column activities of the radionuclides did not derive from sediment resuspension, which would mobilize nearly equal activities of ^{210}Pb and ^{210}Po. The excesses mean that ^{210}Po began to be released from the sediments earlier than was ^{210}Pb, consistent with ^{210}Po's lower scavenging rate in the epilimnion; in general, ^{210}Po seems to have a lower affinity for solids in this lake. The early release of ^{210}Po also has precedents in a number of studies that have documented ^{210}Po remobilization exceeding that of ^{210}Pb (*7–10*).

Iron and Manganese. Bickford Reservoir conforms to the pattern of iron and manganese distribution and fluxes seen in other lakes (e.g., refs 11–17). Within the sediments there is an oxic–anoxic interface above which iron and manganese are oxidized and largely in particulate form, and below which they are reduced and dissolved. In some lakes, including Bickford, this surface passes out of the sediments and into the water column during the summer (Figures 7–9). When this happens, a layer of reprecipitated particulate iron can occur (Figures 9 and 10; ref 13). In Bickford, the main differences between the two transition metals were as follows: (1) manganese levels rose earlier than iron and were elevated in bottom waters even in the presence of low levels of dissolved oxygen, and (2) manganese did not reprecipitate at the oxic–anoxic in-

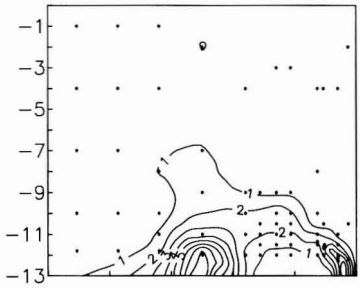

Figure 10. Isopleths of SPM. The contour interval is 1 mg/L. The pattern of SPM distribution is the same as that for particulate iron.

Table III. Hypolimnetic ^{210}Pb Sediment Trap Fluxes

time period	depth, m	^{210}Pb flux, dpm/cm^2·year	Fe flux, mg/cm^2·year
14 Aug–4 Sept[a]	8.3	1.21	
	11.2	1.24	
4 Sept–19 Sept[b]	9.1	0.64	
	11.2	0.90	
19 Sept–26 Sept[c]	9.1	0.52	
	11.2	1.80	
26 Sept–12 Oct[d]	9.1	0.82	0.9
	11.2	2.65	3.7

[a] Oxycline ascended from 12.3 to 10.8 m. [b] Oxycline ascended from 10.8 to 10.4 m. [c] Oxycline ascended from 10.4 to 10.2 m. [d] Oxycline descended from 10.2 to 11.3 m.

terface in the water column.

SPM samples collected from the concentration peak contained 27 ± 13% particulate iron, similar to the 30–40% iron content of particulate iron formed in Esthwaite water (*15*). Assuming that the precipitated ferric iron has the formula $Fe_2O_3 \cdot H_2O$, 43% of the SPM's mass can be accounted for by iron oxyhydroxide. The remainder of the mass probably includes (1) water of hydration, (2) organic matter (*15*), and (3) silicate detritus (watershed clays).

Elevated levels of total iron and manganese were limited to the zone of anoxic water (Figures 7 and 8), and it is tempting to attribute this restriction solely to a barrier to upward transport posed by rapid oxidation, reprecipitation, aggregation, and settling of transition metals at the oxycline. It is important to bear in mind that the observed distribution can also result from the large ratio of epilimnetic to metalimnetic volume. Concentrated bottom waters are substantially diluted when mixed upward into the epilimnion.

On the basis of sediment trap measurements, much of the iron in the hypolimnion was converted to particulate form and returned to the bottom. A sediment trap deployment from 26 September to 12 October 1985 at 9.1 m showed a reducible iron flux of 0.9 mg/cm^2·year while at 11.2 m it was 3.7 mg/cm^2·year, an increase of 2.7 mg/cm^2·year (Table III). This number is comparable to the decrease in the water column Fe inventory over the same depths and time, 5.5 mg/cm^2·year, indicating that a large fraction of the iron was lost as settling particles. There was a similar, but much less dramatic increase with depth in the amount of iron trapped in Esthwaite Water, U.K. (*14*).

Like iron, elevated manganese levels were limited to the metalimnion of Bickford. This was definitely not due to reprecipitation on encountering oxygenated water, since no particulate manganese maximum was observed. Rather, manganese that was transported to the base of the epilimnion was rapidly mixed through the much larger volume of that layer and was quickly diluted.

pH and Alkalinity. Bickford's epilimnion was characterized by alkalinities of a few microequivalents per liter and pH's near 5.7. With depth, pH increased toward neutrality and alkalinities increased to hundreds of microequivalents per liter, due to oxidation of organic matter at the sediment–water interface. From these data it is clear that the release of metals from the sediments was definitely not related to acidification, since Fe, Mn, ^{210}Pb, and ^{210}Po maxima were associated with high alkalinities and pH's. Similarly, White and Driscoll (*18*) documented increases of stable lead in bottom waters of Dart Lake, NY.

Sulfide. In 1985 and 1986, sulfide was generally absent from the water column except in the early fall near the sediment–water interface, where levels rose to a few tenths of a milligram per liter. In Bickford, FeS saturation did not limit iron solubility, as has been observed elsewhere (*19*).

Discussion

The Epilimnion. Time series ^{210}Po and ^{210}Pb data were collected from the water column, streams, and sediment traps at Bickford Reservoir. These were then combined in an epilimnetic mass balance model to yield information on the relative importance of various inputs and outputs and on the rate of uptake and/or release of dissolved radionuclides by solids. The model used was a refinement of the one presented in ref 2. The improvements were as follows: (1) sedimentary fluxes were measured directly by using sediment traps, (2) atmospheric deposition intervals were synchronized with those of water column and stream monitoring, (3) changes in the depth of the thermocline and the volume of the epilimnion were incorporated into the model, and (4) inputs into the epilimnion due to mixing across the thermocline were explicitly considered. Another important difference is that, in the present study, data were collected intensively, but for a shorter time period (June through October). Consequently, the results should not be taken as typical of the full year, but rather may reflect special conditions occuring during the summer.

The mass balance reveals many facts not evident from direct examination of the data. Inputs to the epilimnion from cross-thermocline mixing were low (Table IV). Early in the study period, weak vertical eddy diffusion suppressed this flux despite high levels of radionuclides present in the hypolimnion. Later, erosion of the thermocline hastened transfer of radionuclides upward. Still the contribution of this flux to the epilimnetic mass balance remained small, since the area of the deep part of the lake is equivalent to just a few percent of the lake's surface area. On the other hand, on a per area basis, thermocline erosion was the largest input to the epilimnion in early fall.

Sorption, the rate of conversion of dissolved radionuclides to particulate form, averaged 0.92 ± 0.42 dpm/cm^2·year for ^{210}Pb with a range from 0.32 to 1.55 dpm/cm^2·year, and it was correlated with input by direct precipitation (regression significant at the 98% confidence level). That concentration remains fairly constant, and that sorption correlates with input, suggests that removal may be approximately proportional to ^{210}Pb concentration (*20*, *21*).

The average of calculated ^{210}Pb particle fluxes (Table V) was 1.08 ± 0.42 dpm/cm^2·year with a range from 0.45 to 1.64 dpm/cm^2·year. This average is not significantly different from the average measured sediment trap flux of 0.84 ± 0.23 dpm/cm^2·year or the average scavenging rate described above. The agreement of the calculated sedimentation with the average sediment trap data indicates

Table IV. Mass Balance of Dissolved ^{210}Pb in the epilimnion[a]

	rain	+	inflow	+	thermocline	−	outflow	−	change in storage	=	sorption
14 June											
	0.93 (±0.07)		0.063 (±0.013)		0.000 (±0.000)		0.050 (±0.004)		0.14 (±0.06)		0.80 (±0.09)
4 July											
	0.46 (±0.04)		0.020 (±0.006)		0.000 (±0.000)		0.005 (±0.001)		−0.32 (±0.06)		0.79 (±0.07)
24 July											
	1.30 (±0.10)		0.012 (±0.004)		0.000 (±0.000)		0.001 (±0.000)		−0.06 (±0.03)		1.38 (±0.10)
14 Aug											
	2.00 (±0.08)		0.055 (±0.013)		0.000 (±0.000)		0.038 (±0.003)		0.46 (±0.05)		1.55 (±0.10)
4 Sept											
	0.54 (±0.03)		0.029 (±0.009)		0.000 (±0.000)		0.008 (±0.001)		−0.38 (±0.09)		0.94 (±0.10)
19 Sept											
	0.71 (±0.03)		0.124 (±0.024)		0.000 (±0.000)		0.106 (±0.007)		0.41 (±0.05)		0.32 (±0.06)
9 Oct											
	0.27 (±0.07)		0.041 (±0.010)		0.034 (±0.007)		0.018 (±0.001)		−0.36 (±0.06)		0.69 (±0.10)
24 Oct											

[a] Units: dpm/cm^2·year.

Table V. Mass Balance of Particulate ^{210}Pb in the Epilimnion[a]

	inflow	+	scavenging	+	thermocline	−	change in stor	−	outflow	=	sedimentation: calc	−	sedimentation: meas[b]	=	diff
14 June															
	0.03 (±0.03)		0.80 (±0.09)		0.000 (±0.000)		0.28 (±0.10)		0.097 (±0.007)		0.45 (±0.14)		0.59 (±0.16)		−0.13[c] (±0.21)
4 July															
	0.008 (±0.007)		0.79 (±0.07)		0.000 (±0.000)		−0.54 (±0.10)		0.012 (±0.001)		1.33 (±0.13)		0.61 (±0.16)		0.72 (±0.21)
24 July															
	0.004 (±0.003)		1.38 (±0.10)		0.000 (±0.000)		0.23 (±0.06)		0.006 (±0.000)		1.15 (±0.12)		0.98 (±0.26)		0.17[c] (±0.29)
14 Aug															
	0.02 (±0.02)		1.55 (±0.10)		0.000 (±0.000)		0.34 (±0.10)		0.067 (±0.004)		1.17 (±0.14)		1.24 (±0.33)		−0.07[c] (±0.36)
4 Sept															
	0.012 (±0.009)		0.94 (±0.09)		0.000 (±0.000)		−0.70 (±0.16)		0.014 (±0.001)		1.64 (±0.18)		0.76 (±0.20)		0.88 (±0.27)
19 Sept															
	0.06 (±0.06)		0.32 (±0.06)		0.000 (±0.000)		0.20 (±0.09)		0.119 (±0.009)		(1.07)[d] (±0.43)		0.76 (±0.20)		0.31[c] (±0.48)
9 Oct															
	0.018 (±0.015)		0.69 (±0.10)		0.017 (±0.003)		−0.04 (±0.10)		0.028 (±0.002)		0.74 (±0.14)		0.95 (±0.26)		−0.21[c] (±0.29)
24 Oct															

[a] Units: dpm/cm^2·year. [b] Measured sediment trap flux for comparison with calculated value in previous column. [c] Differences are not statistically significant. [d] The calculated result was not statistically significant. The number is parentheses is the average of the remaining six calculated values.

the reliability of the latter measurements. Particulate ^{210}Po data (Table VI) support the same conclusion.

The equality between scavenging and settling fluxes (Table V) means that, on average, all scavenged ^{210}Pb leaves the water column by means of particle settling. That in turn means that direct uptake by sediments plays only a small role in the epilimnion of Bickford Reservoir. Removal rate constants calculated according to ref 22 support this conclusion. Assuming a particle settling rate of 20 cm/day (*23*) and a diffusive boundary layer thickness of 1000 μm, less than 10% of removal would be expected to occur via direct uptake by bottom sediments.

The behavior of ^{210}Po (Tables VI and VII) differs from that of ^{210}Pb because of its different means of introduction and its different chemical behavior once in the lake. The average dissolved ^{210}Po scavenging rate was 23% of ^{210}Pb scavenging despite their nearly equal water column concentrations ($[^{210}Po]/[^{210}Pb] = 0.96 \pm 0.43$). This difference reflects fundamentally different cycling of the two elements, with Po either having a lower tendency to be scavenged or a greater tendency to be regenerated. Talbot and Andren (*9*) concluded that the lower scavenging flux for ^{210}Po compared to ^{210}Pb in Crystal Lake, WI, reflected a greater degree of Po recycling. This judgment seems to have been based on previous studies of Po and Pb geochemistry in the marine environment, where ^{210}Po has a lower residence time in surface water than does ^{210}Pb, but is regenerated at middepths, producing excesses relative to ^{210}Pb in the thermocline (*7*). The simplest interpretation of both our data and that of Talbot and Andren is that ^{210}Pb is scavenged more rapidly than ^{210}Po, without any water column recycling of ^{210}Po in shallow lakes. Scavenging of ^{210}Pb averaged 2.7 times that of ^{210}Po in Crystal Lake and 4.4 times in Bickford. The ratio of ^{210}Pb to ^{210}Po in settling sediments was 3.2:1 in Bickford and 2.4:1 in Crystal Lake (*24*). There were no consistent occurrences

Table VI. Mass Balance of Particulate ^{210}Po in the Epilimnion[a]

	inflow	+ scavenging	+ support	+ thermocline	− outflow	− decay	− change in stor	= sedimentation calc	− meas[b]	= diff
14 June	0.024 (±0.021)	0.20 (±0.04)	0.092 (±0.010)	0.000 (±0.000)	0.033 (±0.003)	0.028 (±0.004)	−0.04 (±0.06)	0.30 (±0.07)	0.31 (±0.08)	−0.013 (±0.11)
4 July	0.007 (±0.005)	0.20 (±0.03)	0.083 (±0.010)	0.000 (±0.000)	0.007 (±0.001)	0.017 (±0.003)	−0.04 (±0.05)	0.30 (±0.06)	0.33 (±0.09)	−0.023 (±0.11)
24 July	0.004 (±0.002)	0.21 (±0.06)	0.070 (±0.006)	0.000 (±0.000)	0.002 (±0.000)	0.021 (±0.003)	−0.07 (±0.03)	0.33 (±0.07)	0.47 (±0.13)	−0.14[c] (±0.14)
14 Aug	0.020 (±0.016)	0.21 (±0.06)	0.104 (±0.011)	0.000 (±0.000)	0.032 (±0.003)	0.043 (±0.006)	0.28 (±0.07)	0.34 (±0.08)	1.1 (±0.3)	−0.8 (±0.3)
4 Sept	0.010 (±0.007)	0.22 (±0.09)	0.098 (±0.012)	0.000 (±0.000)	0.007 (±0.001)	0.048 (±0.006)	−0.32 (±0.09)	0.59 (±0.13)	0.29 (±0.08)	0.29[c] (±0.15)
19 Sept	0.050 (±0.046)	0.21 (±0.06)	0.082 (±0.009)	0.016 (±0.003)	0.055 (±0.004)	0.052 (±0.006)	0.06 (±0.04)	0.19 (±0.09)	0.27 (±0.07)	−0.08[c] (±0.12)
9 Oct	0.015 (±0.013)	0.22 (±0.08)	0.092 (±0.007)	0.046 (±0.009)	0.016 (±0.001)	0.056 (±0.006)	0.12 (±0.07)	0.34 (±0.08)	0.47 (±0.13)	−0.13[c] (±0.15)
24 Oct										

[a] Units: dpm/cm^2-year. [b] Measured sediment trap flux for comparison with calculated value in previous column. [c] Differences are not statistically significant.

of excess ^{210}Po in either lake except that resulting from releases from the bottom. On the basis of this evidence, shallow lakes seem to differ from the ocean in that (1) ^{210}Pb is preferentially scavenged compared to ^{210}Po by particulate matter in surface waters and (2) ^{210}Po is not regenerated in the water column. In the ocean, ^{210}Po is believed to be actively taken up by phytoplankton, which are eaten by zooplankton, who package the ^{210}Po into rapidly settling (and recycled) fecal pellets. The same mechanism may not dominate in oligotrophic lakes, perhaps because of the greater abundance of nonbiogenic detritus, which can also scavenge the radionuclide. Alternatively, DOC, which is higher in lakes than oceans, is likely to complex quadrivalent Po more effectively than divalent Pb, thereby reducing the efficiency of ^{210}Po scavenging.

The Hypolimnion. ^{210}Pb Distribution and Fluxes. In our data, the most unexpected result is the occurrence of high levels of ^{210}Pb in stratified bottom waters from late summer through early fall. Four pieces of evidence prove that the increase was not caused by resuspension of bottom sediments: (1) ^{210}Po activity exceeded ^{210}Pb through much of this period, (2) SPM levels did not increase in a pattern similar to ^{210}Pb, (3) specific activities of ^{210}Pb were much higher in SPM than in bottom sediments, and (4) much of the increase was in the dissolved form.

Instead, we believe that ^{210}Pb was released from bottom sediments under the influence of reducing conditions caused by anoxia. ^{210}Pb levels were always elevated in anoxic waters (Figures 3 and 9), and they were never high when oxygen was detectable. Elevated ^{210}Pb was observed in 1982 (*2*), 1985, and 1986 when bottom waters went anoxic, but not in 1983 (*2*), when bottom waters contained measurable oxygen all year. If ^{210}Pb were released because of some process accompanying oxygen consumption, e.g., release from oxidized organic matter or production of DOC, then ^{210}Pb levels would have been high in stratified bottom waters containing oxygen.

Under ambient environmental conditions, anoxia does not cause a change in the oxidation state of lead, so ^{210}Pb mobilization must be caused by reduction of some other sedimentary component, presumably the transition metal iron or manganese. This hypothesis is supported by the good correlation between ^{210}Pb and total iron (cf. Figures 4 and 8), and also by the high affinity of iron-rich particulate matter for ^{210}Pb. Figure 11 shows ^{210}Pb partitioning as a function of SPM concentration in the particulate iron maximum near the oxic–anoxic interface. The data lie along a straight line, indicating that ^{210}Pb uptake can be described in terms of a linear partitioning parameter, K_D. The slope of the regression line gives the numerical value of the coefficient as $K_D = 6.3 \times 10^5$ relative to total SPM, or 1.4×10^6 expressed per mass of iron. The high K_D demonstrates that ^{210}Pb has a strong tendency to be associated with iron oxyhydroxides. Adsorbed ^{210}Pb could thus be released from sedimentary iron oxides that are reduced and solubilized by anoxia.

Additional data show that ^{210}Pb indeed comes from the bottom and not from particles settling through the hypolimnion. Sediment trap flux measurements (Table III) combined with sequential leaching experiments (*1*) show that less than half of the documented buildup could have been supplied by remobilization from particles arriving at the top of the stratified zone. More importantly, the particulate ^{210}Pb flux increases with depth in the hypolimnion (Table III), meaning that particles are gaining, not losing, ^{210}Pb as they sink.

Iron oxide particles that form in the oxycline and settle downward carry ^{210}Pb with them, judging from enhanced

Table VII. Mass Balance of Dissolved ^{210}Po in the Epilimnion[a]

	rain	+	inflow	+	support	+	thermocline	−	outflow	−	decay	−	change in stor	=	sorption
14 June															
	0.037 (±0.003)		0.073 (±0.018)		0.048 (±0.006)		0.000 (±0.000)		0.021 (±0.002)		0.028 (±0.004)		−0.09 (±0.04)		0.20 (±0.04)
4 July															
	0.018 (±0.001)		0.025 (±0.005)		0.041 (±0.006)		0.000 (±0.000)		0.002 (±0.000)		0.017 (±0.003)		−0.13 (±0.03)		0.20 (±0.03)
24 July															
	0.052 (±0.004)		0.015 (±0.002)		0.023 (±0.003)		0.000 (±0.000)		0.002 (±0.000)		0.021 (±0.003)		0.19 (±0.03)		(0.21)[b] ±0.06
14 Aug															
	0.080 (±0.003)		0.066 (±0.014)		0.045 (±0.006)		0.000 (±0.000)		0.029 (±0.003)		0.043 (±0.006)		0.19 (±0.05)		(0.21)[b] (±0.06)
4 Sept															
	0.021 (±0.001)		0.036 (±0.006)		0.056 (±0.007)		0.000 (±0.000)		0.008 (±0.001)		0.048 (±0.006)		−0.16 (±0.09)		0.22 (±0.09)
19 Sept															
	0.028 (±0.001)		0.142 (±0.040)		0.062 (±0.005)		0.008 (±0.002)		0.078 (±0.006)		0.052 (±0.006)		0.19 (±0.06)		(0.21)[b] (±0.06)
9 Oct															
	0.011 (±0.003)		0.049 (±0.011)		0.070 (±0.005)		0.023 (±0.005)		0.016 (±0.001)		0.056 (±0.006)		−0.14 (±0.08)		0.22 (±0.08)
24 Oct															

[a] Units: dpm/cm^2·year. [b] Calculated result was not statistically significant. Number in parentheses is the average of the four significant values.

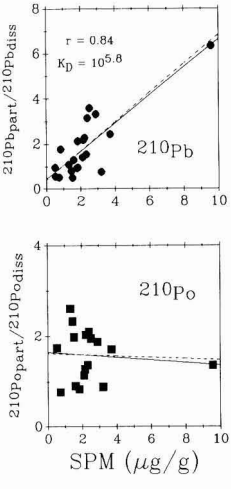

Figure 11. Partitioning of ^{210}Pb and ^{210}Po between particles and solution as a function of SPM concentration. Both particulate and dissolved concentrations are expressed per mass of water, so that the ordinate is dimensionless. The slope of the regression line is equal to K_D. The solid lines are for linear regressions including all the data, and the dashed lines are for regressions excluding the datum for SPM equal to 9.5. Clearly, the single high values do not skew the regression lines. For the ^{210}Pb regression witout the high SPM datum, the linear correlation coefficient is 0.58, which is significant above the 99% level.

accumulation of ^{210}Pb in sediment traps located below the oxycline (Table III). For the period from 14 August to 4 September, both sediment traps were located above the top of the anoxic zone and showed the same flux. During the next two intervals, the oxycline ascended above the lower sediment trap, and there was a significant increase in flux between the two. During the final deployment, thermocline erosion began to cause a deepening of the oxycline, and this process caused the largest measured difference between the ^{210}Pb fluxes above and below the zero oxygen surface. These measurements suggest that the ascending oxycline constitutes a zone where iron oxidizes, precipitates, sorbs ^{210}Pb, aggregates, and settles to the bottom. When the oxycline begins to be eroded downward, this cycle is accelerated by the added supply of metals available in the zone swept out during the descent. The existence of this region of enhanced ^{210}Pb scavenging serves as a barrier at the top of the zone of anoxia and high ^{210}Pb levels and may help to prevent much of the ^{210}Pb released by sediments from escaping into the mixed upper part of the lake.

For some of the samples, low levels of sulfide were detected. The presence of even traces of sulfide raises the possibility that ^{210}Pb may precipitate in the water column because of the extreme insolubility of galena (PbS). Dissolved lead was measured as <5 nM in the Bickford water column, matching world average river water (*25*). Detectable sulfide levels ranged from 0.1 to 0.5 aM (10^{-18} M), based on K_{a2} from ref 26 and our measurements of [H_2S] and pH. The ion product is less than $10^{-26.6}$, exceeding the limit of PbS saturation ($K_{sp} = 10^{-27.5}$, ref 27). Also, the saturation K_{sp} for PbS may, in fact, be lower than $10^{-27.5}$ in view of the recent revision of K_{a2} for H_2S.

Despite possible supersaturation, about half of the ^{210}Pb passed a 0.45-μm filter even for those depth increments with measurable sulfide (Table I). There are several possible explanations for this ostensible lack of PbS precipitation under apparently supersaturated conditions: (1) PbS did, in fact, precipitate, but the particles were small enough to pass through 0.45-μm filters, (2) lead in the water column was bound to colloids or complexed by ligands that outcompete S^{2-}, (3) freshly precipitated PbS may have a higher K_{sp} value than does the well-crystallized mineral [as is the case for FeS (*19*)], or (4) precipitation may be kinetically hindered in some manner (e.g., by slow ligand exchange). Any of the above explanations would mean that ^{210}Pb is not rapidly removed from the water column by particle aggregation and settling; thus, ^{210}Pb would continue to be transported by eddy diffusion as if still dissolved.

Remobilization of ^{210}Pb from sediments (presumably accompanied by release of stable lead) can have significant environmental ramifications. ^{210}Pb dating is of great importance to paleolimnologists and geochemists, and ^{210}Pb mobility raises the possibility of sediment dating errors. Also, sediments are the repository for large quantities of industrial lead discharged to the environment during the past 100 years. Releases to the water column could bring about bioavailability and potential toxicity to aquatic organisms. Because of these possibilities it is crucial to

understand the source, reactions, transport pathways, and fate of the released lead.

In an effort to quantify some of these variables, we attempted to simulate ^{210}Pb distributions using a model similar to the one presented in ref 28. One important difference is that vertical eddy diffusivities were determined by the thermal flux gradient method (*29*). These calculations showed that, during the summer of 1985, vertical turbulent mixing was not an important pathway for transport of ^{210}Pb away from the sediment–water interface to higher levels in the water column.

^{210}Pb not supplied by either remobilization from settling particles or by vertical eddy diffusive transport from sediments could be supplied from sediments via horizontal turbulent diffusion. The importance of horizontal transport was first recognized by Hutchinson (*30*) and has since been confirmed in other lakes (*31*, *28*, *32*). Imboden and Emerson (*31*) measured both vertical and horizontal eddy diffusion coefficients in Greifensee, Switzerland, and found that their ratio ranged from 600 to 6000, with vertical coefficients similar to those measured for Bickford (*29*). If K_x/K_z is similar in Bickford and Greifensee, then horizontal transport is likely to be important to radionuclide distributions.

To test this hypothesis, a simple model was developed based on the following assumptions: (1) a constant rate of ^{210}Pb release from sediments exposed to anoxic bottom water, (2) no release from other sediments, (3) rapid horizontal mixing, (4) no removal of ^{210}Pb from the water column, and (5) no vertical transport. With these assumptions, the increase of ^{210}Pb in the water column can be calculated from the horizontal ^{210}Pb flux:

$$d[^{210}Pb]_z = \frac{F_h A_z \, dt}{V_z} \quad (1)$$

where $d[^{210}Pb]_z$ is the increase in ^{210}Pb concentration over base-line values at depth z (dpm $^{210}Pb/cm^3$), F_h is the horizontal flux of ^{210}Pb per area of sediment (dpm $^{210}Pb/cm^2$·year), A_z is the area of sediment in contact with a layer of the lake centered at depth z (cm^2), dt is the time that water at depth z has been anoxic (year), and V_z is the volume of water in a layer of the lake centered at depth z (cm^3).

According to this model, ^{210}Pb begins to be released from sediments as soon as overlying water becomes anoxic, and the ^{210}Pb then mixes rapidly throughout a thin horizontal layer of the lake water column. ^{210}Pb levels are augmented by increased time of exposure to anoxic bottom water and total sediment surface area and are suppressed by dilution in lake strata with large volumes. Equation 1 can be rearranged to give

$$F_h = \frac{d[^{210}Pb]_z}{dt} \frac{1}{A_z/V_z} \quad (2)$$

Figure 12a is a plot based on eq 2, with the numerator of the right-hand side plotted as a function of the denominator. The abscissa in Figure 12a is a type of time axis, with the data normalized by dilution and flux factors characteristic of each depth layer. This plot allows data from different dates and sampling depths to be compared. The straight-line fit of the data (through the end of September) suggests that this simple model can explain virtually all of the variation in water column ^{210}Pb. The slope of the regression line, 0.7 dpm/cm^2·year, is the constant rate of ^{210}Pb release under reducing conditions and is about equal to the average total input on particles.

Since there seems to be a link between iron and ^{210}Pb releases, it is interesting to apply the constant release–horizontal mixing model to iron (Figure 12b). Two important differences should be noted between parts a and b of Figure 12: (1) the slope of the iron line is steeper than the one for ^{210}Pb compared to average input rates on settling particles, and (2) the iron data fail to fit the model throughout the entire anoxic period, drifting to the right of the line late in the season. The slope of the iron regression line is 10.2 mg/cm^2·year, an order of magnitude greater than the delivery of iron to the sediment water interface by settling particles. This rules out SPM as a major source for the elevated iron levels. The high rate of Fe release from sediments also means that an entire year's input of reducible iron can be remobilized during a 1-mo period of anoxia in the summer. Release of iron from sediments, horizontal transport, precipitation, and settling constitute a kind of sediment focusing that has not been recognized previously (*33*).

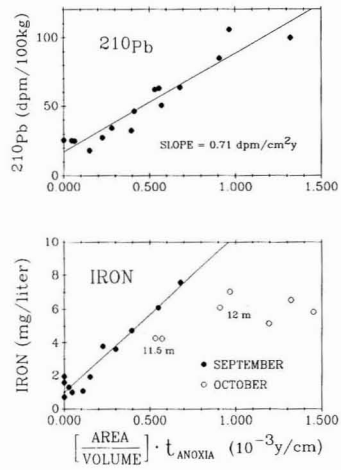

Figure 12. Constant-flux, horizontal-mixing models for (a) ^{210}Pb and (b) iron. The abscissa is the time since the start of anoxia at the depth of each sample normalized by the ratio of sediment area to water column volume at that depth. For ^{210}Pb, the data lie along a straight line, meaning that the rate of release from sediments was constant at all depths during anoxia. The same is true for iron through the beginning of October. Thereafter, data from a given depth lie approximately along a horizontal line, indicating that iron release ceased.

In October, iron data fall to the right of the line, implying an iron deficiency that could result either from a competing removal process or from a slowing or cessation of the rate of iron release by sediments. Neither oxides, sulfides, carbonates, hydroxides, nor phosphates of iron should precipitate under the prevailing water chemistry. Also, since there is not an equivalent effect for ^{210}Pb (Figure 12a), and since there is a high affinity of ^{210}Pb for iron solids (Figure 11), it seems probable that the lower iron in the October samples reflects a decrease in the iron supply rate rather than a removal process. The data therefore suggest that, beginning about 1 October, iron release ended at all depths, signaling an exhaustion of easily reducible metal in near-surface sediments.

The cessation of iron release contrasts sharply with steady ^{210}Pb efflux throughout the anoxic period (Figure 12a,b). The difference means that ^{210}Pb remobilization does not occur solely via liberation from solubilized iron oxyhydroxides, otherwise ^{210}Pb levels would be expected to stabilize at the same time as iron. Instead, an enrichment of oxidized iron in surficial sediments may pose a barrier by adsorbing lead. When anoxia in the overlying water column eliminates this obstacle, ^{210}Pb is free to diffuse from sediment pore waters. This hypothesis is

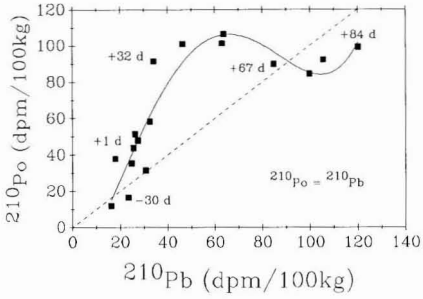

Figure 13. Total ^{210}Po vs total ^{210}Pb in the hypolimnion. Numbers next to symbols refer to the time since the start of anoxia at the depth that the sample was taken. The straight dashed line represents equal activities of the two radionuclides. The solid curved line is a fourth-order regression of the data and shows the trend in the data over time. Shortly before and during the early stages of anoxia, ^{210}Po was released more rapidly than ^{210}Pb, and this trend switched after ~40 days. (Note that for simplicity, many of the data from well before the time of anoxia have been excluded from this graph; these would all plot in the lower left corner of the figure.)

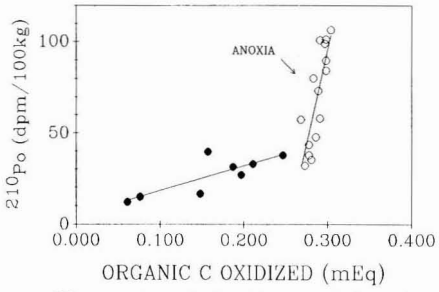

Figure 14. ^{210}Po vs carbon oxidation. The amount of organic carbon oxidized was calculated from the sum of oxygen depletion plus reduced Mn and Fe production, each weighted according to the stoichiometry of the appropriate reaction. The vertical dotted line represents the threshold value of carbon oxidation that depleted all the dissolved oxygen present in the water column. Data to the right of this line correspond to oxygen-depleted samples.

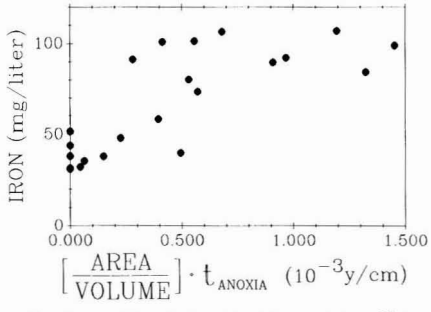

Figure 15. Constant-flux, horizontal-mixing model for ^{210}Po.

consistent with data on sediment solids and pore waters at this site (*1*).

^{210}Po Distribution and Fluxes. The overall pattern of ^{210}Po distribution in the stratified water column is similar to that of ^{210}Pb, but with certain important differences. Like ^{210}Pb, ^{210}Po increases rapidly in the hypolimnion, eventually reaching levels about an order of magnitude higher than in the epilimnion. However, ^{210}Po begins to be released earlier and seems to bear a different relationsip to iron release than does ^{210}Pb.

Remobilization of ^{210}Po into partially oxygen depleted waters has been documented already in a number of studies for both marine and lacustrine environments (*7–10, 34*). In this regard, the results from Bickford up until the time of anoxia follow a well-established pattern; ^{210}Po release without ^{210}Pb, leading to unsupported ^{210}Po. Only under anoxic conditions does ^{210}Pb begin to increase and eventually exceed ^{210}Po (Figure 13). It is clear from this graph that well before anoxia, ^{210}Pb exceeded ^{210}Po. A few weeks before the onset of anoxia, and for several weeks afterward, ^{210}Po increased at a much greater rate than ^{210}Pb and quickly exceeded secular equilibrium. Eventually the situation was reversed—with ^{210}Pb release exceeding that of ^{210}Po—and the data points approach the equilibrium line and pass below it.

Unlike ^{210}Pb, ^{210}Po partitioning does not show a linear dependence on particulate iron concentration (Figure 11). This apparent lack of ^{210}Po adsorption by iron oxyhydroxides, and the documented remobilization of ^{210}Po before iron, suggest that the polonium cycle is not as closely linked to that of iron as is lead.

The early onset of ^{210}Po release and the known association of ^{210}Po and organic matter (*7–9*) raise the possibility that polonium is released, not from transition-metal oxides, but from remineralized organic matter. To test this hypothesis, ^{210}Po was plotted as a function of the amount of organic carbon oxidized (Figure 14). ^{210}Po does increase with organic matter mineralization, but the release rate increases dramatically as soon as the water column becomes anoxic. The sharp inflection implies that ^{210}Po release is related to organic matter oxidation only indirectly. ^{210}Po is associated mainly with some other phase, such as transition metals, whose rate of solubilization would increase with anoxia.

The difference in timing between the release of ^{210}Po and ^{210}Pb still needs explanation, and it is tempting to draw a parallel with the differential behavior of Mn and Fe; manganese is reduced more easily and released somewhat earlier. Unfortunately, it is difficult to distinguish between the influence of these two metals since total ^{210}Po shows a good correlation with either manganese or iron, partly because Fe and Mn correlate with each other to some extent.

An attempt to explain the distribution of ^{210}Po by the constant flux–horizontal mixing model was not successful. Figure 15 shows that ^{210}Po reaced high levels before the onset of anoxia and did not conform to a straight-line relationship like ^{210}Pb (Figure 12a) or Fe (Figure 12b). The failure of the horizontal model to describe ^{210}Po release means that one or more of its assumptions are invalid for this radionuclide. Clearly the assumption of nonrelease from sediments overlain by oxic water is invalid, since ^{210}Po builds up to nearly half its maximum value before complete oxygen depletion. The other assumption that may be violated is that of no removal from the water column.

The different partitioning of ^{210}Po and ^{210}Pb between dissolved and particulate fractions poses an apparent paradox; ^{210}Po is released from settled sediments more readily than ^{210}Pb, but is scavenged more effectively by sediment suspended in the lower water column. In the month from 11 September to 12 October 1985 at a depth of 12 m, 57 ± 8% of the ^{210}Pb but only 29 ± 7% of the ^{210}Po passed a 0.45-μm filter.

One possibility is that polonium occurs in two different oxidation states. In this scenario, ^{210}Po is directly reduced and remobilized, like iron and manganese. Once in the water column it oxidizes and reprecipitates. Polonium occurs in the tetravalent state under oxygenated conditions (*35, 37*), but it can also have valences of −2, +2, and +6. Tetravalent polonium hydroxide is insoluble, so if reduc-

tion of Po(IV) to Po(II) occurs near the same pE as that of the Mn(II)/Mn(IV) couple, and if bivalent polonium is more soluble than tetravalent, then a mechanism could exist for precipitation–remobilization. The redox potential for these two couples is (*37*)

$$MnO_2 + 4H^+ + 2e^- = Mn^{2+} + 2H_2O$$

$$E_h = -0.42 \text{ V} \quad (\text{pH } 7)$$

$$PoO_2 + 4H^+ + 2e^- = Po^{2+} + 2H_2O$$

$$E_h = -0.56 \text{ V} \quad (\text{pH } 7)$$

This analysis does not consider the possible role of speciation of the various oxidation states, and values for the redox potential and hydrolysis constant of Po are only approximate. Still it seems possible that reduction of PoO_2 occurs close to that of MnO_2, thus potentially explaining polonium's behavior in the hypolimnion of Bickford reservoir.

Conclusions

(1) Mass balance calculations showed that direct uptake of ^{210}Pb and ^{210}Po by sediments is negligible compared to removal on settling particles. Transport across the thermocline by eddy diffusion is negligible, but thermocline erosion greatly accelerates this flux so that it becomes dominant on a per area basis.

(2) ^{210}Pb is removed by particles more than 4 times faster than is ^{210}Po. In this way, cycling of these radionuclides in lakes differs from their cycling in the ocean, where Po scavenging is more rapid. The difference may reflect the higher levels of humates and of nonbiogenic detritus in lakes.

(3) Iron increases in the hypolimnion only when oxygen becomes immeasurably low. A peak in SPM and particulate iron forms at the oxycline due to oxidation and precipitation of iron, and most of SPM's mass is attributable to iron oxyhydroxides.

(4) The buildup of iron in the hypolimnion results from reduction in sediments and horizontal transport within the water column. Release from settling particles and vertical mixing fluxes were negligible during the study period. Iron release from sediments ends after 30 days due to depletion of reducible metal. The amount of iron released is equivalent to a year's input on particulate matter; however, most of the released iron is eventually returned to the sediments. The main effect of iron cycling is to chemically focus the metal from shallower to deeper sediments.

(5) ^{210}Pb cycling is closely linked with that of iron. ^{210}Pb is released to the anoxic water column, transported horizontally, and removed along with precipitating Fe at the oxycline. Unlike Fe, ^{210}Pb release continues throughout the entire period of bottom water anoxia, perhaps because it is supplied by diffusion from deeper within sediments.

(6) ^{210}Po is released into suboxic waters resulting in unsupported ^{210}Po. This proves that radionuclide increases are not caused by resuspension, which would yield a ^{210}Po/^{210}Pb ratio near 1.0.

(7) ^{210}Po cycling parallels that of Mn in that both are released in substantial amounts to bottom water that still contains oxygen. Mn also differs from either Fe or ^{210}Pb in that its cycling is not explained by a simple square-wave release function combined with rapid horizontal mixing. It is difficult to establish with certainty the possibility that ^{210}Po correlates with Mn rather than Fe because both of the transition metals correlate with each other to some extent. Po release does not seem to be controlled closely by the amount of organic carbon remineralized by the oxidants O_2, Mn^{4+}, and Fe^{3+}. It is possible that anomalous behavior of Po can be explained by direct reduction of insoluble PoO_2 to soluble Po^{2+} in sediments and subsequent reoxidation or scavenging in the water column.

Acknowledgments

The paper benefited from evaluations by Peter Santschi and three anonymous reviewers.

Registry No. ^{210}Po, 13981-52-7; ^{210}Pb, 14255-04-0; Fe, 7439-89-6; Mn, 7439-96-5.

Literature Cited

(1) Benoit, G.; Hemond, H. F., submitted for publication in *Geochim. Cosmochim. Acta.*
(2) Benoit, G.; Hemond, H. F. *Geochim. Cosmochim. Acta* **1987**, *51*, 1445–1456.
(3) Eshleman, K. N.; Hemond, H. F. *Water Resour. Res.* **1985**, *21*, 1503–1510.
(4) Eshleman, K. N.; Hemond, H. F. *Limnol. Oceanogr.* **1988**, *23*, 174–185.
(5) Hargrave, B. T.; Burns, N. M. *Limnol. Oceanogr.* **1979**, *24*, 1124–1136.
(6) Benoit, G.; Hemond, H. F. *Limnol. Oceanogr.* **1988**, *33*, 1618–1622.
(7) Bacon, M. P.; Spencer, D. W.; Brewer, P. G. *Earth Planet. Sci. Lett.* **1976**, *32*, 277–296.
(8) Bacon, M. P.; Brewer, P. G.; Spencer, D. W.; Murray, J. W.; Goddard, D. J. *Deep-Sea Res.* **1980**, *27A*, 119–135.
(9) Talbot, R. W.; Andren, A. W. *Geochim. Cosmochim. Acta* **1984**, *48*, 2053–2063.
(10) Li, Y.-H.; Santschi, P. H.; Kaufman, A.; Benninger, L. K.; Feely, H. W. *Earth Planet. Sci. Lett.* **1981**, *55*, 217–228.
(11) Mortimer, C. H. *J. Ecol.* **1941**, *29*, 280–329.
(12) Mortimer, C. H. *J. Ecol.* **1942**, *30*, 280–329.
(13) Davison, W.; Heaney, S. I.; Talling, J. F.; Rigg, E. *Schweiz. Z. Hydrol.* **1980**, *42*, 196–224.
(14) Davison, W.; Woof, C.; Rigg, E. *Limnol. Oceanogr.* **1982**, *27*, 987–1003.
(15) Tipping, E.; Woof, C.; Cooke, D. *Geochim. Cosmochim. Acta* **1981**, *45*, 1411–1419.
(16) Sholkovitz, E. R.; Copland, D. *Geochim. Cosmochim. Acta* **1982**, *46*, 393–410.
(17) Sigg, L.; Sturm, M.; Kistler, D. *Limnol. Oceanogr.* **1987**, *32*, 112–130.
(18) White, J. R.; Driscoll, C. T. *Environ. Sci. Technol.* **1985**, *19*, 1182–1187.
(19) Davison, W.; Heaney, S. I. *Limnol. Oceanogr.* **1978**, *23*, 1194–1200.
(20) Hesslein, R. H.; Broecker, W. S.; Schindler, D. W. *Can. J. Fish. Aquat. Sci.* **1980**, *37*, 378–386.
(21) Todd, J. F. Ph.D. Dissertation, Old Dominion University, Norfolk, VA, 1984.
(22) Santschi, P. H.; Nyfeller, U. P.; Anderson, R. F.; Schiff, S. L.; O'Ara, P.; Hesslein, R. H. *Can. J. Fish. Aquat. Sci.* **1986**, *43*, 60–77.
(23) Hesslein, R. H. *Can. J. Fish. Aquat. Sci.* **1987**, *44* (Suppl. 1), 74–82.
(24) Talbot, R. W. Ph.D. Dissertation, Univ. of Wisconsin, Madison, WI, 1981.
(25) Martin, J.-M.; Meybeck, M. *Mar. Chem.* **1979**, *7*, 173–206.
(26) Schonen, M. A. A.; Barnes, H. L. *Geochim. Cosmochim. Acta* **1988**, *52*, 649–654.
(27) Morel, F. M. M. *Principles of Aquatic Chemistry*; Wiley-Interscience: New York, 1983.
(28) Hesslein, R. H. *Can. J. Fish. Aquat. Sci.* **1980**, *37*, 552–558.
(29) Benoit, G.; Hemond, H. F., submitted for publication in *Limnol. Oceanogr.*
(30) Hutchinson, G. E. *A Treatise on Limnology*: *Geography, Physics, and Chemistry*; Wiley Interscience, New York, 1975; Vol. 1.
(31) Imboden, D. M.; Emerson, S. *Limnol. Oceanogr.* **1978**, *23*, 77–90.
(32) Quay, P. D.; Broecker, W. S.; Hesslein, R. H.; Schindler, D. W. *Limnol. Oceanogr.* **1980**, *25*, 201–218.

(33) Hilton, J. *Limnol. Oceanogr.* **1985**, *30*, 1131–1143.
(34) Tanaka, N.; Takeda, Y.; Tsunogai, S. *Geochim. Cosmochim. Acta* **1983**, *47*, 1783–1790.
(35) Figgins, P. E. *The Radiochemistry of Polonium*; National Academy of Science–National Research Council, Office of Technical Services, Dept. of Commerce, Washington, DC, 1961.
(36) Honeyman, B. D.; Santschi, P. H. *J. Mar. Res.* **1989**, *47*, 951–992.
(37) Bard, A. J., Parsons, R., Jordan, J., Eds. *Standard Potentials in Aqueous Solution*; Marcel Dekker: New York, 1985.

Received for review June 26, 1989. Revised manuscript received February 26, 1990. Accepted April 16, 1990. This research was supported in part by the U.S. Geological Survey, the Massachusetts D.W.P.C., the National Wildlife Federation, the Geological Society of America, and an NSF graduate fellowship (G.B.)

Adsorption of Organic Cations to Natural Materials

Bruce J. Brownawell,† Hua Chen, John M. Collier, and John C. Westall*

Department of Chemistry, Oregon State University, Corvallis, Oregon 97331-4003

■ The factors that control the extent of adsorption of amphiphilic organic cations on environmental and pristine surfaces have been studied. The sorbents were kaolinite, montmorillonite, two aquifer materials, and a soil; solutions contained various concentrations of NaCl and $CaCl_2$, at various pH values. The distribution ratio of the dodecylpyridinium was strongly dependent on the nature and concentration of the inorganic cations in solution, but virtually independent of solution pH. The adsorption isotherms were distinctly nonlinear, even at very low surface concentrations of organic cations. A multisite adsorption model has been developed to describe adsorption over a wide range of dodecylpyridinium, NaCl, and $CaCl_2$ concentrations. Two types of adsorption reactions were found to be significant: exchange of pyridinium with an alkali-metal cation, and adsorption of pyridinium with chloride counterion.

Introduction

Amphiphilic organic cations are used in a wide range of consumer and industrial products such as detergents, fabric softeners, dyes, herbicides, emulsifying agents, and additives to drilling muds (*1–3*). These compounds adsorb strongly from aqueous solutions onto soils, sediments, and suspended particles because of favorable hydrophobic and electrostatic interactions with negatively charged surfaces of natural materials. The transport, fate, and biological effects of organic cations are greatly affected by adsorption and by association with suspended and dissolved organic matter (*1, 4*).

Adsorption can have important indirect effects as well: organic cations can effectively displace adsorbed metal ions (*5, 6*), and adsorbed organic cations can increase the affinity of sorbents for hydrophobic compounds (*6–9*). Despite the importance of these compounds, there has not been extensive systematic investigation of their adsorption to natural materials such as soils and sediments.

The adsorption of cationic surfactants on other sorbents, some of which are important constituents or potential analogues of environmental matrices, has been studied in more detail. The sorbent materials that have been studied most extensively include the following: oxides, such as quartz (*10–12*), silica (*13, 14*), and alumina (*15*); AgI sols (*16*); clay minerals (*17, 18*); carbon blacks (*19*); polystyrene latex (*20*); and various textile fibers, which, as organic polyelectrolytes, resemble natural geopolymers in some respects (*21–24*). The adsorption of amphiphilic organic cations has been reviewed by Hough and Rendall (*25*) and Theng (*26*).

There have been additional studies on adsorption of other large organic cations on clays (*26–29*) and other natural materials. Studies of the adsorption of paraquat on sediments (*30*) and of methylacridinium on soils (*31*) illustrate the importance of the clay fraction of natural materials in the adsorption of organic cations.

In this study we seek to characterize the properties of the sorbent and the solvent that affect the distribution of large amphiphilic organic cations in the aquatic environment.

Table I. Cation-Exchange Capacities and Organic Carbon Contents of the Sorbents Used in This Study[a]

sorbent material	organic carbon, %	CEC, mequiv/kg
kaolinite (KGa-1)	0.022	20 (*36*)
Na-montmorillonite (SWy-1)	0.020	764 (*36*)
Borden sand	0.026, 0.020 (*6*)	7.0 (*34*), 23 (*6*)
Lula N6 aquifer material	0.021, 0.033 (*6*)	90 (*6*)
EPA-12 soil	2.12, 2.33 (*35*)	135 (*35*)

[a] Organic carbon contents were determined on a LECO carbon analyzer. Procedures for cation exchange capacity (CEC) determination are given in the references cited.

Methods

Materials. Labeled *N*-[1-^{14}C]dodecylpyridinium (DP) bromide was obtained from Pathfinder Laboratories Inc. (St. Louis, MO). The specific activity was 10.6 Ci/mol, and the purity of the label was greater than 99% as determined by HPLC with radioactivity detection. Solutions of DP used in this study were checked periodically for purity; no evidence of degradation was found. Unlabeled DP was purchased as the chloride monohydrate from Aldrich Chemical and used as received. The critical micelle concentration (CMC) of DP in deionized water is 14.7 mM (*32*). The critical micelle concentrations at 25 °C in 0.01 and 0.1 M NaCl solutions are estimated from the data of Ford et al. (*33*) as 13 and 6.3 mM, respectively.

The sorbents used in this study included low organic carbon aquifer materials, a relatively high organic carbon soil, and pristine clays. Some properties of the sorbents are listed in Table I. A 74–210-μm fraction of aquifer material Borden sand (*6, 34*), isolated by dry-sieving, was used in this work. Lula N6 aquifer material (*6*) was provided by Dermont Bouchard, U.S. EPA. EPA-12 soil (*35*) was provided by Professor John J. Hassett of the University of Illinois. Georgia kaolin (KGa-1) and Wyoming Na-montmorillonite (SWy-1) (*36*) were obtained from

† Present address: Marine Science Research Center, SUNY at Stony Brook, Stony Brook, NY 11794-5000.

 0013-936X/90/0924-1234$02.50/0

Source Clays Repository at the University of Missouri. The deionized water used in all experiments was from a Millipore Milli-Q System, with specific resistivity of approximately 18 MΩ cm.

Equipment. For equilibration and phase separation, a thermostated shaker (New Brunswick Model G-24) and thermostated centrifuge (Beckman Model J2-21) were used. Concentrations of unlabeled DP were determined spectrophotometrically with a Hewlett-Packard Model 8452A UV–visible spectrophotometer. Radioactivity of the labeled compounds were determined with a Beckman Model LS 7800 scintillation counter. Labeled compounds adsorbed to aquifer material or soil were converted to $^{14}CO_2$ with a Harvey Model 300 oxidizer.

Pretreatment of Sorbents. The sorbents were washed several times before use in distribution experiments. The purpose of this step was to equilibrate the sorbent with the electrolyte solution before addition of DP and to reduce the amounts of suspended material that are not separated from the aqueous phase by centrifugation, which can affect the observed distributions of organic compounds in batch adsorption experiments (*37*).

The same general procedure, with minor variations, was used to pretreat the sorbents. A known mass of sorbent (0.050–1.0 g) and 20 mL of electrolyte solution were added to 25-mL Corex glass centrifuge tubes. In general, the mass of sorbent and the composition of the electrolyte solutions were those to be used in the distribution experiments that followed the pretreatment. The mass of sorbent was selected such that the amounts DP in the solution and on the sorbent would be approximately equal; this strategy reduces the likelihood of artifacts arising from incomplete phase separation. The tubes were shaken for periods of 30 min to 6 h at 500 rpm and 25 °C in a thermostated shaker. Then the suspensions were centrifuged for 5–30 min at 5300–9100 rpm (4000–11000*g*). The longer equilibration and centrifugation times were used for clays. The supernatant was removed and replaced with fresh electrolyte solution. This procedure was repeated 5–8 times.

Determination of Distributions. After the sorbents had been pretreated, the suspensions were centrifuged, and the DP was spiked into the particle-free solution in 10–200 μL of 95% ethanol. The purpose of this procedure was to reduce the likelihood of contact between sorbents and localized high concentrations of DP during the spiking. In independent experiments it was determined that the ethanol had no effect on distribution.

The electrolytes were NaCl, NaN_3, and $CaCl_2$. NaN_3 was used in place of NaCl in experiments conducted at low concentration of DP to reduce the possibility of microbial degradation. The tubes, which were sealed with PTFE-lined caps, were shaken for 4 h at 25 °C, after which the aqueous and sorbent phases were separated by centrifugation at 11000*g* for 30–60 min at 25 °C.

After centrifugation, the amounts of alkylpyridinium in the aqueous phase, adsorbed to the sorbent, and adsorbed to the walls of the vessel were determined. The analytical procedures are described below. The concentration distribution ratio, D_c, was calculated from

$$D_c = C_i(\text{s})\ (\mu\text{mol/kg})/C_i(\text{w})\ (\mu\text{M}) \qquad (1)$$

where C_i(s) and C_i(w) are the concentrations of the component i on the sorbent and in the water. The recovery was also calculated from these data.

Analysis for Labeled Pyridinium. Aliquots of the aqueous phase were withdrawn with a graduated glass pipet and transferred to scintillation vials containing 10 mL of Beckman RP scintillation fluid. Then the rest of the solution was carefully removed from the tubes by aspiration and the moist sorbents were freeze-dried and reweighed. The amount of DP on the freeze-dried sorbent was determined by oxidizing two subsamples (10–200 mg) at 900 °C in the oxidizer. The $^{14}CO_2$ was trapped directly in a scintillation vial in a mixture of 5 mL of Packard Carbo-sorb and 5 mL of Permafluor V scintillation fluid. The walls of the centrifuge tubes were then brushed clean, DP was extracted with 20 mL of ethanol on the shaker for 20 min, and aliquots were sampled as described for the aqueous phase. The overall precision for aqueous and sorbent samples was generally better than 2 and 5% RSD, respectively. These procedures produced very good recoveries of DP; the average recovery for all experiments was 97% and the average relative standard deviation within an individual experiment was 1.5%.

Analysis for Unlabeled Pyridinium. Separate analysis of the walls was not performed routinely when experiments were conducted with higher concentrations of unlabeled compounds; adsorption of DP onto centrifuge tube walls from 100 μM solutions was negligible. The concentration of DP was determined by UV spectrophotometry at 260 nM; ϵ_{260} = 4100 AU M^{-1} cm^{-1}. After the remaining aqueous phase was removed from the centrifuge tube, the adsorbed DP was extracted with 20 mL of methanol or 0.01 M HCl in methanol. The tubes were shaken for 1 h and centrifuged; the extract was analyzed for concentration of DP by UV spectrophotometry as above. These procedures resulted in complete recovery of DP adsorbed to Borden sand, Lula aquifer material, and kaolinite clay; recoveries were not complete for montmorillonite. In the latter case, the amount adsorbed was estimated from the difference between final and initial aqueous-phase concentrations.

pH Experiments. The influence of $[H^+]$ on the distribution of alkylpyridinium was examined with several sorbents. Various volumes of 1.0 M NaOH and HCl were added to suspensions of sorbent materials in 20 mL of 0.01 M NaCl or NaN_3. An Orion Model 8102 Ross combination glass electrode, with 3 M KCl outer filling solution, was used for pH determination. The electrode was calibrated with buffers of pH 4.00, 7.00, and 10.00 from Micro Essential Laboratory (Brooklyn, NY).

Sorption Kinetics. Experiments were run to determine the time required for DP to approach equilibrium during adsorption and desorption. For adsorption kinetics, identical tubes were left on the shaker for various times, ranging from 0.5 to 30 h. For desorption kinetics, sorbents were first equilibrated with DP for 4 h. Then the solution and sorbent were separated by centrifugation, and the supernatant was discarded and replaced with the same pyridinium-free electrolyte. The tubes were then shaken concurrently and sampled at various times ranging from 0.5 to 8 h.

There was relatively rapid adsorption equilibrium for DP in experiments conducted with Borden sand, Lula aquifer material, and montmorillonite. The D_c approaches an apparent equilibrium value within 4 h of shaking for the two natural materials, after which D_c remains constant over 24–30 h; adsorption reached apparent equilibrium for montmorillonite within the first 30 min. The release of dodecylpyridinium from the experiment with Lula sorbent was rapid and nearly reversible; the D_c determined after a 1-h desorption step was 7330 compared to a D_c of 5800 after the adsorption step, with approximately the same total amount of DP in the system. For compounds that adsorb with nonlinear isotherms, it is important that the total amount of compound in the system remain constant if distribution ratios are to be compared.

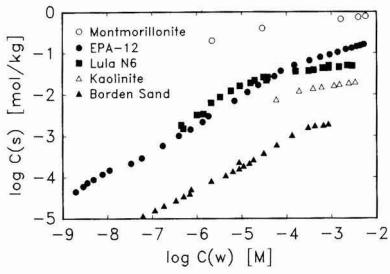

Figure 1. Logarithmic adsorption isotherms of dodecylpyridinium on different materials. Montmorillonite, ratio of solids to liquids [C_s(w)] was 0.0050 kg/L; kaolinite, C_s(w) = 0.025; soil EPA-12, C_s(w) = 0.025; Lula aquifer material, C_s(w) = 0.0025; and Borden sand, C_s(w) = 0.025 or 0.050 kg/L. Solutions contained 0.01 M Na^+.

Results

The objectives of this study were as follows: (i) to characterize the factors that influence the adsorption of a cationic surfactant to natural sorbents; and (ii) to describe the observed adsorption isotherms in terms of mechanistically based adsorption models that can be of use for understanding environmental distributions. We present first the results from experiments in which the adsorption of dodecylpyridinium was determined as a function of sorbent and solution composition. A quantitative interpretation and model follow in the discussion section.

Adsorption Isotherms. The logarithmic adsorption isotherms of DP on five materials are shown in Figure 1. The aqueous phase contained either 0.01 M NaCl or 0.01 M NaN_3; independent tests showed no detectable dependence of adsorption on the anion. The equilibrium concentrations of DP in solution were well below the CMC in all cases.

The affinities of the sorbents for DP, per unit mass of sorbent, follow the order montmorillonite > EPA-12 soil ≈ Lula aquifer material > kaolinite > Borden sand. This order corresponds roughly to the cation-exchange capacities (CECs) of the materials. A judgment about any correlation with organic carbon is hardly warranted, since the organic carbon content of most of these materials is so very low. However, the adsorption affinity of Lula aquifer material is similar to that of EPA-12 despite the 100-fold difference in organic carbon contents.

At concentrations of DP in solution below 125 μM for EPA-12 and Borden sand, and below 20 μM for Lula aquifer material, the logarithmic isotherms (Figure 1) conform to the Freundlich equation:

$$\log C(s) = n \log C(w) + \log K \qquad (2)$$

where K and n are constants. The values of n determined from the slopes of the isotherms in the low-concentration region are 0.63 and 0.58 for EPA-12 and Borden sand, respectively. These low values of n (n = 1 for a linear isotherm) indicate nonlinearity in the isotherms at very low surface coverages. The nonlinearity extends to surface concentrations that are as low as 0.018% of the maximum surface concentration measured in the case of EPA-12 soil. As will be discussed, this nonlinearity is attributed to heterogeneity of adsorption sites.

The higher concentration data from these isotherms are presented on a linear scale in Figure 2. The isotherms approach or reach a plateau, with the exception of the EPA-12 isotherm, in which the concentration adsorbed is still increasing at 7.9 mM DP in solution. The plateau concentrations of DP adsorbed correspond closely, but not strictly, to the reported cation-exchange capacities measured for the five sorbent materials, as can be seen by comparing the plateau values in Figure 2 to the CEC values given in Table I.

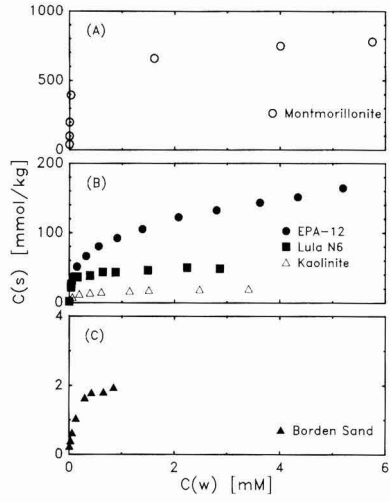

Figure 2. Adsorption isotherms of dodecylpyridinium on different materials. Data are from the high concentration range of Figure 1, plotted here on a linear scale. Note the correspondence between the plateaus of the adsorption isotherms and the cation-exchange capacities listed in Table I. Range of pH values for the data in the isotherms: (A) montmorillonite, pH = 7.13–5.46; (B) kaolinite, pH = 5.39–4.72; soil EPA-12, pH = 7.43–7.00; Lula aquifer material, pH = 6.81–4.49; (C) Borden sand, pH = 9.39–9.02. Solutions contained 0.01 M Na^+; ratios of solids to liquids are given in the legend of Figure 1.

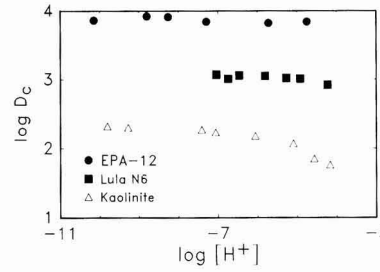

Figure 3. Effect of log [H^+] on the concentration distribution ratio D_c of dodecylpyridinium between aqueous solutions and selected sorbents. EPA-12, C_s(w) = 0.015 kg/L; Lula, C_s(w) = 0.0025; and kaolinite, C_s(w) = 0.0125. Solution contained 0.01 M Na^+. The amounts of dodecylpyridinium adsorbed were nearly constant for EPA-12 and Lula sorbents: C_R(s) = 0.20 and 29 μmol/g, respectively. C_R(s) ranged from 7.6 to 15 μmol/g for kaolinite.

Effect of pH. The effect of [H^+] on the adsorption of DP by EPA-12, Lula aquifer material, and kaolinite is shown in Figure 3. A very small dependence of log D_c on log [H^+] was observed for the heterogeneous sorbents; the slopes ($\Delta \log D_c/\Delta \log [H^+]$) determined from the data in Figure 3 were −0.04 and −0.01 for Lula and EPA-12, respectively. The slight decrease in log D_c with increase in log [H^+] can be attributed either to an increase in surface potential resulting from protonation of pH-dependent surface groups (such as surface hydroxyl groups or organic acid groups) or to ion exchange of H^+ for pyridinium. No independent determination of the amounts of pH-dependent groups was made. The dependence of log D_c on log [H^+] for kaolinite was greater than for the heterogeneous materials. At pH values of <6.06, the slope $\Delta \log D_c/\Delta \log [H^+]$ was −0.23.

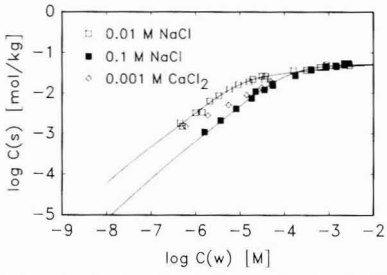

Figure 4. Logarithmic adsorption isotherms of dodecylpyridinium on Lula aquifer material from 0.1 M NaCl, 0.01 M NaCl, and 0.001 M $CaCl_2$. The ratio of solids to liquid was 0.0025 kg/L. The solid lines were computed from the model defined in Table II.

The relation of solution $[H^+]$ to pyridinium adsorption can be viewed from another perspective, that is, the influence of the adsorption of pyridinium on solution $[H^+]$. For example, as the isotherms in Figure 2 were obtained, the solution pH dropped progressively with increasing adsorption of DP. The range of pH over the course of each isotherm is given in the legend of Figure 2. This release of H^+ from the sorbent upon adsorption of DP occurs despite the fact that the sorbents had been preequilibrated with Na^+ solutions. A similar change in pH was observed for adsorption of alkylpyridiniums on Na-montmorillonite (*17*).

Effect of the Electrolyte. The effect of concentration and type of electrolyte on adsorption of DP was examined with two complementary types of data: (i) adsorption isotherms of DP from solutions with different concentrations of salts; and (ii) concentration distribution ratio of DP as a function of concentration of NaCl or $CaCl_2$, with a constant amount of DP in the system. In view of the nonlinearity of the isotherms, the first method is preferable for development of a mechanistic models, while the second provides an estimate of the magnitude of the effect.

The effect of the salt concentration was greater than that of pH. Figure 4 shows the isotherms for adsorption of DP onto Lula aquifer material from 0.01 M NaCl, 0.1 M NaCl, and 0.001 M $CaCl_2$. At low concentrations of organic cation, an increase in the salt concentration decreases the adsorption by a nearly constant factor. At high concentrations of the organic cation, the isotherms merge and cross at surface concentrations that correspond roughly to the CEC. Similar isotherms (not shown) were obtained for Borden sand and kaolinite. It is seen in the figure that 0.001 M Ca^{2+} impedes adsorption of DP more effectively than 0.01 M Na^+.

The effect of NaCl concentration on the adsorption of DP onto EPA-12 soil is shown in Figure 5A. It is similar to that described for Lula aquifer material (Figure 4), except not as pronounced.

The effect of Ca^{2+} on the adsorption of DP onto EPA-12 is shown in Figure 5B. The solutions contained 0.01 M NaN_3 and x $CaCl_2$, with x = 0, 0.6, and 10 mM. The isotherm in the absence of Ca^{2+} is given by the solid line. Addition of 0.6 mM $CaCl_2$ had no significant effect on adsorption. Addition of 10 mM $CaCl_2$ decreased adsorption of DP [$\Delta \log D_c \approx 0.40 - 0.45$, at constant $C_R(w)$]. The isotherms with and without $CaCl_2$ merge at high concentrations of DP.

Experiments in which the amount of DP was kept constant and the concentrations of supporting electrolyte were varied showed effects on adsorption that were similar to those observed in isotherm studies. The effects of added $CaCl_2$ in the presence of 0.01 M NaN_3 on D_c for both

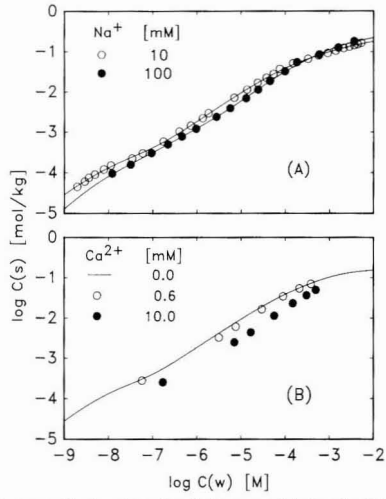

Figure 5. Logarithmic adsorption isotherms of dodecylpyridinium on soil EPA-12 from (A) 0.01 M NaN_3; 0.01 M NaN_3 with 0.09 M NaCl; (B) 0.01 M NaN_3 with 0.0006 M $CaCl_2$; 0.01 M NaN_3 with 0.01 M $CaCl_2$. The solid-to-liquid ratios were 0.025 kg/L in A and 0.0050 kg/L in B. The solid lines in Figure 5A were computed from the model defined in Table III. The line for 0.01 M Na^+ in Figure 5A is reproduced in Figure 5B to allow comparison of isotherms in the presence and absence of added Ca^{2+}.

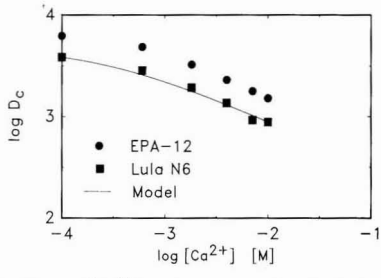

Figure 6. Effect of $[Ca^{2+}]$ on the concentration distribution ratio D_c of dodecylpyridinium on soil EPA-12 and Lula aquifer material. Solutions contained 0.01 M NaN_3 and x M $CaCl_2$. The solid line was computed from the model defined in Table II. The amounts of dodecylpyridinium adsorbed in these experiments were approximately constant at 415 (Lula) and 275 μmol kg^{-1} (EPA-12); the solid-to-liquid ratio was 0.0025 (Lula) and 0.005 kg L^{-1} (EPA-12).

EPA-12 and Lula are illustrated in Figure 6. The effects are similar for both sorbents. The dependence of D_c on $[Ca^{2+}]$ decreases as the Ca^{2+} in solution is masked by the 0.01 M Na^+ background electrolyte. At $[Ca^{2+}]$ above 1 mM, the dependence of log D_c vs log $[Ca^{2+}]$ is approximately linear; the slope, $\Delta \log D_c / \Delta \log [Ca^{2+}]$, is −0.49 and −0.44 for EPA-12 and Lula, respectively.

The influence of NaCl concentration on the adsorption of DP by EPA-12 soil is given in Figure 7. The D_c for DP with EPA-12 soil increases 0.50 log unit as the $[Na^+]$ is increased from 0.01 to 0.1 M. The value of $\Delta \log D_c / \Delta \log [Na^+]$, excluding the lowest Na^+ concentration datum, is −0.62, similar to the values observed for Ca^{2+}.

Discussion

In this study we have determined isotherms for the adsorption of an organic cation on natural sorbents and have examined some of the properties of solution and sorbent that affect the distribution. The following questions are important in the interpretation of these results:

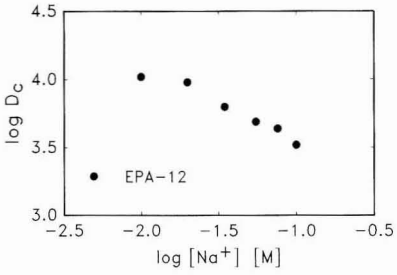

Figure 7. Effect of $[Na^+]$ on the concentration distribution ratio D_c of dodecylpyridinium on soil EPA-12. Solutions contained 0.01 M NaN_3 and x M NaCl. The amounts of dodecylpyridinium adsorbed were approximately constant at 290 μmol kg^{-1}, and the solid-to-liquid ratio was 0.0050 kg L^{-1}.

(i) how can nonlinear isotherms be interpreted quantitatively and mechanistically? (ii) what type of adsorption model can account for the strong dependence of adsorption on electrolyte and relatively weak dependence on pH? (iii) why is there no evidence of hemimicelle formation in the adsorption isotherms for heterogeneous natural materials? and (iv) what properties of sorbent, solvent, and solute are most important in determining the extent of adsorption of amphiphilic organic cations on natural materials?

Nonlinear Isotherms. All of the adsorption isotherms determined in this study were nonlinear, even at very low surface coverages of DP (Figure 1). Causes of isotherm nonlinearity include (i) nonuniformity of energies of adsorption sites, with saturation of high-energy sites; (ii) sorbate–sorbate interactions such as repulsive electrostatic interactions or cooperative chain–chain interactions; and (iii) experimental artifacts that stem from covariation of experimental conditions, such as changes of pH, major ion concentrations, or aggregation of particles, that accompany changes in organic cation concentrations.

For reasons to be discussed, we interpret the nonlinearity of isotherms in these experiments primarily as the result of heterogeneity of sites. Particularly in the low-concentration regions of the isotherms, the changes in pH, concentrations of major ions in solution, and surface charge that accompanied adsorption of the organic cation were too small to account for the isotherm nonlinearity. Thus, at low concentrtions of organic cation, heterogeneity of sites is the preferred explanation. At higher concentrations it is more difficult to exclude the influence of other processes on isotherm nonlinearity.

The nonlinear isotherms are described adequately by the Freundlich equation (*38*) (eq 2) up to surface coverages of 20% of the CEC and, with the possible exception of EPA-12 soil, approach a plateau or saturating level as the concentration is further increased. However, the Freundlich equation provides no clear basis for determining intrinsic adsorption energies or adsorption mechanisms (*39*).

The mechanistic models that were considered for these data were (i) multisite models, (ii) electrostatic models (see refs 40 and 41), and (iii) some combination of the two. Most of the phenomena observed in this study can be explained through the multisite model, with electroneutral reactions and no explicit electrostatic energy term. While this approach is obviously an approximation, it is consistent with a variety of observations, and it is conceptually very simple.

Adsorption Model. The adsorption model that we use is based on the following reactions:

$$R^+ + \overline{NaX} = \overline{RX} + Na^+ \quad K_{RX} \tag{3}$$

$$R^+ + Cl^- + \overline{Y} = \overline{RClY} \quad K_Y \tag{4}$$

$$Ca^{2+} + \overline{2NaX} = \overline{CaX_2} + 2Na^+ \quad K_{CaX_2} \tag{5}$$

where the overbar represents a species associated with the sorbent, X is a negatively charged cation-exchange site, Y is an uncharged site (that could be thought of as a site for hydrophobic adsorption), and R^+ represents the alkylpyridinium. The mass action equations for reactions 3–5 are

$$(R^+)\{\overline{NaX}\}K_{RX} = \{\overline{RX}\}(Na^+) \tag{6}$$

$$(R^+)(Cl^-)\{\overline{Y}\}K_Y = \{\overline{RClY}\} \tag{7}$$

$$(Ca^{2+})\{\overline{NaX}\}^2K_{CaX_2} = \{\overline{CaX_2}\}(Na^+)^2 \tag{8}$$

where (q) represents the activity of species q in solution (mol L^{-1}) and $\{q\}$ represents concentrations of species q on the sorbent (mol kg^{-1}).

The ion-exchange sites X and the adsorption sites Y are subject to the following material balance conditions:

$$T_X = \{\overline{X}\} + \{\overline{NaX}\} + \{\overline{RX}\} + 2\{\overline{CaX_2}\} \tag{9}$$

$$T_Y = \{\overline{Y}\} + \{\overline{RClY}\} \tag{10}$$

where T is the total number of sites (mol kg^{-1}).

Finally, in order to represent the heterogeneous surface, we use not just a single type of ion-exchange site as indicated by X above, but a set of different types of ion-exchange sites (X_1, X_2, ... X_n), each of which obeys its own mass action equations and material balance equations given above. A similar approach can be used for the Y sites (Y_1, Y_2, ... Y_m). Thus the model could be described as a multisite competitive Langmuir model.

The adjustable parameters in the model are the equilibrium constants given by eq 6–8 and the total number of sites given in eq 9 and 10. All parameters were determined with FITEQL (*42*, *43*), a weighted nonlinear least-squares adjustment procedure for multicomponent chemical equilibrium problems. Solution activity coefficients were calculated from the Davies equation and surface activity coefficients were set equal to unity.

Equilibrium Constant Spectrum. To aid in determining the values of the adjustable parameters for the different types of sites, a discrete equilibrium constant spectrum approach was used. In this approach, the values of the equilibrium constants for each type of site (K_1, K_2, ...) are fixed at integral powers of ten (10^0, 10^1, ...) and the total concentrations of each type of site (T_1, T_2, ...) are determined from the experimental data by the nonlinear least-squares procedure. Criteria used in the selection of the range and the interval for the K_i's will be discussed in detail in a future publication. The objective of this approach is to represent the experimental data in terms of a regular distribution of sites, rather than the smallest number of adjustable parameters. This approach facilitates systematic comparison of complex isotherms.

Application of Model. This model was applied first to the adsorption of DP on Lula aquifer material. In the first step, data at two different concentrations of Na^+ (Figure 4) were used to determine the T_{X_i} of the equilibrium constant spectrum; since only one type of Y site was considered, both K_Y and T_Y were determined. The constants are given in Table II, and the isotherms calculated from the constants are given by the lines in Figure 4. The agreement between the model and the data is excellent. In a second step, the competition by Ca^{2+} was taken into the model. The equilibrium constants for exchange of Ca^{2+} with each of the $\overline{NaX_i}$ groups were determined from the

Table II. Equilibrium Constants for Adsorption of Dodecylpyridinium on Lula Aquifer Material

site type	equilibrium constants[a,b] log K_{RX}	log K_{CaX_2}	log K_{YRCl}	total site density, mol kg^{-1}
X_1	5.00	3.00		3.52×10^{-4}
X_2	3.00	0.86		3.15×10^{-2}
Y			5.12	2.08×10^{-2}

[a] Reactions described in text, reactions 3–5. Equilibrium constants valid for 25 ± 2 °C, with aqueous concentrations in mol L^{-1} and concentrations on sorbent in mol kg^{-1}. Properties of sorbents are listed in Table I.

Table III. Equilibrium Constants for Adsorption of Dodecylpyridinium on Soil EPA-12

site type	equilibrium constants[a,b] log K_{RX}	log K_Y	total site density, mol kg^{-1}
X_1	7.00		2.07×10^{-5}
X_2	6.00		1.72×10^{-4}
X_3	4.00		6.20×10^{-4}
X_4	3.00		7.29×10^{-3}
X_5	2.00		4.12×10^{-2}
X_6	1.00		5.36×10^{-2}
Y_1		9.00	1.04×10^{-4}
Y_2		7.00	1.23×10^{-3}
Y_3		5.00	4.46×10^{-2}
Y_4		4.00	8.70×10^{-2}
Y_5		3.00	6.54×10^{-2}

[a] Reactions described in text, reactions 3 and 4. Equilibrium constants valid for 25 ± 2 °C, with aqueous concentrations in mol L^{-1} and concentrations on sorbent in mol kg^{-1}. Properties of sorbents are listed in Table I. [b] Constants are determined by the following procedure: values of K_{RX} and K_Y were set according to the equilibrium constant spectrum approach, and values of T_X and T_Y were determined from data in Figure 5A with FITEQL (*42*, *43*).

Lula data in Figure 6. Again the agreement between the model, represented by the solid line, and the data is excellent.

The same method of data treatment was used for the adsorption of DP on EPA-12, as shown in Figure 5A. The spectrum approach was used for the Y sites as well as for the X sites. The equilibrium constant spectra are given in Table III and the amount adsorbed calculated from the model is given by the lines in Figure 5a. The agreement between the lines and the data is very good.

Certaintly this "discrete equilibrium constant spectrum" approach is subject to the criticism that a model can be fit to any set of data if enough adjustable parameters are used. Furthermore, there is some covariance among the values of the adjustable parameters; the values are not unique, but just one of an infinite number of sets that can be used to represent the data.

However, the advantages of this approach are significant, too. The practical advantage is that the effects of multiple interactions in complex systems can be represented in a way that is completely compatible with chemical equilibrium models used in environmental chemistry. An adsorption isotherm that conforms closely to the Freundlich equation over more than 6 orders of magnitude range in C(w) can be described very well by conventional mass action and material balance equations; these equations have a mechanistic basis, which potentially could be used to understand the factors that influence adsorption.

Another advantage of such a model is that it provides a framework for evaluating quantitatively mechanisms that could be responsible for the phenomena that are observed experimentally, such as, (i) reversal of effect of electrolyte concentration on isotherms near the CEC, (ii) lateral shift of isotherms with salt concentration far below the CEC, (iii) absence of pH effect, (iv) relative effect of Na vs Ca on the isotherms, and (v) absence of evidence for hemimicelle formation. The interpretation of these phenomena in terms of the model will be discussed next.

Reversal of Effect of Electrolyte Concentration. At very low concentrations of DP, the effect of an increase in NaCl concentration is a *decrease* in DP adsorption, as seen in Figures 4 and 5A. This behavior is consistent with simple cation exchange. In contrast, at very high concentrations of DP, the effect of an increase in NaCl concentration is an *increase* in DP adsorption. This increase is observed at surface concentrations near the CEC and is attributed to adsorption of RClY. Higher concentrations of counterions enable more DP to accumulate at the surface. This crossover of adsorption isotherms at approximately the CEC is consistent with the increase in adsorption of DP with ionic strength on vinylon and acetate (*23*, *24*), and counterion adsorption above the "equivalence point" determined for silica (*14*), celluosic fibers (*21*), and montmorillonite (*17*).

Lateral Shift of Isotherms with Electrolyte Concentration. At concentrations far below the CEC, the isotherms of pyridinium on EPA-12 and Lula are seen to shift laterally with changes in electrolyte concentration (Figures 4 and 5A). If adsorption were due exclusively to the cation-exchange reaction (reaction 3) and surface activity coefficients were constant, the isotherms should shift a decade with a decade change in salt concentration. In reality the shift is ~0.7 unit/decade [Na^+] for Lula and 0.3–0.5 unit/decade [Na^+] for EPA-12. This attenuation in the shift is explained through the formation of RClY (reaction 4), which increases with Cl^- concentration, in contrast to the formation of RX, which decreases with Na^+ concentration. Since the formation of RClY is probably related to the hydrophobic effect, it is consistent that the formation of this species is favored on the sorbent with the higher organic carbon content.

Effect of pH. Adsorption to the heterogeneous natural materials is seen to be virtually independent of pH. Therefore pH-dependent sites such as organic carboxylic acid groups or surface hydroxyl groups were not used in the adsorption model.

Effect of Ca(II) vs Na(I). The reduction in adsorption of DP in Ca solutions relative to Na solutions (Figure 4) is explained by the fact that Ca^{2+} competes more effectively for ion-exchange sites of soils and clays. The magnitude of this effet is consistent with energies of ion-exchange reactions, but not consistent with simple attenuation of long-range electrostatic energy as calculated by, for example, the Gouy–Chapman theory.

Hemimicelles. Adsorption isotherms for surfactants on many surfaces exhibit a sharp increase in slope at coverages between 1 and 10% of a calculated monolayer (*11*, *20*, *25*, *44*). The concentration at which this increase in slope occurs is termed the hemimicelle concentration (HMC) (*10*, *44*). Hemimicelles form at surfaces when the attractive hydrophobic interaction between adsorbed molecules becomes significant compared to the interaction between adsorbed molecules and the surface.

No evidence of hemimicelle formation is seen in the isotherms in Figures 1 and 2. The absence of a hemimicelle-formation region in these isotherms is consistent with (i) the heterogeneity of the surface and (ii) the strong interaction between the adsorbed organic cations and the negatively charged surface.

Electrostatic Interactions. Although there is no explicit electrostatic term in the adsorption model, the im-

portance of electrostatic energy is recognized (*40*, *41*) and is perhaps best illustrated by comparing the distribution ratios with EPA-12 soil in this study to distributions of anionic and neutral surfactants of similar size determined with the same material (*45*). The D_c of DP with EPA-12 soil in 0.01 M NaN_3 is found by interpolation to be 2010 mL/g at a C(w) for DP of 1.0 μM from the Freundlich equation. The value of D_c under the same conditions for dodecylbenzenesulfonate is 68.6, and those for tridecyl ethers of poly(ethylene glycol), that is, $C_{13}H_{27}(OCH_2CH_2)_nOH$, with n = 3, 6, and 9, range between 229 and 401.

The adsorption model used in this study does not include an explicit electric double-layer (EDL) model for charge and potential at the sorbent–solution interface. An explicit EDL model is thought not to be necessary for these sorbents since (i) one of the primary adsorption reactions is cation exchange, for which the negative "counterion" is formally *within* the clay; (ii) surface roughness of these heterogeneous natural sorbents argues against description of the interface as a sandwich of discrete planes; and (iii) the lack of pH dependence of the distribution argues against the importance of pH-dependent charge on these sorbents, for which the counter charge might be found in a double layer.

Hydrophobic Interactions. In this study we do not present data for compounds other than dodecylpyridinium; thus it is difficult to say much about the effect of hydrophobicity of the sorbate. However, the magnitude of this effect can be estimated from the effect of alkyl chain length on air–water adsorption or micelle formation. An increase in the hydrocarbon chain length by one CH_2 group leads to a $\Delta G°$ of approximately 2600 J/mol, or a $\Delta \log K \approx 0.46$ (*46*). The dependence of adsorption on the chain length of anionic LAS surfactants on soil is $\Delta \log D_c/\Delta$ n-CH2 or 0.40–0.45 (*45*, *47*). These values are close to those observed for adsorption of cationic surfactants on surfaces of quartz (*44*) and organic polyelectrolytes (*20*, *22*). The effect of different headgroups on adsorption can be related to the effective chain length (*16*). The influence of alkyl chain length diminishes as surface saturation is approached. However, cationic surfactants of longer chain length may be packed more closely in a monolayer (*20*) and are more likely to adsorb in multiple layers (*17*).

Distribution of Organic Cations in the Environment. The results of this study and that of Brown and Combs (*31*) suggest that it may be possible to estimate the environmental distributions of organic cations within reasonable limits, given the CEC of the sorbing phase, the effective chain length or hydrophobicity of the organic cation, and the total concentrations of organic cation and other major ions in the system. Present uncertainties include (i) the generality of the observed adsorption behavior of the three heterogeneous natural materials in this study, (ii) the variability of the distribution of adsorption site energies that can be expected for heterogeneous natural materials, and (iii) the characterization of the adsorption of important metals and other co-ions that compete with organic cations. Complementary studies on the electrophoretic mobilities of natural particles under conditions of variable pH and adsorbed organic cation concentration could provide additional information concerning the validity of the model that we have proposed.

Conclusions

Large amphiphilic organic cations, such as DP, are strongly adsorbed to soils and subsurface materials. Adsorption depends primarily on the CEC of the sorbent, the nature and concentration of the electrolyte, and the concentration and alkyl chain length of the organic cation. Solution pH had little effect on the adsorption of DP on the heterogeneous natural materials studied.

The adsorption isotherms are distinctly nonlinear, even at very low surface concentrations of organic cation. The data conform to the Freundlich equation. This behavior can be described by assuming a heterogeneous mixture of adsorption sites and fitting the data with a summation of Langmuir isotherms. Hemimicelle formation was not apparent in any of the isotherms for adsorption of DP on heterogeneous natural materials.

Maximum or plateau adsorption values of adsorbed DP corresponded roughly to the reported CECs of the sorbent materials. Adsorption was somewhat greater than the CEC for EPA-12 soil; this effect may be related to an increased role of organic matter for high-f_{oc} materials.

The effects of electrolyte type and concentration on adsorption could be explained well with two types of electroneutral reactions: cation exchange and adsorption of the organic cation with an inorganic anion. Ca^{2+} had a larger effect on adsorption than did Na^+, as expected for ion exchange. Competitive adsorption with divalent metal cations will be important in affecting environmental distributions of large organic cations.

Acknowledgments

The technical assistance of Fred B. Rea and Consuelo Carbonell is gratefully acknowledged.

Registry No. DP, 104-73-4; NaCl, 7647-14-5; $CaCl_2$, 10043-52-4; montmorillonite, 1318-93-0.

Literature Cited

(1) Boethling, R. S. *Water Res.* **1984**, *18*, 1061–1076.
(2) Huber, L. H. *J. Am. Oil Chem. Soc.* **1984**, *61*, 377–382.
(3) Greek, B. F.; Layman, P. L. *Chem. Eng. News* **1989**, *67*, 29–49.
(4) Lewis, M. A.; Wee, V. T. *Environ. Toxicol. Chem.* **1983**, *2*, 105–118.
(5) Beveridge, A.; Pickering, W. F. *Water Res.* **1983**, *17*, 215–225.
(6) Bouchard, D. C.; Powell, R. M.; Clark, D. A. *J. Environ. Sci. Health* **1988**, *A23*, 585–601.
(7) Cowan, C. T.; White, D. In *Proceedings of the Ninth National Conference on Clays and Clay Minerals*; Swineford, A., Ed.; Pergamon: New York, 1962; pp 459–467.
(8) Gaynor, J. D.; Volk, V. V. *Weed Sci.* **1976**, *24*, 549–552.
(9) Mortland, M. M.; Shaobai, S.; Boyd, S. A. *Clays Clay Miner.* **1986**, *34*, 581–585.
(10) Fuerstenau, D. W. *J. Phys. Chem.* **1956**, *60*, 981–985.
(11) Takeda, S.; Usui, S. *Colloids Surf.* **1987**, *23*, 15–28.
(12) Schwarz, R.; Heckmann, K.; Strnad, J. *J. Colloid Interface Sci.* **1988**, *124*, 50–56.
(13) Rupprecht, H.; Ullmann, E.; Thoma, K. *Fortschrittsber. Kolloide Polym.* **1971**, *55*, 45–48.
(14) Bijsterbosch, B. H. *J. Colloid Interface Sci.* **1974**, *47*, 186–198.
(15) Fuerstenau, D. W.; Modi, H. J. *J. Electrochem. Soc.* **1959**, *106*, 336–341.
(16) Ottewill, R. H.; Rastogi, M. C. *Trans. Faraday Soc.* **1960**, *56*, 880–892.
(17) Greenland, D. J.; Quirk, J. P. In *Proceedings of the Ninth National Conference on Clays and Clay Minerals*; Swineford, A., Ed.; Pergamon: New York, 1962; pp 484–499.
(18) Law, J. P.; Kunze, G. W. *Soil Sci. Soc. Am. Proc.* **1966**, *30*, 321–327.
(19) Saleeb, F. Z.; Kitchener, J. A. *J. Chem. Soc.* **1965**, 911–917.
(20) Connor, P.; Ottewill, R. H. *J. Colloid Interface Sci.* **1971**, *37*, 642–651.
(21) Sexsmith, F. H.; White, H. J., Jr. *J. Colloid Sci.* **1959**, *14*, 598–618.
(22) Rendall, H. M.; Smith, A. L.; Williams, L. A. *J. Chem. Soc., Faraday Trans.* **1979**, *75*, 669–678.

(23) Sakata, K.; Katayama, A. *J. Colloid Interface Sci.* **1987**, *116*, 177–181.
(24) Sakata, K.; Katayama, A. *J. Colloid Interface Sci.* **1988**, *123*, 129–135.
(25) Hough, D. B.; Rendall, H. M. In *Adsorption from Solution at the Solid/Liquid Interface*; Parfitt, G. D., Rochester, C. H., Eds.; Academic Press: London, 1983; pp 247–319.
(26) Theng, B. K. G. *The Chemistry of Clay—Organic Reactions*; Wiley: New York, 1974; pp 136–238.
(27) Ghosal, D. N.; Mukherjee, S. K. *J. Indian Chem. Soc.* **1972**, *49*, 569–572.
(28) Hayes, M. H. B.; Pick, M. E.; Toms, B. A. *J. Colloid Interface Sci.* **1978**, *65*, 254–265.
(29) Narine, D. R.; Guy, R. D. *Clays Clay Miner.* **1981**, *29*, 205–212.
(30) Karickhoff, S. W.; Brown, D. S. *J. Environ. Qual.* **1978**, *7*, 246–252.
(31) Brown, D. S.; Combs, G. *J. Environ. Qual.* **1985**, *14*, 195–199.
(32) Bayer, O.; Hoffman, H.; Ulbricht, W. In *Surfactants and Solutions*; Mittal, K. L., Bothorel, P., Eds.; Plenum: New York, 1986; Vol. 4, pp 343–348.
(33) Ford, W. P. J.; Ottewill, R. H.; Parreira, H. C. *J. Colloid Interface Sci.* **1966**, *21*, 522–533.
(34) Fuller, C. C.; Davis, J. A. *Geochim. Cosmochim. Acta* **1987**, *51*, 1491–1502.
(35) Hassett, J. J.; Means, J. C.; Banwart, W. L.; Wood, S. G. *Sorption Properties of Sediments and Energy-Related Pollutants*; EPA-600/3-80-041; U.S. Environmental Protection Agency; National Technical Information Service: Springfield, VA, 1980.
(36) van Olphen, H., Fripiat, J. J., Eds. *Data Handbook for Clay Materials and Other Non-Metallic Minerals*; Permagon: New York, 1979.
(37) Gschwend, P. M.; Wu, S.-C. *Environ. Sci. Technol.* **1985**, *19*, 90–69.
(38) Travis, C. C.; Etnier, E. L. *J. Environ. Qual.* **1981**, *10*, 8–17.
(39) Adamson, A. W. *Physical Chemistry of Surfaces*, 3rd ed.; Wiley: New York, 1976; p 389.
(40) Westall, J. In *Geochemical Processes at Mineral Surfaces*; Davis, J. A., Hayes, K. F., Eds.; A Symposium Series 323; American Chemical Society: Washington DC, 1986; pp 54–78.
(41) Westall, J. In *Aquatic Surface Chemistry*; Stumm, W., Ed., Wiley: New York, 1987; pp 3–32.
(42) Westall, J. C. FITEQL: A Computer Program for Determination of Chemical Equilibrium Constants from Equilibrium Data; Version 1.2. Report 82-01; Oregon State University: Corvallis, OR, 1982.
(43) Westall, J. C. FITEQL: A Computer Program for Determination of Chemical Equilibrium Constants from Equilibrium Data; Version 2.0. Report 82-02; Oregon State University: Corvallis, OR, 1982.
(44) Fuerstenau, D. W.; Healy, T. W.; Somasundaran, P. *Trans. Metall. Soc. AIME* **1964**, *229*, 321–325.
(45) Chen, H.; Zhang, W.; Collier, J. M.; Brownawell, B. J.; Westall, J. C., manuscripts in preparation.
(46) Tanford, C. *The Hydrophobic Effect: Formation of Micelles and Biological Membranes*; Wiley-Interscience: New York, 1980; pp 96–105.
(47) Hand, V. C.; Williams, G. K. *Environ. Sci. Technol.* **1987**, *21*, 370–373.

Received for review June 5, 1989. Accepted March 27, 1990. Although the research described in this article has been funded in part by the United States Environmental Protection Agency through assistance agreement CR-814501 to Oregon State University, it has not been subjected to Agency review and therefore does not necessarily reflect the views of the Agency and no official endorsement should be inferred. The grant was administered through the R. S. Kerr Environmental Research Laboratory in Ada, OK.

Structure–Activity Relationships for Biodegradation of Linear Alkylbenzenesulfonates

Robert J. Larson

Environmental Safety Department, The Procter and Gamble Company, Ivorydale Technical Center, Cincinnati, Ohio 45217

■ The kinetics of mineralization of uniformly ^{14}C-ring-labeled linear alkylbenzenesulfonate (LAS) were studied in river water and sediments for a series of pure chain-length homologues and phenyl isomers containing 10–14 carbon atoms in the alkyl chain. Degradation of LAS in river water and sediments showed little variation among different homologues and isomers. Half-lives for mineralization of the benzene ring varied a maximum of 2-fold (15–33 h) and were not significantly different in either water or sediments. Competition experiments indicated that degradation of long- and short-chain homologues occurred independently and was not significantly affected by high concentrations of a competing homologue.

Introduction

Linear alkylbenzenesulfonate (LAS), e.g., **1**, is an anionic surfactant that has been widely used by the detergent industry in laundry and cleaning products. It was initially developed in the mid-1960s as a readily biodegradable replacement for branched-chain alkylbenzenesulfonates (ABS). LAS is currently the major surfactant used in the United States, Western Europe, and Japan, with annual production volumes of approximately 1.4 million tons (*1*).

Since its introduction, the biodegradability of LAS has been studied in a variety of screening test systems (*2–6*).

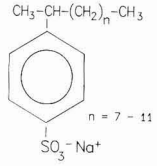

1

Laboratory studies have also been conducted to characterize the metabolic pathway for LAS biodegradation and the influence of LAS structure on biodegradation rates (*1*, *7*). Many of these studies, however, have utilized relatively artificial experimental conditions (e.g., high LAS concentrations, synthetic nutrient media, pure cultures of microorganisms), which do not simulate the conditions found in natural environmental systems. Much of the work has also focused on primary degradation of mixtures of LAS homologues. Relatively little information is available on the kinetics of ultimate biodegradation (mineralization to CO_2) of the LAS benzene ring. This latter step, however, is quite important, since it represents the final step in the LAS biodegradation pathway prior to complete mineralization (*7*).

This paper reports the results of studies to characterize the kinetics of biodegradation of a range of pure chain

Table I. Characterization Data for River Water and Sediment Samples Used in Biodegradation Studies

parameter	value[a]
River Water	
pH	(7.8–8)
total organic carbon, mg/L	(3–5)
total suspended solids, mg/L	(8–160)
hardness (as $CaCo_3$), mg/L	(279–468)
total viable organisms, CFU/mL	(0.8–2.4 × 10^4)
Sediment	
total organic carbon, %	1.0
sand, %	2.2
silt, %	76.8
clay, %	21.0
cation-exchange capacity, mequiv/100 g	15.4

[a] Numbers in parentheses represent range of values for all samples tested.

length LAS homologues in river water and river water/sediment systems. The LAS homologues, which contained 10–14 carbon atoms in the alkyl chain, were uniformly radiolabeled with ^{14}C in the benzene ring. The specific objectives of the study were 3-fold: (1) to characterize the kinetics of mineralization of the LAS benzene ring in river water/sediment systems at microgram per liter concentrations, which approximate realistic environmental levels; (2) to determine the effect of alkyl chain length and phenyl position (point of attachment of the benzene ring to the alkyl chain) on the rate and extent of LAS mineralization; and (3) to determine the effect of high concentrations of suspended solids and competing homologues on the rate and extent of LAS mineralization.

Experimental Section

Materials. A total of 10 different homologues of linear sodium alkyl[U-^{14}C]benzenesulfonate were synthesized by New England Nuclear. Radiochemical purities, as determined by thin-layer chromatography and gas–liquid chromatography with radiochemical detection, were >95%. Specific activities ranged from 12 to 28 μCi/mg (4.2–13.4 mCi/mmol). For five of the LAS materials tested, the alkyl chains were attached to the benzene ring at a single site. These included a C_{10}-2-phenyl LAS, C_{10}-5-phenyl LAS, C_{12}-2-phenyl LAS, C_{12}-6-phenyl LAS, and a C_{14}-2-phenyl LAS. The remaining five materials (C_{10}, C_{11}, C_{12}, C_{13}, and C_{14} LAS) contained a mixture of phenyl distributions typical of commercial LAS. More detailed information on the exact phenyl composition and physiochemical properties of the LAS materials used in testing has been reported previously (*8*).

River water and bottom sediments used in biodegradation studies were collected over a 2-year period from Rapid Creek, a first-order stream located in southwestern South Dakota. A tributary of the Cheyenne River, Rapid Creek has been the subject of comprehensive modeling and monitoring studies to characterize the fate of LAS in aquatic ecosystems (*9*). Water and sediment samples were collected approximately 7 km downstream from the Rapid City municipal wastewater plant, a small (~8 million gal/day) trickling filter facility treating predominantly domestic wastewater. Samples were shipped at 4 °C in 1-gal plastic containers and used for testing within 24 h of collection. Pertinent characterization data for water and sediment samples used in biodegradation studies are given in Table I.

Biodegradation Assays. Biodegradation assays were conducted in a closed flow-through shake flask system as previously described (*10*). Briefly, various concentrations of LAS were added to duplicate or triplicate 2-L Erlenmeyer flasks containing, 1 L of river water or river water with added bottom sediments (1000 mg/L). The [^{14}C]LAS concentrations added to water (5–500 μg/L) and sediment samples (100 μg/g) are in the range of concentrations measured in natural aquatic and benthic environments (*11*). Test flasks were incubated at 24 °C in a constant-temperature room (±2 °C) and constantly agitated on a rotary platform shaker. The head space of test flasks was continuously aerated with CO_2-free air and $^{14}CO_2$ was trapped in external base traps containing 100 mL of 1.5 N KOH. At various intervals, 10-mL aliquots were taken by syringe from each flask and filtered (0.2 μm) to remove particulate matter. The filters were washed with 5 mL of deionized water or 50% ethanol and the 15-mL filtrate was added to 125-mL biometer flasks and acidified with approximately 1 mL of concentrated HCl. After acidification, the $^{14}CO_2$ present in solution as radiolabeled carbonate or bicarbonate was released and trapped in 2 mL of 1.5 N KOH contained in the biometer sidearm. Aliquots from the acidified filtrate (10 mL) and the washed filters were then counted by standard liquid scintillation techniques to quantitate the amount of radiolabel in solution and in microbial biomass, respectively. Aliquots from the biometer sidearm and external base traps (1 mL) were also assayed to determine the amount of $^{14}CO_2$ produced and complete the mass balance of radiolabel at a specific sampling time. Correction factors were used to normalize all disintegrations per minute data to a 10-mL basis (*10*). Biodegradation studies were terminated by the addition of 1.0 mL of concentrated HCl to the test flask. After acidification and quantitation of nonvolatile and volatile radioactivity for mass balance purposes, aliquots (50 mL) from water and sediment/water samples were collected, extracted twice with ethyl ether (60 mL), and evaporated to dryness. The ethyl ether extracts were resuspended in scintillation cocktail and counted to determine the amount of radiolabel (expressed as the percentage of initial ^{14}C activity added) present with the same solubility characteristics as parent LAS.

Data for percent biodegradation as a function of time (expressed as either the amount of ^{14}C converted to $^{14}CO_2$ or the amount of ^{14}C remaining in solution) were analyzed by nonlinear regression models to estimate the pseudo-first-order rate constants for mineralization or removal, normalized for the extent of biodegradation observed. All parameter estimates and their associated 95% confidence intervals were obtained by least-squares analysis using iterative techniques, as previously described (*12*). Half-life ($t_{1/2}$) values (h) for mineralization or removal from solution were calculated from the corresponding pseudo-first-order rate constants (k_1) by the relationship $t_{1/2} = (0.693/k_1) \times 24$.

Results

Biodegradation Kinetics. Typical results of time-course studies to characterize the rate and extent of mineralization of LAS homologues and phenyl isomers in Rapid Creek river water and sediments are shown in Figure 1. The specific data presented are for C_{12}-2-phenyl LAS, tested at two initial concentrations in river water, 10 and 100 μg/L. Similar results, however, were obtained in both water and sediment systems for the other LAS materials tested. In general, final mass balances of radioactivity were high and consistent in different experiments. The overall mean mass balance across 12 separate studies (± standard deviation) was 104 ± 6%, with a range of 96–112%.

In general, $^{14}CO_2$ production and removal of ^{14}C activity from solution exhibited comparable kinetic patterns in all

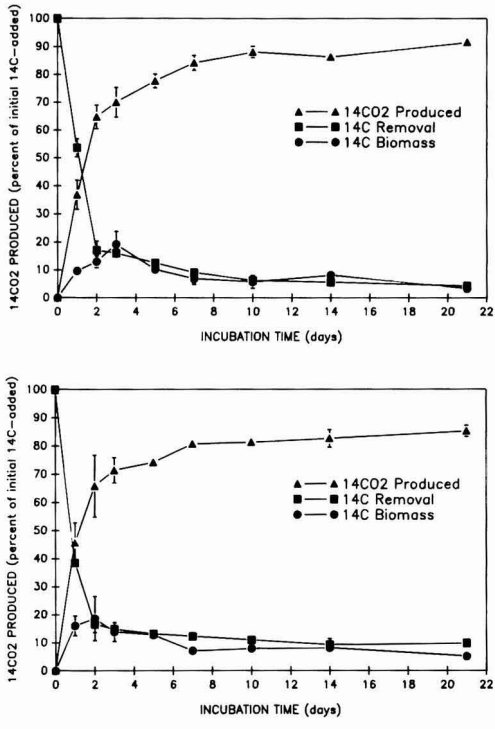

Figure 1. Kinetics of biodegradation of C_{12}-2-phenyl LAS in river water at initial concentrations of 100 (upper) and 10 μg/L (lower). Procedures for measuring $^{14}CO_2$ production, ^{14}C removal, and incorporation of ^{14}C into biomass are described in the Experimental Section. The error bars represent 1 standard deviation from triplicate flasks.

experiments. Lag phases for biodegradation were not observed, and both mineralization and removal could be adequately described by a simple pseudo-first-order kinetic model. The first-order rate constants for mineralization and removal were in good agreement and did not vary significantly ($P < 0.05$) across the 10-fold concentration range tested. The amount of $^{14}CO_2$ produced during LAS degradation consistently reached relatively high values, corresponding to approximately 70–90% of the initial ^{14}C activity added. The remaining ^{14}C activity was equally divided between soluble and biomass fractions, with less than 2% of the residual radioactivity being associated with fractions having the same solubility characteristics as parent LAS.

LAS Homologues and Phenyl Isomers—River Water. Rate constants for biodegradation of LAS homologues and phenyl isomers in Rapid Creek river water are given in Table II. Figure 2 presents an overall summary of the time-course data used to generate the kinetic information given in this table. Plotted are mean values for $^{14}CO_2$ production at a specific time point, averaged across all experiments for the isomers and homologues tested. The error bars represent 1 standard deviation.

In general, rate constants for mineralization of the various LAS homologues and phenyl isomers in river water showed little variation as a function of the length of the alkyl chain or the point of attachment of the benzene ring to the chain. The mean rate constant for mineralization of individual homologues, determined over a 100-fold concentration range (5–500 μg/L) and averaged across five different experiments, was 0.70 day^{-1} with a relative standard deviation (RSD) of 16%. The average half-life

Table II. Kinetic Parameters for Biodegradation of LAS Homologues and Phenyl Isomers in River Water

compound	concn, μg/L	k_1, CO_2 productn, day^{-1}	95% CI
C_{10} LAS	10	0.71	0.54–0.87
	100	0.53	0.42–0.64
	10	0.82	0.59–1.05
	100	0.93	0.75–1.11
C_{11} LAS	10	0.76	0.38–1.13
	100	0.66	0.31–1.00
C_{12} LAS	10	0.68	0.16–1.20
	100	0.77	0.17–1.37
	10	0.81	0.13–1.50
	100	0.79	0.36–1.22
	10	0.61	0.26–0.96
	100	0.62	0.30–0.95
	5	0.60	0.26–0.93
	50	0.77	0.29–1.25
	500	0.74	0.29–1.20
C_{13} LAS	10	0.78	0.22–1.33
	100	0.70	0.40–1.00
C_{14} LAS	10	0.61	0.32–0.90
	100	0.62	0.44–0.79
	10	0.50	0.33–0.68
	100	0.62	0.27–0.97
		0.70 ± 0.11	
C_{10}-2-phenyl LAS	10	1.08	0.19–1.98
	100	0.71	0.48–0.94
C_{10}-5-phenyl LAS	10	0.67	0.26–1.07
	100	0.90	0.75–1.05
C_{12}-2-phenyl LAS	10	0.63	0.42–0.83
	100	0.58	0.30–0.86
C_{12}-6-phenyl LAS	10	0.50	0.22–0.77
	100	*a*	
	10	0.53	0.11–0.94
	100	0.66	0.17–1.15
C_{14}-2-phenyl LAS	10	0.71	0.58–0.84
	100	0.80	0.54–1.06
		0.71 ± 0.17[b]	

[a] Not determined. [b] Mean k_1 value, ± standard deviation, across all experiments.

for mineralization of the different homologues, based on this k_1 value, was ~24 h. The mean rate constant for mineralization of individual phenyl isomers, determined over a 10-fold concentration range (10–100 μg/L) and averaged across four different experiments, was 0.71 day^{-1} with an RSD of 24%. The average half-life for mineralization of different phenyl isomers, based on this k_1 value, was ~23 h.

The low variation in degradation rates for the different LAS homologues is graphically illustrated in Figure 2, which presents single curves for mineralization of the five homologues and isomers as a function of time. Across all experiments, RSD values (error bars) at a specific sampling time generally varied ~15%, with a maximum variation of 40% and a minimum variation of 9%. This range of RSD values is relatively small, given that it reflects a number of sources of variability including different river water samples, different LAS materials, and different LAS concentrations.

LAS Homologues—River Water + Sediment. Rate constants for biodegradation of LAS homologues in Rapid Creek river water containing 1000 mg/L bottom sediments are given in Table III. Figure 3 presents an overall summary of time course data used to generate the kinetic information given in this table. Plotted are mean values for $^{14}CO_2$ production as a function of time for all five homologues tested concurrently in a single experiment at an initial LAS concentration of 100 μg/g of dry sediments.

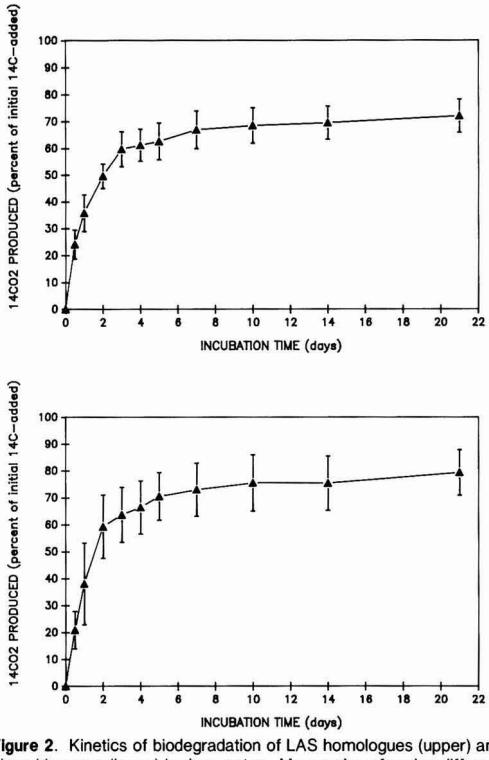

Figure 2. Kinetics of biodegradation of LAS homologues (upper) and phenyl isomers (lower) in river water. Mean values for nine different experiments are plotted and the error bars represent 1 standard deviation.

Table III. Kinetic Parameters for Biodegradation of LAS Homologues in River Sediments

compound[a]	amt sorbed,[b] %	k_1, CO_2 productn, day^{-1}	95% CI
C_{10} LAS	5.2	0.89	0.21–1.57
C_{11} LAS	13.8	0.79	0.27–1.31
C_{12} LAS	31.3	0.86	0.67–1.06
		0.76	0.34–1.18
C_{13} LAS	62.7	0.89	0.17–1.61
C_{14} LAS	77.0	0.72	0.55–0.89
		0.82 ± 0.07[c]	

[a] Initial concentration of LAS homologue, 100 μg/g of dry sediment. [b] At equilibrium (<3h). [c] Mean k_1 value, ± standard deviation, across all experiments.

Overall, the kinetics of biodegradation of LAS homologues in river water containing high levels of suspended sediments were comparable to degradation results observed for homologues and phenyl isomers in river water containing low levels of suspended solids. Biodegradation kinetic measurements were not affected by the kinetics of sorption, since sorption equilibria were rapid and required less than 3 h (*8*). Rate constants for degradation of individual homologues in sediment/water systems showed little variation as a function of alkyl chain length. The mean rate constant for degradation in sediment/water systems (0.82 day^{-1}) was somewhat higher than in river water, but was not significantly different ($P < 0.05$) for the range of LAS materials tested. The average half-life for mineralization of the different homologues in the presence of sediments, based on the mean rate constant, was ~20. Figure 3 graphically summarizes the relatively low variation in sediment degradation rates as a function of LAS chain length. The RSD values (error bars) for all five homologues at a specific sampling time typically varied less than 10%, with a maximum variation of 23% and a minimum variation of 2.5%.

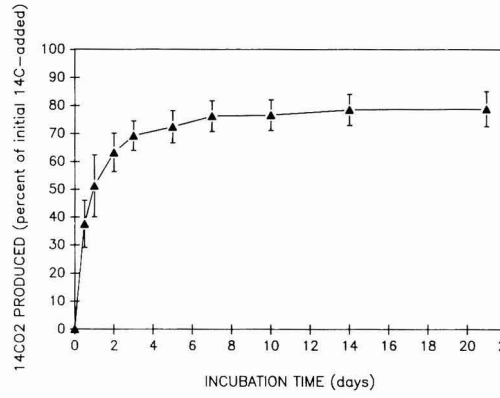

Figure 3. Kinetics of biodegradation of LAS homologues in river water/sediment systems. Mean values for two different experiments are plotted and the error bars represent 1 standard deviation.

Competition Experiments. Table IV summarizes the results of competition studies to characterize the kinetics of degradation of short-chain (C_{10}) and long-chain (C_{14}) LAS homologues in the presence of various concentrations of a competing homologue. Radiolabeled C_{10} or C_{14} LAS were incubated in the presence of equimolar and 10-fold molar excess concentrations of the other unlabeled C_{14} or C_{10} homologue, respectively. The rate and extent of $^{14}CO_2$ production and removal of ^{14}C activity from solution were then followed as a function of time to determine the effect of one competing homologue on the kinetics of biodegradation of the other.

As Table IV indicates, degradation of the labeled C_{10} and C_{14} LAS materials was not significantly affected by the competing unlabeled homologue, even when the latter was present at 10-fold molar excess. The rate and extent of

Table IV. Kinetics of Biodegradation of LAS Homologues in Competition Experiments

^{14}C homologue	^{12}C homologue	concn,[a] mole ratio	k_1, $^{14}CO_2$ productn, day^{-1}	95% CI	extent of $^{14}CO_2$ productn,[b] %	K_1, ^{14}C removal, day^{-1}	95% CI
C_{10} LAS		1	0.72	0.42–1.03	79.8 (0.5)	1.15	0.70–1.60
C_{10} LAS	C_{14} LAS	1:1	0.69	0.46–0.92	77.6 (2.9)	0.89	0.43–1.36
C_{10} LAS	C_{14} LAS	1:10	0.69	0.43–0.95	76.6 (1.2)	0.58	0.33–0.83
C_{14} LAS		1	0.61	0.43–0.78	82.6 (1.3)	0.85	0.68–1.03
C_{14} LAS	C_{10} LAS	1:1	0.56	0.36–0.76	80.7 (0.4)	0.65	0.52–0.79
C_{14} LAS	C_{10} LAS	1:10	0.54	0.29–0.79	82.5 (0.3)	0.90	0.72–1.08

[a] Initial concentration of ^{14}C homologue, 100 μg/L. [b] As percent of initial ^{14}C added at end of experiment (day 16). The values in parentheses represent 1 standard deviation ($n = 3$).

$^{14}CO_2$ production were not significantly different for either material, ($P < 0.05$), and good agreement between degradation results was obtained both within and across treatment groups. Similar results were obtained when removal of ^{14}C activity from solution was used to monitor biodegradation activity. Somewhat larger differences in removal rate constants were observed for the C_{10} and C_{14} homologues in the presence of competing homologue. These differences indicate that high concentrations of the longer chain length homologues may have minor effects on removal of shorter chain length materials. In general, both mineralization and removal rate constants remained relatively constant across all treatment groups. The maximum variation was approximately 2-fold, but typical variations ranged from 4 to 24%.

Discussion

Previous research to characterize the effect of LAS structure on biodegradation of LAS homologues and phenyl isomers has focused almost exclusively on the biotransformation or primary degradation of LAS mixtures (see refs 1 and 7 for thorough reviews). This work has resulted in the formulation of the "distance principle" [first proposed by Swisher (*7*)], which states that primary degradation of LAS homologues and phenyl isomers increases with the length of the alkyl chain, or as the location of the benzenesulfonic group assumes a more terminal position on the alkyl chain. Although preferential degradation of the longer chain lengths and more "outside" phenyl isomers has been observed in several studies, there are notable exceptions to this general rule. Painter and Zabel (*1*) have indicated that the factors controlling relative degradation rates appear to be complex and variable and include the concentration of the LAS homologue or isomer tested, potential inhibitory effects of LAS, presence of competing homologues or isomers, concentrations of suspended solids, and degree of acclimation of the microbial inoculum.

To avoid many of the difficulties cited above, which have hindered past experimental efforts to thoroughly characterize the effect of LAS structure on biodegradation rates, the present studies were conducted utilizing a series of pure chain length LAS homologues and phenyl isomers uniformly radiolabeled with ^{14}C in the benzene ring. The use of ^{14}C-labeled materials allowed degradation measurements to focus on mineralization of the benzenesulfonic moiety, which is the final biodegradation step prior to complete LAS degradation. It also allowed LAS to be tested at microgram per liter concentrations, which approximate realistic environmental levels (*11*). River sediments were included in some studies to determine the effects of suspended solids on degradation rates, and competition experiments were also conducted to determine if degradation rates for one homologue could be adversely affected by high concentrations of a competing homologue. Lastly, all degradation experiments were conducted with river water and sediment samples collected from a natural stream ecosystem with a prior history of continuous exposure to LAS in wastewater effluent. This was done to maximize the potential for obtaining a realistic assemblage of microorganisms already acclimated to LAS and to minimize potential inhibitory effects of LAS on biodegradation activity.

Based on the results of the current studies, neither the length of the alkyl chain nor the point of attachment of the benzenesulfonic group to this chain has significant effects on the rate or extent of LAS degradation in river water/sediment systems. Half-lives for mineralization of the benzene ring varied a maximum of 2-fold (15–33 h) over the range of homologues and isomers tested. These variations were not significantly different when averaged across all experiments. The amount of $^{14}CO_2$ produced during biodegradation assays consistently reached high values (averaging ~80% of the initial radioactivity added), and less than 2% of the residual radioactivity was extractable into solvents specific for parent LAS. The remaining radioactivity was equally divided between soluble and biomass fractions, presumably as transient biodegradation intermediates and cellular components, respectively.

Several recent investigators have also noted a poor correlation between LAS structure and mineralization rates. Ventullo et al. (*13*) found that mineralization rates for a series of [^{14}C]LAS homologues in activated sludge were independent of homologue distribution over a range of alkyl chain lengths (C_{10}–C_{14}). Ward and Larson (*14*) reported similar results in biodegradation studies conducted in sludge-amended surface soils. They found that mineralization rates for [^{14}C]LAS homologues were unaffected by alkyl chain length over a range of C_{10}–C_{14}. Biodegradation half-lives averaged ~20 days across all soil samples tested and were comparable to values obtained for naturally occurring materials typically present in soil environments. Waters et al. (*15*), in an extensive monitoring study conducted in the United Kingdom, also found no preferential degradation of LAS homologues in sludge-amended surface soils. Using HPLC analysis to quantitate specific homologues, they reported half-lives for LAS degradation of 7–22 days. Similar results were obtained by Abe (*16*), who studied the biodegradation and removal of LAS in soil perfusion columns. He found that rates of LAS degradation were independent of homologue distribution and paralleled the biodegradation of total organic carbon in the soil.

Degradation rates for individual LAS homologues were unaffected by the presence of high levels of suspended solids. Mean rate constants in river water containing low levels of suspended solids (0.71 day^{-1}) were comparable to values in river water containing up to 1000 mg/L suspended solids (0.82 day^{-1}), despite the fact significant concentrations of the longer chain length homologues (C_{12}, C_{13}, C_{14}) were bound to particulate matter at the 1000 mg/L level (Table III). The similarity in biodegradation rates in the presence and absence of sediments is probably due to the reversible nature of LAS sorption. Hand and Williams (*8*) found that sorption and desorption of LAS were rapid (<3–<8 h, respectively) and almost completely reversible for both short- (C_{10}) and long- (C_{14}) chain LAS homologues in single-step desorption experiments. This rapid sorption/desorption would allow individual homologues to be degraded equally well in either the bound or unbound form, with degradation rates being independent of sediment levels as long as the kinetics of sorption/desorption were more rapid than the kinetics of biodegradation.

In this study, the kinetics of degradation of short- (C_{10}) and long- (C_{14}) chain LAS homologues were relatively unaffected by the presence of high concentrations of a competing homologue. Previous work by Hand and Williams (*8*) also found that sorption of C_{10} and C_{14} LAS homologues occurred independently below saturation levels and was unaffected by high concentrations (10-fold molar excess) of a competing homologue. Taken together, these results indicate that degradation of individual homologues proceeds independently, due either to specific sorption sites for specific homologues or to a large excess of similar sites. Either mechanism is possible based on the data currently available. Neither mechanism, however, should result in adverse effects on biodegradation rates as long

as the kinetics of sorption are not rate-limiting.

Conclusions

This study has focused on the kinetics of biodegradation (mineralization to CO_2) of 10 ^{14}C-ring-labeled LAS homologues and phenyl isomers in river water and river water/sediment systems at concentrations approximating realistic environmental levels. The homologues and isomers tested bracket the range of materials present in commercial LAS formulations. Based on the results of this study, the following conclusions can be drawn:

(1) Mineralization of LAS homologues and phenyl isomers was extensive (~80%) and followed apparent first-order kinetics in river water and river water/sediment systems. Half-lives for mineralization of the benzene ring ranged from 15 to 33 h.

(2) The rate and extent of mineralization were not significantly affected by the length of the alkyl chain or the point of attachment of the benzene ring to the alkyl chain (phenyl position).

(3) Mineralization rates for individual homologues were not adversely affected by the presence of high concentrations of suspended sediments or competing homologues and biodegradation appeared to occur independently for different homologues.

Acknowledgments

My appreciation is expressed to Daniel H. Davidson for completing the technical aspects of this work.

Registry No. C_{10} LAS, 2627-06-7; C_{11} LAS, 20466-34-6; C_{12} LAS, 2211-98-5; C_{13} LAS, 14356-40-2; C_{14} LAS, 1797-33-7; C_{10}-2-phenyl LAS, 73602-65-0; C_{10}-5-phenyl LAS, 73602-67-2; C_{12}-2-phenyl LAS, 2211-99-6; C_{12}-6-phenyl LAS, 2212-52-4; C_{14}-2-phenyl LAS, 13419-31-3.

Literature Cited

(1) Painter, H. A.; Zabel, T. F. *Review of the Environmental Safety of LAS*; Co 1659-m/1/EV 8658; Water Research Center: Medmenham, UK, 1988; p 1.
(2) Boatman, R. J.; Cunningham, S. C.; Ziegler, D. A. *Environ. Toxicol. Chem.* **1986**, *5*, 233–243.
(3) Gerike, P.; Fischer, W. K. *Ecotoxicol. Environ. Saf.* **1979**, *3*, 159–173.
(4) Gerike, P.; Fischer, W. K. *Ecotoxicol. Environ. Saf.* **1981**, *5*, 45–55.
(5) Larson, R. J. *Appl. Environ. Microbiol.* **1979**, *38*, 1153–1161.
(6) Larson, R. J. *Residue Rev.* **1983**, *85*, 159–171.
(7) Swisher, R. D. *Surfactant Biodegradation*; Marcel Dekker, Inc.: New York, 1987.
(8) Hand, V. C.; Williams, G. K. *Environ. Sci. Technol.* **1987**, *21*, 370–373.
(9) Games, L. M. In *Aquatic Toxicology and Hazard Assessment: Sixth Symposium*; ASTM STP 802; Bishop, W. E., Cardwell, R. D., Heidolph, B. B., Eds.; American Society for Testing and Materials: Philadelphia, PA, 1983; pp 282–299.
(10) Larson, R. J.; Payne, A. G. *Appl. Environ. Microbiol.* **1981**, *41*, 621–627.
(11) De Henau, H.; Matthijs, E.; Hopping, W. D. *Int. J. Environ. Anal. Chem.* **1986**, *26*, 279–293.
(12) Larson, R. J. In *Current Perspectives in Microbial Ecology*; Klug, M. J., Reddy, C. A., Eds.; American Society for Microbiology: Washington, DC, 1984; pp 677–688.
(13) Ventullo, R. M.; Larson, R. J.; Beba, A. D., in press.
(14) Ward, T. E.; Larson, R. J. *Ecotoxicol. Environ. Saf.* **1989**, *17*, 119–130.
(15) Waters, J.; Holt, M. S.; Matthijs. *Tenside, Surfactants, Deterg.* **1989**, *26*, 129–135.
(16) Abe, S. *Nippon Kagaku Kaishi* **1984**, *9*, 1465–1470.

Received for review August 28, 1989. Revised manuscript received February 22, 1990. Accepted March 26, 1990.

Modeling the Bioconcentration of Organic Chemicals in Plants

Stefan Trapp,*,† Michael Matthies,† Irene Scheunert,‡ and Eva M. Topp§

Projektgruppe Umweltgefährdungspotentiale von Chemikalien, Institut für Bodenökologie, and Institut für Ökologische Chemie, Gesellschaft für Strahlen- und Umweltforschung, Ingolstädter Landstrasse 1, D-8042 Neuherberg, West Germany

■ Uptake of several organic chemicals by growing barley was investigated in a closed laboratory model ecosystem (volume 9.4 L). To discriminate between root and foliar uptake, the soil was divided into test soil contaminated with 2 mg/kg ^{14}C-labeled chemicals and unpolluted control soil. Air was exchanged at a rate of 10 mL/min. Concentrations of ^{14}C chemicals in air, soil, roots, and shoots and bioconcentration factors were simulated with a mathematical model based on fugacity. Bioconcentration in the plant is dependent on transfer rates and the ratio of K_{ow} and K_{oc} values. Uptake into foliage is mainly from air for chemicals with a high K_{ow} and a Henry's law constant high enough for volatilization. Chemicals with medium K_{ow} are translocated with the transpiration stream. Metabolites are also taken up. Chemicals in the roots of the barley plants reach equilibrium with the soil, whereas those in foliage are in equilibrium with the air in most cases.

Introduction

The uptake of chemicals into plants is the first step for accumulation in the terrestrial food chain. Chemicals can enter plants via roots or via foliage. Various processes of partitioning, transfer, and transformation that govern uptake have been investigated (*1–11*). Recently a theoretical model was published but not yet validated (*12*). In this paper a model based on fugacity is presented for the calculation of transfer and distribution of chemicals between soil, air, water, and plants. Laboratory experiments with radiolabeled chemicals (*1*) support the results of the model calculation.

Experimental Section

The aim of the laboratory experiments was to yield data on the material balance of chemicals in a soil–water–plant–air model ecosystem including uptake by plants, volatilization, transformation in plants and soil, and the formation of unextractable residues.

Model Ecosystem. The composition of the soil was as follows: particle size distribution, clay (<2 μm) 33.6%, silt (2–63 μm) 27.4%, sand (0.06–2 mm) 32.4%, coarse matter (>2 mm) 6.6%; organic carbon content, 2.06%; soil water content, 30 vol %; pH 6.4 (soil properties measured with methods described in ref 13). The plant was barley (*Hordeum vulgare*). Uptake of chemicals by plants was determined by short-term studies in a closed aerated laboratory apparatus as described elsewhere (*10*). To

† Projektgruppe Umweltgefährdungspotentiale von Chemikalien.
‡ Institut für Bodenökologie.
§ Institut für Ökologische Chemie.

 0013-936X/90/0924-1246$02.50/0

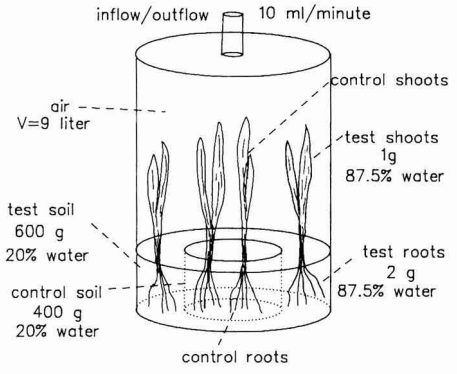

Figure 1. Properties of the model ecosystem.

Table I. Radiopurities of the Test Compounds[a]

chemical	position of the ^{14}C label	radiopurity, %
atrazine	ring at C-2	99.8
triCB	benzene ring	98
tetraCB	benzene ring	>99
dieldrin	chlorinated ring	>99
PCB	dichlorinated ring	>99
HCB	benzene ring	>99
DDT	benzene rings	>99

[a] Abbreviations: triCB, 1,2,4-trichlorobenzene; tetraCB, 1,2,3,5-tetrachlorobenzene; PCB, 2,2′,4,4′,6-pentachlorobiphenyl; HCB, hexachlorobenzene.

discriminate between root and foliar uptake, the soil was divided into contaminated test soil and control soil. A 400-g sample of the control soil was filled into a Petri dish (~11 cm in diameter and 8 cm high) and placed in a desiccator (diameter ~30 cm, volume 9.4 L). Around the dish was placed 600 g of the test soil containing 2 mg/kg (dry weight) ^{14}C-labeled chemicals. Ten barley seeds were plated in the treated test soil to determine the total uptake via both roots and leaves. The untreated control soil in the dish was covered with a plate containing 10 holes where 10 barley grains were seeded. Thus, transfer of chemicals to control soil from the air and hence uptake by control plants from the soil was reduced. Air was pumped through the apparatus at a low rate (10 mL/min). All experiments were carried out in replications (Table III). After 1 week, the desiccator was opened and samples were taken for analysis. The properties of the model ecosystem are shown in Figure 1.

Chemicals. ^{14}C-labeled compounds were either commercially purchased or newly synthesized (*10*, *11*) and purified to radiopurities between 98 and 99.8% (Table I). The ^{14}C-labeled chemicals were mixed with commercially available nonradioactive compounds and solved in acetone by using ultrasound. Before treatment of the soil, the test system was cooled to minimize losses by volatilization. A 500-μL aliquot of the radioactive solution was applied with a Hamilton syringe and mixed into the test soil with a spatula. The application rate was ~1 μCi per test. Altogether, 16 substances were tested in the system (*1*). For the simulations, chemicals with slow conversion rates were selected. The chemicals studied and their physicochemical properties are listed in Table II. Substances were excluded when accurate physicochemical data were not available.

Analytical Methods. Concentrations of ^{14}C-labeled organic compounds in the air of the apparatus were determined by counting ^{14}C trapped in tubes containing

Table II. Physicochemical Properties of the Investigated Chemicals[a]

chemical	log K_{ow}	log K_{oc}	K_{AW}	MW
atrazine	2.71 (*14*)	2.33 (*14*)	8.05×10^{-9}	215.7 (*1*)
triCB	3.98 (*16*)	3.35[b]	0.17 (*17*)	181.5 (*1*)
tetraCB	4.65 (*16*)	3.84[b]	0.1 (*17*)	215.8 (*1*)
dieldrin	5.48 (*18*)	4.44[b]	4.4×10^{-4} (*17*)	380.9 (*1*)
PCB	5.92[c]	4.75[b]	0.0076[d]	326.4 (*1*)
HCB	5.47 (*16*)	4.43[b]	0.054 (*21*)	284.8 (*1*)
DDT	6.19 (*22*)	5.14 (*22*)	2.14×10^{-3} (*17*)	354.5 (*1*)

[a] log K_{ow} is the logarithm of the partition constant between *n*-octanol and water, log K_{oc} is the logarithm of the partition constant between soil organic carbon and water, $K_{AW} = H/(RT)$ and is the dimensionless partition constant between air and water, and MW is the molecular weight. [b] Estimated; ref 22: log K_{oc} = 0.72 log K_{ow} + 0.49. [c] Value for the isomer 2,2′,4,5,5′-PCB (*19*). [d] Value for Aroclor 1254 (*20*).

ethylene glycol monomethyl ether. The glass walls of the apparatus were rinsed with methanol and acetone. The radioactivity of these rinsing solutions was also determined and added to that of the ethylene glycol monomethyl ether. $^{14}CO_2$, which had been formed in small amounts by biomineralization of the chemicals, was trapped in separate tubes containing Carbosorb/Permafluor V 8:12 (Packard). Radioactivity was determined in a liquid scintillation counter (Berthold/Frieseke Betaszint BF 8000) by use of a dioxane-based scintillation liquid. The sum of volatile organic ^{14}C was related to the volume of air passing through the apparatus during the experiment.

Total ^{14}C residues in the soil were determined after Soxhlet extraction of samples with methanol for 48 h. Plants were homogenized with an Ultra Turrax prior to Soxhlet extraction. Radioactivity in extracts was determined in a liquid scintillation counter by use of a dioxane-based scintillation liquid. Unextractable ^{14}C in soil and plants was determined in an automatic sample oxidizer Tri-Carb B 306 (Packard). Thin-layer chromatography was used for the separation and quantification of parent compounds and of conversion products, except for 1,2,4-trichlorobenzene. For this compound, the portion of unchanged parent compound was measured by gas chromatography after cleanup by various partition steps. Conversion ratios were expressed as percent conversion products of total ^{14}C in each sample.

Theoretical Section

The Fugacity Concept. The model for the simulation of the test ecosystem is based on the fugacity concept (*23*, *24*), in which

$$C = fZ \tag{1}$$

where C is the concentration (mol/m^3), f is the fugacity (Pa), and Z is the capacity (mol·m^{-3}·Pa^{-1}) of the chemical.

Capacities of the Compartments. The model system is divided into the compartments air, test soil, test roots, and test shoots, and control soil, control roots, and control shoots (Figure 1). Every compartment has its own capacity Z for a chemical (control soil and control plants have the same properties as test soil and test plants). The Z values are computed as follows.

Air. The capacity of air is the same for all chemicals:

$$Z_A = 1/(RT) \tag{2}$$

in which R is the universal gas constant (J·mol^{-1}·K^{-1}) and T is the temperature (K). Z_A is 4.1×10^{-4} for 20 °C.

Soil. Chemicals may sorb to the organic carbon in the soil, dissolve in the soil solution, or partition into the soil air:

$$Z_S = \rho K_{oc}[C_{org}]Z_w + \theta_W Z_w + \theta_A Z_A \quad (3)$$

where ρ is the bulk density of the soil (1.5 g/cm^3), K_{oc} is the partition constant between soil organic carbon and water (cm^3/g), $[C_{org}]$ is the organic carbon content of the soil (0.0206 g/g of dry soil), θ_W is the volumetric water content of the soil (30 vol %), θ_A is the air-filled pore fraction (20 vol %). Z_w is the capacity of water and is $1/H$, where H is Henry's law constant (m^3·Pa/mol).

Roots. The distribution of chemicals between barley roots and water was measured by Briggs et al. (*3*). It follows

$$Z_R = (10^{(0.77 \log K_{ow} - 1.52)} + W_R)Z_w \quad (4)$$

where W_R is the volumetric water content of the barley roots (87.5%). The first term represents the capacity of the root matrix, the second term (W_R) that for root water. The density of the plant is equal to that of water and does not appear in the equations.

Shoots. The distribution was also measured (*4*):

$$Z_{Sh} = (10^{(0.95 \log K_{ow} - 2.05)} + W_{Sh})Z_w \quad (5)$$

with W_{Sh} is the volumetric water content of the barley shoots (87.5%). This distribution equation can also be derived from *thermodynamic considerations*. Assuming that the partitioning of a chemical between lipid and water is similar to that between *n*-octanol and water we obtain

$$Z_{Sh} = [(\text{lipid content})K_{ow} + W_{Sh}]Z_w \quad (6)$$

With a lipid content of 1% in barley shoots we can write

$$Z_{Sh} = (0.01K_{ow} + W_{Sh})Z_w \quad (7)$$

Equation 7 is nearly identical with eq 5 and can be used for all plants with known lipid and water content. An analogous equation for the distribution into roots is derived in ref 25.

Transfer between Compartments. Other important elements of the model are the transfer values between the compartments. They are also calculated by following the fugacity concept (*15*):

$$N_{ij} = D_{ij}(f_i - f_j) \quad (8)$$

in which N is the flux of chemical between two compartments (mol/s) and D_{ij} is the "conductivity" between compartments i and j (mol·s^{-1}·Pa^{-1}).

Soil–Air. Diffusion takes place in the water or air-filled pores (*15*):

$$D_{SA} = A_{SA}(DG_{eff}Z_A + DW_{eff}Z_w)/Y \quad (9)$$

in which A_{SA} is the area between soil and air (test soil–air 2.21×10^{-2} m^2); DG_{eff} is the effective diffusion constant in air pores of the soil (m^2/s), calculated as $DG_{eff} = DG\theta_A^{1.5}$; DW_{eff} is the effective diffusion constant in water pores of the soil (m^2/s), $DW\theta_W^{1.5}$; DG and DW are the binary diffusion coefficients of the chemical in air and water, respectively, and are estimated with the program DTEST (*26*); Y is the diffusion length (half soil depth, for the test soil 0.009 m). This simplification is justified only for small soil depths. For deeper soils, the transport in the soil must be considered (*27*). The resistance of the air layer is negligible here.

Soil–Roots. The chemical can enter the roots through root growth, with the water taken up by the roots (transpiration stream) and via diffusion.

When roots grow in polluted soil, they take up a part of the soil-borne chemical. It is assumed that the root tips achieve equilibrium with the soil during growth (which means that they have the same fugacity as the soil, i.e., f_R is f_S). This is taken into account in form of a mass flux N_{SR} between soil and growing roots:

$$N_{SR} = (dV_R/dt)Z_R f_S \quad (10)$$

in which dV_R/dt is the change of the root volume with time (3.3×10^{-12} m^3/s). This pathway is important in particular for substances that are immobile in soil.

Chemicals dissolved in the soil water can enter the roots with the water taken up to form the transpiration stream. The accompanying conductivity D_{TST} can be described with

$$D_{TST} = TSTZ_w \quad (11)$$

where TST is the transpiration stream in m^3/s [was not measured, so an average value of 650 L/kg of dry mass of barley was used (*28*)].

Through uptake, a chemical gradient develops in the vicinity of the roots ("deficiency zone"). For phosphorus, zones with a radius of 1.5 mm were found (*29*). Since phosphorus is a fertilizer and is preferentially taken up, this can be regarded as a maximum value for organic chemicals. Chemicals diffuse from outside the deficiency zone to the root surface. Diffusion in soil water can be neglected in this case because the movement of water taken up by roots is much faster. A solution of Fick's law for gaseous diffusion to a root or cylindrical surface is given by (*30*)

$$D_{SR} = DG_{eff}Z_A 2L\pi/\ln(r_2/r_1) \quad (12)$$

in which D_{SR} is the conductivity soil–roots, L is the length of the roots (0.1 m), r_1 is the radius of the roots (0.0003 m), and r_2 is the radius of the deficiency zone added to r_1 (0.0018 m). Water-soluble substances are preferably transported with the water stream into the roots (D_{TST} is larger), whereas chemicals with a high tendency to partition into the vapor phase rapidly diffuse into the roots (D_{SR} is larger). Transport with the transpiration stream occurs in one direction only (into the roots), whereas diffusion can occur in both directions.

Roots–Shoots. The chemical is transported with the transpiration stream. The ratio of the concentration in the transpiration stream C_{TST} to the concentration of the chemical in the external soil solution C_S was expressed by Briggs (*3*) as TSCF (transpiration stream concentration factor):

$$TSCF = C_{TST}/C_S$$

$$TSCF = 0.784 \exp[-(\log K_{ow} - 1.78)^2/2.44] \quad (13)$$

Equation 15 gives a Gaussian curve with a maximum at $\log K_{ow}$ of 1.78.

With the capacity of the soil solution and of the transpiration stream being that of water Z_w, the flux into shoots N_{RSh} can be expressed as

$$N_{RSh} = TST\,TSCFZ_W(f_S - f_{Sh}) \quad (14)$$

Air–Foliage. The transfer depends on the resistances of the air layer, the stomata, and the cuticula. An estimation of the maximum transfer velocity of 0.005 m/s is given in ref 5. This value is for pesticides with a molecular weight of 300 and can be adapted to other molecular weights:

$$D_{AF} = A_F 0.005\sqrt{300/MW}Z_A \quad (15)$$

where A_F is the area of the foliage (70.3×10^{-4} m^2).

For simplicity it is assumed that the plant's growth is linear, i.e., volumes and transfer rates change in a linear

Table III. Measured Concentrations in Plants and Soil

chemical	N^a	C_{plant}, ppm fresh			C_{soil}, ppm dry			recovery, %
		mean	max	min	mean	max	min	
DDT	2	0.875	0.89	0.86	2.16	2.20	2.12	106.6
dieldrin	2	1.24	1.37	1.11	2.075	2.10	2.05	106.95
PCB	2	2.77	2.99	2.54	2.16	2.20	2.12	105.1
HCB	4	2.21	2.43	1.99	1.88	1.93	1.85	96.4
atrazine	2	2.53	2.60	2.46	0.98	0.99	0.97[b]	97.9
triCB	3	1.33	1.80	0.91	0.745	0.78	0.70	69.9
tetraCB	3	3.54	3.79	3.37	1.18	1.22	1.15	96.1

[a] N, number of experiments. [b] Starting concentration in soil 1 ppm. All others 2 ppm.

Table IV. Percent Metabolism and Type of Products Formed

name	% metabolized		% polar		% insoluble		% CO_2
	soil	plant	soil	plant	soil	plant	air
atrazine	14.7	59.5	10.5	48.9	4.2	10.6	0.48
triCB	12.7	47.2	0.95	36.6	11.75	10.6	0.46
tetraCB	4.5	45.6	0.2	40.9	4.3	4.7	0.01
dieldrin	0.4	8.3	0.2	8.1	0.2	0.2	0.01
PCB	0.5	8.3	0.3	8.1	0.2	0.2	0.03
HCB	0.8	0.8	na[a]	na[a]	0.8	0.8	<0.01
DDT	2.9	20.7	2.5	20.4	0.4	0.3	0.01

[a] na, not analyzed.

fashion with the growth, and chemicals in the plant are diluted:

$$f_i(t_1)V_i(t_1) = f_i(t_0)V_i(t_0) \quad (16)$$

in which $f_i(t)$ is the fugacity of the growing compartment at time t and $V_i(t)$ is the accompanying volume.

For every compartment, a *fugacity balance equation* is formulated and solved numerically [level 4 fugacity model (*24*)].

Experimental Results

Concentrations. The primary results are the activities of ^{14}C in the compartments of the model ecosystem. Concentrations in plants (fresh weight) and soil (dry weight) were calculated from the ^{14}C activities assuming no metabolism (Table III). Additionally, the total recovery of ^{14}C is given. All recoveries lie between 96 and 107% except the one for trichlorobenzene. The loss of this substance may be caused by its high fugacity, i.e., by escaping from the model ecosystem.

Metabolism. The activities of ^{14}C in soil and plants consist of the radiolabeled parent compound and the developing radiolabeled metabolites. The fraction of the metabolites can be rather large. They comprise up to 14.7 and 59.5% of the ^{14}C activity found in soil and plants, respectively (Table IV). For atrazine, polar metabolites formed in soil were found to be hydroxylated derivatives of atrazine and of its dealkylated products (*31–33*). For the chlorinated benzenes, the chemical nature of the polar metabolites has not been established. However, since chlorinated anisoles were found as soil metabolites (*34*), it is probable that the polar metabolites are free or conjugated phenols. Within the plants, chemicals can undergo a variety of enzymic reactions (*35*). Some of the tested chemicals are converted to insoluble products and probably bound irreversibly. Only a small portion of the chemicals is degraded ultimately to CO_2 (Table IV). In all cases, the fraction of metabolites in plants is higher than in soil. This indicates faster conversion in the plants. However, polar metabolites formed in soil (e.g., by hydroxylation) may be quickly taken up by the roots and translocated into the shoots. No differentiation between metabolism of parent compounds in plants and metabolism in soil with following uptake of metabolites by plants can be made with the experimental system used.

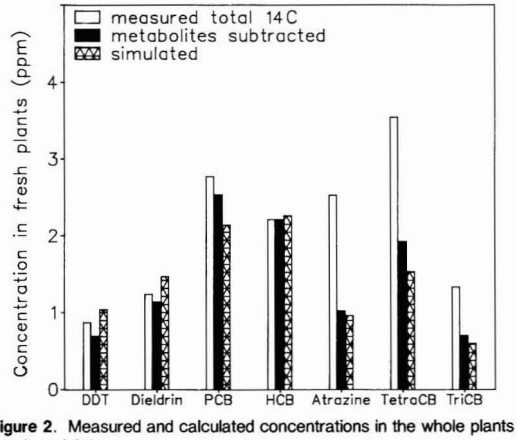

Figure 2. Measured and calculated concentrations in the whole plants (fresh weight).

Comparison between Experimental and Model Results

The model simulations were carried out solely for the parent compounds and not for the metabolites. ^{14}C activities of the metabolites were subtracted from the total ^{14}C found in plants and soil. These concentrations in plants and soil were compared with model simulations multiplied with the recovery rate given in Table III (Figures 2 and 3). The simulated concentrations are in fairly good agreement with the experimental results (differences between 1.7 and 26%). All important processes seem to be considered correctly. The extraordinary conformity of measurement and calculation for some of the soil concentrations, however, has a simple reason: DDT, dieldrin, and PCB change their soil concentration less than 3%, as

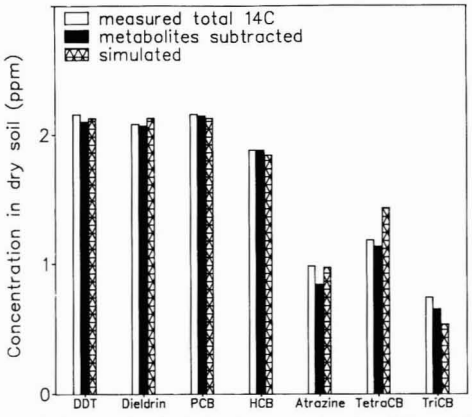

Figure 3. Measured and calculated concentrations in soil (dry weight).

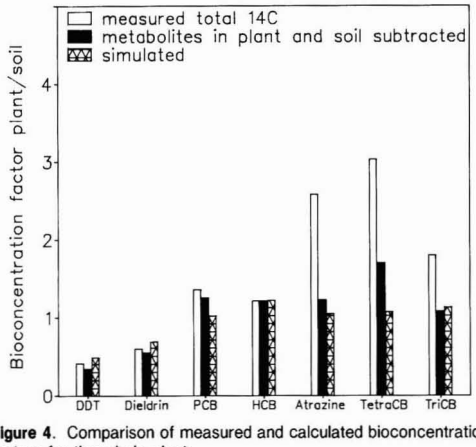

Figure 4. Comparison of measured and calculated bioconcentration factors for the whole plant.

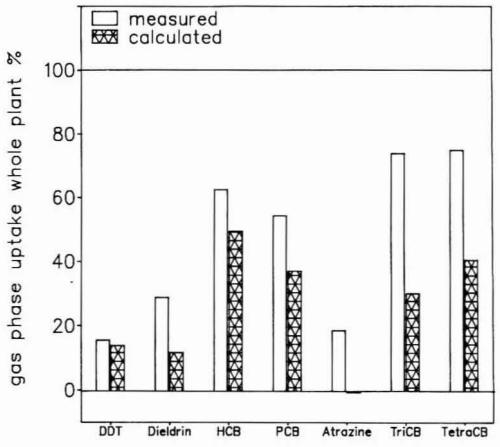

Figure 5. Percentage of uptake via air for the whole plant (measured percentage based on total ^{14}C taken up by plants).

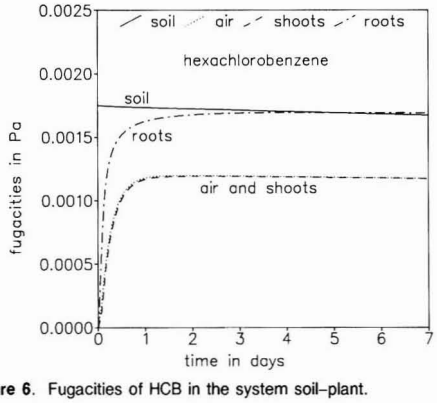

Figure 6. Fugacities of HCB in the system soil–plant.

is predicted by the model, too.

Bioconcentration. The *bioconcentration factor*, BCF, is expressed as

BCF =
concentration in fresh plant/concentration in dry soil

Measured and calculated results are compared in Figure 4. The BCF calculated from the ^{14}C activities is for all chemicals higher than the concentration ratio for the parent compound. The BCF values vary little for the parent compounds. Surprisingly, DDT and dieldrin show the lowest bioconcentration despite their high K_{ow} values. However, they are strongly sorbed to soil and are only transported very slowly with the transpiration stream or by volatilization. Subsequently, BCFs in shoots are low and represent nonequilibrium conditions.

Uptake of Chemicals by Aerial Parts of the Plants. Recently a call for research on this issue was published (*9*). In the experiments, the uptake of chemicals via aerial parts of the plants (GP) was quantified from the concentrations in the control plants. They grew in unpolluted soil and chemicals entered them preferably through the air.

$$GP = C_{\text{control plant}}/C_{\text{test plant}}$$

However, a portion of the chemical might transfer from the air into the unpolluted soil and then into the roots. Thus, the experimental determination of gas-phase uptake led to an overestimation.

In the model simulations, the flux of chemicals from air to shoots was integrated and compared to the total uptake of the plants. Results of experiments and simulations are shown in Figure 5. Experimental results are generally higher than calculated values, but the trend is the same. The result for atrazine is interesting: The model predicts a fast translocation within the plant by the transpiration stream. A small amount of the chemical volatilizes from the foliage into the air. It is not certain whether or not this effect really occurs since the transfer rates are estimated only approximately and direct measurements were not made. The deviations between experimental and calculated gas-phase uptake indicate uncertainties in the determination of the transfer kinetics in the experiments as well as in the model.

Very hydrophobic chemicals enter aerial plant parts from the air (if the Henry's law constant is high enough and volatilization can occur) because they are not translocated with the transpiration stream. The dominating transport from soil into air and then into foliage was also found in other experiments [PCBs (*6*); HCB (*8*); lindane, α-BHC, HCB, DDT, DDE (*7*)].

Fugacities in the System Soil–Air–Plant. The dynamics of the chemicals in the system can be elucidated by calculating the fugacity. Figure 6 shows the fugacities of HCB in soil, roots, air, and shoots. Transfer processes in the small model ecosystem are fast. A near-equilibrium state is reached between the chemical in soil and roots on the one hand and in aerial plant parts and air on the other

(at equilibrium, fugacities are equal). The transfer rates between soil and plant and between air and plant influence the time interval until the equilibrium is reached but not the equilibrium itself. The fugacity in air is always below that of the soil because there is a permanent inflow of unpolluted air into the system.

Sensitivity and Uncertainty Analysis

The purpose of this study was to simulate the uptake of various chemicals into one plant species, namely barley, dependent on the physicochemical properties of the chemicals. One interesting output parameter of the simulation model is the bioconcentration factor BCF. The BCF mainly depends on the ratio of the Z values for the plant, i.e., shoots Z_{Sh} and roots Z_R, and soil Z_S. These Z values are computed by equations using K_{ow}, K_{oc}, and the K_{AW} as input parameters (see Theoretical Section). The sensitivity of the BCF to variations of the physicochemical input parameters was investigated by Monte Carlo simulations, each with 1000 runs. In a first step, the input parameters K_{ow}, K_{oc}, and K_{AW} were randomly and uniformly varied ±50% for the example tetrachlorobenzene (mean values: K_{ow} = 44 668, K_{oc} = 6915, K_{AW} = 0.1). The resulting BCF has a mean value of 1.187 with a coefficient of variation of 44.46% (minimum 0.41, maximum 3.17). The BCF is positively correlated with the K_{ow} (correlation coefficient R = 0.546) and negatively with the K_{oc} (R = −0.767). The correlation to the K_{AW} is weak (R = 0.07).

Many authors showed that the K_{oc} is strongly correlated with the K_{ow} (*36*). Thus, in the following cases only K_{ow} and K_{AW} were varied and the K_{oc} was calculated from the K_{ow} by using various regression equations. The following equations were used:

(a) The equation of *Schwarzenbach* (ref 21; see legend of Table II) gives a K_{oc} with a mean value of 6915. The BCF varies little with a mean value of 1.071 and a coefficient of variation of 3.4% (minimum 0.98, maximum 1.14).

(b) The equation of *Karickhoff* gives higher K_{oc} values (*36*):

$$\log K_{oc} = \log K_{ow} - 0.21$$

With this regression, a mean K_{oc} of 27 564 results, and a mean BCF value of only 0.25 with a coefficient of variation of 5.9% (minimum 0.22, maximum 0.29) is calculated.

(c) The equation of *Briggs* (*36*) is

$$\log K_{oc} = 0.524 \log K_{ow} + 0.855$$

The mean K_{oc} is now only 1937, and a mean BCF of 4.41 with a coefficient of variation of 8.5% (minimum 3.53, maximum 5.22) is calculated.

Equations b and c represent extreme cases. Another established regression is (d) the equation of *Kenega and Goring* (*36*):

$$\log K_{oc} = 0.544 \log K_{ow} + 1.365$$

The mean K_{oc} is 7845 and the mean BCF is 0.91 with a coefficient of variation of 8.1% (minimum 0.73, maximum 1.07).

It can be concluded that the calculated bioconcentration factor plant/soil is less dependent on the absolute values of K_{ow} and K_{oc} than on their ratio. K_{ow} and K_{oc} are uncertain parameters (*37*). A large error can be introduced through incorrect K_{oc} values. The experimental result for the BCF of tetrachlorobenzene is 1.72. The equation of Schwarzenbach gives results in the medium range of possible variations and shows the best agreement with the measured BCF values.

Summary and Conclusions

A model was developed and tested for the simulation of uptake and accumulation of chemicals in plants. The model results are in agreement with laboratory experiments. Therefore, it is concluded that (1) transfer and distribution of organic chemicals in the soil–plant–system can be adequately described and interpreted by using partition and transfer coefficients, the geometry and structure of the system, and the degree of metabolism in soil and plant; (2) the bioconcentration factors fresh plant/dry soil of organic chemicals depend on the transfer coefficients and on the ratio of K_{ow} to K_{oc} values; (3) chemicals with a high partition coefficient K_{ow} enter aerial plant parts via air, if the Henry's law constant is sufficiently high; and (4) the metabolism of chemicals in plants and soil is important, especially when the metabolites are toxic.

The calculation of metabolite behavior is not yet included in the model and is only possible if conversion rates of parent compounds and metabolites and the nature of the products are determined.

Our results are in disagreement with some earlier published studies (*2*, *38*), which reported lower bioconcentration factors of hydrophobic substances. The reason is probably the large uptake from air in our system. In the field, this influence may be smaller. However, the processes of wet and dry deposition of chemicals on foliage then have to be added.

Registry No. TriCB, 120-82-1; TetraCB, 634-90-2; PCB, 39485-83-1; HCB, 118-74-1; DDT, 50-29-3; atrazine, 1912-24-9; dieldrin, 60-57-1.

Literature Cited

(1) Topp, E. M. Aufnahme von Umweltchemikalien in die Pflanze in Abhängigkeit von physikalisch-chemischen Stoffeigenschaften. Doctoral Thesis, Technical University of Munich, FRG, 1986.
(2) Ryan, J. A.; Bell, R. M.; Davidson, J. M.; O'Connor, G. A. *Chemosphere* **1988**, *17*, 2299–2323.
(3) Briggs, G. G.; Bromilow, R. H.; Evans, A. A. *Pestic. Sci.* **1982**, *13*, 495–504.
(4) Briggs, G. G.; Bromilow, R. H.; Evans, A. A.; Williams, M. *Pestic. Sci.* **1983**, *14*, 492–500.
(5) Thompson, N. *Pestic. Sci.* **1983**, *14*, 33–39.
(6) Bacci, E.; Gaggi, C. *Bull. Environ. Contam. Toxicol.* **1985**, *35*, 673–681.
(7) Bacci, E.; Gaggi, C. *Bull. Environ. Contam. Toxicol.* **1986**, *37*, 850–857.
(8) Schroll, R.; Scheunert, I.; Korte, F. In *Aspects methodologiques de l'etude du comportement des pesticides dans le sol*; Jamet, P., Ed.; INRA: Paris, France, 1988.
(9) Travis, C.; Hattemer-Frey, H. *Chemosphere* **1988**, *17*, 277–283.
(10) Kloskowski, R.; Scheunert, I.; Klein, W.; Korte, F. *Chemosphere* **1981**, *10*, 1089–1100.
(11) Topp, E. M.; Scheunert, I.; Attar, A.; Korte, F. *Ecotoxicol. Environ. Saf.* **1986**, *11*, 219–228.
(12) Boersma, L.; Lindstrom, F. T.; McFarlane, C.; McCoy, E. L. *Soil Sci.* **1988**, *146*, 403–417.
(13) Verband Deutscher landwirtschaftlicher Untersuchungs- und Forschungsanstalten, Ed. *Handbuch der landwirtschaftlichen Versuchs- und Untersuchungsmethoden (Methodenbuch Band I Untersuchung von Böden)*, 6th ed.; Vdlufa: Darmstadt, in press.
(14) Brown, D. S.; Flagg, E. W. *J. Environ. Qual.* **1981**, *10*, No. 3.
(15) Mackay, D. *Chemosphere* **1985**, *14*, 335–374.
(16) Doucette, W. J.; Andren, A. W. *Chemosphere* **1988**, *17*, 345–359.
(17) Mackay, D.; Shiu, W. Y. *J. Phys. Chem. Ref. Data* **1981**, *10*, 1175–1199.
(18) Mackay, D. *Environ. Sci. Technol.* **1982**, *16*, 274–278.

(19) Miller, M. M.; Wasik, S. P.; Huang, G. H.; Shiu, W. Y.; Mackay, D. *Environ. Sci. Technol.* **1985**, *19*, 522-529.
(20) Burkhard, L. P.; Armstrong, D. E.; Andren, A. W. *Environ. Sci. Technol.* **1985**, *19*, 590-596.
(21) Nirmalakhandan, N. N.; Speece, R. E. *Environ. Sci. Technol.* **1988**, *22*, 1349-1357.
(22) Schwarzenbach, R. P.; Westall, J. *Environ. Sci. Technol.* **1981**, *15*, 1360-1367.
(23) Mackay, D.; Paterson, S. *Environ. Sci. Technol.* **1981**, *15*, 1006-1014.
(24) Mackay, D. *Environ. Sci. Technol.* **1979**, *13*, 1218-1223.
(25) Paterson, S.; Mackay, D. In *Intermedia Pollutant Transport: Modeling and Field Measurements*; Allen, D. T., Kaplan, I. R., Eds.; Plenum: New York, in press.
(26) Brüggemann, R.; Münzer, B. In *Physical Property Prediction in Organic Chemistry*; Jochum, C., Hicks, M. G., Sunkel, J., Eds.; Springer: Berlin, 1988; pp 303-334.
(27) Matthies, M.; Behrendt, H.; Münzer, B. *EXSOL Modell für den Transport und Verbleib von Stoffen im Boden*; GSF-Bericht 23/87; Gesellschaft für Strahlen- und Umweltforschung Neuherberg, FRG, 1987.
(28) Larcher, W. *Ökologie der Pflanzen*; Eugen Ulmer: Stuttgart, 1984.
(29) Fusseder, A. *Z. Pflanzenernaehr. Bodenkd.* **1985**, *148*, 321-334.
(30) Campbell, G. S. *Soil Physics with BASIC*; Elsevier: Amsterdam, 1985.
(31) Skipper, H. O.; Gilmour, C. M.; Furtick, W. R. *Soil. Sci. Soc. Am. Proc.* **1967**, *31*, 653-656.
(32) Harris, C. I. *J. Agric. Food Chem.* **1967**, *15*, 157-162.
(33) Schiavon, M. *Ecotoxicol. Environ. Saf.* **1988**, *15*, 46-54.
(34) Scheunert, I.; Korte, F. In *Contaminated Soil*; Assink, J. W., van den Brink, W. J., Eds.; Martinus Nijhoff Publishers: Boston, MA 1986; pp 141-143.
(35) Shimabukuro, R. H.; Lamourex, G. L.; Stuart Frear, D. In *Biodegradation of Pesticides*; Matsumura, F., Krishna Murti, C. R., Eds.; Plenum: New York, 1982; pp 21-66.
(36) Lyman, W. J., Reehl, W. F., Rosenblatt, D. H., Eds. *Handbook of Chemical Property Estimation Methods*; MacGraw-Hill: New York, 1982.
(37) Sabljic, A. *Environ. Sci. Technol.* **1987**, *21*, 358-366.
(38) Travis, C. C.; Arms, A. D. *Environ. Sci. Technol.* **1988**, *22*, 271-274.

Received for review August 4, 1989. Revised manuscript received December 28, 1989. Accepted March 22, 1990.

Reduction of Phosphorus and Chlorophyll *a* Concentrations following $CaCO_3$ and $Ca(OH)_2$ Additions to Hypereutrophic Figure Eight Lake, Alberta

Ellie E. Prepas,[1*,‡] Tom P. Murphy,[§] Jan M. Crosby,[‡] Dave T. Walty,[∥] Jit T. Lim,[‡] Jay Babin,[‡,⊥] and Patricia A. Chambers[‡]

Department of Zoology and Meanook Biological Research Station, University of Alberta, Edmonton, Alberta, Canada, T6G 2E9, National Water Research Institute, P.O. Box 5050, Burlington, Ontario, Canada L7R 4A6, Alberta Fish and Wildlife Division, Bag 900-38, Peace River, Alberta, Canada, T0H 2X0, and HydroQual, 4500-16th Avenue, N.W., Calgary, Alberta, Canada, T3B 0M6

■ Lime [$CaCO_3$ or $Ca(OH)_2$] was added a total of four times to hard-water, hypereutrophic, Figure Eight Lake, Alberta. Within 14 days of treatment, chlorophyll *a* concentrations [Chl*a*] decreased to less than half the values measured just prior to treatment; there was no short-term trend in total phosphorus concentrations, $[P]_T$. Chl*a* returned to pretreatment concentrations within 35 days of treatment. Although dissolved oxygen concentrations were very low in the autumn and first winter following lime treatments, under-ice $[P]_T$ were less than half pretreatment values. During the summer following the first lime treatments, $[P]_T$, [Chl*a*], and water clarity improved relative to the other five summers on record; average $[P]_T$ decreased to 30% and [Chl*a*] decreased to 12% of the previous summer's values. The following winter, dissolved oxygen depletion rates were 59% of pretreatment rates. The short-term reduction in [Chl*a*] was likely related to precipitation of growth-limiting nutrients other than phosphorus, such as iron, with the calcite. In contrast, improvements in [Chl*a*] the year following the first lime treatments could be related to lower $[P]_T$ in the water column, as a consequence of increased P-binding capacity of bottom sediments. Lime treatments can enhance water quality in eutrophic hard-water lakes by suppression of growth-limiting nutrients for phytoplankton.

Introduction

In the long term, phosphorus controls algal biomass and production in most freshwater lakes (*1*). For many eutrophic lakes, reductions in algal biomass have been achieved by decreasing the external P load (*2, 3*). External inputs cannot be controlled, however, when the major external source is from P-rich soils and rocks, such as in much of western Canada (*4, 5*). In the Canadian prairies, unsightly algal blooms and associated problems, such as unpleasant odor and winterkill, are common. Low-cost nontoxic approaches to control algal biomass and production are needed for these naturally eutrophic systems.

Calcite precipitation is a natural phenomenon that occurs during the summer in hard-water lakes (*6*). This process reduces algal production by coprecipitation of P and calcium from the surface waters and formation of insoluble hydroxyapatite (*7-11*). Lime additions [$CaCO_3$ and $Ca(OH)_2$] can reduce P concentrations in water by the same principle (*12-14*). $Ca(OH)_2$ is routinely used in wastewater treatment to remove P (*15*). Fly ash, which contains Ca, has been used for some time to retard release of P from lake sediments (*16*). While both $CaCO_3$ and $Ca(OH)_2$ have been used for over 40 years to reduce color [ref 17 used $Ca(OH)_2$·MgO] and more recently to buffer acidified lakes (*18*), only recently has lime been used in the treatment of eutrophic surface waters. In a preliminary study on a small hardwater lake in British Columbia, four relatively low doses of $Ca(OH)_2$ reduced available P and algal biomass (*4*). However, insufficient data were collected to evaluate long-term effects.

In this study, a small hypereutrophic hard-water lake (Figure Eight Lake) in northwestern Alberta was treated with lime [both $CaCO_3$ and $Ca(OH)_2$] to induce calcite precipitation, and water quality was evaluated over a 2-year period.

[‡] University of Alberta.
[§] National Water Research Institute.
[∥] Alberta Fish and Wildlife Division.
[⊥] HydroQual.

 0013-936X/90/0924-1252$02.50/0

Table I. Parameters Measured in Figure Eight Lake Information on Collection and Analysis[a]

Parameter	Method
temperature	0.5- to 1-m intervals; resistance thermometer
light penetration	20-cm-diameter Secchi disk
water samples	0.5- to 2-m intervals; 1.5-L aluminum drop-sleeve water bottle
dissolved oxygen (DO)	ref 21, within 24 h
conductivity	Metrohm E587 conductometer immediately after collection
pH	Metrohm E588 pH meter immediately after collection
total alkalinity	ref 19, within 48 h
color	Hellige aqua tester Model 611A within 7 days
turbidity	Hach turbidimeter Model 2100A within 7 days
Cl, total Fe $[Fe]_T$, SO_4, Na	ref 19, within 1 month
K, Ca (filtered and unfiltered), Mg	ref 19, within 1 month
particulate organic carbon (POC)	ref 19, within 1 month
dissolved inorganic carbon (DIC)	ref 19, within 1 month
$NO_2 + NO_3$	ref 22, within 48 h
total Kjeldahl nitrogen	ref 23, within 48 h
total nitrogen $[N]_T$	sum of total Kjeldahl N, $NO_2 + NO_3$
total phosphorus $[P]_T$	ref 5, within 14 days
total dissolved phosphorus	ref 5, within 14 days
chlorophyll *a* (Chl*a*)	ref(s) 24 and/or 25, within 1 month
phytoplankton species composition	ref 26

[a] Samples were treated and preserved as outlined in refs 19 and 20.

Materials and Methods

Figure Eight Lake was sampled at intervals from 1 day to 2 months from 05 June 1985 to 27 March 1988. Secchi disk data had been collected sporadically in 1980, 1983, and 1984. Two types of information (Table I) were collected from the lake: (1) vertical chemical profiles were constructed from discrete water samples collected over the deepest part of the two deepest basins; and (2) integrated water samples for P and Chl*a* analysis and phytoplankton identification were collected to a depth of 3 m (i.e., the epilimnion) from five representative stations on the lake with weighted Tygon tubing during the open-water period; on each date all integrated samples were pooled. Unless otherwise indicated, all values were calculated from discrete samples, integrated over the top 3 m and volume-weighted over the two basins; average summer values ($X \pm 1$ SE) represent the period 01 June to 31 August. Since an estimate of all Ca in solution was required, Ca data were volume-weighted over the entire water column, rather than just the epilimnion. Under-ice Ca concentrations ([Ca]) were corrected for ions frozen out; it was assumed that all Ca was frozen out of black (i.e., clear) ice (*27*) and the winter volume-weighted [Ca] includes the water equivalent of the black-ice cover. Winter oxygen depletion rates were calculated as outlined in ref 28.

The inflowing stream was sampled during runoff (08 April through 07 May 1986) with an Isco automatic sampler set to collect 500 mL every 12 h; water samples were treated as outlined for lake water samples. Stream discharge was measured with a Price Model 622 current meter. Outflow water quality is assumed to be identical with surface water concentrations in the south basin.

On 16 July 1985, 15 and 16 July 1986, and 23 July 1987, aquatic macrophytes were harvested from six representative sites in the south basin. At each site, all above-sediment tissues were collected from within three quadrats of 0.25 m^2 each, from depths of 1 and 2 m (i.e., maximum depth of macrophyte colonization). Plants were thoroughly rinsed, separated according to species (with the exception of fine-leaved *Potamogeton* spp.), spin-dried and fresh-weighed. Fresh weight was converted to dry weight by division of fresh weight by 9.8 for *Myriophyllum exalbescens*, 7.4 for *Potamogenton richardsonii*, and 10.7 for *Lemna trisulca* (based on data from Figure Eight Lake), and 10 for all other species (*29*). Results are presented as $X \pm 1$ SE for the six sites.

Table II. Lime Additions to Figure Eight Lake, 1986 and 1987[a]

treatment no.	form	date	tonnes added	in-lake concn, $mg \cdot L^{-1}$
1	$CaCO_3$	18 June 1986	15.8	14.0
2	$Ca(OH)_2$	30 July 1986	9.4	8.4
3	$Ca(OH)_2$	08 August 1986	5.4	4.8
4	$CaCO_3$	14 July 1987	22.5	18.2

[a] In-lake concentrations assume lime mixed with entire lake volume (1.122×10^6 m^3).

Ca budgets were calculated by assuming that pretreatment [Ca] in the water column was fairly constant from year to year and all outflow occurred during a 2-week period in April when one-quarter of the lake water was lost each year from what is assumed to be a continuously stirred reactor. Similar assumptions were made in the discussion of DIC, $[Fe]_T$, and $[P]_T$. Aeolian inputs of total P were calculated from measurements made on a central Alberta lake (*30*). Aeolian inputs of Ca and dissolved inorganic carbon (DIC) were estimated from data collected by Alberta Environment. No data are available on groundwater fluxes. The lake is situated in a semiarid region where annual average pan evaporation (581 mm) exceeds precipitation (447 mm).

The computer program PCWATEQ was used to calculate the saturation values of calcite and hydroxyapatite. The program is the 1984 version of the U.S. Geological Survey release of WATEQF (*31*). The critical variables were all obtained from analysis of samples collected in 1986 and 1987. The average charge balance error was 7%.

Lime was added a total of four times to Figure Eight Lake during the summers of 1986 and 1987 (Table II). Two forms of lime were used in 1986 to evaluate the relative effectiveness of each: 0 grind 97% $CaCO_3$ with 80% less than 180 μm and $Ca(OH)_2$ with 90% less than 120 μm was used. The second and third treatments were with low dosages of $Ca(OH)_2$ and occurred 10 days apart to ensure that the pH of the lake water was not unduly elevated. Lime was applied as a slurry, evenly over the lake surface in proportion to water depth. In 1986 it was applied by pumping lake water from a 7.62-cm outlet pump into a wooden hopper with baffles mounted on a small barge (4.8 × 3.3 m deck) powdered by a 9.9-hp outboard motor; bagged lime was poured into the hopper, where it mixed with the lake water, and then flowed into the lake. In 1987 the procedure was modified: the barge was larger (7.3 × 3.7 m deck); lime and lake water were mixed in a slurry box in the center of the barge; the slurry was pumped forward and distributed through two 2.4-m-long booms, one located on each side of the bow.

An aerator, consisting of a 7.6-hp Sutorbilt vertical style blower, 3.8 cm external diameter two-ply compressor hose, and a 200-m section of the hose with 4.2-mm holes at 30-cm intervals serving as the diffuser, was installed in October

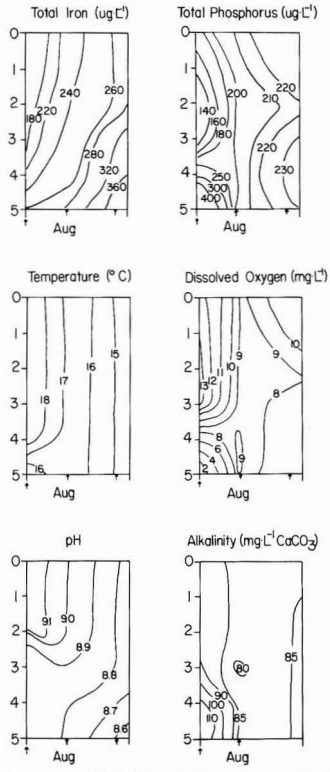

Figure 1. Time-depth distribution of six parameters in August 1985 in the deepest basin of Figure Eight Lake. Arrows on the bottom of each panel indicate sampling dates.

1986 in the deepest part of the south basin.

The Study Lake

Figure Eight Lake has a long history (>30 years) of manipulation in an effort to reduce chronic summer algal blooms and associated winterkill risk to stocked trout. The lake is stocked annually with rainbow trout (*Salmo gairdneri*). Since 1956, at least three different dams have been placed on the outlet to raise lake water levels; increased water levels did not however eliminate winterkill. Since 1973, the outflow has been controlled by an earthfill dam and is drained by a drop inlet spillway. From 1980 through 1984, the lake was treated a total of four times with copper sulfate (average dosage 36 $\mu g \cdot L^{-1}$ Cu), resulting in reduced algal biomass for variable periods. There were some residual effects from the last $CuSO_4$ treatment on chlorophyll concentrations in evidence until October 1985 (*32*), but no residual copper was detected in the water column in 1986 or in 1987. Treatment of eutrophic lakes with $CuSO_4$ is now discontinued in Alberta. The aerator installed in Figure Eight Lake in the fall of 1986 was ineffective the first winter, due to technical problems, and was not used the following winter, until after winter oxygen depletion rates had been established. We do not believe these manipulations interfered with the interpretation of the results presented in this paper.

Figure Eight Lake is a small (36.8 ha), shallow (mean depth 3.1 m) lake situated in P-rich glacial till (long. 56° 18′, lat. 117°54′) 48 km northwest of Peace River, Alberta. The drainage basin is small (4.7 km^2) and covered with aspen–poplar forest; 8% has been cleared for pasture. The lake has three basins: the largest and deepest (maximum depth 6 m) south basin contains 70.5% of the lake water, the other two basins have maximum depths of 5 and 3.5 m and contain 24.3 and 5.2% of the lake water, respectively.

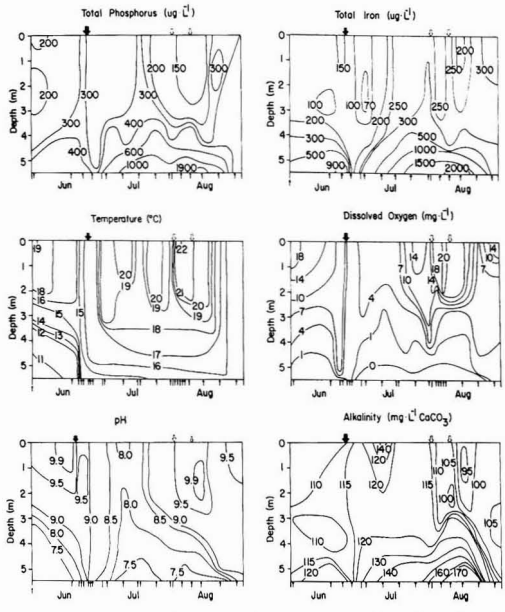

Figure 2. Time-depth distribution of six parameters from June through August 1986 in the deepest basin of Figure Eight Lake. Arrows on top of each panel indicate dates of lime addition, solid arrows indicate $CaCO_3$ treatment, open arrows indicate $Ca(OH)_2$ treatment, and those on the bottom indicate sampling dates.

Channelized surface runoff is limited to one stream, which flows only for a brief period in April; lake water residence time based on surface inputs and outputs only is >4 years. Groundwater, although unmeasured, is likely a significant source of dissolved ions, and a much smaller source of water to the lake (*33*, *34*). Addition of groundwater in the water budget would not likely alter the water residence time reported here in a major way. During the brief period when surface runoff flowed into the lake (64% of the total annual surface inflow entered over 4 days in early April 1986), $[P]_T$ and $[Fe]_T$ in the inflow were each as high as 600 $\mu g \cdot L^{-1}$, during the same period [DIC] and [Ca] both averaged 14 $mg \cdot L^{-1}$.

Figure Eight Lake is a hard-water lake. From June through August 1986, conductivity averaged 215 ± 3 $\mu S \cdot cm^{-1}$, [Ca] 28 ± 0.3 $mg \cdot L^{-1}$, [Mg] 10 ± 0.05 $mg \cdot L^{-1}$, [K] 9 ± 0.07 $mg \cdot L^{-1}$, [Na] 2 ± 0.02 $mg \cdot L^{-1}$, $[HCO_3]$ 107 ± 8 $mg \cdot L^{-1}$, $[CO_3]$ 13 ± 4 $mg \cdot L^{-1}$, $[SO_4]$ 14 ± 0.2 $mg \cdot L^{-1}$, and [Cl] 1 ± 0.08 $mg \cdot L^{-1}$ (pretreatment values, or those unaffected by the treatments).

During the summer, Figure Eight Lake is weakly thermally stratified; water over the bottom sediments frequently is anoxic (Figures 1–3). When the water column is thermally stratified, total P and Fe accumulate over the bottom sediments to concentrations occasionally exceeding 1900 $\mu g \cdot L^{-1}$ for both parameters. In the period monitored prior to lime treatment (i.e., 1985 to mid-June 1986), $[P]_T$ and $[Fe]_T$ in the epilimnion exceeded 200 $\mu g \cdot L^{-1}$ (Figures 1 and 2), and [Chl*a*] and particulate organic carbon [POC] exceeded 150 $\mu g \cdot L^{-1}$ and 7 $mg \cdot L^{-1}$, respectively (Figure 5). The pH increased to 9.9 during the algal bloom in June 1986 (Figure 2). Prior to lime additions, water transparency was generally poor, with Secchi disk readings aver-

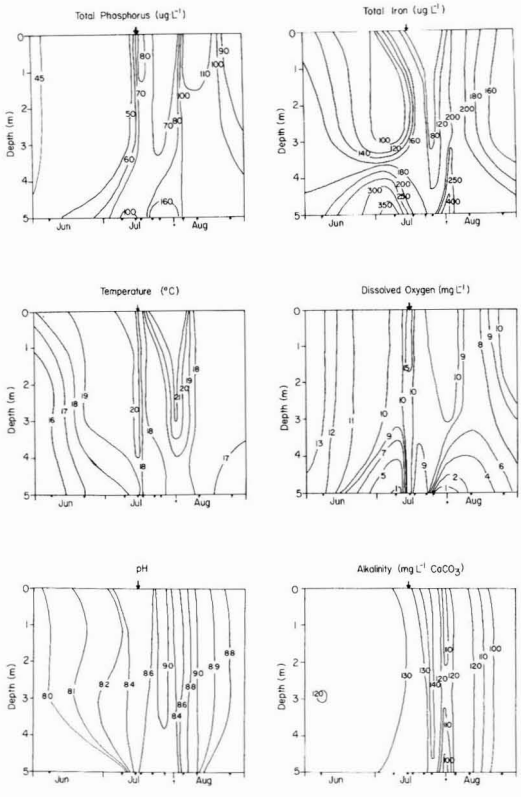

Figure 3. Time-depth distribution of six parameters from June through August 1987 in the deepest basin of Figure Eight Lake. Arrows as in Figure 2.

aging 1 m or less (Figure 6). Although the water was somewhat colored ($X = 28 \pm 2$ mg·L^{-1} Pt, summer 1986), it was not turbid ($X = 5 \pm 0.7$ NTU, same time period); poor transparency was primarily due to algal blooms, dominated (>95%, dry weight) by the blue-green alga, *Aphanizomenon flos-aquae*.

Under-ice oxygen depletion rates were high, from 26 October (date of ice formation) through 18 December 1985 (when average dissolved oxygen [DO] for the whole lake

Table III. Average Volume-Weighted Concentrations (±1 SE) in the Top 3 m of Figure Eight Lake from 01 June to 31 August[a]

chemical	year 1986	year 1987	*P*
total P, μg/L	246 ± 14	75 ± 8	***
Chl*a*, μg/L	96 ± 14	12 ± 7	***
total Fe, μg/L	205 ± 21	146 ± 16	ns
SO_4, mg/L	14 ± 0.2	24 ± 0.6	***
total N, μg/L	2782 ± 197	1021 ± 167	***
alkalinity, mg/L $CaCO_3$	111 ± 2	122 ± 5	
DIC, mg/L	22 ± 1	30 ± 0.4	
Ca,[b] mg/L	28 ± 0.3	37 ± 0.6	***

[a] Results of an unpaired *t* test are indicated as *** ($P \ll 0.01$) or ns (not significant). [b] Whole-lake weighted average.

reached 2.2 mg·L^{-1}; Figure 7) average whole-lake oxygen depletion rates were 0.611 ± 0.036 g of O_2 m^{-2}·day^{-1}. These rates are not significantly different ($P \gg 0.05$) from the under-ice oxygen depletion rate of 0.624 g of O_2 m^{-2}·day^{-1}, predicted from average summer $[P]_T$ in the trophogenic zone and from lake depth (eq 4, ref 28).

Results

There was no clear pattern in changes in $[P]_T$ in the first month following the four lime treatments. After two treatments, epilimnetic $[P]_T$ increased in the short term; thermal mixing redistributed total P from the deeper waters into the epilimnion (Figures 2–4). During the first fall and winter after lime treatments began, $[P]_T$ decreased dramatically. Although [DO] were lower under ice in 1986–1987 than 1985–1986, $[P]_T$ was half that of previous winter values; volume-weighted whole-lake averages were 143 and 281 μg·L^{-1} total P in March 1987 and February 1986, respectively. The under-ice differences at a depth of 1 m below the ice surface were even more spectacular, 60 as compared with 200 μg·L^{-1} total P, respectively, for the dates indicated. By the summer of 1987, average $[P]_T$ decreased to $^1/_3$ of the 1986 value (Table III).

After the first treatment with $CaCO_3$, [Chl*a*] and [POC] decreased substantially (Figure 5). Within 2 weeks, [Chl*a*] had decreased to 2% of pretreatment values in both the euphotic zone and epilimnion, and POC declined to 7% of pretreatment concentrations in the epilimnion. Within five weeks, POC and Chl*a* returned to pretreatment concentrations. After each subsequent lime treatment in 1986,

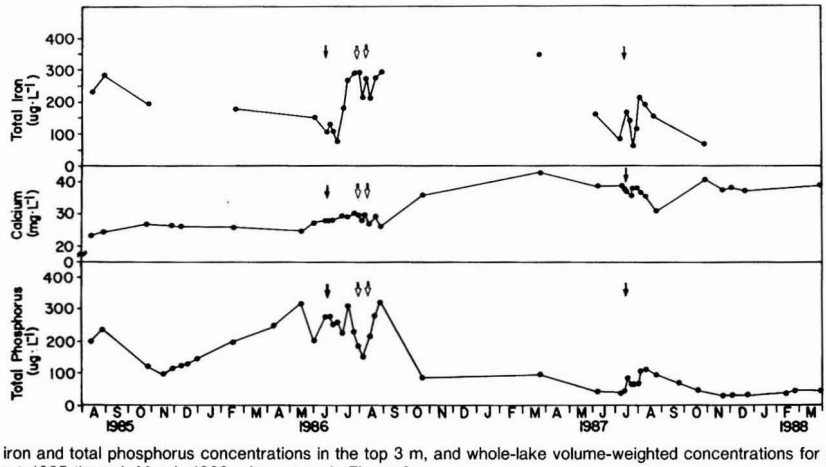

Figure 4. Total iron and total phosphorus concentrations in the top 3 m, and whole-lake volume-weighted concentrations for calcium in Figure Eight Lake, August 1985 through March 1988. Arrows as in Figure 2.

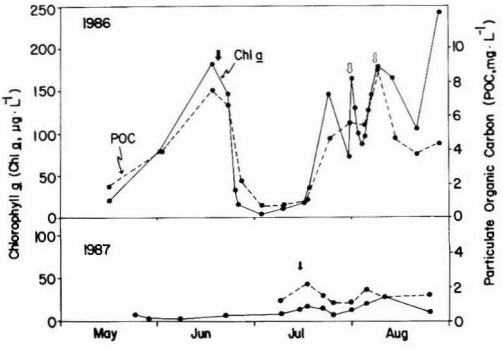

Figure 5. Chlorophyll *a* and particulate organic carbon concentrations from May through August 1986 and 1987. Arrows as in Figure 2.

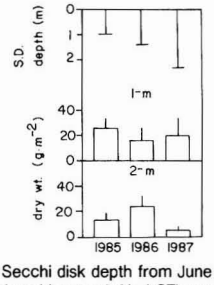

Figure 6. Average Secchi disk depth from June through August and average July macrophyte biomass (with 1 SE) at two depths from 1985 through 1987, Figure Eight Lake.

Chl*a* decreased briefly but quickly returned to pretreatment concentrations.

In the summer of 1987, average [Chl*a*] was 12% of the 1986 value (Table III). Prior to lime treatment in July 1987, Chl*a* was less than 10% of the pretreatment 1986 concentration. In 1987, the decrease in [Chl*a*] and [POC] after $CaCO_3$ treatment was less than in 1986; however, the pattern was similar, with a sharp, but short-term, decrease 10 days after treatment (Figure 5). After the 1987 treatment, the dominant algal taxa shifted from blue-green to green (small flagellates) and diatoms (*Synedra* sp.) for the remainder of the summer. Much improved water clarity in 1987 (Figure 6) coincided with reduced [Chl*a*].

Although average light transparency increased in Figure Eight Lake from 1985 through 1987, July macrophyte biomass did not increase (Figure 6) and at the deeper (2-m depth) sites it declined. Macrophyte species also shifted over the study period. In 1985, prior to lime treatment, the community was dominated by rooted aquatic plants. After treatment, a nonrooted plant, *Lemna trisulca*, represented 70–100% of macrophyte biomass at depths of 1 and 2 m.

$[Fe]_T$ decreased within 5–14 days after each of the four lime treatments to anywhere from 68 to 74% of pretreatment concentrations and then returned to pretreatment values within 16–21 days of treatment (Figure 4). $[Fe]_T$ in the summer of 1987 was slightly, but not significantly, lower than in 1986 (Table III). In the summer of 1986, there was a substantial input of total Fe to the top 3 m of water from the bottom sediments, whereas in 1987 the input was less (Figures 2 and 3). These differences could be related to more complete water column mixing and higher [DO] over the bottom sediments in 1987 than in 1986.

In 1987, $[SO_4]$ and $[N]_T$ reflected reduced algal productivity. For the June through August period, average

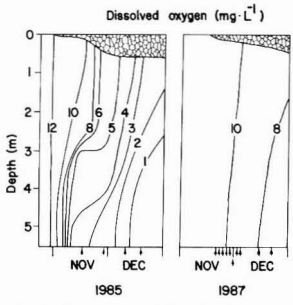

Figure 7. Time-depth distribution of dissolved oxygen during the first 2 months of ice cover in 1985 and 1987, Figure Eight Lake.

$[SO_4]$ in the open water almost doubled (Table III), as a result of less pyrite formation in the bottom sediments (*32*). $[N]_T$ decreased to less than half over the same period (Table III), possibly due to reduced nitrogen fixation (*35*), enhanced sedimentation, and reduced sediment release.

Within 10–14 days after the $CaCO_3$ treatments (Table II), alkalinity in the epilimnion increased an average of 12 mg·L^{-1} $CaCO_3$ and then declined to pretreatment values (Figures 2 and 3). In contrast, within 1 week of each of the two applications of $Ca(OH)_2$, alkalinity decreased an average of 6 mg·L^{-1} $CaCO_3$, due to calcite precipitation. In the long term, both alkalinity and inorganic carbon increased after lime treatment of Figure Eight Lake, alkalinity increased by $^1/_3$ from 1985 (when it was 91 ± 5 mg·L^{-1} $CaCO_3$) to 1987 (Table III). Similarly, [DIC] increased from 1986 to 1987 (Table III). Following the $CaCO_3$ treatments, pH declined; the decrease was greater in 1986 than in 1987 (Figures 2 and 3) because primary production, which slowed in both cases, would have been higher in 1986. These decreases in pH following the $CaCO_3$ treatments likely reflect reduced rates of primary production and increased rates of algal decay. In contrast, after the $Ca(OH)_2$ treatments, pH in the epilimnion increased up to 0.5 pH unit (Figure 2).

[Ca] did not change immediately after the initial treatment, and there were no detectable differences between filtered and unfiltered [Ca]. Rather, added Ca was first lost to the bottom sediments, and then concentrations in the water column increased slowly over the fall and winter of 1986–1987 and remained elevated through March 1988 (Figure 4). [Ca] increased 18% from the summer of 1986 (Table III) to 22 October 1986 (when it was 33.4 mg·L^{-1}) and by another 18% (to 39.6 mg·L^{-1}) by March 1987. [Ca] remained significantly higher throughout the summer of 1987 than in 1986 (Table III). The highest whole-lake value recorded was for October 1987, when [Ca] reached 40.7 mg·L^{-1}. Under ice cover during 1987–1988, [Ca] ranged from 37.2 to 38.8 mg·L^{-1}.

The top 3 m of water in Figure Eight Lake was supersaturated with calcite and hydroxyapatite prior to lime treatment (Figure 8). Within a few days after lime treatment, the additional calcite went to the bottom sediments. During both summer and winter, the water overlying the deep sediments is undersaturated with calcite and hydroxyapatite; thus, both minerals redissolve in the waters overlying these sediments.

Under-ice [DO] did not respond initially to the lime treatments. The fall of 1986 was unusually warm; then winter came suddenly and the lake became ice covered while [DO] was at 45% saturation. An aerator installled in the lake was turned on soon after ice-on in 1986. The aerator was off for sufficient time (14–17 November 1986) to calculate a rough estimate of winter oxygen depletion

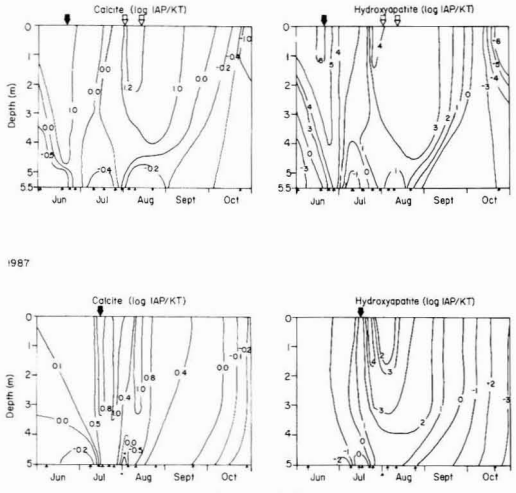

Figure 8. Time-depth distribution of calcite and hydroxapatite saturation (log IAP/*KT*) June through October 1986 (top panel) and 1987 (bottom panel) in the deepest basin of Figure Eight Lake. Arrows as in Figure 2.

rates, 0.54 g of O_2 m^{-2}·day^{-1}; this rate is slightly lower than for the same period 1 year earlier. The aerator was turned off 22 January 1987 when the lake became anoxic. In the fall of 1987, the lake became ice covered while oxygen saturation was close to 100%. Under-ice oxygen depletion rates in 1987–1988 were lower than the previous year (Figure 7), perhaps as a result of lower summer algal biomass. The aerator was not turned on until 30 December 1987. Under-ice oxygen depletion rates from 30 November to 29 December 1987 were 0.363 ± 0.018 g of O_2 m^{-2}·day^{-1} or 59% of, and statistically less (t test, $P \ll 0.01$) than, pretreatment rates.

Lime treatments had no detectable negative impact on invertebrates and vertebrates in Figure Eight Lake. Amphipods returned to Figure Eight Lake in 1986 for the first time since 1980, when the lake was first treated with $CuSO_4$. Stocked rainbow trout thrived in the summer of 1986, and from the summer of 1987 through the following summer (D. Walty, unpublished data).

Discussion

The short-term (i.e., within 2 week) decreases in [Chl*a*] reported for Figure Eight Lake following lime treatments were similar to those observed in Frisken Lake, British Columbia (*4*). Although the British Columbia study also indicated short-term declines in $[P]_T$, we did not observe any consistent changes in $[P]_T$. Short-term reductions in $[P]_T$ in Figure Eight Lake may have been masked by mixing events that incorporated deep P-rich water into the epilimnion (Figures 2 and 3). In contrast, Frisken Lake was permanently thermally stratified in summer, and under these conditions, the impact of lime treatments on total P may be less equivocal. The short-term changes in [Chl*a*] in Figure Eight Lake may be related to precipitation of growth-limiting nutrients other than phosphorus, such as iron, with the calcite (*10*). In contrast, lower [Chl*a*] in the summer following the first lime treatments of Figure Eight Lake are likely related to lower open-water $[P]_T$.

Although the data are insufficient to calculate annual budgets for natural inputs to and outputs from Figure Eight Lake, the following summary can be made for total P, total Fe, Ca, and DIC. The bulk (>90%) of the external total P load comes in a 2-week period with spring runoff while the lake is ice covered but unsafe to sample. How much of that phosphorus stays in the lake relative to loss to the outflow, is unknown (*36*). Because there is relatively little external total P input from May through August, euphotic zone phosphorus dynamics (Figures 1–4) are driven by internal inputs from and losses to the bottom sediments, as documented for another shallow lake in this region (*5*). Similarily, although there are no reliable data on aeolian total Fe inputs, total Fe dynamics in the euphotic zone from May through August are likely driven by internal loading and losses. Calcium inputs in spring runoff could account for >95% of the external inputs, and similarly, most of the external input of DIC likely accompanies spring runoff. In contrast to $[P]_T$ and $[Fe]_T$, which were higher in runoff than in lake water, [Ca] and [DIC] in runoff were lower than those in lake water at Figure Eight Lake. Ca could be an important, but unmeasured, component of groundwater inputs to the lake.

A total of 12.4 mg·L^{-1} Ca was added via the lime treatments to the entire volume of Figure Eight Lake in 1986, and 7.6 mg·L^{-1} Ca was added in 1987. Although the added Ca initially precipitated to the bottom sediments, over the long-term, open-water dissolved [Ca] increased. Our data from 1986 in Figure Eight Lake and from other lakes and dugouts (*37*, *38*) indicate that there is no net change in open water [Ca] the first 1–2 months after treatment when similar amounts of lime are added to hard water. However, by October 1986, an estimated 40% of the added Ca was in solution in Figure Eight Lake, and by March 1987, 90% was in solution (Figure 4). Further, approximately 85% (i.e., 8.2 mg·L^{-1}) of the Ca remaining from the 1986 additions was in the water column in the summer of 1987. Over the winter of 1987–1988, the fraction of the total Ca added in both summers, and still in the water column, decreased to two-thirds. These changes in [Ca] following the lime treatments must be associated with the lower summer pH and thus increased solubility of calcite (Figues 2, 3, and 8), and inputs from the bottom sediments.

The observed changes in total P, Chl*a*, SO_4, and Ca in Figure Eight Lake following the lime treatments are not likely due to natural year-to-year variation in these parameters. The University of Alberta and Alberta Environment have 8 years (1980–1987) of continuous data on water quality parameters in seven lakes, which cover the range of trophic conditions found in this region. In five of the seven long-term study lakes, average summer [Chl*a*] was higher in 1987 than in 1986. These patterns are the opposite of what was observed in Figure Eight Lake. Also, the relative differences between the 1986 and 1987 mean summer [Chl*a*] and $[P]_T$ in Figure Eight Lake are much greater than the maximum differences between years in any of our long-term study lakes. Also, [Ca] and $[SO_4]$ in lakes in this region are relatively constant throughout the year. None of our long-term study lakes had changes in [Ca] and $[SO_4]$ between 1986 and 1987 that were comparable to those in Figure Eight Lake. Thus, we believe the changes described in Figure Eight Lake in 1986 and 1987 were a result of the lime treatments.

The mechanisms involved in the long-term reduction of Chl*a* and total P in lime-treated lakes need further investigation. As calcite is known to adsorb organic matter (*39*), the precipitating calcite may have adsorbed algal cells as was observed in one lake (*10*). These cells could have been weakened by a shortage of biologically available iron, which is essential for photosynthesis and nitrogen fixation by blue-green algae (*40*). After each of the four lime additions, $[Fe]_T$ dropped to approximately $^2/_3$ pretreatment

values in Figure Eight Lake. Alternatively, calcite may have encrusted the algal cells and enhanced precipitation (*41*). The long-term decreases in open water $[P]_T$ were likely due to changes in the phosphorus-binding capacity of the bottom sediments, which could be related to increased calcium concentrations in the bottom sediments of the treated lake (*42*). One unexpected result was that macrophyte populations did not respond significantly to the increased light penetration in Figure Eight Lake (Figure 6). Macrophyte biomass often increases with increased light transparency (*43*). Possible interpretations for our results are that increased Ca in the bottom sediments enhanced apatite formation, or that enhanced calcite precipitation on the leaves blocked light. Further, the shift away from blue-green algae could have beneficial effects on the entire food web.

Lime treatments may be a feasible route to enhance water quality in naturally eutrophic hard-water lakes. Lime is relatively inexpensive; the delivered cost in Alberta runs between $20 and $100 per tonne. The treatments appear to be nontoxic to invertebrates and vertebrates; lime seems to suppress grown-limiting nutrients for phytoplankton for an extended period. More research is required to ascertain the mechanisms involved in the short-term reduction in [Chl*a*], the long-term reduction in open water $[P]_T$, and the responses of macrophyte and phytoplankton communities following lime additions. The appropriate dosage and form required for long-term improvements in water quality must be established, as well as the impact of variation in important parameters such as alkalinity and flushing rate.

Acknowledgments

We thank J. McKague, J. Ghitter, K. Sloman, T. Collette, M. Mawhinney, L. Harris, D. Sasaki, M. Serediak, J. Burke, and G. Hutchinson for field and analytical support. B. Maclock, J. Barica, and the Boreal Institute for Northern Studies supported this project throughout. J. Cole, R. G. Wetzel, D. W. Schindler, J. Curtis, and two anonymous reviewers provided critical comments on various versions of the manuscript.

Registry No. P, 7723-14-0; Chla, 479-61-8; O_2, 7782-44-7; $CaCO_3$, 471-34-1; Fe, 7439-89-6; N_2, 7727-37-9; Ca, 7440-70-2; C, 7440-44-0.

Literature Cited

(1) Schindler, D. W. *Science (Washington, D.C.)* **1974**, *184*, 897–899.
(2) De Pinto, J. V.; Young, T. C.; McIlroy, L. M. *Environ. Sci. Technol.* **1986**, *20*, 752–759.
(3) Dillon, P. J.; Nicholls, K. H.; Robinson, G. W. *Verh. Int. Ver. Theor. Angew. Limnol.* **1978**, *20*, 263–271.
(4) Murphy, T. P.; Hall, K. G.; Northcote, T. G. *Lake Reservoir Manage.* **1988**, *4*, 51–62.
(5) Riley, E. T.; Prepas, E. E. *Can. J. Fish. Aquat. Sci.* **1984**, *41*, 845–855.
(6) Vanderploeg, H. A.; Eadie, B. J.; Lieberg, J. R.; Tarapchak, S. J.; Glover, R. M. *Can. J. Fish. Aquat. Sci.* **1987**, *44*, 1898–1914.
(7) Avnimelech, Y. *Nature* **1980**, *288*, 255–257.
(8) Effler, S. W.; Driscoll, C. T. *Environ. Sci. Technol.* **1985**, *19*, 716–720.
(9) Koschel, R.; Benndorf, J.; Proft, G.; Recknagel, F. *Arch. Hydrobiol.* **1983**, *98*, 380–408.
(10) Murphy, T. P.; Hall, K. J.; Yesaki, I. *Limnol. Oceanogr.* **1983**, *28*, 58–69.
(11) Otsuki, A.; Wetzel, R. G. *Limnol. Oceanogr.* **1972**, *17*, 763–767.
(12) Gessner, F. *Int. Rev. Gesamten Hydrobiol. Hydrogr.* **1939**, *38*, 202–211.
(13) Rubin, A. J. *Chemistry of Wastewater Technology*; Ann Arbor Science: Stoneham, MA, 1978.
(14) Stross, R. G.; Hasler, A. D. *Limnol. Oceanogr.* **1960**, *5*, 265–272.
(15) Shannon, E. E. Presented at the Nutrient Control Seminar, Calgary, AB, February 1980.
(16) Theis, T. L.; McCabe, P. J. *J.—Water Pollut. Control Fed.* **1978**, *50*, 2666–2676.
(17) Johnson, W. E.; Hasler, A. D. *J. Wildl. Manage.* **1954**, *18*, 113–134.
(18) Bengtsson, B.; Dickson, W.; Nyberg, P. *Ambio* **1980**, *9*, 34–36.
(19) Environment Canada *Analytical Methods Manual*; Inland Water Directorate: Ottawa, 1979.
(20) Prepas, E. E.; Trew, D. O. *Can. J. Fish. Aquat. Sci.* **1983**, *40*, 27–35.
(21) Carpenter, J. H. *Limnol. Oceanogr.* **1965**, *10*, 141–143.
(22) Stainton, M. P.; Capel, M. J.; Armstrong, F. A. J. *The Chemical Analysis of Freshwater*, 2nd ed.; Fisheries Environment Canada Special Publication 25, 1977.
(23) D'Elia, C. F.; Steudler, P. A.; Corwin, N. *Limnol. Oceanogr.* **1977**, *22*, 760–764.
(24) Bergmann, M.; Peters, R. H. *Can. J. Fish. Aquat. Sci.* **1980**, *37*, 111–114.
(25) Burnison, B. K. *Can. J. Fish. Aquat. Sci.* **1980**, *37*, 729–733.
(26) Lund, J. W. G.; Kipling, C.; Le Cren, E. D. *Hydrobiologia* **1958**, *11*, 143–170.
(27) Barica, J. *Can. J. Fish. Aquat. Sci.* **1977**, *34*, 2210–2215.
(28) Babin, J.; Prepas, E. E. *Can. J. Fish. Aquat. Sci.* **1985**, *42*, 239–249.
(29) Westlake, D. F. *Mem. Ist. Ital. Idrobiol.* **1965**, *18* (suppl.), 313–322.
(30) Shaw, R. D.; Trimbee, A. M.; Minty, A.; Fricker, H.; Prepas, E. E. *Water, Air, Soil Pollut.* **1989**, *43*, 119–134.
(31) Plummer, L. N.; Jones, B. F.; Truesdell, A. H. WATEQF, a FORTRAN IV version of WATEQ, a computer program for calculating chemical equilibria of natural waters. *Water-Resour. Invest. U.S. Geol. Surv.* **1976**, *No. 76-13*.
(32) Manning, P. G.; Murphy, T. P.; Mayer, T.; Prepas, E. E. *Can. Mineral.* **1988**, *26*, 965–972.
(33) Shaw, R. D.; Prepas, E. E. *J. Hydrol.*, in press.
(34) Shaw, R. D.; Shaw, J. F. H.; Fricker, H.; Prepas, E. E. *Limnol. Oceanogr.*, in press.
(35) Prepas, E. E.; Trimbee, A. M. *Hydrobiologia* **1988**, *159*, 269–276.
(36) Bergman, M. A.; Welch, H. A. *Can. J. Fish. Aquat. Sci.* **1985**, *42*, 1789–1798.
(37) Babin, J.; Prepas, E. E.; Murphy, T. P.; Hamilton, H. R. *Lake Reservoir Manage.* **1989**, *5*, 129–135.
(38) Murphy, T. P.; Prepas, E. E.; Lim, J. T.; Walty, D. T.; Crosby, J. M. *Lake Reservoir Manage.*, in press.
(39) White, W. S.; Wetzel, R. G. *Verh. Int. Ver. Theor. Angew. Limnol.* **1975**, *19*, 330–339.
(40) Howarth, R. W.; Marino, R.; Cole, J. J. *Limnol. Oceanogr.* **1988**, *33*, 688–701.
(41) Wodka, M. C.; Effler, S. W.; Driscoll, C. T. *Limnol. Oceanogr.* **1985**, *30*, 833–843.
(42) Ryan, J.; Curtin, D.; Cheema, M. A. *Soil Sci. Soc. Am. J.* **1984**, *48*, 74–76.
(43) Schindler, D. W. *Can. J. Fish. Aquat. Sci.* **1987**, *44* (Suppl. No. 1), 6–25.

Received for review January 30, 1989. Revised manuscript received September 8, 1989. Accepted April 6, 1990. Funding was provided by a contract from Planning Division, Alberta Environment to E.E.P. and grants from NSERC to E.E.P. and from Bucks for Wildlife to D.T.W.

Environ. Sci. Technol. 1990, 24, 1259–1261

Inferred Effects of Lake Acidification on *Daphnia galeata mendotae*

Wendel Keller,*,† Norman D. Yan,‡ Keith E. Holtze,‡,§ and J. Roger Pitblado‖

Ontario Ministry of the Environment, Sudbury, Ontario, Canada P3E 5P9

Introduction

Large numbers of Canadian Shield lakes have been acidified by the atmospheric deposition of anthropogenic sulfur (*1*). Biological damage attributable to acidification occurs at all levels of aquatic food webs (*2*, *3*); however, documentation of this damage has largely been confined to areas near large point sources of air pollutants (*4*, *5*), to small numbers of study lakes (*6*, *7*), or to experimentally acidified lakes (*8*). Demonstrations of widespread biological effects of acidification have been greatly hampered by the general absence of observations of the occurrence or abundance of important, ubiquitous species in large numbers of lakes ranging widely in acidity, coupled with laboratory determinations of lethal acid thresholds for these species (*9*, *10*). In consequence, it has been necessary to estimate rather than to document the regional extent of biological damage in North America (*11*). In this report we couple determination of the lethal acid threshold of *Daphnia galeata mendotae* Birge, a large, ubiquitous, planktonic crustacean (*12*), with results of extensive lake surveys, to examine if the acidification of lakes in Ontario has resulted in widespread losses of this important member of the zooplankton.

Methods

D. galeata mendotae were collected in zooplankton surveys from four areas of Ontario (termed South-central, Northeastern, Algoma, and Northwestern) spanning a wide range in sulfur deposition regimes (Figure 1). Animals were collected from the South-central lakes on 2–13 occasions per annum, from 1983 to 1985 in a series of metered, 76-μm mesh net hauls through selected depths that were combined to form a composite sample that corrected for the diminution of stratum volume with depth. Animals were collected from the Northeastern (1981), Algoma (1986), and Northwestern (1981) lakes in single, vertical net hauls from 1 m above bottom to the lake surface at a central location in each lake, except in some shallow (<2 m deep) Algoma lakes where horizontal tows were used. Northeastern and Algoma lakes were sampled once. Northwestern lakes were sampled one to three times. All lakes were sampled during the ice-free season. Lakes sampled only once were visited during the summer (mid-June to late August), when *D. galeata mendotae* would be expected to be abundant if present. For the South-central lake samples, biomass was calculated from the measured lengths and abundances of *D. galeata mendotae* determined with a semiautomated system (13). For the other samples, biomass was estimated from animal abundance by using the average dry weight of 8.76 μg/animal observed in the South-central lake set (*14*).

Many Northeastern lakes within about 100 km of Sudbury, Ontario, have been affected by elevated sulfur and trace-metal emissions from the Sudbury smelters (*15*–*17*). To remove the influence of trace-metal deposition associated with these smelters, lakes with Cu concentrations of ≥ 5 μg L^{-1} were eliminated from the data set (*18*, *19*). The other study areas are all distant from Sudbury (>150 km) and from other major point sources of acid and metal emissions. Lakes with pH >7.5 or conductivity >50 μS were also excluded, reducing the final data set to 445 lakes.

Table I. Lethal pH Thresholds for *Daphnia galeata mendotae*

trial	4-day LC50	95% CI
A	5.69	5.47–5.92
B	5.98	5.72–6.24
C	5.95	5.73–6.14
combined	5.85	5.69–6.00

Laboratory cultures of *D. galeata mendotae* were established from a wild population in Red Chalk Lake, a soft water lake (pH 6.3, conductivity 28 μS, calcium 2.6 mg L^{-1}, total aluminum 9 μg L^{-1}, dissolved organic carbon 2.4 mg L^{-1}) in south-central Ontario. Animals were reared for three generations in source lake water prior to initiating assays. Bioassays were conducted at 20 °C in well-aerated Red Chalk Lake water with pH levels adjusted with ultrapure H_2SO_4. For each trial, 10 neonates (<24 h old) were exposed in 500-mL vessels at pH 6.9 (control; aeration explains the higher laboratory pH than in situ pH), 6.0, 5.8, 5.6, 5.4, and 5.2. Solutions were renewed daily to maintain constant pH. With each renewal, animals were fed 10 mL of a 1:1 mixture of *Selenastrum capricornutum* and *Chlorella fusca* containing 4×10^5 cells mL^{-1}. Bioassays were conducted between August and October 1987 under a combination of incandescent and fluorescent lighting with photoperiod adjusted twice monthly to match actual day lengths. Median lethal levels of pH (LC50) were calculated with survival data and H^+ concentrations by probit analysis (*20*) with corrections for control mortality (*21*). Differences among the three trials were examined by using the standard error of the difference (*22*).

Results and Discussion

D. galeata mendotae is a very important zooplankton species in nonacidic lakes in Ontario. It occurred in 44–92% of the lakes with pH >6.0 in each data set, and it was the first to third most important contributor (11–14%) to average herbivorous zooplankton biomass in these lakes. The biomass of *D. galeata mendotae* declined dramatically near pH 6.0 in all the regions with low pH lakes, and it was absent from virtually all lakes with pH <5.5 (Figure 2). This agrees with the observation that *D. galeata mendotae* disappeared in a whole lake acidification experiment at pH ~5.5 (*8*).

Within all the data sets, even the consistently near-neutral Northwestern lakes, the biomass of *D. galeata mendotae* [$\log_{10}(x + 1)$ transformed] was significantly ($p < 0.05$) correlated with pH (Pearson product moment correlation coefficients of 0.22–0.64). In the three data sets with low pH lakes, *D. galeata mendotae* biomass was more strongly correlated with pH than with other limnological characteristics ($\log_{10}$ transformed) reflecting morphometry (area, depth), chemistry (conductivity, aluminum), and

† Ontario Ministry of the Environment, 199 Larch St., Sudbury, Ontario, Canada, P3E 5P9.

‡ Ontario Ministry of the Environment, Dorset Research Centre, P.O. Box 39, Dorset, Ontario, Canada, P0A 1E0.

§ Present address: B.A.R. Environmental, Brock Rd., R.R. 3, Guelph, Ontario, Canada, N1H 6H9.

‖ Geography Department, Laurentian University, Ramsey Lake Rd., Sudbury, Ontario, Canada, P3E 2C6.

0013-936X/90/0924-1259$02.50/0

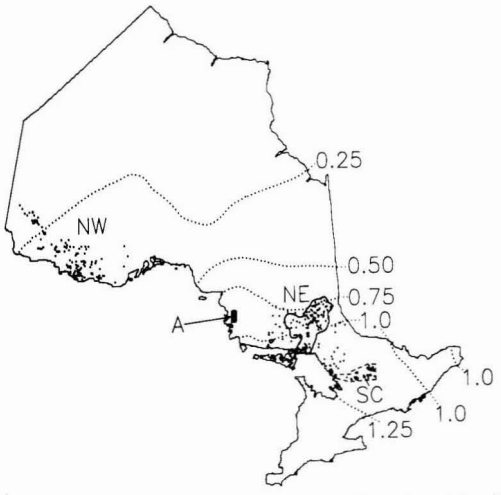

Figure 1. Total sulfur deposition isopleths (dotted lines, in g of S m^{-2} yr^{-1}) in Ontario in 1983 (*27*) and the locations of the study lakes (NW, Northwestern; A, Algoma; NE, Northeastern; SC, South-central). The approximate zone of significant influence by Sudbury on lake chemistry, defined as $SO_4^{2-}/(SO_4^{2-}$ + alkalinity) > 0.7, is indicated by the solid line enclosing many of the Northeastern lakes. The gap in sampling coverage in the immediate Sudbury (S) area results from the exclusion of metal-contaminated lakes from the data set.

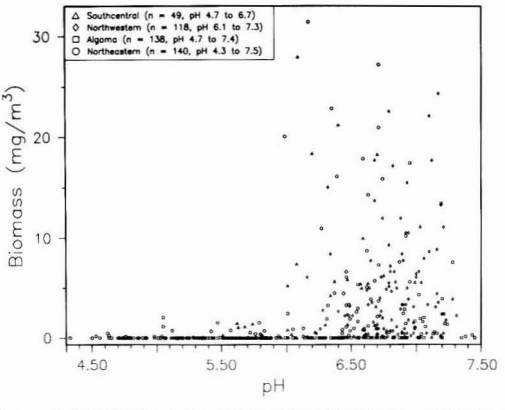

Figure 2. Relationship between lake pH and the biomass of *Daphnia galeata mendotae* in the four zooplankton surveys.

trophic status (total phosphorus, total nitrogen, color/dissolved organic carbon, and Secchi transparency).

Consistent with the survey data, survival of *D. galeata mendotae* was reduced at all pH levels of ≤6.0 in bioassays. No survival was observed at pH ≤5.4. The 4-day LC50 pH values ranged from 5.69 to 5.98 and were not significantly different (Table I). Pooling all the data yielded a 4-day LC50 pH of 5.85, much higher than a value of 4.77 (*23*) previously reported for shorter (48-h) exposures with adult *D. galeata mendotae* in much harder water (calcium 7.8 mg L^{-1}).

If we assume that absence of *D. galeata mendotae* implies disappearance rather than lack of colonization, the close agreement between the calculated lethal acid thresholds (Table I) and the distribution of *D. galeata mendotae* biomass along the environmental pH gradient (Figure 2) strongly suggests that lake acidity is the major factor controlling the biomass of this important zooplankter in acid-sensitive lakes in Ontario. Three observations indicate this is a reasonable assumption. First, Fryer (*24*) has demonstrated that crustacean zooplankton colonize new habitats rapidly. Second, *D. galeata mendotae* has been observed to colonize an acidic lake after water quality improved. *D. galeata mendotae* were never once recorded in the zooplankton of Nelson Lake, 30 km northwest of Sudbury, in 1975 when the pH was 5.7, or in 1976, the first year after the pH was experimentally elevated to 6.5 (*25*). However, after a decade at pH >6.0, *D. galeata mendotae* were observed in every sample collected at monthly intervals over the ice-free seasons of 1985 and 1986 (Keller and Yan, unpublished data). Third, because *D. galeata mendotae* is one of the most commonly observed zooplankton species in nonacidified lakes in all regions of Ontario (*12*, *26*), many colonization sources are available.

Lake acidification in Ontario is attributable to atmospheric sulfur deposition, which is caused by elevated sulfur emissions in North America (*1*). Therefore, our data strongly suggest that widespread damage to *D. galeata mendotae* populations has occurred as a result of anthropogenic influences. This damage commences at comparatively low levels of acidity, near or even above pH 6.0. It is estimated that there are at least 19000 lakes that now have pH levels <6.0 in Ontario (*27*).

Acknowledgments

We thank B. Girard, H. Stahl, and L. Maki for sample collection, W. Geiling for sample enumeration, B. Neary for mapping the Sudbury zone of effect, and P. Dillon and K. Nicholls for comments on the manuscript.

Literature Cited

(1) Neary, B. P.; Dillon, P. J. *Nature* **1988**, *333*, 340.
(2) Haines, T. T. *Trans. Am. Fish. Soc.* **1984**, *110*, 669.
(3) Dillon, P. J.; Yan, N. D.; Harvey, H. H. *Crit. Rev. Environ. Control* **1984**, *13*, 167.
(4) Beamish, R. J.; Harvey, H. H. *J. Fish. Res. Board Can.* **1972**, *29*, 1131.
(5) Sprules, W. G. *J. Fish. Res. Board Can.* **1975**, *32*, 389.
(6) Rooke, J. B.; Mackie, G. L. *Can. J. Fish. Aquat. Sci.* **1984**, *41*, 777.
(7) Stephenson, M.; Mackie, G. L. *Can. J. Fish. Aquat. Sci.* **1986**, *43*, 288.
(8) Schindler, D. W.; et al. *Science* **1985**, *228*, 1395.
(9) Magnuson, J. J.; Baker, J. P.; Rahel, E. J. *Philos. Trans. R. Soc. London* **1984**, *305*, 501.
(10) Mierle, G.; Clark, K.; France, R. *Water, Air, Soil Pollut.* **1986**, *31*, 593.
(11) Schindler, D. W.; Kasian, S. E. M.; Hesslein, R. H. *Environ. Sci. Technol.* **1989**, *23*, 573.
(12) Carter, J. C. H.; Dadswell, M. J.; Roff, J. C.; Sprules, W. G. *Can. J. Zool.* **1980**, *58*, 1355.
(13) Sprules, G. W.; Holtby, L. B.; Griggs, G. *Can. J. Zool.* **1981**, *59*, 1611.
(14) Hitchin, G. G.; Yan, N. D. Crustacean Zooplankton Communities of Muskoka Haliburton Study Lakes: Methods and 1976–1987 Data. Ontario Ministry of the Environment Report DR 83/4; Toronto, Canada, 1983.
(15) Dillon, P. J.; Yan, N. D.; Scheider, W. A.; Conroy, N. *Arch. Hydrobiol. Beih. Ergebn. Limnol.* **1979**, *13*, 317.
(16) Keller, W.; Pitblado, J. R. *Water, Air, Soil Pollut.* **1984**, *23*, 271.
(17) Keller, W.; Pitblado, J. R. *Water, Air, Soil Pollut.* **1986**, *29*, 285.
(18) Ontario Ministry of Environment. Water Management—Goals, Policies, Objectives and Implementation Procedures of the Ministry of the Environment. Ontario Ministry of the Environment Report, Toronto, Canada, 1984.
(19) Winner, R. W. *Water Res.* **1985**, *19*, 449.
(20) Hubert, J. J.; Schoch, P. J. *Probit: An Interactive Program in Basic for Probit Analysis*; Statistical Series No. 1984–160; University of Guelph: Guelph, Canada, 1984.

(21) Abott, W. S. *J. Econ. Entomol.* **1925**, *18*, 265.
(22) Sprague, J. B.; Fogels, A. Watch the y in Bioassay. Environmental Protection Service Technical Report No. EPS-5-AR-77-1, 107–118; Halifax, Canada, 1977.
(23) Price, E. E.; Swift, M. C. *Can. J. Fish. Aquat. Sci.* **1985**, *42*, 1749.
(24) Fryer, G. *Freshwater Biol.* **1985**, *15*, 347.
(25) Yan, N. D.; Scheider, W. A.; Dillon, P. J. *Water Pollut. Res. Can.* **1977**, *12*, 213.
(26) Keller, W.; Pitblado, J. R. *J. Biogeogr.* **1989**, *16*, 249.
(27) Neary, B. P.; Dillon, P. J.; Munro, J. R.; Clark, B. J. The Acidification of Ontario Lakes: An Assessment of their Sensitivity and Current Status with Respect to Biological Damage. Ontario Ministry of the Environment Report, Dorset, Canada, 1990.

Received for review August 28, 1989. Accepted March 8, 1990.

Nonaqueous Ion-Exchange Separation Technique for Use in Bioassay-Directed Fractionation of Complex Mixtures: Application to Wood Smoke Particle Extracts

Douglas A. Bell,*,† Hani Karam,‡ and Richard M. Kamens

Department of Environmental Sciences and Engineering, School of Public Health, University of North Carolina, Chapel Hill, North Carolina 27514

■ We have explored the feasibility of an alternative method for acid/base/neutral separation of atmospheric samples such as wood smoke particle extracts that contain highly polar or acidic organic species. Ion-exchange resins, Amberlyst 15 and Amberlyst 26, were used with organic solvents for fractionating a standard mixture of organic acid, base, and neutral compounds, and a dichloromethane extract from pine wood smoke particles. Total recovery of individual standard compounds was 85–124% and qualitative separation between chemical classes was good. The recovery of wood soot extract through the fractionation system was 107 ± 13%, with 15% in the basic fraction, 55% in the neutral fraction, and 20% and 17% in two acidic fractions. The majority of bacterial mutagenicity (TA98+S9, 49%; TA98-S9, 61%) appeared in the neutral fraction but significant direct-acting mutagenicity (39%) was found in the acidic fractions.

Introduction

Isolation of biologically active chemical fractions and the identification of specific toxic agents from complex environmental mixtures is a difficult technical challenge (*1*). This process, often referred to as bioassay-directed fractionation, requires chemical separation techniques that allow high recovery of total sample mass and individual toxic species (*2*). Application of bioassay-directed fractionation to the polar fractions of wood smoke, which contain 75–90% of the mutagenic activity, has been particularly difficult (*3*). Common chemical separation methods for combustion samples such as normal-phase silica gel HPLC and aqueous-phase acid/base/neutral liquid/liquid partitioning have resulted in low mass recovery of polar compounds and loss of mutagenicity in polar fractions. Bell et al. (*4*) used normal-phase silica gel HPLC to separate dichloromethane extracts from freshly emitted and sunlight-reacted pine wood smoke particles. This method resulted in respective mass recoveries of 76% and 50%, and mutagenicity (TA98+S9) recoveries of 67% and 46%. Nishioka et al. (5) performed acid, base, and neutral fractionation of pine smoke extracts by aqueous-phase liquid/liquid partitioning and observed ~40% mass loss and ~33% mutagenicity loss. Clearly, there is a need for an alternative to these techniques when confronted with highly polar, acidic organic mixtures.

Table I. Recovery of Fractionation Standard Compounds through the Ion-Exchange Separation

	% recovery				
compound	base	neutral	acid	polar acid	total[e]
benzoic acid[a]		16 ± 2	72 ± 2	18 ± 5	106 ± 3
phthalic acid[a] (n = 2)		31 ± 3	33 ± 7	50 ± 8	115 ± 11
dibenzofuran[a]		102 ± 2			102 ± 2
1-naphthol[a]		20 ± 1	76 ± 4	7 ± 3	103 ± 5
9-fluorenone[a]		102 ± 3			102 ± 3
7,8-benzoquinoline[a] (n = 2)	85 ± 3				85 ± 3
4-nitrophenol[b]		2 ± 1	83 ± 7	11 ± 4	96 ± 8
pyrene[a]		104 ± 3			104 ± 3
naphthalic acid anhydride[b]		88 ± 4	11 ± 4	8 ± 3	107 ± 6
benz[a]anthracene-7,12-dione[c]		124 ± 6			124 ± 6

[a] Aldrich, >99%. [b] Chem Service, >99%. [c] Kodak, >99%. [d] Mean of four runs unless otherwise noted. Mean ± SEM. Total mass of standard applied to columns was 12, 24, 30, or 30 mg. This represents a range of ~0.05–0.1 mequiv (~1% of the column capacity). [e] Square root of the sum of the variance for the four fractions converted to percent of the mean.

The goal of this work was to explore the feasibility of a simple, alternative method for chemically separating acidic, basic, and neutral fractions found in pine wood smoke extract while achieving high mass and mutagenicity recovery required for bioassay-directed fractionation. We report here preliminary data on the use of a nonaqueous ion-exchange technique for fractionating a standard mixture of organic acid, base, and neutral compounds, and a dichloromethane extract from pine smoke particles. We have evaluated this scheme with respect to quantitative recovery of authentic chemical standards, mass of wood smoke extract, and mutagenicity. We are currently modifying and refining this technique for use on source emissions from wood stoves, ambient air samples impacted by residential wood stoves and mobile sources, and stack

† Present address: National Research Council, Genetic Toxicology Division, U.S. EPA, Research Triangle Park, NC 27711.
‡ Present address: Triangle Laboratories, Research Triangle Park, NC 27709.

0013-936X/90/0924-1261$02.50/0

samples from municipal waste incinerators.

Materials and Methods

Reagents. High purity grade chloroform, dichloromethane (DCM), tetrahydrofuran (THF), and methanol were purchased from Burdick and Jackson (Muskegon, MI). The macroreticular ion-exchange resins (Amberlyst 15 and Amberlyst 26) were manufactured by Rohm and Hass and obtained from Alfa Products (Danvers, MA). Trifluoroacetic acid and isopropylamine were obtained from Fluka (Ronkonkoma, NY). Source and purity of standard compounds are listed in Table I.

Conditioning of Ion-Exchange Resins. Preparation was similar to that of Bell et al. (6) and Jewell et al. (7). Amberlyst 15, a sulfonic acid cation-exchange resin (capacity 4.7 mequiv/g), was washed with 100 mL of a methanolic potassium hydroxide solution (5% by weight) and then rinsed with 100 mL of methanol. It was then converted to the acid state by slowly adding 100 mL of 5% volume HCl in methanol and stirring for 30 min. The resin was washed with distilled deionized water until the pH of the washing water was neutral. The final step was to Soxhlet extract the resin for 24 h each with methanol, dichloromethane, and a chloroform/5% tetrahydrofuran mixture. The cation-exchange resin was stored in chloroform in the dark in a glass container with a Teflon-lined cap until used.

The anion-exchange resin, Amberlyst 26 (quaternary amine, capacity 4.4 mequiv/g), was washed with 100 mL of 5% HCl in methanol and rinsed with 100 mL of methanol. After being rinsed, the resin was activated by adding 100 mL of 5% methanolic potassium hydroxide solution. The resin was washed with deionized water, Soxhlet extracted sequentially with methanol, DCM, methanol, and DCM, and stored in DCM. Resins should be used within 30 days of conditioning. Approximately 6 g (dry weight) of resin was slurry packed in DCM into a 25-mL buret plugged with glass wool and fitted with a Teflon stopcock. Columns were rinsed with 50 mL of the initial solvent prior to addition of the sample. The quantity of resin used in these separations was estimated to provide greater than 90% excess anion-exchange capacity relative to the sample.

Separation Procedure. A high concentration standard was prepared containing each of the compounds listed in Table I at a concentration of ~6 mg/mL in 10% methanol/DCM and aliquots of this mixture were used for the qualitative and quantitative analysis. The relative amounts of total acidic (40%), basic (10%), and neutral (50%) components reflect the approximate distribution of these chemical classes in wood smoke. Many of these compounds have been identified in wood smoke by Kamens et al. (8) and Ramdahl and Becher (9).

The method reported here is modified from that reported by Jewell et al. (7) and Bell et al. (6). The ion-exchange separation procedure is shown schematically in Figure 1. Fractionation standard (12–30 mg) or wood smoke extract (69.1 mg dissolved in 10% methanol/DCM) was placed on the Amberlyst 15 column. Acids and neutrals were eluted with 50 mL of 20% methanol/DCM. Previous trials suggested that the presence of methanol in the elution solvent was needed to provide sufficient mobile-phase polarity to maintain the polar solutes in solution during the separation.

The retained bases were removed from the resin with 50 mL of 20% volume isopropylamine in methanol. The acid/neutral mixture was concentrated by rotary evaporation to ~1 mL and placed on the anion-exchange column. Neutrals were eluted in 50 mL of 100% DCM.

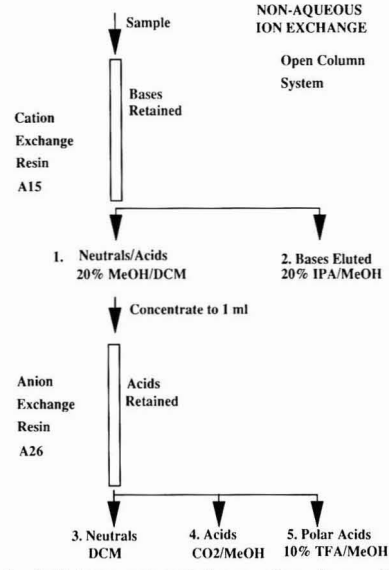

Figure 1. Acid, base, and neutral separation scheme utilizing ion-exchange resins.

Retained acids were then eluted by adding 50 mL of CO_2/methanol solution. This fraction is referred to as the acid fraction. The CO_2/methanol solution was created by bubbling gaseous CO_2 through methanol for ~30 min. The polar acid fraction was collected by eluting with a 10% trifluoroacetic acid/methanol solution. Each elution was carried out at a rate of ~1 mL/min. The volume of solvent used for the wood smoke separation was 75 mL/fraction. Basic and acidic fractions were rotary evaporated just to dryness to remove any remaining isopropylamine, CO_2, or trifluoroacetic acid. They were then redissolved in fresh solvent. Samples to be bioassayed were solvent exchanged into DMSO. Quantitation of compounds in the fractions was by gas chromatography utilizing a 30-m fused-silica J&W, DB 1701 (phenyl(cyanopropyl)methyl) column with hydrogen as carrier gas and a flame ionization detector as described in Kamens et al. (10).

Mutagenicity Assay. Samples were tested by the plate incorporation test with *Salmonella typhimurium* strain TA98 with and without a 10% rat liver homogenate mixture (S9) prepared from Aroclor-induced rats (11, 12). Due to a limitation of mass for most fractions, fractions were tested with duplicate plates at four doses that were chosen by estimating the probable linear dose–response range based on previous testing. Mutagenicity slope values were calculated by simple linear regression using all dose levels.

Results and Discussion

Recovery of Authentic Compounds. Table I summarizes the recovery of authentic compounds through the ion-exchange separation method (four trials). Total recovery of individual compounds in the fractionation standard was high, and qualitative separation between chemical classes was good. There was no overlap of acid or neutral compounds into the base fraction, and the base, benzoquinoline, showed 85% recovery. Good qualitative separation of neutrals was also achieved. With the exception of naphthalic acid anhydride, no neutral compounds appeared in the acid or base fractions. The acidic compound, 4-nitrophenol, appeared almost entirely in the acidic fractions and showed 96% recovery. These data

Table II. Mass Distribution and Recovery for Wood Smoke Particle Extract Sample

sample	mass, mg	% rec
whole	69.1	100.0
base	10.2	14.8
neutral	38.0	55.0
acid	14.2	20.5
polar acid	11.9	17.2
sum	74.3	107.5[a]

[a] The mass measurement error (SD) for individual samples was typically ±7% based on replicate analysis and ±13% for the sum of four samples (square root of the sum of the variances of four samples).

Table III. Mutagenic Potency, Percent Distribution and Mutagenicity Recovery for Wood Smoke Whole Extract and Fractions in TA98

	TA98-S9			TA98+S9		
sample	rev/μg extrt[a]	rev/ fractn[b]	% mutag distribn[c]	rev/μg extrt[a]	rev/ fractn[b]	% mutag distribn[c]
whole extract	0.47	32280	100	1.77	122530	100
base	0.08	820	3	1.35	13730	11
neutral	0.52	19800	61	1.60	60650	49
acid	0.24	3440	11	0.31	4400	4
polar acid	0.76	9060	28	0.72	8550	7
sum of fractions			103			71

[a] Revertants per microgram of extract indicates relative potency of the samples. Mean (n = 3) revertant counts for controls: spontaneous −S9, 26; spontaneous +S9, 31; 3 μg of 2-nitrofluorene, 268; 0.5 μg of 2-aminoanthracene, 477. Calculated slope error for most samples was less than 5%; however, only a single test was performed and typical historical error between repeat tests is ±~15%. [b] Revertants per fraction is (revertants per microgram of extract)(fraction mass)[(potency)(mass)]. [c] Percent mutagenicity distribution is (potency)(mass) as a percent of the unfractionated or whole sample.

suggest that ion-exchange separation may be useful in studies such as Nishioka et al. (*14*), which focused on recovery and identification hydroxynitroarenes in atmospherically reacted samples.

An area of concern in these data is the presence of significant quantities of weak acid species, specifically benzoic acid, 1-naphthol, and phthalic acid in the neutral fraction (16%, 20%, and 31%, respectively). Given that the total milliequivalents of acid in these four separations varied from ~0.05 to 0.1 mequiv (see Table I) and that the total ion-exchange capacity of the column was ~26 mequiv, it is unlikely that breakthrough, or overloading of the column, caused the elution of the weak acids in the neutral fraction.

In additional trials, we explored the hypothesis that the presence of methanol could reduce the selectivity of the anion-exchange resin for weak organic acids. We found that increasing the methanol concentration of the neutral elution solvent to 10% in step 3 (Figure 1) resulted in a dramatic increase (from 16% to 46%) in the quantity of benzoic acid in the neutral fraction. Because many of the acidic components could not be maintained in solution in 100% DCM, elution of the neutrals/acids from the cation resin in step 1 required 20% methanol/DCM. Therefore, we infer from the above results that the presence of residual methanol from step 1, concentrated during the rotory evaporation step, is the reason for the observed lack of selectivity of this ion-exchange resin for weak acids. Ongoing work suggests that a related anion-exchange resin, AG-MP1 (Bio-Rad, Richmond, CA), has better selectivity in the presence of methanol, particularly if used in a solid-phase extraction protocol (*15*).

Wood Smoke Mass Recovery. A wood smoke extract sample was chemically separated, and mass distribution and recovery results are shown in Table II. The recovery of mass through the separation scheme was 107.5 ± 13%. The base, neutral, and acid fractions contained 14.8%, 55%, and 37.7%, respectively, of the fractionated mass. For pine smoke stack sample, Nishioka et al. (*5*) recovered 59% of the mass fractionated using an aqueous-phase liquid/liquid partitioning procedure. Of the total mass fractionated, bases comprised 1.9%, neutrals 29.3%, and acids 27.8%.

Mutagenicity Recovery. The TA98 mutagenic potency, percent distribution, and recovery are shown in Table III. The whole unfractionated pine wood smoke extract was slightly more potent than other samples tested in this laboratory (typical values for TA98: −S9, 0.3 revertants/μg; +S9, 1.2 revertants/μg). The neutral fraction contained the most mutagenicity with or without S9 activation. The acid fractions also contained significant direct-acting (−S9) mutagenicity (11% and 28%). The base fraction had a high S9-dependent mutagenic potency but, due to low mass, contributed relatively little (11%) to the whole sample.

Mutagenicity recovery was calculated from the sum of the percent distribution values for the fractions. These values were 103% and 71%. Variation between recovery of direct-acting and S9-dependent mutagenicity was observed in previous work with a similar separation scheme (*6*) and also during HPLC fractionation of oak combustion particles reacted with NO_2 and O_3 (*8*). Variation in mutagenicity recovery may reflect the combined error in the mutagenicity assay and the mass analysis (estimated at 15–25% for mass and mutagenic potency combined). This suggests that recoveries are within the range of the experimental error.

Mutagenicity testing of method blanks produced no significant response above the spontaneous mutation level, suggesting little effect of the method on the mutagenicity of the fractions. Chromatographic analysis of the method blanks detected a single trace contaminant peak. In addition, small quantities of isopropylamine and trifluoroacetic acid were found in the base and polar acid fractions. The chromatographic contaminant may be related to residual unpolymerized divinylbenzene monomers eluting from the ion-exchange resin. Isopropylamine and trifluoroacetic acid were tested for mutagenicity and did not produce a mutagenic response.

Overall, these data suggest adequate recovery of mass and mutagenicity through this separation scheme and demonstrate the compatibility of the technique with the mutagenicity bioassay. This method appears to be feasible as a primary step in bioassay-directed fractionation, particularly for separating highly polar organic extracts such as wood smoke. Current research is aimed at improving qualitative separation of weak acids by optimizing flow and solvent parameters and exploring additional resin types in a solid-phase extraction protocol. We are also evaluating this method with a variety of highly acidic samples such as particles from a municiple waste incinerator.

Acknowledgments

We thank Drs. L. Claxton and J. Lewtas, U.S. EPA, for their continued support of this project. We also acknowledge the useful suggestions made by M. Nishioka, Battelle Columbus Laboratory, and the excellent technical support of J. Fulcher and C. Braun, University of North Carolina.

Registry No. Amberlyst 15, 9037-24-5; Amberlyst 26, 69865-42-5; benzoic acid, 65-85-0; phthalic acid, 88-99-3; dibenzofuran, 132-64-9; 1-naphthol, 90-15-3; 9-fluorenone, 486-25-9; 7,8-benzoquinoline, 230-27-3; 4-nitrophenol, 100-02-7; pyrene, 129-00-0; naphthalic acid anhydride, 81-84-5; benz[*a*]anthracene-7,12-dione, 2498-66-0.

Literature Cited

(1) Scheutzle, D.; Lewtas, J. *Anal. Chem.* **1986**, *58*, 1060–1067.
(2) Lewtas, J. *Fundam. Appl. Toxicol.* **1988**, *10*, 571–589.
(3) Nishioka, M.; Chuang, C. C.; Peterson, B. A.; Austin A.; Lewtas, J. *Environ. Int.* **1985**, *11*, 137–146.
(4) Bell, D. A.; Kamens, R. M.; Claxton, L. D.; Lewtas, J. Presented at 79th Annual Meeting, Air Pollution Control Association, Minneapolis, MN, 1986; APCA 86-77.4.
(5) Nishioka, M.; Strup, P.; Chuang, C. C.; Cooke, M. Draft final report prepared by Battelle Columbus Laboratories for ORD-USEPA, Contract No. 68-02-2686, Task Directive 134, 1986.
(6) Bell, D. A., Karam, H.; Kamens, R. M. *Proceedings of the 1987 EPA/APCA Symposium on Measurement of Toxic Air Pollutants*; EPA600/9-87-010; Research Triangle Park, NC, 1987; APCA V1P-8, pp 411–415.
(7) Jewell, D. M.; Weber, J. H.; Benger, J. W.; Plancher, H.; Latham, D. R. *Anal. Chem.* **1972**, *44*, 1391.
(8) Kamens, R. M.; Bell, D. A.; Dietrich, A.; Perry, J.; Goodman, R.; Claxton, L. D.; Tejada, S. *Environ. Sci. Technol.* **1985**, *19*, 63–69.
(9) Ramdahl, T.; Becher, G. *Anal. Chim. Acta* **1982**, *144*, 83–91.
(10) Kamens, R. M.; Karam, H.; Guo, J.; Perry, J. M.; Stockburger, L. *Environ. Sci. Technol.* **1989**, *23*, 801–806.
(11) Maron, D.; Ames, B. N. *Mutat. Res.* **1983**, *113*, 173–215.
(12) Claxton, L.; Austin, A.; Kohan, M.; Evans, C. Health Effects Research Laboratory, U.S. EPA, EPA-HERL-0323; 1982.
(13) Kamens, R. M.; Rives, G.; Perry, J.; Bell, D. A.; Paylor, R. E., Jr.; Goodman, R. G.; Claxton, L. D. *Environ. Sci. Technol.* **1984**, *18*, 523–530.
(14) Nishioka, M.; Howard, C.; Contos, D.; Ball, L.; Lewtas, J. *Environ. Sci. Technol.* **1988**, *22*, 908–915.
(15) Bell, D. A.; Williams, R.; Brooks, L.; Thompson, D.; Zwiedinger, R.; Lewtas, J. Presented at the International Conference on the Genetic Toxicology of Complex Mixtures, Washington, DC, 1989; abstract.

Received for review February 1, 1989. Revised manuscript received February 23, 1990. Accepted March 12, 1990. This work was funded wholely by cooperative agreement (CR 812514) and grant (R812256) from the U.S. EPA.

Environ. Sci. Technol. 1990, 24, 1265–1270

Selected Organic Pollutant Emissions from Unvented Kerosene Space Heaters

Gregory W. Traynor,* Michael G. Apte, and Harvey A. Sokol

Indoor Environment Program, Applied Science Division, Lawrence Berkeley Laboratory, University of California, Berkeley, California 94720

Jane C. Chuang

Analytical and Structural Chemistry Center, Battelle Columbus Laboratories, Columbus, Ohio 43201

W. Gene Tucker

Air and Energy Engineering Research Laboratory, U.S. Environmental Protection Agency, Research Triangle Park, North Carolina 27711

Judy L. Mumford

Health Effects Research Laboratory, U.S. Environmental Protection Agency, Research Triangle Park, North Carolina 27711

■ An exploratory study was performed to assess the semivolatile and nonvolatile organic pollutant emission rates from unvented kerosene space heaters. A well-tuned radiant heater and maltuned convective heater were tested for semivolatile and nonvolatile organic pollutant emissions. Each heater was operated in a 27-m^3 chamber with a prescribed on/off pattern. Organic compounds were collected on Teflon-impregnated glass filters backed by XAD-2 resin and analyzed by gas chromatography/mass spectrometry. Pollulant source strengths were calculated by use of a mass balance equation. The results show that kerosene heaters can emit polycyclic aromatic hydrocarbons (PAHs); nitrated PAHs; alkylbenzenes, phthalates; hydronaphthalenes; aliphatic hydrocarbons, alcohols, and ketones; and other organic compounds, some of which are known mutagens.

Introduction

The sale and use of unvented kerosene space heaters have increased dramatically in the United States during the past decade. These heaters have been found to emit a wide variety of pollutants including carbon monoxide, carbon dioxide, nitric oxide, nitrogen dioxide, sulfur dioxide, formaldehyde, and suspended particles (*1–5*). Several studies using a kerosene-fueled turbulent-diffusion continuous-flow combuster showed that many polycyclic aromatic hydrocarbons (PAHs) are emitted during kerosene combustion (*6–8*). Two of these studies also showed that kerosene soot is indirectly mutagenic (*7, 8*), and one showed that essentially all of the indirect mutagenic activity of kerosene soot was due to unnitrated PAH compounds (*8*). Another study revealed that kerosene heaters emit dinitropyrenes, showed kerosene soot to be directly mutagenic, and attributed most of the direct mutagenic activity to the dinitropyrenes (*9*).

The above studies have shown the following: kerosene combustion products can be mutagenic, kerosene combustion can produce PAHs and nitrated PAHs, and much of the mutagenic activity of kerosene soot is likely due to the PAHs and nitrated PAHs. However, it is not known whether the unvented portable kerosene space heaters with wicks commonly used indoors in the United States produce emissions similar to those emitted by turbulent-diffusion kerosene combustors used in laboratory studies (*6–8*) because of the difference in the combustion process. Additionally, it is not known whether unvented kerosene space heaters produce other potentially harmful organic pollutants.

The goal of this exploratory study was to measure selected pollutant emission rates (including PAH and nitrated PAH emission rates) from portable kerosene heaters commonly used in the United States. Two heater/tuning conditions were chosen based, in part, on previously reported particulate emission data (*4*). The previous study showed that particulate emissions from a well-tuned, properly adjusted convective kerosene heater were negligible but that particulate emissions from a well-tuned, properly adjusted radiant heater were not. Therefore, it was reasonable to assume that the organic pollutant emission rates observed from a radiant heater would be higher than the rates from a convective heater. A radiant heater operating under well-tuned, properly adjusted conditions was chosen as the first heater/tuning combination to be tested. The other heater/tuning combination chosen for testing was a convective heater operated under maltuned conditions. This choice was based, in part, on conversations with kerosene heater users and testers, who indicated that a convective heater was more likely to "soot" (i.e., emit a visible stream of particles) than was a radiant heater. The convective heater was maltuned by lifting the exterior shell of the heater by approximately 1 cm, thereby providing excess air to the wick, which probably represents an exaggerated case of maltuning. Multiple tests were conducted on each heater/tuning combination to allow collection of enough pollutant mass for future tests of mutagenic activity.

All experiments were conducted at the Lawrence Berkely Laboratory (LBL). Battelle Columbus Laboratories prepared and analyzed filters, provided clean resins used by LBL, and provided sample extracts to the Health Effects Research Laboratory of the U.S. Environmental Protection Agency for future mutagenicity tests.

Experimental Methods and Test Protocol

Each heater was operated in a 27-m^3 chamber. The chamber walls and ceiling are taped-and-sealed Sheetrock, and the floor is concrete. The heaters were operated intermittently to avoid unrealistically high chamber temperatures. For the five radiant heater tests conducted, the

0013-936X/90/0924-1265$02.50/0

heater was operated for 4 cycles of 1 h on and 1 h off. For the two maltuned convective heater tests, the heater was operated for only 2 cycles of the same 1-h-on/1-h-off pattern. The fuel consumption rates averaged 7000 ± 100 kJ/h for the radiant heater tests and averaged 6900 ± 600 kJ/h for the maltuned convective heater tests (heat content of kerosene, 43.5 kJ/g or 41.2 Btu/g). Two 8-h control tests were also conducted without a heater in operation. The air-exchange rates of the chamber averaged 1.1 ± 0.1 air changes/h for all tests. An average air-exchange rate for each test was computed from the decay curves of either CO or CO_2. The air-exchange rate was dominated by our sampling flow rate.

Pollutant source strengths (mass of pollutants emitted per hour) of particles and organic compound emissions were calculated by the steady-state, mass balance equation. The mass balance equation, arranged to isolate the pollutant source strength, follows:

$$S = V[C\ (a + k) - PaC_o] \qquad (1)$$

where S is the pollutant source strength (mass/h), V is the chamber volume (27 m^3), C is the average indoor pollutant concentration (mass/m^3), a is the average chamber air-exchange rate (h^{-1}), k is the average net rate of removal processes other than airflow, also called "reactivity" rate (h^{-1}), P is the outdoor pollutant penetration factor (dimensionless), and C_o is the average outdoor pollutant concentration (mass/m^3).

Equation 1 is the steady-state version of the indoor air quality mass balance equation developed by Turk (*10*) and used by numerous researchers (e.g., refs 3 and 11–14). The pollutant reactivity rate is the rate that the pollutant reacts with or deposits on indoor surfaces and suspended particles. This rate is often expressed as a first-order removal process similiar to air exchange. The outdoor penetration factor is a number between zero and 1 that reflects pollutant removal caused by the chamber shell as the outdoor air flows into the chamber. A value of 1 implies that there was no pollutant removal by the chamber shell.

Average source strengths determined with eq 1 were multiplied by 2 in order to estimate the pollutant source strengths with the kerosene heater on. Pollutant source strengths for CO, NO, and NO_2 were calculated by using the time-dependent version of eq 1 (*11*) because real-time data, as opposed to time-averaged data, were available for these pollutants. Pollutant emission rates (mass of pollutant emitted per kilojoules of fuel consumed) were calculated by dividing the kerosene heaters' pollutant source strengths by their fuel consumption rates. P was assigned the value of 1.0 for inorganic gases, such as nitrogen dioxide, and 0.4 for particles on the basis of previous research in the same chamber (*12*). Somewhat arbitrarily, P was assumed to be 0.8 for semivolatile organic compounds (SVOCs); however, using a value of 1.0, as for other gaseous compounds, would not significantly alter the emission rate results. The average chamber reactivity/deposition rate, k, was directly determined from real-time decay curves for inorganic gases. For SVOCs and particles, estimates of k were made by rearranging eq 1 and using the indoor/outdoor pollutant ratios measured during control tests (i.e., when $S = 0$), the air-exchange rates measured during control tests, and the estimates for P. The estimates of k ranged from 0.0 to over 2.0 h^{-1} for SVOCs, depending upon the compound or class of compounds, and ranged from 0.0 to 0.4 h^{-1} for particles. For the purpose of estimating pollutant emission rates, k was assigned the value of 1.0 h^{-1} for SVOCs and 0.2 h^{-1} for particles. Since different SVOCs have different reactivity rates, some error will be introduced to the emission rate calculations by using a single k value for all SVOCs.

Table I. Standard Compounds for the Semiquantitative Analyses of Organic Pollutants

compd name	compd class[a]	concn, μg/mL: high level	concn, μg/mL: low level
octane	aliphatic HCs	20	10
decane	aliphatic HCs	20	10
dodecane	aliphatic HCs	20	10
heptadecane	aliphatic HCs	20	10
n-eicosane	aliphatic HCs	20	10
docosane	aliphatic HCs	20	10
naphthalene	PAHs	10	5
phenanthrene	PAHs	10	5
pyrene	PAHs	10	5
chrysene	PAHs	10	5
benzo[*a*]pyrene	PAHs	10	5
benzo[*ghi*]perylene	PAHs	10	5
acridine	N heterocyclic compds	10	5
pentachlorophenol	phenols	10	5
benzoic acid	organic acids	20	10
1,2,4-trimethylbenzene	base–neutral org compds	20	10
di-*n*-ethyl phthalate	phthalates	20	10
di-*n*-butyl phthalate	phthalates	20	10
bis(2-ethylhexyl) phthalate	phthalates	20	10

[a] HCs, hydrocarbons.

Indoor pollutant concentration measurement/collection techniques fell into three categories. First, real-time CO, CO_2, NO, and NO_2 measurements were made with standard outdoor air pollution instruments (*11*). Second, 100-cm^2 Teflon-impregnated glass-fiber filters were used to collect nonvolatile and particle-bound organic compounds. And third, approximately 100 g of XAD-2 resin was placed behind each glass-fiber filter to collect SVOCs (*15*).

Each XAD/filter sampler was operated at an airflow rate of 6.8 m^3/h, and each sample was collected for no more than 8 h. Two samplers were operated inside the chamber, and one was operated outside the chamber. One filter and one XAD cartridge were used per test at each sampling location except for the maltuned convective tests, where heavy soot loading required the use of two filters per test for both indoor sampling systems.

After sample collection, the XAD resin was placed in clean glass jars with Teflon-lined caps, and the filters were folded and wrapped in aluminum foil. The XAD-2 and filter samples were placed in unused clean paint cans that were placed in dry ice mailing boxes. The samples and filter and XAD-2 blanks were shipped from LBL to Battelle Columbus Laboratories, by overnight carriers, where all analyses of the glass-fiber filters and XAD resin were done (*15*).

The glass filters were weighed before and after sample collection to determine the total mass of collected particles, to an estimated precision of 5%. Soluble organic material was removed from the filter and the XAD resin samples by Soxhlet extraction with methylene chloride. After this extraction, aliquots of extracts from XAD samples were removed for total chromatographable organic (TCO) analysis (*16*). TCO analysis yields information on the amounts of organic material with boiling points in the approximate range of 100–400 °C. A gas chromatograph (GC) with a flame ionization detector was used for TCO analysis. The GC was calibrated with mixtures of known concentrations of normal C_8, C_{12}, C_{16}, and C_{20} hydrocarbons. The estimated precision for TCO analysis is 20%.

Table II. Carbon Monoxide, Nitric Oxide, and Nitrogen Dioxide Emission Rates for Tests of Well-Tuned Radiant and Maltuned Convective Heaters

test	average emission rates,[a] μg/kJ CO	NO	NO_2
RAD-1	92 ± 16	0.69 ± 0.16	5.1 ± 0.4
RAD-2	88 ± 11	0.53 ± 0.19	5.0 ± 0.3
RAD-3	77 ± 10	0.69 ± 0.21	5.0 ± 0.3
RAD-4	85 ± 12	0.85 ± 0.24	4.7 ± 0.2
RAD-5	79 ± 4	0.71 ± 0.19	4.6 ± 0.2
MCON-1	22 ± 7	21 ± 3	7.5 ± 1.8
MCON-2	18 ± 4	22 ± 0	5.6 ± 1.6

[a] Radiant (RAD) test averages are from four 1-h burns. Maltuned convective (MCON) test averages are from approximately two 1-h burns. Plus/minus values are standard deviations of the two or four emission rates calculated from each 1-h burn.

Table III. Total Suspended Particulate Mass and GRAV Concentration Results for Filter-Collected Samples for Well-Tuned Radiant and Maltuned Convective Kerosene Heaters

test	mass, μg/m³ in[b]	mass, μg/m³ out[c]	GRAV,[a,d] μg/m³ in[b]	GRAV,[a,d] μg/m³ out[c]
RAD-1	28	18	nm	nm
RAD-2	23	9	nm	nm
RAD-3	24	9	8.2	3.6
RAD-4	14	7	nm	nm
RAD-5	13	2	nm	nm
MCON-1	5300	62	nm	nm
MCON-2	2300	40	100	13
CONTROL-1	5	13	1.6	5.6
CONTROL-2	4	13	nm	nm

[a] GRAV analysis is designed to measure solvent-extractable organics, most of which have boiling points over 300 °C. [b] Refers to the concentrations measured inside the chamber. [c] Refers to the concentrations measured outside the chamber. [d] nm, not measured.

Gravimetric (GRAV) analyses for solvent-extracted organics, most of which have boiling points over 300 °C, were done on selected XAD and filter extracts (*16*). Aliquots of sample extracts were dried and weighed for this analysis. Repeat measurements yielded an average estimated precision of 20% for the GRAV analyses.

Nitrated-PAH and other organic analyses were accomplished with a combined gas chromatograph/mass spectrometer (GC/MS). Analyses were performed by a Finnigan 4500 quadrapole MS equipped with an INCOS 2300 data system and a Finnigan GC. The sample extracts were quantitatively analyzed by an on-column injection, negative chemical ionization (NCI) technique (*17*) for the following nitrated PAHs: 1-nitronaphthalene, 2-nitrofluorene, 9-nitroanthracene, 9-nitrophenanthrene, 6-nitrochrysene, 6-nitrobenzo[*a*]pyrene, 3-nitrofluoranthene, 1-nitropyrene, 1,3-dinitropyrene, 1,6-dinitropyrene, 1,8-dinitropyrene, 2,7-dinitrofluorene, and 2,7-dinitrofluorenone. The accuracy and precision of this technique were within 20%.

The extracts were also analyzed by electron impact (EI) GC/MS to provide tentative determinations of the various classes of compounds in the extracts. The identifications of sample components were accomplished by comparison to reference spectra in the Environmental Protection Agency/National Institutes of Health mass spectral library. The quantitations were based on the surrogate response factors generated from partial calibration curves (two levels, triplicate analyses) of the surrogate standards. The surrogate standards (Table I) were chosen to best represent the range of organic compound classes present in the extracts. The response factor of each standard was used for the same class of compounds (e.g., naphthalene as the standard for all two-ring PAHs). If the identified compounds are not represented by the standards, the response factors are designated as 1. The analysis is called semiquantitative because results are estimated to be accurate only to within a factor of 3–4. However, the precision of the results is on the order of 30%.

The MS was operated at 70 eV and scanned from 50 to 450 amu/s in the EI mode. In the NCI mode, the MS was operated at 150 eV and scanned from 100 to 450 amu/s. Methane was used as the carrier and reagent gas.

Table IV. GRAV and TCO Concentration Results for XAD-Collected Samples for Well-Tuned Radiant and Maltuned Convective Heaters

test	GRAV,[a] μg/m³ in[c]	GRAV,[a] μg/m³ out[d]	TCO,[b] μg/m³ in[c]	TCO,[b] μg/m³ out[d]
RAD-1	490	190	1400	150
RAD-2	360	120	930	190
RAD-3	510	120	4900	370
RAD-4	450	77	1000	92
RAD-5	380	48	1700	130
MCON-1	500	250	2100	400
MCON-2	360	220	950	240
CONTROL-1	99	94	700	290
CONTROL-2	50	29	100	110

[a] GRAV analysis is designed to measure solvent-extractable organics, most of which have boiling points over 300 °C. [b] TCO analysis is designed to measure solvent-extractable organics with boiling points between 100 and 400 °C. [c] Refers to the concentrations measured inside the chamber. [d] Refers to the concentrations measured outside the chamber.

Results and Discussion

Carbon Monoxide, Nitric Oxide, and Nitrogen Dioxide. CO, NO, and NO_2 emission rate results for each test that employed organic pollutant samples are presented in Table II. The emission rate results for the well-tuned radiant heater are consistent with previously published data (*2, 4*). The results for the maltuned convective heater show that total nitrogen oxide ($NO + NO_2 = NO_x$) emissions are 27% lower than for a well-tuned convective heater. A well-tuned heater will emit approximately 15 μg/kJ N (of NO_x) (*4*); the maltuned convective heater emitted approximately 11 μg/kJ N (of NO_x). The CO emissions from the maltuned convective heater were similiar to those from a well-tuned heater. This result is not expected to be universal but is probably unique to the method of maltuning used in this study, that is, supplying excess air to the combustion region.

TCO, GRAV, and TSP Mass. Table III lists the TSP mass and GRAV concentration results for filter-collected samples. Both TSP mass and GRAV concentrations were higher for the maltuned convective heater tests than for the radiant heater tests. However, the ratio of GRAV to TSP mass was much lower for the maltuned convective heater tests than for the radiant heater tests. This observation is consistent with a previously reported observation that increased sooting does not cause a proportionate increase in organic pollutants (*18*).

Table IV lists the GRAV and TCO results for XAD-collected samples. Again, notice that the GRAV and TCO indoor concentrations for the well-tuned radiant and the maltuned convective tests are similiar, despite the great difference in TSP concentrations. Tables III and IV show that kerosene heaters do emit some organic pollutants and

Table V. TCO, GRAV, and TSP[a] Mass Emission Rates for Well-Tuned Radiant and Maltuned Convective Kerosene Heaters

pollutant group	emission rates, ng/kJ		
	RAD-1, -2, -4, -5	RAD-3	MCON-1, -2
TCO-XAD	19	76	23
GRAV-XAD	6	7	6
GRAV-filter	nm[b]	0.07	0.9
TSP	0.2	0.2	40

[a] TSP, total suspended particulate. [b] nm, not measured.

Table VI. Nitrated-PAH Emission Rates from Well-Tuned Radiant and Maltuned Convective Kerosene Space Heaters

compounds	emission rates,[a] ng/kJ		
	RAD-1, -2, -4, -5	RAD-3	MCON-1, -2
1-nitronaphthalene			
XAD	0.04	0.02	0.04
filter	nd	0.0005	0.02
9-nitroanthracene			
XAD	nd	0.008	nd
filter	0.0001	0.0005	0.006
3-nitrofluoranthene (filter only)	0.0003	nd	nd
1-nitropyrene (filter only)	0.0006	0.001	nd

[a] nd, none detected.

that most of the organic pollutants were trapped by the XAD-2 resin. TCO analyses were not performed on the filter-collected samples because compounds with boiling points lower than 300 °C were assumed to pass through the filter to be collected on the XAD-2 resin. As will be discussed later in this report, the assumption applied well to the well-tuned radiant heater tests but not as well to the maltuned convective heater tests, in which the heavy soot loading on the filters trapped a significant fraction of many SVOCs before they reached the XAD.

Nitrated PAHs and Other Organic Compounds. Samples of similar types were combined before organic and nitrated-PAH compound analyses were done; however, XAD samples were not mixed with filter samples. Samples for radiant tests coded RAD-1, RAD-2, RAD-4, and RAD-5 were combined (note that the TCO results for RAD-3 were much higher than for the other radiant tests so RAD-3 was analyzed separately); samples from maltuned convective tests MCON-1 and MCON-2 were combined; and samples from CONTROL-1 and CONTROL-2 were combined. Indoor and outdoor samples were not combined. The final totals were eight XAD-2 and eight filter samples: two indoor radiant, two outdoor radiant, one indoor convective, one outdoor convective, one indoor control, and one outdoor control. Field blanks of glass-fiber filters and XAD-2 were also analyzed. The amounts of pollutants found in the field blanks were subtracted from the results of the test samples.

To conform with previous research on pollutant emissions from combustion appliances, results presented here will be expressed as pollutant emission rates (i.e., mass of pollutant emitted per unit of fuel consumed). Pollutant source strengths (i.e., mass of pollutant emitted per unit of time) can be calculated by multiplying the emission rate values by the kerosene heater fuel consumption rate (approximately 7000 kJ/h for the heaters used in this study). Estimates of indoor air pollutant concentrations can be calculated by rearranging eq 1.

A rough error propagation analysis was conducted on our calculations of pollutant emission rates, using precision estimates for the variables in eq 1, to determine if the emission rates were significantly different from zero. Except where noted, the omission of a source strength value from this paper is the result of one of three possibilities: the pollutant was not sought, the pollutant was sought but not found, or the pollutant emission rate was not significantly different from zero. In the last circumstance, qualitative judgments were used in some cases, for example, when the limit of detection of a compound was only approximately known and no outdoor concentrations were reported.

For comparison with other emission rate tables, the emission rates for TCO, GRAV, and TSP mass are given in Table V.

Table VI lists the emission rates of several nitrated PAHs. The nitrated PAHs searched for were previously discussed. 1-Nitronaphthalene is clearly emitted by the well-tuned radiant and maltuned convective koerosene space heaters and was collected almost entirely on the XAD-2 resin for the radiant heater tests. For the maltuned convective heater tests, 30% of the 1-nitronaphthalene was collected on the filter. This is a result of the heavy loading of fresh soot on the filter, which acted like a collecting resin.

Emissions of 9-nitroanthracene were observed in the XAD fraction of one of the radiant heater tests and in the filter fraction of the maltuned convective test. (Again, the heavy soot loading on the filters in the convective tests captured the 9-nitroanthracene before it reached the XAD). Emissions of 1-nitropyrene were also observed in the filter fraction of both radiant-test samples, whereas only trace amounts of 3-nitrofluoranthene were observed in one of the two series of radiant heater tests in the filter-collected fraction.

Both 3-nitrofluoranthene and 1-nitropyrene have been observed to be somewhat mutagenic (*9*, *19*), but the mutagenic activities of 1-nitronaphthalene and 9-nitroanthracene are low (*19*). Missing from Table VI are the highly mutagenic dinitropyrenes (DNPs), possibly because their emission rates were below the detection limit of the techniques used here. The 1,3-DNP, 1,6-DNP, and 1,8-DNP combined source strengths were measured by another research team to be approximately 0.2 ng/h (*9*). The estimated limit of detection in terms of source strengths for DNPs or other nitrated PAHs investigated for this report is approximately 1.0 ng/h. Future studies could take advantage of various fractionation and cleanup techniques to improve the detection sensitivity for this class of compounds; however, such elaborate techniques were not appropriate for this exploratory study.

Table VII presents pollutant source-strength results for selected organic pollutants emitted from the well-tuned radiant and maltuned convective heaters. Although the table contains more information than can be discussed here, two topics are of particular interest: the differences in relative source strengths among the three test/sample categories and the PAH emissions.

There is a striking difference in relative source strengths between the RAD-1, -2, -4, and -5 tests and the RAD-3 test. The alkylbenzene emissions from the RAD-3 test were much greater than those from the other radiant heater tests, whereas the aliphatic hydrocarbon and aliphatic ketone emissions from the RAD-1, -2, -4, and -5 tests were much greater than those from the RAD-3 test. All five radiant heater tests were experimentally identical, yet the relative emission rates of many compounds observed from the RAD-3 test are dramatically different from the other

Table VII. Selected Organic Pollutant Emission Rates from Well-Tuned Radiant and Maltuned Convective Kerosene Space Heater

compound class	emission rates,[a] ng/kJ RAD-1, -2, -4, -5	RAD-3	MCON-1, -2
PAH			
naphthalene			
XAD-2	8.0	33	3
filter	nd[a]	nd	20
C2, naphthalene (filter only)	nd	nd	4
C3, naphthalene (filter only)	0.2	nd	0.7
phenanthrene (XAD only)	0.3	2	0.9
fluoranthene			
XAD-2	nd	0.1	nd
filter	0.02	0.01	0.3
anthracene (filter only)	nd	nd	0.3
chrysene (filter only)	0.01	nd	nd
indeno[*cd*]pyrene (filter only)	nd	0.02	nd
alkylbenzenes			
XAD-2	13	8700	120
filter	0.3	nd	2
pentachlorophenol			
XAD-2	5	7	nd
filter	0.05	0.2	130
phthalates			
XAD-2	170	470	510
filter	1	3	220
hydronaphthalenes			
decalin (XAD-2 only)	43	150	3
C2, decalin (XAD-2 only)	260	930	270
C1, tetralin			
XAD-2	100	240	170
filter	nd	nd	23
aliphatic hydrocarbons			
XAD-2	220	nd	420
filter	1	0.9	200
aliphatic alcohols			
XAD-2	1400	700	710
filter	0.8	5	85
aliphatic ketones			
XAD-2	96	nd	650
filter	nd	0.2	nd
benzoic acids (filter only)	0.3	nd	nd
aromatic acid (XAD-2 only)	nd	nd	91
fatty acids (filter only)	2	3	32
esters (filter only)	0.9	2	28
miscellaneous			
C1, cyclohexane (XAD-2 only)	nd	75	nd
C2, methoxybenzene (XAD-2 only)	420	nd	nd
C2, ethenylbenzene (XAD-2 only)	nd	96	nd
(chlorophenyl)ethanone (XAD-2 only)	nd	nd	40
acridene (filter only)	nd	nd	0.2
methylpropoxybenzene (filter only)	nd	nd	8
aliphatic amine (filter only)	nd	nd	29

[a] nd, none detected.

radiant tests. This appears to imply that small changes in combustion conditions can result in large changes in pollutant emission rates.

The comparison of the convective-test emissions of many compounds with those of the radiant tests reveals both similarities and differences. The PAH, phthalate, and aliphatic alcohol emissions for the radiant and convective tests are quite similar, yet the aliphatic ketone and, particularly, the pentachlorophenol (PCP) emissions are much greater in the convective tests than in the radiant tests. With regard to PCP emissions, tests were conducted on the kerosene for trace amounts of chlorinated compounds using a GC/MS technique (*20*). The results showed that concentrations of chlorinated compounds were below the detection limit of 10 ppm (*20*). However, ambient chlorine was present in the form of airborne sea salt, and methylene chloride was used near the outside of the chamber before and after the experiments were conducted. Since pentachlorophenol was used as a calibration standard for this analysis and some pentachlorophenol was emitted during the radiant heater tests, we must conclude that the convective heater pentachlorophenol source strength presented in Table VII is valid, although how such a compound could be produced in a kerosene flame is somewhat puzzling. Higher levels of acidic compounds such as ketones, acids, and esters were emitted from the maltuned convective heater than from the well-tuned radiant heater. This result is expected since such acidic compounds are indicative of incomplete combustion. Also of interest is the observation that many SVOCs were trapped by the soot-laden filter during the maltuned convective tests.

Relatively few PAHs were observed to be emitted by the kerosene heaters with the very broad GC/MS scanning technique employed in this study. Other PAHs would probably be found by a more sensitive technique. Our analysis shows naphthalene to be the primary PAH emission from kerosene heaters. Emissions of fluoranthene and indeno[*cd*]pyrene, two slightly mutagenic compounds (*8*, *21*), were also found. Previous research from a turbulent-diffusion, continuous-flow kerosene combuster showed that 18 nonvolatile or particle-bound PAHs were emitted, with naphthalene accounting for only 3% of the particle-bound PAHs (*8*). The earlier study also found that relatively few PAHs (perylene, cyclopenta[*cd*]pyrene, and fluoranthene) accounted for almost all of the indirect mutagenic activity of the kerosene heater soot. Of those mutagenic compounds, only fluoranthene was also observed in this study. A more specific study of PAH emissions using more sensitive techniques is warranted.

Conclusions

This study has confirmed the results of other studies, that is, that the kerosene combustion process can emit PAHs and nitrated PAHs. In addition, kerosene heaters were found to emit many other organic compounds including aliphatic hydrocarbons, alcohols, and ketones; phthalates; and alkylbenzenes.

Pollutant emission rate results, such as those presented here, need to be incorporated into air pollution exposure assessment models. Exposure assessments can then be combined with health effects data to determine the risk associated with exposure to these organic compounds. PAH and nitrated-PAH emissions are sufficiently important to justify additional quantitative studies; furthermore, examinations of other organic compounds of toxicologial significance and of other combustion sources are warranted.

This study revealed that the indoor reactivity rates of some SVOCs were near 2 h^{-1}. This implies that reactivity rates for some SVOCs may be more important than typical residential air–exchange rates for determining indoor

concentrations. Therefore, future studies must quantify the indoor reactivity process for individual SVOCs to allow a better understanding of and quantification of indoor exposures to these compounds.

Acknowledgments

We thank J. Crum, B. Henschel, J. Lewtas, D. Sanchez, and J. White of the U.S. Environmental Protection Agency (Research Triangle Park, NC); W. Gutknecht of the Research Triangle Institute (Research Triangle Park, NC); and A. Carruthers and J. McCann of the Lawrence Berkeley Laboratory for their assistance during various phases of this project.

Literature Cited

(1) Yamanaka, S.; Hirose, H.; Takaoa, S. *Atmos. Environ.* **1979**, *13*, 407–412.
(2) Leaderer, B. P. *Science* **1983**, *218*, 1113–1115.
(3) Ryan, P. B.; Spengler, J. D.; Letz, R. *Atmos. Environ.* **1983**, *17*, 1339–1345.
(4) Traynor, G. W.; Allen, J. R.; Apte, M. G.; Girman, J. R.; Hollowell, C. D. *Environ. Sci. Technol.* **1983**, *17*, 369–371; *Environ. Sci. Technol.* **1985**, *19*, 200, addendum.
(5) Lionel, T.; Martin, R. J.; Brown, N. J. *Environ. Sci. Technol.* **1986**, *20*, 78-85.
(6) Prado, G. P.; Lee, M. L.; Hites, R. A.; Hoult, D. P.; Howard, J. B. *Proceedings of the 16th International Symposium on Combustion*; The Combustion Institute: Cambridge, MA, 1973; pp 649–661.
(7) Skopek, T. R.; Liber, H. L.; Kaden, D. A.; Hites, R. A.; Thilly, W. G. *JNCI, J. Natl. Cancer Inst.* **1979**, *68*, 309–312.
(8) Kaden, D. A.; Hites, R. A.; Thilly, W. G. *Cancer Res.* **1979**, *39*, 4152–4159.
(9) Tokiwa, T.; Nakagawa, R.; Horikawa, K. *Mutat. Res.* **1985**, *157*, 39–47.
(10) Turk A. *ASHRAE J.* **1963**, *5*, 55–58.
(11) Traynor, G. W.; Girman, J. R.; Apte, M. G.; Dillworth, J. F.; White, P. D. *J. Air Pollut. Control Assoc.* **1985**, *35*, 231–237.
(12) Traynor, G. W.; Anthon, D. W.; Hollowell, C. D. *Atmos. Environ.* **1982**, *16*, 2979–2987.
(13) Alzona, J.; Cohen, B. L.; Rudolph, H.; Jow, H. N.; Frohliger, J. O. *Atmos. Environ.* **1979**, *13*, 55–60.
(14) Dockery, D. W.; Spengler, J. D. *Atmos. Environ.* **1981**, *15*, 335–343.
(15) Mumford, J. L.; Harris, D. B.; Williams, K.; Chuang, J. C.; Cooke, M. *Environ. Sci. Technol.* **1987**, *21*, 308–311.
(16) Lentzen, D. E.; Wagoner, D. E.; Estes, E. D.; Gutknecht, W. S. *IERL-RTP Procedures Manual: Level 1 Environmental Assessment*, 2nd ed.; EPA-600/7-78-201; U.S. Environmental Protection Agency: Research Triangle Park, NC, 1978.
(17) Nishioka, M. G.; Petersen, B. A.; Lewtas, J. In *Polynuclear Aromatic Hydrocarbons: Chemical Analyses and Biological Fate*; Cooke, M., Dennis, A. J., Fisher, G. L.; Eds.; Battelle Press: Columbus, OH, 1982; pp 603–612.
(18) Howard, J. B.; Longwell, J. P. In *Polynuclear Aromatic Hydrocarbons: Formation, Metabolism and Measurement*; Cooke, M., Dennis, A. J., Eds.; Battelle Press: Columbus, OH, 1983; pp 27–62.
(19) Rosenkranz, H. S.; Mermelstein, R. *J. Environ. Sci. Health* **1985**, *C3*, 221–272.
(20) Carter Analytical Laboratory, Inc., Campbell, CA.
(21) National Research Council *Polycyclic Aromatic Hydrocarbons: Evaluation of Sources and Effects*, National Academy Press: Washington, DC, 1983; p A-14.

Received for review February 28, 1989. Accepted March 9, 1990. The project was funded by the U.S. Environmental Protection Agency (EPA) under Interagency Agreement DW89930753-01 through the U.S. Department of Energy under Contract No. DE-AC03-76SF00098. Although funded by the EPA, the research described here does not necessarily reflect the views of the Agency, and no official endorsement should be inferred.

New ENVIRONMENTAL Titles

from the American Chemical Society

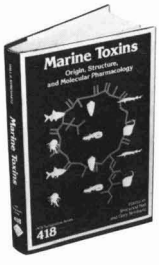

Marine Toxins: Origin, Structure, and Molecular Pharmacology

Sherwood Hall and Gary Strichartz, Editors

Examines the structures of marine toxins, their metabolic origins, and the molecular basis for their toxicity. A description of the sources of marine toxins emphasizes the metabolic pathways responsible for their synthesis. Looks at which features in toxins determine both the distribution of toxic materials among the organs of intoxicated species and the stability, disposition, and biotransformation of those toxins. Investigates the interactions between toxins and their primary sites of action.

ACS Symposium Series No. 418
300 pages (1990) Cloth.
$74.95

Enhanced Biodegradation of Pesticides in the Environment

Kenneth D. Racke and Joel R. Coats, Editors

Offers a comprehensive review of microbial adaptation for pesticide degradation. Includes a general description of enhanced biodegradation as it occurs in an agricultural context; the microbial aspects of enhanced biodegradation, including the genetics, biochemistry, and ecology of pesticide-degrading microorganisms; and the potential impact of enhanced degradation on pesticide fate in aquatic systems and groundwater.

ACS Symposium Series No. 426
296 page (1990) Cloth.
$64.95

Expert Systems for Environmental Applications

Judith M. Hushon, Editor

Provides an ideal introduction to environmental expert systems. Over 65 of the 80 available systems are covered, including GEOTEX, CORA, CADRA, Risk*Assistant*, and Fish Toxicity Prediction. Broader issues, such as success factors for expert systems, verification and validation of environmental expert systems, and the future of expert systems at EPA, are also covered.

ACS Symposium Series No. 431
232 pages (1990) Cloth.
$49.95

Emerging Technologies in Hazardous Waste Management

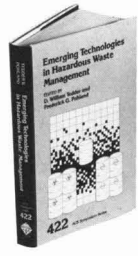

William Tedder and Frederick G. Pohland, Editors

In 22 chapters, this book brings together an array of reports on several technologies related to hazardous waste reduction. Describes developing technologies for treating and managing wastewaters and solid residuals, such as soils and incinerator ashes that are contaminated. Includes chapters on diverse topics such as municipal solid wastes, water purification by radiation, the isolation of organic species and inorganic radionuclides and solvent recycling.

ACS Symposium Series No. 422
416 pages. (1990) Cloth.
$89.95

Now in Print!

Handbook of Chemical Property Estimation Methods

Environmental Behavior of Organic Compounds

Warren J. Lyman, William F. Reehl, and David H. Rosenblatt

Presents simple estimation methods for 26 important properties of organic chemicals that are of environmental concern. Estimations can be obtained quickly using no more than a hand calculator and the Handbook's step-by-step instructions and worked-out examples. Facilitates the study of problematic chemicals in such applications as chemical fate modeling, environmental assessments, priority ranking of large lists of chemicals, chemical spill modeling, chemical process design, and experimental design.

First published by McGraw-Hill Book Company (1982)
960 pages (1990) Cloth.
$49.95

Oxidations in Organic Chemistry

Milos Hudlicky

This volume opens with a discussion of oxidation agents, followed by oxidations of various functional groups, detailed descriptions of the preparations of useful oxidation agents, and specific experimental procedures. The final section provides extensive correlation tables.

ACS Monograph Series No. 186
Estimated 336 pages (1990)
Cloth: $89.95. Paper: $49.95.

Order from: American Chemical Society
Distribution Office, Dept. 60
1155 Sixteenth St. NW, Washington, DC 20036
or call toll free 1-800-227-5558 (in DC 872-4363)
and use your credit card!

Clean solutions for troubled waters.

Environmental sample matrices can be hazardous to your productivity.

If you're struggling to detect water contaminants at the required levels, you'll be glad to know Dionex has an easier way.

Crash the ppb barrier in complex matrices.

Alkali and alkaline earth metals rob ICP spectroscopy of its sensitivity for measuring transition metals in sea water—unless you do a lot of sample prepping.

Couple Dionex Chelation Ion Chromatography to an ICP spectrometer and get those fractional ppb levels with a *direct introduction* of your sea water or acid digest sample.

Find a drop of chromium in a bucket of interferences.

Hexavalent chromium† in waste water is not unlike a needle in a haystack: so elusive, it devours your time.

With our new IC method, incorporating a very high-capacity ion exchange column, non-metallic postcolumn chemistry, and photometric detection, you'll get 0.1 ppb sensitivity and no interferences in a 6-minute analysis.

†Method under EPA review

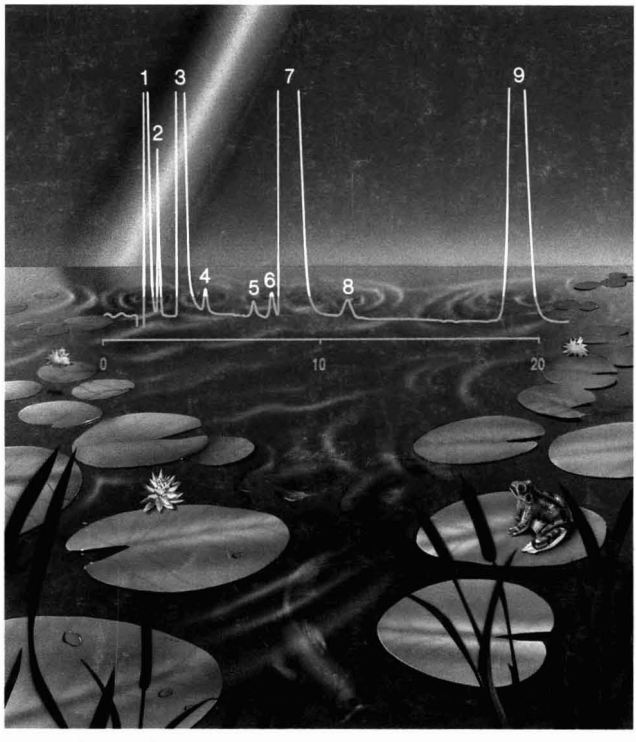

◀Oxy-Halides Detection in Drinking Water†

Adequate separation between the chlorate and nitrate peaks could not be achieved with past anion columns. The new IonPac AS9 column provides the resolution needed for reliable detection of chlorite and chlorate.

Peaks	ppm
1. F^-	5.66
2. ClO_2^-	0.50
3. Cl^-	45.45
4. NO_2^-	0.06
5. Br^-	0.08
6. ClO_3^-	0.14
7. NO_3^-	42.11
8. HPO_4^{2-}	0.17
9. SO_4^{2-}	5.00

Column: IonPac AS9
Eluant: $Na_2CO_3/NaHCO_3$
Detection: Suppressed Conductivity

Direct Metals Detection in Sea Water*

Metal	Detection Limit (ppb) Direct Nebulization[1]	Chelation Concentration[2]
Cd	10	0.1
Co	10	0.1
Cu	10	0.1
Fe	10	0.1
Mn	5	0.1
Ni	10	0.1
Pb	50	0.9
Zn	10	0.1

[1] With background correction
[2] 11 mL concentrated
*IC/ICP under EPA review

Dionex Chelation IC provides a 100-fold improvement in ICP detection limits.

Determine chlorite and chlorate in a single run.

How do you measure oxyhalides in drinking water to the required 0.1 ppm? Until now, with great difficulty and not much reliability. Fortunately, the new, highly selective Dionex IonPac® AS9 column, combined with chemically suppressed conductivity detection, does the job in one easy run.

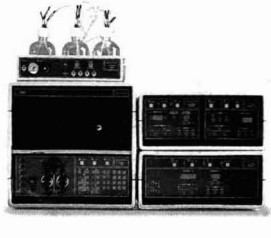

Series 4500i. The right solutions. Right now.

When you want solutions, you need Dionex. Find out how Dionex columns and the Series 4500i Systems can solve your environmental analysis problems—wet or dry. Contact your local Dionex representative or (in U.S.A.) call **1-800-227-1817, ext. 42** today.

Series 4500i
Ion Chromatograph

DIONEX
A BETTER SOLUTION

Dionex Corporation, P.O. Box 3603, Sunnyvale, CA 94088-3603. **Canada** Dionex Canada, Ltd., (416) 855-2551. **England** Dionex (UK) Ltd., (0276) 691722. **West Germany** Dionex GmbH, (06126) 6056. **France** Dionex S.A., (1) 46216666. **Italy** Dionex S.r.l., (06) 3792979. **Netherlands** Dionex B.V., (076) 714800.